UNITED STATES DEPARTMENT OF THE INTERIOR

GEOLOGICAL SURVEY

SUMMARIES OF TECHNICAL REPORTS, VOLUME XVII

Prepared by Participants in

NATIONAL EARTHQUAKE HAZARDS REDUCTION PROGRAM

December 1983

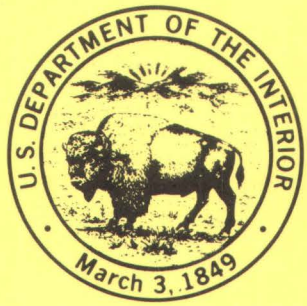

OPEN-FILE REPORT 83-918

This report (map) is preliminary and has not been reviewed for conformity with U.S.Geological Survey editorial standards (and stratigraphic nomenclature). Any use of trade names is for descriptive purposes only and does not imply endorsement by the U.S.G.S.

Menlo Park, California

1983

INSTRUCTIONS FOR PREPARATION OF SUMMARY REPORTS

1. Use 8 1/2" x 11" paper for both text and figures.

2. Leave at least 1" wide margins at top, sides and bottom.

3. Type headings at top of first page. Headings should include:

    a. Project title

    b. Contract, grant or project number

    c. Name of Principal Investigator(s)

    d. Name and address of institution

    e. Telephone number(s) of Principal Investigator(s)

4. Original copies of text and figures are required. No xerox copies.

5. Type figure captions on the same page as the figure.

6. Only type on one side of the paper.

7. Type all text single spaced.

8. Do not use staples.

9. All figures must be in black and white. No color figures (color, weak or grey lines will not photo-reproduce).

UNITED STATES
DEPARTMENT OF THE INTERIOR
GEOLOGICAL SURVEY

SUMMARIES OF TECHNICAL REPORTS, VOLUME XVII

Prepared by Participants in

NATIONAL EARTHQUAKE HAZARDS REDUCTION PROGRAM

Compiled by

Muriel L. Jacobson

The research results described in the following summaries were submitted by the investigators on October 20, 1983 and cover the 6-month period from April 1, 1983 through September 30, 1983. These reports include both work performed under contracts administered by the Geological Survey and work by members of the Geological Survey. The report summaries are grouped into the four major elements of the National Earthquake Hazards Reduction Program:

Earthquake Hazards and Risk Assessment (H)
Robert D. Brown, Jr., Coordinator
U.S. Geological Survey
345 Middlefield Road, MS-77
Menlo Park, CA 94025

Earthquake Prediction (P)
James H. Dieterich, Coordinator
U.S. Geological Survey
345 Middlefield Road, MS-77
Menlo Park, California 94025

Global Seismology (G)
Eric R. Engdahl, Coordinator
U.S. Geological Survey
Denver Federal Center, MS-967
Denver, Colorado 80225

Induced Seismicity (IS)
Mark D. Zoback, Coordinator
U.S. Geological Survey
345 Middlefield Road, MS-77
Menlo Park, California 94025

Open File Report No. 83-918

This report has not been reviewed for conformity with USGS editorial standards and stratigraphic nomenclature. Parts of it were prepared under contract to the U.S. Geological Survey and the opinions and conclusions expressed herein do not necessarily represent those of the USGS. Any use of trade names is for descriptive purposes only and does not imply endorsement by the USGS.

The data and interpretations in these progress reports may be reevaluated by the investigators upon completion of the research. Readers who wish to cite findings described herein should confirm their accuracy with the author.

CONTENTS

Earthquake Hazards Reduction Program

Page

I. Earthquake Hazards and Risk Assessment (H)

Objective 1. Establish an accurate and reliable national earthquake data base.---------- 1

Objective 2. Delineate and evaluate earthquake hazards and risk in the United States on a national scale.---------- 9

Objective 3. Delineate and evaluate earthquake hazards and risk in earthquake-prone urbanized regions in the western United States.---------- 16

Objective 4. Delineate and evaluate earthquake hazards and risk in earthquake-prone regions in the eastern United States.---------- 66

Objective 5. Improve capability to evaluate earthquake potential and predict character of surface faulting.---------- 93

Objective 6. Improve capability to predict character of damaging ground shaking.---------- 145

Objective 7. Improve capability to predict incidence, nature and extent of earthquake-induced ground failures, particularly landsliding and liquefaction.--------- 167

Objective 8. Improve capability to predict earthquake losses.--- 181

II. Earthquake Prediction (P)

Objective 1. Obtain pertinent geophysical observations and attempt to predict great or very damaging earthquakes.

Operate seismic networks and analyze data to determine character of seismicity preceding major earthquakes.

Measure and interpret geodetic strain and elevation changes in regions of high seismic potential, especially in seismic gaps.---------- 186

Page

Objective 2. Obtain definitive data that may reflect precursory changes near the source of moderately large earthquakes. Short term variations in the strain field prior to moderate or large earthquakes require careful documentation in association with other phenomena.

Measure strain and tilt near-continuously to search for short term variations preceding large earthquakes. Complete development of system for stable, continuous monitoring of strain.

Monitor radon emanation water properties and level in wells, especially in close association with other monitoring systems. Monitor apparent resistivity, magnetic field to determine whether precursory variations in these fields occur. Monitor variations in seismic velocity and attenuation within the (San Andreas) fault zone.---------- 324

Objective 3. Provide a physical basis for short-term earthquake predictions through understanding the mechanics of faulting.

Develop theoretical and experimental models to guide and be tested against observations of strain, seismicity, variations in properties of the seismic source, etc., prior to large earthquakes.---------- 400

Objective 4. Determine the geometry, boundary conditions, and constitutive relations of seismically active regions to identify the physical conditions accompanying earthquakes.

Measure physical properties including stress, temperature, elastic and anelastic properties, pore pressure, and material properties of the seismogenic zone and the surrounding region.---------- 447

III. Global Seismology (G)

Objective 1. Operate, maintain, and improve standard networks of seismographic stations.---------- 479

Objective 2. Provide seismological data and information services to the public and to the research community.------- 498

Objective 3. Improve seismological data services through basic and applied research and through application of advances in earthquake source specification and data analysis and management.---------- 500

Page

IV. Induced Seismicity Studies (IS)

Objective 1. Establish a physical basis for understanding the tectonic response to induced changes in pore pressure or loading in specific geologic and tectonic environments.---------- 507

Index 1: Alphabetized by Principal Investigator---------- 534

Index 2: Alphabetized by Institution---------- 539

Reanalysis of Instrumentally-Recorded U.S. Earthquakes

9920-01901

J. W. Dewey
Branch of Global Seismology and Geomagnetism
U.S. Geological Survey
Denver Federal Center, MS 967
Denver, Colorado 80225
(303) 234-4041

Investigations

1. Relocate instrumentally recorded U.S. earthquakes using the method of joint hypocenter determination (JHD) or the master event method, using subsidiary phases (Pg, S, Lg) in addition to first arriving P-waves, using regional travel-time tables, and expressing the uncertainty of the computed hypocenter in terms of confidence ellipsoids on the hypocentral coordinates.

2. Evaluate the implications of the revised hypocenters on regional tectonics and seismic risk.

Results

1. Dave Gordon has completed relocation of approximately 270 instrumentally recorded earthquakes that occurred in the central United States. The earthquakes were those with mblg greater than 3.0 that occurred through 1980 and that were recorded by enough seismographs that they could be located by least squares inversion of phase arrival-times. The earliest such shocks in the central U.S. occurred in 1931. Figure 1 shows relocated shocks from the central Mississippi River valley, including the New Madrid seismic zone. Approximately two-thirds of the shocks in figure 1 occurred prior to the installation of the Southeast Missouri Regional Seismic Network (Saint Louis University) in 1974, but the network data provide the means to calibrate the locations of the pre-network shocks. Gordon has shown that most of the pre-network shocks occurred in source regions defined since 1974 by microearthquake epicenters located by the regional network. The revised epicenters also suggest a north trending lineament centered on Marked Tree (fig. 1) that has not been previously recognized. For the entire central United States, the deepest reliably-determined hypocenters are those beneath southern Illinois in the area bounded by 37.8 degrees N, 38.8 degrees N, 87.8 degrees W, and 88.8 degrees W. Four of these hypocenters, which are also those estimated to be most precise, have focal depths between 20 and 25 km.

2. Jim Dewey has examined properties of selected source regions of midplate earthquakes worldwide in light of hypotheses on the characteristics of the source of the 1886 Charleston earthquake. Data from the other midplate source regions suggest that the Charleston region is more likely to experience a strong earthquake in future decades than a random midplate site, but that strong eastern U.S. earthquakes will also occur in the future at sites that have not previously experienced strong earthquakes. Data from the other regions do not provide conclusive seismological or geological guidelines for identifying sources of future strong earthquakes in the absence of a historical record of strong earthquakes. In particular, most of the other strong

midplate earthquakes were not clearly associated with prominent pre-existing faults. However, the relatively shallow focal depths of most midplate earathquakes and the fact that many of the midplate sources show a general correlation with regional geologic structure, even if they cannot be assigned to specific mapped faults, support the view that the sites of strong midplate earthquakes are determined by pre-existing geological structure. For several midplate earthquakes, the size of the aftershock zone was much larger than the size of the mainshock fault rupture; by implication, the aftershock zone of the 1886 Charleston earthquake may have been much larger than the causative fault of the earthquake.

Reports

Dewey, J. W. 1983, Relocation of instrumentally recorded pre-1974 earthquakes in the South Carolina region. In Gohn, G.S., ed., Studies related to the Charleston, South Carolina, earthquake of 1886—Tectonics and seismicity: U.S. Geological Survey Professional Paper 1313, p. Q1-Q9.

Dewey, J. W., 1983, A global search of continental midplate seismic regions for specific characteristics bearing on the 1886 Charleston earthquake, in Proceedings of the Workshop on the 1886 Charleston Earathquake and its Implications for Today, Charleston, South Carolina, May 23-26, 1983: U.S. Geological Survey Open File Report, in press.

Gordon, D. W., 1983, Revised hypocenters and correlation of seismicity and tectonics in the Central United States: St. Louis, Saint Louis University, Ph.D. dissertation, 199 p.

Gordon, D. W., 1983, Seismicity and plate tectonic remnants in the Central Stable Region of the United States, Program and Abstracts of the 55th Annual Meeting of the Eastern Section of the Seismological Society of America, September 19-21, Mohonk Mountain House, New York.

Figure 1. Revised epicenters of instrumental earthquakes with $m_{bLg} \geq 3.0$ in the Central Mississippi Valley through 1980. Each epicenter is marked by an octagon surrounded by the associated 95% confidence ellipse.

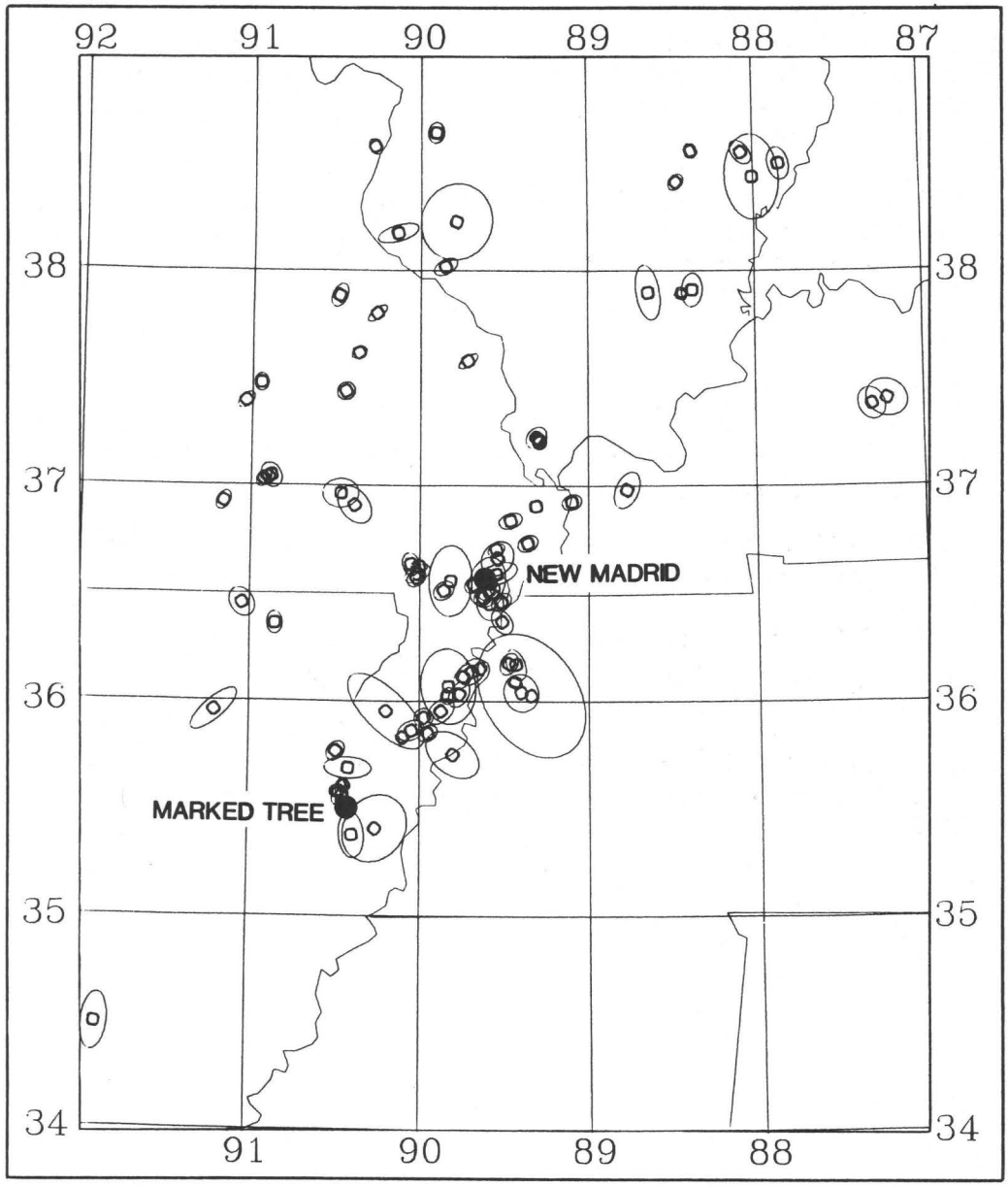

The Historical Seismicity of Central United States: 1811-1928

14-08-0001-21251

Ronald L. Street
Department of Geology
University of Kentucky
Lexington, KY 40506
(606) 257-4777

The purpose of this project is to document in detail, the larger earthquakes known to have occurred in the general region about the junction of the Mississippi and Ohio river valleys. Eighty-three earthquakes, listed in Table 1, have been selected for this study on the basis of their reported felt area and epicentral location. Felt areas and epicentral locations have been initially assumed to be the same as those given by Nuttli (1979) and Street (1980a). Once documentation has been completed, felt areas, epicentral locations, and m_{bLg} magnitudes will be revised where necessary.

Progress in the study is summarized in Table 1. The percentage of documentation completed for each earthquake being studied is indicated by state. The letters C and N in the table stand for "Complete", and "Not Applicable", respectively.

References

Nuttli, O. W. (1979). Seismicity of the central United States, Reviews in Eng. Geology, IV, 67-93.

Street, R. (1980a). The southern Illinois earthquake of September 27, 1891, Bull. Seism. Soc. Am., 70, 915-920.

Street, R. (1980b). A Compilation of Accounts Describing the Mississippi Valley Earthquakes of 1811-1812: Part I, EERC #330, 08/S82/1980, 247 p.

Street, R. (1982). A contribution to the documentation of the 1811-1812 Mississippi Valley earthquake sequence, Earthquake Notes, 53, 39-52.

LIST OF EARTHQUAKES

1811-1927

DATE *mo-day-yr*	TIME *hr-min*	LAT/LONG *n w*	FELT AREA *sq ki*	AR	IL	IN	KY (*states*)	MO	OH	TN
12-16-1811	08:15	36.0/90.0	5000000.*							
01-23-1812	15	36.3/89.6	5000000.*		*See Street (1980b, 1982)					
02-07-1812	09:45	36.5/89.6	5000000.*							
07-05-1827	11:30	38.3/85.8	430000.	N	80	80	C	C	N	80
02-04-1833		42.3/85.6	20000.							
06-09-1838	14:45	38.5/89.0	500000.		80	50	C	20	N	C
12-28-1841					50	N	--		N	
01-05-1843	02:45	35.5/90.5	1500000.	50	80	50	C	80	80	
02-17-1843	05	35.5/90.5	250000.	50			C		N	
08-09-1843		35.6/87.1	40000.				--			
12-18-1853		36.6/89.2	100000.	C			--			
02-28-1854		37.6/84.5	20000.	N	N	N	C	N	N	N
11-09-1856		36.6/89.5	80000.				--			
10-08-1857	10	38.7/89.2	200000.		90	90	C	C	N	N
08-07-1860	15:30	37.8/87.5	80000.		90	20	C		N	20
07-17-1865	15	36.5/89.5	250000.		50	N	C		N	20
05-03-1873	21	36.0/89.6	30000.		C	N	50	C	N	20
06-18-1875	13:43	40.2/84.0	100000.	N	C	20	80	N	10	N
10-07-1875		36.1/89.6	50000.			N	10		N	
09-25-1876	06:15	38.5/87.8	150000.	N	80	10	C	N	C	N
07-15-1877	00:40	36.8/89.7	65000.		30	N	C		N	
03-12-1878	10	36.8/89.1	40000.(?)		C	N	C		N	
11-19-1878	05:52	36.7/89.3	350000.	50	80	N	C	20	N	50
07-14-1880	02:30	35.3/90.3	25000.		C	N	--		N	
07-28-1882		37.6/90.6	25000.		90		--		N	

09-27-1882	10:20	39.0/89.5	100000.	N	70	20	C	20	N	C
10-15-1882	05:50	39.0/89.5	20000.	N	50	N	C	50	N	N
10-15-1882	10:35	39.0/89.5	20000.	N	50	N	C	50	N	N
01-11-1883	07:12	37.0/89.2	200000.	50	70	20	C		N	50
07-14-1883	07:30	37.0/89.1	25000.				--			
12-05-1883	15:20	36.3/91.2	250000.	50	80	N	--		N	
09-19-1884	20:14	40.7/84.1	320000.	N	50		C	N	10	
03-18-1886	05:59	37.0/89.2	45000.	C	80	N	C	20	N	C
02-06-1887	22:15	38.7/87.5	170000.	N	80	C	C	50	N	C
08-02-1887	18:36	37.0/89.2	170000.	50	80	C	C	50	N	50
09-27-1891	04:55	37.0/89.2	500000.	C	80	80	C	80	C	50
10-31-1895	11:08	37.0/89.4	2500000.	C	50	50	C	20	20	20
04-26-1897	04	35.8/89.6	20000.			N	--		N	
06-14-1898	15:20	36.0/89.4	120000.		C		70		N	50
04-30-1899	02:05	38.8/87.0	100000.	N	C	80	C	N	80	N
02-15-1901	00:15	36.0/90.0	30000.		50	N	C	50	N	20
01-24-1902	10:48	38.6/90.2	130000.	C	80	N	C	50	N	N
02-09-1903	00:21	37.8/89.3	180000.	C	80		C	30	N	
10-05-1903	02:56	37.0/90.0	120000.	C	C	N	C	20	N	C
11-04-1903	18:18	36.9/89.3	340000.	C	80	80	C	50	N	50
11-04-1903	19:14	36.9/89.3	340000.	C	80	80	C	50	N	50
11-27-1903	09:20	36.5/89.5	180000.	C	80		C		N	C
08-22-1905	05:08	36.8/89.6	325000.	C	80	80	C	C	50	C
12-28-1908	21:15	37.0/89.0	80000.	N	80	30	C		N	40
05-26-1909	14:42	42.5/89.0	800000.				C	50		
07-19-1909	04:34	40.2/90.0	100000.	N	80	N	N	50	N	N
08-16-1909	22:45	38.3/90.1	45000.	N	50	C	N		N	N
09-22-1909										
09-27-1909	09:45	39.5/87.4	250000.				N	50		
10-23-1909	07:10	37.0/89.5	125000.	C	80	80	C	50	C	80
03-31-1911				50	C	N	N	N	N	
01-02-1912	16:21	41.5/88.5	150000.	N	50	80	N	80	N	N
12-07-1915	18:40	36.7/89.1	120000.	C	80	80	C	50	N	50
05-21-1916	18:34	36.6/89.5	20000.	N	70	N	C	20	N	N
04-09-1917	20:52	38.1/90.2	550000	C	70		C	50	N	30

06-09-1917	13:14	36.8/90.4	45000.		70	N	--	50	N	
10-04-1918							--			
10-16-1918	02:15	36.0/89.2	100000.	50	80	N	C	50	N	80
05-25-1919	09:45	38.4/87.5	65000.	C	80		C	50	N	C
05-01-1920	15:15	38.5/89.5	60000.	N	80	N	N	50	N	N
03-14-1921	12:15	39.5/87.5	65000.	N	50		50	N	N	N
01-11-1922	03:42	37.9/87.8	25000.	N	80		C		N	N
03-22-1922	22:30	37.3/88.9	150000.		80		C		N	20
03-23-1922	21:45	37.0/88.9	50000.		80		C		N	20
03-30-1922	16:53	36.1/89.6	40000.		50	N	C		N	50
11-27-1922	03:31	37.8/88.5	130000.	N			C		N	C
10-28-1923	17:10	35.5/90.4	120000.	C	C	N	C		N	50
11-26-1923	23:25	35.5/90.4	23000.	50	50				N	
01-01-1924	03:05	35.4/90.3	150000.	C	80		C		N	50
04-02-1924	11:18	37.0/89.1	80000.		80	N	C		N	80
06-07-1924	05:42	36.4/89.5	25000.	N	N	N	C		N	
04-27-1925	04:05	38.3/87.6	250000.	N	80		C		50	C
09-02-1925	11:55	37.8/87.5	200000.		80		C		80	C
09-20-1925	09	37.8/87.5	25000.	N	C		C		N	C
06-20-1926				50	80		--			50
05-07-1927	08:28	35.7/90.6	300000.	C	80	N	C		N	50
07-20-1927		35.8/86.0	180000.		50		--	50		
08-13-1927	16:10	36.4/89.5	65000.	N	N	N	C		N	80

National Earthquake Catalog

9920-02648

J. N. Taggart
Branch of Global Seismology and Geomagnetism
U.S. Geological Survey
Denver Federal Center, MS967
Denver, Colorado 80225
(303) 234-5079

Investigations

1. Continued compilation of intensity data for early California and Alaska earthquakes.

2. Investigated the aftershock sequence of the March 10, 1933, Long Beach earthquake.

3. Developed a compressed, integer-structured database that can be rapidly searched.

Results

1. Carol Thomasson and Jim Taggart edited and checked about 2,400 corrections to 10,700 southern California local shock listings for 1932-1959. About one-half of these corrections are reference listings, but the other half represent new intensity data. Several hundred events also were added to the Alaska database, mostly for the period 1880-1912. Karen Meagher continued to collect and collate data on historical California earthquakes from newspapers, Seismological Notes, United States Earthquakes, and other published sources.

2. Willie Lee and Jim Thorsen reinterpreted original seismograms of the aftershocks of the March 10, 1933, Long Beach earthquake. They augmented the permanent station data with arrival times from a temporary seismograph station. Hypocenter relocations were obtained for about 60 of several hundred aftershocks that were recorded by three or more stations. Plots of the hypocenters suggest that velocities differ noticeably on the two sides of the Long Beach fault. The main problems in this investigation are the determination of station clock corrections and the development of an adequate model of crustal velocities.

3. Jim Taggart developed a new, compressed National Earthquake Catalog database on the VAX 11/780 computer. An indexed key for each earthquake, consisting of pseudo-Julian date and origin time, is stored as a seven-character string of three integers to a precision of 0.1 msec. Other basic parameters, such as coordinates, depth, magnitudes, intensity and hypocenter statistics, are stored as real or integer numbers to facilitate rapid comparisons against the selected search criteria. Local network event parameters are included in the main database. A large number of bit flags point to keyed secondary files of less common data, such as tsunami information and location of waveform data. Use of coded byte integers in the new database reduced storage requirements by more than a factor of two compared with storage of the same information in ASCII format.

Regional and National Seismic Hazard and Risk Assessment

9950-01207

S. T. Algermissen
Branch of Engineering Geology and Tectonics
U.S. Geological Survey
Denver Federal Center, MS 966
Denver, CO 80225
(303) 234-4014

Investigations

1. A field party was dispatched following the May 2, 1983 Coalinga, California earthquake to systematically survey building damage in the Coalinga area. Buildings, both damaged and undamaged, were catalogued in order that percent loss can be estimated for buildings within each structural classification.

2. Assessment of long return-period earthquake ground motion for the eastern United States continued. Consequences of modeling five seismotectonic hypotheses that relate eastern U.S. seismicity to geologic structures or geologic processes are being investigated in terms of differences in resulting regional probabilistic ground motion values. The statistical significance of various source zones was investigated in terms of their capacity to describe the spatial distribution of earthquakes in the eastern United States.

3. The magnitude and distance dependence of the standard deviation of ground motion attenuation statistical variability was investigated using a simple rupture model.

4. A graphical technique for showing the relative contribution of various magnitudes to the exceedances of a given ground motion value in probabilistic seismic hazard analysis was developed.

5. The dependence of maximum magnitude of Benioff zone earthquakes on various characteristics of the subduction zone was investigated using a variety of multivariate analysis techniques.

6. Assessment of sensitivity of regional probabilistic ground motion values to changes in the input parameters of finite fault rupture model, ground motion attenuation function, and magnitude-frequency relationship has been summarized in a series of papers for journal publication.

7. A new pattern-recognition algorithm has been developed and programmed. The algorithm seeks to discriminate areas having high potential for large earthquakes from areas having low potential for large earthquakes based on a number of geographic, geologic and topographic similarities or dissimilarities.

8. Development of a series of efficient computer programs for digitizing and plotting seismicity data is continuing.

9. Investigation of efficient data processing techniques for collecting and analyzing earthquake damage data is continuing, particularly with respect to the new methodology employed in collecting damage data following the May 2, 1983 Coalinga, California earthquake.

10. Reanalysis of earthquake damage data from the 1971 San Fernando earthquake in an effort to extract possible characteristic site-dependent building damage.

11. A computer program is being developed under contract to water resources division for use in seismic hazard evaluation of dam sites.

12. Assessment of potential for earthquake-induced liquefaction and other ground effects for damaging earthquakes in the Mississippi Valley in connection with a FEMA supported disaster preparedness study in the Midwest.

Results

1. Observations and preliminary results of the Coalinga, California damage investigation have been summarized in an article submitted to a special volume devoted to the earthquake and its effects being published by the California Division of Mines and Geology.

2. A text is in preparation describing tectonic and seismotectonic models used in developing seismic source zones for long return-period earthquake hazard evaluation in the eastern United States. A salient conclusion from this work is that the variability in ground motion estimates is dominated by uncertainty in ground motion attenuation and not configuration of the seismic source zones.

3. The simple rupture model predicts significant decrease in that part of the variability due to the rupture source with increasing magnitude and distance. Therefore, at relatively large distances, knowledge of site characteristics can greatly reduce total ground motion variability for large earthquakes.

4. For several velocity attenuation functions, the exceedances are dominated by the effects of earthquakes between magnitude 5.5 to 6.5

5. Results of this investigation did not show improvement over a regression on two of the characteristics.

6. Results of probabilistic ground motion sensitivity studies have been submitted for journal publication. One paper has been published and is listed below.

7. Evaluation of the new pattern recognition algorithm is in progress.

8. A report that estimates economic loss in the Los Angeles, California, area due to a recurrence of historical earthquakes and postulated future earthquakes is in preparation.

9. Reduction of Coalinga damage data is in progress. A preliminary report is in press.

Reports

Algermissen, S. T., and Steinbrugge, K. V., 1984, Seismic hazard and risk assessment: some case histories, the Geneva Papers on Risk and Insurance, 9 (No. 30, January 1984), Assoc. Internationale pour l'Etude de l'Economie de l'Assurance, Geneva, pp. 8-26.

Bender, B., 1983, Maximum likelihood estimation of b values for magnitude grouped data: Seismological Society of America Bulletin, v. 73, pp. 831-851.

Bender, B., submitted, A two state model for seismic hazard analysis: Seismological Society of America Bulletin.

Bender, B., submitted, Seismic hazard estimation using a finite fault rupture model: Seismological Society of America Bulletin.

Hopper, M. G., Thenhaus, P. C., Barnhard, L. M., and Algermissen, S. T., in press, Damage survey in Coalinga, California for the earthquake of May 2, 1983, in, California Division of Mines and Geology special report on the Coalinga earthquake.

Seismic Hazard Studies: Anchorage, AK

9950-01205

A. F. Espinosa
Branch of Engineering Geology and Tectonics
U.S. Geological Survey
Denver Federal Center, MS 966
Denver, CO 80225
(303) 234-5077

Investigations

1. Data analysis of 128 NTS events recorded at near- and intermediate-epicentral distances on accelerograph stystems is in progress.

2. A report entitled "Earthquake Catalog for Peru," by L. A. Casaverde, A. F. Espinosa, J. Michael and J. Vargas Neumann, is in the process of being written.

3. Regional attenuation relations have been derived for the contiguous United States using Lg-waves. The $M_b(L_g)$ scaling laws take into account the variation of the dissipation factor (Q) in different regions of the U.S.A. A paper is being written on this subject which has a direct impact on other regional scaling laws and on seismic risk studies.

4. A damage evaluation for the City of Anchorage, sustained from the 1964 Alaskan earthquake, is being performed with damage data which have not been published previously. This information and local surficial geological data is planned to be used in order to evaluate transfer function amplification curves in Anchorage and to ascertain any existing correlation between damage and soil conditions in the area.

5. A "completeness" of the seismicity catalog is being investigated in order to use lower magnitude thresholds in (a) spatial and magnitude-temporal distribution of shallow ($h \leq 33$ km) and intermediate ($34 \leq h \leq 100$ km) seismicity ($M_s \geq 5.5$) occurring within a specified area in the period of time which uses (a) historical and (b) instrumentally recorded earthquakes. B-values are being determined likewise for the region under study. This effort is part of the seismicity study being carried out in this project for the Anchorage and vicinity region in Alaska.

Reports

Espinosa, A. F., and Michael, J., 1983, P_g-wave data-base tabulation recorded on the: ILRSM stations in the conterminous United States, II New England Stations: U.S. Geological Survey Open-File Report 83-590, 75 p.

Investigation of Seismic Wave Propagation for Determination of Crustal Structure

9950-01896

S. T. Harding
Branch of Engineering Geology and Tectonics
U.S. Geological Survey
Denver Federal Center, MS 966
Denver, CO 80225
(303) 234-5087

Investigations

1. Conducted high resolution seismic reflection survey over recent faults.
   a. An east west line through the city of Nephi, Utah, in order to determine movement on the Wasatch Fault.
   b. Across the fault scarp at Willow Creek north of Nephi, Utah.
   c. Across the fault scarp at Hobble Creek south of Provo, Utah.
   d. Across the East Bench Fault along Interstate 80 in Salt Lake City, Utah.

Results

Rough processing on all these lines have been completed. The data shows that the Mini-Sosie energy source yields results in populated areas without to many problems. We were able to operate throughout the city of Nephi without disturbing any property. The profile along the interstate indicates the method is useful to gather data where the traffic volume is extremely high.

Data Processing, Golden

9950-02088

R. B. Park
Branch of Engineering Geology and Tectonics
U.S. Geological Survey
Denver Federal Center, MS 966
Denver, CO 80225
(303) 234-5070

Investigations

The purpose of this project is to provide the day to day management and systems maintenance and development for the Golden Data Processing Center. The center supports Golden based Office of Earthquakes, Volcanoes and Engineering investigators with a variety of computer services. The systems include a PDP 11/70, several PDP 11/03's and PDP 11/23's, a VAX/780 and two PDP 11/34's. Total memory is 6.4 mbytes and disk space will be approximately 2.2 G bytes. Peripherals include four plotters, eight mag-tape units, an analog tape unit, five line printers, 5 CRT terminals with graphics and a Summagraphic digitizing table. Dial-up is available on all the major systems and hardwire lines are available for user terminals on the upper floors of the building. Users may access any of the systems through a Gandalf terminal switch. Operating systems used are RSX11 (11/34's), Unix (11/70), RT11 (LSI's) and VMS (VAX).

The three major systems are shared by the Branch of Global Seismicity and Geomagnetism and the Branch of Engineering Geology and Tectonics.

Results

Computation performed is primarily related to the Global Seismology and Hazards programs; however, work is also done for the Induced Seismicity and Prediction programs as well as for DARPA, ACDA, MMS, U.S. Bureau of Reclamation, and AFTAC among others.

In Global Seismology and Geomagnetism, the data center is central to nearly every project. The monitoring and reporting of seismic events by the National Earthquake Information Service is 100 percent supported by the center. Their products are, of course, a primary data source for international seismic research and have implications for hazard assessment and prediction research as well as nuclear test ban treaties. Digital time series analysis of Global Digital Seismograph Network data is also 100 percent supported by the data center. This data is used to augment NEIS activities as well as for research into routine estimation of earthquake source parameters. The data center is also intimately related to the automatic detection of events recorded by telemetered U.S. stations and the cataloging of U.S. seismicty, both under development.

In Engineering Geology and Tectonics, the data center supports research in assessing seismic risk and the construction of national risk maps. It also provides capability for digitizing analog chart recordings and maps as well as analog tape. Also, most if not all of the research computing related to the hazards program are supported by the data center.

The data center also supports equipment for online digital monitoring of Nevada seismicity. Also it provides capability for processing seismic data recorded on field analog and digital cassette tape in various formats. Under development is a portable microprocessor based system to be used by the field investigations group to do preliminary analysis and editing of temporary local networks and the GOES Satellite Event Detect System. Recent acquisitions include the replacement of the PDP 11/40 used for analog input with a PDP 11/34, expansion of the Nevada Network 11/34 for collection of Western Slope data for the U.S. Bureau of Reclamation, a second Versatec plotter and a Tektronix 4014 graphic system.

Ground Response Along the Wasatch Front

9950-01919

K. W. King
Branch of Engineering Geology and Tectonics
U.S. Geological Survey
Denver Federal Center, MS 966
Denver, CO 80225

(303) 234-5087

Investigations

The objective is to improve fundamental knowledge about how the ground response along the Wasatch front correlates with the local and regional geology. Data have been acquired in the Salt Lake City, Ogden, Provo, urban areas along the Wasatch front as well as in two other urban areas, Logan and Cedar City, which provide a comparison. If possible a field experiment is planned to explain an area of anomalously low-ground responses in the Ogden area. A seismic study was made to discern the difference between surface and subsurface ground motions in a waste repository site. A seismic study was made on the effects of induced seismic energy from road construction on adobe construction and archaeological ruins.

Results

1. The activities in the Wasatch area this fiscal year are designed to prepare and to publish data reports and journal manuscripts and to develop equipment for future experiments. One such publication is the forthcoming 3d International Conference on Microzonation. The Wasatch data report is 99 percent complete (in reiteration from CTR). The equipment specifications are finalized.

2. Induced seismic motions were documented on adobe construction and analyzed. Preliminary reports were made to the Federal Highway Administration and the National Park Service.

Reports

Hays, W. W., and King, K. W., 1982, Zoning of the earthquake ground shaking hazard along the Wasatch fault zone, Utah [abs.]: International Conference on Microzonation, 3d, Seattle, July 1982.

King, K. W., 1982, A study of surface and subsurface ground motion at Calico Hills, Nevada Test Site: U.S. Geological Survey Open-File Report 82-1044, 19 p.

King, K. W., Hays, W. W., and McDermott, P. J., Wasatch front urban area seismic response data report: U.S. Geological Survey Open-File Report 83-452, 70 p. (Has not been released thru U.S. Geological Survey Open-File Services Section, 10/19/83.)

Alaska Seismic Studies

9930-01162

John C. Lahr
Christopher D. Stephens
Branch of Seismology
U. S. Geological Survey
345 Middlefield Road, MS 77
Menlo Park, California 94025
(415) 323-8111, ext. 2510

Investigations

1) Continued collection and analysis of data from the high-gain short-period seismic network extending across southern Alaska from Juneau to Cook Inlet and inland across the Chugach Mountains. A new station was installed 20 km northeast of Icy Bay above a persistent source of aftershocks of the 1979 St. Elias earthquake. This station will improve depth control and also aid in resolving focal mechanisms.

   With funding from the Division of Geological and Geophysical Surveys of the State of Alaska, four seismic stations, which had been terminated in 1982 due to funding considerations, are again being recorded. These stations are particularly important for coverage of the northern Prince William Sound region which experienced two magnitude 6 earthquakes this past summer.

2) Continued monitoring of the region around the proposed Bradley Lake hydroelectric project on the Kenai Peninsula, a cooperative effort with the Alaska Power Authority. Two new stations were installed about 40 km southwest of Bradley Lake to help in detection and location of crustal activity that has been observed there during the past few years.

3) The USGS operates 43 strong motion instruments in Alaska, including 13 between Icy Bay and Cordova in the area of the Yakataga seismic gap. Fourteen of these are connected to the high-gain station telemetry network so that absolute trigger time can be obtained. Maintenance of the remaining instruments is shared between this project and the Engineering Seismology and Geology Branch.

Results

1) During the past six months data processing has remained on schedule. Preliminary hypocenters have been determined for earthquakes that occurred in March - July, 1983 (Figure 1) and parts of August and September. For the interval March - July, prominent aftershock sequences following four shallow (depth less than 35 km) intermediate-

sized shocks of magnitude 5.1 m_b or larger increased the average monthly rate of events to 410, about 15% higher than for the previous six month period. The four mainshocks include a 5.3 m_b* event on March 30 located near the Duke River segment of the Denali fault system in Canada, a 5.9 m_b event on June 28 in the aftershock zone of the 1979 St. Elias earthquake (7.1 M_S), a magnitude 6.3 M_S event on July 12 beneath the Columbia Glacier north of Prince William Sound, and a second event in the St. Elias aftershock zone on July 15 that had a magnitude of 5.1 m_b. The three largest events within the western part of the network during this time all had magnitudes of 4.7 m_b. Two of these events were located between 80 and 90 km depth in the Benioff zone west of Cook Inlet, and one occurred at a depth of about 20 km beneath western Prince William Sound. Near the end of June, a small swarm of earthquakes of coda-duration magnitude 3.5 and smaller occurred beneath the continental margin about 75 km southeast of Yakutat Bay. This area is characterized by a relatively low rate of activity and the last known swarm occurred in 1974.

2) On July 12, 1983 a magnitude 6.3 M_S earthquake occurred at about 30 km depth beneath the Columbia Glacier north of Prince William Sound and was felt throughout much of southern Alaska and as far east as Whitehorse, Canada. This is the largest earthquake to occur in the Prince William Sound region since the 1964 Alaska earthquake. Epicenters of aftershocks that occurred within 24 hours following the mainshock define a northeast-striking zone about 20 km long and 8 km wide (Figure 2, left). On September 7, a magnitude 6.1 M_S shock occurred at the southwest end of the aftershock zone of the July 12 mainshock at a depth of about 30 km (Figure 2, left). The first 24 hours of aftershock activity from the September 7 shock is confined to a zone of approximately equal lateral dimensions about 10 km across and has little overlap with the aftershock zone of the July 12 event. In the first ten days following the July 12 shock three aftershocks of magnitude 3.5 M_L or larger occurred, and the largest aftershock prior to the September 7 shock was a magnitude 4.0 M_L event on August 4.

In contrast, seven aftershocks of the September 7 event that occurred in the first 10 days following the mainshock had magnitudes of 3.5 M_L or larger, and the largest aftershock was a 5.0 m_b shock three hours after the mainshock. A few temporary seismograph stations surrounding the epicentral area were deployed after each mainshock. Hypocenters of aftershocks from the July 12 event that were located using the temporary stations define a fault plane about 25 km long dipping about 70° to the northwest between depths of about 22 and 32 km (Figure 2, right). P-wave first-motions obtained from regional and some teleseismic

* Surface-wave (M_S) and body-wave (m_b) magnitudes and felt reports were obtained from the Preliminary Determination of Epicenters of the USGS National Earthquake Information Service. Local magnitudes (M_L) are those reported by the Alaska Tsumani Warning Center in Palmer, Alaska.

stations indicate normal faulting for the mechanism of the July 12 mainshock. P-wave first motions for the September 7 shock indicate that this event also involved normal faulting, but a preliminary look at relative amplitudes of P, pP, and sP phases recorded atlong-period teleseismic stations suggests that the nodal planes of this event may be significantly rotated with respect to the July 12 event. No obvious foreshock activity to the July 12 shock is evident in the pattern of coda-duration magnitude 2 and larger earthquakes that occurred in the area of the aftershock zone for a period at least two years prior to the earthquake. It is inferred that the Columbia Bay events occurred in the subducted Pacific plate. To test this hypothesis we are seeking direct seismological evidence of a subhorizontal velocity contrast that may indicate the interface between the subducting and overthrust plates.

3) The July 12, 1983 earthquake near Columbia Glacier (6.3 M_S) triggered several strong-motion instruments in southern Alaska and produced the largest recorded acceleration known for Alaska, 0.32 g on the horizontal component of the Valdez High School accelerograph (Personal communication, G. Brady, USGS, 1983), which is located about 40 km to the east of the closest point on the burried fault rupture. The M_S 6.1 companion shock of September 7, 1983 registered a much lower acceleration, 0.07 g, at the Valdez High School.

Three other earthquakes also triggered strong-motion instruments in southern Alaska. A magnitude 5.9 m_b shock that occurred on June 28, 1983 at 12 km depth east of Icy Bay triggered an instrument at GYO, about 13 km to the west. A preliminary estimate of 0.11 g was obtained for the maximum horizontal acceleration on this record. A second instrument near Icy Bay was triggered between August 26, 1982 and July 27, 1983 and recorded a maximum horizontal acceleration of 0.18 g, but as yet the identifiction of the causative event is uncertain. Simlarly, the event which triggered an instrument at the site BRLK on the Kenai Peninsula and produced a maximum horizontal acceleration of 0.08 g between June 24, 1982 and June 26, 1983 is uncertain.

4) Since 1974, when the regional seismograph network began operating in the eastern Gulf of Alaska, earthquakes of magnitude 4.5 m_b and larger have occurred frequently along the eastern and southern boundaries of the Yakgataga seismic gap. Within the gap, however, the two largest events have had magnitudes of about 4. Both shocks were located about 100 km west of the aftershock zone of the 1979 St. Elias earthquake (7.1 M_S) that occurred along the eastern boundary of the gap, and both occurred within 9 months of the St. Elias mainshock. In the first 8 1/2 months of 1983 seven earthquakes of magnitude 5 m_b and larger have occurred in a 200-km wide zone around the Yakataga seismic gap, more than in any one year period since 1970-71. At the microearthquake level, within a relatively quiet zone extending from Icy Bay westward to eastern Prince William Sound, the pattern of activity has remained relatively stable since 1974, with prominent concentrations beneath the Copper River Delta and Waxell Ridge. Considering the short seismic

history and complex tectonics of the region, the uniqueness and significance of the elevated level of activity at magnitudes larger than 5 are difficult to evaluate.

Reports

Blackford, M. E., and Fogleman, K. A., 1983, Focal mechanism of the July 12, 1983 Columbia Glacier, Alaska earthquake [abs.]: EOS, Transactions of the American Geophysical Union, v. 64, [in press].

Fogleman, K. A., Stephens, C. D., Lahr, J. C., Rogers, J. A., Cancilla, R. S., Roy Tam, Freiberg, J. A., and Melnick, J. P., 1983, Catalog of earthquakes in southern Alaska, April - June 1980: U. S. Geological Survey Open-File Report 83-14, 54 p.

Fogleman, K. A., Stephens, C. D., Lahr, J. C., Rogers, J. A., Cancilla, R. S., Roy Tam, Helton, S. M., Freiberg, J. A., and Melnick, J. P., 1983, Catalog of earthquakes in southern Alaska, July - September 1980: U. S. Geological Survey Open-File Report 83-15, 54 p.

Lahr, J. C., Stephens, C. D., 1983, Eastern Gulf of Alaska seismicity: Final report to the National Oceanic and Atmospheric Administration for July 1, 1975 through September 30, 1981: U. S. Geological Survey Open-File Report 83-592, 49 p.

Page, R. A., Stephens, C. D., and Fogleman, K. A., 1983, Columbia Bay, Alaska earthquakes of 1983 [abs.]: EOS, Transactions of the American Geophysical Union, v. 64, [in press].

Stephens, C. D., Fogleman, K. A., Lahr, J. C., and Page, R. A., 1983, The Wrangell Benioff, southern Alaska: submitted to Geology.

Stephens, C. D., Lahr, J. C., Page, R. A., and Rogers, J. A., 1983, Review of earthquake activity and current status of seismic monitoring in the region of the Bradley Lake Hydroelectric Project, southern Kenai Peninsula, Alaska: December 1981- May 1983: U. S. Geological Survey Open-File Report 83-744, 25 p.

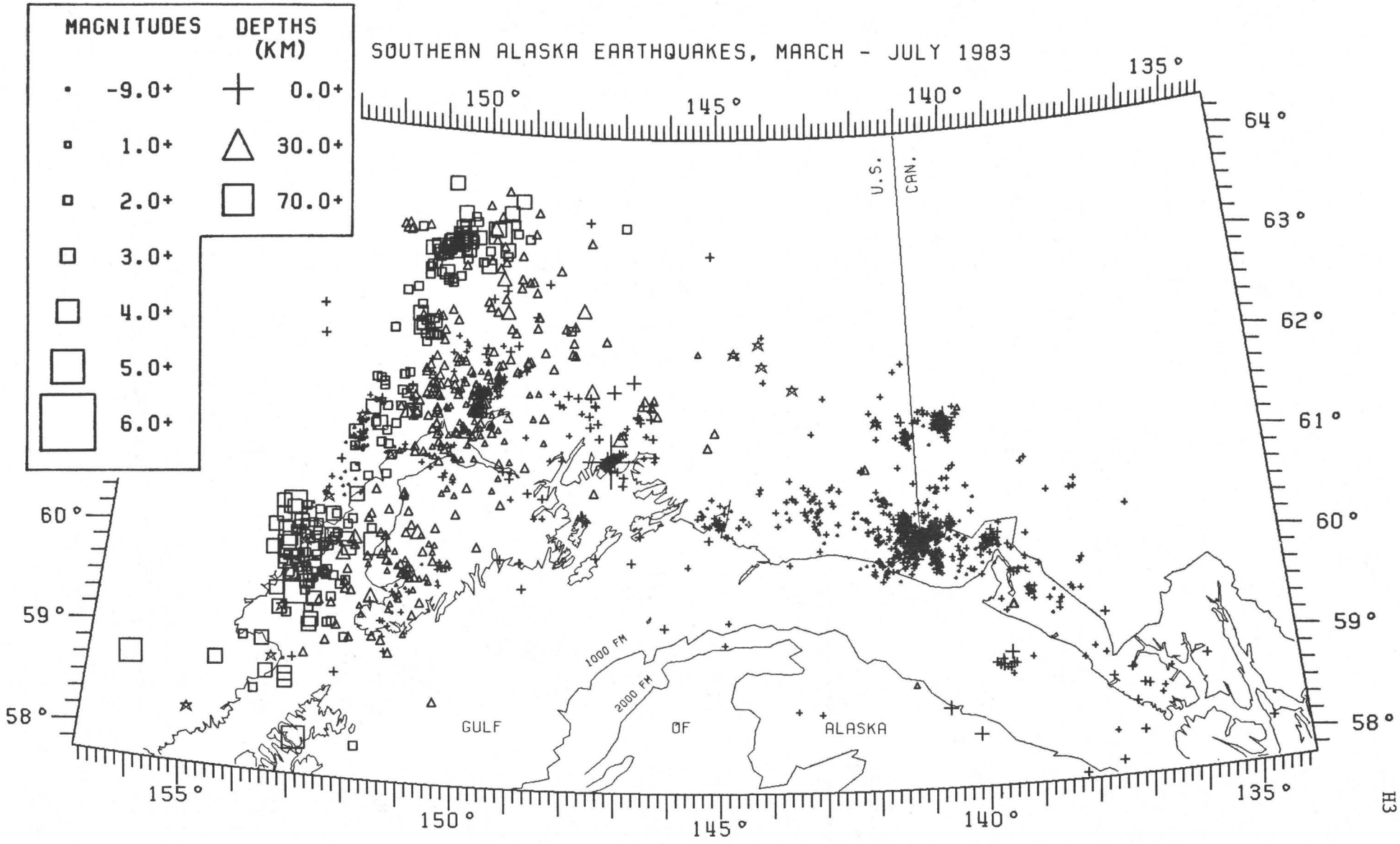

Figure 1. Seismicity in southern Alaska from March through July 1983. Stars indicate Quaternary volcanoes.

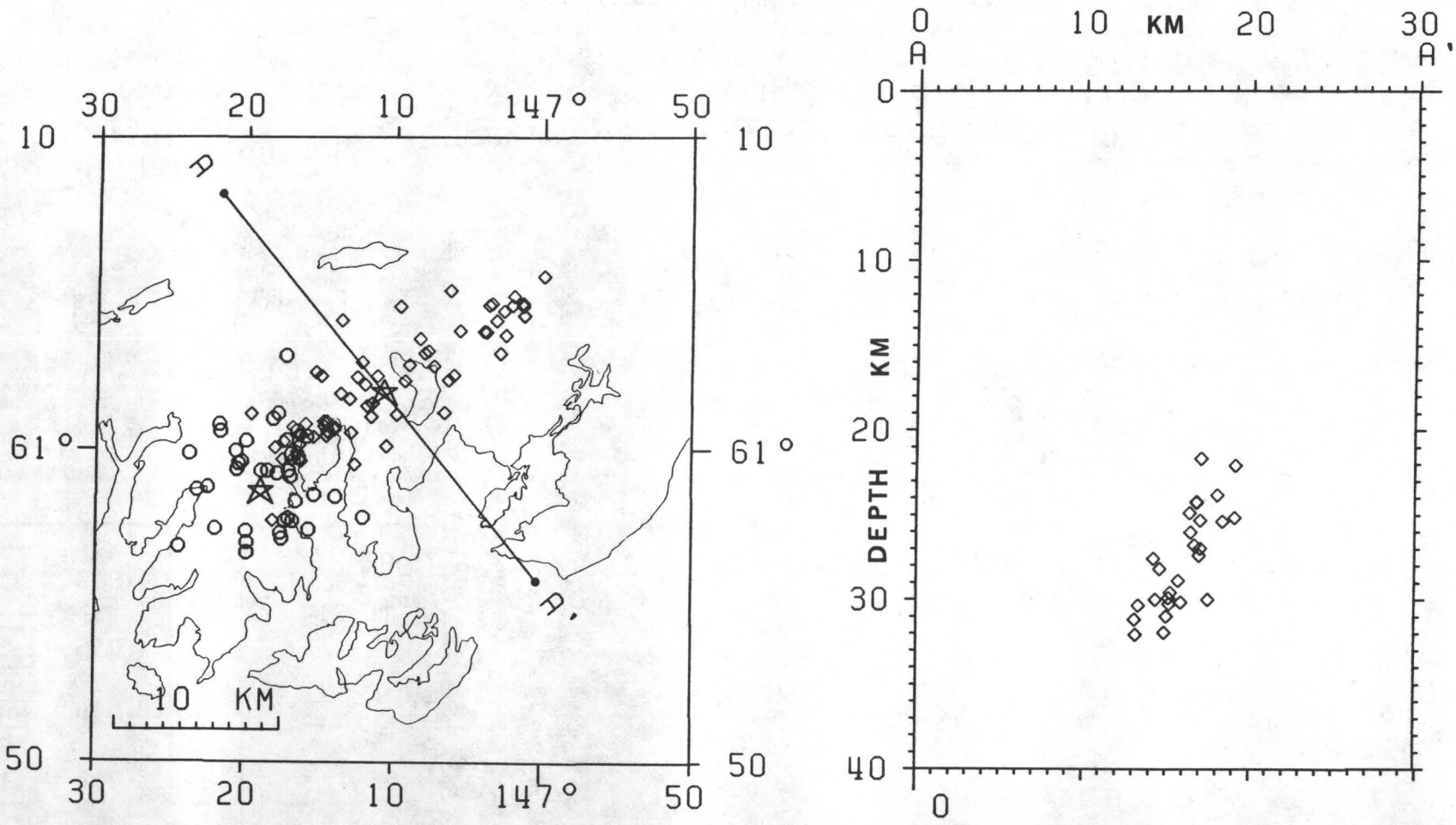

Figure 2. (left) Earthquake sequences of July and September, 1983. Symbols are: upper right star - July 12 epicenter; diamonds - aftershocks of July 12 event; lower left star - September 7 epicenter; and circles - afetrshocks of September 7 event. (right) Well located aftershocks of July 12 event projected onto the plane A - A'.

Applications of Mathematical Modeling

9540-03301

Robert K. Mark
Branch of Western Regional Geology
345 Middlefield Road, MS 75
Menlo Park, CA 94025
(415) 323-8111, ext. 2059

Investigations

1. Continued studies of historic crustal deformation based on the results of repeated levelings and both continuous and discontinuous sea-level measurements, and how this deformation may be related to the late Cenozoic tectonics of selected parts of California and adjacent states.

2. Reinstituted evaluations of the magnitude and predictability of various types of systematic error in geodetic leveling based on an examination of the historic record.

3. Completed statistical study of the relations among surface faulting parameters and earthquake magnitude.

Results

1. Intensive review by Robert E. Powell of an earlier submitted report on "An early-20th-century uplift in southern California" disclosed an inconsistency in our previously reported chronology of the growth of this feature that significantly alters the relation between its growth and at least one large temporally associated earthquake. Specifically, reexamination of the data and recovery of additional data now indicates that the first major spasm of uplift began sometime after March 1905 and probably was largely over by the following spring and, hence, prior to the 1906 San Francisco earthquake. Whether in fact these phenomenon are mechanically related is uncertain, but it is difficult to dismiss their association as the product of chance.

Reports

Gilmore, T. D., and Castle, R. O., 1983, Tectonic preservation of the divide between the Salton basin and the Gulf of California: Geology, v. 11, no. 8, p. 474-477.

Earthquake Hazards Studies, Upper Santa Ana valley and Adjacent Areas, Southern California

9540-01616

Jonathan C. Matti
Branch of Western Regional Geology
U. S. Geological Survey
345 Middlefield Road, MS 75
Menlo Park, California 94025
(415) 323-8111 ext. 2358, 2353

Investigations

1. Studies of the Quaternary history of the upper Santa Ana River Valley. Emphasis currently is on: (a) generation of liquefaction susceptibility and liquefaction opportunity maps; and (b) the three-dimensional distribution of the valley fill and its lithologic, lithofacies, and pedogenic character.

2. Neotectonic studies of the Crafton Hills-Yucaipa Valley, Banning, and San Andreas fault zones. The study has focused on: (a) mapping fault strands that deform crystalline basement rocks, Tertiary sedimentary rocks, and Quaternary surficial units; (b) identification of Quaternary units to establish Quaternary depositional patterns and the relative ages of displacements along various fault strands; and (c) interpreting inter-relationships between the Banning fault system and the south branch of the San Andreas fault.

Results

1. Scott E. Carson and J. C. Matti conducted a program of subsurface exploratory boring in the San Bernardino Valley. The drilling program supports our ongoing evaluation of liquefaction potential within the upper Santa Ana River Valley region, and is designed to provide a hands-on basis for evaluating subsurface geotechnical data compiled from many other sources. At each of 27 sites we drilled two borings. An initial boring by solid-stem continuous-flight augering techniques allowed us to obtain textural and stratigraphic data to depths averaging 60 ft subsurface. A second boring employed hollow-stem augering techniques that allowed us to conduct standard penetration tests with a split-spoon sampler at predetermined intervals selected on the basis of the results of the continuous-flight augering. Drilling activities utilized a U.S. Geological Survey drill rig operated by S. Shaler.

The 27 drill sites within the San Bernardino Valley are located in three major alluvial provinces: distal flood-plain deposits of the Santa Ana River, alluvial-fan deposits prograding southward from the San Bernardino Mts., and braided-channel deposits of the Cajon-Lytle Creek terrace. Drilling results suggest that each depositional province is characterized by a unique physical stratigraphy. (1) Santa Ana flood-plain deposits in the vicinity of metropolitan San Bernardino consist of abundant clay and fine silt interlayered with fining-upward cycles having coarse fractions in the fine-to medium-sand class. Gravelly sand layers are uncommon. (2) The prograding alluvial-fan deposits are characterized by sand and gravelly sand, with minor silt. (3) Braided-channel deposits of the Cajon-Lytle Creek terrace are characterized by sand and gravelly sand in proximal settings, and sand, silt, and clay in

distal settings. At some sites, vertical changes in stratigraphy indicate that the geographic positions of these three depositional provinces may have shifted through time, presumably in response to late Quaternary climatic changes but possibly also in response to tectonics.

We presently are interpreting liquefaction susceptibility patterns at the 27 sites. Preliminary facts and interpretations include the following: (1) The zone of shallow ground water underlying metropolitan San Bernardino embraces mainly the distal parts of the three alluvial provinces--domains where sediments most likely will be fine grained and well sorted; (2) stratal successions at many of the drill sites within the shallow-water zone contain large amounts of clay and clayey silt--sediment layers that are not likely to experience liquefaction themselves, but that could confine ground water contained in adjacent saturated sand layers; (3) loose, cohesionless layers of silt and sand occur in the stratal record of all 27 sides; (4) thicknesses of individual sand layers vary from a few inches to a several feet; (5) the presence of buried paleosols in some borings and a trend toward increased penetration resistance below 20-30 ft subsurface suggest that although surface sediments may be relatively young and unconsolidated, older sediments that are well consolidated can be encountered at depths as shallow as 20 ft subsurface.

2. J. C. Matti and J. W. Harden are conducting studies of alluvial stratigraphy, fault geomorphology, and soil development in the Yucaipa Valley-Oak Glen Valley district. Quaternary sediment in this district consists mainly of Pleistocene alluvium. Holocene deposits are minimal, and consist of late Holocene and Recent sediments occurring in incised washes and stream bottoms or on small alluvial fans emanating from nearby uplands. Pleistocene alluvium is represented by two major facies: (1) valley-filling alluvial deposits that occupy the axes of Oak Glen and Yucaipa Valleys, and (2) older-fan deposits that emanated from local mountain sources. The valley-filling facies was deposited by stream systems that flowed westward and southward down the axes of Oak Glen and Yucaipa Valley. The older-fan facies represents alluvial cones that interfingered with the valley-filling alluvium.

Qualitative soil-profile data indicate that most of the Pleistocene valley-filling and older-fan units are capped by soils comparable in development to Snelling/Ramona soils of the Riverbank Formation in the San Joaquin Valley. There, Riverbank-type soils have an age range of about 130,000 to 400,000 y.b.p. However, this age span cannot be applied indiscriminately to Riverbank-type soils in Yucaipa Valley because similar rates of soil formation between the Great Valley and southern California have not been demonstrated, and soil-genesis rates in Yucaipa Valley may be more rapid. Our pedogenic studies are incomplete, but preliminary observations suggest three conclusions: (1) more than one late Pleistocene fill event having Riverbank-type soils may be present in the valley-filling and older-fan facies; (2) latest Pleistocene and early Holocene fills are not abundant--instead, this time interval seems to be represented by degradational modification of Riverbank-type surfaces, accompanied by warping and faulting of these surfaces and by local deposition of thin post-Riverbank veneers; (3) the Yucaipa Valley-Oak Glen Valley district does not have an extensive record of Holocene depositional fills.

The older-fan facies in Yucaipa Valley provides data that bear on the late Quaternary history of the south branch of the San Andreas fault southeast

of Mill Creek. Along the 3.5-mile reach of the fault between Mill Creek and Wilson Creek, the older-fan facies forms a fringe of alluvial deposits that is separated from bedrock of Yucaipa Ridge by the south branch. Along this 3.5-mile reach, the older-fan facies consists almost entirely of sandstone and conglomerate clasts derived from the Potato Sandstone (the Mill Creek beds of some workers), a distinctive late Tertiary sedimentary unit that crops out only on Yucaipa Ridge. Preliminary mapping, soil descriptions, and paleocurrent analyses within the older-fan facies suggest two preliminary conclusions. (1) Relative to their bedrock source areas, the older-fan deposits containing Potato Sandstone clasts presently crop out in geographic locations not much different from those in which they were originally deposited. Right-lateral displacements on the south branch have not offset the older-fan facies by more than a few thousand feet from their Potato Sandstone source rocks. (2) The older-fan deposits have soil-profile characteristics comparable to Riverbank soils. Thus, the south branch southeast of Mill Creek has not produced significant right-lateral displacements during late Pleistocene and Holocene time--that is, since the development of Riverbank-type soils.

These interpretations can be used to understand the origin of normal faulting in the Yucaipa Valley area--a zone of extension localized in a region where right-lateral and reverse faulting are the most obvious expressions of crustal deformation. In an earlier summary report, Morton and Matti (1982) defined the Crafton Hills horst-and-graben complex as a series of northeast-trending normal faults associated with the Crafton Hills bedrock uplift. Subsequent mapping by Matti in Yucaipa Valley has identified additional east- and northeast-oriented normal faults that break the late Pleistocene and Holocene valley-filling and older-fan facies. Thus, extensional faulting in this region is more widespread than originally identified, and occurs in alluvial fills of the valleys as well as marginal to the Crafton Hills bedrock horst. These fault patterns lend credence to the notion that the Crafton Hills-Yucaipa Valley horst-and-graben complex is a significant tectonic element that must be factored into the overall mosaic of crustal-block boundaries in southern California.

The Crafton Hills-Yucaipa Valley horst-and-graben complex apparently has been forming during late Pleistocene and Holocene time as the San Bernardino Valley moves northwestward away from the region of a knot in the San Andreas fault system. This knot, a region of compressional strain centered in San Gorgonio Pass, is a zone of Quaternary Banning-B and Banning-C reverse and thrust faulting that extends as far west as the Calimesa area (Morton and Matti, 1981; Matti and Morton, 1982). As the San Bernardino Valley moves northwestward away from the knot region, the crust appears to be breaking up and pulling apart in the vicinity of the Craton Hills-Yucaipa Valley horst-and-graben complex.

Central to this interpretation is the apparent contrast in amount and rate of right-slip on the south branch of the San Andreas fault between Cajon Pass and Yucaipa Valley. The San Bernardino Valley presently is moving northwestward via right-lateral displacements on the south branch. In Cajon Pass, 30 miles northwest of Yucaipa Valley, late Pleistocene and Holocene displacements on the south branch and Holocene slip rates of 20-25 mm/year are well documented (Weldon and Sieh, 1981). Between Cajon Pass and Mill Creek, right-lateral displacements along the south branch are evidenced by well developed right-lateral physiography along the fault trace, and slip rates comparable to

those in Cajon Pass may apply in the vicinity of San Bernardino (Rasmussen, 1982). However, late Quaternary right slip on the south branch apparently has been negligible along that portion of the fault that extends southeast from the vicinity of Mill Creek. This interpretation is suggested by (1) the absence of well-developed fault physiography along the south branch between Mill Creek and Banning Canyon, and by (2) evidence for negligible right-lateral displacements on the south branch as recorded by late Pleistocene older-fan deposits in Yucaipa Valley. If this contrast along the south branch is real, then elimination of right slip between Cajon Pass and Mill Creek requires that strain be taken up on other fault systems.

A model for late Quaternary crustal tectonics in this part of southern California must integrate the roles of at least four fault systems: the San Jacinto fault, the south branch of the San Andreas fault, the Crafton Hills-Yucaipa Valley horst-and-graben complex, and the Banning fault system. One possible model incorporates the following components (fig. 1). (1) The northwest-oriented triangle of the San Bernardino Valley is moving northwestward at slip rates that fall from 25 mm in the Cajon Pass district to minimal in the vicinity of Mill Creek. (2) The Perris block is moving northwestward along the San Jacinto fault. (3) North of the latitude of lower San Timoteo Canyon, northwestward movement of both the Perris block and the San Bernardino Valley suggests that the two provinces intermittently behave as a single unit along this stretch of the San Jacinto fault--a relationship that requires the San Bernardino Valley to be attached intermittently to the Perris block. South of the latitude of lower San Timoteo Canyon, the Perris block is sliding past the San Timoteo Badlands by slip on the San Jacinto. (4) The Crafton Hills-Yucaipa Valley horst-and-graben complex pulls apart in the wake of northwestward movement of the San Bernardino Valley. (5) If the San Bernardino Valley can become attached to the Perris block, that portion of the San Jacinto fault that traverses the San Bernardino Valley at times must be locked up and quiescent in terms of large earthquakes. This hypothesis could account for the seismic-slip gap hypothesized for this portion of the San Jacinto fault by Thatcher and others (1975).

Referenes cited

Matti, Jonathan C., and Morton, Douglas M., 1982, Geologic history of the Banning fault zone, southern California: Geological Society of America Abstracts with Porgrams, v. 14, no. 4, p. 184.

Morton, Douglas M., and Matti, Jonathan C., 1981, Earthquake hazards studies, Upper Santa Ana Valley and adjacent areas, southern California: in Summaries of Technical Reports, v. XI, pp. 70-72, U.S. Geological Survey Open-File Report 81-167.

Morton, Douglas M., and Matti, Jonathan C., 1982, Earthquake hazards studies, upper Santa Ana River Valley and adjacent areas, southern California: in Summaries of Technical Reports, v. XIII, p. 51-54, U.S. Geological Survey Open-File Report 82-65.

Rasmussen, G. A., 1982, Geologic hazards and rate of movement along the south branch of the San Andreas fault, San Bernardino, California, Field trip no. 4, Geologic hazards along the San Andreas fault system, San Bernardino-Hemet-Elsinore, California: in Cooper, J. A., compiler, Neotectonics in southern California, Guidebook, Geological Society of America, Cordilleran Section Annual Meeting, 78th, Anaheim, California, p. 109-114.

Thatcher, Wayne, Hileman, James, A., and Hanks, Thomas C., 1975, Seismic Slip distribution along the San Jacinto Fault zone, Southern California, and its implications: Geological Society of America Bulletin, v. 86, p. 1140-1146.

Weldon, Ray, and Sieh, Kerry, 1981, Offset rate and possible timing of Recent earthquakes on the San Andreas fault in Cajon Pass, California: EOS, Transactions of the American Geophysics Union, v. 62, no. 45, p. 1048.

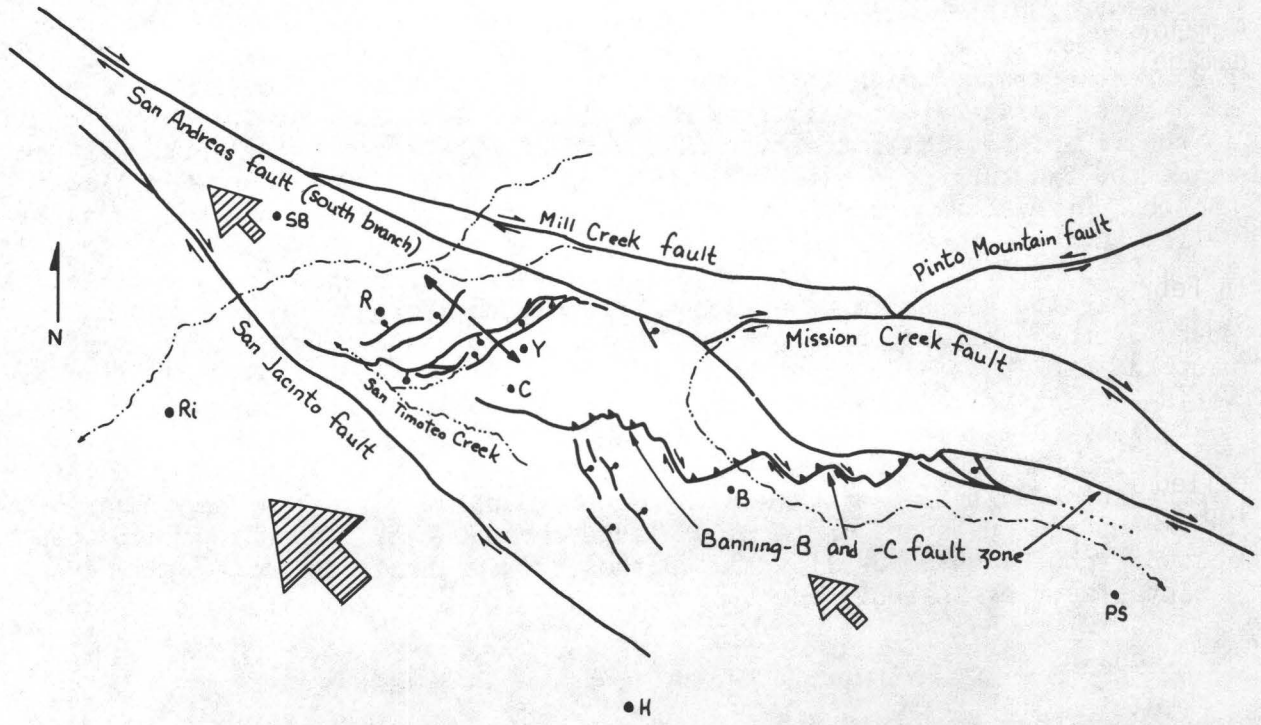

Figure 1.--Schematic diagram illustrating relations between faults and crustal blocks in the vicinity of Yucaipa Valley, southern California. B, Banning; C, Calimesa; H, Hemet; R, Redlands; Ri, Riverside; SB, San Bernardino; Y, Yucaipa. Large ruled arrows indicate the relative motion of crustal blocks. Large solid arrows near Yucaipa indicate crustal extension in the Crafton Hills-Yucaipa Valley horst-and-graben complex.

Earthquake Hazard Maps for Selected Earthquake Scenarios San Francisco Bay Area

14-08-0001-21226

Jeanne B. Perkins
Association of Bay Area Governments
Hotel Claremont
Berkeley, California 94705
(415) 841-9730

INTRODUCTION

A major earthquake in the San Francisco Bay Area will cause property damage, personal injury and death, and serious economic and social disruption. Earthquake hazard and risk maps play a key part in efforts to minimize these losses; organizations and people can use the maps (a) to develop ways to mitigate the mapped hazards through land use management and structural measures as well as (b) to develop loss estimates to enhance emergency response programs.

In February 1979, ABAG began a series of four projects to (1) use its computer-based geographic information system to produce maps of several types of earthquake hazards and (2) develop innovative methods of using these maps for hazard mitigation. The maps of maximum ground shaking intensity and risk of damage from ground shaking produced by ABAG prior to this contract have three major inadequacies. First, the availability of detailed geologic mapping in digital form for only part of the Bay Area has led to the maps being of uneven quality throughout the region. Second, the availability of more accurate fault location information in July 1983 has rendered some parts of the ground shaking maps out of date. Last, and most significantly, the existing maps are a composite of the risks of ground shaking associated with many different earthquakes. Maps for selected individual earthquakes are also needed for certain applications.

Therefore, ABAG has expanded the area for which detailed mapping of geologic materials is available in digital form to cover all nine Bay Area counties. In addition, fault trace and fault study zone mapping available in July 1983 has been incorporated into ABAG's existing computer files of these data. The fault and geology files will then be combined with seismologic data on ground shaking attenuation, the effects of local geology on intensity, and the recurrence intervals of major earthquakes to refine the ground shaking risk maps produced in earlier contracts, as well as to produce a series of intensity maps for selected earthquake events. Finally, a series of maps showing hazards associated with liquefaction, dam failure and tsunami inundation (based on work in previous contracts) similar in format to the ground shaking intensity maps will be produced at a scale appropriate for most users for comparison with those intensity maps. ABAG plans to continue its successful program of extensive documentation and user interaction to ensure the continued

and appropriate use of these maps by federal, state and local government, other ABAG programs, transportation and utility groups, and the private sector. ABAG, as the comprehensive regional planning agency for the Bay Area, is uniquely qualified to provide this service.

PROJECT COMPONENTS

1. Basic Data Map File Development and Refinement

2. Hazard Map File Development and Refinement

3. Research Applications and Report Preparation

DISCUSSION OF RESEARCH PROGRESS

1. Basic Data Map File Development and Refinement

A. Geologic Mapping - Detailed bedrock geology maps have been collected for those areas of the San Francisco Bay region not already available in digital form as part of ABAG's computer-based geographic information system. These maps (available from U.S. Geologic Survey work at scales of 1:24,000 and 1:62,500) have been redrafted to remove all but boundary information. Data codes have been recorded on the maps; map border inconsistencies and unit labeling omissions have been resolved by coordinating with the map authors. These drafted and coded maps have been digitized, and the digitized lines and codes edited. These lines have then been converted to hectare cells, and the resulting cell file mapped and edited. Finally, this new information has been combined with the existing geologic cell file to obtain a complete revised file.

B. Fault Special Studies Zones Mapping - Revised Alquist-Priolo Special Studies Zone Maps were obtained from the California Division of Mines and Geology (CDMG). These maps (at a scale of 1:24,000) were compared with other maps already in the computer data base and necessary revisions noted. Data codes were assigned for faults not appearing on the maps digitized for earlier contracts. These codes were drafted on the maps. The maps were then digitized and the digitized lines and codes edited. These lines were then converted to cells and the resulting file mapped and edited. Finally, the cell file was combined with fault study zone data from earlier contracts to produce this complete revised file.

C. Fault Trace Mapping - The fault trace file currently available for only those faults not zoned by the State Geologist was expanded to include the most current data on fault trace locations for those zoned. Again, data codes were assigned. The lines were digitized and edited, and the data combined with the data from earlier contracts.

2. Hazard Map File Development and Refinement

A. New Data - New data affecting the intensity map modeling process have been examined. The focus of this effort has been in two directions. First, project staff have worked to determine how to assess the effect of such data on the eventual production of casualty and loss estimates for selected earthquake scenarios. Second, data on appropriate intensity increments for additional geologic units mapped have been obtained from USGS researchers. Identifying appropriate geologic units has involved the preparation of a master geologic explanation (including 278 units) for the nine-county San Francisco Bay Area.

B. Scenario Earthquakes - Ten scenario earthquakes have been selected for analysis and map preparation at 1:250,000.

C. Additional Maps - By the end of this project (December 31, 1983), the following ten additional maps will be produced at 1:250,000:

- o maximum ground shaking intensity map;
- o three risk of damage (or cumulative damage potential) maps for three building types;
- o two fault maps (one of fault traces used in the intensity map modeling and one of existing Alquist-Priolo Special Studies Zones);
- o geologic materials map (grouped into units with similar average predicted seismic properties);
- o liquefaction susceptibility map and liquefaction potential map; and
- o dam failure inundation areas.

3. Research Applications and Report Preparations

A. Interaction - Much effort is being made to ensure that the findings of this work are effectively communicated to a variety of professionals working for and with government, lifeline and transportation agencies, and private businesses and industries. Continuing interaction has been occurring with people who use the system or are interested in developing similar capabilities in both the public and private sectors, including the Bay Area Water Resources Council, Region 9 of the Federal Highway Administration, the State of Washington Office of Emergency Services, the Southern California Earthquake Preparedness Project, Cal Poly State University - San Luis Obispo, FIRESCOPE, Dames and Moore, URS/John Blume and Associates, BSD, Inc., Pacific Gas and Electric Company, the Santa Clara County Earthquake/Disaster Task Force and the Bay Area Earthquake Study.

Additional related information has been supplied to the cities of Saratoga, Pacifica and Oakland. Information on the hazard mapping has appeared in the Contra Costa Times and its sister newspapers. Phone and in-person information requests by individual homeowners and businesses (including tape storage and insurance companies) have also been fulfilled.

B. Documentation - A series of eighteen working papers and a user's guide previously developed to document the hazard mapping capabilities are being expanded to include the documentation of this contract. Information on the cumulative damage potential or risk maps has been reworked, has completed technical review, and has been forwarded to the Technical Reports Unit of USGS for publication in the Miscellaneous Field Studies Report series.

EARTHQUAKE RESEARCH IN THE WESTERN GREAT BASIN

Contract 14-08-0001-21248

Alan Ryall and Ute Vetter
Seismological Laboratory
University of Nevada
Reno, NV 89557-0018
(702) 784-4975

1. Research Program

This program supports continued operation of a seismic network in the western Great Basin of Nevada and eastern California, and research focused on: (1) seismicity and focal mechanisms associated with magma injection in Long Valley caldera; (2) geometry of magma bodies in Long Valley caldera; (3) stress changes associated with systematic changes in focal mechanism with depth in the Great Basin; (4) premonitory seismicity patterns preceding the 1980 Mammoth Lakes earthquakes; (5) possible precursory seismicity patterns in the White Mountains gap; (6) evaluation of the contribution that high-quality digital broadband seismic stations can make to regional network-seismic studies. Progress in selected areas of this program is described below.

2. Results

A. Location of Magma Bodies in Long Valley Caldera

In an extension of earlier work by this Laboratory C. O. Sanders has completed a detailed investigation of the shadowing of seismic S-waves by magma bodies within Long Valley caldera. To map the subsurface geometry of the magma bodies, Sanders used recordings of 281 small earthquakes that occurred around the southern boundary of the caldera, in the depth range 1-15 km. With over 1,200 normal and anomalous ray paths through the caldera, Sanders has located two massive magma bodies in the central and northwest parts of the caldera, as well as two apparently dispersed (e.g., dike swarm) bodies in the southern caldera and beneath Lake Crowley. The locations of these bodies are shown on Figure 1, with contours indicating approximate depth to the top of the magma. The central magma body extends from 4.5 to at least 13 km depth and the northwest body is probably as shallow as 5.5 km. The northwest and central bodies are below the perimeter of the resurgent dome and probably connect at depth greater than about 8 km beneath the center of the dome. The shallower parts of these magma bodies and the southern anomalous area also lie beneath the medial graben of the caldera, suggesting that structural features seen at the surface of the valley are related to magmatic processes at depth. Sanders' work was summarized in a preliminary report with F. Ryall in the August 1983 issue of Geophysical Research Letters, and a more extensive paper has been submitted to the Journal of Geophysical Research.

B. Systematic Change in Focal Mechanism with Depth

An investigation by U. Vetter and A. Ryall, of systematic changes in earthquake focal mechanisms with depth, was published in the October 1983 issue of the Journal of Geophysical Research. In general the observed change in mechanism, from strike-slip at shallow depth to oblique-slip in the middle crust, is interpreted as the result of increasing overburden pressure, resulting in rotation of the maximum compressive stress from horizontal at depths less than about 6 km to almost vertical at depths greater than 9 km. The study includes an estimate of principal stresses as a function of depth.

Fault-plane solutions for the Long Valley sequence were included in a paper by U. Vetter and A. Ryall, on Seismological Investigations of Volcanic and Tectonic Processes in the Western Great Basin, presented at the Geothermal Resources Council Symposium on "The Role of Heat in the Development of Energy and Mineral Resources in the Northern Basin and Range Province." The paper will be published in the Proceedings of this Symposium. Another paper, summarizing the earlier results and presenting an additional 84 new mechanisms, has been submitted to Annales Geophysicae.

In an extension of this research we are studying the mechanisms of the M = 6+ shocks in May 1980 -- earthquakes that B. Julian has concluded were caused by mechanisms of the "compensated linear vector dipole" type, possibly due to the formation of dikes. Our analysis indicates that the large earthquakes were multiple events, increasing in size and possibly in depth with time, and suggesting that Julian's data set was contaminated by mixing first-arrival observations from different events.

C. Seismic Network Operation

During the last half of 1982 the University of Nevada installed five additional seismic stations in the southwest part of the caldera, to provide coverage of an area where spasmodic tremor has been observed on at least eight occasions. Responsibility for operating these stations was later taken over by the US Geological Survey and our equipment was moved to new locations. The present configuration of the network is shown on Figure 2. Within the next month station GLM will be removed and two new stations will be installed to provide better coverage in the area between stations CLK and SCH.

In addition to the analog stations shown on Figure 2, the University has developed and tested an experimental digital seismic station for remote operation. The digital station provides broadband (0.05-30 Hz), wide dynamic-range (96 dB) signals from a three-component set of seismometers and the data are telemetered in a gain-ranged digital format to a central facility where they are recorded continuously. One of these stations has been operating at our station MNA (upper right corner of Figure 2) since May 1983 and another will be installed between stations LUL, MMC and MON in the area north of Mono Lake during October. Digital data from the two stations will be used to study spectral characteristics of normal and anomalous signals that have propagated through the caldera.

Analysis of the Mammoth Lakes earthquake data is complete through mid-July 1983. We are now in the final stages of hiring a postdoctoral fellow, and one of his initial assignments will be to determine sets of station corrections appropriate for different parts of the Long Valley epicentral zone, assemble our entire data base for that sequence, and systematically relocate all the events that have occurred there since October 1978.

3. Reports

Ryall, A. and F. Ryall (1983). Spasmodic tremor and possible magma injection in Long Valley caldera, eastern California, Science, 219, 1432-1433.

Sanders, C. O. (1983). Location and configuration of magma bodies beneath Long Valley, California, determined from anomalous earthquake signals, submitted to Jour. Geophys. Res.

Sanders, C. O. and F. Ryall (1983). Geometry of magma bodies beneath Long Valley, California, determined from anomalous earthquake signals, Geophys. Res. Letters, 10, 690-692.

Vetter, U. and A. Ryall (1983). Systematic change of focal mechanism with depth in the western Great Basin, Jour. Geophys. Res., 88, 8237-8250.

Vetter, U. and A. Ryall (1983). Seismological investigations of volcanic and tectonic processes in the western Great Basin, Proc. Geothermal Resources Council Symposium on the Role of Heat in the Development of Energy and Mineral Resources in the Northern Basin and Range Province, in press.

Vetter, U. and A. Ryall (1983). Focal mechanisms and crustal stress patterns in western Nevada and eastern California, submitted to Annales Geophysicae.

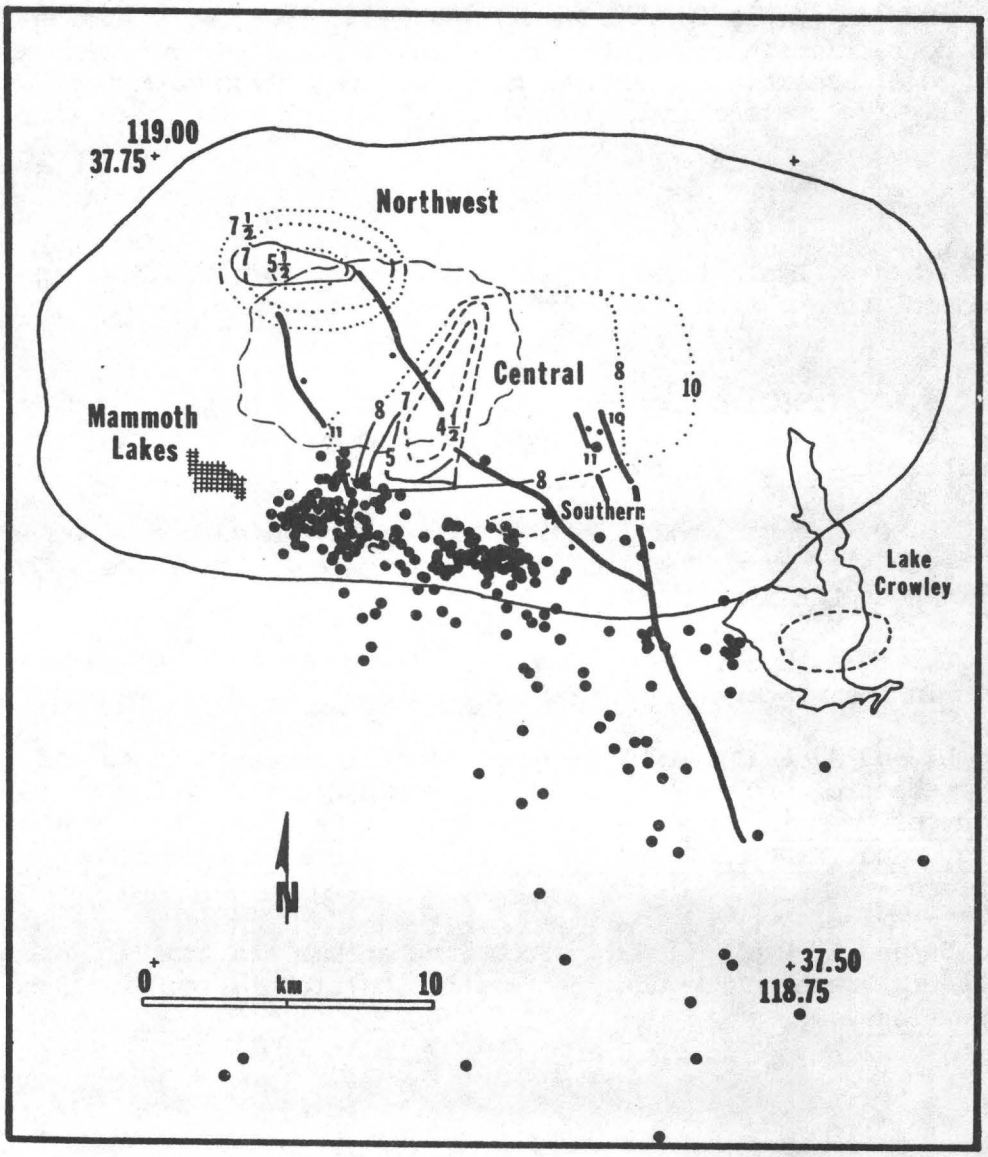

Figure 1. Map of Long Valley Caldera showing epicenters of earthquakes (dots) used to study the geometry of magma bodies, and the location of magma bodies inferred from the analysis. For the central magma body the solid lines are well-located boundaries and the dashed or dotted lines are more interpretive. Depths to the top of magma bodies are given where possible by contours. Major faults in and near the caldera are shown by heavy lines and the outline of the resurgent dome is shown by long dashes.

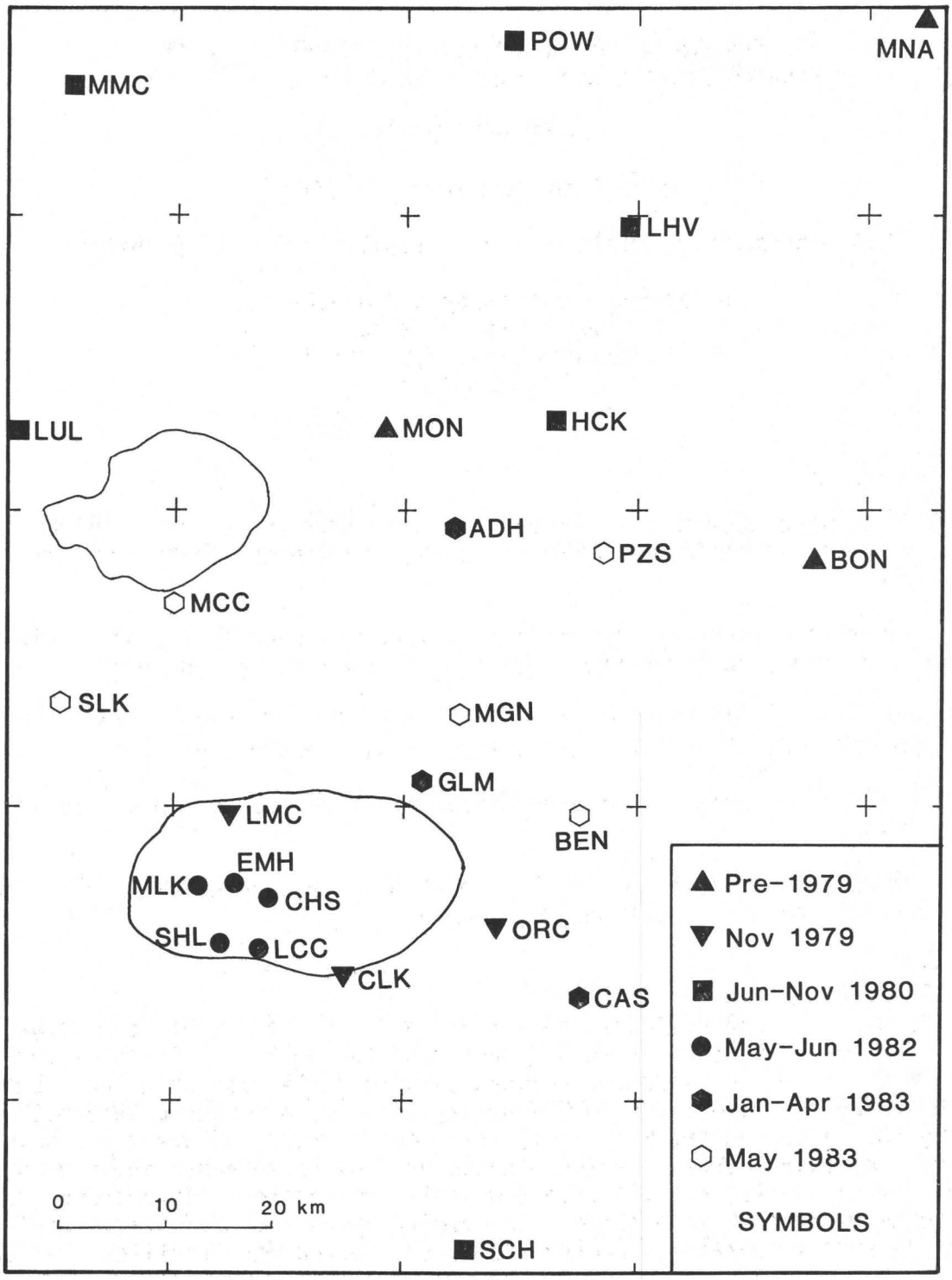

Figure 2. Seismic stations of the Long Valley-Mono Craters seismic network as of September 1983. Different symbols indicate the dates stations began operation.

Earthquake Hazard and Prediction Research in the Wasatch Front/Southern Intermountain Seismic Belt

14-08-0001-21184

April 1 to September 30, 1983

R.B. Smith, W. J. Arabasz, J.C. Pechmann, and W.D. Richins*

Department of Geology and Geophysics
University of Utah
Salt Lake City, Utah 84112
(801)581-6274

Investigations

1. Subsurface geometry and kinematics of normal fault zones based on seismic reflection, earthquake data, and thermal-mechanical modeling.

2. Subsurface geometry of active faulting--and correlation of seismicity with fine structure--based on earthquake field studies.

3. Comparison of strain release across the Wasatch Front from seismic-moment-tensor and geodetic-strain information

4. Studies of earthquake source characteristics using local network data.

5. University of Utah network operations and seismicity for the period: April 1-September 30, 1983.

Results

1. As part of a broad investigation of the correlation of earthquakes and surface faulting in the interior of the Western U.S. Cordillera, more than 1500 km of industry-donated seismic reflection data have been interpreted and reveal the following styles of late Cenozoic deformation along the eastern Great Basin: (1) the wide-spread development of asymmetric eastward-tilted basins bounded by low- to moderate-angle planar and listric faults, and (2) five low-angle reflections interpreted as detachments stacked en echelon. Seismicity appears to correlate chiefly with "blind" subsurface structures seen on reflection profiles rather

*The following individuals also contributed significantly to this project during the report period: H. M. Benz, R. L. Bruhn, S. M. Jackson, D. R. Julander, E. McPherson, G. E. Randall and C. Renggli.

than with mapped surface faults.. A structural style of low-angle and listric faulting cannot be easily reconciled with the classic brittle failure theory, but the interpreted termination of normal faults above deeper low-angle reflections suggest the possibility of pre-existing zones of weakness, i.e. ancient detachments or zones of ductile deformation, that may terminate or bound earthquake zones. Rheologic models for the Basin-Range suggest the depth of frictional/quasi-plastic transition may be as shallow as 7 km. One plausible explanation for the difference between the steep attitudes of faults inferred from fault plane solutions and the gentle to moderate fault dips observed in the seismic reflection data is that abundant earthquakes occur at depths above the brittle/ductile transition where the seismic regime for frictional sliding dominates; below this depth, fault planes may flatten and accommodate aseismic, quasi-plastic strain release. Details are described by Smith and Bruhn (1983).

2. During September 1983 a six-week, fifty-station microearthquake survey was conducted in the seismically active Hansel Valley-Pocatello Valley region, north of the Great Salt Lake in northern Utah. This experiment was a cooperative project between the University of Utah and Peter Molnar of MIT and included the participation of Dr. Geoffrey King, Cambridge University, and Dr. Dennis Hautzfield, Grenoble University. Forty analog, smoked-paper-recording seismographs and 10 three-component digital seismographs (loaned to us by Dr. R. P. Meyer, University of Wisconsin) were installed in the study area as a means of determining high-resolution hypocenters and single-event fault plane solutions for small earthquakes. The average station spacing was ca. 2-3 km. A primary objective of the survey was to obtain precise hypocenter information and to investigate source properties in an area where industry-donated seismic reflection data suggest the presence of a subsurface low-angle detachment. The experiment data are currently being analyzed.

3. We have examined the detailed distribution of strain release across the Wasatch Front and the surrounding area by comparing strain rates derived from seismic moment tensors of historic earthquakes and from geodetically-derived horizontal strain components. For this study the Wasatch Front study area was divided into subareas, each with similar Cenozoic geology and assumed homogeneous strain. Moment tensors were estimated for each subarea using observed seismicity rates, applicable moment-magnitude relationships, and fault-plane solutions. These moment tensors provide an estimate of strain rate and an area-averaged synthetic fault-plane solution for each subarea.

Preliminary tests of the method indicate that the synthetic fault-plane solutions for subregions of the Wasatch Front are consistent within 18^{0} of observed focal mechanisms within the subregions. T-axes show a general east-west strike with much less scatter than the corresponding P-axes.

Strain rates were calculated as follows:

1) Hansel Valley, Utah; maximum extensional strain$_1$ = 6.9×10^{-16} s^{-1}, maximum compressional strain = -6.4×10^{-16} s^{-1}

2) East Cache fault zone; maximum extensional strain = 5.7×10^{-18} s^{-1}, maximum compressional strain = -5.9×10^{-18} s^{-1}

These seismic moment rates are similar to those determined from observed geodetic measurements (Snay, Smith and Soler, in press) that suggest E-W extensional strain-rates of ca. 10^{-15} s^{-1} for the central Wasatch Front. The higher seismically derived rates for the Hansel Valley area are consistent with the relatively higher frequency of occurrence of magnitude 6+ earthquakes in that area. Applications to the Wasatch Front urban corridor are continuing.

4. An interactive computer program was developed and tested for determining instrument-corrected spectra of P- and S-waves recorded digitally by the University of Utah seismic network and for estimating seismic moment from these spectra. Systematic development of a software library for analysis of digital seismic data from the network is in progress.

5. During the six-month period: April 1-September 30, 1983, 372 earthquakes were located within the Utah region (Figure 1). The largest event was a magnitude 4.0 earthquake (not reported felt), located approximately 20 km northeast of Dinosaur National Monument (NE of Vernal), on September 24, 1983. Felt earthquakes during the report period included the following: (1) M3.2 near Hanksville, Utah (May 3, 1983), (2) M2.9 near Mona, Utah (June 9, 1983), and (3) M2.9 east of Croydon, Utah, in Morgan Canyon (August 29, 1983). Near Soda Springs, Idaho, seismicity continued as part of a swarm sequence that peaked in October 1982 ($M_L \leq 4.7$).

Reports and Publications

Julander, D. R., 1983, Seismicity and correlation with fine structure in the Sevier Valley area of the Basin and Range-Colorado Plateau transition, south-central Utah, M.S. Thesis, University of Utah, Salt Lake City, 143 pp.

Richins, W.D., Arabasz, W. J. and Langer, C.J., 1983, Episodic earthquake swarms near Soda Springs, Idaho: Correlation with local structure and regional tectonics (preprint).

Smith, R. B., 1983, Structural style and deformation accompanying intraplate tectonics of the basin-range: inferences for thermal and mechanical properties of an extending lithosphere (abs.), Programme and Abstracts, Int. Union Geod. Geophys., XVII General Assembly, Hamburg, August 1983.

Smith, R. B. and Bruhn, R. L., 1983, Intraplate extensional tectonics of the western U.S. Cordillera: Inferences on structural style from seismic reflection data, regional tectonics and thermal-mechanical models of brittle/ductile deformation (submitted to Jour. Geophys. Res.).

Swing, M. D., 1983, Calibration of a three-component S-13 seismometer station with application to synthetic seismograms, M.S. Thesis, University of Utah, Salt Lake City.

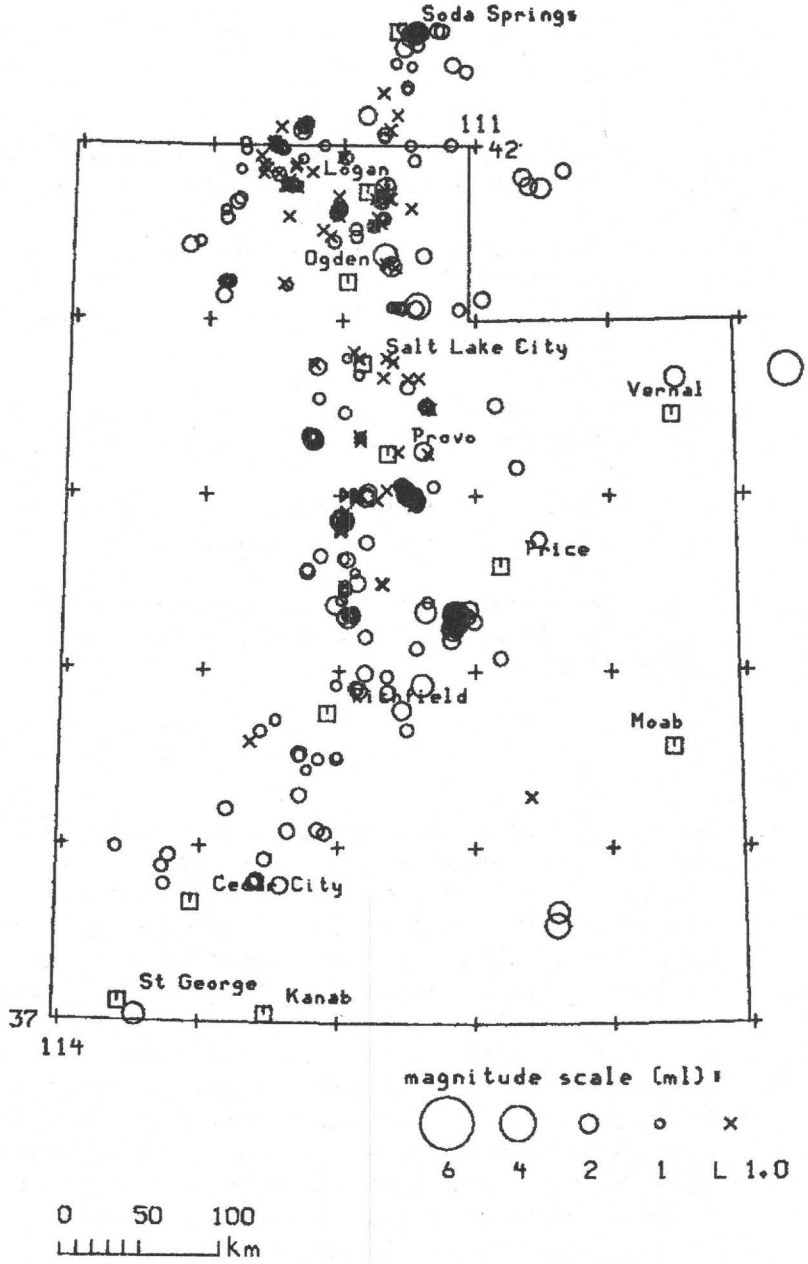

Figure 1. Epicenters of earthquakes in the Utah region during the period April 1 to September 30, 1983.

Quaternary Framework for Earthquake Studies Los Angeles, California

9540-01611

John C. Tinsley
Branch of Western Regional Geology
U. S. Geological Survey
345 Middlefield Road, MS 75
Menlo Park, California 94025
(415) 323-8111, x 2037

Investigations

1. Conducted exploratory drilling studies of near-surface Quaternary deposits at sites near (a) University High School in west Los Angeles, (b) on the site of former lakes located northest of the Baldwin Hills near Ballona Gap, and (c) in the Long Beach-San Pedro area. These studies will provide datable materials, stratigraphic information, and depths to buried soil horizons having significance for regional Quaternary stratigraphic studies in the Los Angeles Basin. (J. Tinsley-D. Ponti)

2. Continued loading into the USGS VAX/computer geotechnical data from the Pasadena, Burbank, and Van Nuys 7.5' quadrangles (M. Nicholson, J. Tinsley).

3. Continued 1/24,000 geomorphic/photogeologic/soil stratigraphic mapping of the surficial geology in the Los Angeles area (J. Tinsley).

4. Continued preparing and revising drafts of several chapters for inclusion in the U.S.G.S. Professional Paper describing earthquake hazards in the greater Los Angeles region.

Results

1. (a) An exploratory borehole at University High School, West Los Angeles, CA, revealed a sequence of two buried soils, each characterized by a rubified (reddened) argillic horizon, preserved beneath a thin accumulation of Holocene deposits and fill. These deposits and soils occur along elements of the Santa Monica fault zone on the lower block, and may constrain estimates of the vertical component of displacement across this fault zone. Pending chemical analyses to facilitate definitive comparisons among profiles, the buried profiles encountered in the borehole appear to correspond to relict and buried soil profiles exposed nearby, across the fault, on the upper block. These studies will not constrain the timing of any most recent movements nor will we derive precise earthquake recurrence data. We can obtain some estimate of the late Pleistocene fault activity, provided the soil correlations withstand chemical testing and we can show that the soil-bearing deposits are faulted and are not a sedimentary drape formed on an earlier scarp.

(b) Carbonaceous sediments recovered from a borehole located at the intersection of Cochran and Roseland streets in Los Angeles can be radiometrically dated using ^{14}C analytical techniques. These carbonaceous deposits unconformably overlie a red, clay-rich deposit that probably is a buried argillic horizon formed on a late Pleistocene topographic surface near Ballona Gap north of the Baldwin Hills. The carbonaceous sediments may be of paludal or of lacustrine origin and may bear ultimately on rates of late Pleistocene deformation of the Baldwin Hills.

(c) (With Daniel J. Ponti and K. R. Lajoie) Three shallow borings were drilled to obtain samples from shell-bearing horizons that may be equivalents of either the Palos Verdes Sand or of older shell beds within the San Pedro Formation. One objective of Ponti's study is to devise a means to relate surface outcrops of fossil-bearing deposits to their subsurface correlatives. If the correlations can be established, Ponti will have a means to analyze deformation of a late Pleistocene datum along the Newport-Inglewood and the Palos Verdes fault zones.

2. Data base compilation is 80% complete in the Van Nuys and Burbank quadrangles.

3. Surficial geologic mapping is 95% complete and 50% of that is field-checked in the Los Angeles basin area.

4. Of the six contributions (chapters) to the Los Angeles earthquake hazards professional paper of which Tinsley is author or co-author, three chapters are in technical review, two chapters are in pre-review, author-draft status, and one chapter is to hatch imminently.

Reports

1. Yerkes, R. F., Ellsworth, W. L., and Tinsley, J. C., 1983, Triggered reverse fault and earthquake due to crustal unloading, northwest Transverse Ranges, California: Geology, v. 11, no. 5, p. 287-291.

2. Ziony, J. I. and Tinsley, J. C., 1983, Mapping the earthquake hazards of the Los Angeles Region: Earthquake Information Bulletin, volume 15, Number 4, p. 134-141.

USGS/Alaska Division of Geological & Geophysical Surveys Cooperative Earthquake Hazards Project; Geotechnical Studies in the Upper Cook Inlet Region, AK

14-08-0001-A-0024

Randall G. Updike
Alaska Division of Geological and Geophysical Surveys
P.O. Box 772116
Eagle River, Alaska 99577
(907) 688-3555

Investigations

The Upper Cook Inlet area of south-central Alaska, which includes the Anchorage and Matanuska-Susitna Municipalities, is the most populous area of the state and sustained considerable damage and loss of life as a result of the 1964 Prince William Sound Earthquake. Much of the destruction was attributed to massive ground failure of Quaternary soils. Subsequent to the investigations conducted in the years immediately following that major event, very little research has been performed on earthquake hazards in the region. The present study involves (1) determination of present-day susceptability for ground failure due to liquefaction or sensitive clay collapse in response to a seismic event, (2) mapping of soil units having failure potential, (3) establishing and updating an engineering soils data bank of geotechnical borehole logs and associated test results for the region, and (4) mapping the extent and adjacent geology of active faults within the region.

Results

(1) The Quaternary geology of north Anchorage (Government Hill-Anchorage Port) and south Anchorage have been mapped in three-dimensions at a scale of 1:10,000 to a depth of 50 m below sea level. This includes the detailed mapping of the Bootlegger Cove Formation which consists of eight engineering geologic facies, each having a distinct geotechnical parametric signature. Geologic cross-sections and derivative maps showing facies distributions, formational structure, and thicknesses are included. Presently, the downtown Anchorage area is being mapped in the same detail and at the same scale. Four manuscripts are at this time in press with the USGS and ADGGS related to the completed mapping. When completed, these maps will encompass all areas of historic seismic ground failure problems.

(2) State-of-the-art laboratory testing on the Bootlegger Cove Formation has been seriously lacking since the early efforts immediately after the 1964 earthquake. I have initiated a series of testing programs at two high-rise building sites in downtown Anchorage. The studies include: (a) a series of deep geotechnical stratigraphic boreholes, (b) a laboratory program of static engineering tests on undisturbed core samples to calibrate the stratigraphy of the sites, (c) cyclic triaxial tests, (d) resonant column tests, (e) cyclic simple shear tests, and (f) scanninng electron microscope fabric studies. Independent runs of the SHAKE program were made before and after the dynamic testing to assess modeling accuracy. Multiple publications are forthcoming.

(3) The truck-mounted Ertec electric cone penetration testing system (CPT) has been utilized in the vicinity of (a) the Anchorage Port, (b) Government Hill landslide, (c) Fourth Avenue landslide, (d) L Steet landslide, (e) Turnagain Heights landslide, and (e) Knik River tidal floodplain. Objectives were to (1) enhance subsurface stratigraphic data, (2) characterize the Bootlegger Cove Formation facies relative to CPT parameters, (3) calibrate the Anchorage soils with respect to CPT-SPT relationships, and (4) assess liquefaction susceptability of sands. ADGGS and USGS publications of the results are in various stages of completion.

(4) Bedrock and surficial geologic mapping has been underway for two years along the west front of the Chugach Mountains, at a scale of 1:25,000. A primary objective of that mapping has been to identifiy active faults along the trend of the Border Ranges Fault System. Two high angle normal fault scarps, believed to be splays of that system have been mapped traversing both the McHugh Complex (Jurassic/Cretaceous) bedrock and Holocene glacial and periglacial surficial deposits. The bedrock and surficial geology of three quads along the west front of the Chugach Mountain Front are complete; two additional quads are scheduled for FY84.

(5) The engineering soils data bank for Anchorage and vicinity has now been on line for five years and is continuously being updated with new borehole and testing information provided by municipal, state and federal agencies, and by industry. Presently the information for several thousand sites has been catalogued and is being stored in the original report format. These data are critical to the success of the detailed three-dimensional mapping underway in the Anchorage area.

Reports

Updike, R.G., Cole, D.A., and Ulery, C.A., 1982, Shear moduli and damping ratios for the Bootlegger Cove Formation as determined by resonant column testing: Alaska Division of Geological and Geophysical Surveys Geologic Report 73, p. 7-12.

Updike, R.G., 1982, Engineering geologic facies of the Bootleggger Cove Formation, Anchorage, Alaska (Abst.): Geological Society of America Annual Meeting, New Orleans, Abstracts with Programs, p. 636.

Updike, R.G. and Ulery, C.A., 1983, Preliminary geologic map of the Anchorage B-6NW (Eklutna Lake) Quadrangle, Alaska: Alaska Division of Geological and Geophysical Surveys Report of Investigation 83-8.

Reger, R.D., and Updike, R.G., 1983, Upper Cook Inlet Region and the Matanuska Valley, Guidebook to Permafrost and Quaternary geology: International Conference on Permafrost, Fairbanks, Guidebook 1, Alaska Division of Geological and Geophysical Surveys, p. 185-263.

Updike, R.G., 1983, Seismic liquefaction potential in the Anchorage area, south-central Alaska (Abst.): Symposium on Liquefiable Deposits in the western United States, Geological Society of America, Rocky Mountain/Cordilleran Sections Annual Meetings, Salt Lake City, Abstracts with Programs, p. 374.

Updike, R.G., 1983, Inclinometer strain analyses of Anchorage landslides, 1965-1980: Alaska Division of Geological and Geophysical Surveys Professional Report 80, 141 p.

Hydrogen Release from Active Faults

21264

R. H. Ware

CIRES
University of Colorado
Boulder, CO 80309
(303) 492-8028

Investigations

Gas samples have been collected on various faults in the western US and the concentration of hydrogen gas has been determined using gas chromotography. This investigation was stimulated by reports of high hydrogen concentrations in soil gas samples collected on faults in Japan by Wakita et al (Science, 210, p188, 1980), and Sugisaki et al (Chemical Geology, 36, p217, 1982). The initial approach was to complete a broad survey of various fault regimes to identify those faults associated with hydrogen emanation. Subsequent studies will focus on the generating mechanism.

Soil gas collection and hydrogen detection

Reliable sampling and analysis procedures have been developed. An inverted PVC can with a small rubber septum on the top is used to collect soil gas samples. Gas is then withdrawn through the septum with a valved gas syringe and is returned to the lab where it is injected into a gas chromatograph. A sensitized electron capture detector easily detects hydrogen in ambient air (0.5ppm) using a 0.1ml sample. Methane in ambient air (1ppm) is also detected. Each sample can be analyzed in several minutes.

Negative results

Hydrogen and methane concentrations not exceeding those found in ambient air were found in gas samples collected on the following faults:

1. San Andreas fault, central California. Twenty one sites ranging from Parkfield to San Juan Bautista were sampled in January, 1983. Soil gas was taken from inverted cans installed by C. Y. King to monitor radon on the fault. Transportation and advice were provided by the courtesy of Calvin Walkingstick.

2. Coalinga earthquake, central California. Two samples were taken from inverted cans buried along surface cracks near the epicenter several days after the event. Samples were collected by Robert L. Brewer and Gary Fuis assisted with the logistics.

3. San Fernando fault, southern California. Three samples were collected in January, 1983, from a surface rupture of the 1971 San Fernando earthquake. Cans were buried in sandy clay and decomposed granite.

4. San Andreas fault, southern California. Five samples were taken near Big Pine at the Apple Tree campground, in June, 1983. This was the site of the 1857 Fort Tejon surface rupture. Advice on this site and the San Fernando site was kindly provided by Clarence Allen.

5. Colorado faults. Samples were collected in July, 1983, from the Four Mile Canyon, Rock River, Cottonwood Ridge and Carter Lake faults, including sedimentary and granite exposures. Locations were suggested and identified by Bill Braddock.

6. Greece. Six samples were taken on the main rupture of the 1891 Alchionides earthquake where it intersects the coast about 3 km E of Sxina. All were buried in loose debris made up of limestone fragments (up to 5 cm) and soil. Samples were collected by Max Wyss in September, 1983.

Positive results

1. Hebgen Lake, Montana. Six samples were collected in October, 1983, on a scarp of the normal fault from the 1959 Hebgen Lake earthquake. Two had elevated levels of hydrogen (15 and 80ppm) and methane (up to 100ppm), the others had ambient levels. A thorough investigation of this fault is called for.

2. Burro Mountain, central California. Four samples were taken from cans placed over gases bubbling from shallow water in Burro Creek, in July, 1983. Hydrogen concentration was 50% and methane 5%. This was verified by Bill Evans (USGS) using an independent gas chromatographic analysis. This area is essentially composed of dunnite. The gradual conversion of the associated ferrous hydroxide into magnetite is a possible source of the hydrogen, which emanates from local cracks, fissures and faults. A return to this area for a follow up study is warranted.

Geothermal Seismotectonic Studies

9930-02097

Craig S. Weaver
Branch of Seismology
U. S. Geological Survey
Geophysics Program AK-50
University of Washington
Seattle, Washington 98195
(206) 442-0627

Investigations

1. Analysis of the seismicity and volcanism patterns of the Pacific Northwest in an effort to develop an improved tectonic model that will be useful in updating earthquake hazards in the region. (Weaver, Michaelson, Yelin)

2. Continued acquisition of seismicity data along the Washington coast, directly above the interface between the North American plate and the subducting Juan de Fuca plate. (Weaver, UW contract)

3. Examine the hypothesis: Given a simple Coulomb failure criterion for a pre-existing fault and a range of values for the effective principal stresses, could the faults and slip directions that have been observed in northwestern Washington be the result of a stress field characterized by northeast compression. (Yelin)

4. Continued seismic monitoring of the Mount St. Helens area, including Spirit Lake (where the stability of the debris dam formed on May 18, 1980 is an issue) and Elk Lake (where seismicity remains at elevated levels an elevated level 30 months after the February 14, 1981 earthquake). (Weaver, Grant, UW contract).

Results

1. Pronounced differences in the earthquake distribution, style and volume of late Cenozoic and Quaternary volcanism, and the teleseismic P-wave delay pattern occur between Mount Rainier and Mount Hood. No sub-crustal earthquakes are observed south of Mount Rainier, and south of Mount Hood, few crustal earthquakes are known. Volcanism is much more widespread south of Mount Rainier than to the north. As these changes are sharp and nearly co-incident with each other, we have interpreted these changes as reflecting segmentation of the Juan de Fuca plate, with the plate dipping more steeply beneath northern Oregon than beneath Washington. The steeper dip beneath Oregon has allowed extensional tectonics to develop south of Mount Hood, and as a consequence this area is characterized by high heat flow, extensive volcanism, and normal faulting. In contrast, horizontal

compression dominates the tectonics north of Mount Rainier, where strike-slip faulting and only two isolated Quaternary volcanoes are found. The area between Mount Hood and Mount Rainier, where the change in plate dip is proposed, is transitional, with aspects of both compressional and extensional tectonics observed.

2. Earthquakes beneath the Olympic Peninsula can be divided into two groups: shallow crustal seismicity (depths 20 km at the coast to 30 km on the eastern Olympic Peninsula), and a deep group. This deep group is 5-10 km thick, and the zone dips to the east at an angle of about 108o9. At the coast, where the separation between the two zones is poorly defined, the top of the deep group is at a depth of 25 km. The top of the deep group is at about 45 km depth on the eastern edge of the Olympic Peninsula. The deep events appear to be occurring in the upper part of the subducting oceanic lithosphere. Focal mechanisms for the deep suite of events show primarily normal faulting with the P axes normal to the slab and the T axes displaying a range of angles within the slab; however, the average T axis is in the down-dip direction. These small magnitude earthquakes with down-dip tension axes are consistent with the slab sinking under its own weight.

3. Only occassional earthquake activity has occurred during the past six months near Spirit Lake, and all events have been of magnitude 2.0 or less. Focal mechanisms for two clusters of earthquakes beneath Windy Ridge (the northeast striking ridge immediately south of Spirit Lake) show strike-slip faulting on vertical planes. The P-axis orientation for these two focal mechanisms is N. 408o9 E., consistent with the regional stresses determined for southwestern Washington. West of Spirit Lake, focal mechanisms have been determined along the St. Helens seismic zone (SHZ) between Mount St. Helens and the location of the Elk Lake aftershock zone (a distance of about 15 km). Focal mechanisms are consistent with those along the SHZ at Elk Lake and south of Mount St. Helens, as they show strike-slip faulting on north-south striking fault planes.

Reports

Weaver, C. S., Zollweg, J. E., and Malone, S. D., 1983, Deep earthquakes beneath Mount St. Helens: Evidence for magmatic gas transport?: Science, v. 221, p. 1391-1394.

Malone, S. D., Boyko, C., and Weaver, C. S., 1983, Seismic precursors to the Mount St. Helens eruptions in 1981 and 1982: Science, v. 221, p. 1376-1378.

Swanson, D. A., Casadevall, T. J., Dzurisin, D., Malone, S. D., Newhall, C. G., and Weaver, C. S., 1983, Predicting eruptions at Mount St. Helens, June 1980 through December 1982: Science, v. 221, p. 1369-1376.

Weaver, C. S., 1983, Seismicity and seismotectonic boundaries in Washington (abs): Earthquake Notes, v. 54, p. 40.

Yelin, T. S., 1983, Possible block tectonics in northwestern Washington (abs): Earthquake Notes, v. 54, p. 40-41.

Taber, J. J. and Weaver, C. S., 1983, Seismicity of the Olympic Peninsula, Washington (abs): Earthquake Notes, v. 54, p. 41.

Michaelson, C. A. and Weaver, C. S., 1983, Deep earthquakes under the Puget Sound basin (abs): Earthquake Notes, v. 54, p. 41-42.

Grant, W. C., Weaver, C. S., and Zollweg, J. E., 1983, Temporal variation of the magnitude-frequency relation at Elk Lake, Washington (abs): Earthquake Notes, v. 54, p. 42.

Tectonic-tilt Measurements Using Lake Levels

9950-02396

Spencer H. Wood and Kirk Vincent
Branch of Engineering Geology and Tectonics
U.S. Geological Survey
Mailing address: Department of Geology and Geophysics
Boise State University
Boise, Idaho 83725
(208) 385-3629 or 385-1631

Investigations

1.Analysis of leveling data along the Wasatch Front:

Geodetic leveling data along the northern Wasatch Fault was examined for evidence of vertical tectonic movement. Estimates were made of possible systematic errors in determining elevations on the older National Geodetic Survey (NGS) and USGS level lines. A cooperative study was initiated with the National Geodetic Survey (J.Till and E. Balazs) to recalculate elevations using new rod-calibrations and also applying a correction for refraction. Original field notes of NGS and USGS lines are being coded for recalculation and also for inclusion in the format (Pfeifer and Morrison, 1980) of the national vertical control data set.

2.Releveling across the Wasatch Fault:

The 23-km level line that crosses the Wasatch Fault in Weber Canyon (near Ogden) was releveled by the NGS in September, 1983. This line was previously leveled in 1958 by the NGS and in 1974 and 1978 by the USGS. The 1983 releveling goes from Ogden, Utah to Evansen, Wyoming. A closed-loop spur line was extended west of Weber Canyon to the town of Roy, Utah in order to monitor the pattern of vertical deformation indicated by earlier releveling (Figure 1). Results of the releveling are not yet available.

3.Lake-level measurements on the Great Salt Lake:

Two new measuring sites were established in September,1983 to detect vertical movement closer to the Wasatch Fault One site near Farmington is within 3 km of the fault trace (Figure 2). Previous measuring sites of lake levels referenced to bench marks had been established at 4 sites around the lake in September, 1982. The lake has risen about 6 ft this year and flooded causeway barriers which may allow a level reference surface to be established over much of the lake.

4.Lake-level measurements on the Kenai Peninsula and Southeast Alaska (Kirk Vincent):

Measurements of land-surface tilt were made using simultaneouly recorded lake levels on each of the the following lakes during August, 1983: Kenai, Skilak, Tustamena Lakes on the Kenai Peninsula, Eyak Lake near Cordova, and Harlequin Lake near Yakutat.

Results

Elevation change along the Wasatch Front from leveling data:

Repeated first-order geodetic leveling in 1953 and 1967 along the Wasatch front shows elevation changes on the order of 11 cm that are consistant with strain accumulation along the Wasatch fault zone (Wood and Bucknam, 1983). This rate of strain is larger than indicated by the long-term rates of Holocene strain derived from exploratory trenching of the fault and paleoseismicity studies reported by Swan and others (1980).

The possibility that the contemporary elevation changes can be attributed to systematic errors in the leveling data cannot yet be dismissed. Systematic errors caused by refraction of the sight lines, when long-sight distances were used over terrain with significant near-surface temperature gradients ($1^{o}C/m$) may explain some of the elevation change. An estimate was made of the possible refraction error by the method suggested by Pelton and Smith(1982). For the 1958 NGS line in Weber Canyon a calculation was made assuming a 60-m sight length and a temperature differance of $2.3^{o}C$ between points 0.5 and 2.5m above the ground. Such conditions would lead to an elevation difference along the 23-km line that was 7 cm too small because of refraction of the sight line. This is about the elevation difference that is determined from differencing the 1958 and 1974 elevations. The 1974 and 1978/79 USGS leveling along the same line agree so closely with one another that errors are not suspected for these later derived elevations along the line.

If the leveling data is taken at face value, the observed elevation changes can be interpreted as ground-surface tilting of a zone about 12-km wide centered along the Wasatch fault zone. Beyond this zone, the Salt Lake Valley and the Wasatch Mountains appear to move largely as rigid blocks. This result suggests that efforts to monitor accumulating surface tilt should be concentrated within this 12-km zone. On this basis, lake-level monitoring sites for detecting ground surface tilt are being established closer to the fault (figure 2).

Work is underway to re-calculate the older leveling data using methods developed by Holdahl (1982). In addition, the leveling route that crosses the Wasatch Fault zone was releveled by the NGS in September 1983 using proceedures developed over the past few years to minimize systematic errors that have been suspected in earlier studies of crustal deformation derived from leveling data. Many old marks had to be re-established or reset because of this year's floods. New bench marks were also established and leveled west of the original route in order to establish a longer base line for monitoring the indicated pattern of vertical crustal movement on the Wasatch Fault in the vicinity of Ogden (figure 1).

References

Holdahl, S.R.,1982, Recomputation of vertical crustal motions near Palmdale, California, 1959-1975: Journal of Geophysical Research, v.87, p.9374-9388.

Pelton, J.R. , and Smith, R.B., 1982, Contemporary vertical surface displacements in Yellowstone National Park: Journal of Geophysical Research, v.87, p. 2745-2761.

Pfeifer, L., and Morrison, N.L.,1980, Input formats and specifications of the National Geodetic Survey data base, Volume II, vertical control base: NOAA Manual NOS NGS 2.

Swan, F. H. , III, Schwartz, D.P., and Cluff, L.S., 1980, Recurrence of moderate-to-large magnitude earthquakes produced by surface faulting on the Wasatch Fault zone, Utah: Bulletin of the Seismological Society of America, v.70, p. 1431-1462.

Reports

Wood, S.H., and Bucknam, R.C., 1983,Vertical Movement on the Wasatch Fault Zone, Northern Utah (abs.): Earthquake Notes, v. 54, no.1, p. 102 (Annual Meeting of the Seismological Society of America, Salt Lake City, Utah)

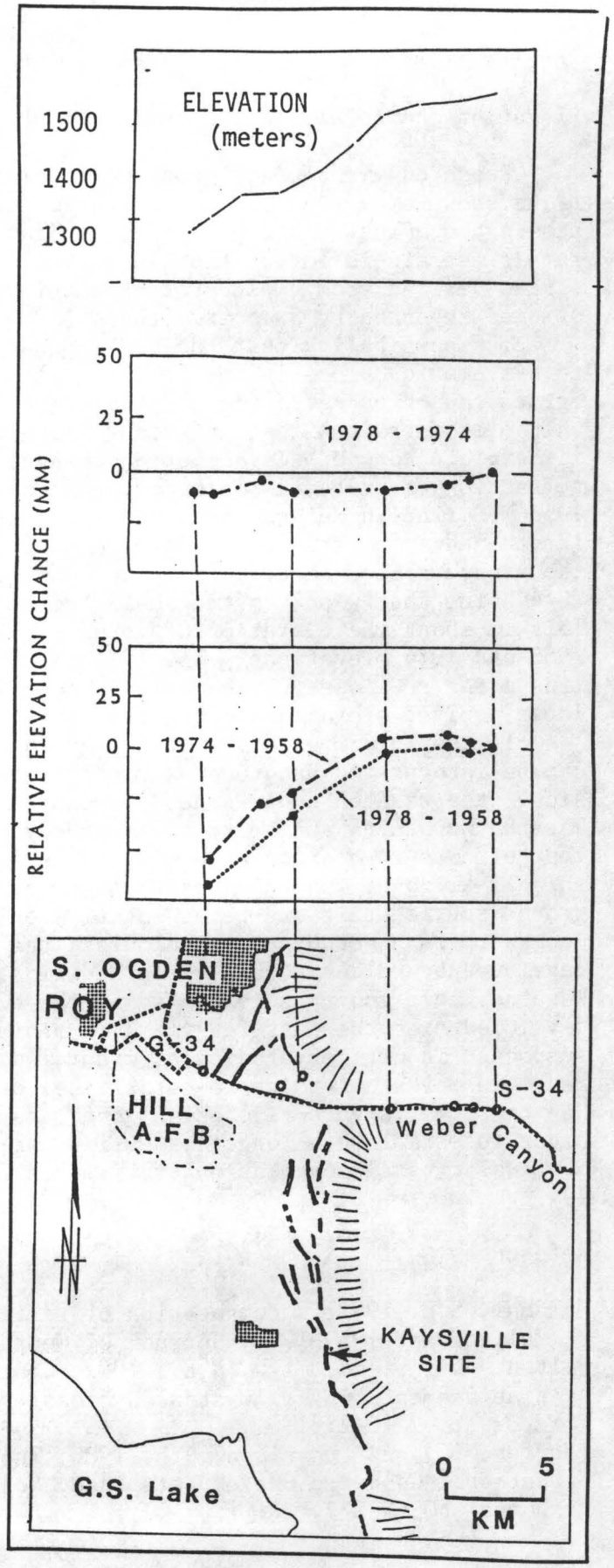

Figure 1. Map showing the 1958 NGS route and the 1974 and 1978/79 USGS leveling route across the Wasatch fault zone near Ogden, Utah. Route of the 1983 NGS leveling is shown with a dotted line. Graphs show the apparent changes in elevation detected by the earlier surveys and the elevation profile along the route. Of most interest is the 11-km segment showing a ground-surface tilt of about 7 microradians centered on the crossing of the Wasatch fault.

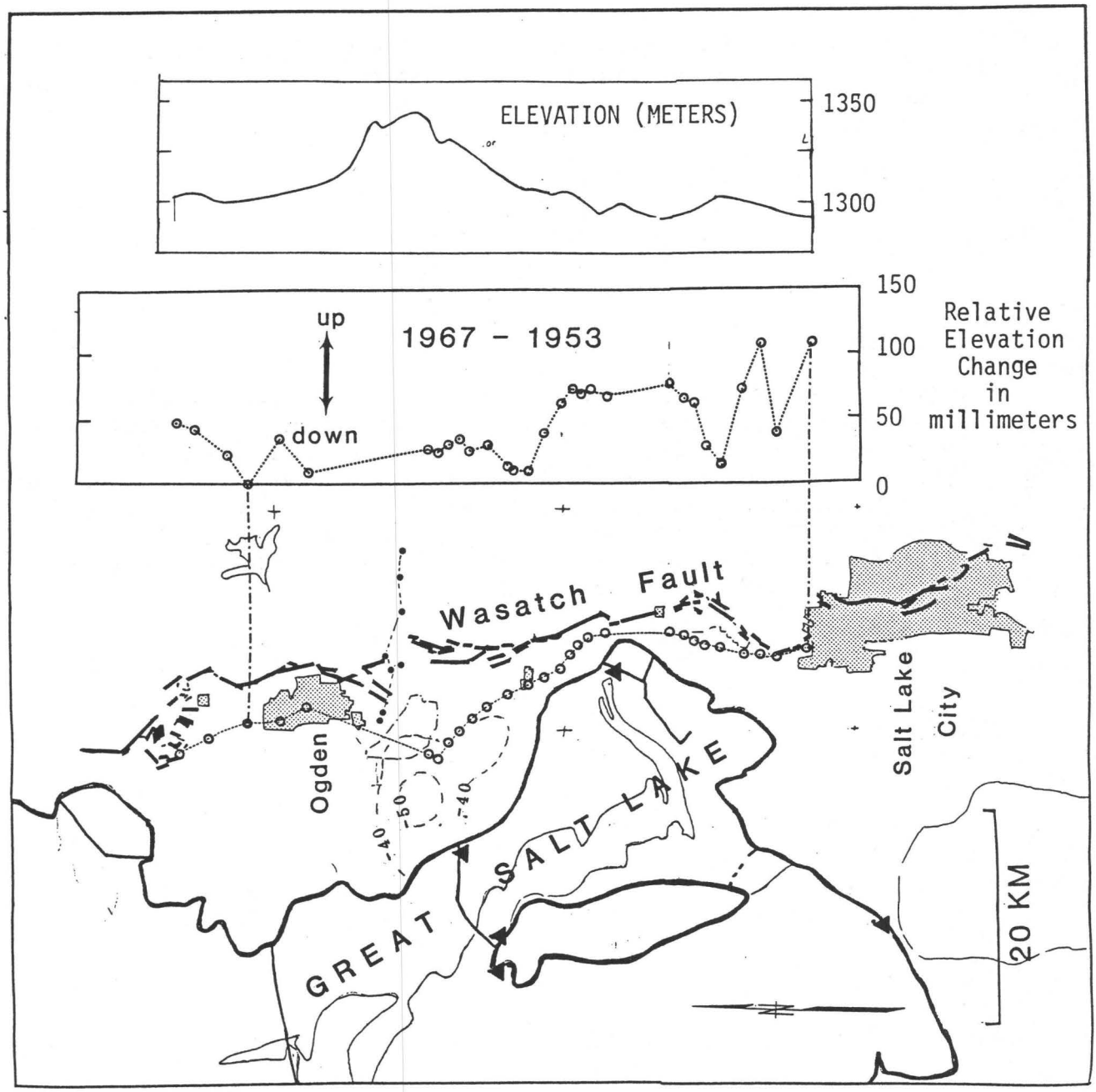

Figure 2. Map and profiles of apparent elevation change and elevation along the Wasatch Front based upon first-order NGS leveling in 1953 and 1967. The profiled elevation changes show that the elevation change and ground-surface tilt is greatest near the fault zone, and are diminished as the level line becomes more distant from the fault zone. Annotated contours southwest of Ogden outline an area of piezometric-level declines in the Weber-delta-area aquifers where minor subsidence might be suspected. Contour values are in feet of water level decline (preliminary and unpublished data from T. Arno, Water Resources Division, U. S. Geological Survey)

Potentially Active Reverse Faults of Eastern Ventura Basin, Los Angeles County, California

14-08-0001-21279

Robert S. Yeats
James McDougall
Department of Geology
Oregon State University
Corvallis, Oregon 97331

Investigations

Field mapping of critical fault localities was completed during the summer. Cross sections are now being constructed to incorporate subsurface and surface geology. The Oak Canyon oil field contains considerable detailed information bearing on the problem of reverse faults west of the San Gabriel fault. At the present time, it appears that we will be able to work out a fault history which will show that some of the faults are potentially active and others are not. Open-file surface geologic maps of Whitaker Peak and Valverde 7½ minute quadrangles are being completed.

Earthquake Hazards Studies, Metropolitan Los Angeles-Western Transverse Ranges Region

9540-02907

R. F. Yerkes
Branch of Western Regional Geology
U. S. Geological Survey
345 Middlefield Road, MS 75
Menlo Park, California 94025
(415) 323-8111 ext. 2350

Investigations and results

1. Historic earthquake data (W. H. K. Lee; Lee spent about half the planned 1/4 time on this investigation). Continued evaluation of unpublished data on 1933 Long Beach earthquake; systematic re-reading of P and S arrival times using microfilms of original seismograms, especially records from previously unread La Jolla and Santa Barbara stations. Continued organizing, evaluating, and merging phase data from several sources for southern California earthquakes.

2. Earthquake hazard studies (Yerkes). Reviewed surficial and shallow subsurface (oil well) geology of Coalinga area, petroleum and groundwater withdrawal, and reservoir fluid pressures. Preliminary evidence indicates presence of pressures up to 70% of geostatic at depths below 1/2 km in structurally high part of Coalinga Nose, thus extending northwestward the record of abnormally high fluid pressures documented by Berry (1973; in AAPG Bull. 57-7, p. 1219-1249) for the Kettleman Hills-Lost Hills chain.

3. Late Cenozoic ashes (A.M. Sarna-Wojcicki):

a. Continued investigations reported previously (items a-c, p. 48, vol. XVI).

b. We have identified the Nomlaki Tuff[1] at two new localities in southern California (tables 1 and 2): (1) from surface outcrops of the lower member of the marine Fernando Formation, near the town of Olive, in southeastern Los Angeles basin (in coop. with Thane McCulloh, formerly of WRG, Seattle, Wash.), and (2) from a shallow subsurface core in old alluvium near Romoland, in Perris Valley, about 60 km to the east of the first locality (in coop. with Doug Morton, ORG, Reston).

The Nomlaki Tuff, a widespread mid-Pliocene age and stratigraphic marker, was erupted about 3.4 m.y. ago, in the southern Cascade Range of northern California (Evernden and others, 1964; Sarna-Wojcicki, 1976). We have identified this tephra layer previously in southern California in the "Repetto Beds" of the Malaga Cove area, north of Palos Verdes Peninsula, where it is exposed above sea lavel (p. 117, vol. IX), and from subsurface core samples obtained near Santa Fe Springs in the L.A. basin (p. 71, vol. XII).

[1]Member of the Tehama and Tuscan Formations, in northwestern and northeastern Sacramento Valley, respectively, in northern California.

Data for electron-microprobe and energy-dispersive X-ray fluorescence analyses are given below (tables 1 and 2).

Table 1. Electron-microprobe analysis of volcanic glass of the 3.4-m.y.-old Nomlaki Tuff (Member of the Tehama and Tuscan Formations) and glass from correlative tephra layers. Analysis of the 0.73-m.y.-old Bishop ash bed are shown for comparison. C. E. Meyer. USGS, Menlo Park, Analyst.

Sample No.	SiO_2	Al_2O_3	Fe_2O_3	MgO	CaO	BaO	TiO_2	Na_2O	K_2O
1. Olive-1	76.95	12.77	1.10	0.18	0.98	0.10	0.21	3.94	3.59
2. 82W14	76.97	12.63	1.14	0.18	0.97	0.11	0.22	4.05	3.57
3. MLG-1	76.41	13.10	1.21	0.21	0.98	0.10	0.21	4.36	3.22
4. Bell-60	78.22	12.82	1.07	0.16	0.87	0.12	0.21	4.26	2.08
5. 758-314	77.51	13.00	1.07	0.19	0.93	0.11	0.22	3.54	3.29
6. BID-1	76.44	13.32	1.15	0.18	1.03	0.11	0.23	3.98	3.39
7. Bishop	77.37	12.72	0.75	0.04	0.45	0.00	0.06	3.34	5.22

1. Sample from near Olive, L.A. basin.
2. Sample from Perris Valley, southeastern California.
3. Sample from Malaga Cove area, north of Palos Verdes Peninsula, California.
4. Sample from subsurface, Santa Fe Springs, L.A. basin.
5. Nomlaki Tuff Member, type loc., west Sacramento Valley, California.
6. Nomlaki Tuff Member, east Sacramento Valley, California.
7. Bishop ash, north of Bishop, east-central California.

Table 2. Energy-dispersive X-ray fluorescence analysis of volcanic glass of the 3.4-m.y.-old Nomlaki Tuff Member (of the Tehama and Tuscan Formations) and glass of correlative tephra layers. Analyses of the 0.73-m.y.-old Bishop ash bed are shown for comparison. Values given are spectral intensity ratios for each of the elements. J. L. Slate, USGS, analyst. Sample numbers and locations are the same as in table 1.

Sample No.	Ca	Ti	Mn	Fe	Rb	Sr	Y	Zr	Nb
1. Olive-1	64	222	179	866	1269	1508	633	2791	526
2. 82W14	64	218	171	853	1306	1486	618	2728	525
5. 758-314	67	218	175	869	1202	1474	608	2764	487
7. Bishop	47	89	189	797	2258	303	964	1605	883

Reports

Sarna-Wojcicki, A. M., Meyer, C. E., Bowman, H. R., Hall, N. T., Russell, P. C., Woodward, M. J., and Slate, J. L., Correlation of the Rockland ash bed, a middle Pleistocene stratigraphic marker in northern and central California and western Nevada. Approved journal article submitted to Quaternary Research.

Sarna-Wojcicki, A. M., Meyer, C. E., and Slate, J. L., Applications of tephrochronology and tephrostratigraphy to Quaternary chronology, stratigraphy, and tectonics in the Western United States. Abstract for International Symposium on Recent Crustal Movements of the Pacific Region, Wellington, New Zealand. Accepted.

Lajoie, K. R., Sarna-Wojcicki, A. M., Kennedy, G. M., Mathieson, S. A., McCrory, P. A., Morrison, S. A., and Stephens, T. A., Late Quaternary Coastal Tectonics of the Pacific Coast of the United States. Abstract for International Symposium on Recent Crustal Movements of the Pacific Region, Wellington, New Zealand. Accepted.

Lajoie, K. R., Kennedy, G. L., Mathieson, S. A, Sarna-Wojcicki, A. M., Morrison, S. A., and Tobish, M. K., 1983. Emergent Holocene Marine Terraces Cape Mendocino and Ventura, California, U.S.A. Abstract, Conference on Holocene Shorelines, Japan.

Yerkes, R. F., Ellsworth, W. L., and Tinsley, J. C., 1983, Triggered reverse fault and earthquake due to crustal unloading, northwest Transverse Ranges, California: Geology, v. 11, p. 287-291, May, 1983.

Yerkes, R. F., and Williams, K. M., Shallow stress changes due to withdrawal of liquid from oil fields in the Coalinga area, California: 5 pages incluing 2 tables, 1 figure. Submitted to CDMG.

Segall, P., Reasenberg, P. and Yerkes, R..F., Crustal stress changes and subsidence resulting from fluid withdrawal in the epicentral region of the 1983 Coalinga earthquake (abs.). Submitted to AGU.

Earthquake Hazards
Puget Sound, Washington

9540-02197

J.C. Yount
Branch of Western Regional Geology
U.S. Geological Survey
345 Middlefield Road
Menlo Park, California 94025
(415) 323-8111 x2905

Investigations

Studies of earthquake hazards in Puget Sound have been directed toward three main topics during the life of this project (1980-1983):

1. Developing an understanding of the seismotectonic setting of Puget Sound and the major tectonic forces responsible for earthquakes in the region.

2. Determining the nature and distribution of geologic materials that control seismic ground shaking in Puget Sound.

3. Investigating the properties, particularly of glaciogenic materials, that control liquification during seismic shaking.

Results

1. Geologic mapping and compilation of pertinent geophysical information have delineated the basic tectonic framework for the Puget Sound region. Puget Sound is broken into a series of roughly equidimensional basins bounded by prismatic west to northwest trending bedrock highs. Quaternary sediments thicken in the basins and thin over bedrock highs, suggesting, but not proving, that basin margin tectonism is still going on. Radiocarbon dating of uplifted marine deposits along the south side of the Seattle Basin confirms recent uplift along the Seattle-Bremerton Fault as young as 1350 to 3260 years ago.

   Examination of the seismicity of Puget Sound reveals no clear relationship between shallow earthquakes and any of the basin margin structures cutting the area. Focal mechanisms indicating north-south compression in the upper 30 kilometers of the crust are consistent, however, with northward translation of the North America Plate relative to the Pacific Plate, with accompanying buttressing against Vancouver Island. The deep (greater than 35 km) earthquakes define an east-dipping slab buckled into an east-plunging antiform beneath Puget Sound. This feature is interpreted to be the subducted Juan de Fuca Plate. Seismicity beneath the Olympic Peninsula, the presence of over-consolidated late Quaternary muds outcropping on the Washington continental slope, and results of geodetic leveling across Puget Sound, all support the fact that subduction is going on at the present time.

The 1949 Olympia earthquake (M=7.1) and the 1965 Seattle earthquake (M=6.5) were apparently generated by tensional breaking of the descending Juan de Fuca Plate beneath Puget Sound.

2. Geologic mapping and subsurface investigation of the Quaternary deposits indicate that the distribution and nature of the various stratigraphic units are highly variable. Owing to repeated glaciation of the region and subsequent re-development of the major fluvial drainage systems during the Quaternary, sedimentary units of contrasting lithology and physical properties often nest younger into older along steep contacts. This configuration makes simplified plane layer models of seismic ground shaking impossible to apply to this region. It further explains the enigmatic patterns of strong ground motion observed during past earthquakes in Puget Sound.

3. Analysis of boreholes in the Seattle South 7 1/2 minute Quadrangle indicates that mappable glacial and nonglacial units have physical properties (grain size, water content, standard penetration) unique enough to permit gross delineation of liquifaction potential for the region based on the distribution of geologic units and elevation of the water table. As there is no reason to postulate an earthquake along any well-defined structure in the region, it must be assumed that the causitive earthquake can occur anywhere in the region beneath a depth of 50 kilometers. Thus the map of liquifaction potential of materials is in effect, a liquifaction susceptibility map.

Reports (1980-1983)

Published

Dethier, D. P., Safioles, S. A., and Minard, J. P., 1982, Preliminary Geologic Map of the Maxwelton Quadrangle, Island County, Washington: U.S. Geological Survey Open-File Report 82-192, scale 1:24,000.

Dethier, D. P., and Whetten, J. T., 1980, Preliminary geologic map of the Clear Lake SW quadrangle, Skagit and Snohomish Counties, Washington: U.S. Geological Survey Open-File Report 80-825, scale 1:24,000.

Dethier, D. P., Whetten, J. T., and Carroll, P. R., 1980, Preliminary geologic map of the Clear Lake SE quadrangle Skagit County, Washington: U.S. Geological Survey Open-File Report 80-303.

Gower, H. D., 1980, Bedrock geologic and Quaternary tectonic map of the Port Townsend area, Washington: U.S. Geological Survey Open-File Report 80-1174.

Minard, J. P, 1980, Distribution and description of the geologic units in the Snohomish quadrangle, Washington: U.S. Geological Survey Open-File Report 80-2013, scale 1:24,000.

Minard, J. P., 1981, Distribution and description of the geologic units in the Maltby quadrangle, Snohomish and King Counties, Washington: U.S. Geological Survey, Open-File Report 81-100, scale 1:24,000.

Minard, J. P., 1981, Distribution and description of the geologic units in the Bothell quadrangle, Snohomish and King Counties, Washington: U.S. Geological Survey Open-File Report 81-106, scale 1:24,000.

Minard, J. P., 1981, Distribution and description of the geologic units in the Everett quadrangle, Snohomish County, Washington: U.S. Geological Survey Open-File Report 81-248, scale 1:24,000.

Minard, J. P., 1982, Distribution and description of the geologic units in the Mukilteo quadrangle, Snohomish County, Washington: U.S. Geological Survey Miscellaneous Field Investigations Map, MF 1438, scale 1:24,000.

Wagner, H. C., and Wiley, M. C., 1980, Preliminary map of offshore geology in the Protection Island-Point Partridge area northern Puget Sound Washington: U.S. Geological Survey Open-File Report 80-548.

Whetten, J. T., Dethier, D. P., Carroll, P. R., 1980, Preliminary geologic map of the Clear Lake NW quadrangle, Skagit County, Washington: U.S. Geological Survey Open-File Report 80-247.

Yount, J. C. and Crosson, R. S., eds., 1983, Earthquake Hazards of the Puget Sound Region, Washington: Proceedings of Workshop XIV, National Earthquake Hazards Reduction Program: U.S. Geological Survey Open-File Report 83-19, 306 p.

Yount, J. C., and Gower, H. D., 1981, Seismotectonic model for the Puget Sound Region of Washington State: Geological Society of America Abstracts with Programs, v. 13, no. 2, p. 115.

Yount, J. C., Marcus, K. L., and Mozley, P. S., 1980, Radiocarbon-dated localities from the Puget Sound Lowland, Washington: U.S. Geological Survey Open-File Report 80-780.

In press (Directors approval received)

Minard, J. P., Distribution and description of the geologic units in the Edmonds East and adjoining eastern part of the Edmonds West Quadrangles, Snohomish and King counties, Washington: U.S. Geological Survey Miscellaneous Investigations Map, scale 1:24,000.

Minard, J. P., Distribution and description of the geologic units in the Kirkland quadrangle, King County, Washington: U.S. Geological Survey Miscellaneous Investigations Map, scale 1:24,000.

Salter, A. F., Yount, J. C. and Dembroff, G. R., Locations of Radiocarbon-Dated Samples from the State of Washington: U.S. Geological Survey Miscellaneous Investigations Maps, scale 1:250,000 and 1:500,000.

Whetten, J. T., Carroll, P. I., Gower, H. D., Brown, E. H., and Pessl, Fred, Jr., 1983, Bedrock geologic map of the Port Townsend quadrangle, Washington: U.S. Geological Survey Miscellaneous Field Investigations, Map I-1198, scale 1:100,000.

Yount, J. C., Dembroff, G. R. and Barats, G. M., Depth-to-Bedrock, Seattle 1:100,000 Quadrangle: U.S. Geological Survey Miscellaneous Investigations Map, scale 1:100,000.

Regional Syntheses of Earthquake Hazards in Southern California

9910-03012

Joseph I. Ziony
Branch of Engineering Seismology and Geology
U. S. Geological Survey
345 Middlefield Road, MS-77
Menlo Park, California 94025
(415) 323-8111, ext. 2944

Investigations

1. Analysis of the geologic and seismologic character of late Quaternary faults of the Los Angeles region, as determined from published and unpublished sources and from limited field investigations, continued. Our emphasis is on obtaining: (a) quantitative data on offsets of deposits or geomorphic features younger than about 700,000 years in order to provide a reasonably uniform basis for estimating rates of geologically-recent slip along individual faults, and (b) geologic constraints on the recurrence of large earthquakes. The long-term objectives are to estimate the relative activity of these faults, and, where possible, their earthquake and surface faulting potential.

2. Coordination of the preparation of a professional paper on the earthquake hazards of the Los Angeles region continued. This comprehensive report will summarize the current methods and conclusions of USGS investigators concerning the major earthquake-hazard factors for the region.

Results

1. Systematic areal differences in fault slip rates across the Los Angeles region are confirmed by newly acquired or revised data on offset late Quaternary markers. Average rates in the tens of millimeters per year characterize the San Andreas and San Jacinto faults, but are much less for the other active faults. Within the Transverse Ranges province, the highest values are associated with the belt of late Quaternary faults that extend diagonally across the province from near Santa Barbara to near San Bernardino. This belt within the Ventura basin is broad and is composed of numerous faults with individual slip rates of about 1-2 mm/yr. The belt narrows to the east, and slip is concentrated on fewer strands. Thus, the faults forming the southern boundary of the Transverse Ranges eastward from Pasadena have late Quaternary slip rates as great as 6 mm/yr. In contrast, faults along the southern boundary of the Transverse Range province between the Channel Islands and Pasadena, have rates of slip less than 1 mm/yr.

   Rates on the northwest-trending fault zones west from the San Jacinto fault are poorly constrained by late Quaternary data. We provisionally infer average rates of about 1 mm/yr each for the Elsinore, Newport-Inglewood and Palos Verdes Hills fault zones; these value are compatible with the sparse data on rates of vertical separation known along these faults. Furthermore, displaced late Pleistocene shorelines near La Jolla (Kern, 1977) suggest a slip rate of 1.2-1.4 mm/yr for the Rose Canyon fault, the likely southern continuation of the Newport-Inglewood zone.

2. Final drafts for all of the chapters of the Los Angeles professional paper are nearly complete. As a demonstration of the various hazard-evaluation methods discussed in the volume, the contributors jointly are evaluating the geologically controlled effects expected from a postulated M 6.5 earthquake generated by strike slip along the northern part of the Newport-Inglewood zone.

   Predicted effects include:

   --secondary faulting (normal-oblique slip) at the ground surface along one or more exposed late Quaternary faults in the Baldwin and Rosecrans Hills. Possible subsurface slip along reverse faults near the Dominguez Hills.

   --shaking intensities of Modified Mercalli intensity VII distributed widely throughout the Los Angeles basin and the San Fernando Valley, with scattered sectors of intensity VIII to distances of 18 km or so from the surface trace of the fault zone.

   --strong shaking lasting about 10 seconds. Strong directivity effects on ground motion values are expected if the subsurface tectonic rupture propagates northwestward from the postulated epicenter, with some components of peak velocity an order-of-magnitude higher near Century City than at Long Beach airport. Predictive maps showing the areal distribution of peak acceleration, peak velocity, and response spectral values are being prepared.

   --liquefaction in highly susceptible saturated Holocene alluvial sediments as distant as 17 km from the earthquake source zone. Areas most susceptible to liquefaction-type ground failure include parts of the southern San Fernando Valley, the coastal and harbor areas of Long Beach and Marina Del Rey, and the recent floodplains of the Ballona, Dominguez, and Santa Ana gaps.

   --earthquake-triggered landslides. Numerous disrupted failures (rock/soil falls and slides) will be most common in upland areas within 41 km of the northern Newport-Inglewood zone, but a few may occur as distant as 112 km on highly susceptible slopes. A few coherent slope failures (deep-seated slumps and block-glides) may occur.

   --minor seiching in enclosed small bodies of surface water, and fluctuations in levels of groundwater in some wells.

Reports

Clark, M. M., Harms, K. K., Lienkaemper, J. J., and Ziony, J. I., 1983, Late Quaternary slip rates for California faults [abs.]: International Symposium on Recent Crustal Movements, February 9-14, 1984, Wellington, New Zealand. (Approved by Director).

Ziony, J. I., and Tinsley, J. C., 1983, Mapping the earthquake hazards of the Los Angeles region: Earthquake Information Bulletin, v. 15, no. 4, p. 134-141.

An Investigation of Holocene Neotectonic Deformations in the Charleston South Carolina Region Compared to Areas to the North and to the South

3-9900-5067

D.J. Colquhoun
University of South Carolina
Department of Geology
Columbia, South Carolina 29208
(803) 777-2600

Investigations

1. Investigations proceeded to the north of Charleston, South Carolina in the vicinity of Georgetown, and to the south of Charleston, South Carolina in the vicinity of Edisto Island areas as well as in the Charleston vicinity to measure sea-level indicators in Holocene marsh stratigraphy and to date sea-level positions during the Holocene for comparison.

Both coring using a slightly modified dutch gouge auger and vibracoring techniques were employed.

In addition, archeological site investigations in estuarine areas were conducted in the Charleston and Edisto Island areas to complement studies conducted in the previous year in the Georgetown area.

Results

1. Winyah Bay (Georgetown)

40 dutch auger cores were taken along the Pee Dee and Waccamaw Rivers. Significant peat bodies for dating purposes were finally located approximately six miles east of Georgetown. Two vibracores were taken and three samples are being submitted for dating to add to the information obtained last year (Colquhoun 1982b). A total of 30 man days were expended in the field.

2. Charleston Area

47 dutch gouge auger cores were obtained in the Wando and Stono Rivers. Intertidal basal peats were found in the Wando River but not in the Stono. Two samples have been submitted for dating to add to the information reported last year (Colquhoun 1982).

An intensive investigation of interriverine archeological sites was conducted in the Stono River area for comparison with previously conducted investigations in the Wando area. These areas lie athwart the postulated Charleston fault depicted in Tertiary stratigraphic investigations as in Colquhoun, 1982b or microseismal studies as in Talwani, 1982. 30 man days were expended in the field.

3. Edisto Island Area

118 dutch gouge auger cores and 17 vibracores were obtained in and surrounding the North Edisto estuary. Ten intertidal basal peat samples have been submitted for dating. This area which had received the least attention last year has now been investigated to approximately the same effort as the Charleston and Georgetown regions. Approximately 65 man days field work were expended. In addition an intensive interriverine archeological site investigation was conducted, and re-examination of several estuarine shell middens was accomplished.

Ongoing Investigations

Diatom analysis of all samples to be dated is proceeding and an additional thirteen samples are being selected on a priority basis for submission within two weeks. Pollen analyses are proceeding.

The final report will be written during November and submitted.

Reports

Colquhoun, D.J., Brooks, M.J., Brown, J.G., and Stone, P.A., 1983, Correlation between sea level and climatic change in the middle Holocene of the southeastern United States; Inter-union Commission on the Lithosphere, XVIII General Assembly, Hamburg August 15-27, 1983, Programme and Abstracts, p. 89.

Colquhoun, D.J., Brooks, M.J., Brown, J.C., and Stone, P.A., 1983 Correlation between sea level and climatic change in the middle Holocene of the southeastern Unitec States; International symposium on coastal evolution in the Holocene, Tokyo, Japan, August 29-31, 1983, Abstracts of papers.

Brooks, M.J., Colquhoun, D.J., Brown, J.G., Stone, P. A., 1983, Sea level change, estuarine developement and temporal variability in Woodland period subsistence-settlement patterning on the lower Coastal Plain of South Carolina; abstract to be presented at the Southeastern Archeological Assembly on November 11, 1983.

References

Colquhoun, D.J., 1982, An investigation of Holocene Neotectonic Deformation in the Charleston, South Carolina region, compared to areas to the north and to the south: U.S. Geol. Survey, Summaries of Technical Reports, v. 15, p. 78-82.

Talwani, P., 1982, Internally consistent pattern of seismicity near Charleston, South Carolina: Geology, v. 10, p. 654-658.

Seismotectonics of Northeastern United States

9950-02093

W. H. Diment
Branch of Engineering Geology and Tectonics
U.S. Geological Survey
Denver Federal Center, MS 966
Denver, CO 80225
(303) 234-5087

Investigations

Work on this project was temporarily recessed during this report period due to other commitments. Progress on reports is indicated below.

Reports

Diment, W. H., Urban, T. C., and Muller, O. H., 1983, Notes on the thickness of the seismogenic layer in the eastern United States and its relation to seismicity: Geological Society of America Abstracts with Programs, v. 15, no. 5, p. 138.

Muller, O. H., Diment, W. H., and Urban, T. C., 1983, The geophysical nature of the Adirondack Mountain block--relation to seismicity: Geological Society of America Abstracts with Programs, v. 15, no. 5, p. 124.

Urban, T. C., and Diment, W. H., 1983, Thermal conductivity profiles of the Appalachian Basin--Application to identification of anomalous geothermal conditions and to estimation of deep temperatures: Geological Society of America Abstracts with Programs, v. 15, no. 5, p. 197.

Diment, W. H., McKeown, F. A., and Thenhaus, P. C., 1983, Northeastern United States seismic source zones--Summary of workshop, convened September 10-11, 1980, in Thenhaus, P. C., ed., Summary of seismic regional source zones of parts of the conterminous United States, convened by the U.S. Geological Survey 1979-1980, Golden, Colorado: U.S. Geological Survey Circular 898 (in press).

Diment, W. H., and Urban, T. C., 1983, A simple method for detecting anomalous fluid motions in boreholes from continuous temperature logs: Geothermal Resources Council Transactions, v. 7 (accepted).

Thenhaus, P. C., Ziony, J. I., Diment, W. H., Hopper, M. G., Perkins, D. M., Hanson, S. L., and Algermissen, S. T., 1983, Probabilistic estimates of maximum seismic horizontal ground acceleration on rock in Alaska and the adjacent outer continental shelf: Seismological Society of America Bulletin (CTR).

Urban, T. C., and Diment, W. H., 1983, The thermal regime of the shallow sediments of Clear Lake, California, in Sims, J. D., ed., Quaternary history of Clear Lake, California: Geological Society of America Special Paper (CTR).

A Study of Source Parameters of Large Northeastern Earthquakes

14-08-0001-21295

John E. Ebel
Dept. of Geology & Geophysics
Boston College
381 Concord Road
Weston, Massachusetts 02193
(617) 899-0950

Objective: During the first half of the 20th century, several relatively large earthquakes took place in northeastern North America. The events, which occurred in 1925 near La Malbaie, Quebec (M=6.8), in 1935 near Timiskaming, Quebec (M=6.3), in 1939 near La Malbaie, Quebec (M=5.2), in 1940 near Ossipee, New Hampshire (M=5.6), and in 1944 near Massena, New York (M=6.0), were recorded widely by seismographs in North America, South America and Europe. The purpose of this study is to use synthetic seismogram analysis techniques to determine the source parameters (focal mechanism, depth, source time function, stress drop and seismic moment) for each event. This information can then be used to help investigate the cause of moderately-large earthquakes in northeastern North America.

Data Acquisition and Analysis: The first six months of work on this project have been filled with preparations to do the data analysis. These have included.

1. Efforts to contact observatories world wide to obtain originals or copies of seismograms of each of these earthquakes. Over 50 seismograms of varying quality have been acquired, although in a number of cases several inquires had to be made before replies and seismograms from foreign observatories were sent. Most of the seismograms have useful surface wave information, but only about 10% are of sufficient quality to be useful for a body wave analysis. Efforts to procure more seismograms are still being made.

2. Calculations of instrument responses. Much effort has been expended in trying to document the proper instrument types and responses used in recording the seismograms. For many instruments clear, easily available documentation exists. In other cases, discussions of some instrument operations and response have been more difficult to find. This work is near completion and programs to calculate the impulse responses of mechanical and electromagnetic instruments have been written.

3. Synthetic seismogram programs have been adapted to the Boston College VAX 11/780 computer. The synthetic seismogram programs have been rewritten to make them compatible with the Boston College VAX computer as well as to allow the input and analysis of the old seismograms. These modifications have been recently tested and appear to be working properly.

4. A number of seismograms of the 1925 and 1935 earthquakes have been digitized for analysis. More seismograms for these earthquakes as well as seismograms of other earthquakes still must be digitized.

5. High frequency seismograms recorded within 8° of the 1935 earthquake have been digitized and low-pass filtered in an effort to analyze the $P_{n\ell}$ waves. This work has met with very limited initial success.

Preliminary Results: Most of the work performed to date has been to prepare the data and analysis programs. However, testing some of the data in analysis programs has indicated that both the 1925 and 1935 earthquakes were predominantly thrust events with hypocenters of about 8 km depth. The particular values of strike, dip and rake as well as the values of other source parameters have not yet been resolved.

Whole Waveform Inversion of Regional Digitial Seismic Data

14-08-0001-20640

Robert B. Herrmann
Department of Earth and Atmospheric Sciences
Saint Louis University
P.O. Box 8099 Laclede Station
St. Louis, MO 63156
(314) 658-3131

Goals

1. Investigate the possibility of using high frequency regional network data for the direct inversion for focal mechanism and seismic moment by waveform inversion.

Investigations

1. We have acquired the USGS data sets from the New Brunswick and Monticello Reservoir earthquakes. Most time has been spent with the New Brunswick data set learning how to process the data. Data are first low pass filtered and compared to synthetics passed through the same instrument and filter. A systematic search is made for source parameters of depth, strike, dip and slip using C. Langstons Cagniard-de Hoop program.

Results

1. Results are premature since we are still learning how to process the data and are beginning to appreciate the effects of unknown crustal structure, even at distances as short as 10 km.

Mississippi Valley Seismotectonics

9950-01504

Frank McKeown
Branch of Engineering Geology and Tectonics
U.S. Geological Survey
Denver Federal Center, MS 966
Denver, CO 80226
(303) 234-5087

Investigations

1. Processing and interpretation of seismic reflection data recorded on the R/V Neecho on the Mississippi River was continued intermittently.

2. Digitization of Cretaceous and Tertiary reflectors on seismic reflection profiles in the New Madrid region was nearly completed.

3. Organization of level line data and preparations to analyze it were continued.

4. A quantitative geomorphic study of streams in the southeastern part of the Ozark uplift was continued.

5. Two hundred miles of seismic reflection profiling data were purchased under a sole source contract.

Results

1. Illustrations and text describing interpretations of the Mississippi River seismic reflection data is nearly complete.

2. Computer programs to manipulate and plot level line data were tested on hypothetical and real data. The programs are ready for use to analyze hundreds of miles of level line data obtained in the upper Mississippi embayment region.

3. Digitized stream profile data were used to calculate stream gradient indices, and second derivatives of semilog plots of stream profiles. These parameters were plotted on maps for contouring. In addition, a subenvelope map was constructed from the profile data. Preliminary interpretation of some of the geomorphic and geologic data supplied by E. Glick and B. Haley suggests that the gradients and sinuosity of some streams west and north of the buried Newport pluton may be related to nonlithologic factors. An unexpected result was that profiles of several streams have inflections at the locations of some faults. Available geologic data for these locations do not indicate that the inflections are the result of a change in lithology across the faults. Field examination will be required to determine the cause of the inflections.

4. Cursory examination of the purchased seismic reflection profiles indicates that it will be possible to delimit within a few kilometers a major deeply buried structural zone which appears to be closely related to the principal northeast-trending zone of seismicity in the New Madrid region.

Northeastern U.S. Seismicity and Tectonics

9510-02388

Nicholas M. Ratcliffe

Branch of Eastern Regional Geology

U.S. Geological Survey, National Center, MS 925

Reston, Va. 22092 (703) 860-6406

Investigations:

1. Vibroseis profiling of Ramapo seismic zone and gravity survey.
2. Bedrock mapping and coring New Jersey and New York along planned vibroseis routes.
3. Gravity and structural studies of the Newark Basin.

Results:

1. Approximately 65 km of 12-fold seismic reflection data across the Newark Basin in New Jersey and Rockland County, New York, were collected in August, in cooperation with John Costain of Virginia Tech. (Figure 1). A line north of Princeton, New Jersey, appears to contain excellent reflectors within and beneath the Triassic-Jurassic basin and beneath basement gneiss to the west of the basin. The line of section extends from Schooley Mountain, past Oldwick, N.J., to Sommerville, N.J. Seismicity along this line includes the Schooley Mountain earthquake swarm and the Oldwick Magnitude 2.8 event of February 1983.

2. Drill coring of the border fault of the Newark Basin in the line of the vibroseis section at Oldwick reveals a surface dip of 35°E. or SE for Flemington fault from two continuously cored holes. Analysis of the fault structures suggest that the latest movement on the Flemington was extensional, and perhaps oblique-normal. Coring of the Ramapo fault at Bernardsville was completed in August and a strike of N35°E. and a dip 40° SE is indicated from three continuously cored holes and from trenching of the fault zone.

3. Detailed gravity traverse was conducted along the route of the vibroseis line in New Jersey by Wendy Rosov and Ken Kodoma of Lehigh University.

4. Bedrock mapping in the northern Hudson Highlands in Poughquagh quadrangle has defined the distribution and attitude of semi-ductile shear zones in the gneiss basement north of Annsville, N.Y., in an area affected by repeated low level seismicity. The January 8, 1983, magnitude 3.0 Whaley Lake event (Figure 1) occurred within the mapped area and could have been generated on one of these semi-ductile shear zones at depth of 4 or 5 km. A vibroseis line across this part of the Ramapo seismic zone is planned for FY 84 (Figure 1).

5. Structural sections of the northern end of Newark Basin based on our field data show rather shallow sediment thicknesses ranging from 0 to 3 km that agree in part with the preliminary results of Wendy Rosov and Ken Kodoma of Lehigh University from two dimensional models of the gravity data collected by Rosov and Marty Kane in a dense grid across the basin in Rockland County, N.Y.

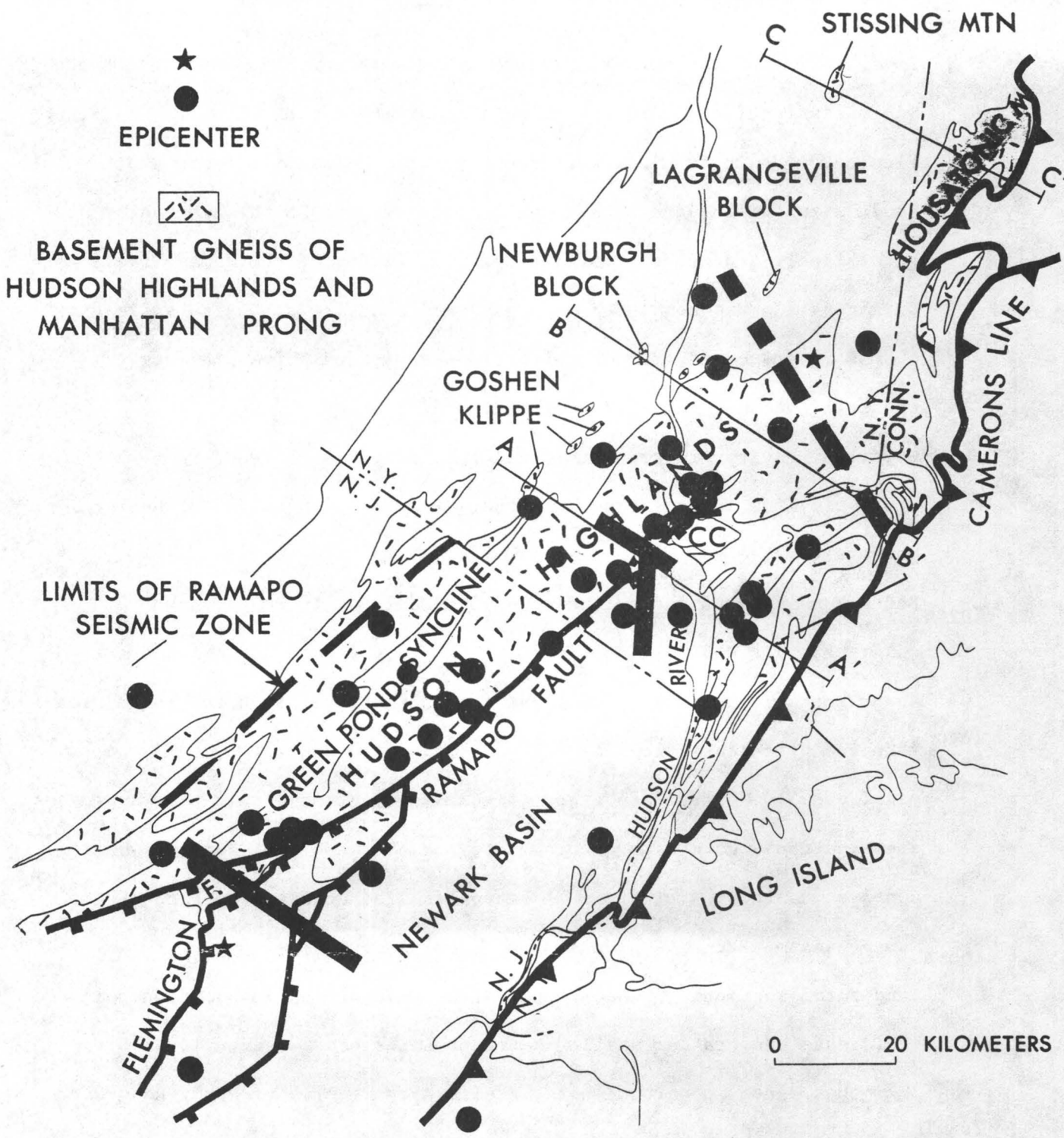

RAMAPO SEISMIC ZONE

Figure 1. Location of seismic reflection profiles across Ramapo and Flemington fault completed in August 1983. Dashed line shows profile to be run in FY 84. Stars show location of Oldwick and Whaley Lake events $M_{2.8}$ and M_3 respectively of January and February 1983.

Earthquake Hazard Studies in Southeast Missouri

14-08-0001-21262

William Stauder
Robert B. Herrmann
Department of Earth and Atmospheric Sciences
Saint Louis University
P.O. Box 8099 Laclede Station
St. Louis, MO 63156
(314) 658-3131

Goals

1. Monitor seismic activity in the New Madrid Seismic Zone, using data from a 60 station regional seismic array sponsored by the USGS and the USNRC.

2. Conduct research on eastern United States seismic sources using array and supplemental data.

Investigations

1. The project consists of monitoring data from a network of 32 USGS and 16 NRC seismograph stations located in the central Mississippi Valley. In addition telemetered data from eight Tennessee Earthquake Information Center stations in the southern part of the New Madrid Seismic Zone will be recorded digitally. The seismic data are also recorded on 16mm film and on a PDP 11/34 digital computer. Since the initial deployment of seismograph stations in July, 1974 1967 earthquakes have been located through the end of July, 1983. These earthquakes are plotted with sizes scaled to magnitude in the attached figure. The earthquakes include not only those located by the SLU network, but also those locted by the TEIC, University of Kentucky and University of Michigan networks. The regional data base is not yet complete. The locations of all contributing stations are also plotted. Operation, analysis and publication of quarterly bulletins are an ongoing task. Cooperative arrangements with other organizations, such as the Tennessee Earthquake Information Center and the University of Kentucky, have been made in order to make the quarterly published Central Mississippi Valley Seismic Bulletin as complete as possible.

2. The implementation of advanced analysis tools on the PDP 11/70 and improved detection codes on the PDP 11/34 is progressing. A technique for guaranteeing long triggers has been successfully implemented. We now obtain long triggers for larger events. The technique does not yield long triggers for noise triggers.

Results

1. During the second quarter of 1983, 35 earthquakes have been located, including 1 event with $m_{bLg} > 4.0$.

2. Major research results are listed in the papers below.

Publications

Herrmann, R. B. and A. Kijko (1983). Short period Lg magnitudes: Instrument, attenuation and source effects, Bull. Seism. Soc. Am. (in press).

Herrmann, R. B. (1982). The relevance of regional networks for the siting of critical facilities, Earthquake Notes 53, 37-48.

Stauder, W. et al (1982). Central Mississippi Valley Earthquakes - 1980, Earthquake Notes 53, 53-56.

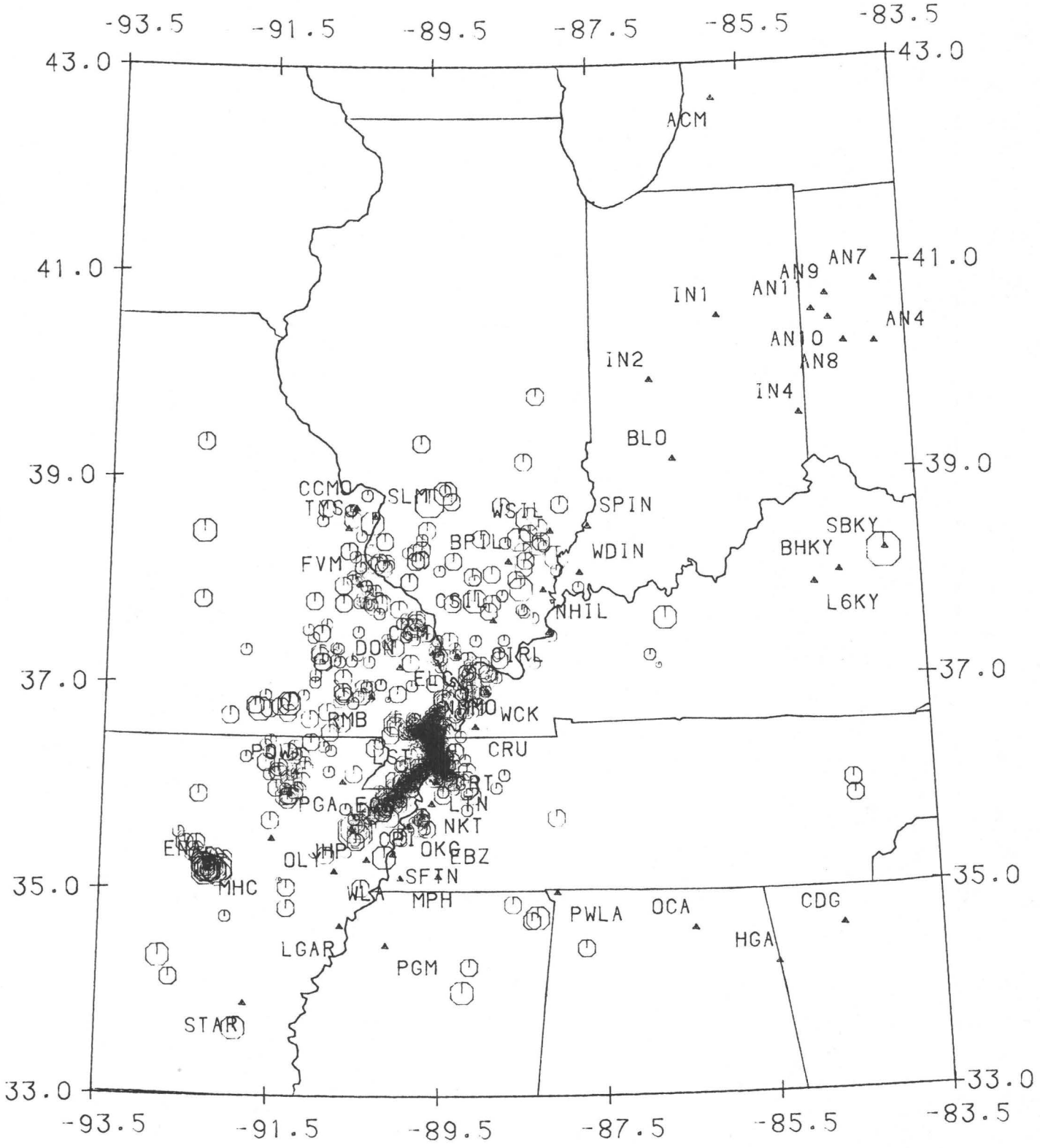
-93.5
-91.5
-89.5
-87.5
-85.5
-83.5
43.0
41.0
39.0
37.0
35.0
33.0
ACM
AN7
AN9
AN1
IN1
AN4
AN10
AN8
IN2
IN4
BLO
SPIN
SBKY
BHKY
L6KY
WDIN
NHIL
CCMO
SLM
WSIL
BPLO
FVM
DON
CIRL
RMB
WCK
CRU
LIN
NKT
OKG
EBZ
SFIN
MPH
OLY
JHP
MHC
WLA
LGAR
PGM
STAR
PWLA
OCA
HGA
CDG

Earthquake Hazard Studies near Charleston, South Carolina

Contract No. 14-08-0001-21334

Pradeep Talwani
Geology Department
University of South Carolina
Columbia, S.C. 29208
(803) 777-6449

Investigations

1. Search for paleoliquefaction sites near Charleston, S.C., to try and establish recurrence rates of large earthquakes.

2. Evaluation of releveling data near Charleston, S.C.

3. Detailed gravity surveys in the South Carolina Coastal Plain.

Results

1. The site of a sand blow associated with the 1886 Charleston earthquake was discovered near Ravenel, S.C. (approximately 30 km SW of Charleston). A series of trenches (Fig. 1) were excavated on June 28, 1983 to reveal this sand blow. The ejected sands crosscut approximately 6.5 ft of unconsolidated Pleistocene sediments. The source unit is composed of well-sorted, fine grained orthoquartzite, which lies below the water table (at a depth of about 6 ft below the ground surface in summer, and less than 2 ft in winter). The sand was extruded in dikes varying in thickness from about 1" to 9" over the main vent. About 300 ft of trench faces were mapped and logs prepared to determine the spatial and stratigraphic relationships. Extensive sampling was carried out to obtain materials for age dating and other analyses. Additionally, eleven power-auger holes were put down in order to map the extent and geometry of the source unit and the depth to the Pleistocene-Pliocene unconformity. The source sand was found to lie at a depth of 7.5 ft below the ground surface and was about 9 ft thick. Figure 2 shows a trench wall map of face CC'. Surficial soil clasts slumped into the clean sand attesting to its fluid state during injection. The extent of the sand blow is shown in Figure 1. On the surface the thickness of the sand blow below the blow layer varies from about 9" in the middle to about 2" on the periphery.

No obvious older sand blow feature was found in the trenches.

2. Interpretation of instrumentally recorded recent seismicity led to the discovery of the Ashley River fault (ARF, Fig. 3), Talwani (1982). The earthquake activity is associated with a shallow (4-7 km), NW striking reverse fault with the SW side upthrown. Shallow (to 500 ft) stratigraphic data by Colquhoun also defined this fault near the surface. However, the stratigraphic data indicated that in the Cenozoic period the

SW side of ARF was downthrown. To resolve the discrepancy, releveling data in the area were analyzed. Figure 4 shows the location of portions of first order leveling lines in the area. The Columbia-Lane-Charleston line and the Savannah-Yemassee-Charleston line have a tie point at F67. The two most recent dates of leveling on each of these lines are 1960/61 and 1979; and 1960 and 1974, respectively. To compare the two lines, elevation change rates were computed.

Preliminary results show a general subsidence of 2 mm/year near Lane increasing to about 4 mm/year near F67. This increase in subsidence rate towards the Atlantic coast has been noted by earlier workers in various locations on the Atlantic seaboard. However to the west of the tie point, on crossing the Ashley River and approximately to the Edisto River - Greenpond area, there is a marked decrease in subsidence rate. This anomalous decrease in subsidence (or relative uplift) is supportive of the uplift inferred from fault plane solutions. It is also in accordance with uplift inferred from geomorphic data. Shallow subsurface geology has revealed that the Edisto River used to flow to the SE towards the Ashley River as recently as about 120,000 years, and it changed its course to the south possibly due to uplift in the region between the rivers. Thus the preliminary releveling data are supportive of earlier inferences of a local uplift in the area - possibly causing the seismicity near Charleston.

3. Interpretation of the aeromagnetic data to the NW of the Ashley River fault (ARF) suggests the presence of a NW trending block in the Coastal Plain. The SW side of this block appears (in the aeromagnetic data) to be collinear with ARF. To determine the reality of this observation and the depth extent, etc., detailed gravity survey was carried out in the Coastal Plain, covering an area of 7700 sq km. These data are being analyzed at present.

Reports

Cox, J., and Talwani, P., 1983, Discovery of the first seismically induced paleoliquefaction site near Charleston, South Carolina: Eastern Section Annual Meeting, Seismological Society of America, New Paltz, New York, September 1983.

Talwani, P., 1983, A block tectonics model to explain seismicity in southeastern U.S.: Spring meeting of American Geophysical Union, Baltimore, Maryland, EOS Trans. Am. Geophys. Union 64 (29), p. 466.

References

Talwani, P., 1982, Internally consistent pattern of seismicity near Charleston, South Carolina, Geology, 10 (12), p. 654-658.

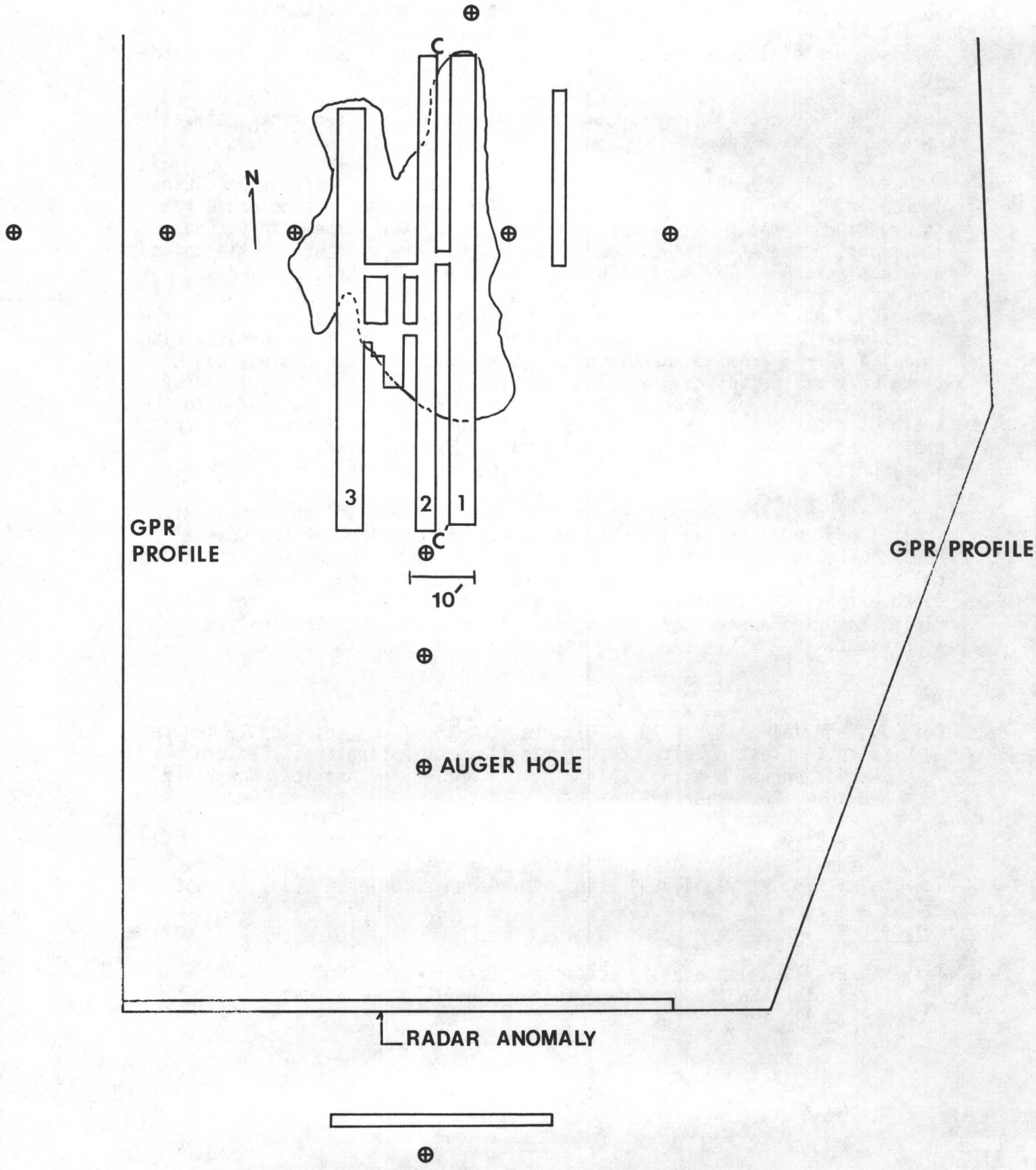

Figure 1. Map view of trenches showing outline of extruded sand.

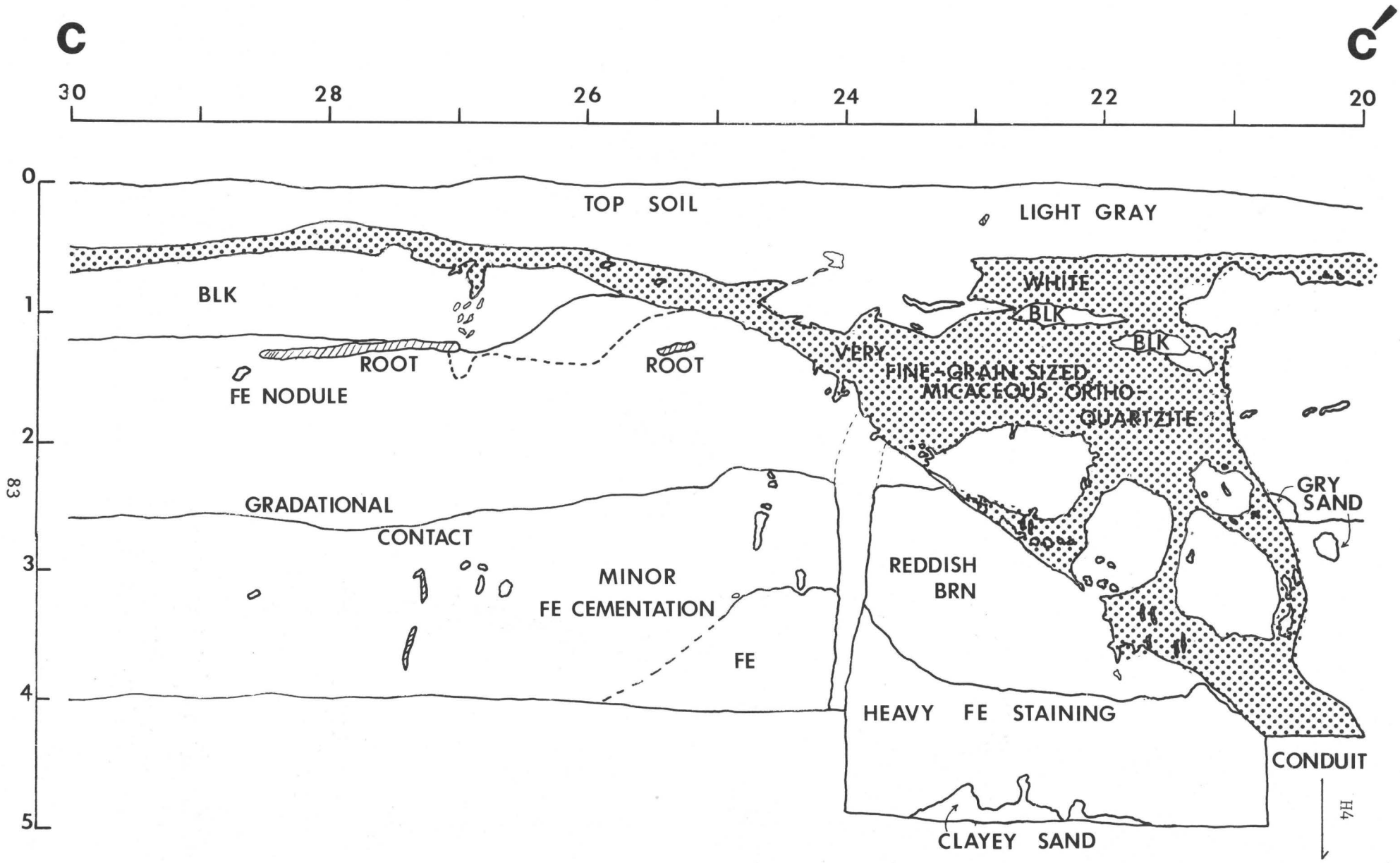

Figure 2. Trench wall map to show the sand blow cutting across shallow sediments.

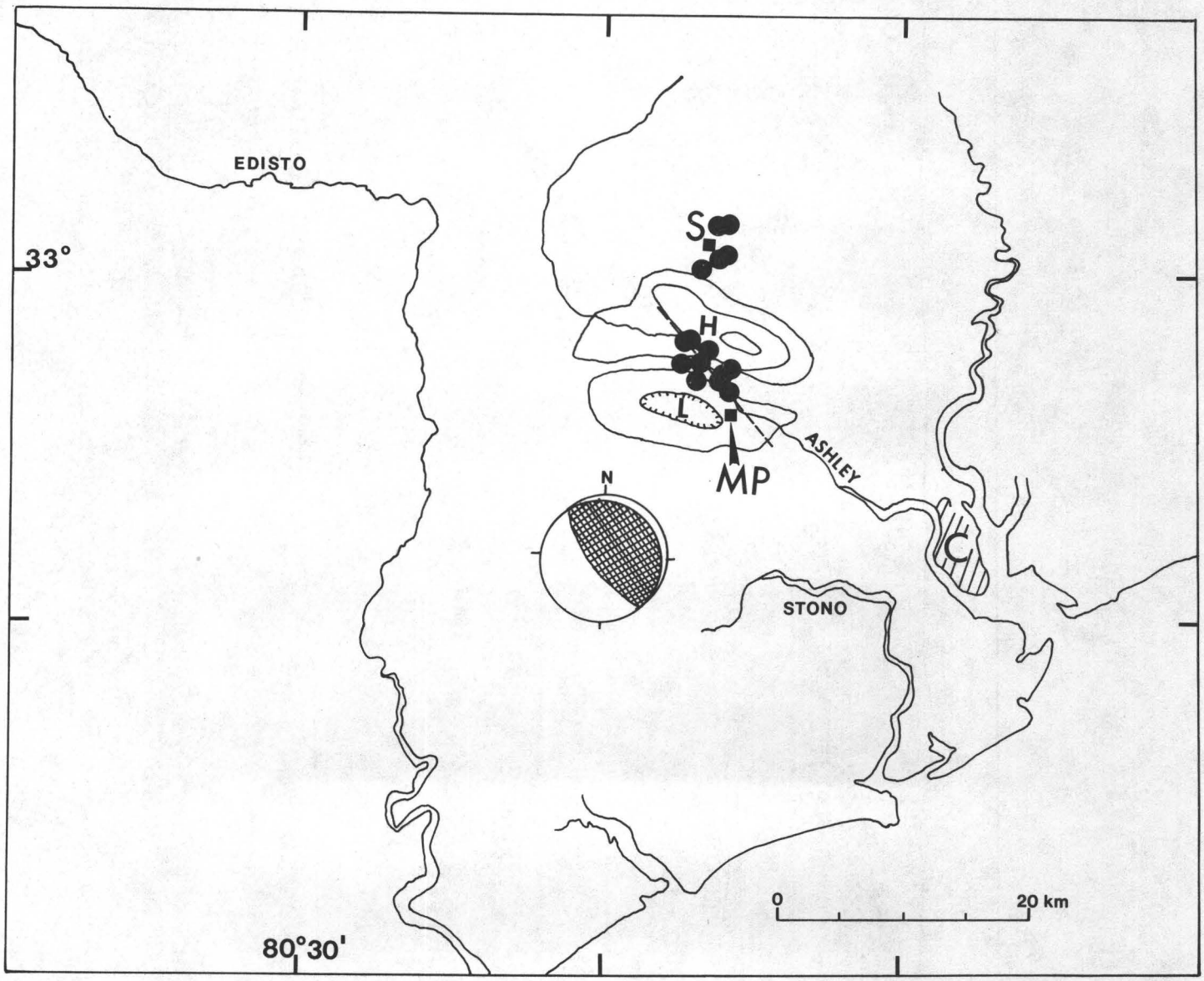

Figure 3. Showing location of Ashley River fault (ARF) (dashed), and shallow (4-7 km) seismicity. The fault is associated with a local aeromagnetic high (H) and low (L). S, C, and MP are Summerville, Charleston, and Middleton Place, respectively.

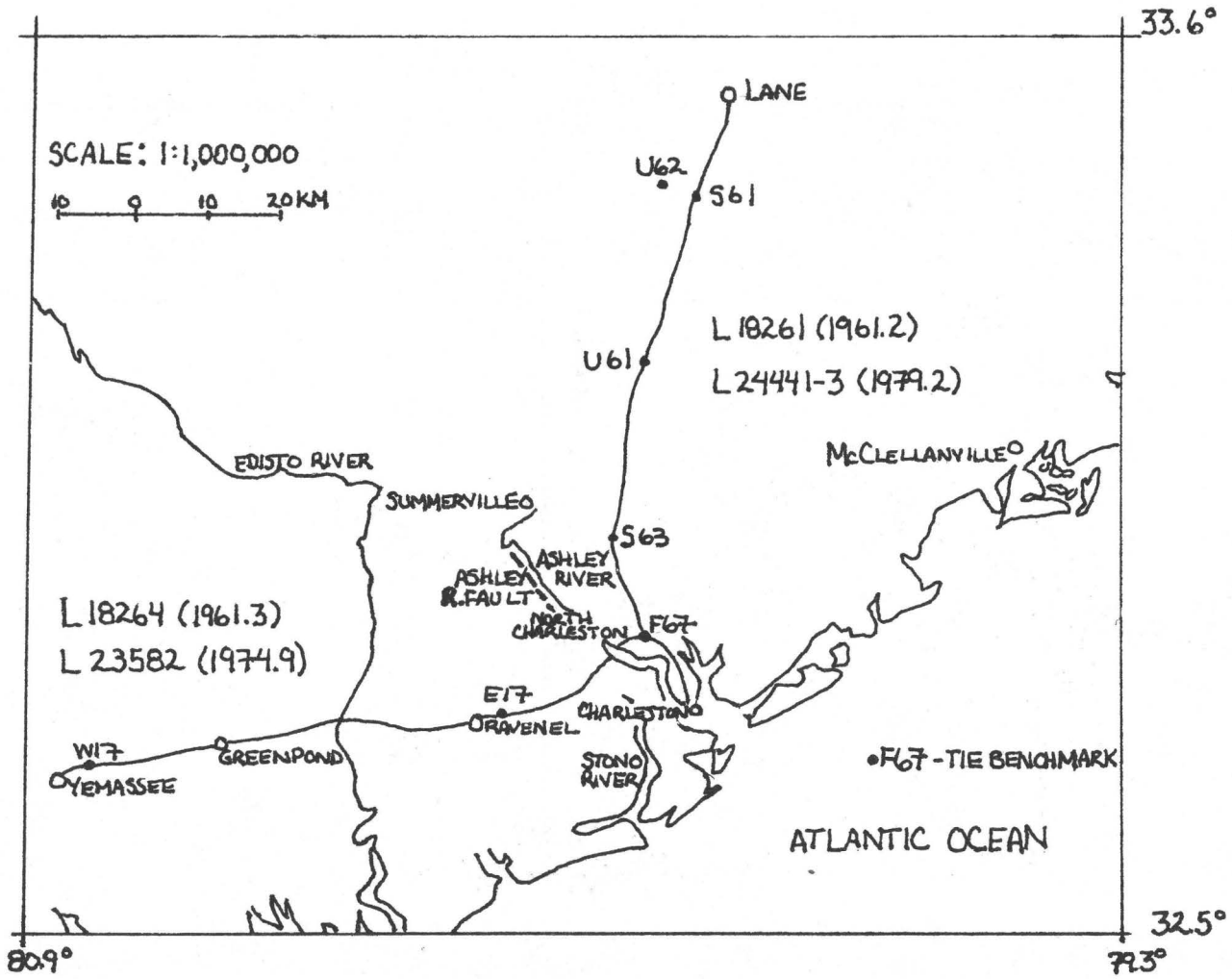

Figure 4. Location of first order leveling lines.

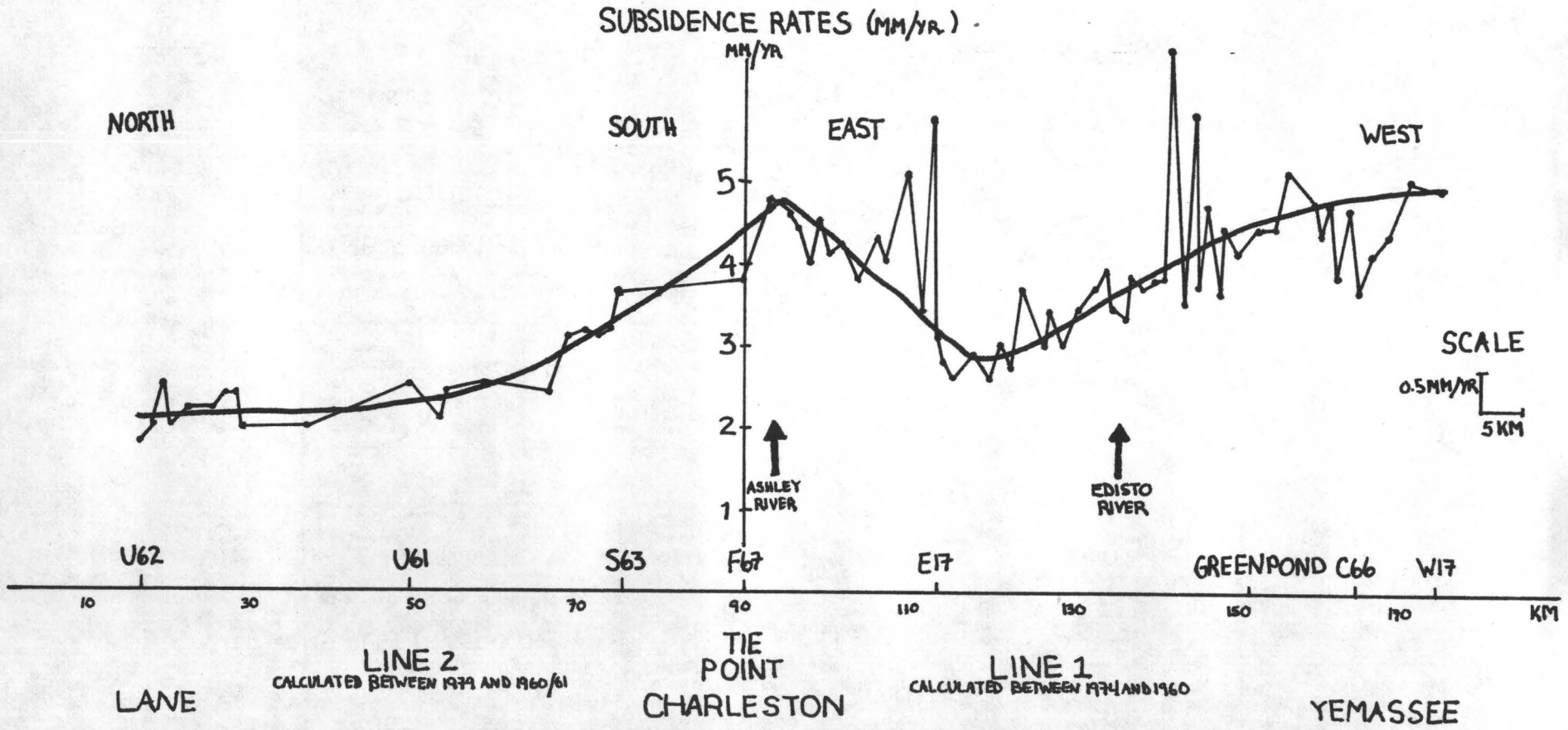

Figure 5. Subsidence rates along leveling lines.

Source Characteristics of Recent Earthquakes in the Northeastern United States - Implications for Earthquake Hazards

Contract No. 14-08-0001-21284

M. Nafi Toksöz and Jay J. Pulli
Earth Resources Laboratory
Massachusetts Institute of Technology
42 Carleton St.
Cambridge, MA 02142
(617) 253-6382

Investigations:

1) Determination of the source mechanism of the January 9, 1982 New Brunswick earthquake.

2) Determination of the source mechanism of the January 19, 1982 Gaza, NH earthquake.

3) Measurement of seismic wave attenuation in the northeastern US using the New Brunswick and New Hampshire earthquakes as sources.

4) Determination of intensity and particle velocity attenuation models for New England using data from the New Brunswick and New Hampshire earthquakes.

5) Comparison of the strong motion records for the Gaza, NH earthquake with the ground motion attenuation models derived for New England.

Results:

1) The source mechanism of the New Brunswick earthquake of January 9, 1982 (m_b=5.7, Ms=4.8) was studied using teleseismic short and long period body waveforms (P and SH) from the GDSN, WWSSN, and Canadian networks[1]. Inversion of the body wave data indicates thrust faulting at a depth of 7 km with nodal planes striking in the N-S direction (strike 3°, dip 34°, rake 95°; see Fig. 1). The seismic moment was 1.5E24 dyne*cm. The source time function has a duration of less than 1 sec and can be resolved only by the short period data. If t*=0.6 sec, then the source time function has a duration of 0.9 sec, and the inferred fault radius is about 2 km with a stress drop between 60 and 120 bars. If t*=1.0 sec, then the source time function has a duration of 0.2 sec with a stress drop as high as 900 bars. A moment tensor inversion was also performed using the amplitude spectra of Rayleigh waves in the period range

between 68 and 26 seconds[2]. The residuals of the inversion plotted as a function of depth indicate a minimum at a depth of 8 km. The resulting moment tensor shows dip-slip faulting with no strike-slip motion. The nodal planes are oriented in a N-S direction and dip at an angle of about 45°. The scalar seismic moment obtained by diagonalizing the moment tensor is 1.1E24 dyne*cm.

2) The Gaza, NH earthquake of January 19, 1982 was of magnitude 4.6 (m_b) and produced intensity V (M.M.) effects in the epicentral area. To locate this earthquake and its aftershocks[3], we chose a subset of the six closest stations which surround the epicenter and used a crustal model developed specifically for this area[4]. The location we have obtained is: lat. 43.52, long. -71.61, depth 3 km. The main shock was then used as a master event for a joint hypocentral location of the aftershocks[3,4]. The five largest aftershocks all fall within an area of 2 km in extent and trending NE. Focal depths of the aftershocks are all less than 2 km. Twenty-four reliable P-wave first motions were used to determine the focal mechanism of the main shock[3]. The fault plane solution shows right-lateral strike-slip faulting (see Fig. 2). The preferred fault plane strikes approximately N20E and dips 80° to the east. The auxiliary plane strikes N100E and dips 75° to the north. Results of the inversion of the teleseismic P-wave at the short period station ANMO indicate a seismic moment of 3E22 dyne*cm and a focal depth of 3.4 km. The source time function is shorter or equal to the resolution limit of the data, which is about 0.2 sec[3].

3) The attenuation of coda waves was measured as a function of frequency using short period digital recordings of the New Brunswick and New Hampshire earthquakes[5]. The frequency band of interest was 0.75 to 10 Hz. Qc was found to obey the relationship

$$Qc(f)=660(f)^{0.40} \qquad (1)$$

in this frequency band.

4) Data from the New Brunswick and New Hampshire earthquakes were used to compute intensity and particle velocity attenuation models for New England[6]. The intensity attenuation model obtained is

$$I(r,m_b)=-1.43+1.79(m_b)-0.0018(r)-1.83[\mathrm{Log}(r)] \qquad (2)$$

where r is the epicentral distance in km (see Fig. 3). Combining this equation with a site intensity - particle velocity correlation for medium sites[8], we obtain the velocity attenuation model

$$\mathrm{Log}[v(r,m_b)]=-2.34+0.739(m_b)-0.001(r)-0.756[\mathrm{Log}(r)] \qquad (3)$$

where v is the peak horizontal velocity in cm/sec (see Fig. 4)

5) Integrated strong motion records from the Gaza, NH earthquake were

used to check the applicability of equation (3) [6,7]. The comparisons are shown in Figure 5. Equation (3) closely predicts the particle velocities observed for the Gaza earthquake at epicentral distances from 7 to 100 km.

Reports:

1. Nabelek, J., Suarez, G., and Toksöz, M.N. (1982), Source parameters of the New Brunswick earthquake of January 9, 1982 from inversion of teleseismic body and surface waves, ***abstract***, *Earthquake Notes*, *53*, No. 3, 28

2. Suarez, G. and Nabelek, J. (1983), The January 9, 1982 New Brunswick earthquake: a moment tensor inversion from the amplitude spectra of Rayleigh waves, presented at the Eastern SSA Meeting, New Paltz, NY, September 19-21

3. Pulli, J.J., Nabelek, J.L., and Sauber, J.M. (1983), Source parameters of the January 19, 1982 Gaza, NH earthquake, presented at the Eastern SSA Meeting, New Paltz, NY, September 19-21

4. Curtin, P.L., Pulli, J.J., and Godkin, C.B. (1983), A new crustal model for central New England - implications for hypocentral calculations and fault plane solutions, presented at the Eastern SSA Meeting, New Paltz, NY, September 19-21

5. Pulli, J.J. (1983), Seismicity, Earthquake Mechanisms, and Seismic Wave Attenuation in the Northeastern United States, *PhD Thesis*, Massachusetts Institute of Technology, 398 pp.

6. Klimkiewicz, G.C. and Pulli, J.J. (1983), Ground motion attenuation models for New England, ***abstract***, *Earthquake Notes*, *54*, No. 1, 10-11

7. Pulli, J.J. and Toksöz, M.N. (1982), Attenuation of strong ground motion in New England, ***abstract***, *Earthquake Notes*, *53*, No.3, 32

Reference:

8. McGuire, R.K. (1977), The use of intensity data in seismic hazard analysis, *Proc. 6th World Conf. on Earthquake Engr.*, New Delhi, vol. 2, 353-358

FIGURE 1

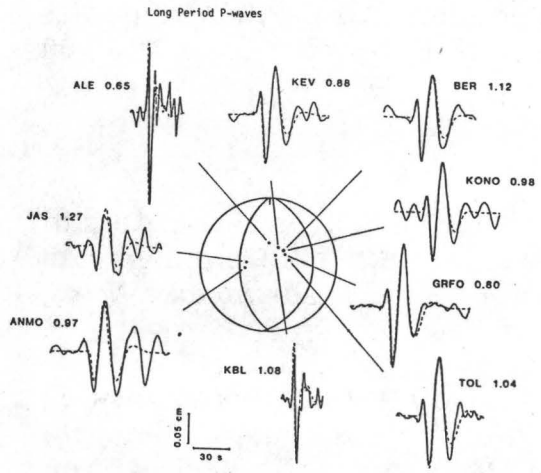

FIGURE 2

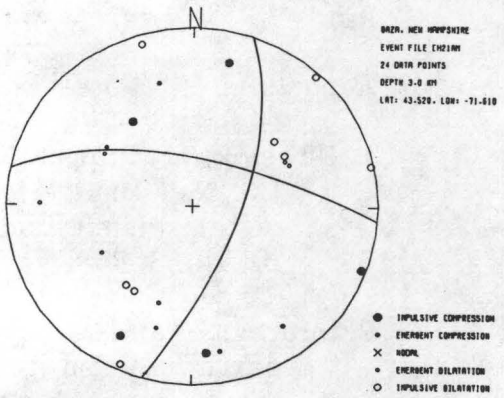

FIGURE 3

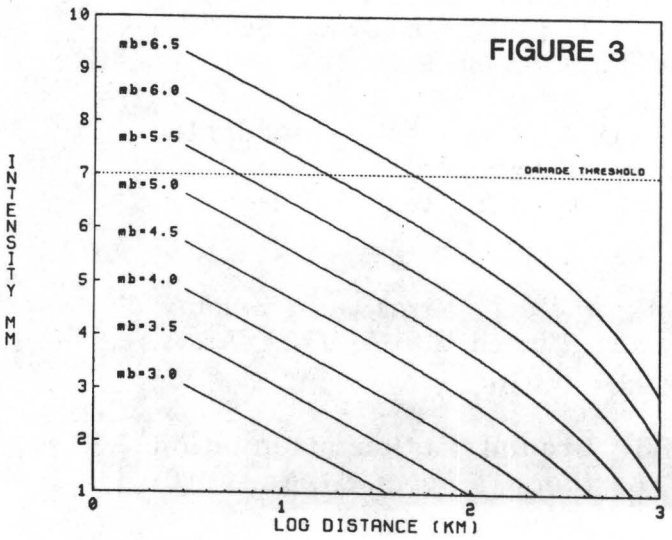

FIGURE 4

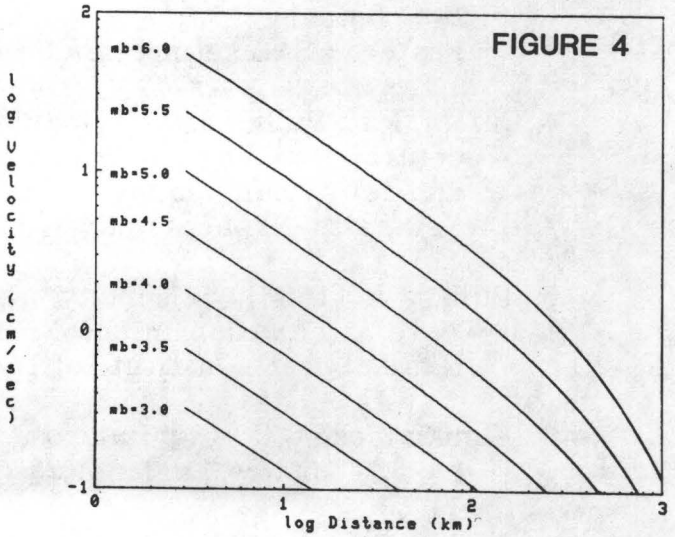

FIGURE 5

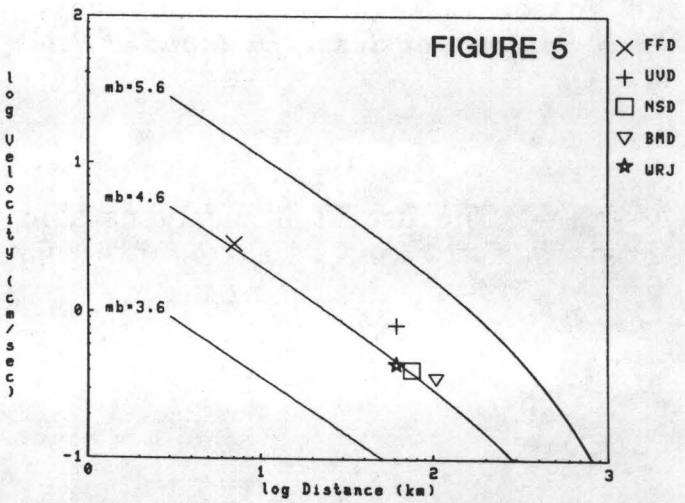

Structural Framework of Eastern United States Seismic Zones

9950-02653

R. L. Wheeler
Branch of Engineering Geology and Tectonics
U.S. Geological Survey
Denver Federal Center, MS 966
Denver, CO 80225
(303) 234-5087

Investigations

The overall project goal is to help provide a geologic basis for hazard evaluation in the East. The justification for a geologic basis is that the record of seismicity is too sparse to characterize hazard by itself. The strategy is to identify types of structures or structural associations that are seismogenic, and to map their areas of occurrence. Work included compilation and interpretation of a map of known continental rifts, grabens, and other extended terranes in the central and southeastern United States, to test the suggested association between damaging seismicity and rifts. See Results and Reports.

Results

A hypothesis offered by several workers to explain the seismicity of the Charleston region is that of seismic reactivation of a large, narrow, northwest-trending weak zone that crosses most or all of South Carolina. The main basis for the hypothesis is the observed alignment of the Blake Spur fracture zone (BSFZ) with the diffuse seismicity of Bollinger's South Carolina-Georgia seismic zone (SCGSZ). All forms of the hypothesis state or assume that the weak zone can be recognized by examination of presently available geological, seismological, and geophysical maps.

New data, analytical results, and interpretations contradict this hypothesis of a narrow weak zone in four ways. (1) Offshore geophysical data provide no evidence that the BSFZ extends closer to land than about 150 km. The most likely landward projection of the BSFZ would intersect the coastline at least 100 km southwest of the Charleston-area seismicity. (2) Despite efforts designed to detect offshore seismicity in the Charleston region, none is known to have occurred since the start of the historical record in 1698. (3) Despite frequent statements that onshore seismicity aligns northwest-southeast across South Carolina, no such alignment has been demonstrated to exist. The various sets of epicentral locations cited as evidence of such an alignment are either too inaccurate to provide objective support for a subjective perception of alignment, distorted by incompleteness and by the probable presence of quarry and highway blasts, or derived from too few independent seismic sources to distinguish the suggested alignment from a random pattern. (4) The known and likely complexities of the geologic evolution of the southeast make

it unlikely that a narrow weak zone could have been preserved across South Carolina, in any form that could be recognized at the present state of geologic mapping and other knowledge.

Reports

Wheeler, R. L., 1983, Earthquake hazard zoning in the central and eastern United States: Improvements based on new geologic foundations [abs.]: Earthquake Notes, v. 54, no. 1, p. 8.

Neotectonics of the North Frontal Fault System of the San Bernardino Mountains, Southern California

Contract No. 14-08-0001-19754

Clarence R. Allen and Kristian E. Meisling
Seismological Laboratory, California Institute of Technology
Pasadena, California 91125 (213-356-6904)

Investigations and results

This project is now completed, and following is the abstract of the Final Technical Report.

The north frontal fault system of the San Bernardino Mountains is made up of a number of disparate structural elements, each of which accommodates range-front deformation in a manner dictated by its geometry. A two-stage history of late Cenozoic structural development is proposed for the northwestern San Bernardino Mountains: the range was first uplifted on low-angle structures and later modified by high-angle faulting. Evidence for Pliocene onset of deformation and uplift in the westernmost San Bernardino Mountains is found in the provenance and character of the associated sediments.

Thrusting uplifted the northern range front during a pulse of deformation spanning late Pliocene through middle Pleistocene time. Uplift in the westernmost San Bernardino Mountains was accomplished contemporaneously by tilting, warping, and arching. Nature and timing of deformation were consistent with the hypothesized formation of a transpressional welt across the San Andreas fault, which may have affected both the San Bernardino and San Gabriel Mountains.

High-angle faulting replaced thrusting and warping as the dominant style of deformation in the northwestern San Bernardino Mountains beginning in middle to late Pleistocene time. Pleistocene left-lateral faulting in the westernmost San Bernardino Mountains has accomplished north-south crustal shortening by squeezing the San Bernardino block eastward. Northwest-trending right-lateral faults, characteristic of the Mojave block prior to range-front uplift, have reasserted and incorporated themselves in the complex zone of range-front deformation. Local extension resulting in minor graben formation appears to have been associated with lateral motion on the north frontal fault zone in Fifteenmile Valley (Sky Hi Ranch fault zone) and the Cleghorn fault zone.

Arcuate patterns of faulting in the western San Bernardino Mountains can be explained in terms of the pattern of faulting predicted for secondary faults near the end of a strike-slip fault. In this case the "end effect" would be produced by a change in the slip rate on the San Andreas fault in Cajon Pass, possibly related to motion on the San Jacinto fault. All faulting in the study area is interpreted as the product of compression across the San Andreas fault.

A weathered erosion surface was developed on the crystalline terrane over most of the area in response to humid conditions during the late Mio-

cene(?), at which time the region was characterized by an upland surface of subdued relief. This weathered erosion surface is a useful index to structural deformation in the northwestern San Bernardino Mountains.

Late Cenozoic stratigraphy constrains the timing of deformation and uplift in the northwestern San Bernardino Mountains. The late Miocene to Pliocene(?) Crowder Formation was deposited by drainages carrying distinctive volcanic and metamorphic clasts from the Victorville area southward, across the site of the western San Bernardino Mountains. The late Miocene beds of the Punchbowl Formation are faulted against the lower Crowder Formation, but are overlain by the upper Crowder Formation. The Punchbowl and Crowder Formations share the same age and paleocurrent direction, yet differ markedly in sediment character and provenance. The relationship between these two units remains an unsolved stratigraphic problem, which seemingly requires substantial lateral structural translation.

The middle to late Pliocene onset of deformation and uplift is recorded in the stratigraphic sequence by the appearance of fine-grained sediments, new clast lithologies, and northerly paleocurrent directions. The volcanogenic eastern facies of the Crowder(?) Formation is believed to be a syntectonic deposit indicative of ponding that accompanied the reveral in drainage direction brought on by incipient uplift of the western San Bernardino Mountains. The fine grained, lacustrine character of the Harold Formation can be interpreted in the same way; the base of the Harold Formation is <2.75 my old on the basis of paleomagnetic constraints. The Old Woman Sandstone in Lucerne Valley records an abrupt change from fine-grained sediments indicative of incipient uplift to coarse, angular debris signalling the emergence of the range front as a topographic element. The influx of range-front debris is estimated to have occurred <2.5 my ago. Several small, deformed patches of fine-grained sediment in Arrastre Canyon appear to be of similar origin.

The Quaternary stratigraphy of the western San Bernardino Mountains is dominated by the Harold Formation, Shoemaker Gravel, and Older Alluvium, which underlie the Victorville Fan. These units were shed northeast off the San Gabriel and western San Bernardino Mountains, and record their uplift. The Harold Formation contains the earliest appearance of San Gabriel Mountains crystalline basement lithology within the stratigraphy of the Mojave block. The Victorville Fan sequence is believed to be time-transgressive, reflecting the northwestward movement of the San Gabriel Mountains crystalline terrane along the San Andreas fault.

The Older Alluvium capping the Shoemaker Gravel in Cajon Pass records the Brunhes/Matuyama polarity reversal of 730,000 y B.P. The Older Alluvium can be divided into dissected and undissected facies believed to predate and postdate the polarity transition respectively. This crude chronology can be extended to sediments on the flanks of the Ord Mountains that define a late Pleistocene drainage system tributary to the ancestral Mojave River. The Pleistocene units contain evidence of progressive growth and integration of drainage in the western San Bernardino Mountains in response to uplift during Pleistocene time.

Detailed geologic mapping in the northwestern San Bernardino Mountains permits slip rates and offsets to be calculated for important range-front faults. The Cleghorn fault has a cumulative left-lateral offset of 3.5 to 4.0 kilometers, and a slip rate of about 3.0 mm/yr. The Sky Hi Ranch fault zone

has a late Pleistocene right-lateral offset of approximately 0.5 kilometers, with a slip-rate on the order of 1 mm/yr. The faults along the west flank of the Ord Mountains have a vertical slip-rate of less than 1 mm/yr.

The Cleghorn fault is classified as "active," under the criteria set forth by the State of California in the Alquist-Priolo Act of 1972, and is considered capable of a M_s 6.8 earthquake. Parts of the north frontal fault system on the west flank of the Ord Mountains and the Sky High Ranch fault zone are classified as "potentially active," in the terminology of the Alquist-Priolo Act, and are thought to be capable of a M_s 6.6 to 6.8 event. The Tunnel Ridge lineament and Arrastre Canyon Narrows fault zones are considered tentatively active, and should be examined in detail prior to development of adjoining areas. Clearly, the San Andreas fault poses the greatest seismic hazard to the communities in the study area.

Publications and Reports

Meisling, K. E., 1983, Neotectonics of the north frontal fault system of the San Bernardino Mountains, southern California: Cajon Pass to Lucerne Valley: Unpub. Ph.D. thesis, California Institute of Technology, 394 p.

Meisling, K. E., and Weldon, R. J., 1982, The late-Cenozoic structure and stratigraphy of the western San Bernardino Mountains: Geologic Excursions in the Transverse Ranges, Geol. Soc. America, Cordilleran Sect., 78th Ann. Mtg., Guidebook, p. 75-81.

Meisling, K. E., and Weldon, R. J., 1982, Slip-rate, offset and history of the Cleghorn fault, western San Bernardino Mountains, southern California [abstract]: Geol. Soc. America Abstracts with Programs, v. 14, p. 215.

Weldon, R. J., and Meisling, K. E., 1982, Late Cenozoic tectonics in the western San Bernardino Mts; Implications for the uplift and offset of the central Transverse Ranges [abstract]: Geol. Soc. America Abstracts with Programs, v. 14, p. 243.

Weldon, R. J., Meisling, K. E., Allen, C. R., and Sieh, K. E., 1981, Neotectonics of the Silverwood Lake area: Unpub. Rept. to California Dept. Water Resources, 22 p., 11 figs., 1 map.

Regional and Local Hazards Mapping in the Eastern Great Basin

9950-01738

R. E. Anderson
Branch of Engineering Geology and Tectonics
U.S. Geological Survey
Denver Federal Center, MS 966
Denver, CO 80225
(303) 234-5109

Investigations

1. Collect, process, and interpret high-resolution seismic reflection profiles across selected faults in the eastern Great Basin (S. T. Harding and A. J. Crone).

2. Study fault scarps in the Sevier Desert basin near the Drum Mountains (A. J. Crone).

3. Study paleostress in central Utah using fault-slip data collected from exposed faults (R. E. Anderson).

Results

1. The second phase of continuing efforts to collect high-resolution seismic reflection profiles across young scarps in Utah yielded data across (1) the East Bench fault in Salt Lake City, (2) the Wasatch fault near Hobble Creek, Mona, and Nephi, and (3) along a line extending from an existing high-resolution profile near Clear Lake in the Sevier Desert basin. The 1.5-km-long line across the East Bench fault was run along Interstate 80 and demonstrates the exciting capability of effectively operating the high-resolution system in a culturally noisy urban environment. Preliminary interpretation of the profile shows reflectors at 60- to 180-m depth with apparent down-to-the west normal fault offsets and an associated antithetic offset in the vicinity of the East Bench fault. The estimated vertical displacement across the entire zone is about 46 m. A 4.2-km-long east-west line through the town of Nephi shows several prominent breaks in shallow reflectors (60-120 m) in the basin-fill sediments west of the Wasatch Front. East of the mountain front, the profile shows a set of shallow (60-m), subhorizontal reflectors in Salt Creek Canyon. These subhorizontal reflectors are paradoxical because exposed bedrock along that part of the profile is highly distorted and steep dips are common. Brute stacks of data from the Hobble Creek and Mona sites contain strong shallow reflections but the data is insufficiently processed to permit any interpretations.

2. In conjunction with landform modification studies being conducted by Hanks and others, a 69-m-long trench was excavated across a fault scarp with a surface offset of 7.2 m and the adjacent antithetic fault. The trench reveals a stratigraphic throw of 6.8 m on the main fault and 1.1 m on the antithetic fault. The scarp profile indicates that the scarp is the result of a single surface-faulting event. The stratigraphy of the post-

faulting colluvial deposits show that most, if not all, of the present scarp topography is the product of a single, large, surface-faulting event. However, near the base of the colluvial wedge, a decrease in cobble and boulder content, slight changes in apparent dips of bedding, and a subtle increase in the degree of induration all suggest the possibility of an early, small surface-faulting event.

3. Fault-slip data were collected from several major faults in the transition zone between the Colorado Plateau and Basin and Range provinces near Richfield, Utah, including: (1) the Teasdale and Thousand Lakes faults in Emery County, (2) the Paradise fault in Wayne County, and (3) several major faults including the Sevier fault and faults that cross Salina Canyon in Sevier County. The area is of special interest because focal mechanisms determined from microseismicity studies are dominated by strike slip whereas previously available geologic data would predict dip-slip fault events. The youngest displacements on the Paradise fault, the faults that cross Salina Canyon, and graben-bounding faults in the Pavant Range appear to be mainly dip slip consistent with the regional geology. Some faults west of the townsite of Sevier are predominantly strike slip consistent with the seismicity. Many other faults, including the Sevier and Thousand Lakes faults, appear to be capable of strike-slip, or dip-slip displacements. This study represents the first known documentation of major strike-slip faulting in the area. Additional field studies are planned.

Reports

Anderson, R. E., 1983, Cenozoic structural history of selected areas in the eastern Great Basin, Nevada-Utah: U.S. Geological Survey Open-File Report 83-504, 47 p.

Anderson, R. E., Zoback, M. L., and Thompson, G. A., 1983, Implications of selected subsurface data on the structural form and evolution of some basins in the northern Basin and Range province, Nevada and Utah: Geological Society of America Bulletin, v. 94, p. 1055-1072.

Crone, A. J., and Harding, S. T., High-resolution reflection profiles in the Sevier Desert basin, western Utah--Application to earthquake studies: submitted to Geology.

Zoback, M. L., 1983, Structure and Cenozoic tectonism along the Wasatch fault zone, Utah: Geological Society of America Memoir 157, p. 3-27.

Surface Faulting Studies

M. G. Bonilla
Branch of Engineering Seismology and Geology
U. S. Geological Survey
345 Middlefield Road, MS-77
Menlo Park, California 94025
(415) 323-8111, ext. 2245

Investigations

The investigations were focused on the study of: (a) statistical data related to surface faulting, in collaboration with J. J. Lienkaemper and R. K. Mark, and (b) the appearance of active faults in exploratory trenches.

Results

A manuscript titled "Statistical relations among earthquake magnitude, surface rupture length, and surface fault displacement" was prepared by Bonilla, Mark, and Lienkaemper and is being revised after technical review. Leinkaemper is revising his manuscript on magnitude of the earthquakes associated with the surface faulting.

Data on more than 100 trench exposures across active faults were compiled in preliminary form. A computer program was developed to interactively tabulate the data. Analysis of the data will provide quantitative guidelines on the effect that material penetrated and amount of fault displacement can have on our ability to recognize faults in trenches and to date fault displacements.

Reports

None.

Fault Activity and Recurrence Intervals, Whittier Fault, Los Angeles Basin

Contract No. 14-08-0001-21368

L. R. Cann and F. B. Leighton
Leighton and Associates, Inc.
1151 Duryea Avenue
Irvine, California 92714
(714) 556-1421

Investigations

The proposed objectives of this investigation are:

1. Selection and logging of fault trenches on the Whittier fault segment west of Brea Canyon.

2. Obtain more definitive data that might be applied to analysis of recurrence intervals along the Whittier fault.

3. Improve the technique and tools used for estimating earthquake recurrence intervals on the Whittier fault.

4. Expand the data base on the characteristics of surface faulting, including the distribution of slip in time and space, in relation to the size, depth and tectonic setting of associated earthquakes.

5. Estimate quantitatively the frequency of occurrence and maximum magnitude of potential earthquakes on the Whittier fault.

Results

No results were available for publication at the date of submittal of this summary.

Late Quaternary Slip Rates on Active Faults of California

9910-03554

Malcolm M. Clark
Branch of Engineering Seismology and Geology
345 Middlefield Road, MS 77
Menlo Park, CA 94025
(415) 323-8111, ext. 2591

Investigations

1. Compile a table and map (1:1,000,000) of late Quaternary slip rates for faults of California from published and unpublished data. The following USGS geologists act as evaluators and compilers for specific regions: north Coast Ranges, J. J. Lienkaemper, K. R. Lajoie, M. J. Rymer; south Coast Ranges, K. R. Lajoie, K. K. Harms, J. D. Sims, J. A. Perkins; Transverse Ranges and L.A. Basin, J. I. Ziony, A. M. Sarna-Wojcicki, J. C. Matti, J. C. Tinsley; Peninsular Ranges, J. I. Ziony; Salton Trough, R. V. Sharp; Mojave Desert, Great Basin, and eastern Sierra Nevada, M. M. Clark; Cascade-Modoc Plateau, K. K. Harms, and D. S. Harwood. Edited by K. K. Harms, J. J. Lienkaemper, M. M. Clark, and J. I. Ziony.

2. Search out and record surface ruptures associated with the M 6.5 Coalinga, California, earthquake of May 2, 1983, and its aftershocks. Place monuments along Nunez fault to record subsequent slip and creep. Initiate investigation of late Quaternary displacement along the Nunez fault using trenches, geologic mapping, and geomorphic analysis (M. J. Rymer, K. K. Harms, M. M. Clark, J. J. Lienkaemper).

3. Determine age of five nested fluvial terraces of Tres Pinos Creek at Calaveras fault, south of Hollister, California. Formation of these terraces is related to lateral and vertical displacement along the Calaveras fault. The investigation concentrates on detailed soil descriptions and analyses, plus ^{14}C dating, and will yield late Quaternary slip rates. The resulting dated soil sequence will also be useful in other slip-rate studies nearby and in the San Francisco Bay region. T. C. Hanks and R. E. Wallace will investigate the relation of inter-terrace scarp profiles to scarp age at this site (J. W. Harden, K. K. Harms, S. N. Hoose, M. M. Clark).

Results

1. Evaluation of more than 160 determinations from geologic evidence of late Quaternary slip rate for faults in California indicates relatively consistent values for a given style of faulting within major structural-physiographic provinces but distinctly different values between some provinces. The table below summarizes the range of late Quaternary slip rates for major faults of different tectonic style within each province. These rates were either calculated or compiled by U.S. Geological Survey geologists from published and unpublished data of varying reliability. Although slip rates for many late Quaternary faults have not yet been accurately determined, the rates obtained suggest that

regional differences are real. The San Andreas fault is listed separately from the provinces it passes through.

RANGE OF SLIP RATE (mm/yr)

	DOMINANT STYLE FOR FAULTS MEASURED			
PROVINCE	RIGHT LATERAL	LEFT LATERAL	REVERSE	NORMAL
Coast Ranges----------	1-10	--	0.2-2	--
Transverse Ranges-------	--	0.5-2	0.5-6	0.3-2.4
Peninsular Ranges-------	1->12	--	0.5-1	?
Salton Trough----------	2-20	--	--	--
Mojave Desert----------	?	1-10	--	0.001-.006
Western Sierra Nevada---	--	--	?	0.005
Great Basin/E. S. Nev.--	1-2	--	--	0.1-2.5
Cascade-Modoc----------	--	--	--	0.5
San Andreas fault-------	10-50	--	--	--

2. (See R. V. Sharp, this volume, about immediate post-earthquake investigation).

A 3.3 km right-reverse surface rupture was mapped by Michael Rymer, Katherine Harms, and Malcolm Clark along the newly named Nunez fault, which is located about 12 km northwest of Coalinga and 14 km west of the May 2, 1983 M = 6.5 mainshock of the Coalinga sequence. The surface rupture formed at the time of a shallow M = 5.2 aftershock approximately 40 days after the mainshock. Four later aftershocks increased the displacement and extended this rupture southward. Releveling of arrays along the north half of the Nunez faulta after the M = 6, July 22 aftershock showed renewed slip at different localities in inverse porportion to initial slip at each locality. The largest change was 3 cm vertically and 2 cm horizontally near the north end of the rupture. The Nunez fault trends north-south and dips 65° east; in contrast, faults inferred to be active during the mainshock, have northwest-southeast trends, but were not associated with ground rupture.

The June 11, surface faulting involved two N-S echelon segments separated by a right step of 0.3 km. Sense of movement along the north half of the surface rupture is dominantly reverse, east side relatively up. A right-lateral component, minor in the north half of the rupture, becomes

dominant in the south half. Maximum measured reverse and right-lateral components of 1983 slip measured in the fault plane in the north half are 66 and 20 cm, respectively, and in the south half 8 and 11 cm, respectively. Only the southern third of the fault was identified before these earthquakes, and the fault was not known to have Holocene activity. Exposures in streams and a roadcut show offsets of strata greater than those of 1983 along both segments of the fault, indicating that all of the new faulting was along pre-existing traces. Strata are offset vertically from prehistoric slip events at least 24 m about 0.3 km from the north end of the fault.

3. In September 1983 several soil pits were excavated 4-5 m deep in each of the four oldest terraces of Tres Pinos Creek that lie northeast of the Calaveras fault and in three terraces that lie southwest of the fault. The pits yielded charcoal specimens for ^{14}C dating and revealed measurable changes with age in soil properties. Qualitative preliminary assessment of degree of soil development suggests that the next-to-oldest terrace northeast of the fault is more than 100,000 years old. Soil development on terraces on both sides of the fault also suggests significant uplift on the southwest side of the fault at this location.

Reports

Clark, M. M., Harms, K. K., Lienkaemper, J. J., Perkins, J. A., Rymer, M. J., Sharp, R. V., 1983, The May 2, 1983, Earthquake at Coalinga, California: The search for surface faulting, in R. D. Borcherdt, compiler, The Coalinga earthquake sequence commencing May 2, 1983: U.S. Geological Survey Open-File Report 83-571, p. 8-11.

Holocene Behavior of the Hayward-Calaveras Fault System, San Francisco Bay Area, California

20555

W. R. Cotton, N. T. Hall, and E. A. Hay
Foothill-DeAnza Community College District
Los Altos Hills, California 94022
(415) 948-8590

Investigation

The intention of this program was to locate and evaluate sites along the Hayward and Calaveras faults that contain detailed, decipherable, and datable Holocene records of slip.

Results

1. The initial phase of the investigation was to conduct a systematic analysis of historic information pertaining to seismic events on the Hayward and Calaveras faults. All available surface and subsurface records from previous investigations were compiled, and in conjunction with detailed photo reconnaissance, several sites were selected for field evaluation.

2. Two sites for trenching were selected on the Calaveras fault. Both locations, one east of Leavesly Rd. in Gilroy, and the other near San Felipe Lake and Highway 152, were selected because they met the technical criteria we developed to recognize a site with high research potential, and also because they could be positioned to intersect known surface ruptures created during the 1979 Coyote Lake earthquakes. Several excavations at each site failed to reveal data useful in establishing discrete slip events, or slip-rates.

3. One trenching site was selected on the creeping segment of the Hayward fault. It is located just south of the Fremont Civic Center. The master trace of the fault was a well-defined meter-wide zone in the subsurface, and the characteristic "left-stepping" surface ruptures that are commonly seen along right-lateral-slip creeping fault zones could be traced downward into this zone. The strike of the Hayward fault at this locality is about N30W, yet the splays that rise from this trend rotate in a clockwise direction as they propagate upward. Their strikes vary considerably, but typically they range between N10E and N40E, with dips between 80° and vertical (see attached figures of the fault zone shown in both map view and structure section view). This pattern of clockwise rotated tensional rupture splays near a master trace (along which horizontal shears produce the dominant strain) may be an important indicator of creep along a strike-slip fault. The zone of en echelon tensional fractures is also marked by a downward penetration of dark soil materials into the underlying sediments at the fault.

No evidence of discrete or multiple seismic events were seen at this site, and no radiocarbon determinations were conducted.

Reports

Hay, E. A., Hall. N. T., and Cotton, W. R., 1983, Evidence for Non-1906-Like Earthquakes on the San Andreas Fault, Dogtown, California: Association of Engineering Geologists, Abstracts and Program, p. 73.

Hay, E. A., Hall, N. T., and Cotton, W. R., 1983, The Pleito Fault: Late Neogene Activity: Guidebook of the Transverse Ranges, California (Don Fife, Editor), South Coast Geological Society, 5 pages, in press.

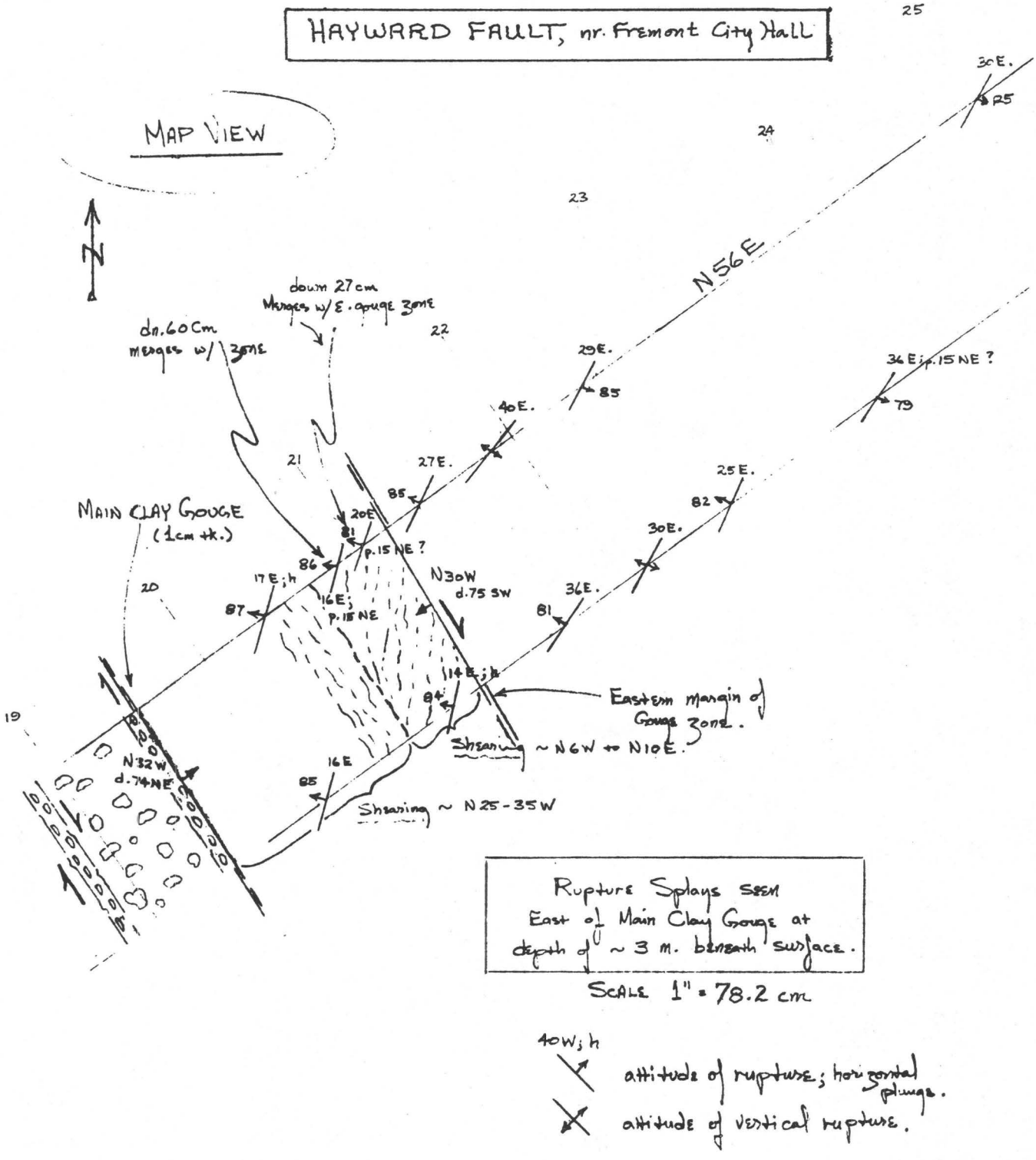
HAYWARD FAULT, nr. Fremont City Hall
MAP VIEW
N
down 27cm
Merges w/ E. gouge zone
dn. 60 cm
merges w/ zone
MAIN CLAY GOUGE
(1cm th.)
N56E
30E.
R5
29E.
85
36E; p.15 NE ?
79
40E.
27E.
85
25E.
82
30E.
36E.
81
20E
81
p.15 NE ?
86
17E; h
87
16E;
p.15 NE
N30W
d.75 SW
14E; h
84
Eastern margin of
Gouge Zone.
Shearing ~ N6W to N10E.
16E
85
Shearing ~ N25-35W
N32W
d.74NE
21
22
23
24
25
20
19
Rupture Splays seen
East of Main Clay Gouge at
depth of ~ 3 m. beneath surface.
SCALE 1" = 78.2 cm
40W; h
attitude of rupture; horizontal plunge.
attitude of vertical rupture.

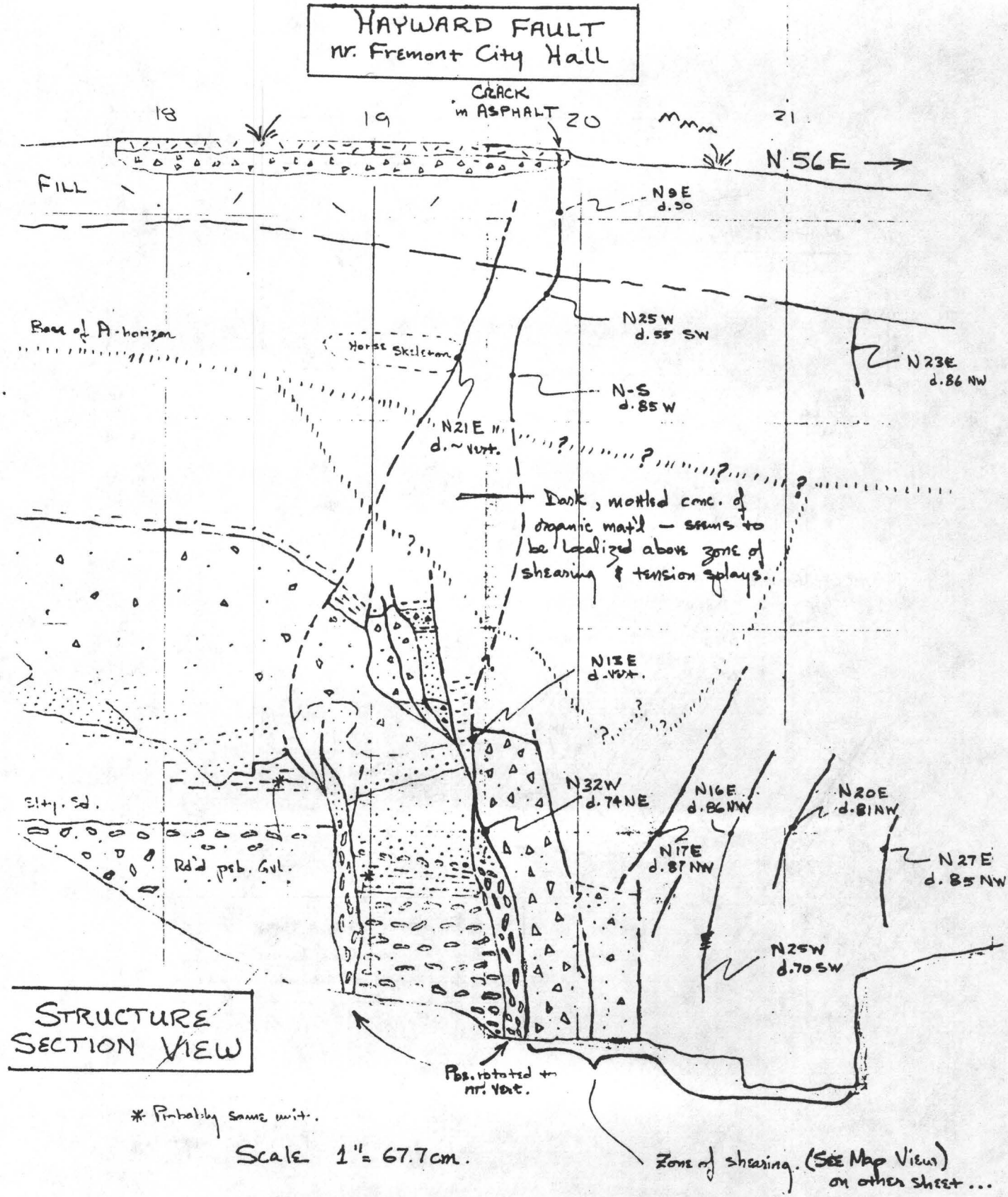
HAYWARD FAULT
nr. Fremont City Hall
CRACK in ASPHALT
18
19
20
21
N56E
FILL
N9E d.90
Base of A-horizon
Horse skeleton
N25W d.55 SW
N23E d.86 NW
N-S d.85 W
N21E ± d.~vert.
Dark, mottled conc. of organic mat'l — seems to be localized above zone of shearing & tension splays.
N13E d.vert.
N32W d.74NE
N16E d.86NW
N20E d.81NW
N17E d.87NW
N27E d.85NW
N25W d.70SW
Silty Sd.
Rd'd peb. Gvl.
STRUCTURE SECTION VIEW
Pebs. rotated to nr. vert.
* Probably same unit.
Scale 1" = 67.7cm.
Zone of shearing. (SEE Map View) on other sheet...

Holocene Styles of Surface Faulting Along the Creeping Segment of the San Andreas Fault, San Juan Bautista to Cholame, California

21335

W. R. Cotton, N. T. Hall, and E. A. Hay
Foothill-DeAnza Community College District
Los Altos Hills, California 94022

Investigation

This project is designed to recognize and evaluate localities along the creeping segment of the San Andreas fault capable of yielding information about 1) characteristics of the style of rupturing in a creeping segment (as opposed to locked segments), 2) slip rates for creep that extend back into pre-historic time, and 3) recurrence interval determinations if discrete rupture events are recognizable.

Results

1. The initial phase of this investigation was to conduct a systematic analysis of the USGS detailed mapping between San Juan Bautista and Cholame, and to augment this review by aerial photographic reconnaissance. Several sites were then selected for field evaluation.

2. The major site selected for subsurface investigation was on the ranch of Fred Flook located at the northwestern end of Bitterwater Valley east of King City. The trenching was conducted at a site between a Foothill College monument array and USGS creepmeters which currently are indicating minimum creep rates of 27-29 mm/yr. Here the active trace of the San Andreas fault is marked by a broad linear trench or swale which stretches across a Holocene alluvial fan. Thalwegs of buried channels which cross the creeping zone reveal that a 10 meter-wide shallow graben coincident with the surface trough has developed along the creeping zone. The vertical component of subsurface deformation (as seen in older sedimentary layers) is greater than that seen in the topography.

3. Five horizons that potentially are able to yield creep-rate determinations were recognized at the Flook Ranch site. A fence, the banks of a modern stream valley, and three different stream channels exposed in the subsurface all lend themselves to this task. The fence was constructed in 1908± (Brown and Wallace 1968) and its offset yields an average creep rate of 35 mm/yr. since then. The modern stream banks are offset a minimum of 11 feet, and there is basis for suggesting that the gullying process that created them began in the year 1885 (Leopold and Miller, 1956). If this is the case, the average creep rate since then has been 34 mm/yr. Three paleostream channels, located by extensive

trenching, are shown as A-A', A-A", and B-B' on the accompanying trench location map of the Flook Ranch site. A-A' is offset approximately 20 feet, B-B' approximately 30 feet, and A-A" approximately 90 feet. Eight charcoal samples have been submitted for age determinations using conventional radiocarbon techniques, and several very small specimens will be evaluated in the near future using the recently developed accelerator technique. It is our hope to extend creep-rate estimates back several hundreds of years once these determinations are received.

4. Two trenches were excavated at a site on the San Andreas fault near Cholame Creek, just north of Highway 46. Although ruptures were recognized in the subsurface, the location was abandoned for lack of relationships capable of establishing discrete slip events or slip-rates.

References

Brown, R. D., Jr., and Wallace, R. E., 1968, Current and historic fault movement along the San Andreas fault between Paicines and Camp Dix, California: Proceedings of Conference on Geologic Problems of San Andreas Fault System (Wm. R. Dickinson and A. Grantz, Editors, p. 22-41).

Leopold, L. B., and Miller, J. P., 1956, Ephemeral streams-hydraulic factors and their relation to the drainage net: USGS Prof. Paper 282-A, 36 pp.

Reports

Hay, E. A., Hall, N. T., and Cotton, W. R., 1983, Evidence for Non-1906-Like Earthquakes on the San Andreas Fault, Dogtown, California: Association of Engineering Geologists, Abstracts and Program, p. 73.

Hay, E. A., Hall, N. T., and Cotton, W. R., 1983, The Pleito Fault: Late Neogene Activity: Guidebook of the Transverse Ranges, California (Don Fife, Editor), South Coast Geological Society, 5 pages, in press.

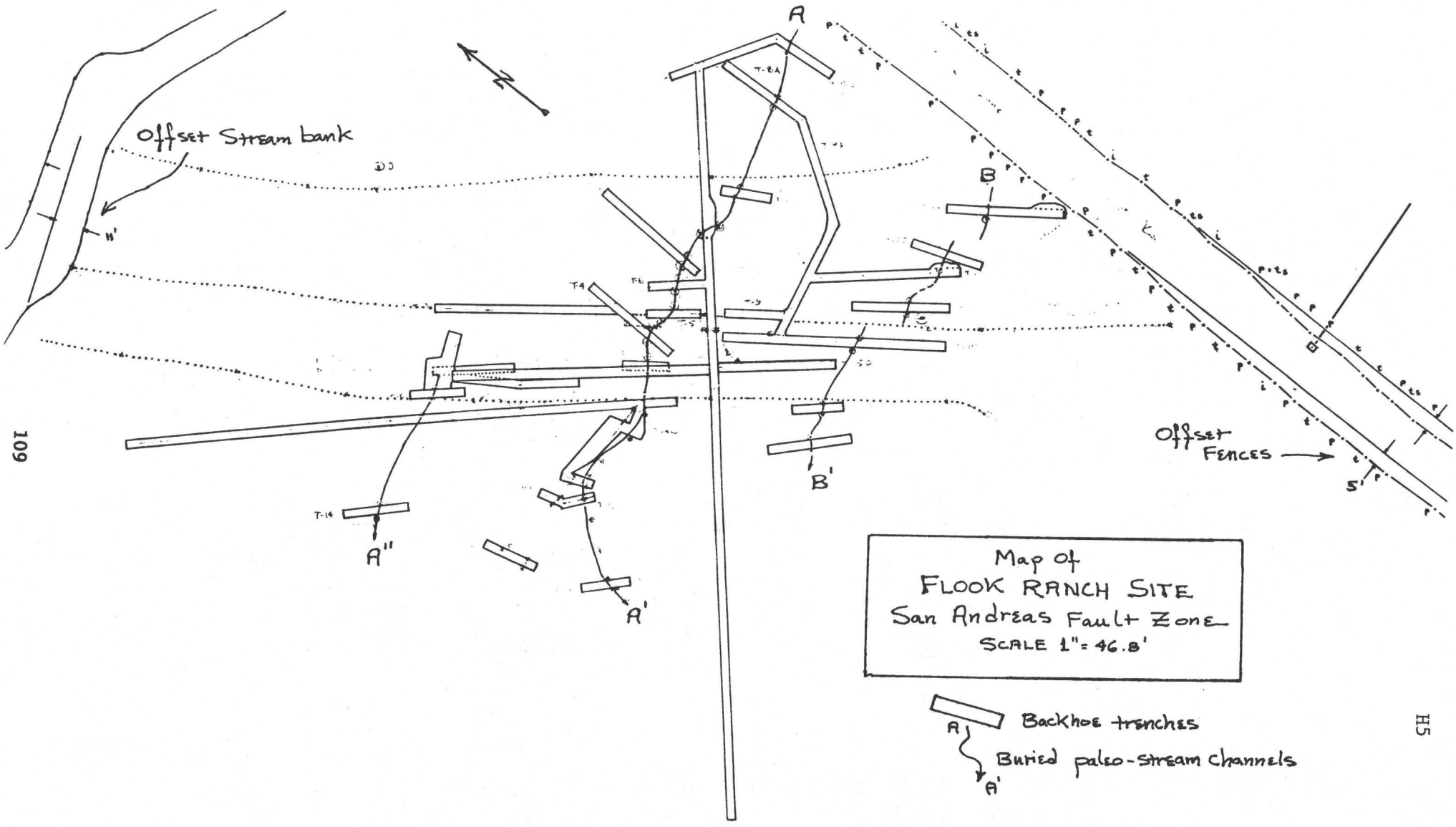
A
B
B'
A''
A'
Offset Stream bank
Offset Fences
N
Map of
FLOOK RANCH SITE
San Andreas Fault Zone
SCALE 1" = 46.8'
Backhoe trenches
Buried paleo-stream channels

PALOS VERDES FAULT ZONE
EARTHQUAKE POTENTIAL AND SURFACE FAULTING

14-08-0001-21304

P.D. Guptill and S.T. Freeman
Woodward-Clyde Consultants
203 North Golden Circle Drive
Santa Ana, California 92705
(714) 835-6886

Investigations

Field studies of the Palos Verdes fault and related secondary faulting on the Palos Verdes Peninsula are in progress. The object of the field studies is to locate fault traces and evaluate offsets of late Quaternary geologic units. The methods being used include describing the youngest marine terraces, drilling and sampling, and trenching across fault traces.

Results

1. Sets of aerial photographs from 1929, 1945 and 1979 have been analized for geomorphic forms related to faulting. Two suspected fault traces have been identified and transferred to the 1979 aerial photographs and onto topographic maps. One fault trace is believed to be that of the Palos Verdes fault, the other to an antithetic fault south of the Palos Verdes fault.

2. Late Pleistocene marine deposits have been located and sampled from two locations along the northeast side of the Palos Verdes Hills. At one location in the Chandler Sand Pit, the youngest terrace is offset by minor secondary faulting and is tilted toward the northeast at approximately 15 to 18 degrees. Three borings have been drilled north of the Chandler Pit through the youngest terrace to test for continuity across the Palos Verdes fault trace and to locate the fault. Additional borings are planned to continue searching for the presence or absence of a major offset in the marine deposits.

3. Trenching is planned for late 1983 and early 1984 once final sites have been selected.

Detailed Analysis of 1906 Faulting in Marin County, California

21242

N. T. Hall, W. R. Cotton, and E. A. Hay

Foothill-DeAnza Community College District
El Monte Road, Los Altos Hills, California 94022
(415) 948-8590

Investigation

The investigation is being focused on a 12 kilometer segment of the 1906 trace of the San Andreas fault. The research area lies between the Marin County localities of Dogtown and the Vedanta Retreat, and is an area where Holocene activity along the fault has occurred in a narrow zone. The investigation is designed to produce a set of detailed geologic and geomorphic maps of the seismotectonic features. This information will be augmented by the rich historic record of the 1906 faulting that was compiled by G. K. Gilbert shortly after the 1906 earthquake.

Results

1. The initial phase of the investigation has been completed. This work included collecting and compiling topographic and geologic base maps and reports. Aerial photographs have been flown along the entire segment of the fault from Bolinas Lagoon to Tomales Bay. The photographs were flown at a scale of 1:4,800 and 1:2,400 and were both black and white and colored transparency images. The timing of the photographs was in mid-April in order to delineate any moisture-controlled vegetation that might be related to recent faulting. A total of 110 new stereoscopic photographs were flown for the project. The photographs are being used to make detailed photogeologic/geomorphic strip maps along the 1906 trace.

2. It is the intention of this investigation to undertake a thorough search for trenching sites with a decipherable paleoseismic record in the San Andreas rift valley of Marin County. We will prepare large-scale (1" = 500', C.I. = 10') topographic base maps of selected portions of the rift valley between Dogtown and the Vedanta Retreat area that are underlain by Holocene deposits. Data plotted on these maps will include the location of (1) the traces active in 1906; (2) additional traces active in Late Quaternary time; (3) camera stations for Gilbert's 1906-7 photographs and other historic data; (4) significant geomorphic features; and (5) Holocene deposits cut or bounded by active fault traces. We will evaluate and rank the potential of each site of Holocene deposits for containing an event-by-event record of pre-1906 movements on the San Andreas fault.

Reports

Hay, E. A., Hall, N. T., and Cotton, W. R., 1983, Evidence for Non-1906-Like Earthquakes on the San Andreas Fault, Dogtown, California: Association of Engineering Geologists, Abstracts and Program, p. 73.

Hay, E. A., Hall, N. T., and Cotton, W. R., 1983, The Pleito Fault: Late Neogene Activity: Guidebook of the Transverse Ranges, California (Don Fife, Editor), South Coast Geological Society, 5 pages, in press.

Tectonics of Central and Northern California

9910-01290

William P. Irwin
Branch of Engineering Seismology and Geology
U. S. Geological Survey
345 Middlefield Road, MS 77
Menlo Park, CA 94025
415 323-8111, ext. 2065

Investigations

1. Relations between seismicity and crustal out-gassing of carbon dioxide: collaboration with Ivan Barnes.

2. Paleomagnetic study of Permian and younger strata of the Eastern Klamath terrane: collaboration with E. A. Mankinen and C. S. Gromme.

3. Tectonic accretion of terranes of northern California: collaboration with C. D. Blome, M. C. Blake, and J. P. Albers.

Results

Tectonic analysis of the Klamath Mountains has included a study of the distribution of the granitoid plutonic rocks in terms of the allochthonous terrane concept. Published isotopic ages are available for most of the major plutons. These ages, when analyzed in context with various tectonic aspects of the region, suggest that the plutons tend to be arranged in numerous belts (Fig. 1). The postulated plutonic belts generally follow the trend of the various terranes of the Klamath Mountains province, but most are not clearly continuous throughout the length of a given terrane. The trend of the plutonic belts in the NE part of the province is NE-SW, virtually at right angles to the NW-SE trend of the belts in the SW part of the province (Fig. 1). This change in trend occurs across a vaguely defined NW-trending zone, and is accompanied by other changes in the plutonic belts as well as by major changes in other regional geologic features.

The plutonic belts range in age from Ordovician to Early Cretaceous. Those of Paleozoic age (Alpine gabbro, Skookum Gulch, Mule Mountain, and McCloud belts) are all included in the Eastern Klamath terrane. To the west the belts are Jurassic and Cretaceous in age and, with some exceptions, are successively younger oceanward. However, the youngest plutonic belt (Shasta Bally) is mostly in the Eastern Klamath terrane and partly overprints the oldest plutonic belt (Alpine gabbro).

Some of the plutonic belts are thought to have formed in island arcs, perhaps quite distant from the North American continent. These are similar in age and composition to the volcanic strata of their host terrane and form comagmatic pairs (McCloud belt-Dekkas Andesite, Mule Mountain stock-Balaklala

Rhyolite, and Ironside Mountain belt-Hayfork Bally Meta-andesite). Except for the McCloud, these belts are thought to have formed before the host terrane accreted to its neighboring terrane. The McCloud is unusual in that it represents a second magmatic cycle in the Eastern Klamath terrane; it is a postaccretion belt in relation to the Devonian suturing of the Central Metamorphic terrane, but is a preaccretion belt in relation to the Jurassic terranes W of the Central Metamorphic terrane.

Other plutonic belts of the province are significantly younger than their host rocks. They are considered to be postaccretion belts in places where some of the plutons crosscut the suture between the host and an adjacent terrane, or where the suture is known to be older than the plutons on the basis of other regional geologic considerations.

Reports

Irwin, W. P., 1983, Review of "Orogeny", Mkiyashiro, A., Aki, K., Sengor, A. M. C., eds., Wiley: Journal Precambrian Research, in press.

Irwin, W. P., 1983, Preaccretion and postaccretion plutonic belts in allochthonous terranes of the Klamath Mountains, California and Oregon: Circum-Pacific Terrane Conference, August 28 - September 2, Stanford University, Stanford, Calif., 3 p. in press.

Irwin, W. P., Mankinen, E. A., and Gromme, C. S., 1983, Paleomagnetism in the Klamath Mountains, California and Oregon: Circum-Pacific Terrane Conference, August 28 - September 2, Stanford University, Stanford, Calif., 4 p. in press.

Blome, C. D., and Irwin, W. P., 1983, Tectonic significance of Late Paleozoic to Jurassic radiolarians from the North Fork terrane, Klamath Mountains, California, in Pre-Jurassic rocks in western North American suspect terranes, Stevens, C. H., ed.: Society of Economic Mineralogists and Paleontologists, Pacific Section, p. 77-89.

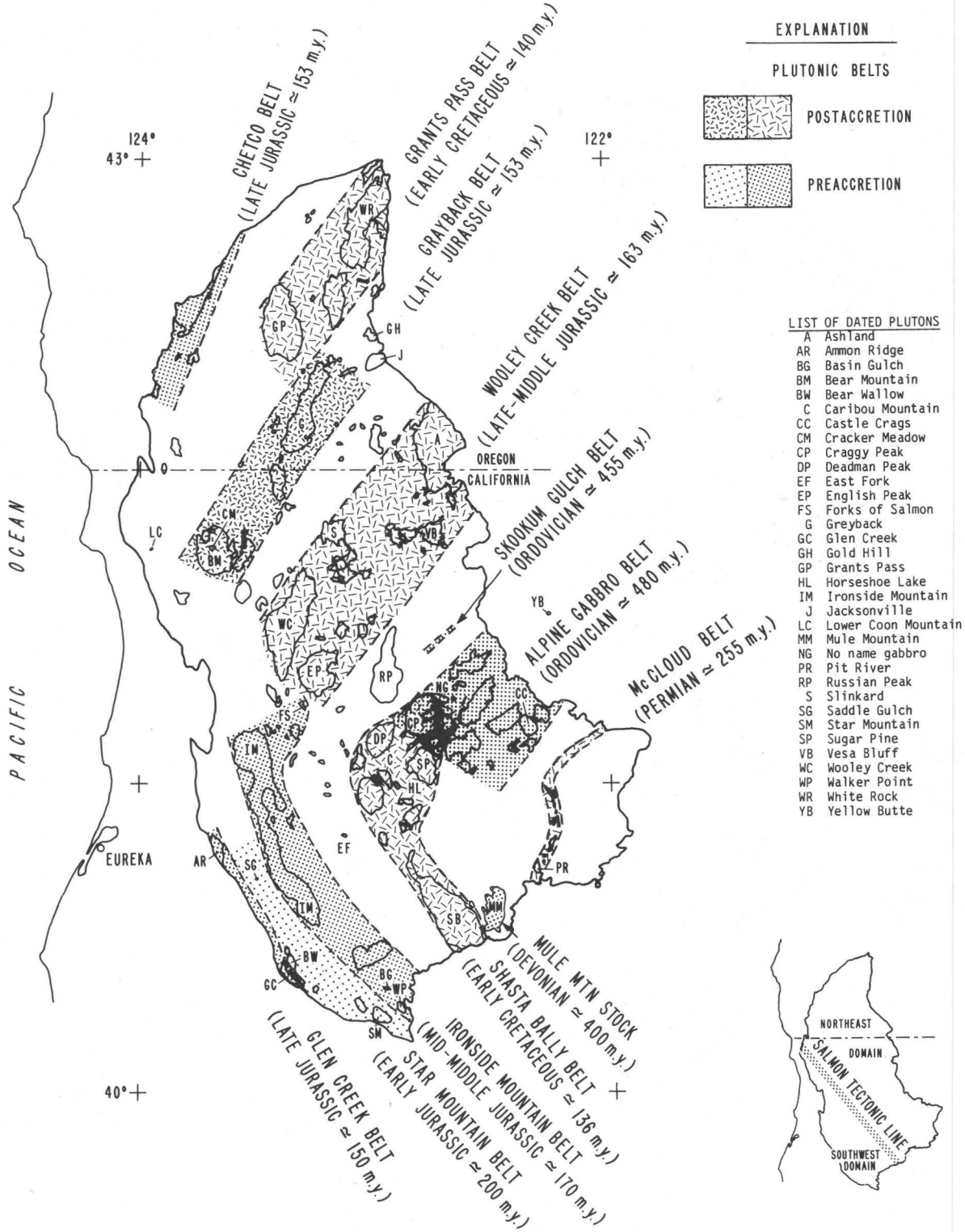

Figure 1 Map of Klamath Moutains province showing outlines of major plutons and the trends of the plutonic belts. Ultramafic ophiolitic rocks are not shown. Letter symbols on map correspond to names in list of dated plutons. The scale of Harland and others (A geologic time scale: London, England, Cambridge University Press, 131 p., 1982) was used for correlating the isotopic ages with geologic time.

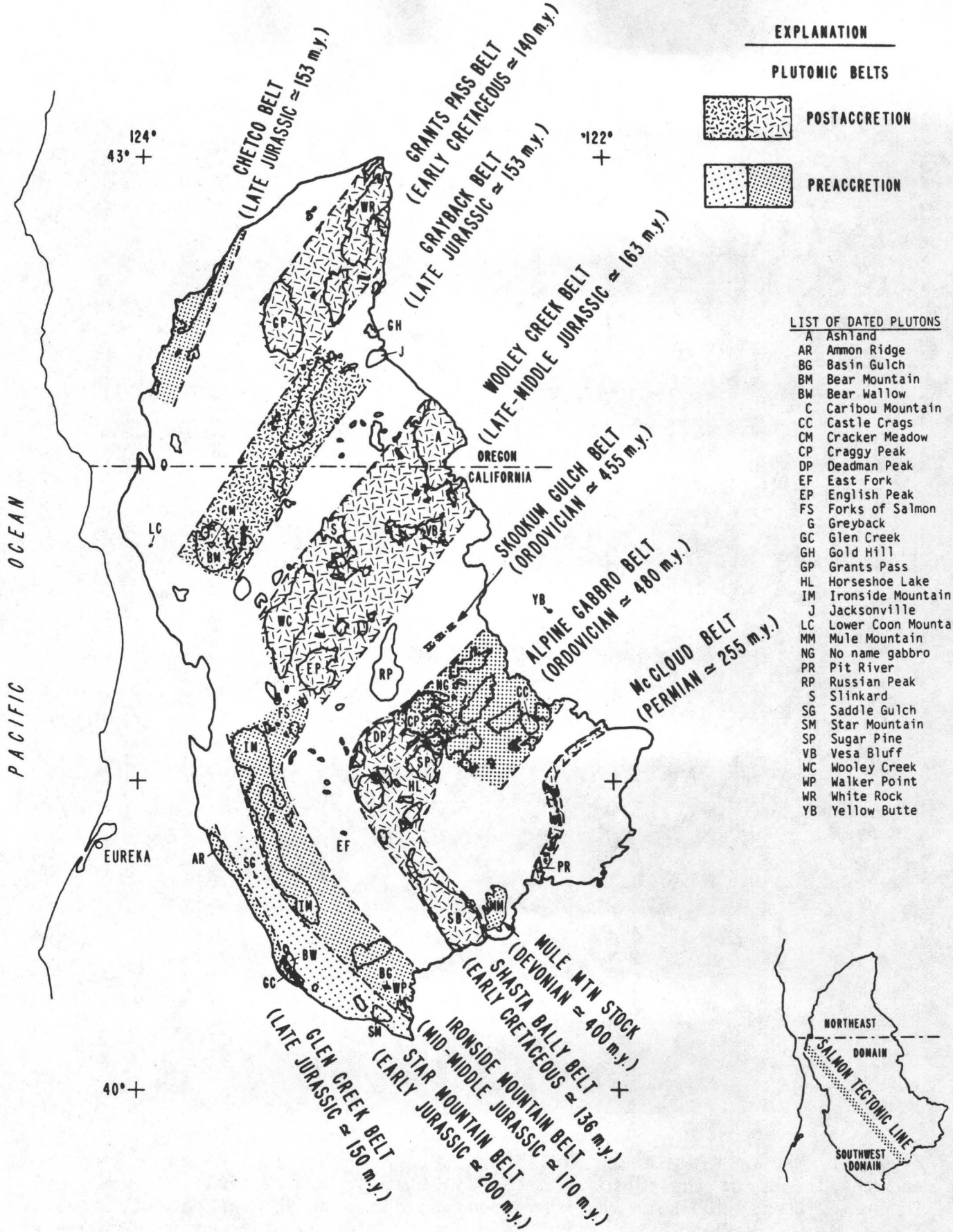

Figure 1 Map of Klamath Moutains province showing outlines of major plutons and the trends of the plutonic belts. Ultramafic ophiolitic rocks are not shown. Letter symbols on map correspond to names in list of dated plutons. The scale of Harland and others (A geologic time scale: London, England, Cambridge University Press, 131 p., 1982) was used for correlating the isotopic ages with geologic time.

Coastal Tectonics, Western U.S.

9940-01623

Kenneth R. Lajoie
Branch of Engineering Seismology and Geology
U.S. Geological Survey
345 Middlefield Road, M/S 77
Menlo Park, CA 94025
(415) 323-8111, ext. 2642

Investigations

1. The objectives of this project are to determine patterns and rates of Quaternary crustal deformation and ground response in the coastal area of the western United States by mapping and dating marine terraces and associated marine and alluvial deposits, and evaluating geotechnical data from marine and alluvial deposits in deep sedimentary basins.

Project personnel are Dan Ponti, Scott Mathieson and Patricia McCrory.

Results

1. Sea cliff erosion caused by heavy winter storms exposed new Holocene fault traces in the San Gregorio fault zone south of Año Nuevo (San Mateo County, CA). A marine wave-cut platform (105 ka?) and overlying Holocene alluvial sediments and soils are displaced across these traces. The lack of precise stratigraphic correlation in the alluvial sediments across the fault trace indicates lateral displacement prevailed. Data from the new traces agree with data from previously mapped Holocene traces in the fault zone.

2. With Gerald Weber (Santa Cruz), Charles Repenning (USGS) and Steve Robinson (USGS) dated peaty beds interbedded with dune deposits recently exposed by wave erosion in the west-shore cliffs of Año Nuevo (San Mateo County, CA). The ^{14}C dates, which range from 0-29 ka B.P., help provide age control for Holocene faults in this area.

3. Sea cliff erosion along the San Mateo coast during heavy winter storms (1982/1983) was controlled by tectonic setting. In tectonically depressed areas where unconsolidated alluvium and marine terrace deposits are exposed to wave attack near sea level, cliff erosion was the most severe.

4. With Yoko Ota (Yokohama National University) and Kelvin Berryman (New Zealand Geological Survey) collected marine shells from recently exposed wave-cut platforms of emergent Holocene terraces at Big Flat in northern California near the Mendocino triple junction. Radiocarbon dates (Steve Robinson, USGS) agree with ages of these terraces derived solely by graphical methods using an assumed Holocene sea level curve. This agreement indicates this assumed datum is correct and that several dated samples from emergent beach ridges are reworked. The derived uplift rate is 4.0 m/ka, at least one order of magnitude higher than uplift rates for most of the California coast.

5. Attended Penrose (Winnemucca, Nevada) and GSA Meeting (Salt Lake City, Utah).

A. Observations and dates of the most prominent high shorelines in the Bonneville and Lahonton Basins confirm my previous correlation of the features with the 13-12 ka shoreline in Mono Basin, CA. These shorelines provide a precise datum for assessing tectonic and isostatic movements of the earth's crust throughout the Great Basin. All appear to have been formed during a true late Pleistocene Pluvial event in the Great Basin.

B. Ron Spencer (Calgary) confirmed a suspected correlation of a thin tephra layer in a core from Great Salt Lake with tephra bed 15 in the Wilson Creek beds of Mono Basin, CA dated at about 28 ka B.P. A wood sample just below the tephra layer in the core yields a ^{14}C age of 29 ka B.P., which agrees well with the dates (Lajoie, Robison) from Mono Basin.

6. With Joe Liddicoat (New York) and Steve Lund (USC) initiated a detailed paleomagnetic study of the Wilson Creek beds in Mono Basin, CA. Initial results by Lund from the south shore of Mono Lake yield a complete secular variation curve for the upper part of the Wilson Creek beds that matches the curve from similar-aged deposits in the eastern United States. This curve can be used to assess the amount of section missing from the slightly disturbed type section of the Wilson Creek beds on the northwest shore of the lake.

7. With Dan Ponti, mapped and sampled steeply dipping marine terrace deposits on the northwest side of the Palos Verdes Peninsula (south of the Palos Verdes fault) in Los Angeles Co., CA. If borings penetrate these deposits north of the fault, the age and displacement rate of the fault can be determined.

8. Attended International Symposium on Coastal Evolution in the Holocene in Tokyo, Japan.

A. No Holocene eustatic sea level curve presented at this conference had significant oscillations over the past 6-5 ka B.P. The assumed curve used on the west coast of the United States as a tectonic datum is probably correct.

B. Data presented by S. Kaizuka (Tokyo) documents an uplift rate of 20 cm/yr over the past 800 years for the volcanic island of Iwo Jima. Uplift of this terraced island has been steady, not episodic; the terraces are cut by storms, not formed by coseismic uplift events. These data indicate that it is incorrect to assume that all steps on emergent Holocene terraces represent major earthquakes. The numerous steps on the emergent Holocene terraces at Ocean House and Big Flat (northern California), and at Ventura (southern California) probably represent both storm and coseismic events.

Reports

Hanks, T. C., Bucknam, R. C., Lajoie, K. R., and Wallace, R. E., 1983, Modification of Wave-cut and Faulting-controlled Landforms: Journal, Geophysical Research.

Lajoie, K. R., and Mathieson, S. A., 1983, Comparison of rate of sea-cliff-retreat during the 1982 and 1983 winter storms with the breakwater-induced rate increase from 1960 to 1980, Half Moon Bay, California [abs.]: GSA Annual Meeting, Indianapolis, Indiana, October 31-November 3, 1983.

Lajoie, K. R., Kennedy, G. L., Mathieson, S. A., Sarna-Wojcicki, A. M., Morrison, S. A., and Tobish, M. K., 1983, Emergent Holocene marine terraces at Cape Mendocino and Ventura, California, USA [abs.]: International Symposium on Development of Holocene Shorelines, Tokyo, Japan, September 28-30, 1983.

Mathieson, S. A., and Lajoie, K. R., 1983, Cliff-retreat increase due to a problem enhanced by the storms of 1982 and 1983, San Mateo County, California: The Half Moon Bay Breakwater [abs.]: Annual Meeting, Association of Engineering Geologists, San Diego, California, October 4-6, 1983.

Soil Dating Techniques, Western Region
9540-02192

Michael N. Machette
Branch of Western Regional Geology
U.S. Geological Survey
345 Middlefield Road, MS 75
Menlo Park, California 94025
(303) 234-3131 (Denver)

Purpose: To establish a data base for soil chronosequences as correlation and dating tools for Quaternary surficial deposits in the western United States.

Strategy: To identify and study soil chronosequences with age control from varied climatic and geologic environments, in order to determine which soil properties are useful indicators and how rates of soil development vary in different climates and types of parent materials.

Current personnel: M. N. Machette, J. W. Harden, M. C. Reheis (WAE), E. M. Taylor (WAE), and Glenn Dembroff (WAE). On contract: M. J. Singer, A. J. Busacca, J. R. Aniku, and Peter Janitzky (University of California at Davis); M. L. Gillam (University of Colorado at Boulder); D. P. Dethier (Williams College, Massachusetts). With contributions from A. J. Busacca (Washington State University at Pullman), R. M. Burke (Humboldt State College at Arcata), and P. W. Birkeland (Univ. of Colorado at Boulder).

Investigations

1. Manuscripts are being prepared and will cover the Quaternary stratigraphy, age control, and basic soil information (including appendices of soil and laboratory data) for each soil chronosequence investigated by the project (proposed as a U.S. Geological Survey Bulletin series). As of this report period, the following chronosequence chapters are in peer review: Merced River, Calif. (Harden); northern Rock Creek Basin, Montana (Reheis); Kane Fans, Wyoming (Reheis); Beaver basin, Utah (Machette); Cowlitz River, Washington (Dethier).

2. Revision (after peer review) of a laboratory manual is in progress. The manual describes the field chemical, mineralogical, and physical analyses of samples collected during this study. (Singer, Janitzky, Busacca, Harden, Ko, Machette, Meixner, Reheis, Taylor, and Walker).

3. Machette submitted a manuscript describing the feasibility, techniques, and results of thermoluminescence dating of soil carbonate from two areas in New Mexico (Rodd May, coauthor).

4. Machette is revising (after peer review) a manuscript summarizing the Quaternary tectonic history of the La Jencia fault, central Rio Grande rift of New Mexico. This study utilizes soil stratigraphy and scarp morphology to determine the amount of Quaternary displacement and paleoseismicity of the fault.

5. Harden conducted two new field investigations south of Hollister, California in cooperation with J. D. Sims and M. M. Clark. Soils were described and sampled for assessing ages of deposits associated with slip-rate studies underway in Office of Earthquake, Volcanoes, and Engineering.

Results

1. Gillam completed soil sampling and geologic mapping of the terrace sequence along the Animas River. She found the 600,000-yr-old Lava Creek ash bed in the Farmington area, thus providing a positive statigraphic tie to numerous localities of the same ash bed in the Durango area, about 50 km to the north.

2. Reheis completed geologic mapping of terrace and fan deposits in the northern Big Horn basin and collected a new locality of the 2-m.y.-old Huckleberry Ridge ash bed.

3. Singer, Aniku, and Janitzky completed laboratory analysis of samples from the Santa Cruz and Ano Nuevo chronosequences.

4. This is the final report of the project, therefore we will summarize some major contributions that this project has made to the Earthquake Hazards Reduction Program. (Original project chief was D. E. Marchand until his death in 1981).

   A. Geologic age control for the chronosequences

   One of the major goals of this project was to locate, establish, or develop well-dated successions of Quaternary surficial deposits that can serve as local reference sections for future mapping efforts in the western United States. Age control for the uppermost Pleistocene (10,000-40,000 yrs B.P.) and Holocene deposits (less than 10,000 yrs B.P.) comes mainly from charcoal, organic matter, wood, or fossils that have been dated by ^{14}C methods. Many deposits in the 40,000 to 600,000 yr range have been dated for this project by the uranium-trend method (developed by John Rosholt, U.S.G.S.), which provides dates for deposits that otherwise are difficult to date by ^{14}C or other radiometric methods. In the Ventura and Honcut Creek areas we also have amino-acid racemization ratios and uranium-series determinations that provide additional age control.

   We have found volcanic ash beds associated with many of the fluvial deposits in the region. The more widespread of these ashes have been radiometrically dated as 450,000 yrs old (the Rockland ash bed; California and Nevada), 620,000 yrs old (the Lava Creek-B ash bed; western U.S), 730,000 (the Bishop ash bed; western U.S.); and about 2.0 m.y. old (the Huckleberry Ridge ash bed; western U.S.). These ash beds provide well-dated, essentially instantaneous time markers for many of the deposits of the chronosequences. Most of the chronosequences span at least 500,000 years, and the Rock Creek (Montana), Merced River and Honcut Creek (California), and Animas River (Colorado and New Mexico) chronosequences cover a large portion of the Quaternary and late Pliocene.

B. Investigation of soil properties as a function of time

Harden developed and published a soil-development index which numerically rates soil field-properties for their degree of development. The index works well for most of the chronosequences of this project and can be applied to most geologic investigations where soil descriptions are available. The index is now being used for age control in studies on rates of fault offset. This index combines as many as ten soil field-properties, including clay films, texture plus wet consistence, rubification (increase in color hue and chroma), color paling (decrease in hue and chroma), structure, dry consistence, moist consistence, melanization (decrease in color value), color-lightening (increase in color value) and pH. Individual quantified field properties, as well as the integrated index, are used for age calibrations and age estmates.

Busacca, Harden, and Reheis have discovered significant chemical transformations in various size-separates of soils, in which X-ray fluorescence data are plotted against time. From the Honcut chronosequence, Busacca concluded that silt fractions in andesitic, central California soils suffer a profound loss of most major elements (Ca, Mg, Na, Fe, Al) as a result of mineral dissolution. Harden also documented very similar dissolution and loss trends in sands and whole-soil fractions of granitic soils of the Merced chronosequence; only the fine (silt-plus-clay) fraction indicated net gains of certain elements (Fe, Al, Ti). Reheis, in a study of soils in the continental, subarctic climate of the northern Big Horn basin, found net gains of most elements (Ca, Mg, Na, Fe, Al) in the fine fraction, thereby contrasting the rates of element removal in the drier continental regions of California. Zr was found by all 3 workers to be the most stable constituent. Total chemical analysis of size separates appears to be a rapid, accurate means of documenting fundamental soil processes. These comparative studies indicate important contrasts in soils of different climates, specifically the differences in rates of mineral dissolution, reprecipitation and removal by leaching. To date, element-loss rates are the most reproducable, systematic measure of soil development in varying climatic settings and are a valuable tool for correlating and dating late Cenozoic deposits.

C. Methods manual for inter-regional chronosequence studies

In addition to establishing a large data base soil field-properties, this project formulated a series of standardized laboratory procedures for analyzing physical, chemical, and mineralogical properties of soils. A comprehesive, cookbook-style laboratory manual describing these procedures is being prepared in association with our colleques at the University of California at Davis. The manual will provide guidelines for future analyses of soils, which would be compatible with the our current data base. Our data base includes 14 chronosequences from varying climates and parent materials, 215 soil profiles, and about 1200 samples, with a total of about 12,000 separate analyses.

D. Eolian contributions to soils

Our results indicate that eolian influx of materials imparts major pedogenic features to soils in semiarid to arid regions. Carbonate, gypsic and possibly argillic (clay) horizons in these soils appear to have inherited significant masses of these constituents, as compared to masses formed in situ by mineral transformations. Most of the pedogenic $CaCO_3$ in semiarid to arid soils in the southwestern U. S. is derived from a combination of airborne calcareous dust and rain-dissolved Ca^{++} and CO_3^{--} ions. Machette has found that the rate of carbonate accumulation in the Southwestern U.S. commonly varies by a factor of 2 to 4 over broad regions in response to variations in Ca^{++} influx rates and the annual distribution and amounts of precipitation. The total weight of secondary calcium carbonate per unit area of soil accumulates with time and is an important measure of soil development in these areas. The volumes of pedogenic carbonate can be used to estimate the age of deposits (given calibration by a dated chronosequence), to correlate soils formed in Quaternary surficial deposits over broad regions, and to date episodes of movement on faults.

Reheis has shown that the pervasive gypsum in soils of the Kane-fan chronosequence of the northern Big Horn basin has an eolian source. By parallel logic then, much of the clay in semiarid soils might also be of eolian origin, rather than dervived from in situ mineral weathering. Thus, the rates of clay accumulation in argillic horizons also might be expected to vary in semiarid regions in response to rainfall and dustfall patterns, as was found for rates of calcium carbonate accumulation.

Reports (published or approved)

Burke, R. M., and Birkeland, P. W., in press, Holocene and late Pleistocene glaciation of the mountains of the western United States (abs.), in H. E. Wright and S. C. Porter, eds., Proceedings of the 1982 International Quaternary Association (INQUA), Moscow: International Quaternary Association, v. xx, no. xx, p. xx-xx.

Busacca, A. J., 1983, Weathering of elements from silt-sized primary minerals in a soil chronosequence, Sacramento Valley (abs.): American Society of Agronomy, Crop Science Society of America, and Soil Science Society of America Abstracts, Annual Meeting, August 14-19, 1983, Washingtion, D.C.

Busacca, A. J., Aniku, J. R., and Singer, M. J., Dispersion of soils by a cup-type ultrasonic method that eliminates probe contact and titanium contamination: submitted to Soil Science Society of America Journal, 20 ms. p.

Harden, J. W., 1983, Order and rates of element loss form central-California soils (abs.): American Society of Agronomy, Crop Science Society of America, and Soil Science Society of America Abstracts, Annual Meeting, August 14-19, 1983, Washingtion, D.C.

Harden, J. W., and Taylor, E. M., A quantitative comparison of soil development in four climatic regimes: Accepted by Quaternary Research (6/83).

Machette, M. N., Late Cenozoic geology of the Beaver Basin, south-central Utah: Geological Society of America Bulletin, 43 p., 7 figures, 1 table (directors approval 9/7/83, submitted to GSA 9/20/83).

Machette, M. N., 1983, Geologic map of the southwest quarter of the Beaver quadrangle, Beaver County, Utah: U.S. Geological Survey Miscellaneous Investigations Map I-1444, scale 1:24,000.

Machette, M. N., and Personius, S. F., Quaternary and Pliocene faults in the eastern part of the Aztec and western part of the Raton 1° x 2° quadrangles, northern New Mexico: U.S. Geological Survey Miscellaneous Field Studies Map 1465-B, scale 1:250,000 (branch approval 9/20/83).

Machette, M. N., and Steven, T. A., 1983, Geologic map of the northwest quarter of the Beaver quadrangle, Beaver County: U.S. Geological Survey Miscellaneous Investigations Map I-1445, scale 1:24,000.

Machette, M. N., Steven, T. A., Cunningham, C. G., and Anderson, J. J., 1983, Geologic map of the Beaver quadrangle, Beaver and Piute Counties, Utah: U.S. Geological Survey Miscellaneous Investigations Map I-1520, scale 1:50,000 (in press).

Machette, M. N., and Colman, S. M., 1983, Age and distribution of Quaternary faults in the Rio Grande rift: Evidence from morphometric analysis of fault scarps: Geological Society of America Abstracts with Program, v. 15, no. 5, p. 320.

Machette, M. N., Harper-Tervet, Jan, and Timbel, N. R, Calcic soils and calcretes of the southwestern United States, in Weide, D. L., and Farber, M. L., eds., Surficial Deposits of the Southwestern United States: Geological Society of America Special Paper, 58 ms. p (Directors approval 4/83)

Reheis, M. C., 1983, Glaciofluvial origin and drainage history revealed by terraces in the northern Bighorn basin, Montana (abs.): Geological Society of America Abstracts with Program, v. 15, no. 5, p. 431.

Basement Tectonic Framework Studies
Southern Sierra Nevada, California

9910-02191

Donald C. Ross
Branch Of Engineering Seismology and Geology
345 Middlefield Road, Mail Stop 77
Menlo Park, California 94025
(415) 323-8111, ext. 2341

Investigations

1. Revision and updating of a Professional Paper manuscript on metamorphic and plutonic rocks of the southernmost Sierra Nevada, California (manuscript now being edited in Branch of Western Technical Reports).

2. Final revision of Professional Paper manuscript titled: "Possible correlations of basement rocks across the San Andreas, San Gregorio-Hosgri, and Rinconada-Reliz-King City faults, California" (manuscript has now received Director's approval and is being processed for publication).

3. Examination of mafic plutonic rocks along the Sierra Nevada Foothills from Porterville north to the Fresno area.

4. Selected and submitted samples of plutonic rocks from the southern Sierra Nevada to Ivan Barnes' laboratory for ^{18}O determinations. In addition, in cooperation with David Sams (California Institute of Technology), granitic and high-grade metamorphic samples from the southern Sierra Nevada for which U-Ob zircon ages have been determined, were also submitted for ^{18}O determination.

5. Petrographic study of granitic and metamorphic rocks and modal analysis of granitic rocks from the 1982 field season in the area near the Kern Canyon fault zone.

Results

1. Preliminary results of ^{18}O determinations on high-grade metamorphic rocks of the southernmost Sierra Nevada show that some hypersthene granulite is strongly enriched with values as high as +13 to +15 ($\delta^{18}O$ SMOW), which indicates either a sedimentary protolith or considerable contamination of an igneous protolith by sedimentary material. Associated quartzofeldspathic gneiss is also similarly enriched and reflects a similar sedimentary origin. Conversely some of the hornblende-rich amphibolite shows values of +6.5 to +9 ($\delta^{18}O$ SMOW), which suggests that these rocks are meta-igneous. These preliminary ^{18}O determinations suggest that the metamorphic rocks of the southernmost Sierra Nevada, which may represent a batholithic root zone, reflect a complex parentage and cannot be characterized solely as refractory granitic melt residium.

2. The Professional Paper on "correlations" listed above under Investigations, is essentially my final report on a several year reconnaissance study of the basement rocks of the Salinian block. The following statement destined to be eventually in the Monthly List of Publications summarizes the results of that study: "A reconstruction that treats the Salinian block as a fault-derived fragment of the Sierra Nevada is supported by the similarity of some basement rock features between the central Salinian block and the southern Sierra Nevada. However, documented movements on currently recognized faults are not great enough to accommodate all of the Salinian block basement into the Sierra Nevada. Additional movement on faults yet to be discovered, or transportation of the Salinian block as an exotic from a considerable distance seem to be called for."

3. Examination of the hypersthene-bearing tonalitic rocks of the Academy pluton (about 30 km northeast of Fresno, California) both in the field and in thin section, points out strong similarities to the hypersthene-bearing rocks in the tonalite of Bear Valley Springs in the southernmost Sierra Nevada. The absence of associated high-grade metamorphic rocks in the Academy area, however, suggests that those hypersthene-bearing tonalite exposures represent shallower crustal depths than are represented by the hypersthene-bearing tonalite and high-grade metamorphic terrane of the southern Sierra Nevada.

Reports

Ross, D. C., 1983, Hornblende-rich, high-grade metamorphic terranes in the southernmost Sierra Nevada, California, and implications for crustal depths and batholith roots: U.S. Geological Survey Open-File Report 83-465, 51 p.

_____1983, Petrographic (thin section) notes on selected samples from hornblende-rich metamorphic terranes in the southernmost Sierra Nevada, California: U.S. Geological Survey Open-File Report 83-587, 36 p.

_____1983, The Salinian block--a structurally displaced granitic block in the California Coast Ranges: in Roddick, J. A., ed., Circum-Pacific plutonic terranes; Geological Society of America Memoir 159, p. 255-264.

Tephrochronology

9540-01947

Andrei M. Sarna-Wojcicki
Branch of Western Regional Geology
U.S. Geological Survey
345 Middlefield Road, MS 75
Menlo Park, California 94025
(415) 323-8111 ext. 2745

Continued sampling, chemical and petrographic analysis, and fission-track age dating of tephra (ashes and tuffs) of young geological age in order to provide age control for studies of recent tectonism and volcanism in California, Nevada, Oregon, and Washington, and to provide independent calibration for other age dating techniques. Neutron-activation, X-ray fluorescence, and electron microprobe analyses of separated volcanic glass and crystals are used in combination with petrographic characteristics to identify widespread tephra units of known radiometric age. New tephra units identified by chemical and petrographic analyses are dated by appropriate radiometric age dating methods (with C. E. Meyer, Janet Ziegler, J. R. Rivera, Gail McCoy, and John Diaz, BWRG).

Investigations

1) Continued work on specific teprochronologic problems in Nevada, the western coastal states of the conterminous U.S., and the northeastern Pacific Ocean adjacent to the continent (see item 1, Summary of Technical reports, v. XV, Jan., 1983, p. 154-156, U.S.G.S. OFR 83-90).

2) We have identified the widespread, circa 1.8-m.y.-old Huckleberry Ridge ash bed (table 1) at two new localities in the western U.S. At the first locality, the ash bed is in the marine Falor Formation, in Humboldt County, northwestern California, and represents the westernmost documented on-land locality of this ash bed found to date. We have previously identified this ash from a core sample of DSDP hole 36, located about 500 km west of Cape Mendocino, in the northeastern Pacific Ocean; in the core, the ash is stratigraphically close to the position of the Pliocene-Pleistocene boundary, as determined from independent biostratigraphic evidence (item 4, p. 155, vol. XV, 1983, and fig. 1. p. 108, vol. XVI, 1983). Identification of this ash bed places time constraints on rates of faulting and deformation in the tectonically-active Humboldt basin (coop. with Gary Carver, Humboldt State Univ.). At the second locality, near Soldier Peak, Nevada, tentative identification of this ash constrains the age of older alluvium containing the ash (table 1) (coop. with Art Snoke, Univ. of South Carolina).

We have some difficulty in distinguishing the Huckleberry Ridge ash bed from the closely-related, 0.6-m.y.-old Lava Creek-B ash bed on the basis of electron-microprobe analysis alone (small differences in iron and calcium can sometimes be used; table 1), and we are conducting further analysis by energy-dispersive X-ray fluorescence and neutron activation (coop with G. A. Izett, ORG, and R. E. Wilcox, BCMR).

3). Our data from electron-probe analysis (table 2) indicate that a fresh, white, 2-cm-thick ash bed in the uppermost marine San Joaquin Formation in the Kettleman Hills of western San Joaquin Valley, California, correlates well with the Ishi Tuff Member (of the volcanic and fluvio-volcanic Tuscan Formation) of northeastern Sacramento Valley, Calif., some 475 km to the north. We also correlate the Ishi Tuff Member locally within the Tuscan Formation over distances of as much as 80 km (coop. with D. S. Harwood, BWRG). In the Tuscan Formation, the Ishi Tuff has been dated at 2.0 m.y. (K-Ar) and 2.4 m.y. (fission-track) (D. S. Harwood, oral commun., 1983), an age substantially in agreement with a 2.2 m.y. fission-track date obtained previously by Obradovich and others (1979) on a tephra layer in a stratigraphic position similar to that of our white, 2-cm-thick ash, in the Kettleman Hills. The Ishi Tuff Member is situated stratigraphically above the Nomlaki Tuff Member (of the Tuscan and Tehama Formation) at both the Sacramento and San Joaquin Valley localities. At the former locality, the Nomlaki Tuff Member is near the base of the Tuscan Formation, while at the latter locality, near the middle of the San Joaquin Formation. The Nomlaki Tuff Member has been dated at 3.4 m.y. (K-Ar; Evernden and others, 1964), and the isotopic ages and stratigraphic relationships of the Ishi and Nomlaki Tuff Members help to confirm our chemical correlations.

Reports

Sarna-Wojcicki, A. M., Meyer, C. E., Bowman, H. R., Hall, N. T., Russell, P. C., Woodward, M. J., and Slate, J. L., Correlation of the Rockland ash bed, a middle Pleistocene stratigraphic marker in northern and central California and western Nevada. Approved journal article submitted to Quaternary Research.

Sarna-Wojcicki, A. M., Meyer, C. E., and Slate, J. L., Applications of tephrochronology and tephrostratigraphy to Quaternary chronology, stratigraphy, and tectonics in the Western United States. Abstract for International Symposium on Recent Crustal Movements of the Pacific Region, Wellington, New Zealand. Accepted.

Lajoie, K. R., Sarna-Wojcicki, A. M., Kennedy, G. M., Mathieson, S. A., McCrory, P. A., Morrison, S. A., and Stephens, T. A., Late Quaternary Coastal Tectonics of the Pacific Coast of the United States. Abstract for International Symposium on Recent Crustal Movements of the Pacific Region, Wellington, New Zealand. Accepted.

Lajoie, K. R., Kennedy, G. L., Mathieson, S. A., Sarna-Wojcicki, A. M., Morrison, S. A., and Tobish, M. K., 1983, Emergent Holocene Marine Terraces Cape Mendocino and Ventura, California, U.S.A. Abstract, Conference on Holocene Shorelines, Japan.

Table 1. Electron microprobe analyses of glass of the Huckleberry Ridge ash bed and the Lava Creek-B ash beds, western United States. Concentrations are given in oxide weight percent, recalculated on a fluid-free basis. Original totals are given on the right (T_o). C. E. Meyer, USGS, Menlo Park, analyst.

		SiO_2	Al_2O_3	Fe_2O_3	MgO	MnO	CaO	TiO_2	Na_2O	K_2O	T_o
					Huckleberry Ridge ash bed						
1.	HPA-1	76.68	12.26	1.71	0.02	0.04	0.57	0.12	3.59	5.00	94.67
2.	DSDP-36	76.15	12.43	1.80	0.03	0.06	0.59	0.13	3.60	5.04	94.68
3.	VA-2-1982	77.07	12.12	1.64	0.01	0.04	0.58	0.10	3.48	4.97	94.54
4.	BEAVER-1	76.30	12.27	1.80	0.02	0.04	0.55	0.09	3.55	5.20	93.85
5.	TECO-12B1	76.08	12.33	1.82	0.03	0.05	0.61	0.14	3.45	5.28	94.93
6.	68W98	76.78	12.14	1.71	0.03	0.04	0.57	0.11	3.50	5.12	94.64
					Lava Creek-B ash bed						
7.	67W104	77.02	12.10	1.55	0.03	0.04	0.52	0.10	3.66	4.99	94.85

1. Ash near base of marine Falor Fm., Hatfield Prairie, Humboldt Co., California (Gary Carver, coll.).
2. Ash in DSDP core 36, W. of Gorda Ridge, at 37m depth, at approx. the Pliocene-Pleistocene boundary.
3. Ash in old alluvium, Soldier Peak, eastern Nevada (Arthur Snoke, coll.).
4. Ash from old alluvium, Beaver basin, southwestern Utah (Mike Machette, coll.).
5. Ash C from lake beds of Pleistocene Lake Tecopa, southeastern California.
6. Ash from old alluvium, Borchers paleofauna loc., Kansas (R. E. Wilcox, coll.).
7. Ash from old alluvium, Onion Creek, eastern Utah (R. E. Wilcox, coll.).

Table 2. Electron microprobe analysis of volcanic glass of the Ishi Tuff (Member of the Tuscan Formation), and correlative ash bed from the top of the San Joaquin Formation, Kettleman Hills, western San Joaquin Valley, California. An analysis of the older Nomlaki Tuff (member of the Tuscan and Tehama Formations is given for comparison. Concentrations are given in oxide weight percent, recalculated on a fluid-free basis. Original totals are given on the right (T_o). C. E. Meyer, USGS, Menlo Park, analyst.

		SiO_2	Al_2O_3	Fe_2O_3	MgO	MnO	CaO	TiO_2	Na_2O	K_2O	T_o
					Ishi Tuff (Member of the Tuscan Formation)						
1.	KT-11A	78.47	12.16	0.86	0.14	0.04	0.77	0.16	3.59	3.81	93.56
2.	KT-11B	78.81	11.95	0.90	0.14	0.03	0.78	0.18	3.57	3.74	93.87
3.	RS-2	77.58	12.71	0.85	0.14	0.02	0.75	0.15	3.49	4.11	94.97
4.	RS-2	77.31	12.79	0.84	0.16	0.02	0.74	0.15	3.38	4.39	94.39
5.	MILL-10	77.61	12.69	0.83	0.14	0.04	0.75	0.16	3.51	4.08	95.28
					Nomlaki Tuff (Member of the Tuscan and Tehama Formations)						
6.	758-314D	76.93	12.82	1.11	0.18	0.05	0.95	0.20	4.06	3.60	94.67
7.	758-324	77.03	12.71	1.10	0.18	0.02	0.98	0.22	3.98	3.52	96.33

1, 2 Samples from San Joaquin Formation, Kettleman Hills, SW San Joaquin Valley.
3-5 Samples from the Tuscan Formation, NE Sacramento Valley.
6,7 Samples from the Tehama Formation, NW Sacramento Valley.

Salton Trough Tectonics and Quaternary Faulting

9940-01292
Robert V. Sharp
Branch of Engineering Seismology and Geology
U.S. Geological Survey
345 Middlefield Road, MS 77
Menlo Park, California 94025
(415) 323-8111, ext. 2596

Investigations

1. Monitoring level changes of near-field monuments at sites on the San Jacinto fault zone and San Andreas fault.

2. Continuation of trenching of the Imperial fault at the California - Baja California international boundary.

3. Search for surface faulting associated with the May 2, 1983 earthquake near Coalinga, California.

Results

1. Vertical ground deformation across the northern Coyote Creek fault near Middle Willows and the San Andreas fault near the Salton Sea has continued, but the cumulative signals over more than two years show considerable, and apparently partly seasonal fluctuation. Figure 1 shows the cumulative elevation changes for the two arrays from late 1980 to early 1983. The most recent change on the Coyote Creek fault represents the largest signal observed there to date, but it followed a nearly complete collapse of the nearly as large earlier deformation. The strength of the latest elevation change may be related to the unusually high rainfall of the 1982-1983 winter season. Over the same period of time, however, the cumulative signal at the San Andreas fault diminished slightly, unlike its behavior in the two previous winters. Each array shows a net secular rise over the period of observation, and this may reflect a dipslip component of subsurface creep. For these sections of these faults, surficial horizontal creep has been established only for the San Andreas fault. To date, there is no suggestion of surficial dipslip movement in the leveling data for either fault.

2. Deepening of trenches to the water table has revealed evidence of the first displacement event(s) older than the 1940 movement on the Imperial fault. The right-lateral component of the older offset is greater than 23 m, and its age is presently constrained by ^{14}C dating to pre - A.D. 1300. A bed older than the dated stratum contains shells which soon will provide a better constraint on the time of the pre - 1940 event(s).

3. This report briefly describes efforts by M. M. Clark, K. K. Harms, J. J. Lienkaemper, J. A. Perkins, M. J. Rymer, and R. V. Sharp of the Branch of Engineering Seismology and Geology to determine whether surface faulting accompanied the May 2, 1983, main shock at Coalinga. The ground search for evidence of faulting began on the morning of May 3, and continued to May 7; other brief investigations were made on May 10 and May 24-25.

An aerial search on the morning of May 3 extended from the San Andreas fault near Mustang Ridge eastward to Interstate 5 and from Avenal northward to Black Mountain. Rockfalls, landslides, slumps, and related secondary fractures were seen from the air, but no fault ruptures were identified. Nearby parts of the San Andreas and other known faults were air- and ground-checked to see if they sustained sympathetic movement due to shaking or stress changes.

Although fissures and cracks were found by ground search at many places within about 10 km of the instrumental epicenter, none appeared to represent new faulting. Indeed, the epicentral region was notable because of the scarcity of both previously identified faults and lineaments on the ground surface that could have reflected preexisting fault structures.

In interpreting the observed cracks, we applied the following criteria to distinguish tectonic faulting from cracking due to other processes:

1. That there be net displacement across the crack features or, alternatively, that purely extensional opening on steeply dipping cracks be insufficient evidence of faulting (which by definition requires displacement parallel to its surface).

2. That the style of faulting or sense of displacement of suspected faults persists, or at least varies in some consistent way, along the length of the crack feature.

3. That the cracks not be readily explainable by other processes restricted to near the surface (for example, slumps parallel to a free face of a nearby channel or an artificial fill).

Our ground search concentrated in the epicentral area because of the abundance of new fissures and cracks there. A preliminary focal mechanism provided by USGS seismologists at the beginning of our ground search suggested, however, that a far-ranging regional inspection should be made, particularly along the eastern margin of the Coast Ranges. Because of the shallow dip of one of the possible focal planes, ground checks along pavements were made to a considerable distance eastward into the San Joaquin Valley.

One characteristic of many fissures and cracks that were found either in the epicentral area, which overlies an anticlinal structure, or on the alluviated surface immediately to the southwest deserves comment. The trends of many of these breaks were oriented in the northwest quadrant, approximately parallel to the nearby Coast Range regional strike and the limbs of the anticline. The consistent orientation of many of the cracks might be explained in various ways--one of the most likely being that the preexisting structure of both buried and exposed sedimentary beds might have controlled the orientation of new breaks. Bedding-controlled topography buried under young alluvium also may have guided differential compaction boundaries expressed at the surface as fissures with downdropping on one side.

Several kinds of surficial processes combined with strong ground shaking probably account for the recently created fractures that were observed on

the ground surface after the May 2 main shock near Coalinga. None of the fracturing, however, was considered to be caused by tectonic displacements on deeply rooted fault structues.

After this field investigation and following a strong aftershock on June 11, a new fault break was discovered on a mountain slope about 10 km northwest of Coalinga. Another field investigation commenced, and its results are reported by M. M. Clark elsewhere in this volume.

Reports

Clark, M. M., Harms, K. K., Lienkaemper, J. J., Perkins, J. A., Rymer, M. J., and Sharp, R. V., 1983, The May 2, 1983, earthquake at Coalinga, California: The search for surface faulting, in Borchardt, R. D., ed., The Coalinga earthquake sequence commencing May 2, 1983, U.S. Geological Survey Open-File Report 83-511, p. 8-11.

Sharp, R. V., 1983, History of late Holocene slip on the Imperial fault, southern California: A subsurface geologic study by excavation [abs.]: International Symposium on recent crustal movements, Pacific Region, Wellington, New Zealand (1984).

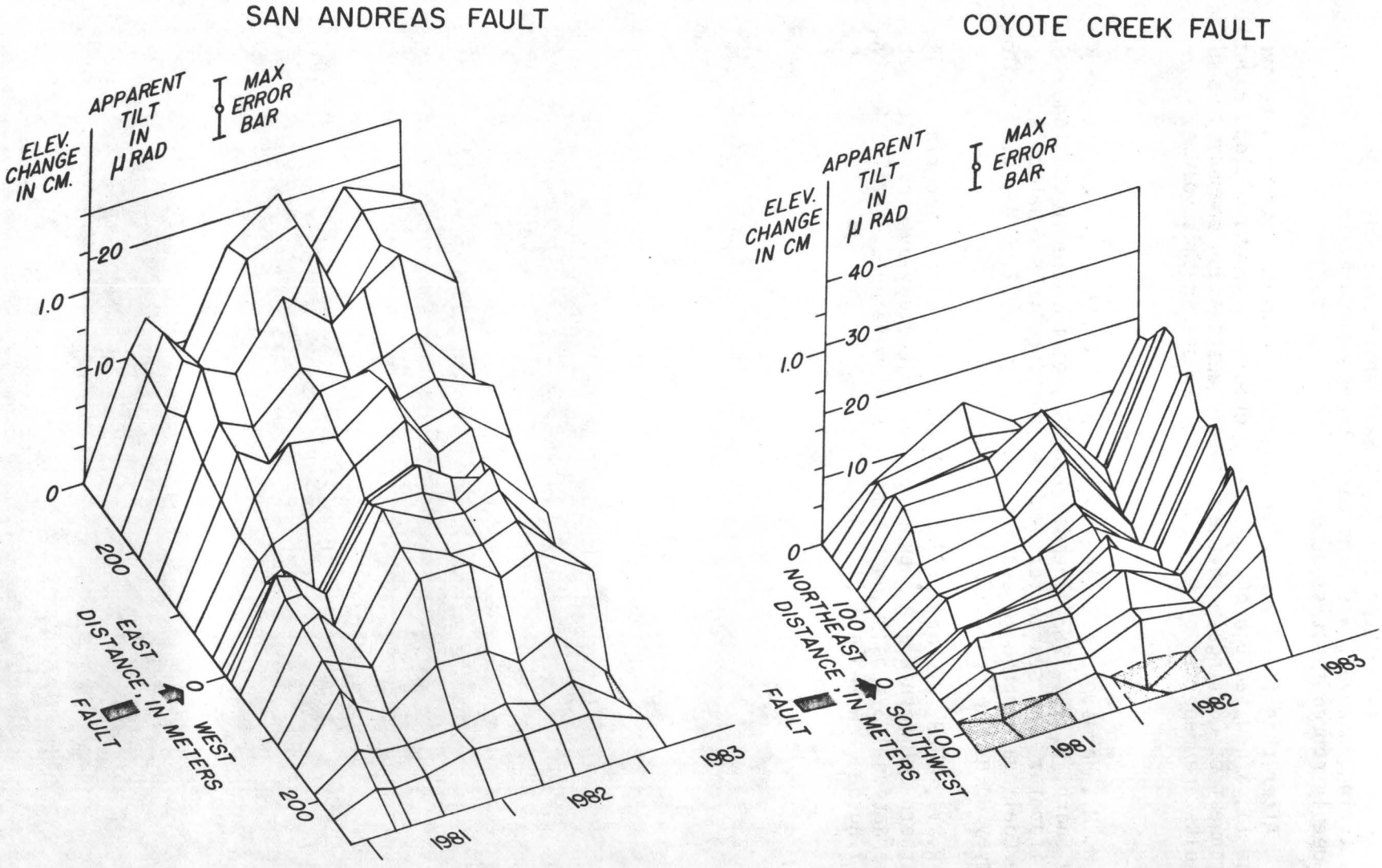

Figure 1. Elevation changes across the two faults. Stippled areas represent negative values.

Late Holocene Behavior of the San Andreas Fault

14-08-0001-21275

Kerry Sieh
Division of Geological and Planetary Siences
California Institute of Technology
Pasadena, CA 91125
(213) 356-6115

Investigations

We have continued our geologic studies of the San Andreas fault system in southern California. Specifically, we have continued mapping along the San Jacinto fault and the San Andreas fault near San Bernardino.

Results

Geologic mapping, radiocarbon and soils analyses continue to improve our understanding of the late Pleistocene and Holocene rates of slip and character of slip along the San Andreas and related faults of the Cajon Creek-Mill Creek region north of San Bernardino.

Reports

Several manuscripts have been submitted, revised, resubmitted, and/or re-revised.

Sieh, K. (in press). Lateral Offsets and Revised Dates of Large Prehistoric Earthquakes at Pallett Creek, Southern California.

Sieh, K., and R. Jahns (in press, GSA Bulletin). Holocene Activity of the San Andreas Fault at Wallace Creek, California.

Weldon, R., and K. Sieh (to be submitted, GSA Bulletin). Holocene and late Pleistocene History of the San Andreas Fault near Cajon Pass, Southern California.

Earthquake Hazard of the Red River Fault and Related Faults Deduced from Geological Field Studies in Western Yunnan Province, P.R.C.

14-08-0001-21289

Kerry Sieh
Division of Geological and Planetary Sciences 170-25
California Institute of Technology
Pasadena, CA 91125

Investigations

I and graduate student, Ray Weldon, spent the period from mid-March to mid-June in the People's Republic of China as guests of the Yunnan Bureau of Seismology (Kunming) and State Seismological Bureau (Beijing). With several Chinese geologists from the YSB, we investigated Quaternary tectonism in Yunnan Province, which borders on Vietnam, Laos, and Burma (Fig. 1). The potential for loss of life from earthquakes is very high in this province, but understanding of seismogenic faults is quite limited. We attempted to determine slip rates and recurrence intervals for faults Clarence Allen and I identified during our field work in in 1981 as being particularly hazardous. In addition, we attempted to gain a better overall understanding of the seismotectonics of southern China and its part in the ongoing collision of India and Asia.

Results

We discovered a site along the right-lateral Red River Fault (Sieh et al., 1982; Allen et al., in press) which contains a record of the past 5 large earthquakes. The site is nestled within a small stream channel, which is offset 50 m by the fault, near Gasa (Fig. 1). Scarp breccias which have collapsed onto a gradually accumulating, peaty and clayey channel fill record dateable fault-slip events. Other dateable geological units will enable us to calculate a fault-slip rate. I suspect a rate of a few mm/yr and an average recurrence interval of about 500-1000 years, but these data must await radiocarbon analysis of the samples. I am currently negotiating with the Chinese for delivery of the radiocarbon samples to the U.S.

We also began work on a large normal fault near Xiaguan (Fig. 1) which was recognized only recently as an active normal fault. Several Tang dynasty (1000-year old) walls show no clear offset where they cross the fault zone, and yet late Holocene alluvial fans have experienced repeated episodes of faulting. Radiocarbon analyses will help pin down the dates of activity of this fault.

Reports

Allen, C.R., A.R. Gillespie, Han Yuan, K.E. Sieh, Zhang Buckun, and Zhu Chengnan, (in press, GSA Bulletin). Red River and Associated Faults, Yunnan Province China: Quaternary Geology, Slip Rates, and Seismic Hazard.

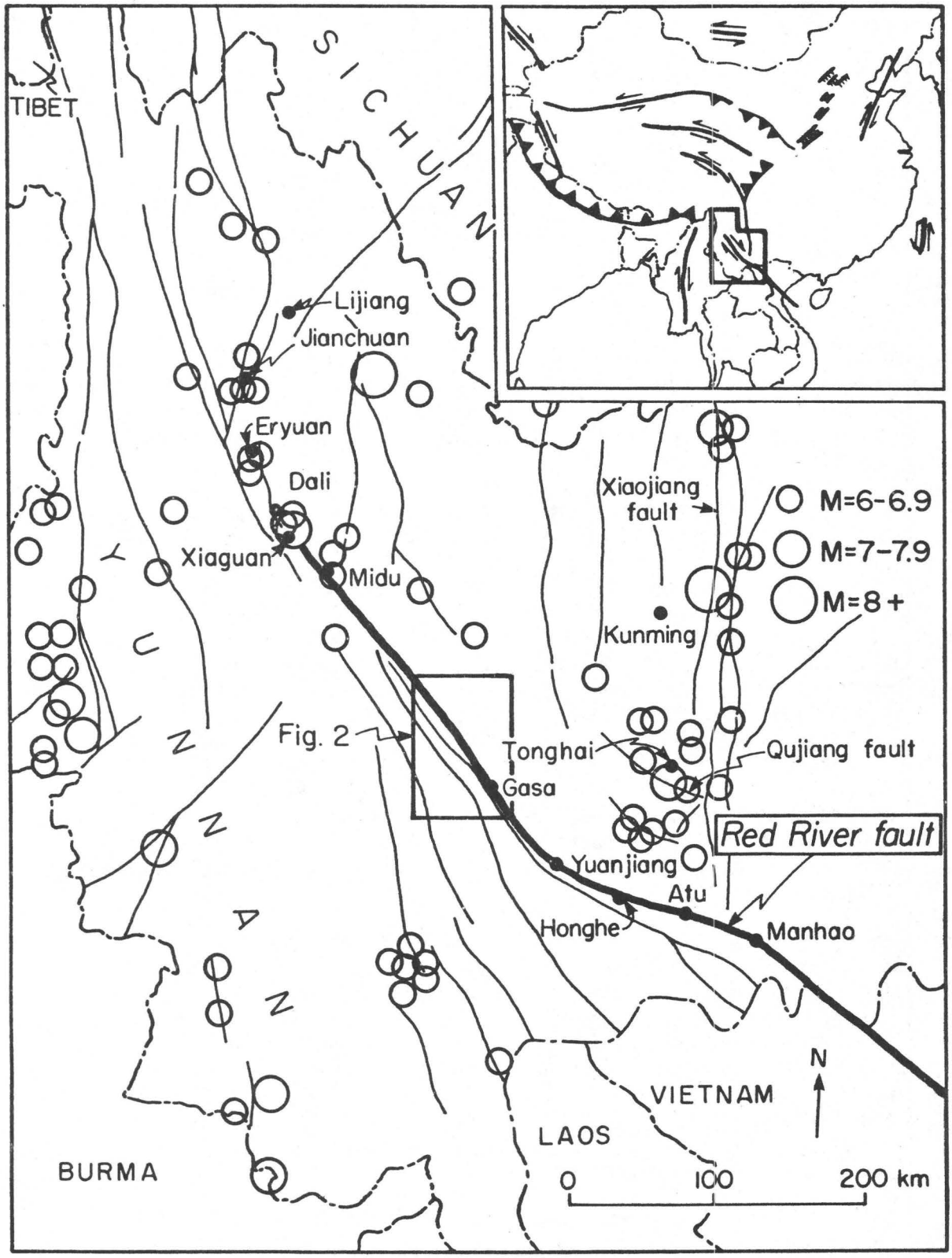
TIBET
SICHUAN
Lijiang
Jianchuan
Eryuan
Dali
Xiaguan
Midu
Xiaojiang fault
M=6-6.9
M=7-7.9
M=8+
Kunming
Fig. 2
Tonghai
Gasa
Qujiang fault
Red River fault
Yuanjiang
Atu
Honghe
Manhao
YUNNAN
VIETNAM
LAOS
BURMA
N
0
100
200 km

Detailed Geologic Studies, Central San Andreas Fault Zone

9910-01294

John D. Sims
Branch of Engineering Seismology and Geology
U. S. Geological Survey
345 Middlefield Road, MS-77
Menlo Park, California 94025
(415) 323-8111, ext. 2252

Investigations

1. Detailed geologic field investigations of structure, and surficial and bedrock deposits were conducted in and adjacent to the central section of the San Andreas fault zone (San Juan Bautista to Wallace Creek, Carrizo Plain) to determine horizontal and vertical slip rates and the detailed tectonic environment of the zone.

2. Detailed field searching for ground rupture associated with the May 2 Coalinga earthquake, reported by M. Clark elsewhere in this volume.

Results

1. Alluvial terraces cut by the San Andres Fault (SAF) at Parkfield were reevaluated for their potential to yield Holocene slip rates following the trending of alluvial terraces at Melendy Ranch, studies by Perkins and Sims. As a result of the experience gained in trenches at the Melendy Ranch site three sites were identified in the area around Parkfield. One site was chosen for trenching commencing 10 October, 1983. A second site will be trenched in the summer 1984. Mapping and structural analysis continues in the Middle Mountain area NW of Parkfield. The detailed mapping in progress suggests that the Gold Hill fault does not enter the San Andreas Fault at Parkfield but continues parallel up Little Cholame Creek to the east of the SAF.

2. Regional and site-specific studies by J. A. Perkins at the terraces along San Benito River continue to be at primary interest in the northern area of study. During this report period work was concentrated on site-specific trench and geomorphic analyses at the terraces at Melendy Ranch, approximately 36 km southeast of Hollister. At Melendy Ranch four terraces are transected by the San Andreas fault, however, only the oldest two terrace scarps exhibit offset (reported in earlier Semi-Annual Technical Reports). A single 40-m-long trench was excavated across the t_2-t_3 terrace scarp to recover datable material and detail the stratigraphy at these deposits.

   Numerous charcoal samples were recovered from both the t_2 and t_3 terraces, five of which were submitted for ^{14}C dating. The next youngest terrace (t_1) exhibits no offset and was trenched to identify subsurface offset features, recover charcoal, and to detail the stratigraphy. Three trenches were excavated on the t_1 surface: a 15 m-long trench across the fault was excavated to identify the main trace and to recover charcoal;

fault was excavated to identify the main trace and to recover charcoal; and two 20 m-long trenches parallel to the fault were excavated to determine offset features and recover charcoal. Three unique features were identified in both parallel trenches that yield offsets of 17.0 m, 17.5 m, and 17.6 m. Twelve charcoal samples were recovered from the t_1 terrace deposits, five of which were submitted for ^{14}C age determinations. Approximately 75 m of trenches were excavated on the youngest terrace, t_0. Cultural features such as barbwire, shoes, bolts, and porcelain were recovered from depths up to 2 meters in the t_0 deposits. This surface was not intensely studied owing to its very young age (100 yr). Data reduction and compilation of trench data is nearly complete and reports are currently being written.

Reports

Perkins, J. A., and Sims, J. D., 1983, Late Holocene deformation of river terraces, central San Andreas fault, California [abs.]: International Symposium on Recent Crustal Movements of the Pacific Region, Wellington, New Zealand, February 9-14, 1984.

Clark, M. M., Harms, K. K., Lienkaemper, J. J., Perkins, J. A., Rymer, M. J., and Sharp, R. V., The May 2, 1983 Earthquake at Coalinga, California: The search for surface faulting: in Borchardt, R. D., ed., The Coalinga earthquake sequence commencing May 2, 1983, United States Geological Survey Open-File Report 83-511, p. 8-11.

Tectonic Analysis of Active Faults

9900-01270

Robert E. Wallace
Office of Earthquakes, Volcanoes and Engineering
345 Middlefield Road, MS 77
Menlo Park, California 94025
(415) 323-8111, ext. 2751

Investigations

1. Analysis of fault scarp data in northcentral Nevada and overview analysis of paleoseismicity and tectonics of the Basin and Range province.

2. Evaluation of fault scarps and tectonics of the central Nevada and eastern California seismic belts.

3. Tectonic Geomorphology. A Penrose Conference under the auspices of the Geological Society of America.

4. Active Tectonics--Impact on Society. A project under the auspices of the Geophysics Study Group, National Research Council, National Academy of Sciences.

Results

1. Together with William B. Bull, University of Arizona, I served as co-convener of a Penrose Conference on Tectonic Geomorphology in April 1983 under the auspices of the Geological Society of America. Topics discussed included tectonic effects on fluvial systems and marine terraces, soil dating, analytical modelling especially of fault scarps, and the use of geomorphology in general to identify and evaluate tectonic activity. Special emphasis was paid to the interaction of the rates of tectonics and geomorphic processes.

2. Under the auspices of the Geophysics Study Group, National Research Council, National Academy of Science, a project titled "Active Tectonics--Impact on Society" was started. I will serve as chairman of the project. A symposium will be held at the December 1983 meeting of the American Geophysical Union meeting in San Francisco at which seventeen papers are scheduled. Manuscripts for a volume to be published by NRC/NAS are to be completed in the spring of 1984 and the volume is expected to go to press later in 1984.

3. The White Mountain - Mono Lake seismic gap appears to be the most likely site for a future M=7-8 earthquake within the central Nevada and eastern California seismic belts. Evidence for this conclusion includes: (1) the demonstrated capability of the state of stress in the region to generate earthquakes of M-6; (2) the large volume of crust prepared to generate earthquakes, as indicated by the 7-km-wide ring of seismicity surrounding much of the gap area; (3) regional stress changes indicated by reactivation of the resurgent dome in Long Valley caldera; and (4) a general increase of seismicity in the region.

The Sierran range front faults such as at Lundy and the Hilton Creek fault, as well as the northward continuation of the fault that generated the 1872 earthquake are major candidates, acting either independently or in some combination, to generate the next M 7-8 earthquake.

4. The White Mountain-Mono Lake seismic gap was evaluated as to where large earthquakes had been generated in addition to 1872 within the past 10,000 years (Holocene) by a reconnaissance search for young fault scarps. A summary follows:

- o ADOBE VALLEY LINEAMENT. No young fault scarps were found along this 40 km lineament, even though the lineament is conspicuous in LANDSAT images.

- o WEST FLANK WHITE MOUNTAINS. (a) A set of young scarps extends from Black Canyon north to Coldwater Canyon a length of about 20 km. Some of the scarps may be early Holocene. Datable volcanic ash was found in Poleta Canyon. (b) A gap containing no young scarps lies along a 45 km reach of the range front from about Coldwater Canyon to Montgomery Creek. This site is a good candidate for a M 7.5 earthquake. Uplift rates are rapid here. (c) Conspicuous young scarps (probably of Holocene age) were found in Queen Valley at the northern end of the range.

- o FISH LAKE VALLEY. Young scarps extend for at least 50 km along the east flank of the White Mountains. Spectacular scarps more than 100 feet high are near Dyer. Much, possibly all, of the scarp height was formed prior to Holocene.

- o DEEP SPRINGS VALLEY. A very young Holocene scarp lies along the southeast side of Deep Springs Valley. This may be only a few hundred to a few thousand years old.

- o EUREKA VALLEY. Only a few short segments of young scarps were found here on the west flank of the Last Chance Range north of Hanging Rock Canyon. The rest of the north end of Eureka Valley is devoid of Holocene scarps.

- o BLIND SPRINGS HILL TO CHIDAGO CANYON. Despite many faults that cut Bishop Tuff (700 K years) no scarps clearly of Holocene age were found. A short segment of fault on east flank of Blind Springs Hill is marked by a lineament of vegetation.

Arguments can be made both for the concept that the faults segment represented by Holocene scarps will produce the next large earthquake or that the gaps between the Holocene scarps will be the most likely sites.

Reports

Wallace, R. E., 1983, Active tectonics--impact on society [Abs.]: American Geophysical Union Meeting, December 1983, San Francisco, California

Wallace, R. E., Hill, D. P., Ryall, A. S., and Cockerham, R. S., 1983, Potential for large earthquakes in the central Nevada-eastern California seismic belt [Abs.]: Seismological Society of America Meeting, Salt Lake City, Utah, May 2-4, 1983

Wallace, R. E., 1983, Patterns and timing of late Quaternary faulting in the Great Basin Province and relation to some regional tectonic features: Proceedings Volume, Chapman Conference, Snowbird, Utah, 1982.

Wallace, R. E. and Whitney, R. A., 1983, Late Quaternary history of the Stillwater Seismic Gap, Nevada: Bulletin of the Seismological Society of America (in press).

Wallace, R. E., Davis, J. F., and McNally, Karen C., 1983, Terms for expressing earthquake potential, prediction and probability: Bulletin Seismological Society of America (in press).

Wallace, R. E., 1983, Review of "The Road to Jamarillo: Critical Years of the Revolution in Earth Science" by William Glen: Elsevier Publishing Co., The Netherlands.

Wallace, R. E., and Schulz, S. S., 1983, Aerial views in color of the San Andreas fault, California: U.S. Geological Survey Open-File Report 83-98.

Schulz, S. S., and Wallace, R. E., 1983, The San Andreas Fault: U.S. Geological Survey Leaflet (in press)

Wesson, R. L., and Wallace, R. E., 1983, Preparing for the next great earthquake in California: Scientific American (in press).

Wallace, R. E., 1983, Tangshan, six years later: Earthquake Information Bulletin, May-June 1983, v. 15, n. 3, p. 102-107.

Geophysical and Tectonic Investigations of the Intermountain Seismic Belt

9930-02664
Mary Lou Zoback
U. S. Geological Survey
Branch of Seismology
345 Middlefield Road, Mail Stop 77
Menlo Park, California 94025
(415) 323-8111, ext. 2367

Investigations

1) Compilation and analysis of principal stress data for the North American plate.

2) Analysis of seismic reflection and gravity data from the Sevier Desert basin in central Utah.

3) Evaluation of the style and faulting for numerous basins in the Northern Basin and Range Province using seismic reflection and gravity data.

4) Collaboration with Jason Saleeby (California Institute of Technology) and others in construction of Continental Ocean Transect C-2 crossing the Northern Basin and Range Province.

Results

1. A file of prinicpal stress data determined from focal mechanisms, in situ stress measurements, and geologic stress indicators, has been created. The file covers the entire North American plate and includes the data from the conterminous United States compiled by Zoback and Zoback (JGR, 1980) as well as all new data published since that compilation. Mara Schiltz, using available plotting software, has developed the capability to plot the stress data on any standard map projection.

   Zoback and others (1983) used this updated compilation and seismicity data in an investigation of mid-plate deformation of the North American plate. They found that a comparison of oceanic and continental deformation reveals similar levels and patterns of seismicity in the two regions. Major events in both regions appear clustered and can often be associated with pre-existing structural and/or topographic features. Individual seismic zones are generally widely dispersed. Large contrasts in available short-term (Holocene or Quaternary) and long-term (post-Paleozoic or post-Mesozoic) deformation rates indicate that sites of deformation probably migrate with time and suggest that stress and strain buildup in intraplate regions may be non-uniform both spatially and temporally.

The state of stress in much of the intraplate region of North America east of the Rocky Mountain front is dominated by horizontal compression oriented NE-SW to ENE-WSW. The major exception to this pattern of NE-SW compression occurs along the Atlantic and the northeastern Canada passive margin where the maximum horizontal compressive stress appears to be oriented NW-SE. In these areas local forces possibly arising from lateral contrasts in lithosphere structure and density as well as remanent effects of deglaciation may dominate the stress field. However, finite-element modeling, both global and for the North American plate alone, suggests that the primary source of the intraplate NE-SW compression is a ridge-push force from the Mid-Atlantic ridge. The possible role of drag forces acting on the base of the lithosphere cannot be well constrained at present.

Data from the stress file were also used to produce a map of stress orientations to be included in a Geodynamic Map of the Circum-Pacific Map Series together with free-air gravity, seismicity, and focal mechanism data. George Moore, U. S. Geological Survey, is Chief coordinator of the map.

2. A gently westward-dipping detachment surface has been shown by the COCORP seismic reflectin data to be concealed at depth beneath a broad area of west-central Utah. This detachment surface separates large-magnitude brittle extension above from a seemingly stable underlying block. Recently acquired seismic reflection profiles have been interpreted together with well, gravity, and previously published reflection data (McDonald, 1976), to help define both the shallow structure of the detachment surface and the upper-plate extensional structure in the Sevier Desert area. An updip projection of the detachment surface intersects the ground surface near the east edge of the Sevier Desert, along the west margins of the Pavant and Canyon Ranges. The detachment surface dips 3°-7° W beneath the Sevier Desert and reaches a maximum depth of about 12 km near the Cricket and Drum Mountains, which form the west margin of the Sevier Desert. Onstrike reversal in dip of normal fault zones along the west margin require transverse zones within the upper plate. An analysis of the stratigraphy in one deep well in the Sevier Desert indicate that extensional block faulting of the upper plate began during late Miocene time (Lindsey and others, 1981) and was preceded by a broad late Oligocene evaporite basin which was possibly related to earlier movement on the detachment. Occurrence of Quaternary and Holocene fault scarps in the Sevier Desert (Bucknam and Anderson, 1979) along fault zones that merge downward into the detachment surface suggests recent movement on that surface. A tentative correlation of upper-plate pre-Tertiary rocks with those exposed in ranges to the east of the Sevier Desert indicates a minimum displacement of 45 km on the detachment surface. Preliminary analysis of available well data suggests that the detachment does not coincide with any of the major thrust faults mapped to the east of the Sevier Desert.

3. A review of seismic reflection data from the Great Basin indicates three general modes of modern basin formation: (A) relatively simple asymmetric sags bounded by one or more major steep (60°) planar normal faults, (B) tilted ramps associated with moderately to deeply penetrating listric normal faults, and (C) assemblages of complexly deformed subbasins associated with both listric and planar normal faults that sole into a gently dipping detachment surface. Faults of each mode are known to be active, as evidenced by historical, Holocene, or lateset Pleistocene surface ruptures. Reflection data from north-central Nevada indicate that many of the high temperature hot spring systems in this area are situated along normal fault zones bounding basins of mode A. The concentration of geothermal activity in both north-central and northwestern Nevada coincides generally with a region of higher than normal heat flow for the province and a relatively high rate and density of Quaternary faulting and seismicity. These facts, together with the obervation that most hot springs occur along range-front fault zones, have led to the popular interpretation that these hot-spring systems probably are large the result of metoric water circulating along the relatively steep fault zones to moderate depths (3-5 km) in the warm crust of the area. In contrast, reflection data from central Utah and from the Raft River geothermal area in southwesetern Idaho indicate that some of the geothermal systems in these regions are associated with basins and faults of mode C, important components of which are low-angle (5°-35° dip) detachment faults at depths of less than 4 km. The transport of both geothermal water and magma across these detachment faults however, implies structural continunity between the upper and lower plates. Quaternary faulting is also prevalent in the central Utah geothermal systems; however, in contrast to central Nevada, many of the Utah geothermal areas (excluding the Raft River area) are related to young volcanic features.

4. As part of a collaborative effort on Transect C-2 of the U. S. Geodynamics Program, the investigator compiled and interpreted gravity and magnetic profiles and crustal structure across the Northern Great Basin and Colorado Plateau.

Reports

Zoback, M. L., 1983a, Shallow structure of the Sevier Desert detachment, Geological Society of America, Abstracts with Programs: v. 15, no. 5, p. 287.

Zoback, M. L., 1983b, Structural style along the Sevier frontal thrust zone in central Utah: Geological Society of America, Abstracts with Program: v. 15, no. 5, p. 377.

Zoback, M. L. and Anderson, R. E., 1983, Style of Basin-Range faulting as inferred from seismic reflection data in the Great Basin, Nevada and Utah: Geothermal Resources Council Transactions, in press.

Zoback, M. L., Nishenko, S. P., Richardson, R. M., Hasegawa, H. S., and Zoback, M. D., 1983, Mid-plate stress, deformation, and seismicity, in Vogt, P. R., and Tucholke, B., eds., Decade of North American Geology, North Atlantic volume, in press.

Physical Constraints on Source of Ground Motion

9910-01915

D. J. Andrews
Branch of Engineering Seismology
U.S. Geological Survey
345 Middlefield Road, MS 77
Menlo Park, California 94025
(415) 323 8111 ext. 2752

Investigations

A numerical boundary integral (Green function) method is being adapted for use with a generalized frictional sliding law on a fault plane.

Results

The numerical boundary integral method used by Hamano and Das for calculating dynamic brittle crack growth can be adapted for use with any frictional sliding law on a plane interface in an elastic medium. Two unknown functions on the fault plane, slip u and traction T, are determined by two relations between them, (1) the response of the elastic half spaces on each side of the fault plane and (2) the frictional constitutive law of the fault plane. In each element of the fault plane at each time step the Das-Hamano method provides a linear relation between slip and traction,

$$u + C\,T = L$$

where the "local compliance" C is the discretized Green function at the source point, and the "load" L is the convolution of the discretized Green function with past values of traction. Any constitutive relation between slip and traction can complete the solution.

For each element of the fault plane the logic for starting and stopping slip is handled by analogy to plastic yielding. Implementation of this logic requires that slip be saved from the immediately preceding time step. A trial value of traction is found assuming no increment in slip in the current time step, and this is the solution if the frictional traction is not exceeded. Otherwise slip is incremented so that traction equals the frictional traction. Frictional traction may be a function of slip, slip rate, or slip history, as in Ruina's friction law with memory. Calculations with slip- weakening friction in plane strain confirm results I found previously by a finite difference method. Calculating spatial convolutions via Fourier transforms reduces computer time by a large factor.

Report

Andrews, D. J., 1983, On combining the Das-Hamano numerical method with a generalized frictional sliding law [abs.]: AGU Fall Meeting.

National Strong Motion Data Center

9910-02085

Lawrence M. Baker
Branch of Engineering Seismology and Geology
U. S. Geological Survey, MS-77
345 Middlefield Road
Menlo Park, California 94025
(415) 323-8111, ext. 2982

Investigations

The goals of the National Strong Motion Data Center are to:

1) Develop a strong capability for processing, analyzing, and disseminating all strong motion data collected on the National Strong Motion Network and portable arrays;

2) Support research projects in the Branch of Engineering Seismology and Geology by providing programming and computer support for computation of numerical models;

3) Provide digitizing and processing capabilities rapidly in the event of an earthquake as an aid to earthquake investigations.

Results

The National Strong Motion Data Center consists of a Digital Equipment Corporation PDP-11/70 minicomputer and associated peripherals running under the vendor supplied real-time operating system, RSX-11M-Plus, and a field deployable LSI-11/23 microcomputer system for locating and plotting aftershock sequences on-site. CPU time used during the 6 month period between April 1, 1983 and September 30, 1983 for the PDP-11/70 was 845 hours--approximately 7 hours per day averaged over a five day work week.

The PDP-11/70 is connected to several smaller computers (including the LSI-11/23) as well as the Office VAX-11/780 for file transfers, remote file access, and remote terminal access across the network. Real-time data are transmitted across this network to maintain up-to-date records of seismic activity on the larger office computers for interactive inquiry and analysis.

Data collected during this six month period were from the strong motion experiment in the Anza desert in southern California (approximately 150 events), the aftershock sequence in New Brunswick, Canada (approximately 150 events), and the aftershock sequence from the Coalinga, California earthquake (approximately 26,000 records from 1,500 events).

Reports

None.

Office of Earthquakes, Volcanoes, and Engineering Analysis Center

9910-03430

Lawrence M. Baker

Branch of Engineering Seismology and Geology
U. S. Geological Survey, MS-77
345 Middlefield Road
Menlo Park, California 94025
(415) 323-8111, ext. 2982

Investigations

The objective of this project is to provide computer support of research projects in the Office of Earthquakes, Volcanoes, and Engineering (OEVE). The OEVE/VAX Analysis Center consists of a Digital Equipment Corporation VAX-11/780 minicomputer and associated peripherals. The facility serves a diverse user community from all the branches in the OEVE in Menlo Park. Users have access to VAX Fortran, VAX PL/1 and VAX C compilers for executing their programs.

Results

There are 180 user accounts on the VAX-11/780. From April 1 to September 30, the average number of CPU hours used per day was 6.3.

Reports

None.

H6

INVESTIGATION OF REGIONAL MOMENT-MAGNITUDE RELATION AND SHEAR WAVE ATTENUATION IN ALASKA FROM CODA WAVE SEISMIC DATA

3-9900-01268

N. N. Biswas
Geophysical Institute
University of Alaska
Fairbanks, Alaska 99701

K. Aki
Department of Earth, Atmospheric and Planetary Sciences
Massachusetts Institute of Technology
Cambridge, Massachusetts 02139

SUMMARY

The effects of multiple scattering on coda waves have been investigated by an extension of the single scattering theory. The contributions to the coda power due to multiple scattering from a uniform distribution of isotropic scatterers in two and three-dimensional infinite elastic media have been numerically evaluated. The results show that at longer lapse time (time measured from the origin time) the effects of multiple scattering need to be considered. These effects start to become important at the lapse time $t_c = 0.65\ (n_0\ \sigma\ u)^{-1}$ in three-dimensional medium compared to $t_c = 0.8\ (n_0\ \sigma\ u)^{-1}$ for two-dimensional medium. Here n_0, σ and u are the number of scatterers in unit area, average cross section of scatterers and velocity of the medium respectively.

The coda wave studies further extended to the analysis of data. In these studies, coda amplitude decay rates as a function of lapse time for two moderate size Alaskan earthquakes are related to their known values of seismic moments. This relation is then used to compute seismic moments from coda wave data for a selected group of small earthquakes located in the greater Fairbanks, Alaska seismic zone. The computed values of moment appear to be consistent with the local magnitudes. Next, with the moment and magnitude data, an empirical moment-magnitude relation is obtained for central and southcentral Alaska. This relation is similar to those for central and northern California proposed by others. Computation for Q values in the frequency (f) band 1.03-1.5 Hz for central and southcentral Alaska with local coda wave data yielded values in the range from about 160 to 290. The minimum of Q(f) appears to be in the frequency interval from 0.5 to 1.5 Hz. Moreover, Q values (f = 1 Hz) in the above range have been recently reported by others for areas in the western United States having similar tectonic history as the Alaskan study area.

References

Gao, L. S., L. C. Lee, N. N. Biswas and K. Aki, 1983. Comparison of single multiple scattering effects on coda waves, Bull. Seism. Soc. Am., 73, 377-389.

Gao, L. A., N. N. Biswas, L. C. Lee and K. Aki, 1983. Effects of multiple scattering on coda waves in three-dimensional medium, in press.

Biswas, N. N. and K. Aki, 1983. Characteristics of coda waves: central and southcentral Alaska, in press.

Global Accelerograph Program (GAP)

9910-02689

R. D. Borcherdt
Branch of Engineering Seismology and Geology
U. S. Geological Survey
345 Middlefield Road, MS-77
Menlo Park, California 94025
(415) 323-8111, ext. 2755

Investigations

The objective of this program is to obtain critically needed records of damaging levels of ground motion close to the source of earthquakes of magnitude M 6.5 and greater.

During the second half of FY 83, the following activities were carried out:

(1) Negotiation of formal GAP agreements with counterpart agencies in countries with significant earthquake potential was continued.

(2) Field deployments of a General Earthquake Observation System (GEOS) were carried out near New Castle, New Brunswick, and Newcombe, New York.

Results

The prototype GAP agreement developed for the program identifies the following primary activity elements: (1) continued long-term strong-motion data and information exchange between the U. S. Geological Survey and the agency(ies) identified in the host country; 2) the rapid exchange (preferably as soon as possible--within 1-4 days following damaging events) of scientific teams to investigate engineering and scientific effects of large earthquakes in the U. S. and the host country; and 3) the rapid deployment of U. S. personnel and instruments to the host country after a large earthquake (M 7.5 and greater) has occurred to record large (M 6.5 and greater) aftershocks. In some cases, the installation and long-term operation of a permanent network of strong-motion instruments in the host country shall also be considered under the agreement.

(1) Negotiation of agreements is proceeding, but not as quickly as desired. Changes in foreign government officials has in some cases required renegotiation of agreements.

(2) Final modifications of GEOS based on field deployment experience are being incorporated.

(3) Wide dynamic range, broad frequency band-width data sets were collected near New Castle, New Brunswick, and Newcombe, New York using the General Earthquake Observation System (GEOS). An example is attached.

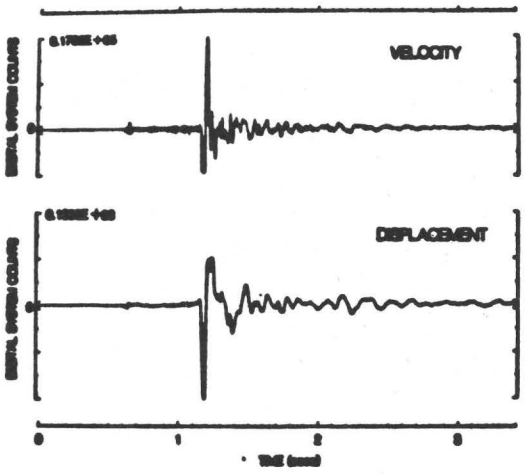

Figure 1. Velocity (upper trace) and inferred displacement (lower trace) for a small aftershock recorded in New Brunswick, Canada. Velocity trace was recorded at 1200 sps.

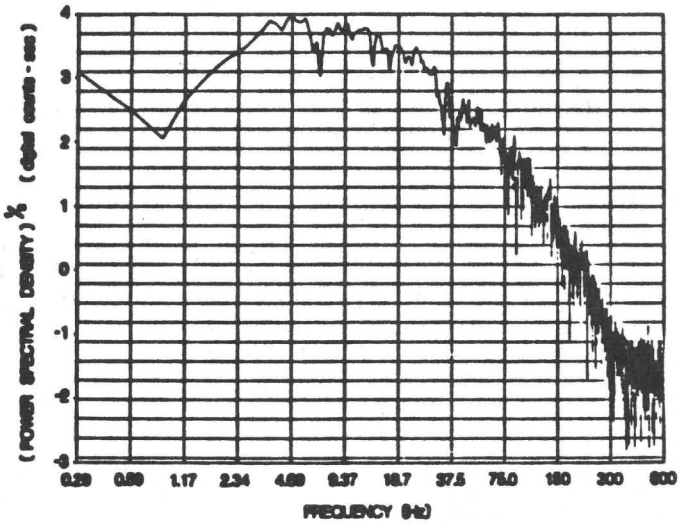

Figure 2. Displacement spectra computed for lower trace. Frequency bandwidth (600 Hz Nyquist) and dynamic range (>90 dB) of signal recorded on GEOS are indicated.

Reports

Maxwell, G. L., Jensen, E. G., Borcherdt, R. D., Fletcher, J. P., McClearn, R., Van Schaack, J. R., and Warrick, R. E., 1983, GEOS [abs.]: American Geophysical Union Fall Meeting, December 5-14, 1983, San Francisco, California.

Borcherdt, R. D., Jensen, E. G., Maxwell, G. L., Fletcher, J. P., McClearn, R., Van Schaack, J. R., and Warrick, R. E., 1983, A General Earthquake Observation System (GEOS) [abs.]: Workshop on Portable Digital Seismograph Development, Los Altos, California, October 1983.

Borcherdt, R. D., Mueller, C. S., and Wennerberg, L. G., 1983, Effects of Local Geological Conditions on Strong-Ground Motions in the Vicinity of Coalinga, California: Workshop on "Site-Specific Effects of Soil and Rock on Ground Motion and the Implications for Earthquake-Resistant Design": Santa Fe, New Mexico, July 26-28, 1983.

Nonlinear Soil Response at Imperial Valley Recording Sites

9910-03390

Albert T. F. Chen
Branch of Engineering Seismology and Geology
U.S. Geological Survey, MS-74
345 Middlefield Road
Menlo Park, CA 94025
(415) 323-8111, Ext. 2605

Investigations

(1). Completed a parametric study of seismic response at Stations 6 and 7 of the El Centro Strong Motion Array.

(2). Initiated a study of using an effective stress approach for computation of nonlinear response of sand deposits during earthquakes and for assessment of liquefaction potential.

Results

(1). In order to reach the recorded peak accelerations during the 1979 Imperial Valley earthquake, the strength values used in nonlinear response analyses would have to equal or exceed twice the strength values determined from static triaxial test results or cone penetration records.

(2). Transmitting boundary conditions are helpful and often used in estimating seismic response of very thick sediments. However, in nonlinear response analyses, cautions must be exercised in assigning a transmitting boundary so that the assumption of having an elastic half-space as the base can be justified. Analyses of response at Stations 6 and 7 suggested that the boundary should be located at the depth with the highest strength value rather than at the depth with the highest contrast in accoustical impedance.

Reports

There were no reports this period.

Hybrid Ray-Mode Method for Synthetic Seismology

Contract No. 14-08-0001-20572

Leopold B. Felsen
Department of Electrical Engineering and Computer Science
Microwave Research Institute
Polytechnic Institute of New York
Farmingdale, NY 11735
(516) 454-5073

Investigations

1. In an asymptotic ray theory (ART) program for SH motion at the surface of a two-layer earth model consisting of a sediment, whose velocity profile increases monotonically with depth, above a homogeneous semi-infinite bedrock, the failure along transitional rays was repaired through replacement of these ray fields by groups of modal fields. The transitional ray fields were of three types: a) caustic forming rays guided along the sediment surface without encountering the bottom; b) the bottom glancing ray; c) the critically reflected ray.

2. A reference solution was generated by numerical evaluation of the exact generalized ray integrals for the transitional rays.

Results

1. Comparison of ART with the reference solution confirmed the failure of the former in the various transitional ranges.

2. Modal substitution for the caustic forming and bottom glancing rays was found to repair the ART deficiency and to be numerically more efficient than computation of the generalized ray integrals.

3. For the critically reflected ray, modal substitution also worked, but in a numerically less efficient manner than direct computation of the generalized ray integral. However, this circumstance may be due to the fact that for the parameters used in the calculation, the critically reflected and bottom glancing rays happened to be in close proximity.

4. The calculations established the validity of the modal substitution method and its greater numerical efficiency, at least for two types of transitional rays, when compared with direct computation of the generalized ray integral.

Reports

A final report is in preparation.

Strong Ground Motion Studies
Application to Puget Sound

Contract No. 14-08-0001-21306

David M. Hadley and George R. Mellman
Sierra Geophysics, Inc.
15446 Bell-Red Road
Redmond, WA 98052
(206) 881-8833

Investigations

The Puget Sound region is a metropolitan area with a potentially significant earthquake hazard. Earthquakes of magnitude 7.1 (1949) and 6.5 (1965) have occurred in the immediate vicinity at depths of 50-60 Km. Given the tectonic setting of the region it is impossible to exclude the possibility that larger events will affect the region in the future.

The ground response at a particular site is dependent upon the characteristics of the source, gross path propagational effects and near site response. Past modeling studies of the strong ground records from the 1965 earthquake (Langston, 1981) demonstrate that the three-dimensional geologic structure of this region profoundly affects the observed motions. Hence, the first goal of this study is to develop and assess the adequacy of current three-dimensional geologic structural models for use in modeling the observed motions from the 1965 event (both recorded motions and isoseismal distribution). Assuming the geologic model can be refined to the point of adequately predicting past experience, the second goal is to estimate the expected ground response from earthquakes spanning a range of hypocentral locations and magnitudes.

Results

The first step in this project is an extensive review of the geological and geophysical literature to develop the best possible model for the region. This work is currently in progress. We expect to begin developing a digital three-dimensional model within the next month. The principal elements of the model include: (1) Low velocity surficial sediments (fill and recent alluvium); (2) Higher velocity, compacted glacial tills; (3) Basement; (4) Mid crustal and moho horizons. The digital model will contain the topography of each geologic layer and the estimated velocities, densities and attenuation (damping).

After developing a digital geologic model we will use an extensive raytracing package developed at Sierra to model wave propagation (both P and S) in a three-dimensional geologic structure. As an example of this modeling, Figure 1 shows a single interface (basement topography, depth ~ 1 Km) and a seismic source located at a depth of 8 Km. The raypaths show the bounce points of the first internal reflection. Figure 2 shows the synthetic seismogram for the direct arrival and the first

few multiples. A simple wavelet has been convolved with the impulse response at each station. This figure illustrates several important observations. By noting the arrival times of the direct phase, it is clear that station 6 is at the closest epicentral distance to the source. Nonetheless, despite geometrical spreading, the direct arrival at the more distant first station is nearly twice as large. This results from the effects of focusing by geologic structure. The large second arrival (first multiple) illustrates the effects of critical reflections within the basin. Note the phase shift that occurs between stations 11 and 12 and the very large near-critical reflections at stations 16-18. These modeling results are in good agreement with many observations that three-dimensional geologic structure introduces significant variations (factors of 2-3) in the amplitude and duration of strong ground motions. This modeling package will be used to model the observed strong ground motions in the Puget Sound region.

References

Langston, C.A., 1981, A Study of Puget Sound Strong Ground Motions, Bull. Seis. Soc. Am., 71, 883-904.

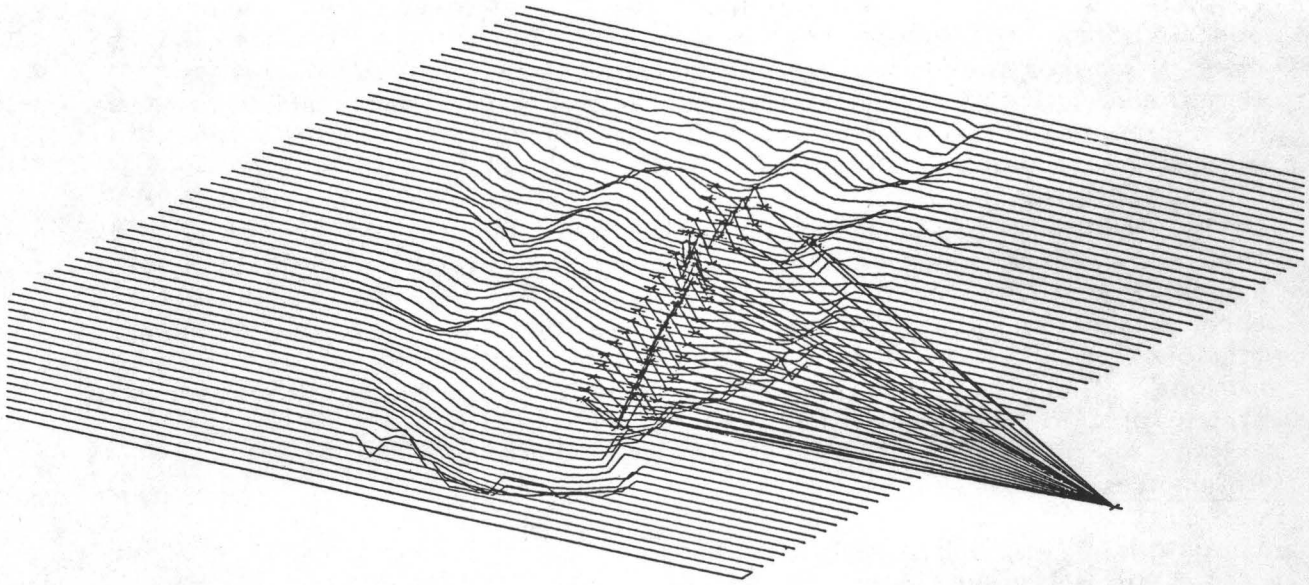

Figure 1. First multiple raypaths from earthquake source to a profile of receivers. The small X's on each ray shows the point where each raypath enters the sedimentary layer, reflects at the surface, the basement, and stops at the receiver.

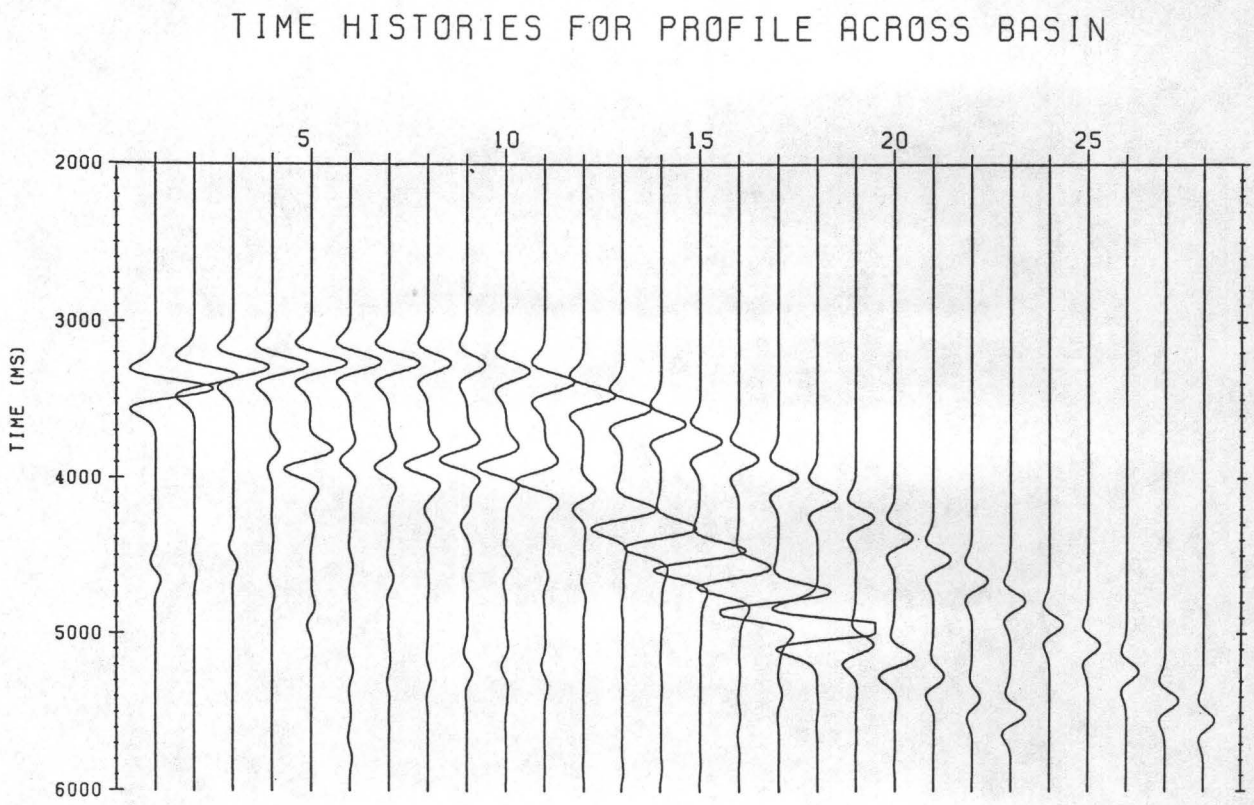

Figure 2. Synthetic seismograms for the direct and first few multiple reflections for the profile shown in Figure 1. Note the large amplitudes and phase shifts of the secondary arrivals.

Estimating Strong Ground Motion for Engineering Design and Seismic Zonation

9910-01168

W. B. Joyner
D. M. Boore

Office of Earthquake Studies
Branch of Engineering Seismology and Geology
U. S. Geological Survey, MS-77
345 Middlefield Road
Menlo Park, California 94025
(415) 323-8111, ext. 2754, 2698

Investigations

1. Analysis of strong-motion data leading to the development of predictive equations for strong-motion parameters and development of methodology for making predictive maps of strong ground motion.

2. Cooperation with professional groups in the development of code provisions for earthquake resistance.

3. Study of the scaling of earthquake spectra.

Results

1. We have developed a scaling law for earthquake spectra that is applicable above the critical moment corresponding to rupture of the entire width of the seismogenic zone. Below the critical moment the proposed scaling law agrees with the Hanks-McGuire model, which has had impressive success in predicting measures of strong ground motion over a broad range in moment magnitude. The predictions of the proposed law are consistent with strong-motion data for shallow earthquakes in Western North America, within the scatter of the data and the uncertainty of the parameters of the proposed law.

Reports

Boore, D. M., and Joyner, W. B., 1983, Ground motions and response spectra at soil sites from seismological models of radiated spectra: Workshop on "Site-Specific Effects of Soil and Rock on Ground Motion and the Implications for Earthquake-Resistant Design": Santa Fe, New Mexico, July 26-28, 1983.

Seismological Field Investigations

9950-01539

C. J. Langer
Branch Engineering Geology and Tectonics
U.S. Geological Survey
Denver Federal Center, MS 966
Denver, CO 80225
(303) 234-5091

Investigation

North Yemen aftershock study--regional investigation of aftershocks resulting from the magnitude 6.0 (m_b, M_s) earthquake of December 13, 1982.

Results

The magnitude 6.0 Yemen earthquake of December 13, 1982, occurred in a densely populated area of the southwestern Arabian Peninsula, about 75 km south of Sanáa, capitol city of the Yemen Arab Republic (YAR). Because of the widespread destruction throughout much of Dhamār province; accounts of thousands dead, injured, and homeless; and various reports of ground fissuring and possible volcanic activity, the Ministry of Petroleum and Mineral Resources, Kingdom of Saudi Arabia, organized a post-earthquake investigations team to study the earthquake and its effects. The U.S. Geological Survey was requested to participate in this effort and was responsible for the installation and operation of 11 portable seismographs to monitor and locate the aftershocks and compute their source parameters. During the period between December 29, 1982, and January 11, 1983, 14 sites that surrounded the epicentral region were occupied and several thousand aftershocks were recorded at all stations. The unusually high level of seismic activity observed after more than 2 weeks following the main shock was completely unexpected and provided an excellent data set for locating about 250 aftershock hypocenters. The principal aftershock zone lies between Mábar and Dhamār, is approximately 17 km long, 10 km wide, and trends roughly N. 25° W. Depth of the hypocenters generally range from near surface to 7 km. The aftershock trend is in good agreement with the strike of observed extensional cracking as documented by George Plafker.

Four composite fault plane solutions (CFPS) were computed for subzones of the aftershock region using short-period P-wave first-motion data. All of these CFPS's indicate normal faulting along northwest-striking fault planes. In each case the axes of maximum compressive stress (pressure axes) are oriented near vertical and the axes of minimum compressive stress (tension axes) are near horizontal and strike northeast-southwest. Thus, the dominant active tectonic process throughout the aftershock region is normal faulting in response to the northeast-southwest extension that is consistent with and may be related to the relative movement of the Arabian plate to the northeast, away from the Nubian plate to the west and Somalian plate to the south.

Reports

Bollinger, G. A., Adams, M. J., Henrisey, R. F., and Langer, C. J., 1983, The Denver earthquake sequence of March-April, 1981: Earthquake Notes (in press).

Langer, S. J., and Merghelani, H. M., 1983, Aftershocks of the Yemen earthquake of December 13, 1982--A detailed study from locally recorded data [abs.]: Earthquake Notes, v. 54, no. 1, p. 20.

Richins, W. D., Arabasz, W. J., and Langer, C. J., 1983, Episodic earthquake swarms ($M_L \leq 4.7$) near Soda Springs, Idaho, 1981-1982--Correlation with local structure and regional tectonics [abs.]: Earthquake notes, v. 54, no. 1, p. 99.

Spence, W., and Langer, C. J., 1984, The seismic gap filling, 1974 Peru aftershock series represents a well-ordered process of stress release: Journal of Geophysical Research (in press).

Effect of Lateral Heterogenieties on Strong Ground Motion

14-08-0001-21257

C.A. Langston
440 Deike Building
Department of Geosciences
The Pennsylvania State University
University Park, PA 16802
(814) 865-0083

Investigations

1. Simulation of high frequency strong ground motions over plausible three-dimensional geologic structure is being performed using a ray tracing method. The scheme for tracing rays is being modified to include point sources in or near the structure of interest.

2. Calculation of strong ground motions over models of geologic structures in the Puget sound area for shallow sources is being performed to compliment previous simulations involving deep sources.

3. A study of anomalous site effects in the Pasadena, California area for the San Fernando earthquake is underway to examine the role of incidence angle and azimuth on amplification using the ray technique.

Results

Theoretical work has been completed on algorithms needed to modify the existing incident plane wave ray tracing technique to include dislocation point sources. We are also proceeding to investigate the "Gaussian beam" technique for calculating amplitudes, particularly near caustics. This technique shows much promise in cutting computational expense since an exact ray trace is not needed.

Reports

Lee, Jia-Ju, and C.A. Langston. Wave propagation in a three-dimensional circular basin. Bull. Seis. Soc. Am., in press.

Langston, C.A. and Jia-Ju Lee. Effect of structure geometry on strong ground motions: The Duwamish River Valley, Seattle, Washington. Bull. Seis. Soc. Am., in press.

"ESTIMATION OF SEISMIC GROUND MOTION IN NORTHERN UTAH"

Contract No. 14-08-0001-19825
Robin K. McGuire
Dames & Moore
1626 Cole Blvd.
Golden, Colorado 80401
Tel. 303-232-6262

Modified Mercalli (MM) intensity data in the Rocky Mountain Region provide a starting point for estimating strong ground motion in northern Utah. The available intensity data are used to calibrate attenuation equations in which site intensity near the source is constrained to equal preselected values. California strong motion data provide correlations between peak parameters (ground acceleration, ground velocity, and spectral velocity), MM intensity, and distance. These correlations, when combined with the region-specific MM intensity attenuation relation, yield quantitative estimates of ground motion which are generally consistent with other studies. The estimates are also consistent with the one available strong motion record for the northern Utah region.

Post-Earthquake Shaking Effects and Fault Creep

9910-03027

Robert Nason
Branch of Engineering Seismology and Geology
U. S. Geological Survey, MS-77
345 Middlefield Road
Menlo Park, California 94025
(415) 323-8111, ext. 2760

Investigations

1. The literature of major earthquakes has been examined in order to learn of observations of seismic intensity in fault zones elsewhere in the world.

Results

1. Careful investigations of earthquakes in Algeria, Guatemala, Iran and Turkey have found that the damage to native masonry buildings in the fault zone is approximately the same as the damage at a distance from the fault.

Reports

None.

Strong Ground Motion Focusing in Sedimentary Basins

14-08-0001-21258

J. A. Rial
C. F. Richter Seismological Laboratory
University of California, Santa Cruz
Santa Cruz, CA 95064
(408) 429-4548

Investigations

1. Time and frequency domain reconnaissance analyses of the accelerograms of the 1979 Imperial Valley, Oroville, 1975, and San Fernando, 1971 earthquakes to identify instances of caustics and focusing affecting (amplifying) the ground motion.

2. Quantification of the effects of focusing. Development of computer codes to establish the location and frequency dependence of focusing phenomena due to the lens-like effects of sedimentary basins.

Results

1. All the USGS array stations accelerograms of the Imperial Valley, 1979 earthquake have been analyzed in the time and frequency domains. Special emphasis has been made on the comparative study of the records from station 6 of the Imperial Valley array. Some important results are:

a) The peak vertical acceleration (1.7 g) is more than likely the result of convergence and focusing of P-wave energy at this locality, and not of reverberation. This is at variance with results reported by Mueller et al. (1982), where one of the important points raised concerns the coda amplification at station 6. We believe that only sections of the coda are amplified because small aftershocks are present. These sections are amplified with respect to other sections of the same record, free of aftershocks. Reverberation, as claimed by Mueller et al. (1982), would not produce the strong horizontal components associated with the 1.7 g vertical acceleration peak. It would, besides, lengthen the duration of the strong motion there. The vertical record at station 6 has the shortest duration of all the group of stations in its neighborhood. The resonant peaks causative of the 13-15 Hz reverberations are indeed observed in the spectrum, but they are not associated with the peak acceleration. The 1.7 g acceleration peak occurs at 9 hz. The Fourier spectrum of the vertical component at station 6 shows a marked increase in spectral amplitude starting at about 1 Hz and culminating at 9 Hz. This build-up of spectral energy is typical of caustics, not of isolated reverberation or resonant peaks.

b) Particle motions (hodographs) have been analyzed as a function

of frequency and reveal the fact that most if not all the energy arriving at the time of the 1.7 g peak is a P-wave. By band-pass filtering the accelerograms, the main shock P, SV and SH arrivals are clearly identified. Their polarization is in perfect agreement with the focal mechanism.

c) Accelerograms from the Oroville, 1975 earthquake processed so far show strong variations in waveform and frequency content that appears controlled by the geological setting of the recording station. Records from the San Fernando, 1971 earthquake are currently being processed.

2. A computer code has been developed to trace rays across three dimensional heterogeneous media with irregular boundaries. The display of the results is being worked out presently in order to apply it to Los Angeles basin and Imperial Valley. Computer codes to simulate the effects of sedimentary basins on pulse-like signals have been developed using the Kirchhoff formalism (Scott and Helmberger, 1983). An extension of this code is now being developed to compute synthetic particle motions (hodographs) at places where caustics or focusing occurs. It is hoped that from these synthetic particle motion plots, the shape and possibly the depth of the basin causing the focusing can be estimated.

References

Mueller, C. S., D. M. Boore, and R. L. Porcella, 1983, Detailed study of site amplification at El Centro strong-motion array station 6, Proc. of the Third Int. Conf. on Earthquake Microzonification, 1, convened Seattle, Washington, 413-424.

Scott, P., and D. V. Helmberger, 1983, Applications of the Kirchhoff-Helmholtz integral to problems in seismology, Geophys. Jour. R. A. S., 72, 237-254.

Strong Ground Motion Prediction in Realistic Earth Structures

9910-03010

P. Spudich/T. Heaton
Branch of Engineering Seismology and Geology
U. S. Geological Survey
345 Middlefield Road, MS-77
Menlo Park, California 94025
(415) 323-8111, ext. 2395

Investigations

1. Investigation of the seismic potential associated with subduction off the coast of Washington and Oregon.

2. A study of the teleseismic body waveforms recorded from the May 2, 1983 Coalinga earthquake.

3. Development of a method for rapid calculation of high frequency body-wave synthetic seismograms for large earthquakes.

Results

1. Although there is good evidence of present-day convergence between the Juan de Fuca and North American plates at a rate of about 3 to 4 cm/year, there are no historic reports of large shallow thrust earthquakes that are usually associated with active subduction zones. Furthermore, there is very little seismicity observed along the shallow portion of the Juan de Fuca subduction zone. These observations have been used by some to conclude that subduction is occurring aseismically and by others to conclude that the plate boundary is presently locked. In order to further investigate these possibilities, we compare the characteristics of subduction of the Juan de Fuca plate with those of other subduction zones. We find that the Juan de Fuca subduction zones shares many features with other subduction zones that experience great earthquakes, while several features indicative of aseismic subduction are absent. The age of the subducted Juan de Fuca plate is very young (10-15 my) and the corresponding characteristics of subduction appear to be typical of the subduction of young lithosphere. Specifically, subduction of young lithosphere is often associated with the following features: (1) shallow-dipping Benioff-Wadati seismicity zone; (2) absence of an active back-arc basin; (3) shallow oceanic trench; (4) the presence of an accretionary prism; (5) up-lift of the overthrusting plate; (6) temporal seismic quiescence; (7) and finally, the occurence of very large shallow subduction earthquakes. All features, except the last, appear to be present for the Juan de Fuca subduction zone. Thus, we feel that there is sufficient evidence to warrant further study of the possibility of a great subduction zone earthquake in the Pacific Northwest.

2. Long-period, vertical P-waves from 15 WWSSN and Canadian stations in the distance range from 30° to 90° were modeled to obtain estimates of the source parameters for the May 2, 1983 Coalinga earthquake. The best

fitting focal mechanism is: Strike = 297 ± 5°, dip = 64 ± 1°, rake = 70 ± 10°. The moment is estimated to be 3.8 ± 1.5 x 10^{25} dyne-cm with a rupture duration of 5 ± 1 sec. The depth is estimated at 12 ± 2 k.m. The emergent character of the teleseismic short-period P-waves suggests that the rupture started with a 2 sec. interval of less energetic faulting.

3. In collaboration with L. N. Frazer of the Hawaii Institute of Geophysics, we have developed a method for using ray theory to calculate high frequency body-wave synthetic seismograms for large earthquakes. If one assumes that most of the high frequency seismic waves generated by an earthquake originate at the rupture front, and if one further assumes that direct body waves such as P and S carry most of this energy, then synthetic seismograms may be calculated by doing a series of line integrals on the fault plane, rather than the usual surface integrals that are typically done. The theory describing this method may be applied in laterally varying media. We have written computer codes which use this method for arbitrarily complicated earthquake ruptures in laterally homogeneous media. Initial tests using a Haskell fault model in a whole space and a quasidynamical source in a vertically varying media give excellent results. When completed, this method may be a powerful and economical tool for predicting high frequency earthquake ground motions in geologically complex (i.e. realistic) structures.

Reports

Heaton, T. H., and Kanamori, H., (1983). Seismic potential associated with subduction in the northwestern United States, Earthquake Notes, 54, no. 2.

Heaton, T. H., and Kanamori, H., (1983). Subduction in the northwestern United States seismic or aseismic? EOS, 64, no. 45.

Hartzell, S. H., and Heaton, T. H., (1983). Teleseismic mechanism of the May 2, 1983 Coalinga, California, earthquake from long period P-waves, CDMG Special Report, the 1983 Coalinga, California earthquake.

Spudich, P., and Frazer L. N., 1983, High frequency synthetic seismograms for earthquakes: theory and examples [abs.]: American Geophysical Union Fall Meeting, December 5-10, 1983, San Francisco, CA.

Aftershock Investigations and Geotechnical Studies

9910-02089

Richard E. Warrick
Eugene D. Sembera

Branch of Engineering Seismology and Geology
345 Middlefield Road, MS 77
Menlo Park, CA 94025
(415) 323-8111, ext. 2757

Investigations

1. The development of techniques for the improvement of field data acquisition, specifically in the application of triggered digital recording systems to aftershock studies.

2. Improvement in the methods used in generating recording and interpretation of shear waves in downhole surveys.

Results

1a. Gene Sembera continued to maintain, install and operate the DR-100 and GEOS recording systems. Field deployment included the Coalinga aftershock series in May (Borcherdt), the New Brunswick, Canada experiments in July (Cranswick), the Massachusetts experiments in August (Liu) and the New Mexico-Nevada tests in September (King).

1b. Coyn Criley assisted Bob McClearn, Gray Jensen and others in assembling GEOS systems and in field investigations at Coalinga.

2a. A trigger circuit was developed for the Nimbus System to reduce false triggers and to improve trigger time stability.

2b. A scouting and permitting trip to the Mammoth Lakes region was made with Archuleta to locate a site for the deep borehole in the McGee Creek area.

Reports

Maxwell, G. L., Jensen, E. G., Borcherdt, R. D., Fletcher, J. P., McClearn, R., Van Schaack, J. R., and Warrick, R. E., 1983, GEOS [abs.]: American Geophysical Union Fall Meeting, December 5-14, 1983, San Francisco, CA.

Development of a Liquefaction Potential Map for Salt Lake County, Utah

Contract No. 14-08-0001-19910

Loren R. Anderson
Department of Civil & Environmental Engineering
Utah State University
Logan, UT 84322
(801) 753-5119

Jeffrey R. Keaton
Dames & Moore
250 East Broadway
Suite 200
SLC, UT 84111
(801) 521-9255

As part of the U.S. Geological Survey's Earthquake Hazard Reduction program a "Liquefaction Potential Map" has been prepared for Salt Lake County, Utah. Liquefaction potential was evaluated from existing subsurface data and from a supplementary subsurface investigation performed as one of the tasks in this study. All of the data used in this study are summarized on base maps of the study area.

The liquefaction potential is classified as high, moderate, low and very low depending on the probability that a critical acceleration will be exceeded in 100 years. The critical acceleration for a given location is defined as the lowest value of the maximum ground surface acceleration required to induce liquefaction. The categories of high, moderate, low and very low correspond to probabilities of exceeding the critical acceleration in the ranges of greater than 50 percent, 10 to 50 percent, 5 to 10 percent and less than 5 percent, respectively.

The critical acceleration was computed using the method proposed by Seed (1983). This method is based on a correlation between the standard penetration test and the cyclic shear stress ratio required to cause liquefaction. Standard penetration blow counts were adjusted to account for the silt content in liquefaction susceptible soils.

The soil data and standard penetration data were obtained from the results of previous subsurface investigations as well as from a supplementary investigation that was conducted as part of this study. The supplementary investigation included both conventional soil borings with standard penetration tests and cone penetrometer tests. Fifty four cone penetrometer soundings were made throughout the study area. A number of these soundings were located adjacent to borings where standard penetration tests were performed so that a correlation could be made between the cone penetrometer test and the standard penetration test.

In the process of assessing the liquefaction potential in Salt Lake County four maps were developed and presented in the final report: (1) Soil

Data and Ground Water Map, (2) Critical Acceleration and Ground Slope Map, (3) Geologic Ground Failure Map and (4) Liquefaction Potential Map. These maps summarize all of the pertinent data that was obtained as well as the final results of the study.

Although the liquefaction potential was defined on the basis of the critical accelerations calculated from the results of standard penetration tests and cone penetrometer tests an interpretation of the surficial geologic conditions was required to draw the final boundaries delineating areas of high, moderate, low and very low liquefaction potential.

The Liquefaction Potential Map of the final report shows that for a significant portion of Salt Lake County the probability of exceeding the critical acceleration in 100 years is greater than 50 percent. Hence, liquefaction induced ground failure is a significant seismic hazard.

Development of a Liquefaction Potential Map for Utah County, Utah

Contract No. 14-08-0001-21359

Loren R. Anderson
Department of Civil & Environmental Engineering
Utah State University
Logan, UT 84322
(801) 753-5119

Jeffrey R. Keaton
Dames & Moore
250 East Broadway
Suite 200
SLC, UT 84111
(801) 521-9255

A liquefaction potential map is being compiled for Utah County, Utah. The map is being developed from existing data that is available in the files of private consulting firms and government agencies . The existing data will be supplemented by drilling test borings and making cone penetrometer soundings.

Standard penetration test (SPT) results have been obtained from soil boring data. The blow count, N_1, corrected to an overburden pressure of 1 Ton/ft^2, and the relationshp proposed by Seed (1983) are being used to obtain the cyclic stress ratio, $(\tau/\bar{\sigma}_o)$, required to cause liquefaction. The critical acceleration (that required to cause liquefaction), can then be computed by the method suggested by Seed (1983).

$$a_{max} = \frac{\left(\frac{\tau_{ave}}{\bar{\sigma}_o}\right)}{\left(\frac{\bar{\sigma}_o}{\sigma_o}\right)} \left(\frac{g}{0.65 r_d}\right)$$

where,

a_{max} = maximum acceleration at ground surface

$\left(\frac{\tau_{ave}}{\bar{\sigma}_o}\right)$ = cyclic stress ratio required to cause liquefaction

σ_o = total overburden pressure on sand layer under consideration

$\bar{\sigma}_o$ = effective overburden pressure on sand layer under consideration

r_d = a stress reduction factor varying from a value of 1.0 at the groundsurface to 0.9 at a depth of 30 feet

For silt and silty fine sand it is necessary to correct the SPT blow count to account for the influence of the fines on the blow count and the

liquefaction susceptibility. this correction is applied by the method suggested by Seed (1983).

The liquefaction potential will be classified as high, moderate, low and very low depending on the probability that the critical acceleration will be exceeded in 100 years. The critical acceleration for a given location is defined as the lowest value of the maximum ground surface acceleration required to induce liquefaction. The categories of high, moderate, low and very low correspond to probabilities of exceeding the critical acceleration in the ranges of greater that 50 percent, 10 to 50 percent, 5 to 10 percent and less than 5 percent, respectively.

After the critical acceleration have been computed and plotted on a map for all boring and penetrometer sounding locations, boundaries will be drawn delineating zones of high, moderate, low and very low liquefaction potential. In establishing the boundaries consideration will be given to the geologic conditions throughout the area.

All boring locations have been digitized and stored on magnetic tape along with the boring log information. This information will be used to produce computer generated maps that summarize the data.

In assessing the Liquefaction Potential in Utah County, Utah, four maps will be developed: (1) Soil Data and Ground Water Map, (2) Critical Acceleration and Ground Slope Map, (3) Geologic Ground Failure Map and (4) Liquefaction Potential Map. The Liquefaction Potential Map will identify areas of high, moderate, low and very low liquefaction susceptibility, and will be used in conjunction with the soil data and ground slope maps to suggest the most likely type of liquefaction induced ground failure.

Seismic Slope Stability

9950-03391

David K. Keefer
U.S. Geological Survey
Branch of Engineering Geology and Tectonics
345 Middlefield Road MS 98
Menlo Park, California 94025
(415) 856-7115

Investigations

1. Continued development of quantitative methods for predicting earthquake-induced landslides on a regional scale.

2. Conducted field investigation of landslides following the May 2, 1983, Coalinga, California earthquake.

3. Conducted studies and hazard evaluations of debris flows and other landslides caused by high precipitation and rapid snowmelt along the Wasatch Front in Utah.

4. Conducted reconnaissance in the Mammoth Lakes, California area to locate a site for simultaneous monitoring of strong motion and dynamic pore pressures in saturated alluvial sediments from earthquakes on the boundary of the Long Valley Caldera. The site chosen was situated near the zone of seismic activity that began in January 1983, near Sherwin Creek, and on an active alluvial plain underlain by saturated sands more than 10 m deep.

5. As a continuation of work on earthquake-induced landslides in the New Madrid seismic zone, conducted field investigation in western Tennessee and Kentucky. The goals of this field investigation were 1) to field-check airphoto landslide inventory map; 2) to observe geomorphic and stratigraphic relationships; and 3) to investigate and describe in detail selected landslides for analysis.

Results

1. In our previous work, we have developed quantitative measures of the stability of slopes under seismic conditions. We have also devised methods for estimating the probability of failure of slopes of a given stability as a function of the severity of seismic shaking as measured by strong-motion accelerograph records. However, the development of regional methods for predicting earthquake-induced landsliding has been hampered by the lack of a reliable method for estimating the severity of seismic shaking as a function of earthquake magnitude and source distance. Magnitude/distance relationships have been published for peak acceleration, but the peak acceleration alone is not a reliable predictor of slope failure. To remedy this lack, we have developed an empirical relationship between Arias intensity, an instrumentally based seismic severity measure (previously established as a reliable predictor of slope failure), the source distance, and the size of the earthquake as measured on the moment-magnitude scale.

From the published literature, we compiled the moment-magnitude, source distance, and Arias intensity for 31 strong-motion recordings of California earthquakes. By making certain assumptions, we developed the following relationship:

$$\log I_a = -4.1 + 1.0\,M - 2 \log r$$

where: I_a = Arias intensity (m/s); M = moment-magnitude; and, r = source distance (km). This relation provides the best fit to the strong-motion data with a standard deviation = 0.44. This new empirical relationship can be directly related to our previously developed relationships between I_a and the probability of failure of slopes with given stabilities.

2. The Coalinga earthquake (M=6.5) triggered several types of landslides in the hills northwest of Coalinga. Our reconnaissance showed that the most numerous landslides were rock falls and rock slides. Along Los Gatos Creek, rock falls had volumes of as much as several hundred cubic meters. These rock falls originated in a massive but weakly cemented cliff-forming sandstone in the Panoche Formation. Several rotational slumps also occurred; the largest observed, along Los Gatos Creek about 12 km northwest of Coalinga, was about 200,000 m^3 in volume and involved loose, dry, slightly cemented sand. Several slumps also occurred nearby in the highway fill of Los Gatos Creek Road. Lateral spreading and small sand boils occurred in a few localities in sandbars in Los Gatos Creek. These features, associated with liquefaction, were limited to a sand and silt deposit, 0.6 m thick, that overlies coarse gravel in the river channel. Many cut-and-fill oil-well pads in the Anticline Ridge area north of Coalinga sustained rock and soil falls from the cut slopes and cracks and slumps in the outer edges of the fill forming the pads. Vibrational compaction also created small scarps and cracks around concrete pump aprons.

3. Six piezometers were emplaced at the Mammoth Lakes site at depths from 2.5 m to 20 m in saturated alluvial sediments. The piezometers were emplaced in a circular array 12 m in diameter; they were equally spaced around a circle the center of which will eventually be occupied by a downhole strong-motion accelerometer and a surface accelerometer. The purpose of the permanent site is to record acceleration and pore-water pressure during earthquakes that cause liquefaction in the saturated sandy sediments.

4. Sixty percent of the landslides mapped from airphotos in the New Madrid area were accessible and were field checked. The accuracy of the airphoto map was shown to be good, but significant improvement resulted from this field calibration. Stratigraphic relationships were observed and recorded throughout the field area; samples of each unit were collected for classification and determination of index properties. Profiles of eight landslides were obtained, and three of these landslides were studied in greater detail by hand-augered borings, large-scale mapping of landslide features, and collection of material for dating.

Reports

Harp, E. L., Sarmiento, John, and Cranswick, Edward, Seismic-induced pore-water pressure records from the Mammoth Lakes, California, earthquake sequence of May 25-28, 1980: Submitted to Seismological Society of America Bulletin, 12 p., 8 figs.

Harp, E. L., Wilson, R. C., and Keefer, D. K., 1983, Landslides and related ground failures from the May 2, 1983, Coalinga, California earthquake (abs.): Association of Engineering Geologists 26 Annual Meeting, San Diego, California, Coalinga Earthquake Symposium.

Keefer, D. K., in press, Rock avalanches caused by earthquakes--source characteristics: Science (Accepted for publication).

Keefer, D. K., Harp, E. L., and Wilson, R. C., 1983, Landslides and related ground failures, in Borcherdt, R. D., compiler, The Coalinga earthquake sequence commencing May 2, 1983: U.S. Geological Survey Open-File Report 83-511, p. 12-19.

Mavko, G. M., and Harp, E. L., Analysis of wave-induced pore pressure changes: Submitted to Seismological Society of America Bulletin, 22 p., 4 figs.

Wilson, R. C., and Keefer, D. K., 1983, Dynamic analysis of a slope failure from the August 6, 1979, Coyote Lake, California, earthquake: Seismological Society of America Bulletin, v. 73, no. 3, p. 863-877.

CPT Pore-Pressure Measurements and SPT Hammer - Energy Calibration

14-08-0001-19105 No. 3 H7

Geoffrey R. Martin, Bruce J. Douglas, Andrew I. Strutynsky

Ertec, Inc.
3777 Long Beach Blvd.
Long Beach, California 90807
(213) 595-6111

As an extension to our study for the U.S.G.S., titled "Evaluation of the Cone Penetrometer for Liquefaction Hazard Assessment", The Earth Technology Corporation has measured the input energy of the various SPT hammers used in the previous study. Piezometric CPT to define static and dynamic pore pressure response to cone penetration has been performed using two different designs of piezo elements. All of these measurements are intended to supplement the previous data base allowing increased refinement of the CPT-liquefaction potential method.

Energy measurements have been taken of the trip and donut SPT hammers used for the previous study. Additional SPT energy data on 3 types of safety hammers, using two different drilling rig types (rope around the cat head, and spool-off winch) have also been obtained.

Piezometric CPT soundings measuring dynamic and static pore pressure response have been performed at the San Diego, Heber Road, and Salinas, California sites. Two different designs of piezometric elements were used. These designs were: 1) a tip sensing piezometric element which incorporates transducer inlet ports on the face of the conical tip of the cone instrument; and 2) a side sensing piezometric element which incorporates transducer inlet ports just behind the conical tip, but before the friction sleeve of the cone instrument. Different dynamic pore pressure response is obtained depending on the design used.

The results of these SPT calibration tests are being used to calibrate the CPT-liquefaction potential predictive method and to enhance the data base describing United States Average Energy used in the SPT. The piezometric CPT results will be used to assess the value and effectiveness of pore-pressure measurement with regard to liquefaction potential evaluations.

EVALUATION OF LIQUEFACTION OPPORTUNITY AND LIQUEFACTION POTENTIAL IN THE SAN DIEGO, CALIFORNIA URBAN AREA

14-08-0001-20607

M.S. Power, A.W. Dawson, I.M. Idriss,
R.R. Youngs, and K.J. Coppersmith

Woodward-Clyde Consultants
One Walnut Creek Center
100 Pringle Avenue
Walnut Creek, CA 94596
(415) 945-3000

3467 Kurtz Street
San Diego, CA 92110
(714) 224-2911

Investigations

1. Liquefaction potential of the San Diego, California urban area is assessed in this study. This assessment is based on the liquefaction susceptibility and liquefaction opportunity of the area. Liquefaction susceptibility is the relative likelihood that a geologic unit would undergo liquefaction and ground failure during intense seismic shaking; this was assessed for the San Diego area during a previous Woodward-Clyde Consultants study (Power and others, 1982a, 1982b). Liquefaction opportunity, which is evaluated in this study, is a function of the seismicity of the area and the frequency of occurrence of earthquake ground motions capable of causing liquefaction in susceptible materials. When liquefaction susceptibility and liquefaction opportunity are combined, the liquefaction potential of an area can be assessed.

2. Potentially significant sources of earthquakes in the San Diego region are identified and characterized with respect to the parameters necessary for probabilistic seismic hazard analyses (e.g. fault geometry, maximum earthquake magnitude, and earthquake recurrence). The uncertainty in each of these parameters is accounted for through the use of a probabilistic approach (Coppersmith and Youngs, 1982, 1983) in which input parameters are assigned conditional probabilities that reflect the relative degree of confidence in each parameter.

3. A seismic hazard analysis is conducted to calculate the annual mean number of events that exceed certain acceleration levels as a result of the occurrence of earthquakes of specified magnitudes. This analysis is based on the information for each of the potentially significant seismic sources.

4. The probability of occurrence of liquefaction during a specified time period is assessed using two different methods.

In the first method, developed by T.L. Youd and D.M. Perkins, the occurrence of liquefaction in susceptible soils is related to distance from fault sources and the magnitudes of the earthquakes that orginate on the individual faults. The second method is based on a correlation developed by H.B. Seed and I.M. Idriss. In this correlation, the liquefaction criterion is expressed as curves of peak ground acceleration required to cause liquefaction versus the standard penetration resistance of the soil deposit. The normalized standard penetration test data was obtained for the study area during the previous study of liquefaction susceptibility (Power and others, 1982a).

Results

1. The tectonic setting and historic seismicity of the San Diego region are reviewed in this study. Based on this review, fourteen potentially significant fault sources are identified and characterized. Geologic and geophysical data are used to define fault length, fault dip and down-dip width. The maximum earthquake magnitude on each fault is assessed using fault dimensions. The frequency of occurrence of earthquakes of various magnitudes is estimated for each fault is based on geologic slip rate.

2. Ground acceleration levels for three different return periods are estimated at locations throughout the study area . The ranges of acceleration values obtained are: 0.10-0.15 g for a 100-year return period; 0.20-0.30 g for a 500-year return period; and 0.35-0.55 for a 2500 year return period.

3. Preliminary findings indicate a return period for liquefaction on the order of several hundred to a few thousand years.

References

Coppersmith, K.J. and Youngs, R.R. (1982), Probabilistic Earthquake Source Definition for Seismic Exposure Analyses (abstract): Earthquake Notes Vol. 53, No. 1, January-March, p. 67.

Coppersmith, K.J. and Youngs, R.R. (1983), Source Characterization for Seismic Hazard Analyses within Intraplate Tectonic Environments (abstract): Earthquake Notes Vol. 54, No. 1, January-March, p. 7.

Power, M.S., Dawson, A.W., Streiff, D.W., Perman, R.C., and Berger, V. (1982a), Evaluation of Liquefaction Susceptibility in the San Diego, California Urban Area: Final technical report prepared for the U.S. Geological Survey under Contract No. 14-08-0001-19110 by Woodward-Clyde Consultants, San Diego, California.

Power, M.S., Dawson, A.W., Streiff, D.W., Perman, R.C., and Haley, S.C. (1982b), Evaluation of Liquefaction Susceptibility in the San Diego, California Urban Area: Proceedings of the Third International Earthquake Microzonation Conference, Seattle, June 28-July 1, 1982.

EXTENSION OF LIQUEFACTION CRITERIA FOR SILTY SOILS AND EVALUATION OF POST-CYCLIC BEHAVIOR

14-08-0001-20565

Sukhmander Singh
Robert Y. Chew

Dames & Moore
500 Sansome Street
San Francisco, CA 94111
(415) 433-0700

Investigations

1. Existing data on the cyclic strength characteristics of silty soils were collected and compared with that of sands. An evaluation of the data was made to develop a liquefaction criteria for silts.

Results

1. Silts undergo strains in a manner different than the sands. There is usually a steady buildup of strains right from the start of the test and it appears to be not too strongly associated with the buildup of the pore pressure as it is in case of sands. In most cases the 5 percent and 10 percent double amplitude axial strain develop before the time pore pressures become equal to confirming pressure.

2. In most pure silt samples, the trend of pore pressure development was different than in case of sands such that it takes large numbers of cycles of loading to reach one hundred percent pore pressure ratio. The presence of sand contents can, however, offset this effect, and silts with significant percent of fine sands can have dramatic rise in pore pressures.

3. Silts, even after reaching one hundred percent pore pressure ratios, do not deform as rapidly as sands.

4. It is suggested that the liquefaction criteria of "one hundred percent pore pressure ratio with strain potential" used for sand may not be applicable for silts which usually develop large strains well before one hundred percent pore pressure ratio is reached. For sandy silts the criteria should be based on actual observation of the sample behavior during cyclic loading. For clayey silts, the above mentioned criteria for pure silts can also be applied.

Liquefaction Investigations

9910-01629

T. Leslie Youd
Branch of Engineering Seismology and Geology
U.S. Geological Survey MS 98
Menlo Park, CA 94025
(415) 856-7117

Investigations

1. With John Tinsley, Branch of Western Regional Geology, continued compilation of liquefaction potential maps for Los Angeles Basin area.

2. Continued investigation of liquefaction potential of debris in the blockages impounding Spirit, Castle Creek, and Cold Water lakes north of Mount St. Helens. Drilled sites at Spirit and Castle Creek lakes, took samples, and installed sensors for monitoring ground motions and pore-water pressures.

3. Selected and explored a site in the Mammoth Lakes area, California to be instrumentation for monitoring of ground motion and pore-water pressures as the site responds during future earthquakes. This area has experienced several magnitude 5 to 6 earthquakes in the past few years and the probability is high that more earthquakes of this size will strike in the next few years.

4. Continued studies of sites in the Imperial Valley, California where liquefaction occurred during earthquakes in 1979 and 1981.

Results

A four-pronged investigation of liquefaction susceptibility of debris blockages impounding Spirit, Castle Creek, and Cold Water lakes north of Mount St. Helens was undertaken. These blockages are composed materials deposited during the May 18, 1980 eruption of the mountain. The deposits are primarily debris avalanche material, but the Spirit Lake blockage also contains blast, ash-cloud, and pyroclastic-flow materials. If any one of these blockages should fail, severe flooding could occur downstream along the Toutle, Cowlitz and Columbia rivers. The four different approaches to evaluate liquefaction susceptibility are as follows: 1. Standard penetration test (SPT) data were collected and are being compared with standard engineering criteria to estimate the susceptibility of the material. The SPT tests were primarily made by the U.S. Army Corps of Engineers during drilling investigations at the Spirit Lake blockage. The debris avalanche material is very coarse, containing large fractions of gravel, cobbles, and boulders. The validity of SPT data in such coarse material is questionable, hence the need for other evaluation techniques. 2. Cyclically loaded triaxial compression tests were made on reconstituted samples of debris avalanche material at the USGS geotechnical laboratory in Menlo Park, California. Only the material fraction containing sand-size and smaller particles could be tested. Hence, the results of these tests are also questionable. 3. Shear-wave velocity and shear modulus profiles were

developed for each of the blockages from spectral analysis of surface waves generated by hammer impacts on the blockages. From this information, shear strain amplitudes in the deposits can be calcualted for probable earthquakes in the region. These amplitudes can then be compared with threshold strains for initiation of excess pore-water pressures in the material to evaluate liquefaction susceptibility. Laboratory tests to estimate threshold strains for the debris avalanche material are being conducted on reconstituted samples in the soils engineering laboratory at Rensselaer Polytechnic Institute. Contracts were awarded to the University of Texas for the surface wave measurements and the development of the shear-wave velocity profiles, and to Rensselaer Polytechnic Institute to determine threshold strain values. 4. To measure actual ground-motion and pore-water pressure response of the Spirit Lake and Castle Creek blockages, strong-motion seismometers were installed at the surface and at a 30-meter depth and 3 to 4 pore-pressure transducers were installed below the present water in each blockage. The transducers were placed at depths between 24 m and 30 m. If a moderate- or larger-size earthquake should strike the area, these monitoring devices would provide direct information for evaluating the response and liquefaction susceptibility of the blockages. The instrumentation would also provide data for evaluating the postearthquake stability of the blockages. These studies are still in progress and final analyses are yet to be made.

Reports

No reports were published during this reporting period.

Stochastic Models for Earthquake Occurrence

14-08-0001-19155
A. S. Kiremidjian and T. Anagnos
Department of Civil Engineering
Stanford University, Stanford, CA 94305
Tel. (415) 497-4164

The objectives of this study are: (1) to critically review existing seismic hazard models; (2) review current geophysical theories on patterns of occurrence of earthquake events; (3) develop stochastic models to incorporate the geophysical theories into a seismic hazard analysis; and (4) apply the models to various regions for model verification purposes.

Two representations of the earthquake generating mechanism are studied, specifically, the time-predictable recurrence model and the slip-predictable recurrence model proposed by Shimazaki and Nakata (1980). Assumptions of the time-predictable model are that an earthquake occurs on a fault when the stress, accumulating at some constant rate, reaches a threshold level. The time to the next earthquake is then proportional to the size of the previous event and inversely proportional to the rate of stress accumulation. This behavior is shown schematically in Figure 1. Assumptions of the slip-predictable model are that stress accumulates at a constant rate and the size of the next earthquake depends on the elapsed time since the last occurrence. At the time of an earthquake occurrence all of the accumulated stress is released as shown in Figure 2. For both hypotheses the time between events can be related to the cumulative coseismic slip and the average slip rate on the fault (see Figures 1 and 2).

The time-predictable and slip-predictable representations of earthquake sequences enable the prediction of either the time of occurrence or the size of the next event, but not both. Thus both models have some random aspect which prevents a complete deterministic description of the time, location and size of future occurrences. Stochastic model representations were developed for the two hypotheses in order to incorporate randomness and uncertainty in input parameters such as slip rate, average displacement resulting from an earthquake, and the distribution of earthquake magnitudes. The stochastic representations are Markov renewal models, consequently the estimated probabilities of occurrence are based on one-step temporal dependence.

The time-predictable model was applied to a section of the San Andreas fault that ruptured during the 1906 earthquake. Probabilities of occurrence and the expected number of events in time t were computed using data from Ellsworth et al. (1981). The model was found to be sensitive to variations in the slip rate and the smallest magnitude considered in the analysis. It is insensitive to the number of discrete stress levels and the Gutenberg-Richter b value used as a parameter in the probabilistic magnitude distribution. The effect of the shape of

the magnitude and interarrival time probability distributions on the hazard estimates needs further study. The slip-predictable model was applied to a 1700 km section of the Middle America Trench along the west coast of Mexico. Data from Wang et al. (1982) and McNally and Minster (1981) was used to estimate parameters of the stochastic model representation. Probabilities of occurrence and the expected number of events in time t were computed using two proposed slip rates. Comparison with forecasts from the Poisson model showed that occurrence probabilities estimated from the Poisson model may be too large for short durations since the last earthquake and may underestimate the hazard for longer durations.

The results of this investigation have been submitted to the U.S. Geological Survey as an open-file report. A further development will be to include spatial dependence in the stochastic model formulations.

References

1. Ellsworth, W.L., Lindh, A.G., Prescott, W.H. and D.G. Herd (1981). The 1906 San Francisco Earthquake and the Seismic Cylce, Earthquake Prediction, Maurice Ewing Series, 4, A.G.U., 126-140.

2. McNally, K.C. and J.B. Minster (1981). Nonuniform Seismic Slip Rates Along the Middle America Trench, J. Geoph. Res., V86, 4949-4959.

3. Shimazaki K. and T. Nakata (1980). Time-Predictable Recurrence for Large Earthquakes, Geoph. Res. Lett., V7, 279-282.

4. Wang, S.C., McNally, K.C. and R.J. Geller (1982). Seismic Strain Release Along the Middle America Trench, Mexico, Geoph. Res. Lett., V9, 182-185.

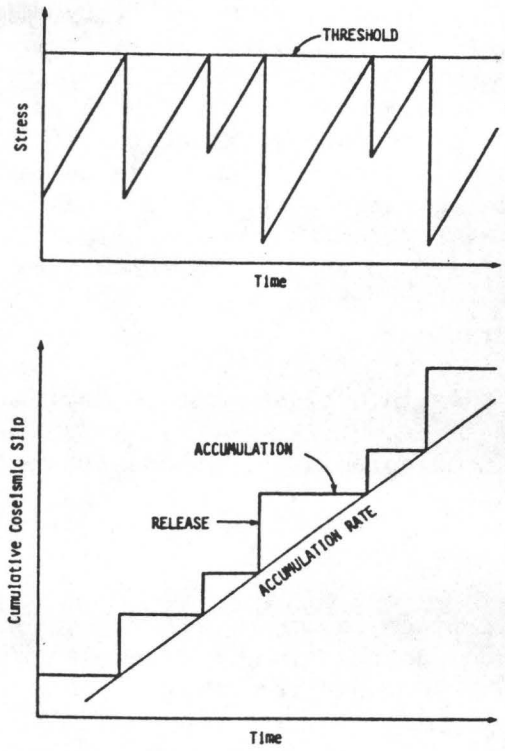

Figure 1

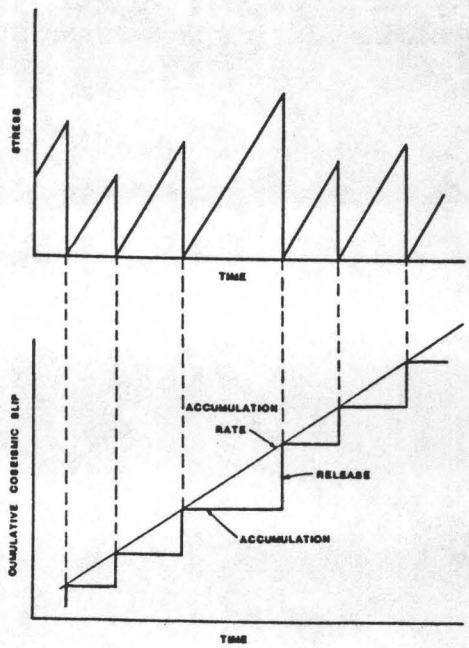

Figure 2

A COMPUTERIZED METHOD FOR PREDICTING EARTHQUAKE LOSSES IN URBAN AREAS
(Final Technical Report for Phase II)

Contract No. 14-08-0001-20629

by
Onder Kustu
David D. Miller
Roger E. Scholl

URS/John A. Blume & Associates, Engineers
130 Jessie Street (at New Montgomery)
San Francisco, California 94105
(415) 397-2525

This report presents the results of Phase II of a three-phase research program currently being conducted by URS/John A. Blume & Associates, Engineers, for the United States Geological Survey. The overall objective of the program is to develop a comprehensive and practical method for predicting earthquake-caused losses in urban areas, to compile the data necessary for its application, and to demonstrate its practicability. The objective of Phase II was to complete the development of the theoretical methodology introduced in Phase I, write a computer program to automate the application of the methodology, develop the necessary damage models for structures in urban areas, and determine through parametric studies the sensitivity of loss predictions to certain parameters.

The following are the essential tasks in the methodology:

- Definition of the Problem
  - -- Definition of the urban area
  - -- Definition of the purpose and scope of prediction
- Definition of the Global Coordinate System
- Modeling the Seismic Hazard
  - -- Definition of the seismic environment
  - -- Definition of ground motion zones
  - -- Estimation of site ground motion
- Modeling the Urban System
  - -- Inventory models
  - -- Damageability models
- Computation of Losses
  - -- Prediction of earthquake losses
  - -- Determination of loss statistics

Defining the problem means setting limits to the urban area to be analyzed, whether several blocks or several counties, and specifying the reason for predicting damage to that area and the form the results should take.

To predict damage to an urban area, it is necessary to consider both structural response and damageability characteristics of the structures

in the area and the expected ground motion. To describe both the seismic hazard and urban system models, the analyst must define a uniform coordinate system.

The ground motion is modeled by identifying all earthquake sources that will have significant effect on the urban area and estimating the extent of the ground motion each one will produce. This process is made easier by dividing the urban area into ground motion zones.

Next, an analyst must determine what classes of buildings and special structures are found in the urban area and how susceptible they are to damage from earthquake motion. Information needed to model the number of structures in a class and their replacement value is available from federal, local, and private sources and can be supplemented in various ways. This report presents a building classification scheme and associated damage models developed by expert judgment.

The final prediction of earthquake losses is computed probabilistically through the use of a simulation procedure, which is an approximate method of solution using Monte Carlo techniques. This procedure has been automated by the computer program SIMPLE. Using the mean, standard deviation, and probability density function of the computed losses, total loss predictions can be made at any desired level of confidence.

Crustal Tilt in Southern California

14-08-0001-21358

Thomas J. Ahrens, Co-PI
Don L. Anderson, Co-PI
Seismological Laboratory
California Institute of Technology
Pasadena, California 91125
(213) 356-6906, 356-6901

Scope

Observation of crustal deformation in Southern California via an array of instruments may, in time, provide an understanding and criteria for recognition of tectonic processes which are related to preseismic, co-seismic and past seismic processes. With this perspective a series of instruments which senses strain were all sited in a tunnel in bedrock called the Dalton Geophysical Observatory along the southern slope of the San Gabriel mountains (Fig. 1 - map) in 1980.

In addition to carbon filament, vibrating wire and strain meters and a water tube tiltmeter, a short base-line tiltmeter, supported under the present contract, was installed. Although the present contract technically deals only with the Dalton Tunnel instrument we have examined two component signals also from two other sites in southern California (Kresge and Lake Hughes) which have been operating intermittently but concurrently during periods in 1982. As indicated in Fig. 1 these stations are within 75 km of one another. The periods of operation of these three instruments are shown in Fig. 2. The Lake Hughes station is a unique borehole installation. All three stations record the semidiurnal earth tide (Figs. 3-5). These figures demonstrate that the earth, tilt, tide, correlates, as expected, with the local ocean tide signal. However, the Kresge station which is nearly a surface installation only shows a dominant diurnal, probably solar insolation induced signal of usually ~0.5 μradian peak to peak amplitude. Some analysis of the limited data available for a portion of 1982 indicate no regional tilt anomalies were detected simultaneously over the periods indicated in Fig. 2. More analysis will be carried out regarding coherence of the data and examining the question of whether the flexural rigidity of the crust due to tidal loading has remained effectively constant under each station for the periods where we have adequate data.

It should be also noted that in the case of Kresge only, a strong, ~0.1 μrad, semidiurnal tidal signal is observed when the thermal signal is subdued due to cloudy weather. At present we cannot explain the better than expected correlation of the tidal E-W tilt signal at Kresge with the ~N-S signal at Lakes Hughes (actually N38^{o}W).

Unfortunately, largely due to a one year hiatus in funding of this project, both Lake Hughes and Dalton are not now operating. We expect both stations to become operational this winter.

Report prepared by: Wayne Miller, Thomas Ahrens, and Don L. Anderson

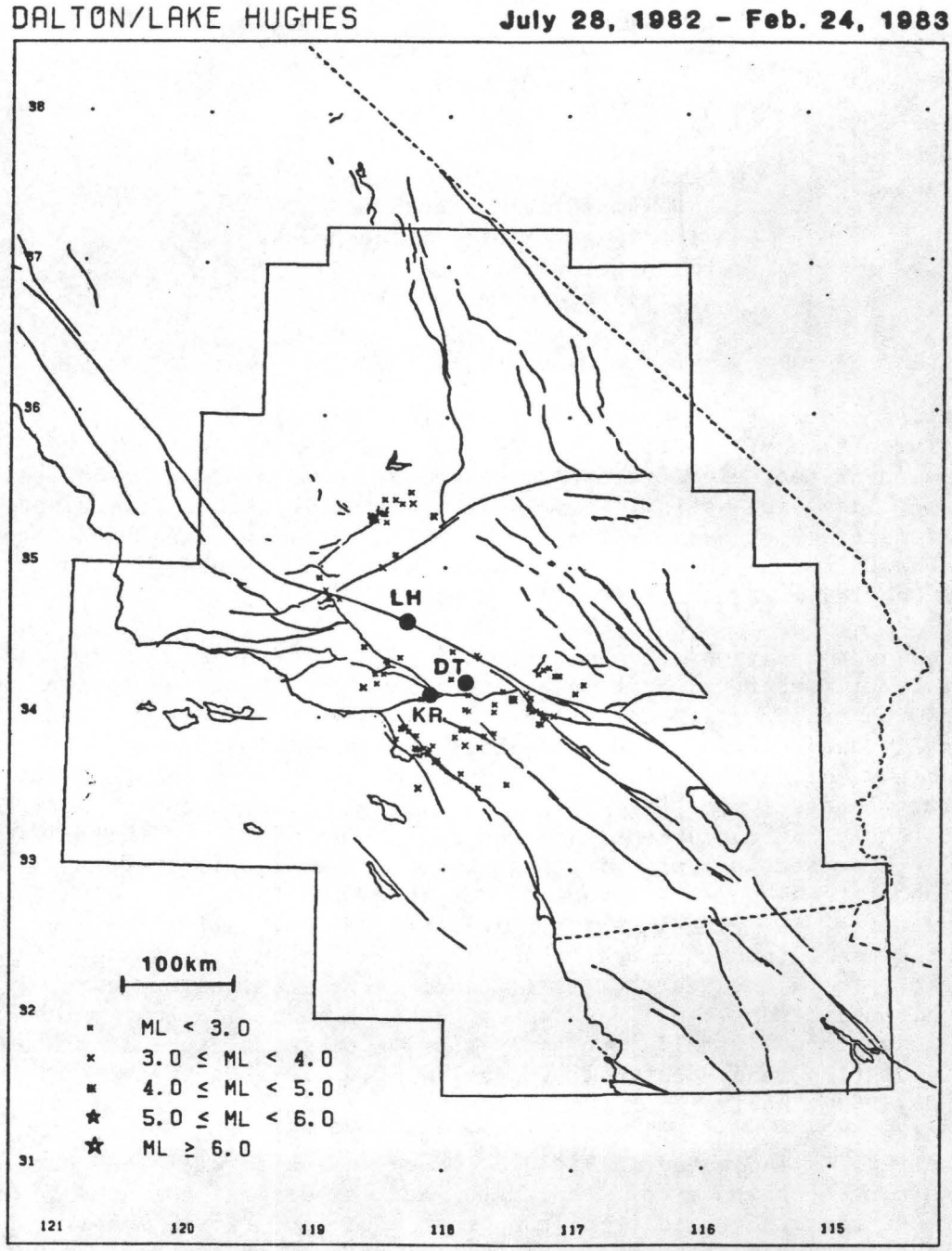

Earthquakes Within One Degree of the DALTON, LAKE HUGHES and KRESGE Sites

Figure 1. Locations of the Dalton Tunnel (DT), Kresge Tunnel (KR) and Lake Hughes borehole (LH) tiltmeters. Also shown are earthquakes within one degree of the sites which occurred during the period of operation. The range of earthquake varied from Richter magnitude 2.0 to 4.1.

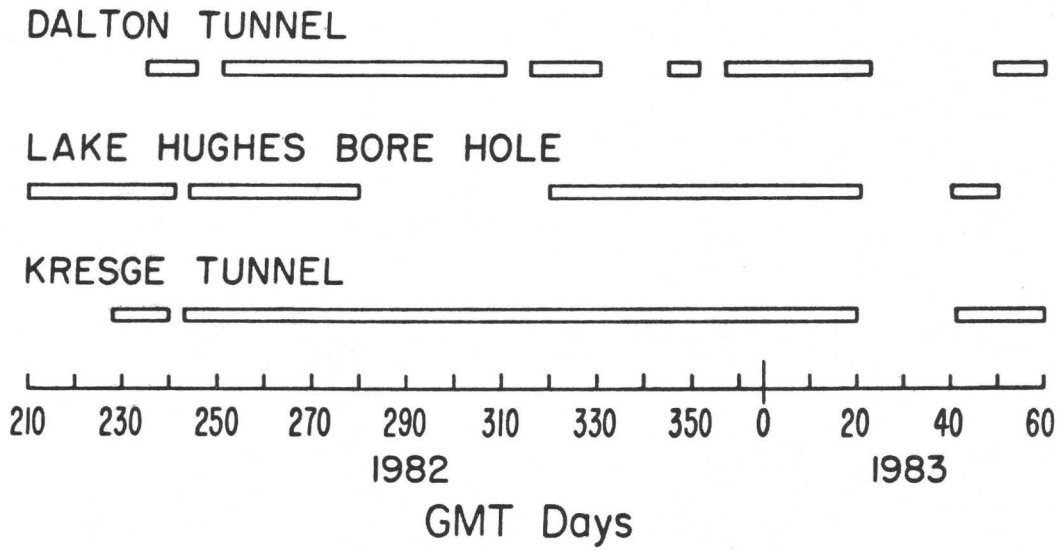

Figure 2. Periods of operation of the tiltmeters. Data are telemetered from the sites to the Seismological Lab. over common dial-up telephone lines. Short gaps in the data are due to telemetry problems. The large gap in the Lake Hughes data was due to damage at the site caused by a lightning strike. The large common gap was due to a failure associated with the computer which automatically retrieves the data from each site.

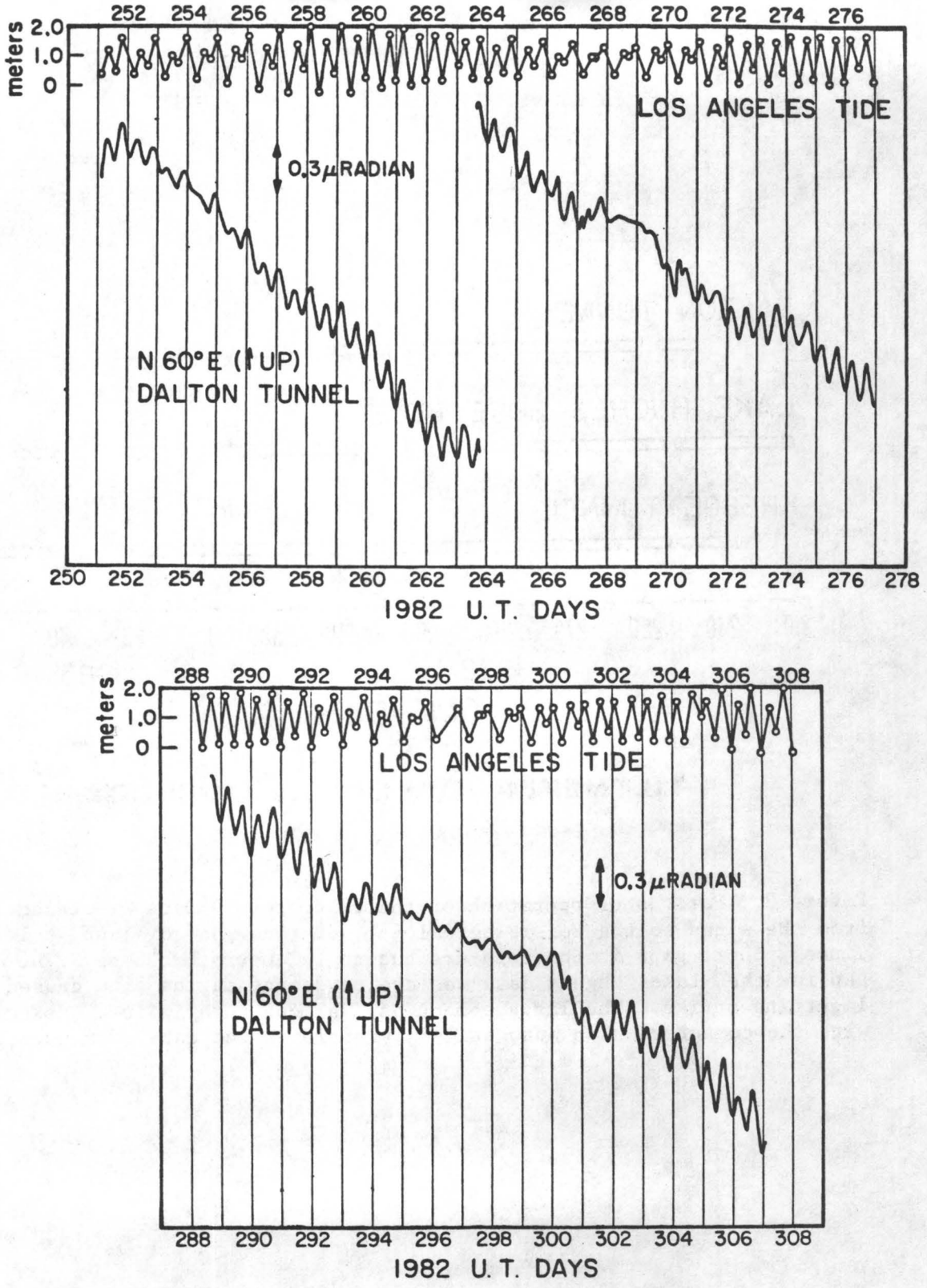

Figure 3. A comparison of the Dalton semidiurnal tilt signal and the U.S. Dept. of Commerce tide data for the Los Angeles Harbor. A strong correlation is clearly evident.

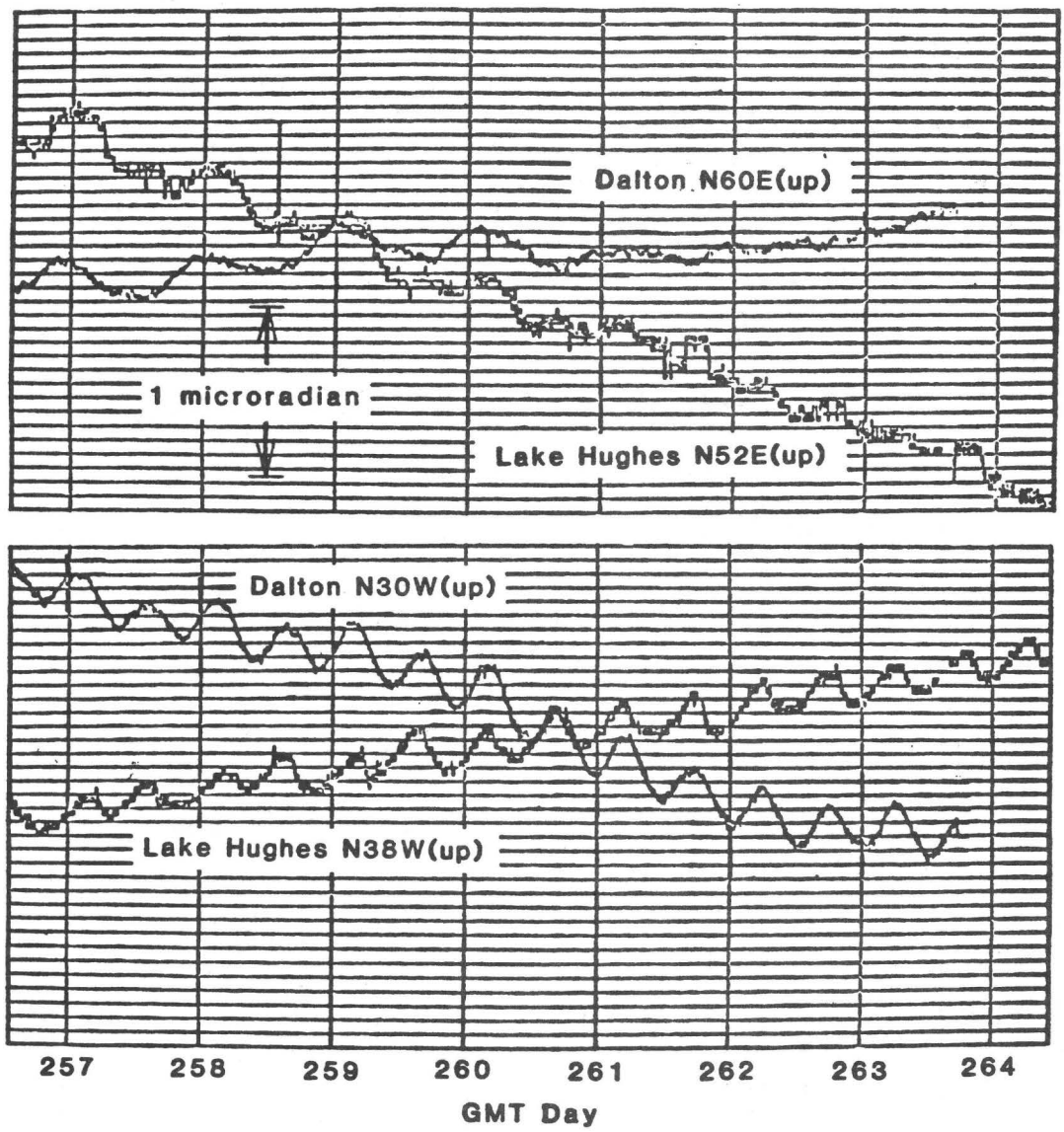

Tilt at Dalton Tunnel and Lake Hughes Borehole

Figure 4. A comparison of the tilt signals at the Dalton Tunnel and Lake Hughes borehole shows good correlation on both axes. These figures also demonstrate the clear separation of the diurnal and semidiurnal signals.

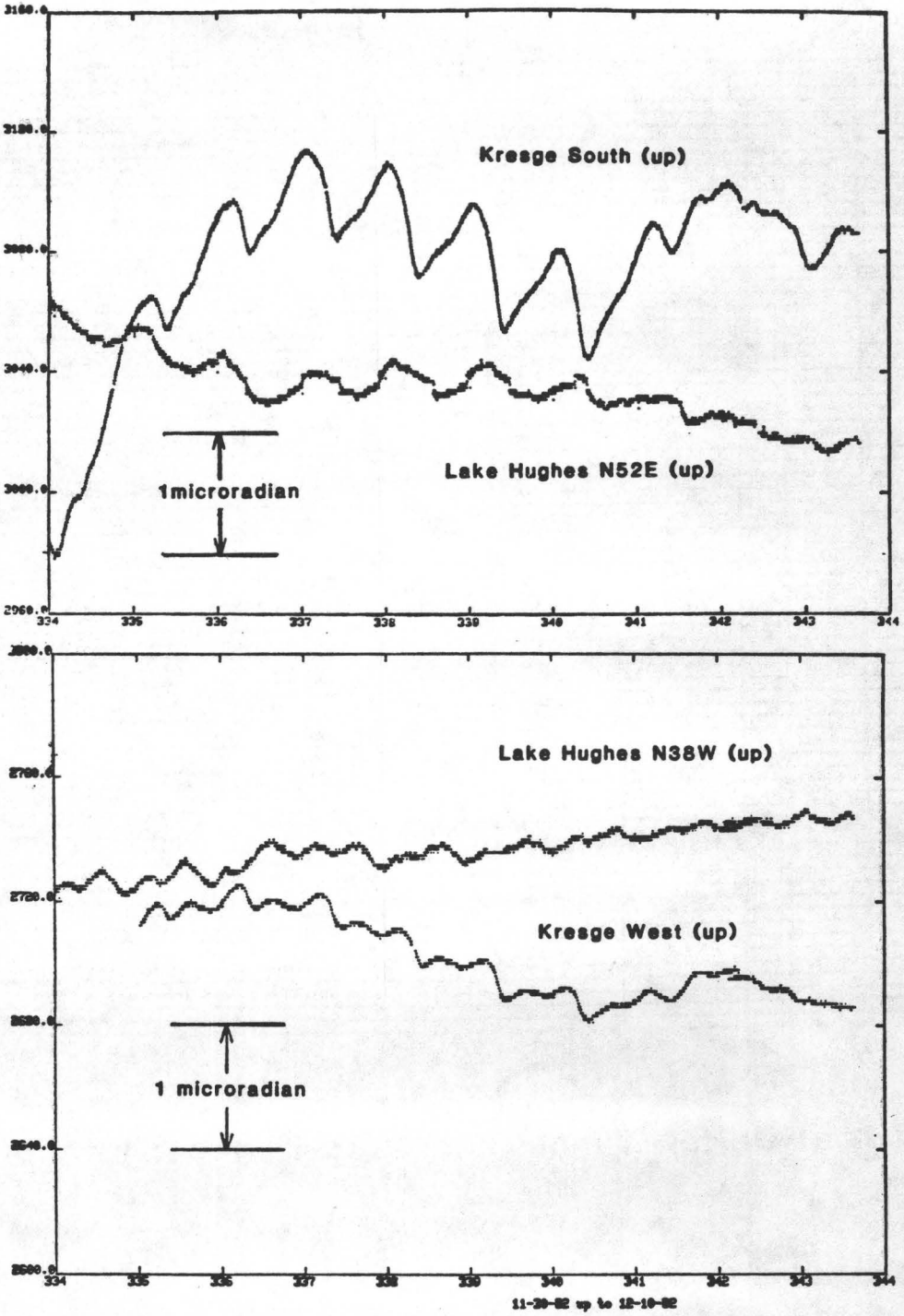

Tilt Comparison, Kresge vs Lake Hughes

Figure 5. A comparison of the tilt signals from the Kresge Tunnel and Lake Hughes borehole. The Kresge site is nearly a surface installation and the semidiurnal signal can only be observed when the apparently solar insolation signal is subdued due to cloudy weather. Again, the separation of diurnal and semidiurnal signals is evident.

ANALYSIS OF CENTRAL CALIFORNIA NETWORK DATA AND EARTHQUAKE PREDICTION

U.S.G.S. Contract Number 14-08-0001-21292

Principle Investigator: Keiiti Aki
Massachusetts Institute of Technology
77 Massachusetts Ave., Cambridge, MA 02139 (617)253-6397

INVESTIGATIONS

Coda wave techniques have been used to recover the average path effect (Q_β) of the lithosphere under Japan by Aki (1980), who used a single-station method based on eliminating the source effect from S waves by the use of coda spectra (Aki and Chouet, 1975; Rautian and Khalturin, 1978). We seek to extend this method to a multi-station data set which means that site as well as source effects must be taken into account. The long range goals of this study include the characterization of the attenuative properties of the study region on a path by path basis, and the recovery of valuable source and site effect information.

From the work of Aki and Chouet (1975), Tsujiura (1978) and Rautian and Khalturin (1978), it is well established that the coda power spectrum can be written as:

$$A_{ij}^{c} = \langle Site(i,f) \rangle_{\vartheta} \cdot \langle Source(j,f) \rangle_{\vartheta} \cdot P(f,t)$$

where f=frequency, t is measured from the origin time and $\langle\rangle_{\vartheta}$ represents an directional average. $Site(i,f)$ is the local site effect at station i, $Source(j,f)$ is the effect of source j, and $P(f,t)$ is the coda decay which only depends on medium properties and not on i, j. By comparing measurements of coda power all taken at a constant lapse time from the origin time, information about the source and site effects can be extracted.

The S wave amplitude spectrum can be written as:

$$A_{ij}^{s} = Site(i,f,\vartheta_{ij}) \cdot Source(j,f,\vartheta_{ij}) \cdot \left[\frac{\exp\left(\frac{-2\pi f T_{ij}}{Q_\beta(f)}\right)}{X_{ij}^2} \right]$$

where Xij is the distance and Tij is the S travel time between source j and station i. The ϑij represent possible dependence on wave path direction. To study the path effect (Q_β) we form the following quotient and call it the S-to-coda ratio;

$$R_{ij}(f)=\frac{A_{ij}^{s}(f)\cdot X_{ij}^{2}}{A_{ij}^{c}(f,t_o)}$$

from which the directionally averaged source and station site effect on S waves have been removed. The ratio still contains the directionally dependent portions of the source and site effects which may be removed by applying an appropriate correction, or by smoothing over various stations and sources. An average Q_β correction can also be included.

RESULTS

We are currently working with records from 12 USGS low-gain 3-component stations and over 80 high-gain vertical stations located in Central California. The low-gain records are used to study the S wave, while the high-gain records are used to study the coda of the same earthquake. Data from 14 earthquakes (magnitudes 2.5 to 3.3) have been examined; nine of these are aftershocks of the Coyote Lake earthquake of 1979. Our results allow the following conclusions to be drawn:

(1) The S-to-coda ratio seems to be dominated by conditions close to the emergence point of the ray path. Azimuthal effects were ignored by looking at ratios from groups of stations along similar azimuths from Coyote Lake. Stations lying above low velocity anomalies, often associated with sediment filled graben structures in the upper crust (Zandt, 1978) produced lower ratios, indicating more attenuative paths. The lowest ratios were observed for paths emerging in the San Andreas fault zone at the Stone Canyon station.

(2) The S-to-coda ratio has been used to estimate a regional average of Q_β, which agrees quite well with the Q of coda waves as shown in Figure 1. Regional Q_β is found as in Aki (1980); coda Qc is calculated from the temporal decay of the coda waves using Sato's (1977) model. In previous studies, the coincidence of shear and coda Q have lent support to the idea that coda waves are backscattered S waves.

(3) The source effect of coda waves is similar to results from previous single-station studies in Central California. Chouet (1975) found that the coda source factor for many

earthquakes near Stone Canyon, California, showed only slight low frequency flattening and poorly defined corner frequencies. We have obtained similar results at Stone Canyon and at other stations as well, thus reducing the possibility that the strange coda source factor may be due to the station site effect.

(4) The station site effect is inversely correlated with velocity fluctuations in the upper crust. Coda power measurements for a single earthquake show a remarkably strong inverse correlation with velocities in the upper 10 km. of the earth's crust as determined by Zandt (1978). The correlation is best at low frequencies, 0.75-3.0 Hz. Site effect highs often correlate with low velocity sediment filled graben structures. An example is the area near the junction of the San Andreas and Calaveras faults, extending southeast into Bear Valley. Site effect lows are seen in well consolidated geologic terraine like the granitic Gabilan mountain range. Relative coda power at 1.5 Hz. is shown in Figure 2. Stations in the Bear Valley area show coda amplitudes as much as 7-8 times larger than those in the Gabilan mountains.

(5) A pronounced low station site effect at low frequencies does not always remain low relative to other stations at higher frequencies (>6 Hz.). This is especially true for stations in the Gabilan range.

REFERENCES

Aki, K. (1980). Attenuation of shear waves in the lithosphere for frequencies from 0.05 to 25 Hz, *Phys. Earth Planet. Interiors*, *21*, 50-60.

Aki, K. and B. Chouet (1975). Origin of coda waves: Source, attenuation and scattering effects, *J. Geophys. Res.*, *80*, 3322-3342.

Rautian, T.G., and V.I. Khalturin (1978). The use of the coda for determination of earthquake source spectrum, *Bull. Seismol. Soc. Am.*, *68*, 923-948.

Sato, H. (1977). Energy propagation including scattering effect; single isotropic scattering approximation, *J. Phys. Earth*, *25* 27-41.

Tsujiura, M. (1978). Spectral analysis of coda waves of local earthquakes, *Bull. Earthq. Res. Inst. Univ. of Tokyo*, *53*, 1-48.

Zandt, G. (1978). Study of three-dimensional heterogeneity beneath seismic arrays in Central California and Yellowstone, Wyoming, Ph.D. thesis, M.I.T., Cambridge, Massachusetts.

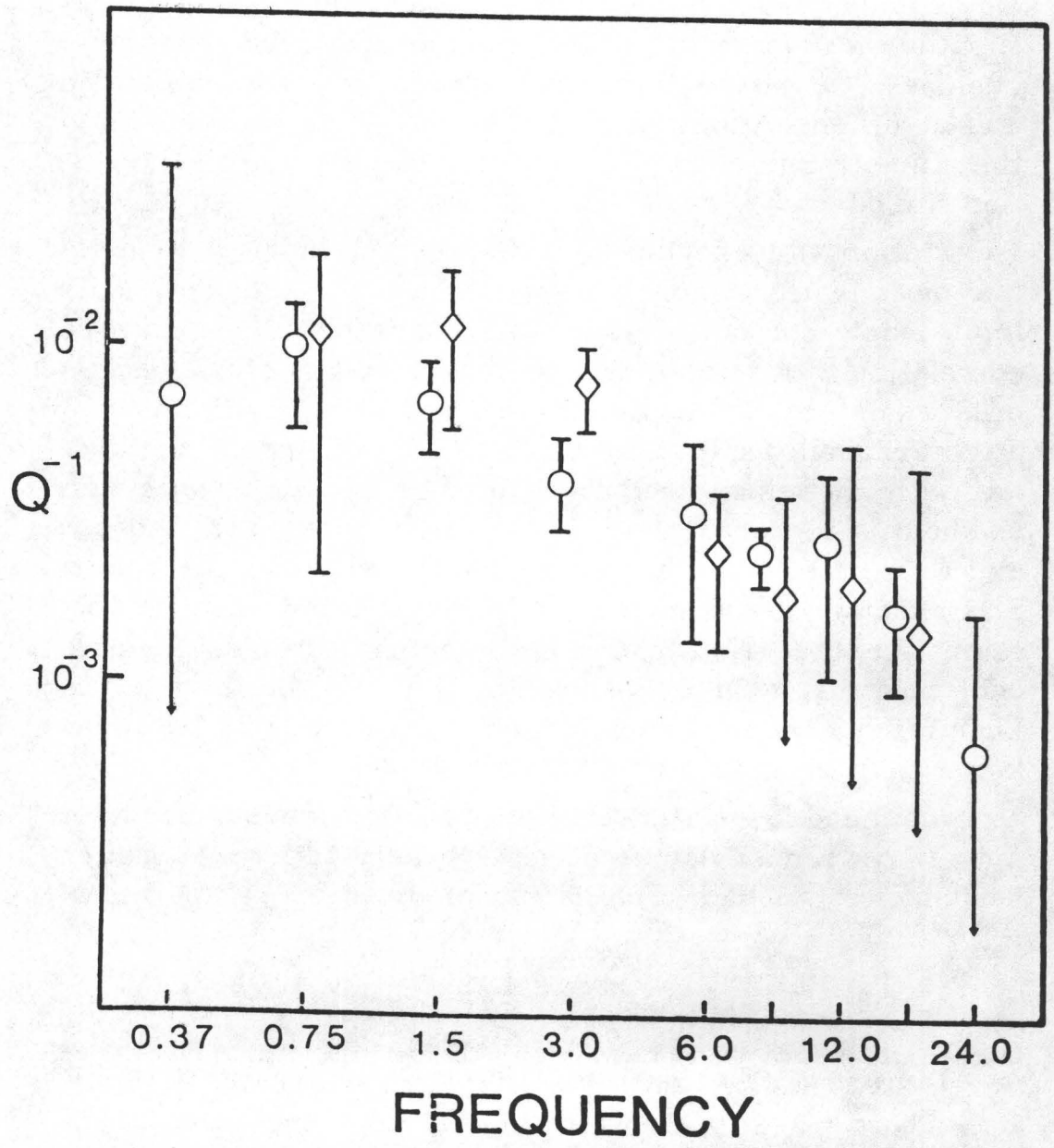

Figure 1

1/Q of S waves (diamonds) and coda waves (circles) against frequency in Hz. $Q\beta$ is taken from the variation of 50 S-to-coda ratios with distance; Q_c is an average of over 400 observations of coda decay with time. Error bars represent the 90% confidence limits of the results.

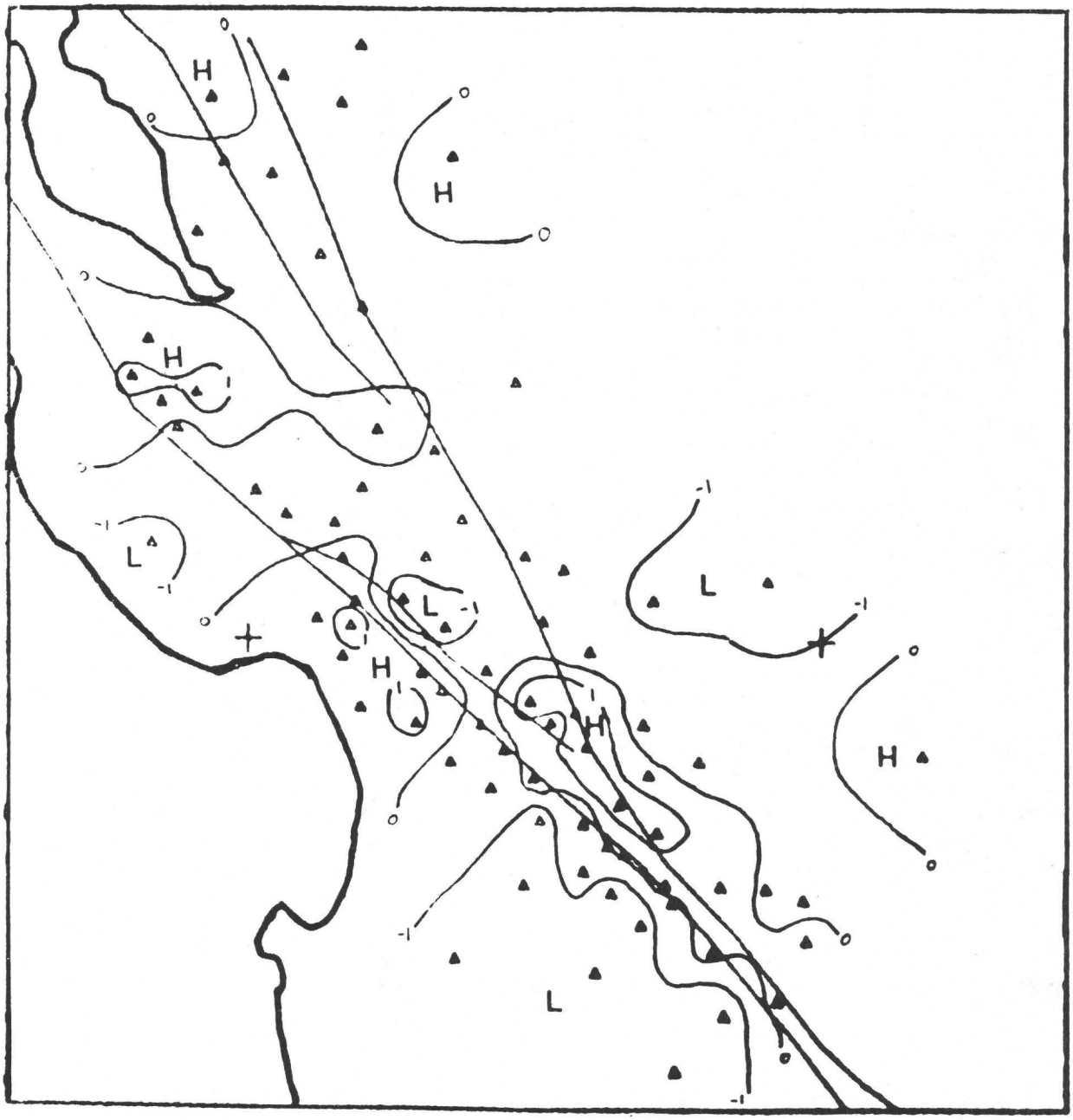

Figure 2

Map of the study area showing the site effect at 1.5 Hz after removal of the mean for 13 earthquakes including 8 Coyote Lake aftershocks. Contours represent ln(relative amplitude); stations are shown as triangles. At this frequency there is a strong inverse correlation with velocity anomalies observed in the upper crust.

Southern California Seismic Arrays

Contract No. 14-08-0001-21209

Clarence R. Allen
Seismological Laboratory, California Institute of Technology
Pasadena, California 91125 (213-356-6904)

Investigations

This semi-annual report summary covers the six month period from 1 April 1983 to 30 September 1983. The contract's purpose is the partial support of the joint Caltech-USGS Southern California Seismographic Network, which is also supported by other groups as well as by direct USGS funding through its own employees at Caltech. Other supporting groups during the report period include the California Division of Mines and Geology and the Caltech Earthquake Research Affiliates. According to the contract, the primary visible product will be a joint USGS-Caltech catalog of earthquakes in the southern California region; quarterly epicenter maps and preliminary catalogs are also required and have been submitted as due during the contract period. About 250 preliminary catalogs are routinely distributed to interested parties.

Results

Figure 1 shows the epicenters of all cataloged shocks that have been located during the 6-month period from 1 January 1983 to 30 June 1983. This is not exactly the same interval as that of the reporting period but follows sequentially the data of the last semi-annual report and reflects that fact that earthquake data analysis is necessarily somewhat delayed. With new data-processing software recently implemented, such delays should be reduced in the future, and hopefully we can be up-to-date by the time of the next semi-annual summary. Some of the seismic highlights during the January to June 1983 period are as follows:

Number of earthquakes currently entered in catalog: 4,656
Number of earthquakes of M = 3.0 and greater: 444
Number of earthquakes of M = 4.0 and greater: 49
Number of earthquakes of M = 5.0 and greater: 7 [all Mammoth or Coalinga, technically outside of network area (Fig. 1)]
Largest shock within network area (29 June 1983, offshore San Diego): 4.6
Largest nearby shock: (2 May 1983, Coalinga): 6.3
Smallest felt earthquake (14 June 1983, Thousand Oaks): 2.2

This has been a period of relatively normal activity within the network area, although the nearby Coalinga earthquake of 2 May was of significant scientific and engineering interest. A series of small shocks southeast of Niland attracted attention, because they lie on the southeastward-projected trace of the San Andreas fault but in an area where no definitive surface evidence of the fault trace has been identified. Activity remained high, as it has for several years, in the Mammoth and Coso areas.

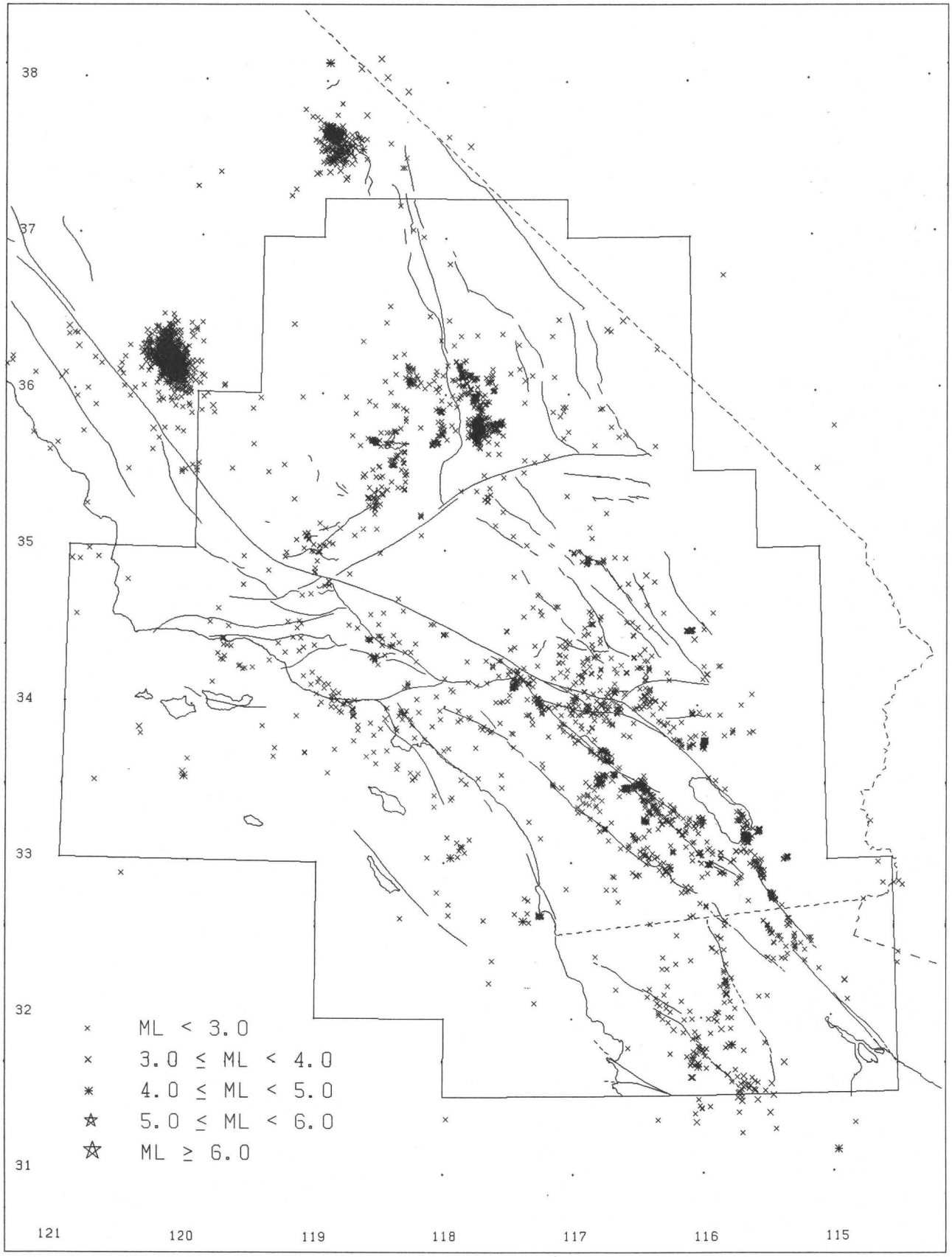

Fig. 1.--Epicenters of larger earthquakes in the southern California region, 1 January 1983 to 30 June 1983.

Creep and Strain Studies in Southern California

Contract No. 14-08-0001-21212

Clarence R. Allen and Kerry E. Sieh
Seismological Laboratory, California Institute of Technology
Pasadena, California 91125 (213-356-6904)

Investigations

This semi-annual report summary covers the six-month period from 1 April 1983 to 30 September 1983. The contract's purpose is to monitor creepmeters, displacement meters, and alignment arrays across active faults in the southern California region. Primary emphasis focuses on faults in the Coachella and Imperial Valleys.

During the reporting period, resurveys of theodolite alignment arrays were carried out at BERTRAM, CAMERON, COLTON, RED CANYON, WATERMAN CANYON, and SANTA ANA WASH. Nail-file arrays were resurveyed at ANDERHOLT, ROSS ROAD, and WORTHINGTON ROAD. Creepmeters were serviced and strip-chart records collected at NORTH SHORE, MECCA BEACH, SUPERSTITION HILLS, HARRIS ROAD, ROSS ROAD, HEBER ROAD, and TUTTLE RANCH. In addition, new displacement meters were installed at TWISSELMAN RANCH (near Bitterwater) and JACK RANCH (Cholame Valley). Thus 4 displacement meters are now installed along the San Andreas fault--at MECCA BEACH, LOST LAKE (Cajon Pass), and the two new localities. One instrument remains to be installed.

Results

Graduate student John Louie has recently completed a systematic reanalysis of all geodetic data obtained since the program started in 1967, and during the past summer, undergraduate student Paul Haase has systematically reevaluated all recent creepmeter records, as well as carrying out laboratory tests on the effectiveness of the existing field instrumentation. The following summarizes these results.

Imperial fault.--The Imperial fault has historically been the locus both of occasional large slips of as much as 6 m during significant local earthquakes (e.g., 1940 and 1979) and of episodic creep events, which are often associated with no recorded local seismic activity. The three alignment arrays across the Imperial fault have shown diverse results: the southernmost array at the international border (ALL AMERICAN CANAL) has shown no firm evidence of total lateral movement greater than 1 cm during the 16-yr life of the array. Northwest 18 km along the fault at HIGHWAY 80, however, some 54 cm of slip has taken place during the same period, including about 23 cm during the 1979 earthquake alone. The long-term slip rate here between 1967 and 1979 was about 3 mm/yr. Still farther northwest, the array at WORTHINGTON ROAD has given results similar to those at HIGHWAY 80. Subsidence on the eastern side of the fault during the 1979 event was measured at 2 locations, amounting to 6 cm at HIGHWAY 80 and 11 cm at WORTHINGTON ROAD. Vertical displacement continued at WORTHINGTON ROAD to the end of 1980, although it decayed faster than the horizontal afterslip. Three continuously recording creepmeters between the two

southernmost arrays document the high rates of slip along the south-central section of the fault. The creepmeters at ROSS ROAD and HEBER ROAD indicate that afterslip due to the 1979 earthquake is continuing there, with several displacement events (usually not coincident at the two stations) larger than 2 mm having occurred at each location since the 1979 event. The afterslip is decaying, with the events continuing to occur at larger intervals rather than decreasing in size. Analysis shows that only about 50% of the total slip can be attributed to such events; the remaining slip apparently takes place either continuously (as true "creep") or as events smaller than the detection threshold of about 0.1 mm. Post-seismic slip at rates greater than that prior to 1979 continued on the Imperial fault for more than 3 years only at these 2 locations. There is a large discrepancy between the measured post-seismic slip and the moment-derived slip, based on recorded seismicity, which seems to rule out a Maxwellian viscoelastic explanation for the surface afterslip.

Brawley fault.--The creepmeter at HARRIS ROAD has shown less than 5 mm of right-lateral slip since May 1980. Similarly, the alignment array at KEYSTONE ROAD, although showing 1-2 cm of horizontal slip and 8-9 cm of vertical slip (down to the west) during the 1979 earthquake, has shown no subsequent resolvable slip.

The distribution of post-1979 deformation on the Imperial and Brawley faults presents a curious picture. In the center of the southern half of the mapped surface break, the creepmeters across the Imperial fault at HEBER ROAD and ROSS ROAD show that afterslip is still continuing and will probably remain above the preseismic slip rate of 5 mm/yr for at least 6-10 years, despite the fact that this area displayed more coseismic slip than fault segments farther north. These northern segments, along with the segment at TUTTLE RANCH to the south, displayed afterslip which decayed within two years. Where post-seismic dip slip is resolvable, as at WORTHINGTON ROAD, it decayed even more rapidly.

Unnamed fault near Dixieland.--An array was established in 1970 across a northwest-trending zone of cracks that developed in the desert floor about 2 km west of Dixieland (on the west border of the Imperial Valley). Although these cracks were initially thought to be of subsidence origin, it is now clear on the basis of surveys through 1979 (when the array was destroyed by road construction) that an average of 3 mm/yr of right-lateral displacement was taking place across the zone of cracks. It is perhaps significant that this locality is nearly on a line projected between the southeastern end of the Coyote Creek fault (1968 rupture) and the northwestern end of the Cerro Prieto fault in Mexico--an interval in which no active fault has heretofore been mapped but which shows a linear pattern of recorded seismic activity.

Superstition Hills fault.--The SUPERSTITION HILLS alignment array demonstrates that, since the displacement triggered by the 1968 Borrego Mountain earthquake, no more than 5 mm of slip could have occurred up to May 1977, when the array became unusable. The nearby creepmeter, however, showed about 1 cm of right-lateral slip during the interval including the 1979 Imperial Valley earthquake, but no slip of greater than 1 mm has occurred since that time.

San Andreas fault in Coachella Valley.--Geodetic measurements continue to confirm the recent surprising observation that creep or episodic slip is taking place along the San Andreas southeast from San Gorgonio Pass to its apparent termination near the Salton Sea. This is surprising because of the very low to nil seismicity along this segment of the fault, marking it as a

possible seismic gap. The northernmost array at DEVERS HILL (across the Banning member of the San Andreas zone) has shown a relatively consistent slip rate of 2.0 mm/yr since its establishment in 1970. Progressing southeastward, the array at INDIO HILLS has shown an average slip rate of 1.8 mm/yr since 1977, the array at DILLON ROAD 2.2 mm/yr since 1970, the array at RED CANYON 3.1 mm/yr since 1977 and 1.7 mm/yr since 1967, and the array at BERTRAM variable slip possibly as much as 2 mm/yr at times but quiescent since 1979. All of these arrays except for DEVERS HILL show highly variable rates with time, increasingly influenced to the south by events in the Imperial Valley. The creepmeter at NORTH SHORE has not recorded any continuous creep or events larger than 1 mm from the time of its installation in 1970 to the present, although it lies between RED CANYON and BERTRAM, and despite a few measurements from the nearby NORTH SHORE alignment array that indicated a possible 1 mm/yr of slip. The nearby telemetered creepmeter at MECCA BEACH went into service in 1981 and has not reliably measured any motion greater than 1 mm up to the last servicing in May 1983. Thus it is increasingly clear that creep and/or episodic slip is taking place along at least 90 km of the the San Andreas fault in the Coachella Valley-Salton Sea region, but in a manner which is highly variable in both space and time. Due to the very low seismicity, the moment-derived slip is, of course, far lower than the observed surficial slip.

Coyote Creek fault.--This southeastward diverging extension of the San Jacinto fault system--locus of the 1968 Borrego Mountain earthquake--has the highest slip rate observed on any fault in southern California, averaging 5.8 mm/yr in some 12 resurveys since establishment of the BAILEYS WELL array in 1970. During this period, however, there have been two 1-2-yr intervals of apparent quiescence. The slip derived from the cumulative moment of seismicity along the fault trace shows similar periods of quiescence but is at least an order of magnitude less than the observed slip. This suggests that non-elastic slip is predominant on the Coyote Creek fault between large earthquakes and may control the minor seismicity.

San Jacinto fault.--Only two arrays across the San Jacinto fault have survived, those at COLTON and ANZA, which represent a rather unsatisfactory sampling of the 180-km-long fault. No overall creep exceeding 1 mm/yr has taken place since 1973 within the array at COLTON, near San Bernardino, although isolated creep events of up to a few millimeters could have occurred during this period. The ANZA array is squarely within the Anza seismic gap, and its correspondence to the rest of the fault zone is therefore questionable. Unstable monuments make this array difficult to evaluate, but between 1977 and 1983 the data suggest no creep greater than 1 mm/yr or episodic slip of greater than 1 cm. More than 2 mm/yr of creep is unlikely since 1973. It is, in fact, likely that no slip has occurred at this locality since 1973.

San Andreas fault northwest of San Gorgonio Pass.--Six alignment arrays in this "big bend" segment of the San Andreas fault between San Bernardino and Palmdale provide a good sample: SANTA ANA CANYON, WATERMAN CANYON, CAJON, BIG PINES, PALLETT CREEK, and UNA LAKE. These arrays provide convincing evidence that, despite continuing slip along the same fault zone in the Coachella Valley to the southeast, neither significant creep nor large episodic displacements have taken place along this segment of the fault since 1970. Creep of 0.2 to 1.0 mm/yr, and episodic slips of 5 to 20 mm could, however, have gone undetected at individual arrays.

Garlock fault.--The southwesternmost array across the Garlock fault, at CAMERON, has consistently shown left-lateral slip at an average rate of 3.7 mm/yr since its establishment in 1971. The slip may total as much as 6 mm/yr over a still wider zone. An NGS array 50 km southwest, near the junction of the San Andreas and Garlock faults, confirms continuing left-lateral slip on this southwestern segment of the fault. But 66 km along the fault northeast of CAMERON, our array at RAND provides good evidence for little if any continuing slip; over 12 years, the slip rate has not exceeded 0.1 mm/yr, nor have episodic displacements of greater than 1 mm occurred. Still 30 km farther northeast along the fault at CHRISTMAS CANYON, results are similar, at least through the last resurvey in 1980. A recently completed seismicity study of the Garlock fault by graduate student Luciana Astiz indicates that the seismicity pattern of the fault, as well as its geometry and fracture pattern, are consistent with the observed spatial variations in slip rates. The moment-derived slip rate from 50 years of seismic recording along the southwestern segment is, however, not as high as the slip rate derived either from the alignment array or from the Holocene geologic history.

On-Line Seismic Processing

9970-02940

Rex Allen
Branch of Seismology
U.S. Geological Survey
345 Middlefield Road, MS 77
Menlo Park, California 94025
(415) 323-8111 ext 2240

Investigations and Results

The Menlo Park real-time processor (RTP) is now the principal source of seismic data for its part of CALNET. In the past the RTP data were used to supplement the hand-picks from film. The procedure now is to use the RTP data as the primary source, and to supplement them by hand picks only where required because of malfunction or obvious poor performance by the RTP. The improved performance of the RTP which makes this change possible is largely due to the critical evaluation and suggestions we have received from users of the data, such as Jerry Eaton, Mitch Pitt, and Al Lindh.

An improved coda-length measurement algorithm was developed in cooperation with Lindh which is based on the decay rates of the seismic coda, rather than the actual measured time of return to noise level. The method is similar to that investigated by Carl Johnson in his thesis, but is suitable for use 'on the fly' in real-time systems. It provides by far the most accurate magnitude measurements we have yet achieved, and in addition, the decay slope measurement has proved to be a very powerful discriminant against noise bursts and 'glitches' on the telephone lines. Briefly, the method consists of taking averages of the absolute value of the seismic signal in two-second windows at selected intervals during an earthquake, and using these to calculate a coda decay time. The method allows the treatment of events longer than 141 seconds, the arbitrary cutoff point for the RTP observation of an event, and has thus extended our range of magnitude measurement to about 4.5.

Two new systems for use with the Yellowstone Net and at Mammoth have been completed, and will be delivered as soon as the installation sites are ready for them. The Yellowstone processor will be installed at the University of Utah in Salt Lake City, and the Mammoth unit at a location yet to be determined.

The Menlo Park RTP hardware has behaved reasonably well during this period, but Ellis and Rodriguez fight a continuing series of minor rearguard skirmishes against advancing age of the equipment and the inevitable newly-discovered bugs in hardware or software. We have begun to plan for the next version (Mark II) of the RTP, and are evaluating the processors now available. We hope that the Mark II can be built with a minimum of custom hardware, and our preliminary investigations are very encouraging.

Seismological Data Processing

9930-03354

Barbara Bekins

Branch of Seismology
U.S. Geological Survey
345 Middlefield Rd. MS 77
Menlo Park, California, 94025
(415) 323-8111 ext. 2965

Investigations

Computer data processing is absolutely necessary in modern seismological research; digital seismic data can be analyzed in no other way, and problems of earthquakes and seismic wave propagation usually require numerical solution. On the other hand, the interface between computers and people usually makes data processing unnecessarily difficult. The purpose of this project is to develop and operate a simple, powerful, well human-engineered computer data processing system and to write general application programs to meet the needs of scientists in the earthquake prediction program and monitor earthquakes in northern California.

Results

The PDP11-70 UNIX system has continued to operate smoothly, and performs a large amount of computing for program projects. Some current statistics:

233	registered users
637976	1024-byte disk storage blocks used
40	different users per weekday
177	average hours login time per day

Recent events of particular importance include:

The real-time Ppicker is operating smoothly and has been modified to determine magnitudes. In addition to sending out an alarm when there is high activity at Mammoth, it sends an alarm whenever there is an event with an average coda length greater than 120 seconds.

The Operating system has been updated to Berkeley version 2.9. Many users are now using the job control interpreter which conveniently allows them to start and stop processes running on their terminal.

The 11/70 computer will be upgraded to a Vax 11/750 in December of 1983. This will allow large programs to run without overlays. In addition, the Berkeley 4.2 operating system may be run on the Vax. This is a very efficient system, whose development is funded by ARPA.

Also two 414 MB winchester disk drives and a 9900 controller have been purchased from System Industries Corp. These will replace the RP06 disks which are expensive to maintain and about the speed, and increase the capacity on the system by 100%. Hopefully this will alleviate the chronic disk space shortage on the 11/70 system.

Finally, Ethernet hardware and user communication software have been ordered to form a high speed connection between the 11/750 UNIX system and the office Vax 11/780 VMS system. This will allow file transfers, remote logins (where someone on a terminal connected to one of the machines may login across the network to the other), and remote job execution (where a job may be submitted on on machine to run on another).

SEISMIC HAZARD AND EARTHQUAKE PREDICTION IN NORTHWEST MEXICO AND THE CALIFORNIA-MEXICO BORDER REGION: A COOPERATIVE U.S.-MEXICO STUDY

14-08-0001-19852 & 21337

James N. Brune and Michael S. Reichle
Institute of Geophysics and Planetary Physics
Scripps Institution of Oceanography (A025)
University of California, San Diego
La Jolla, California 92093
(619) 452-2890

A comparative study of northern Baja California and Imperial Valley - Mexicali Valley historic earthquakes was started in order to better understand how different source and propagation path properties contribute to the observed differences in the areas of damaging intensities and in the spectral source parameters. Initial regional spectral analyses inferred low stress drops for northern Gulf of California - Salton Trough events and high stress drops for San Miguel fault (northern Baja California) events. More recent studies using local records have noted high stress drop events in the Salton Trough. This raises the question of whether the observed regional differences are indeed source effects or are due to propagation path differences.

Two events, one from the Mexicali Valley and one from the San Miguel fault, which were recorded on local digital stations and at Pasadena, were analyzed for average path attenuation using spectral ratios of the S waves. The path from the San Miguel event to Pasadena is primarily through the southern California batholith. An average Q_s of 350 was calculated. The path from the Mexicali Valley event is more complex, including portions of the Salton Trough and the batholith. A path-averaged Q_s of 170 suggests a somewhat lower Q_s for the Salton Trough itself.

These preliminary estimates of regional variations in attenuation were included in analyses of the 1954 and 1956 San Miguel earthquakes, and the 1979 and 1980 Salton Trough earthquakes. Regional strong motion records provided high frequency data. The low frequency spectral level was determined from the teleseismic seismic moments. The Q differences had little effect on the estimate of corner frequency and, hence, on the calculated stress drop. The spectral values at higher frequencies, around 1-2 Hz, were affected by factors of 2-4 for Salton Trough events and only 1.5-2 for San Miguel events. Since much of the ground-shaking damage from larger earthquakes seems to result from frequencies near 1 to 4 Hz or so, both the greater high frequency excitation of San Miguel fault earthquakes and the lower path attenuation along the batholith appear to contribute to the greater areal extent of damaging intensities from those events.

VERY LONG BASELINE INTERFEROMETRIC GEODESY WITH GPS SATELLITES

Contract No. 14-08-0001-19864

Prof. Charles C. Counselman III
Massachusetts Institute of Technology
Department of Earth, Atmospheric and Planetary Sciences
Cambridge, MA 02139
Telephone (617) 253-7902

Introduction

For geophysical research, and especially for earthquake-predictive research, a surveying instrument that could determine geodetic-monument positions accurately in all three dimensions would be extremely useful. Such an instrument might be used, for example, to monitor a network of monuments that extended along both sides of an active fault, or that surrounded a volcano. For geophysical purposes, measurement accuracies of the order of 1 part in 10^7 (corresponding to 1 centimeter in 100 kilometers) or even 10^8 (1 cm in 1000 km) are desired. Such accuracies, we believe, are obtainable with portable surveying instruments that receive radio signals from the earth-orbiting satellites of the Global Positioning System (GPS) [reference (1)], and that process these signals in an interferometric mode.

The purpose of our work under this contract is "to determine the accuracy with which the lengths and the relative directions of very long baselines can be determined with a GPS-based interferometry system." [Ref. (2)] The work has two parts: first, to see how well the geocentric orbits of the satellites can be determined; and second, given knowledge of the orbits, to see how accurately we can determine the baseline vector between monuments that are occupied by portable receivers.

For the purpose of orbit determination, the satellites can be tracked by receivers stationed at well-known locations. The tracking data from these receivers can be analyzed to determine the orbits. The resulting ephemerides can then be used in separate analyses of data collected by portable receivers at geophysically interesting sites. An alternate approach, more complicated but theoretically more accurate, is to analyze the data from all receivers simultaneously. We have tested both approaches.

Accomplishments

We have used GPS interferometry to measure baseline vectors of various lengths, from 124 meters to 845 kilometers. Our measurement results have been compared with independent determinations by other measurement techniques, in order to

test accuracy. The other techniques have included conventional surveying methods (tape, EDM, theodolite, precise level) for the shorter baselines, and Transit satellite and radio-astronomical VLBI for the longest baseline. The level of accuracy indicated by the most reliable of these comparisons has been about 1 part in 10^6 or better for baselines longer than about 1 km. [See references (3)-(6).]

The accuracies of our baseline measurements have been limited by two factors: (i) uncertainty in the orbits of the satellites, and (ii) ionospheric refraction effects on the signals received by the portable receivers. The main cause of the orbital uncertainty, we believe, has been instability of the (Cesium-beam) frequency standards that have been used at the tracking stations. This source of error can be reduced by the use of more stable standards, such as hydrogen masers, at the tracking stations. There is no need to employ stable frequency standards with the portable receivers. The effect of the ionosphere on the portable-receiver observations can be virtually eliminated if these receivers observe the GPS signals in both of the two frequency bands that are transmitted. Dual-band receivers have recently become available.

Plans

During October, 1983, we will install dual-band satellite-tracking receivers at two hydrogen-maser-equipped sites: the NEROC Haystack Observatory in Massachusetts, and the U.S. Naval Observatory in Richmond, Florida. In the near future, we will outfit other maser-equipped sites with dual-band tracking receivers, beginning with the G.R. Agassiz Station in Ft. Davis, Texas. With the data from at least three of these tracking sites, we should be able to determine the satellite orbits at the level of 1 part in 10^7 or better. Then, to test our ability to determine baseline vectors with portable receivers, we will measure baselines that are known already to within less than 1 part in 10^7 from radio-astronomical VLBI observations.

References

1. Parkinson, B. W., "Overview" (Introduction to GPS Special Issue), Navigation, vol. 25. no. 2, Summer 1978; see also other articles in this issue.

2. Counselman III, C. C., and Shapiro, I. I., "Very Long Baseline Interferometric Geodesy with GPS Satellites," unsolicited proposal submitted to the U.S.G.S. Earthquake Hazards Reduction Program, September 30, 1980; basis of the present contract.

3. Counselman III, C. C., et al., "Centimeter-Level Relative Positioning with GPS," Journal of Surveying Engineering, vol. 109, pp. 81-89, August 1983.

The following papers were presented at the XVIII General Assembly of the International Union of Geodesy and Geophysics, International Association of Geodesy Symposium d, Hamburg, Federal Republic of Germany, August 15-27, 1983, and may be printed in the Proceedings of the Symposium, and/or in the Bulletin Geodesique, in the near future:

4. Bock, Y., et al., "Geodetic Accuracy of the Macrometer Model V-1000"

5. Goad, C. C., and Remondi, B. W., "Initial Relative Positioning Results Using the Global Positioning System"

6. Hothem, L. D., et al., "Analyses of Doppler, Satellite Laser, VLBI, and Terrestrial Coordinate Systems"

Search for Electromagnetic Precursors to Earthquakes

110212

W. D. Daily
Engineering Research Division
Lawrence Livermore National Laboratory
P. O. Box 5504, L-156
Livermore, CA 94550
(415) 422-8623

Investigations

1. A prototype, low frequency, broad band radio receiver has been constructed and field tested. Ambient electromagnetic noise levels from 0.1-1 kHz, 1-10 kHz and 10-100 kHz were monitored for about five months to evaluate the system performance and to understand signal variations.

2. A field deployable system has been built based on the prototype performance evaluation.

Results

1. One field deployable broad band receiver has been completed. Work is about 60% complete on construction of four other identical systems. Each system records on paper tape and digital magnetic tape integrated signal strength in three frequency bands: 0.2-1 kHz, 1-10 kHz, 10-100 kHz. System design is so that unattended operation is possible for one month intervals.

2. The completed field system has not yet been deployed. This will be accomplished during October 1983.

3. Four sites have been chosen for deployment such that a broad representative area along the San Andreas fault system can be monitored. The sites are at Coyote Lake, Parkfield, Bear Valley, and Pinion Flat.

4. The fifth receiving system will be used as a spare or be deployed at Long Valley, California.

Theodolite Measurements of Creep Rates on San Francisco Bay Region Faults

Contract No. 14-08-0001-21260

Jon S. Galehouse
San Francisco State University
San Francisco, CA 94132
(415) 469-1204

We bagan to measure creep rates on various faults in the San Francisco Bay region in September 1979. The total amount of slip is determined by noting changes in angles between sets of measurements taken across a fault at different times. This triangulation method uses a theodolite set up over a fixed point used as an instrument station on one side of a fault, a traverse target set up over another fixed point used as an orientation station on the same side of the fault as the theodolite, and a second traverse target set up over a fixed point on the opposite side of the fault. The theodolite is used to measure the angle formed by the three fixed points to the nearest tenth of a second. Each day that a measurement set is done, the angle is measured 12 times and the average determined. The amount of slip between measurements can be calculated trigonometrically using the change in average angle.

We presently have theodolite measurement sites at 19 localities on faults in the Bay region. Most of the distances between our fixed points on opposite sides of the faults range from 75-215 meters; consequently, we can monitor a much wider slip zone than can be done using standard creepmeters. The precision of our measurement method is such that we can detect with confidence any movement more than a millimeter or two between successive measurement days. We measure most of our sites about once every two months.

The following is a brief summary of our results thus far:

Seal Cove fault - We began our measurements on the Seal Cove fault in San Mateo County in November 1979. For the past four years, the Seal Cove fault has been moving at an average rate ofabout 1.2 millimeters per year in a right-lateral sense. It is difficult to ascertain whether the real tectonic displacement is uniform or episodic inasmuch as seasonal effects involving apparent left-lateral slip occur toward the end of each calendar year.

San Andreas fault - Since March 1980, our site on the San Andreas fault in South San Francisco has shown virtually no net slip, indicating that the San Andreas fault is virtually locked in the San Francisco area. Our site in the Point Arena area has averaged slightly more than one millimeter per year of right-lateral slip from January 1981 to February 1983.

Calaveras fault - We began monitoring the Calaveras fault at two sites in the Hollister area in September and October 1979. Slip in this area is quite

episodic, with times of relatively rapid right-lateral movement alternating with times of little net movement. The times and amounts of relatively rapid movement and the times of little movement are often different for the two sites. For the past four years, there has been an overall average of about 8.5 millimeters per year of right-lateral slip at our site within the City of Hollister and about 14 millimeters per year for our site 2.3 kilometers to the northwest. These results indicate that the Calaveras fault in the Hollister area is the most rapidly creeping fault in the greater San Francisco Bay region. In contrast, our site in San Ramon, near the northwesterly terminus of the Calaveras fault, has averaged only about one millimeter per year of right-lateral slip for the past two and one-half years.

Rodgers Creek fault - Since we began our measurements on the Rodgers Creek fault in Santa Rosa in August 1980, there has been an overall net right-lateral slip of several millimeters. However, our results show large variations in the amounts and directions of movement from one measurement day to another which are probably due to seasonal and/or gravity-controlled mass movement effects, not tectonic slip.

West Napa fault - Since we began our measurements on the West Napa fault in the City of Napa in July 1980, there has been no overall net movement. Similarly to our results for the Rodgers Creek fault, however, large variations up to nearly a centimeter have occurred in both a right-lateral and a left-lateral sense between measurement days. The magnitude of these nontectonic effects is obscuring any tectonic slip that may be occurring. We hope that continued monitoring of these North Bay faults over a longer period of time will help clarify the situation.

Hayward fault - We began our measurements on the Hayward fault in late September 1979 at sites in Fremont and Union City. In the four years since then, the average rate of right-lateral slip has been about 5.0 millimeters per year in Fremont and about 4.4 millimeters per year in Union City. Periodic aberrations involving apparent left-lateral slip have also occurred at both these sites. Unpublished U.S.G.S. creepmeter data suggest a similar net rate of movement in this area and also show aberrations in direction of movement.

We began measuring two sites within the City of Hayward in June 1980. In more than three years since then, the average rate of right-lateral movement has been about 5.1 and about 4.1 millimeters per year at the two sites. U.S.G.S. creepmeters in Hayward show a similar rate of movement over this same time interval.

We began measurements in San Pablo near the northwestern terminus of the Hayward fault in August 1980. After three years, the average rate of movement has been about 4.0 millimeters per year in a right-lateral sense. However, changes between measurement days of up to nearly a centimeter in both a right-lateral and a left-lateral sense suggest that non-tectonic effects are also present at this site.

It may be significant that four of our five sites on the Hayward fault have shown a higher than average rate of right-lateral movement since August 1982, with sites in Fremont, Hayward, and San Pablo showing especially increased rates of movement since January 1983.

Concord fault - We began our measurements at two sites on the Concord fault in the City of Concord in September 1979. Both sites showed about a centimeter of right-lateral slip during October and November 1979, perhaps the greatest amount of movement in a short period of time on this fault in the past two decades. In the four years since this rapid slip, both sites have shown additional right-lateral movement at a rate of only about one millimeter per year.

Antioch fault - We began our measurements at the more southeasterly of our two original sites on the Antioch fault in the City of Antioch in January 1980. During the next 27 months, we measured a net right-lateral displacement of nearly two centimeters. However, large changes in both a right-lateral and a left-lateral sense occurred between measurement days. Three times left-lateral displacement occurred toward the end of one calendar year and/or beginning of the next. We had to abandon this site in April 1982 because of logistic problems. The more northwesterly of our original sites is located where the fault zone appears to be less specifically delineated. In more than three years since May 1980, we have measured a net displacement of about four millimeters in a left-lateral sense. Much subsidence and mass movement creep appear to be occurring both inside and outside the Antioch fault zone and it is probable that these nontectonic movements have influenced our theodolite results at these two sites. We have recently established a new site on the Antioch fault just southeast of the City of Antioch and hope to have significant results soon.

Papers Presented:

Brown, B. D. and Galehouse, J. S., 1983, Triangulation survey methodology for monitoring of earthquake fault creep in the San Francisco Bay region: Third Annual Meeting, Association of North Bay Scientists, Eureka, CA.

Galehouse, J. S., 1983, An earthquake prediction effort in the San Francisco Bay area: Fall 1983 Conference, National Association of Geology Teachers - Far Western Section, Coalinga, CA.

Papers Published:

Galehouse, J. S., Brown, B. D., Pierce, B., and Thordsen, J. J., 1982, Changes in movement rates on certain East Bay faults: in Proceedings - Conference on Earthquake Hazards in the Eastern San Francisco Bay Area; Hart, E. W., Hirschfeld, S. E., and Schulz, S. S., editors; Special Publication 62, Calif. Div. Mines and Geology, pp. 239-250.

PIEZOMAGNETIC MONITORING IN THE SOUTH PACIFIC REGION.

14-0800001-17771

Michael T. Gladwin
Department of physics
University of Queensland
St.Lucia,4067
AUSTRALIA

1.INVESTIGATIONS. This project has established an array of microprocessor controlled remote monitoring stations in a region of very high shallow seismicity in the South Pacific Ocean. The 25 stations are currently equipped with 0.25nT proton precession magnetometers which sample the earth field synchronously across the array every five minutes. Stations return collected data every three hours via satellite, and are equipped with reserve printers to permit collection of data taken during satellite outages. The data set is complete for eleven stations from July 1980, and for the remaining 14 stations from July 1981 and includes an extensive set of station diagnostics. Stations are visited annually for maintenance.

2.RESULTS

A. In contrast with the results reported to date in California by Mueller and Johnston, piezomagnetic monitoring in the south Pacific array is totally feasible at the 0.5nT level. The standard deviation of hourly means of simple station differences shows little increase with station separation out to several hundred kilometers. This is shown in figure 1. The Californian array seems severely limited in its predictive capability at separations beyond 50 km, where for large events, in the scale range of 100 to 300 km, anomalies of several nT would be required for unambiguous detection.

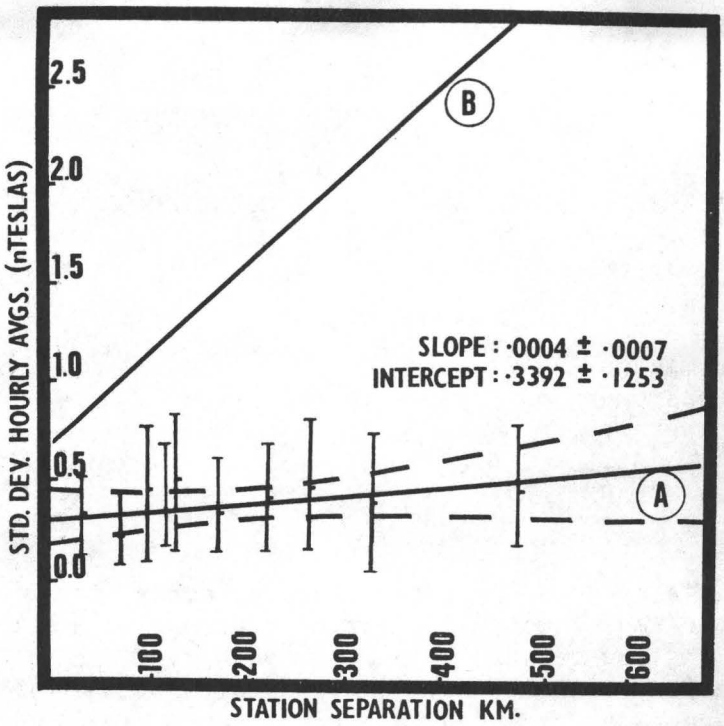

Figure 1. Comparison of Standard Deviations of hourly averages of differences as a function of station separation for the South Pacific array (data A) and for the Californian data (line B). The negligible slope of the South Pacific data enhances the array predictive capability.

B. Two events have occurred in the past twelve months in the northern part of the array. The first, on day 244 of 1982, was a dip slip event (mb =5.9, ms=6.4, depth=45km). The second event, also dip slip, occurred on day 077 of 1983. It was reported in P.D.E. as mb=6.4, ms=7.9, depth 88km. The location of these events in relation to the five nearest stations is shown in figure 2. Changes in the magnetic field at each of the stations for the period spanning these events are shown in figure 3. For a total field shift to be included it must be documented in differences with all nearest neighbours, and differences between these neighbours are required to remain stationary relative to each other. Only shifts greater than 1.0nT are included. The following conclusions have been drawn:

1. The two epicentres were sufficiently close to the stations Nissan and Manga to show piezomagnetic anomalies.

2. That no obvious coseismic shift occurred for either earthquake.

3. That with only one exception, the magnetic events during this period occurred asynchronously at the various stations (eg day 070 at Nis, day 080 at Man or again the sequence 280 at Nis, 320 at Nam, 335 at Rab, 340 at Nis, 345 at Buk, 365 at Nam etc).

4. All shifts occurred with rapid onsets at the stations shown. It should be noted that piezomagnetic monitoring stations are most sensitive to stresses in the 5 to 10 km volume immediately surrounding the station.

5. If the asynchronous and rapid onset of these changes reflect changes of stress in the region of the detection site , there is clear evidence of aseismic propagation of stress fields in the area at drift velocities in the range 5 to 15 km per day.

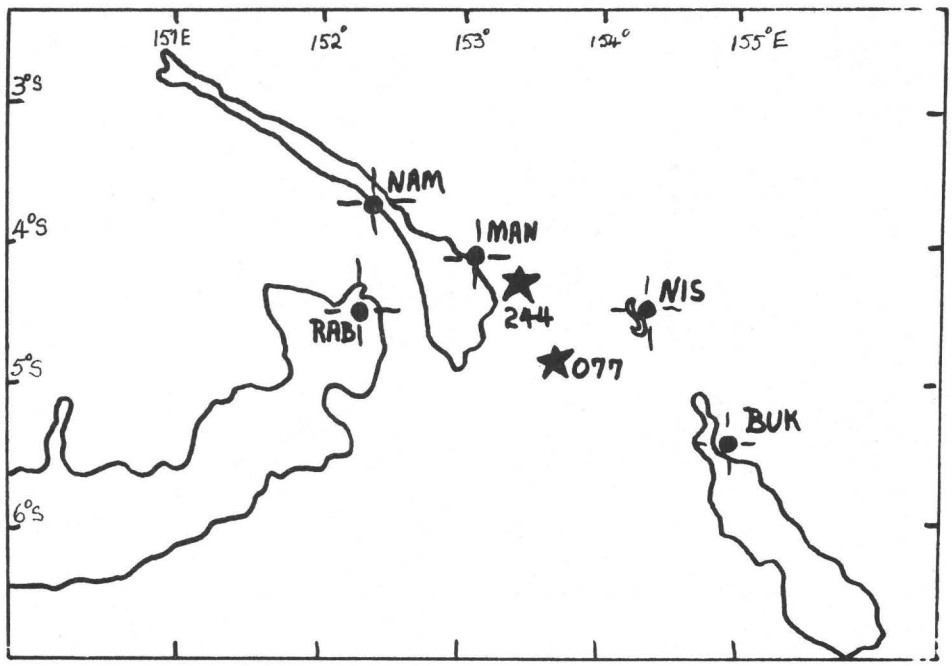

Figure 2. Location of five nearest stations to the two events considered.

6. That the scale of the phenomena we are observing relates well to earthquakes of magnitude about 7.

7. That in the six month period prior to 1982, there were no equivalent shifts on any of the stations shown.

8. That it is inappropriate to use simple elastic approximations in modelling large event piezomagnetics. All evidence in the present data indicates that large scale propagation of aseismic stress fields occur prior to large events. These propagation phenomena are probably related to the production of stress concentrations responsible for large seismic events.

9. That greater success in piezomagnetic modelling for earthquake studies may be obtained by abandoning the simple consideration of quasi static elastic strain fields centered on the final event in favour of an attempt to model the dynamics of the stress accumulation process preceeding rupture.

10. That further sequences of events need to be investigated to verify the generality of these observations. U.S.G.S. has terminated its interest in the program but it is probable that at least one further sequence will be documented in the next twelve months. Comparisons with the Californian array will be continued for as long as a high percentage of the 25 field sites remain fully operational.

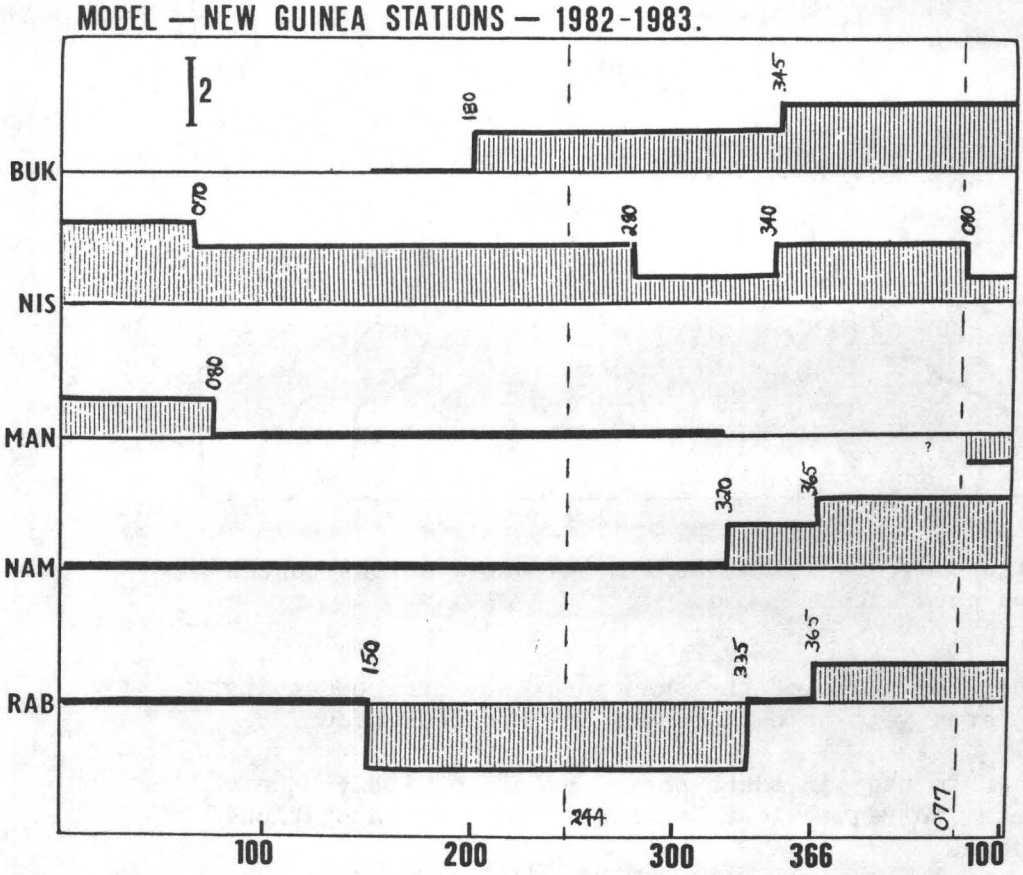

Figure 3. Total field shifts shown as a function of time for the two events. The numbers identify the days on which shifts occurred. Earthquakes occurred on day 244, 1982, and day 077,1983.

Central California Network Operations

9930-01891

Wes Hall
OFFICE OF EARTHQUAKES, VOLCANOES, AND ENGINEERING
Branch of Seismology
345 Middlefield Road, Mail Stop 77
Menlo Park, California 94025
(415) 323-8111, ext. 2509

Investigations

1. Maintenance and recording of 385 seismograph stations, located in northern California and Oregon. The area covered is approximately 83,000 square miles. Recording 20 tiltmeter, 4 strain meter, and 18 creepmeter sites.

Results

1. Began new outside maintenance contract for seismic network in northern and southern California. The contract was awarded to the Stanwick Corporation.

2. Installed four new permanent stations in the Coalinga area following major earthquake.

3. Upgraded the Mammoth Lakes seismic array. Fabricated and installed equipment for 14 sites.

4. Upgraded the Shasta, Lassen Network, installed four new antenna towers.

5. Began installation of new microwave equipment at Mission Peak.

6. Extensive involvement in RTP data output.

7. Assembled approximately 100 DC/DC converters for use in VCO's and summing amps.

Support of the Southern California Geophysical Data and Analysis Center

14-08-0001-21216

David G. Harkrider
Seismological Laboratory, 252-21
California Institute of Technology
Pasadena, California 91125

This report covers the six-month period from April 1, 1983 to September 30, 1983.

Goals

1. This contract supports the data collecting and processing activities of the CEDAR (Caltech Earthquake Detection and Recording) and CROSS (Caltech Remote Observatory Support System) systems at the Seismological Laboratory.

Results

1. CEDAR

The CEDAR system was originally developed and supported by this contract and its predecessors (contracts #14-08-0001-16629, 17642, 18330, and 19267), and is now an element of the joint USGS-Caltech SCARLET system (Southern California Array for Research on Local Earthquakes and Teleseisms). Its product is a component of the results produced by the contract "Southern California Seismic Arrays", contract #14-08-0001-19268, i.e., the recording and processing of earthquake data effecting a digitized data base of seismic events stored on "Archive" 800 PBI magnetic tapes.

2. CROSS

This contract supplies continuing operational support for CROSS developed under the predecessor contracts (given above). During this reporting period fourteen data login (TIM) units have been maintained on site.

Stations currently in operation:

SITE LOCATION	TYPE OF MEASUREMENT	PRINCIPAL INVESTIGATOR
Anza (AZ)	water well	Lamar/Merifield
Caltech campus (RO)	tilt	T. Ahrens
Hollister (HO)	tellurics	T. A. Madden
Kresge Lab. (KR)	tilt	Test site
Lake Hughes (LH)	tilt, meteorology	T. Ahrens, T. Henyey
Palmdale (PD)	tellurics	T. A. Madden
Palmdale (PM)	water well baro. pressure	Lamar/Merifield
Palmdale (GP)	water well	Lamar/Merifield
Palmdale (AQ)	water well	Lamar/Merifield
Ocotillo Wells (OW)	water well	Lamar/Merifield
Borrego Springs (BS)	water well	Lamar/Merifield
Pallett Creek (PC)	water well	Lamar/Merifield
Mecca Beach (MC)	tilt,creep	C. Allen
Dalton tunnel (DT)	tilt, meteorology	T. Ahrens

Note: Some sites listed in previous reports have been removed from service by the P.I.'s for operational reasons. The Fairmont (FM) site is now being telemetered by the USC P.I.'s own system.

The data at these Southern California sites are collected once or twice a day via a telephone telemetry polling procedure and are being accumulated as a data base on the Caltech Seismological Laboratory PRIME computing system. For non-Caltech investigators the data is made available on hard copy, magnetic tape or via a modem port into the PRIME computer through which investigators may transmit the data to devices at their location by telephone.

Analysis of Seismic Data from the Shumagin Seismic Gap, Alaska

14-08-0001-21299

Egill Hauksson and Klaus H. Jacob
Lamont-Doherty Geological Observatory of Columbia University
Palisades, New York 10964
(914) 359-2900

Investigations

Analyze seismic data from the Shumagin seismic gap in the eastern Aleutians. The available catalogue of the Shumagin seismic network is used to identify possibly precursory spatial and/or temporal clustering of seismicity. Changes in the state of stress adjacent to the plate boundary that may be precursors to a great earthquake are assessed by searching for changes in seismicity and by determining focal mechanisms.

Results

M_S = 5.0 to 6.5 earthquakes that occurred primarily in 1974, 1979 and 1983 contribute to an approximate doughnut pattern surrounding the Shumagin seismic gap. This pattern that may signal the imminence of a great Shumagin earthquake can be inferred both from local network and from teleseismic earthquake locations in the region. The pattern shows higher levels of activity near the eastern and western ends of the seismic gap and along the downdip end of the main thrust zone. The temporal behavior of the seismicity is characterized by a burst of activity in 1978 and 1979 and a low or average level of activity from 1980 to January 1983 (see Figure 1). The burst of seismicity and a simultaneous tilt event suggest that shallow crustal seismicity, and possibly the occurrence of moderate-size ($M_S < 6.0$) earthquakes may be strongly influenced by temporal changes in the rate of aseismic plate subduction down-dip from the brittle, shallow portion of the main thrust zone. Temporal correlation of seismicity with other parameters including tilt from short leveling lines and sea-level monitors, and with volcanicity may enhance the probability gain of future prediction efforts.

Composite focal mechanisms have been determined from high quality data recorded by the Shumagin seismic network in 1981 (see Figure 2). The main results indicate: 1) shallow angle thrusting near the down dip end of the main thrust zone; 2) down-dip compression between 50 to 120 km depth in the upper plane of the double Benioff zone; 3) a diffuse zone of down-dip tension that coincides with the lower plane of the double Benioff zone; 4) dominantly down-dip tension between 120 to 170 km depth and compression from 170 to 250 km depth. In addition, a number of fault plane solutions that had not been identified previously in the Shumagin region show complex low-angle thrusting near the lower edge of the main thrust zone. Also, earthquakes that have similar hypocenters within the slab can have P- and T-axis that differ in orientation by as much as 90°.

Several independent lines of evidence such as doubling of the rate of microseismicity and tilt reversal observed on short leveling lines indicate that an aseismic slip event may have occurred along the Benioff zone between 20 and 70 km depth in 1978-79 (Beavan et al., 1983). During this slip event Reyners and Coles (1982) reported downdip tension in the upper plane of the Benioff zone, although the slip event had not been identified at that time. The change from downdip tension in the upper plane in 1978/79 as compared to downdip compression in 1981 suggests that the slip event strongly affected the state of stress within the Benioff zone. Hence, stresses generated by episodic subduction below the main thrust zone may at times dominate over thermal or other stress sources.

References

Beavan, J., E. Hauksson, S. R. McNutt, R. Bilham, and K. H. Jacob, Tilt and seismicity changes in the Shumagin seismic gap, Science, 222, 322-325, 1983.

Habermann R. E., Teleseismic detection in the Aleutian Island Arc, J. Geophys. Res., 88, 5056-5046, 1983.

Reyners, M., and K. Coles, Fine structure of the dipping seismic zone and subduction mechanics in the Shumagin Islands, Alaska, J. Geophys. Res., 87, 356-366, 1982.

Reports

Hauksson, E., Regular or precursory seismicity, 1973-1983, in the Shumagin seismic gap, Alaska?, EOS, Trans. AGU, 64, p. 258, 1983.

Dobb, S., and E. Hauksson, Temporal variations in patterns of stress within the subducted slab in the Shumagin gap, Alaska?, submitted for 1983 Fall AGU Meeting, 1983.

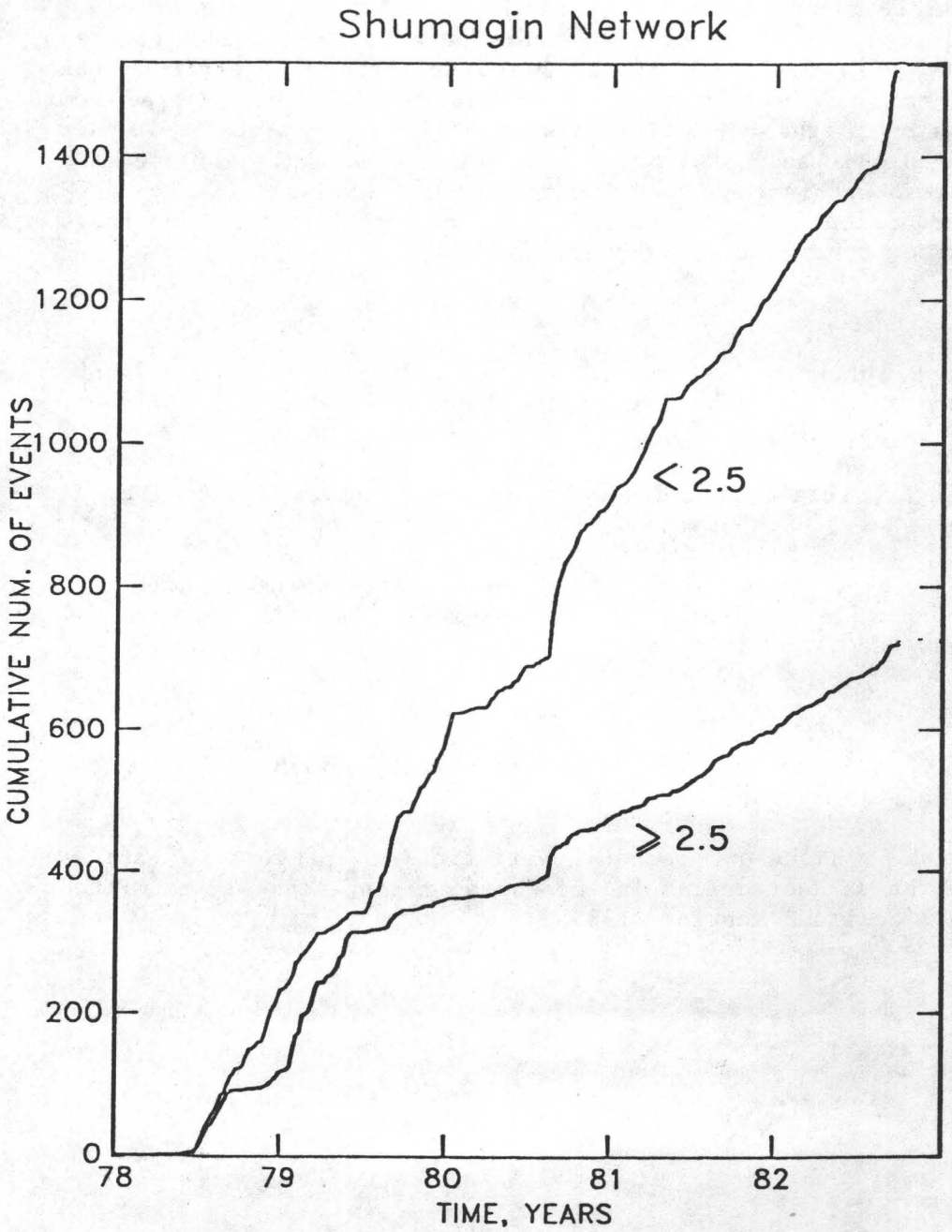

Figure 1. Cumulative number of earthquakes recorded by the Shumagin network from 1978-1982. Techniques and computer programs developed by Habermann (1983) are used to show that for earthquakes of $M \geq 2.5$ there was a significantly higher rate of seismicity in 1978-1979 than there was in 1980-1981.

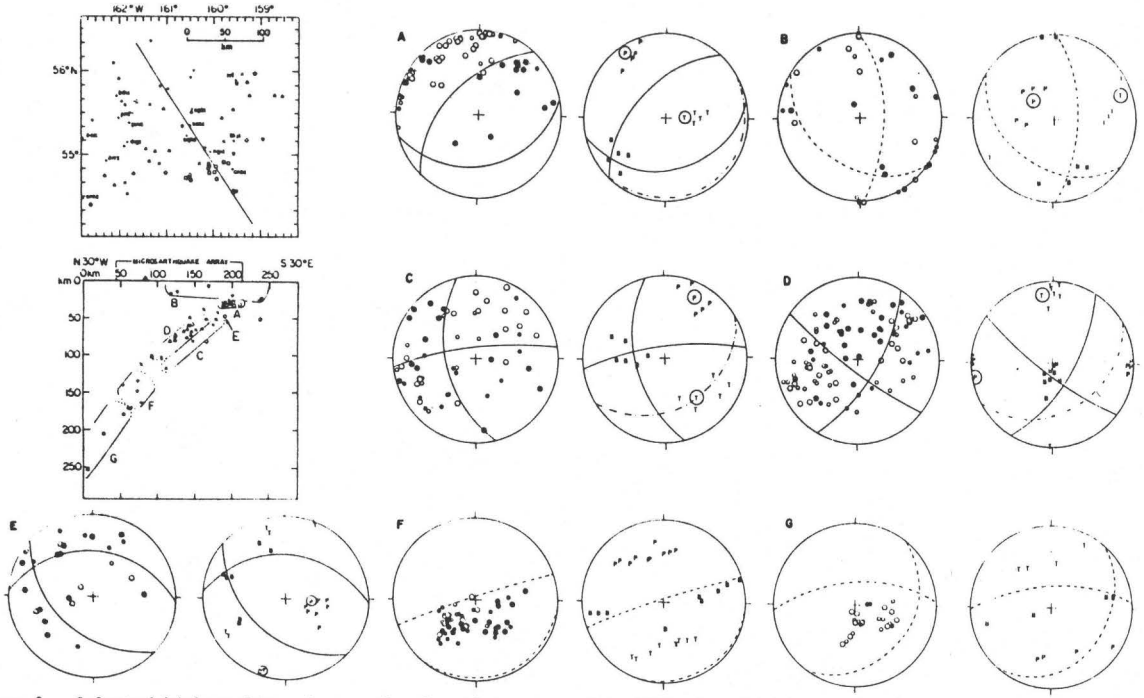

Figure 2. Selected high quality microearthquakes that occurred in 1981, for which composite focal mechanisms have been determined; see map and depth section in left-hand diagram. In the depth section regions A-G correspond to upper hemisphere focal mechanisms A-G shown to the right. Open symbols represent dilatational and solid symbols represent compressional P-wave first motions. Small symbols indicate less reliable readings. Next to each focal mechanism a stereogram of all possible P and T axis is shown, which is determined by allowing for a given number of inconsistencies in each solution. Dashed curves are less well constrained possible fault planes. Dashed-dot curves indicate the approximate dip of the Benioff zone where the respective group of microearthquakes is occurring.

Search for Precursors to Earthquakes in the Vanuatu Island Arc by Monitoring Tilt and Seismicity

14-08-0001-18350

Bryan L. Isacks
Department of Geological Sciences
Cornell University
Ithaca, New York 14853

Investigations

1. During the past year the monitoring network continued to operate with the cooperation of French scientists and technicians of ORSTOM. The network includes twenty seismograph stations distributed along 500 km of the island arc, seven bubble level tiltmeter stations, two periodically releveled arrays of benchmarks, and a two-component, 100 M water-tube tiltmeter. Our investigations have focused primarily on analyses of the seismicity data that has now accumulated for 5 years. The tiltmeter monitoring has been improved to increase the sensitivity of the instruments to possible short period (minutes to hours) precursory signals.

Results

1. During the past year no large earthquake occurred within or near the network. The largest shock occurred on March 12, 1983 about 40 km south of the tilt and seismograph stations on Efate island. The event has a thrust-type focal mechanism typical of an interplate earthquake, a magnitude (Ms) of 5.9, and a moment of 1.7×10^{25} dyne-cm. This event is located south of the 1979 and 1981 events. Its aftershock sequence did not exhibit the remarkable spatial expansion that characterized the 1979 and 1981 episodes. The mainshock was preceded during a period of several weeks by an unusual cluster of small events located within the subducted slab down-dip of the hypocenter.

In August of 1983 the nest of frequent shallow activity located northwest of Efate island activated with a swarm of events including three with magnitudes (Ms) greater than five (5.2, 5.5, and 5.7). No obvious precursory signals are seen on the tiltmeter records for these or for the March 1983 event.

Shallow, upper plate activity continued in the eastern part of the Aoba Basin near the islands of Maewo and Pentecost. Three events with magnitudes Ms near 5.5 occurred during the past year and all had thrust type mechanisms consistent with horizontal compressive stress oriented perpendicular to the arc in the region where the D'Entrecasteaux "fracture zone" is being subducted. These could be part of a long term preseismic pattern possibly characteristic of this region of the arc as suggested by Marthelot (1983).

2. The locations of small events from the 20 station network continue to document the time-space distribution of seismicity in the arc. Monthly bulletins are produced by ORSTOM together with computer tapes of P and S times and location data. ORSTOM has replaced HYPO71 by HYPOINVERSE for hypocenter location, and has rerun previous locations with the new program. From September 1982 through August 1983, 2681 hypocenters were located at an

average of 223 per month. Monthly totals varied between 138 to 400 events. Magnitudes are routinely assigned using a coda duration scale tied to the teleseismic m_b scale. Magnitudes as small as about 2-2.5 are located.

3. Further analysis of the 1979 and 1981 sequences showed that particularly intense concentrations of epicenters, clustering within regions of dimensions of 10 km or less, characterized the aftershock and foreshock activity of the three events of the sequences. In each case "hot spots" of the preceding event were reactivated in the aftershock sequence of the following event. These concentrations seem to mark particular locations in space and may coincide with specific structures in the plate boundary. Further studies of these "hot spots" through detailed studies of precise relative location and similarity of waveforms is being undertaken.

4. In cooperation with J.L. Chatelain and R. Prevot of ORSTOM, study of the variation of "b" values in time has revealed interesting increases before the large events in 1979 and 1981. During the 5 year sample considered these fluctuations are the most remarkable recorded within an area approximately 1 degree square around the large events. The sample is sufficiently long to suggest a background level of "b" between about 0.6 to 1.1. In the case of the August, 1979 sequence "b" increased to about 1.5 for about three months preceding the events and returned to normal just before the sequence started. In the case of the August, 1981 earthquake, two sharp increases ("b"$\approx$2) occurred, each of about 1-2 months duration. One occurred about 1 year preceding the event and the second about 4 months preceding the Ms=7 mainshock. In addition to examining the statistical significance of the fluctuations, we are examining the time-space structure of the activity comprising the large increases in b. No obvious swarm, for example, produces the anomaly.

5. Substantial new recordings have been obtained with the long baseline (100 m) half-filled water tube tiltmeter with the new continuously recording water level monitors at two of the four end points. Additional recorders at the other two end points were installed in September 1983. This system gives good resolution of short period tilt changes. Seiches in the tubes are recorded and are generally of small amplitude. However, the tsunami from the large Tongan earthquake of Dec. 19, 1983 excited particularly large amplitude and long duration seiche activity in the tubes. The bubble level stations continue to operate with the addition of high-pass filtered recording to increase the sensitivity of these units to possible short-period precursors (minutes to hours). These instruments are essentially "strong motion" monitors waiting for a significant event. Only the Efate leveling array was releveled during the past year. The results do not show any significant tilting since the last leveling, which continues the pattern of little secular tilt change during the past 4 years.

Reports

Wray, S.T., R.K. Cardwell, B.L. Isacks, E. Coudert, and J.-L. Chatelain, 1983, Detailed seismicity observations in the forearc region of a convergent plate boundary: Malekula Island, Vanuatu, (Abst.), EOS Trans., AGU, 64, 264, 1983.

Chatelain, J.-L., R.K. Cardwell, and B.L. Isacks, 1983, Expansion of the aftershock zone following the Vanuatu (New Hebrides) earthquake of 15 July, 1981, Geophys. Res. Lett., 10, 385-388.

Marthelot, J.M., 1983, Patterns of seismicity in the Vanuatu (New Hebrides) arc: Regional variations and systematic evolution, Ph.D. Thesis, Cornell University, Ithaca, NY.

Earthquake Prediction in Chile: Cooperative Program with the University of Chile

14-08-0001-20583

Bryan Isacks
Cornell University
Department of Geological Sciences
Ithaca, NY 14853
(607) 256-2307

John Kelleher
Redwood Research, Inc.
801 N. Humboldt St., #407
San Mateo, CA 94401

Investigations

1. Studies of the locations and focal mechanisms of earthquakes in the region of the interplate boundary are being undertaken to define the geometry of the interplate boundary, the distribution of intraplate deformation, and the relations of these to the generation of large shallow earthquakes. Focal mechanism solutions and accurate hypocentral depths for earthquakes with magnitudes (Ms) greater than about 5.7, obtained by comparisons of recorded and synthesized long-period P waves, are combined with selected high-quality locations of smaller events to better resolve the distribution of events and focal mechanism types in and around the Chilean interplate boundary. These data are combined with topographic, bathymetric, geological and geophysical data to resolve in more detail the tectonics of the interplate boundary and, in particular, to examine along-strike variations in the mechanical interaction of the plates.

2. The time-space distribution of shallow earthquakes occurring during the last 20 years is being studied with teleseismic data in relation to the rupture zone of great earthquakes defined by Kelleher along the Chile margin. We seek to place the past 20 years of seismicity in the perspective of the cycle of major interplate slippage and to resolve spatial patterns of seismicity preceding several large (but not great) Chilean earthquakes which occurred during the past 20 years.

3. Kelleher will work in Santiago with Chilean seismologists during November-December of 1983 examining and upgrading both historic and instrumental data. This work is aimed at improved understanding of large earthquake occurrence based on both long-term patterns and short term indications of pre-seismicity.

Results

1. A complete set of focal mechanisms and a nearly complete set of accurate depths have been compiled for shallow earthquakes with magnitudes (Ms) greater than 5.7 that occurred in Chile during the period 1962-1981. Slip vectors from interplate thrust earthquakes are consistent and agree with the direction of plate convergence inferred from global data. Vertical sections perpendicular to the plate boundary show a clear interplate zone above 60 km

depth. Its dip and position relative to the trench do not vary much along strike from the latitudes of Northern Chile through 37°S, although the dip of the Benioff zone at intermediate depths varies from 30° in Northern (18°S-27°S latitude) and South-Central (33°S-37°S) Chile to flat in Central Chile (27°S-33°S). The major changes in dip of the descending slab between these three segments occurs below the interplate seismic zone, at approximately 75-100 km depth. Scattered tensional mechanisms are observed within the shallow part of the descending plate, 25-30 km beneath (not down-dip from) the interplate zone. The forearc region of the upper plate is remarkably aseismic.

A spatial clustering of shallow earthquakes with thrust-type mechanisms is located near 38°S. The locations of these events indicates an anomalously shallow dipping interplate boundary compared to that farther north, if the events occur along the interplate boundary. Due to the absence of activity south of that zone there is uncertainty as to whether the interplate boundary actually has a flatter dip and a larger downdip length there than to the north or if the 38°S cluster lies in the upper plate. This anomalous cluster is very interesting because it lies at the northern end of the great 1960 earthquake.

2. In terms of the cycle of recurrence of earthquakes along the Chilean plate margin, the last 20 year period is part of the interseismic phase of the earthquake cycle. The largest events during the 20 year period (Ms=7.5-7.9) occurred at the ends of the rupture zones of the great shocks that happened previously in this century. The largest events at the ends of the historical rupture zones are at the sites of intense seismicity generally (including, for example, the Ms=7.1 October 4, 1983 earthquake). These areas should be the focus of more detailed work using local data. During the past 20 years there is a striking lack of activity throughout the 1960 rupture zone for both large and small earthquakes. Another particularly quiescent zone is located between 34° and 37°S. Between 27° and 33°S, coinciding with the region of nearly flat subduction at depth, the shallow activity near the interplate boundary is characterized by a clustering of events in space and time, both as swarm activity and as aftershocks.

Seismicity preceding several large earthquakes is being examined in more detail. For several years before a subduction related event in 1981 a striking lineation of seismicity occurred at an angle of about 45° to the trench axis. Epicenter locations imply that this pattern occurred within the underthrust oceanic plate. The pattern is quite similar to others which preceded events in Japan, the New Hebrides, and San Fernando, California.

Reports

Kadinsky-Cade, K. and B. Isacks, 1983, Shallow structure of the Benioff zone in Chile, EOS Trans. AGU, Vol. 64, No. 18, p. 264.

CRUSTAL DEFORMATION OBSERVATORY, PART A
14-08-0001-21237

David D. Jackson
Institute of Geophysics and Space Physics
University of California
Los Angeles, California 90024
(213) 825-0421

OBJECTIVES

The Crustal Deformation Observatory is a cooperative project whose goal is to develop and test advanced methods for observing crustal deformation, and to compile an accurate record of such deformation at one site in southern California. The UCLA role is primarily data analysis. The site is the Pinon Flat Observatory (PFO), located between the San Andreas and San Jacinto faults near Palm Desert, CA. PFO is operated by UCSD.

We have measured tilt at PFO using both continuously recording tiltmeters and geodetic leveling. No tectonic tilt has occurred there since 1981, to within an uncertainty of about 0.3 microrad/yr.

CONTINUOUS TILTMETER OBSERVATIONS

We have now analysed 517 days of tilt data from three long baseline fluid tiltmeters at Pinon Flat Observatory, California The tiltmeter data are shown in Figure 1. The most stable tilt record shows a linear trend of 0.2 microrad per year. This may be due to tilting or instrumental drift or a combination of both. The other tiltmeters are less stable and their records contain transients as large as 0.8 microrad over a period of only 50 days. There are obvious temperature effects, but they are not consistent over the entire time period. Apparently, the nature of the temperature sensitivity has changed with time, for all of the tiltmeters. Consequently, the correlation between tilt and temperature is significant for some time periods for some tiltmeters, but not for the entire time period for any of the tiltmeters.

Since 29 Jan 83 we have measured vertical displacements at both ends of two of these tiltmeters so we can now measure tilt with respect to reference points at 25m depth. Spectra of the various tilt records are shown in Figure 2. Tidal amplitudes of the various records agree to within 5% rms and the tidal phases agree to within 3.5 deg rms.

LEVELING

UCSB has carried out 12 leveling surveys at PFO since 13 Oct 79. Six of these surveys, from 25 Jan 81 to 2 Aug 83, have included the end points of the UCSD tiltmeter as monuments. Results for these six surveys are shown in Figure 3. The inferred tilt rate is -0.15 +/- 0.19 microrad/yr, consistent with a lack of tectonic tilt. For the other monuments, random benchmark motions of up to 1mm cause the dominant errors in the leveling data.

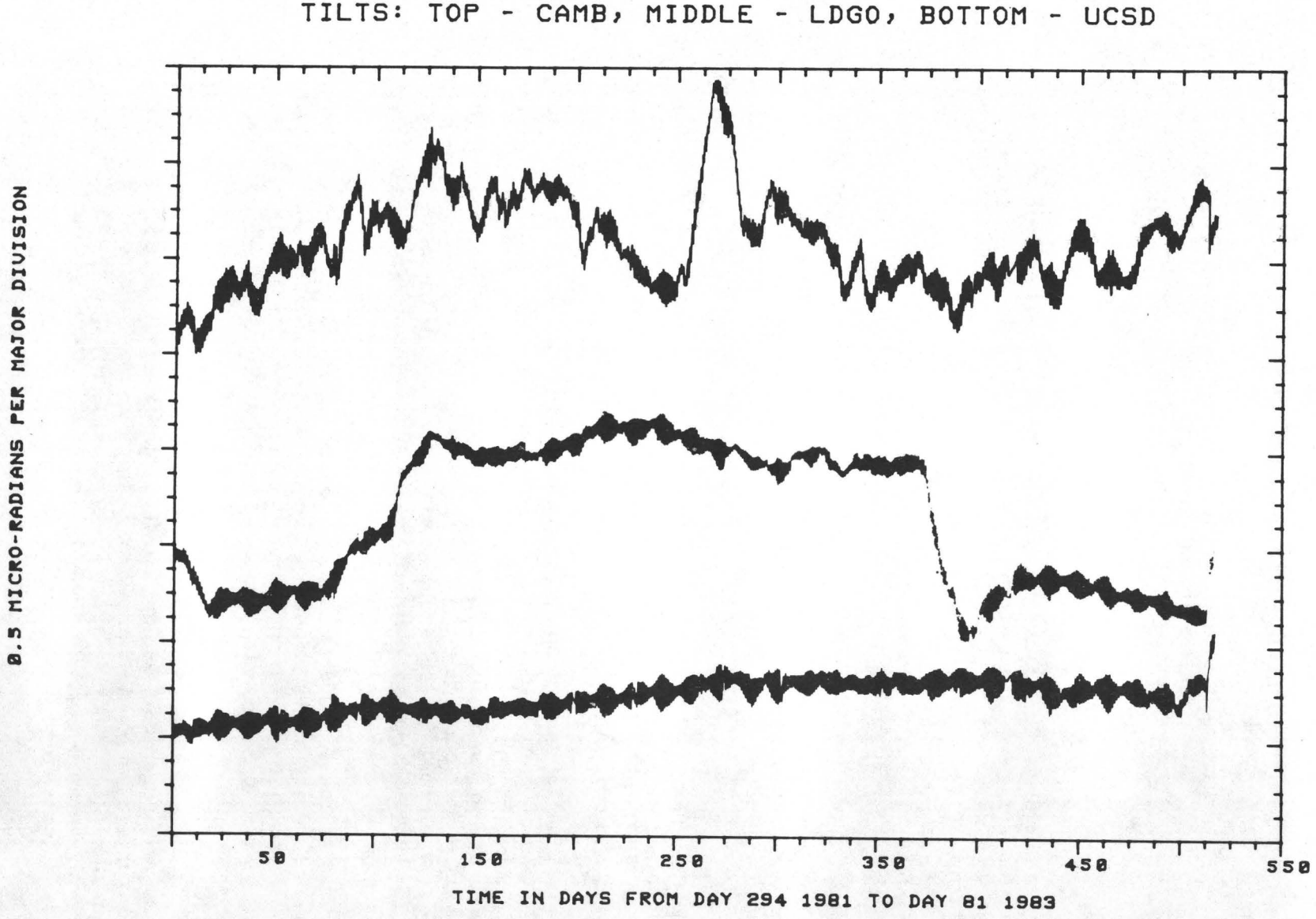

Figure 1. Tilt vs. time inferred from Cambridge, Lamont Doherty Geological Observatory, and UCSD tiltmeters. Positive tilt is down to the east.

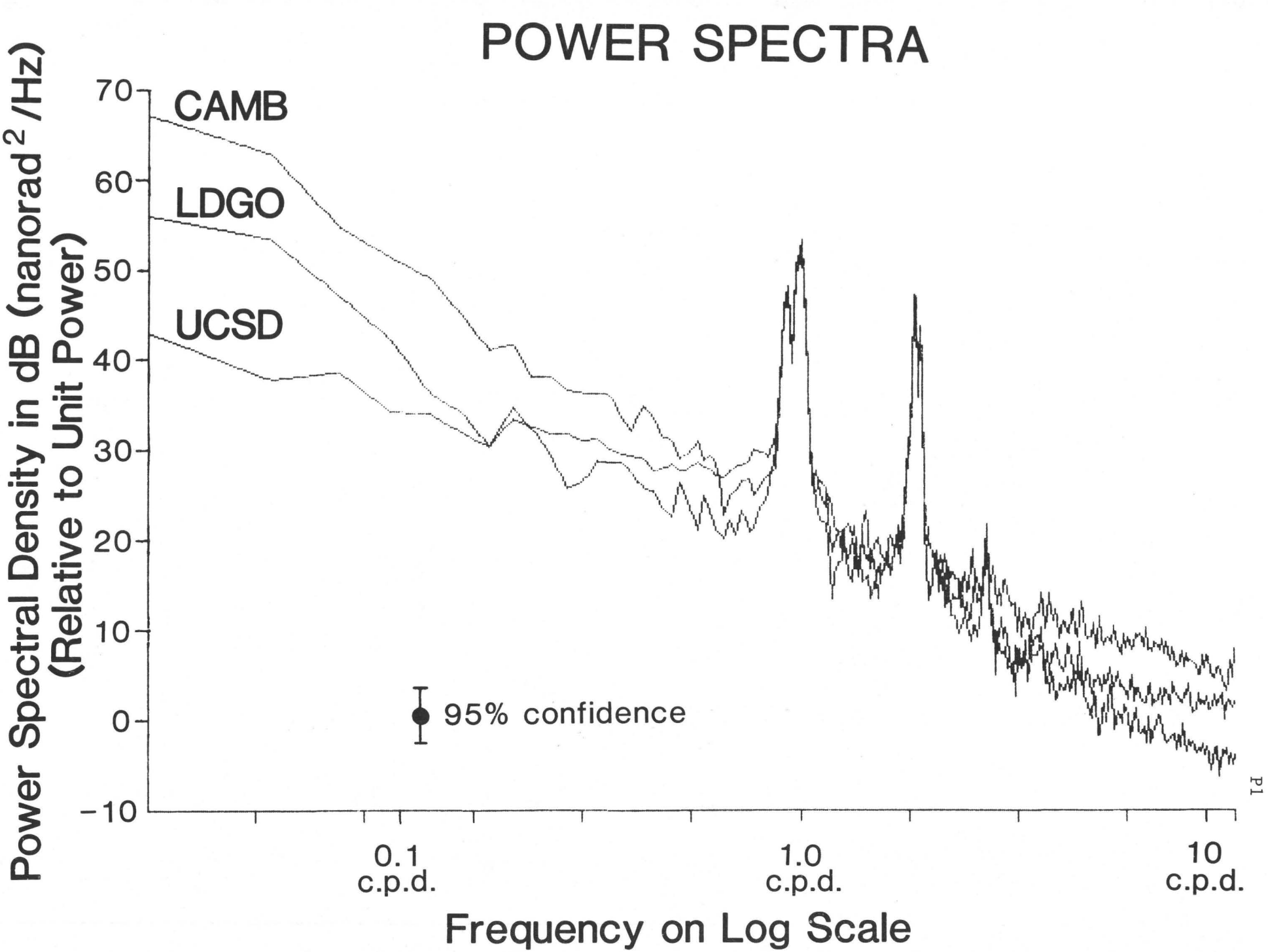

Figure 2. Power spectra of tilt records.

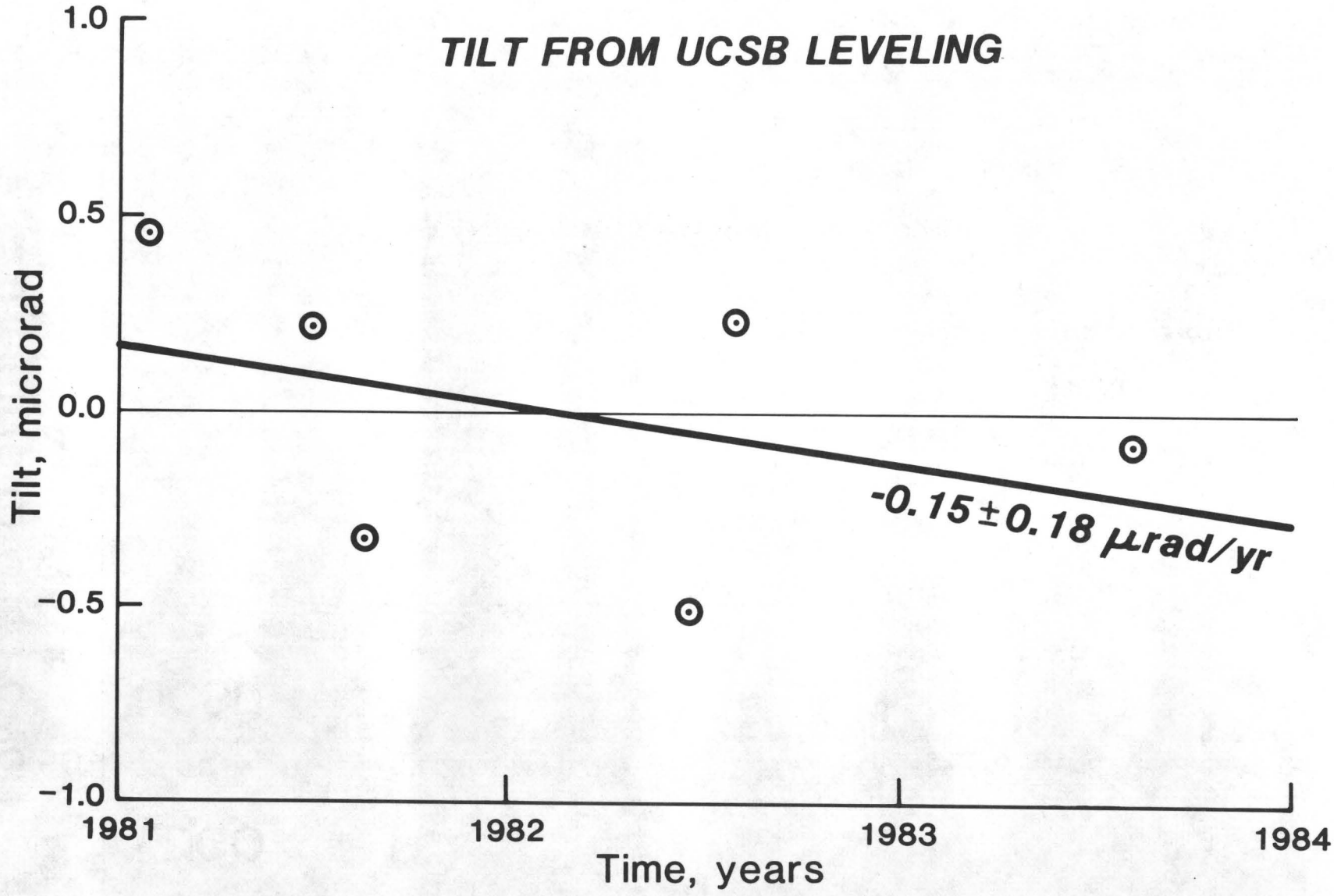

Figure 3. Tilt vs. time inferred from leveling to tiltmeter piers. Positive tilt is down to the east.

Instrument Development and Quality Control

9930-01726

E. Gray Jensen
Branch of Seismology
U.S. Geological Survey
345 Middlefield Road - M/S 77
Menlo Park, California 94025
(415) 323-8111, ext. 2050

Investigations

This project supports other projects in the Office of Earthquake, Volcanoes and Engineering by designing and developing new instrumentation and by evaluating and improving existing equipment in order to maintain high quality in the data acquired by the Office. During this period some personnel from this project were assigned to the GEOS project (9940-03009) or a part-time basis.

Results

A Gandalf terminal switching unit has been installed and is operational. This unit allows a number of terminals to be connected to any of several different computers via keyboard request. The emergency backup power generator is now installed and completely operational. This will provide power for critical seismic and geophysical recording and monitoring functions in the event of a blackout. A PDP 11/44 for monitoring Chinese seismic telemetry, which was tested here, has been moved to China. It is currently being put into full operation. Assistance was provided in evaluating and upgrading telemetry and recording equipment in Guatemala.

This group also assisted in the establishment of an emergency communications system in the Mammoth Lakes area. Equipment for microwave transmission of seismic telemetry has been acquired and installation has begun. Equipment to aid development of board-level microprocessor systems to be used in a number of future projects has been acquired. Specifications for a satellite telemetry system for low-frequency geophysical data has been provided and appropriate equipment has been ordered to implement such a system. This system will allow direct transmission of data from the field site to this office via satellite.

Both the Seismic Cassette Recording (SCR) system and the GEOS system have been maintained through field programs in several locations including Mammoth Lakes, Coalinga and Nevada. Two hundred discriminators have been tuned and put into operations. Repair or alignment of 50 radio transmitters or receivers and calibration of 60 seismometers was performed during this period.

Southern California Cooperative Seismic Network

9930-01174

Carl Johnson
Branch of Seismology
U.S.Geological Survey
Seismological Laboratory 252-21
Pasadena, California 91125
(213) 356-6957

Investigations

1. Routine processing using stations of the southern California cooperative seismic network was continued for the period April through September 1983. Routine analysis includes the timing of phases, event location and preliminary catalog production using the newly developed CUSP analysis system.

2. The development of the CUSP routine analysis system was continued. The data capture function was completed during March. Preliminary testing at Menlo Park has demonstrated a system capacity of 510 seismic channels at a sampling rate of 100 hz. This provides a throughput of 51,000 samples per second requiring roughly 50% of available CPU time for detection and spooling of detected events to digital magnetic tape. Completion of the analysis portion of the CUSP system is anticipated during the third quarter.

Results

1. The analysis portion of the CUSP routine analysis package became operational. The CUSP system is basically an event driven process control system based on a relational data base developed in-house. Aggragate throughput capabilities now exceed 20 events/hour so that little difficulty is expected in analyzing the annual load of about 20,000 earthquakes in the region covered by the Southern California Seismic Network.

SEISMIC PARAMETERS OF THE ARKANSAS EARTHQUAKE SWARM

14-08-0001-21245

A.C. Johnston
A.G. Metzger
Tennessee Earthquake Information Center
Memphis State University
Memphis, TN 38152
(901) 454-2007

1. Summary of the Swarm

The central Arkansas earthquake swarm began quite suddenly in January, 1982. As of this writing (August, 1983), it is still active. An estimated 30-35,000 earthquakes with magnitudes ranging from approximately -4 to 4.5 have been recorded by a network of portable seismographs installed and maintained by the Tennessee Earthquake Information Center (TEIC). During this time 116 earthquakes have been confirmed as felt. Fifty-eight of the earthquakes had magnitudes greater than 2.5, the most recent being a magnitude 2.9 event on 31 July, 1983. Figure 1 is a daily histogram of the first 18 months of swarm activity.

2. Investigations and Results

The objective of this project is to determine to the maximum extent possible the basic seismic parameters of the Arkansas earthquake swarm. Toward this goal the following tasks have been accomplished.

(a) Development of a local crustal velocity model. Based on several seismic reflection profiles and well-log data supplied by ARCO Oil and Gas Company, this model yields rapid solution convergence and very low (<.1 sec) RMS residuals.

(b) Development of a calibrated duration magnitude scale. The scale is calibrated against the central U.S. m_{bLg} formula for events $1.5 < M_d < 4.5$ and linearly extrapolated to smaller magnitudes.

(c) Compilation of a master event file. The file will be used to study the temporal sequencing of earthquake cycles involving (i) foreshocks/main shocks/aftershocks; (ii) main shocks/aftershocks only; (iii) sub-swarms within the overall swarm; (iiii) degree of randomness of the swarm activity. Approximately 9,500 events (of a total probably exceeding 30,000) have been entered on computer disk file. File parameters include date, time of occurrence to the nearest second, and magnitude of each event.

(d) Hypocenter and (e) Focal mechanism determinations. More than 600 earthquakes have been located including 57 of the events with magnitudes exceeding 2.5, and four significant foreshock-main shock-aftershock sequences.

Eighty-eight of a total of 880 recorded events that occurred between 23 June and 5 July, 1982 have been located, combining digital data from the U.S. Geological Survey network and analog data from the TEIC network (Chiu et al., 1983). A composite fault plane solution for the events before 26 June indicates thrust faulting, with a large component of strike-slip. The nodal planes strike NNE and WNW. Three major (but different) sequences are involved. A magnitude 3.0 event 26 June was virtually an isolated event with few foreshocks or aftershocks. On 30 June, a magnitude 3.2 event had very few foreshocks but numerous aftershocks. Many foreshocks and aftershocks were associated with the magnitude 3.8 earthquake that occurred on 5 July. Focal mechanisms for the 30 June and 05 July sequences both indicate predominantly strike-slip faulting, with the nodal planes striking NNE and WNW. Distinct source zones all within the overall swarm source volume could be resolved for each sequence. Depths for all hypocenters ranged between four and seven kilometers.

Almost 900 earthquakes were recorded in the 23-25 February, 1982, sequence which had a magnitude 3.8 event as the main shock. Four hundred well constrained solutions (epicentral uncertainty <1.0 km) were obtained from this set. Epicentral maps and cross-sections indicate that almost the entire source volume defined by A or B quality hypocenters was active throughout the sequence. However, the events with positive magnitudes were confined to a much smaller volume. Composite fault plane solutions were constructed for sequential time intervals and for spatial subdivisions. The predominant mode of faulting is strike-slip with a small component of dip-slip: either right-lateral slip on a NNE trending plane that dips SE or left-lateral slip on a WNW trending plane that dips NE. The earlier events, however, and those located north and west of the main activity showed predominantly normal faulting. There is strong evidence from the focal mechanisms and cross-sections that more than one fault is active and that more than one mode of faulting is occurring.

3. Reports and Publications

Chiu, Jer-Ming, Arch C. Johnston and Ann G. Metzger (1983) Seismic parameters of the 1982 central Arkansas earthquake swarm, Earthquake Notes, 54, p. 85 (abst.)

Haar, L.C., J.B. Fletcher, E.Sembarra and A.C. Johnston (1982) A preliminary analysis of digital seismograms from the Arkansas earthquake swarm of 1982, EOS, Trans. Am. Geophys. Union, 63, p.1024 (abst.)

Johnston, Arch C. (1982b) The midcontinent's largest earthquake swarm, Earthquake Notes, 53, p. 20 (abst.)

Johnston, Arch C. (1982c) Arkansas' earthquake laboratory, EOS, Trans. Am. Geophys. Union, 63, pp. 1209-1210.

Metzger, Ann G. (1982) Current tectonics of a continental suture zone: the 1982 central Arkansas earthquake swarm, Geol. Soc. Am., Abst. w.Prog, 14, p. 564 (abst.)

Metzger, Ann G. (1983) A detailed study of a major foreshock-main shock-aftershock sequence of the 1982-83 Arkansas earthquake swarm, unpublished M.S. Thesis, Memphis State Univ., Memphis, TN, 117 p.

TEIC Special Report #8: The Central Arkansas Earthquake Swarm: Part I, 12 Jan 82-12 Jul 82; Part II, 12 Jul 82-12 Jan 83; Part III, 12 Jan 83-12 Jul 83 (1982-83). Tenn. Earthquake Information Center, Memphis State Univ., Memphis, TN.

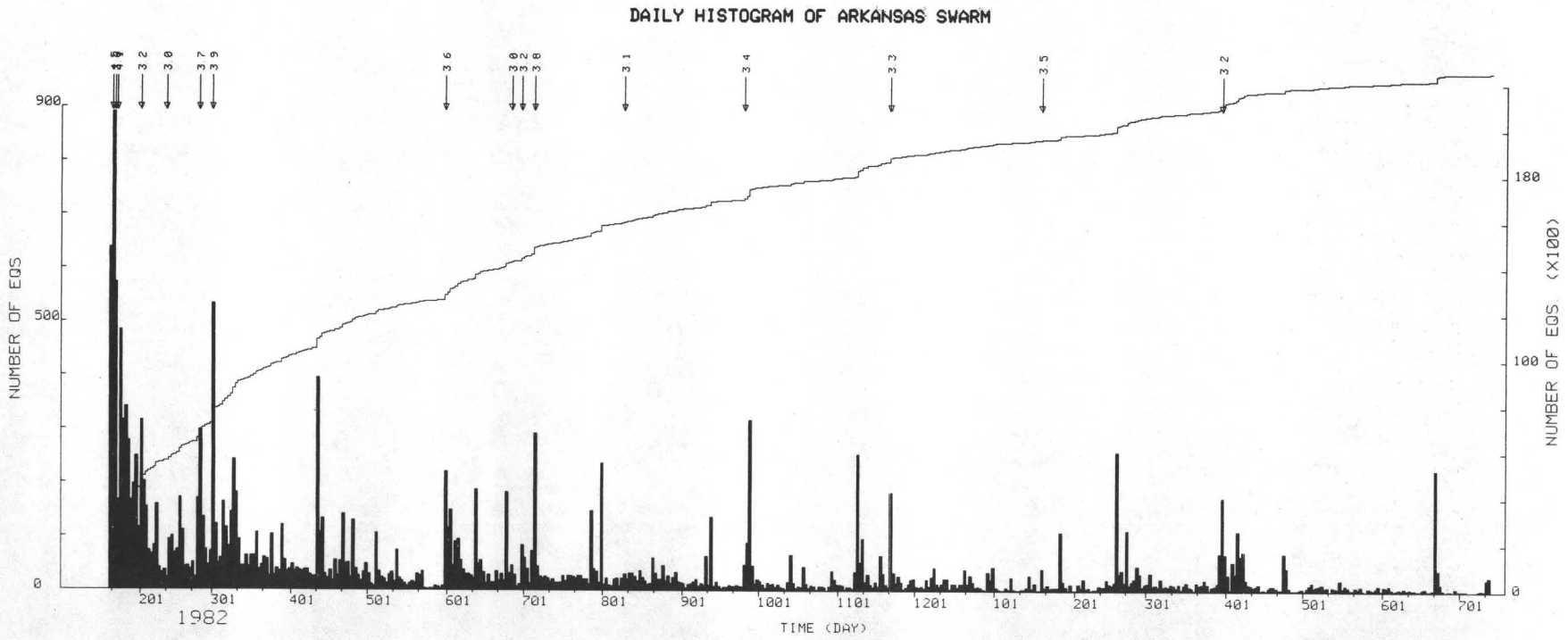

Figure 1. A cumulative event curve and a histogram of the first 18 months of the Arkansas swarm.

Earthquake and Seismicity Research using SCARLET and CEDAR

Contract No. 14-08-0001-21210

Hiroo Kanamori, Clarence R. Allen, Robert W. Clayton
Seismological Laboratory, California Institute of Technology
Pasadena, California 91125 (213-356-6914)

Investigations

We made a seismotectonic analysis of the Anza seismic gap, San Jacinto Fault Zone, Southern California, using SCARLET data.

Results

The San Jacinto fault is a major member of the San Andreas fault system and is the most historically active fault zone in southern California. A section of the San Jacinto fault near the town of Anza is an historic seismic gap. Small earthquake epicenters defind a 22 kilometer quiescent segment of fault bounded to the northwest and southeast by regions of relatively high seismicity. Recent moderate earthquakes on and near the San Jacinto fault in the gap and their relatively depressed aftershock activity indicate that the fault is seismogenic and highly stressed but locked by some mechanism. The locked nature of the fault may be due to relatively high compressive stress normal to the fault resulting from the convergent geometries of the local, active, discontinuous faults and the oblique orientation of the regional maximum compressive stress. A swarm of small earthquakes in the crustal block 13 kilometers southwest of the Anza gap near the Cahuilla Valley released stress in an area which was previously highly active before the 1918 (M 6.8) and 1937 (M_L 6.0) earthquakes. The uniqueness of the timing of this increased seismiciy near Cahuilla before the nearby (closer than 35 kilometers) large earthquakes and the recent swarm suggest that the ground beneath Cahuilla may be acting as a stress-meter signaling the presence of high stresses before large local earthquakes. The length of the quiescent fault segment suggests potential for about an M 6.5 earthquake if the entire segment ruptures at once.

Figure 1 shows P-wave first motion source mechanisms for selected earthquakes near Anza.

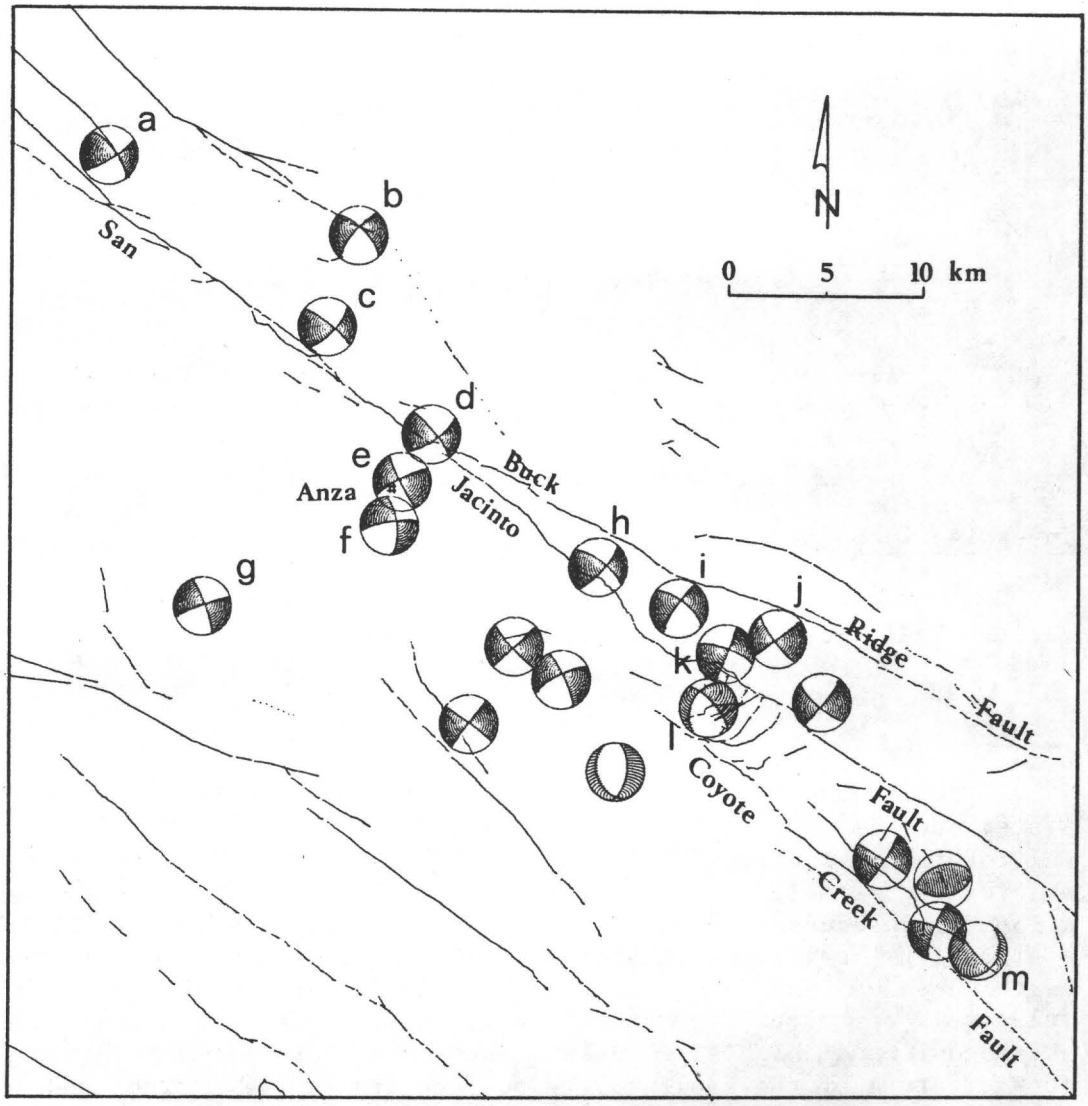

Figure 1 shows P-wave first motion source mechanisms for selected earthquakes near Anza.

Seismological Study on Rupture Mode of Seismic Gaps

Contract No. 14-08-0001-21223

Hiroo Kanamori
Seismological Laboratory, California Institute of Technology
Pasadena, California 91125 (213-356-6914)

Investigations

We made a detailed study on a seismic doublet which occurred in a seismic gap near Ometepec, Guerrero, Mexico. On the basis of this study, we investigated a relation between the repeat time and the size of the characteristic earthquakes that have occurred along the Mexican subduction zone.

Results

On June 7, 1982 an earthquake doublet occurred in a gap near Ometepec, Guerrero, Mexico which had been given a high seismic potential. The two earthquakes (first event: M_s=6.9, M_b=6.0, 16.3°N, 98.4°W, d=25 km; second event M_s=7.0, M_b=6.3, 16.4°N, 98.5°W, 8 km) of the doublet occurred within five hours of each other.

We determine the source parameters of these events by inverting surface wave data at a period of 256 s. The results are for the first event, strike = 116°, dip = 77°, slip = 88° and seismic moment of 2.8×10^{26} dyne-cm, and for the second event strike = 116°, dip - 78°, slip = 89° and seismic moment of 2.8×10^{26} dyne-cm. Modeling of long-period P waves suggests that the first event has a depth of 20 km and is represented by a single trapezoidal source time function with an effective duration of 6 seconds. The second event is best modelled by two sources at depths of 15 and 10 km. The combined effective source duration time for the two sources is about 10 seconds. The ratio of the seismic moment obtained from body waves to that from surface waves is about 0.5 for the first event and 1 for the second. Adding the seismic moment of the two events and considering the first week aftershock area, 3200 km^2, the stress drop is about 4 bars. These results suggest that the first event that involved a deeper asperity caused an incremental stress change large enough to trigger the second event. If the two events of the doublet broke distinct areas of the subduction zone, the coseismic slip is 0.58 m, and accounts for about 25% of the total plate motion between the Cocos plate and the North America plate accumulated since the last large earthquake in the region.

Other doublets similar to the Ometepec doublet have occurred along the Middle America Trench during the past 70 years. A regional distribution of comparable-size asperities may be responsible for this relatively frequent occurrence of doublets and for the simplicity of earthquakes in the region. The high convergence rate, which produces rapid strain accumulation and short recurrence intervals for large earthquakes, and the smooth sea-floor subducted along the Middle America Trench may contribute to the homogeneous distribution of comparable size asperities.

We found a relation, Log T $\sim$ 1/3 log M_o (T is the average recurrence time and M_o is the average seismic moment) for large earthquakes along the subduction zone in the Guerrero-Oaxaca region where the convergence rate and the properties of the subducted plate are considered relatively uniform. A simple asperity model predicts this relation.

PRE-SEISMICITY AND INFERRED STRESS ACCUMULATION FOR STRIKE-SLIP EARTHQUAKES

Contract: #14-08-0001-21282
John Kelleher
Redwood Research, Inc.
801 N. Humboldt Street, #407
San Mateo, California 94401
415-342-8276

Investigations: This study examines the patterns of seismic activity before recent shocks in California. Two features receive special investigation. 1) Prior to rupture there often appears on one or both sides of the ruptured surface block-like regions of quiescence defined by swarms and lineations in seismicity. 2) Before several events there developed a migration in seismicity across or around one of the nearby quiescent blocks. These examples of migrations are few in number but their similar geometry suggest that certain classes of earthquakes may require the completion of a simple geometric pattern of stress accumulation for rupture.

Results: The major result to date is that the patterns of pre-seismicity for strike-slip earthquakes appear to be influenced and hopefully can be classified by the local geometry and structure in the vicinity of the fault zone. The strongest examples of block-like quiescence are associated with earthquakes where the ruptured surface is along the border of a basin such as those near Livermore, Parkfield and possibly Anza. Some of these features appear to be pull-apart basis, while others appear to have some other extensional origin. An understanding of this pattern of pre-seismicity may have wide application because many of the largest strike-slip earthquakes have, in fact, initiated near a basin of some sort. Examples include the 1958 Fairweather, 1906 San Francisco, 1976 Guatemala and the 1939 Anatolian earthquakes.

Migrations of seismic activity around or across tectonic blocks suggest that for at least some earthquakes an important late stage in stress accumulation may develop with simple geometry. Finite element modelling indicates that the geometry of migration is controlled primarily by the character of the coupling along the boundaries of the tectonic block. Because the numerous possibilities suggested by this result, the usefulness of migrations in identifying the state of stress may be limited to earthquake reoccurrences in the same location.

A Field Study of Earthquake Prediction Methods in the Central Aleutian Islands

14-08-0001-21230

C. Kisslinger
S. Billington

Cooperative Institute for Research in Environmental Sciences
Box 449, University of Colorado
Boulder, Colorado 80309
(303) 492-8028

Network Status and Recent Seismicity.

The regular summer maintenance trip for 1983 was confined to work that could be done at the receiving sites and at the Observatory. The westernmost stations (AK2, AK3, AK4) remain inoperative and cannot be serviced until a helicopter is available. The impact of a more limited network is that coverage of small events ($M_D < 2.5$) in the western part of the zone is less effective.

Hypocenters for 292 local earthquakes were determined with the network during January through July, 1983. For the most part, the distribution of hypocenters was the same as that defined during the preceding eight years of observation, but with a resurgence of shallow back-arc activity under Adagdak, an extinct volcano on the northeast corner of Adak Island. The seismic activity during the first seven months of 1983 is unusual in that there were only half as many earthquakes located as during the same time period last year. This is a manifestation of an apparent decrease is seismicity that started in about September, 1982. We are following this situation closely to try to determine whether there is only an apparent decrease in seismicity resulting from some aspect of the network's operation, or whether a real decrease in seismicity exists. The latter possibility could be precursory to a major event yet to come. The decrease in rate of occurrence appears in all magnitude bands, including events strong enough to be located teleseismically and reported in the USGS Preliminary Determination of Epicenters.

Three earthquakes with m_b 5.0 or greater occurred during the seven months. Two of these were intermediate-depth events (116 and 130 km depths) and one (m_b 5.3) occurred in the region we term "SW2". The SW2 region is one of particular interest. Moderate-sized earthquakes have been occurring there with generally increasing magnitude and rate of occurrence as a function of time, during the time period from August 1974 (network startup) to the present (Figure 1), suggesting higher ambient stress and possibily showing an asperity on the main thrust zone. The build-up of activity during the past three years and the evidence for high stress indicate that SW2 may be a nucleation point for a strong earthquake in the near future. Preliminary work suggests that small earthquakes in this region are of larger average magnitude than in other local regions (Figure 2).

Revised Focal Depths and Velocity Model.

A technique suggested by Hales *et al.* (1981), for determining hypocenters that are relatively independent of the velocity model originally used to locate the earthquakes, was applied to a carefully selected set of earthquakes located with the Adak network. For this technique, the origin times are taken from the Wadati diagram for each event and the epicentral distances from the standard hypocenter solution are assumed to be correct. A straight-ray interpretation, based on the

use of a single average velocity from the hypocenter to the surface, is then used to determine the average velocity and the depth from the slope and intercept of the linear X^2-T^2 plot.

The revised depths confirm that the sharp cutoff of the shallower main thrust zone activity at 26 km, seen in the routine Adak hypocenter set, is an artifact of the velocity model used in routine locations. Routine depths are found to be systematically too shallow by a mean amount of 4.5 km, with origin times 0.16 sec too early.

The velocities derived in this study agree with those in the standard model for depths below 80 km, but are higher than the standard values at shallower depths. The two models can be reconciled by invoking small gradients of velocity in the uppermost three layers (upper 26 km), but this result is not unique. The results also indicate local variations of the shallower velocites within the Adak seismic zone.

Shallow Earthquakes Seaward of the Main Thrust Zone.

South of Adak there is a group of shallow earthquakes, seaward of and spatially separated from the main zone of shallow interplate thrust earthquakes. Almost all of these earthquakes are located either under Hawley Ridge (a major forearc bathymetric structure) or under its extension to the east and west. Hypocenters for these earthquakes were determined from the Adak network for the period from 1975 through June, 1983, and from teleseismic data (Engdahl *et al.*, 1983) using Joint Hypocenter Determination for the period 1964 through 1982. One nodal plane from the focal mechanism solution corresponds to a very shallow-dipping thrust plane, suggesting that the earthquakes occur on the very shallow-dipping plate interface under the ridge, rather than within the ridge structure.

In contrast to the main thrust zone earthquakes farther north, the Hawley Ridge earthquakes occur in temporal swarms, each with tightly clustered epicenters. Moreover, the data suggest that the temporal swarms occur episodically, with individual sources becoming activated at roughly five year intervals. That earthquakes occur under Hawley Ridge, but not in the area between the ridge and the main thrust zone, may be due to the additional localized load of Hawley Ridge acting on the plate interface.

Adak Canyon Seismotectonics.

The Adak Canyon region (between Adak Island and Kanaga Island to the west) has been the subject of special interest from the beginning of this project. The canyon itself is tectonically significant. In addition an M_S 7.1 earthquake occurred there in 1971. Since then, the epicentral region has been remarkable devoid of events strong enough to be located teleseismically. In spite of this absence of moderate-to-strong events, small earthquakes occur in this place just as they do throughout the whole Adak thrust zone region. Therefore, the occurrence of an m_b 5.8 earthquake there on June 4, 1982, raises the possibility that this is the first event in a sequence that will end with another big one.

Our solution for the focal mechanism for the 1982 Adak Canyon earthquake is for a thrust mechanism, in which the strike of the two nodal planes is roughly northeast, and the planes dip 41° northwest and 51° southeast. The solution was based on long-period teleseismic P-wave first motions and S-wave polarizations, on the local network P-wave first motions for the earthquake, and on the most common set of local network P-wave first motions for small earthquakes in the epicentral region. The solution differs only slightly from that determined for the USGS (monthly PDEs) from teleseismic long-period waveform matching. Teleseismic

waveform matching and ray-tracing (E. R. Engdahl, personal communication, 1982) both set the depth at 35 km.

Hypocenters were re-determined for all local events within 20 km epicentral distance of the main shock which occurred in 1981 and 1982, using the master event technique with the main shock hypocenter as master. About one-half of the events lie in a plane which matches the northwest-dipping nodal plane of the focal mechanism solution for the main shock. These events include many of the aftershocks, but the plane was active before the earthquake also. In our work to date, we have seen no pattern in the temporal distribution of these events which suggests a precursor to the event. Nor have we been able to document any change in the focal mechanism of small events in the region prior to the main shock, using both the methods of SV/P amplitude ratios (Kisslinger *et al.*, 1982) and of P-wave first-motion patterns (Billington, 1982).

Publications

Bowman, J. R. (1982), Anomalous properties of small earthquakes preceding larger earthquakes near Adak, Alaska (abstr.), *EOS*, 63, 1043.

Bowman, J. R., and C. Kisslinger (1984), A test of foreshock occurrence in the central Aleutian Island Arc, accepted for publication in *Bull. Seism. Soc. Amer.*, Feb, 1984.

Engdahl, E. R., and S. Billington (1983), Short-period depth phases observed from subduction-zone earthquakes (abstr.), *EOS*, 64, 254.

Engdahl, E. R., J. W. Dewey, and S. Billington (1983), Features of subduction-zone seismicity in the central Aleutian Islands (abstr.), presented at XVIII General Assembly, IUGG, Hamburg, F.R.G.

Kisslinger, C., J. R. Bowman, and R. E. Habermann (1983), Seismicity patterns, foreshocks and variations in focal mechanisms as premonitory phenomena, Aleutian Islands (abstr.), presented at XVIII General Assembly, IUGG, Hamburg, F.R.G.

Kisslinger, C., S. Billington, J. R. Bowman, A. Silliman, and J. Pohlman (1983), Seismotectonics above the main thrust zone, central Aleutian Islands (abstr.), presented at XVIII General Assembly, IUGG, Hamburg, F.R.G.

Li, V., and C. Kisslinger (1984), Stress transfer and nonlinear stress accumulation at subduction-type plate boundaries - Application to the Aleutians, submitted to *Pure Appl. Geophys.*

Toth, T., and C. Kisslinger (1984), Revised focal depths and velocity model for local earthquakes in the Adak seismic zone, submitted to *Bull. Seism. Soc. Amer.*.

References

Billington, S. (1982), A method to objectively sort P-wave first-motion data for composite focal mechanism solutions, *Bull. Seism. Soc. Amer.*,**72,** 399-411.

Engdahl, E. R., J. W. Dewey, and S. Billington (1983), Features of subduction-zone seismicity in the central Aleutian Islands, in preparation.

Hales, A. L., D. J. Muirhead, and L. Maki-Lopez (1981), The times of origin and depths of focus of intermediate and deep focus earthquakes: model calculations, *Bull. Seism. Soc. Amer.*, **71,** 1529-1552.

Kisslinger, C., J. R. Bowman, And K. Koch (1982), Determination of focal mechanism from SV/P amplitude ratios at small distances, *Phys. Earth Planet. Int.*, **30,** 172-176.

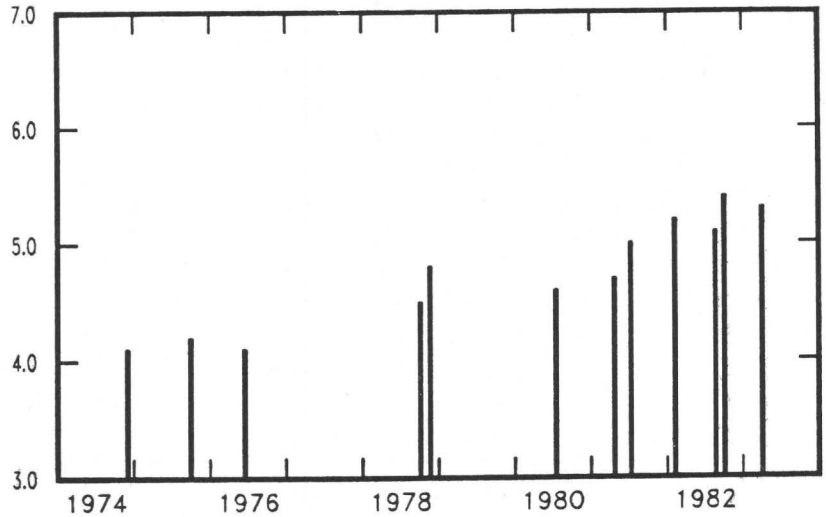

Figure 1: Earthquakes located within the SW2 region. The vertical axis is m_b as given in the USGS Preliminary Determination of Epicenters (PDEs). The time period covered is from August, 1974, through July, 1983.

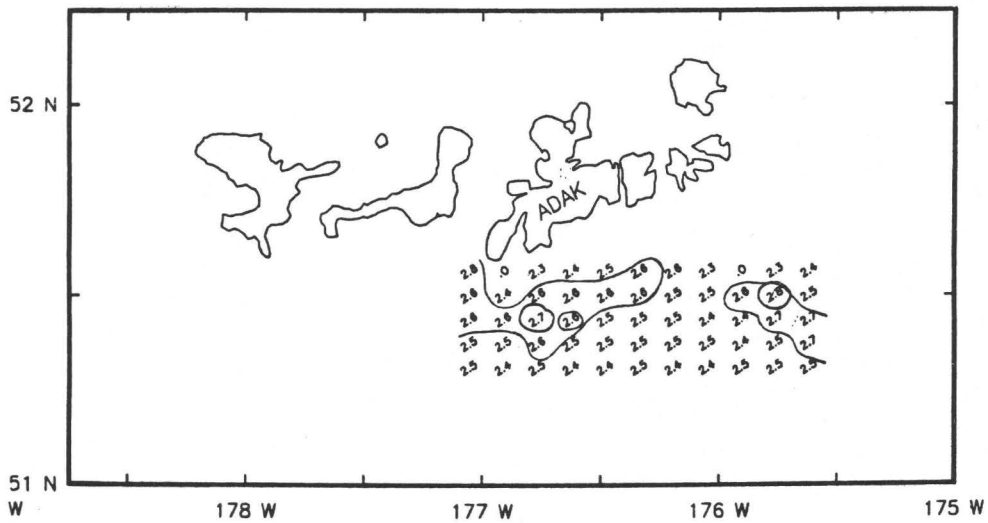

AVERAGE MAGNITUDE IN 10 km
RADIUS SPHERES FOR EVENTS $2.2 \leq M_D \leq 3.8$

Figure 2: Map of average values of duration magnitude (M_D) for events on the main thrust zone south of Adak and east of Adak Canyon. The islands on which the Adak network is located are shown. The average magnitudes were calculated for spherical volumes with 10-km radii, centered on a plane through the center of SW2, and dipping 45° to the north (approximating the thrust zone). The circled value of 2.6 (south of Adak Island) is roughly in the center of the SW2 region. The contours mark regions in which the average duration magnitude is greater than or equal to 2.6.

Seismic Data Library

9930-01501

W. H. K. Lee
U. S. Geological Survey
Branch of Seismology
345 Middlefield Road, Mail Stop 77
Menlo Park, California 94025
(415) 323-8111, ext. 2630

This is a non-research project and its main objective is to provide access of seismic data to the seismological community. This Seismic Data Libráry was started by Jack Pfluke at the Earthquake Mechanism Laboratory before they joined the Geological Survey. Over the past ten years, we have built up one of the world's largest collections of seismograms (almost all on microfilm) and related materials.

Recent major additions to this library included a microfilm copy of over 30,000 seismograms recorded at the University of Tokyo, Tokyo, Japan from 1900 through 1940.

Microearthquake Data Analysis

9930-01173

W. H. K. Lee
Office of Earthquakes, Volcanoes, and Engineering
Branch of Seismology
345 Middlefield Road, Mail Stop 77
Menlo Park, California 94025
(415) 323-8111, ext. 2630

Investigations

The primary focus of this project is the development of state-of-the-art computation methods for analysis of data from microearthquake networks. For the past six months I have been recovering from my illness and mostly working part-time.

A computer-based system for organizing earthquake-related data has been put into routine operation. This system edits, archives, and backups earthquake data sets, and allows users to query and retrieve archived data sets. Details of the system are given in Lee et al. (1983).

I have also investigated the feasibility of a proposal by Kei Aki to systematically monitor seismic parameters in California for earthquake prediction purposes. Aki proposed (1) to divide California into rectangular blocks with a linear dimension of a few kilometers and to keep track of blocks sampled by the ray paths through 3-dimensional simultaneous inversions of arrival times, and (2) to perform coda waves analysis for working out the source/site and attenuation effects and then compute attenuation of S-waves for blocks defined in (1) using S to coda ratios.

Results

(1) A system for routine editing, archiving and retrieving earthquake data sets has been put into operation.
(2) An analysis of Aki's proposal in terms of computation and processing indicated that about 200 gigaflops (billions of floating point operations) are required per year. Such a large-scale computation can be implemented using current available computers within about one year at a cost of about $100,000.

Reports

Lee, W. H. K., Scharre, D. L., and Crane, G. R., 1983. A computer-based system for organizing earthquake-related data, U. S. Geological Survey Open-File Report 83-518, 28 pp.

Lee, W. H. K., and Meyers, H., 1983. Historical Seismogram Filming Project: some reflections after five years (abstract), Regional Workshop of IASPEI/UNESCO Working Group on Historical Seismograms, Hamburg, Germany, August 18-19, 1983.

Northern California Network Processing

9930-01160

Fredrick W. Lester
Branch of Seismology
U. S. Geological Survey
345 Middlefield Road M/S 77
Menlo Park, California 94025
(415) 323-8111, ext. 2149

Investigations

Signals from 430 stations of the multipurpose Northern California Seismic Network (Calnet) are telemetered continuously to the central laboratory facility in Menlo Park where they are recorded, reduced, and analyzed to determine the origin times, magnitudes, and hypocenters of the earthquakes that occur in or near the network. Data on these events are presented in the forms of lists, computer tape and mass data files, and maps to summarize the seismic history of the region and to provide the basic data for further research in seismicity, earthquake hazards, and earthquake mechanics and prediction. A magnetic tape library of "dubbed" unprocessed records of the network for significant local earthquakes and teleseisms is maintained to facilitate further detailed studies of crust and upper mantle structure and physical properties, and of the mechanics of earthquake sources.

Results

1. Figure 1 shows the seismic activity of Northern California for the period April 1, 1983 through September 30, 1983. The 9805 earthquakes plotted are all reliable locations using 4 or more phase readings in the solution. The phase readings were obtained either by hand timing or by the Real Time Picker (RTP) or they are a combination of both sources. The Coast Ranges have been screened for quarrys and those data have been eliminated. Identification of quarrys in the Sierra Nevada Foothills is a constant problem so that all quarry data have not yet been eliminated from the catalog. We feel that the catalog of location data maintained by Calnet is relatively complete for earthquakes M 1.5 and larger.

2. Data for the second half of calendar year 1982 are completely processed and have been prepared for open-file publication in October 1983. Processing of data for the first half of calendar years 1978 and 1983 is nearly complete and the data will be open-filed in the fall of 1983.

3. On May 2, 1983 a magnitude 6.5 earthquake occurred 12 kilometers northeast of Coalinga, California. This event, the largest recorded in the area in historic time, was followed by more than 7000 aftershocks. Figure 2 shows 5620 well located aftershocks. Aftershocks are still continuing to occur, but at a much diminished rate. There have been 8 aftershocks magnitude 5

and larger, the largest of which was magnitude 6.2 and occurred on July 21. In response to this sequence of events 4 new permanent seismic stations were installed to augment the existing network, and provide needed data from the sparsely instrumented eastern edge of the zone of aftershocks.

The zone of aftershocks is approximately centered on the main shock and is roughly 35 kilometers long and 15 kilometers wide, with its long axis striking about N 52° W. Preliminary analysis of the first 3 months of aftershock data indicates that this region is underlain by a complex geologic structure which is characterized by an almost complete lack of surface expression. Focal mechanism plots indicate the occurrence of either thrust faulting or high angle reverse faulting due to subhorizontal crustal compression. A careful ground search of the area shortly after the main shock revealed no observable surface faulting that could be related to tectonic displacements on major fault structures.

An early examination of older seismic data from this region indicates that the Coalinga aftershocks have filled a seismic gap between clusters of aftershocks that occurred in 1976, 1980, and 1982. There appear to be other prominent seismic gaps in the region which deserve further study. An investigation is currently underway to more closely examine the causative mechanism for these earthquakes and to determine the relationship of these earthquakes to the tectonic processes and geologic framework of the area. Complete results of this investigation will be presented as part of a forthcoming U.S. Geological Survey Professional Paper.

4. As a result of the Volcano Hazards Notice released on May 27, 1982, for the Long Valley caldera (LVC) area of eastern California special attention has been placed on the monitoring of seismic activity. Figure 3 shows 2324 earthquakes located in the region since April 1, 1983. Seismic activity for the last 6 months can be characterized by low level seismicity which is occasionally punctuated by small swarms, both in and out of the caldera. These swarms typically last between 1 and 3 hours and produce a few tens of events.

   Analysis of seismic data from the January 1983 earthquake swarm near Mammoth Lakes indicates that the earthquakes were probably associated with the injection of magma into the ring-dike system along the south moat of the LVC. Trilateration data collected since July 1982 from a network that spans the caldera indicate deformation of the network that is consistent with about 0.2 meter of right-lateral slip along, and 0.4 meter of extension across the rupture surface defined by the January 1983 hypocenters. The rupture surface is a vertical rectangle, 8.5 kilometers long, striking N 65° W and extending from the surface to a depth of 8 kilometers. The northwest corner of the rupture surface is 3 kilometers east of Mammoth Lakes. Focal mechanism plots are consistent with the observed deformation in that they indicate both dip-slip and strike-slip movement and have nearly horizontal NE-SW orientation of the T-axes.

5. On August 29, 1983 a moderate earthquake (M_L 5.5) occurred 24 kilometers northwest of San Simeon, California. It was preceded by 3 foreshocks on August 28, the largest of which was magnitude 3.5. Figure 4 shows three foreshocks and 121 aftershocks located in a cluster around the mainshock. A focal mechanism plot for the main shock indicates that the earthquake occurred 8.4 kilometers deep on a fault striking N 41° W and dipping 54° to the northeast. A projection of this fault plane to the surface would be coincident with the Simeon Fault as it is mapped offshore to the west of the epicenter. Indicated movement was oblique-right slip, with the east side up. An investigation is currently underway to determine the relationship of these events to the regional seismicity along this part of the coast.

Reports

Cockerham, R. S., 1983, Evidence for a 180-km-long subducted slap beneath northern California, BSSA (in press).

Cockerham, R. S., and Savage, J., 1983, Earthquake swarm in Long Valley caldera, California, January 1983 (abs.) submitted to the AGU Fall Meeting.

Eaton, J. P., 1983, Seismic setting, location, and focal mechanism, in The Coalinga earthquake sequence commencing May 2, 1983, U.S. Geological Survey Open-File Report 83-511, p. 20-26.

Eaton, J. P., Cockerham, R. S., and Lester, F. W., 1983, Study of the May 2, 1983 Coalinga earthquake and its aftershocks, based on the U.S. Geological Survey seismic network in northern California (in press), in California Division of Mines and Geology Special Report.

Kissling, E., Cockerham, R. S., and Ellsworth, W. L., 1983, Structure of the Long Valley caldera region as interpreted from seismic data, (abs.) submitted to the AGU Fall Meeting.

Savage, J. C., and Cockerham, R. S., 1983, Earthquake Swarm in Long Valley caldera, California, January 1983: Evidence for dike intrusion, JGR (in press).

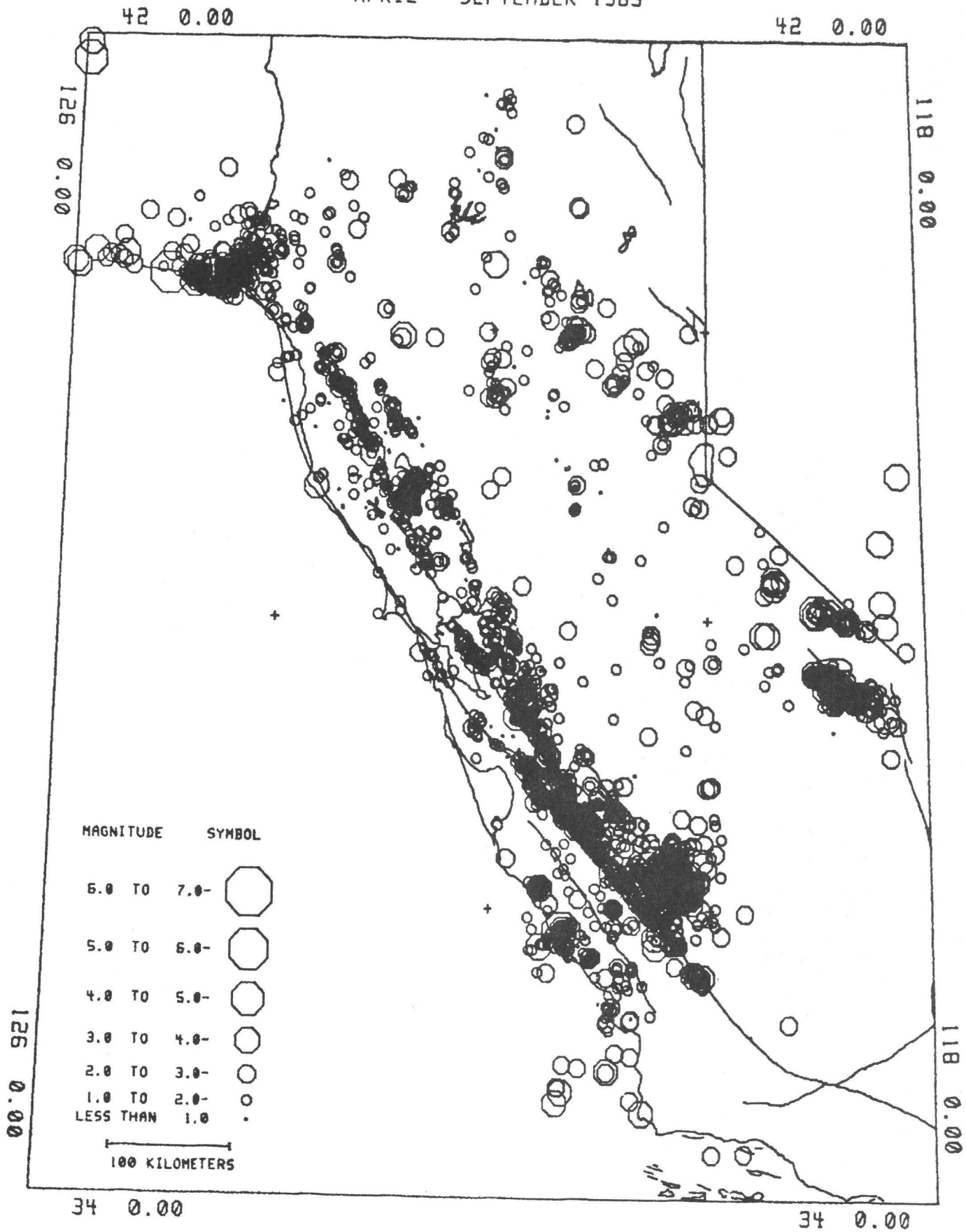
NORTHERN CALIFORINIA SEISMICITY P1
APRIL - SEPTEMBER 1983
42 0.00
42 0.00
126 0.00
118 0.00
126 0.00
118 0.00
34 0.00
34 0.00
MAGNITUDE SYMBOL
6.0 TO 7.0-
5.0 TO 6.0-
4.0 TO 5.0-
3.0 TO 4.0-
2.0 TO 3.0-
1.0 TO 2.0-
LESS THAN 1.0
100 KILOMETERS

FIGURE 1

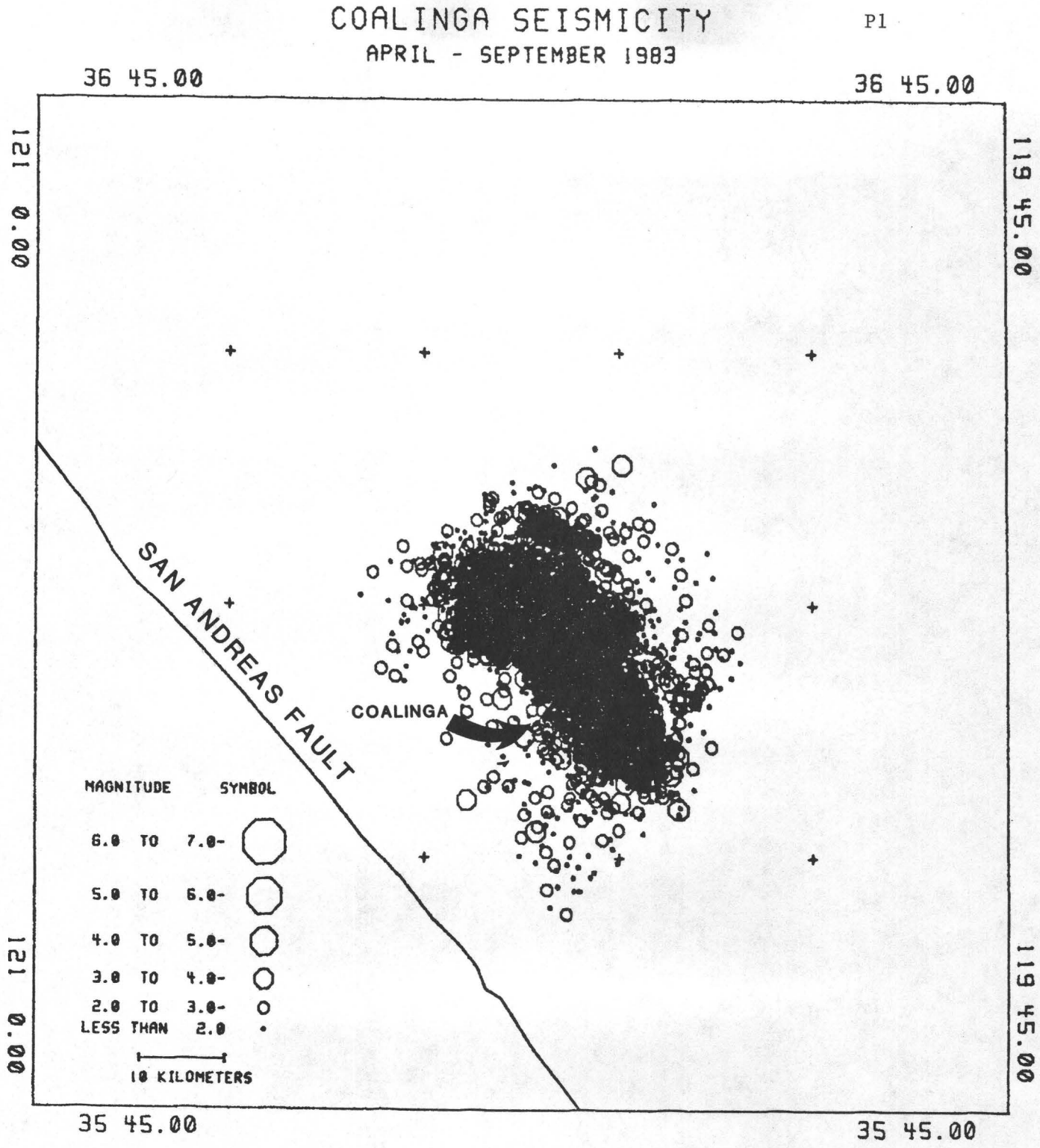
COALINGA SEISMICITY
APRIL - SEPTEMBER 1983
P1
36 45.00
36 45.00
121 00.0
119 45.00
SAN ANDREAS FAULT
COALINGA
MAGNITUDE SYMBOL
6.0 TO 7.0-
5.0 TO 6.0-
4.0 TO 5.0-
3.0 TO 4.0-
2.0 TO 3.0-
LESS THAN 2.0
10 KILOMETERS
35 45.00
35 45.00

FIGURE 2

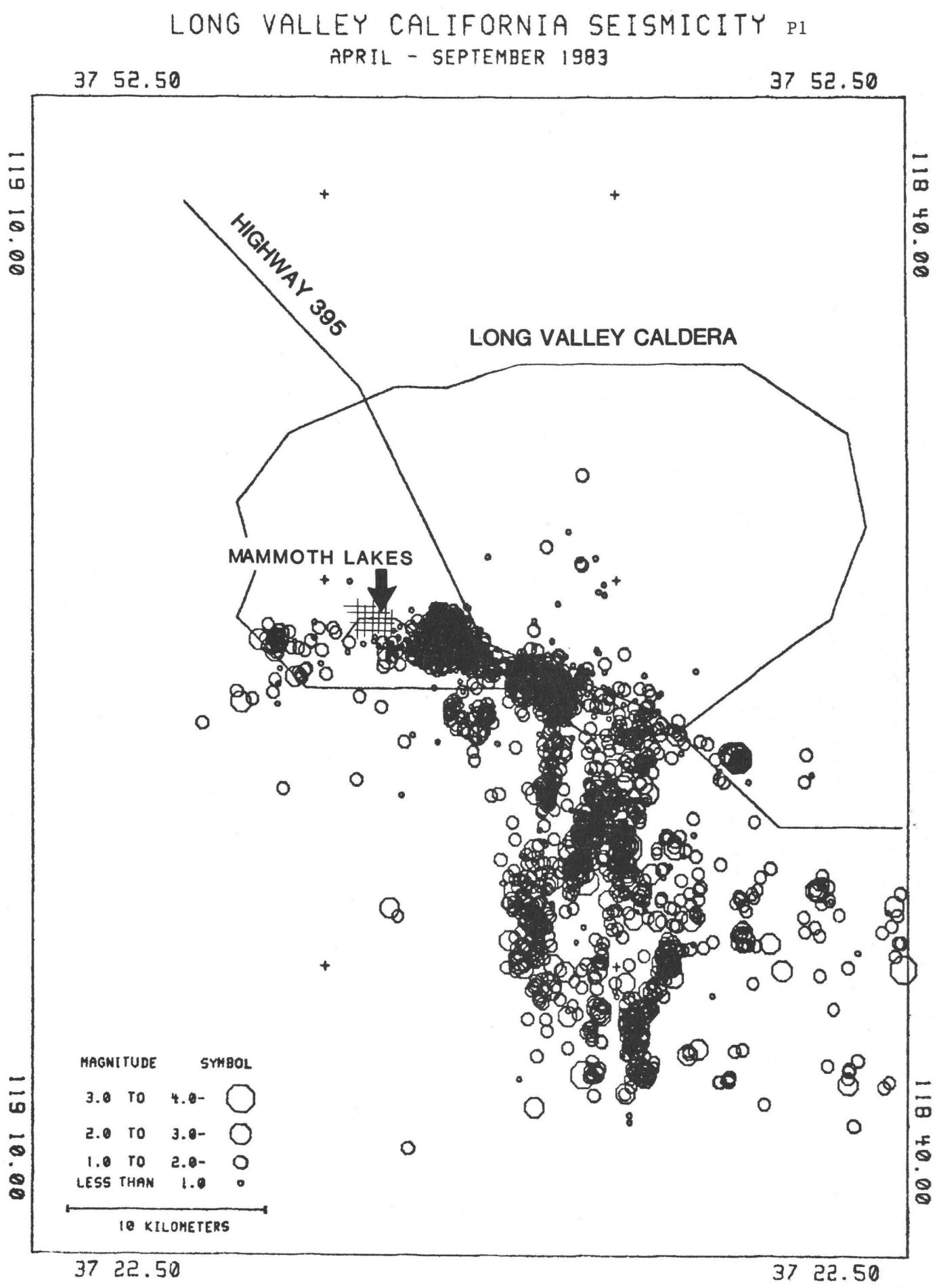
LONG VALLEY CALIFORNIA SEISMICITY P1
APRIL - SEPTEMBER 1983
37 52.50
37 52.50
119 10.00
118 40.00
HIGHWAY 395
LONG VALLEY CALDERA
MAMMOTH LAKES
MAGNITUDE SYMBOL
3.0 TO 4.0-
2.0 TO 3.0-
1.0 TO 2.0-
LESS THAN 1.0
10 KILOMETERS
37 22.50
37 22.50
119 10.00
118 40.00

FIGURE 3

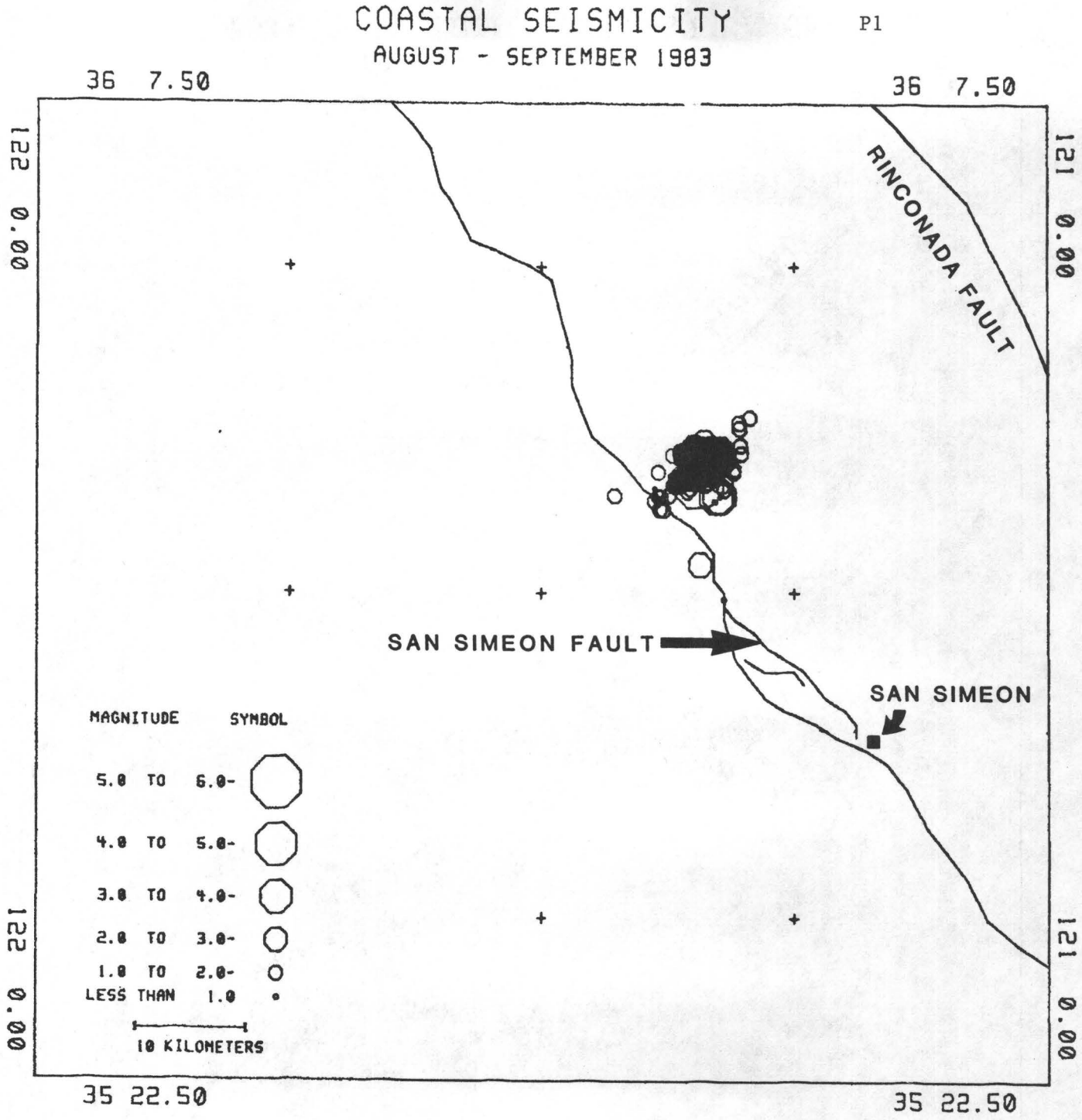
COASTAL SEISMICITY
P1
AUGUST - SEPTEMBER 1983
36 7.50
36 7.50
121 00.0
121 0.00
RINCONADA FAULT
SAN SIMEON FAULT
SAN SIMEON
MAGNITUDE SYMBOL
5.0 TO 6.0-
4.0 TO 5.0-
3.0 TO 4.0-
2.0 TO 3.0-
1.0 TO 2.0-
LESS THAN 1.0
10 KILOMETERS
121 00.0
121 0.00
35 22.50
35 22.50

FIGURE 4

Parkfield Seismicity Project

9930-02098

Allan Lindh
Branch of Seismology
U.S. Geological Survey
345 Middlefield Road - MS 77
Menlo Park, CA 94025
(415) 323-8111, ext. 2042

Investigations and Results

A simple statistical approach (first suggested by Aki [1964]) is used to translate long term recurrence and historic seismicity data into probabilities of earthquake occurrence along the San Andreas fault system. Following Kasahara (1974), a Gaussian distribution is assumed for the interevent times; a standard deviation of 30% of the mean interevent time is assumed as an approximation to the observed scatter. The conditional probability of an earthquake within some future time period, given that one has not yet occurred, is calculated by assuming the shape of the Gaussian remains unchanged; for the case considered here this is functionally equivalent to assuming a Weibull distribution (Hagiwara, 1974).

The resulting probability distribution is consistent with more subjective, qualitative estimates of risk. Annual probabilities of characteristic events (M 6-8) on various fault segments, are in the 1-4% range for most of southern California. A much lower probability is obtained along most of the 1906 break in northern California. Higher probabilities for events of about magnitude 6 are estimated for the San Juan Bautista and Parkfield areas, at the two ends of the creeping section of the San Andreas fault in central California. At Parkfield, the probability of a repeat within the next decade of the 1966 event is estimated to be about 70%.

Because of the high probability of a moderate event at Parkfield in the next 10 years, the U. S. Geological Survey, in cooperation with the Division of Mines and Geology of the State of California, the Department of Terrestial Magnetism at the Carnegie Institute, and with L. M. Slater of the University of Colorado, has initiated an earthquake prediction experiment in the Parkfield region. A detailed study of available seismic data and historical accounts indicates that the last five Parkfield events were probably identical; since their interevent times varied by a factor of three, they do not appear to conform to the time-predictable model (Shimazaki and Nagata, 1978). However a simple extension of the time predictable model to include a finite probablity of an earthquake occurring before the failure stress is reached satisfies the data and is consistent with other observations at Parkfield.

From a detailed study of the microseismicity in the hypocentral region of the 1966 earthquakes we infer that failure initiated within a small area on the fault (a few km on a side) centered at about 9 km depth. This area has been seismically quiet for the past decade, although clusters of M 3 events have occurred near its periphery. Some of these M 3-4 events have static stress drops about 3 times those of events in adjacent regions. One objective of the experiment underway at Parkfield is to monitor the seismicity of this small fault patch as precisely as possible, in hopes of identifying any foreshocks (or other seismic precursors), and understanding the processes leading up to the next moderate earthquake.

A 256 channel, micro-processor based, seismic real-time processor (RTP) has been in operation on the stations of the U.S. Geological Survey's central California micro-earthquake network (CALNET) for several years (Allen, 1982). One practical difficulty that has been encountered is the estimation of earthquake size on this system; in particular, the signals are usually clipped in the vicinity of the S wave, and associated large amplitude shear wave arrivals, severely limiting the routine use of peak amplitude based magnitudes. Robust coda length alogrithms have also proven difficult to implement, particularly for events of M 4 and larger.

We have recently implemented a more appropriate and stable magnitude algorithm on the RTP, based on the work of Johnson (1978) on off-line digital processing. The basic measurement is the average absolute value (A) of the digital seismogram on successive 2 second windows. To maintain continuity with past data sets these measurements are used to define a coda length T, where T is the time (in seconds) after the P wave arrival time, at which A first falls below 60 mvolts (out of the standard CALNET seismic system).

The RTP also outputs 6 values of A taken between the time the signal falls below the clipping level and T. These amplitudes are fit with a function of the form $A = A_1 T^{-Q}$; A_1 and Q are tabulated for each arrival. The integral of this function, following the S arrival time, provides a stable and very robust measure of earthquake size; the log of the integral appears to correlate well with log moment. These numbers also provide a powerful means of filtering out non-earthquakes; noise events turn out to have very different "shapes", as reflected in the average values of Q for each event. As more powerful microprocessors become available, an obvious extension of this approach is to determine the coda shape, and area, for several different passbands, in principle allowing the calculation of "stress-drop-like" source properties.

Geodetic Strain Monitoring

9960-02156

Art McGarr
Branch of Tectonophysics
U.S. Geological Survey
345 Middlefield Road, M/S 77
Menlo Park, California 94025

Investigations

Two-color laser geodimeters are used to survey, repeatedly, geodetic networks within selected tectonically active regions of California.

Results

1. During the period March-June 1983 a geodetic network was established across the southern moat of the Long Valley caldera near Mammoth Lakes, California (Figure 1). Surveying with the new Terrameter, which was accepted in May 1983, commenced at Long Valley in late June and continued on more or less a nightly basis until the end of July. Further surveys of this network were performed in September and October. The network includes instrument set-up points at CASA and MINER and numerous reflector sites (Figure 1). The results through the beginning of October indicate predominantly east-west extension at a rate of approximately 5 ppm/a (Figure 2). Each of the subnetworks, corresponding to the instrument sites at CASA and MINER, are consistent in showing a substantial and steady rate of east-west extension, although the strain rate of the MINER subnetwork appears somewhat higher.

   Duing the summer of 1983 a decision was made to monitor the deformation over this network on a continuous basis throughout the year. To allow surveying during the winter an observatory has been constructed on CASA and four small shelters for permanent reflectors are currently under construction.

2. Two-color measurements of the Pearblossom network, southeast of Palmdale, California, have continued. Results through the middle of September 1983 are shown in Figure 3 where we see that no remarkable strain episodes were detected during the last six months. The rate of shear strain accumulation, which was quite high during 1982, has been much lower since the end of January 1983. Note also that the total areal dilatation accumulated since the end of October 1980 is insignificant. Measurements over this network continue to be made with the two-color geodimeter owned by Dr. Larry Slater of CIRES, University of Colorado.

The Pearblossom installation was also used during May and August, 1983, to determine instrument constants and stabilities of the two Terrameters owned by the USGS.

Reports

Langbein, J. O., McGarr, A., Johnston, M. J. S., and Harsh, P. W., Geodetic measurements of post-seismic crustal deformation following the 1979 Imperial Valley earthquake, California, Bull. Seismol. Soc. Am., 73, 1203-1224, 1983.

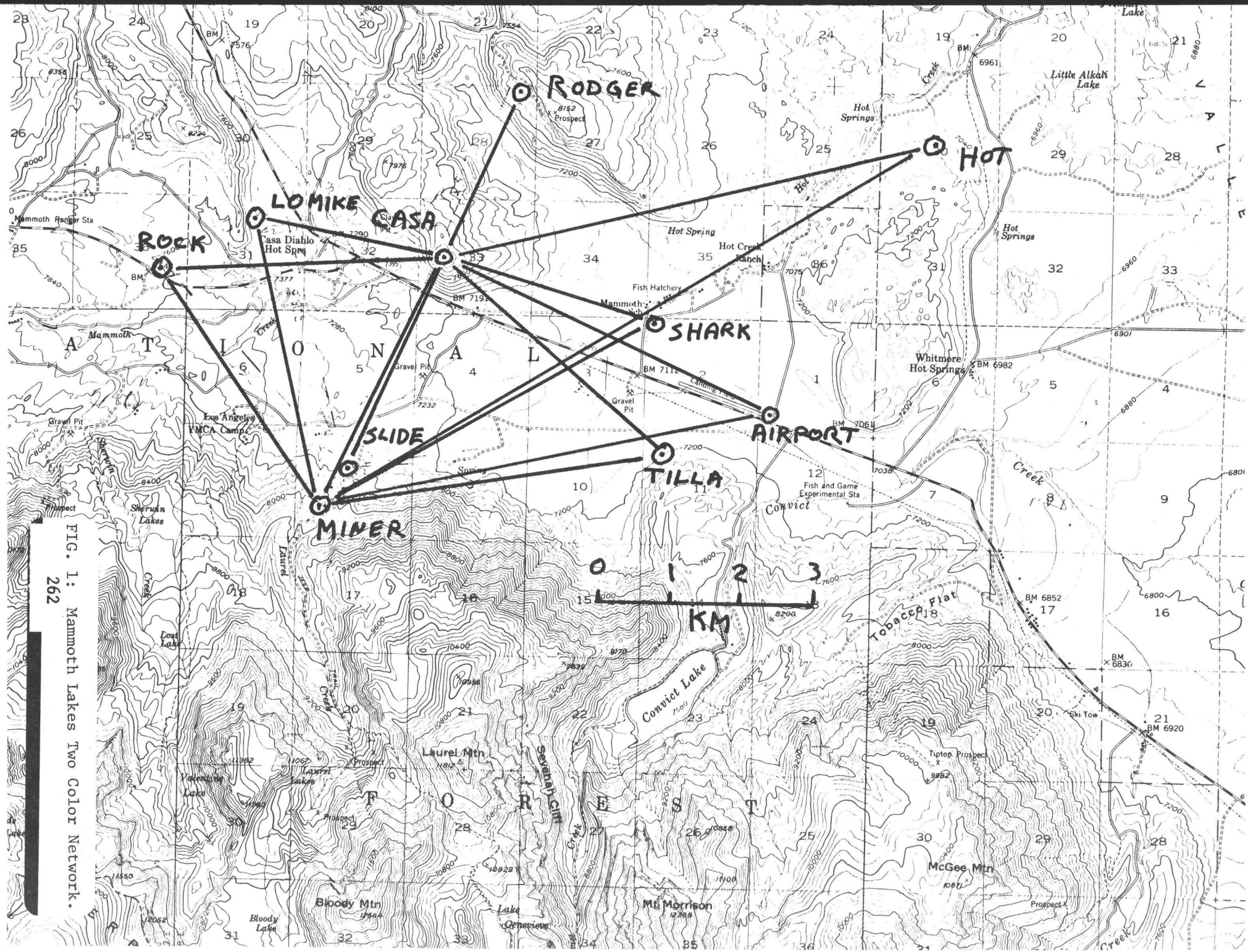
RODGER
LOMIKE
CASA
ROCK
HOT
SHARK
SLIDE
AIRPORT
TILLA
MINER
0 1 2 3
KM
Mammoth Ranger Sta
Casa Diablo Hot Spgs
Hot Springs
Hot Creek Ranch
Fish Hatchery
Mammoth Sch
Whitmore Hot Springs
Gravel Pit
Los Angeles YMCA Camp
Fish and Game Experimental Sta
Convict
Convict Lake
Tobacco Flat
Sherwin Lakes
Laurel Mtn
Bloody Mtn
Mt Morrison
McGee Mtn
Lake Genevieve
Little Alkali Lake
Ski Tow
Tiptop Prospect
Prospect
BM 6852
BM 6961
BM 7061
BM 6982
BM 6920
BM 6836
BM 7191
BM 7112
Mammoth
Creek
Laurel
Lost Lake
Valentine Lake
Laurel Lakes
Bloody Lake
Seven Mile Cliff
Lake
Creek
Hot
Creek
Hot Springs
Creek
Creek
Creek

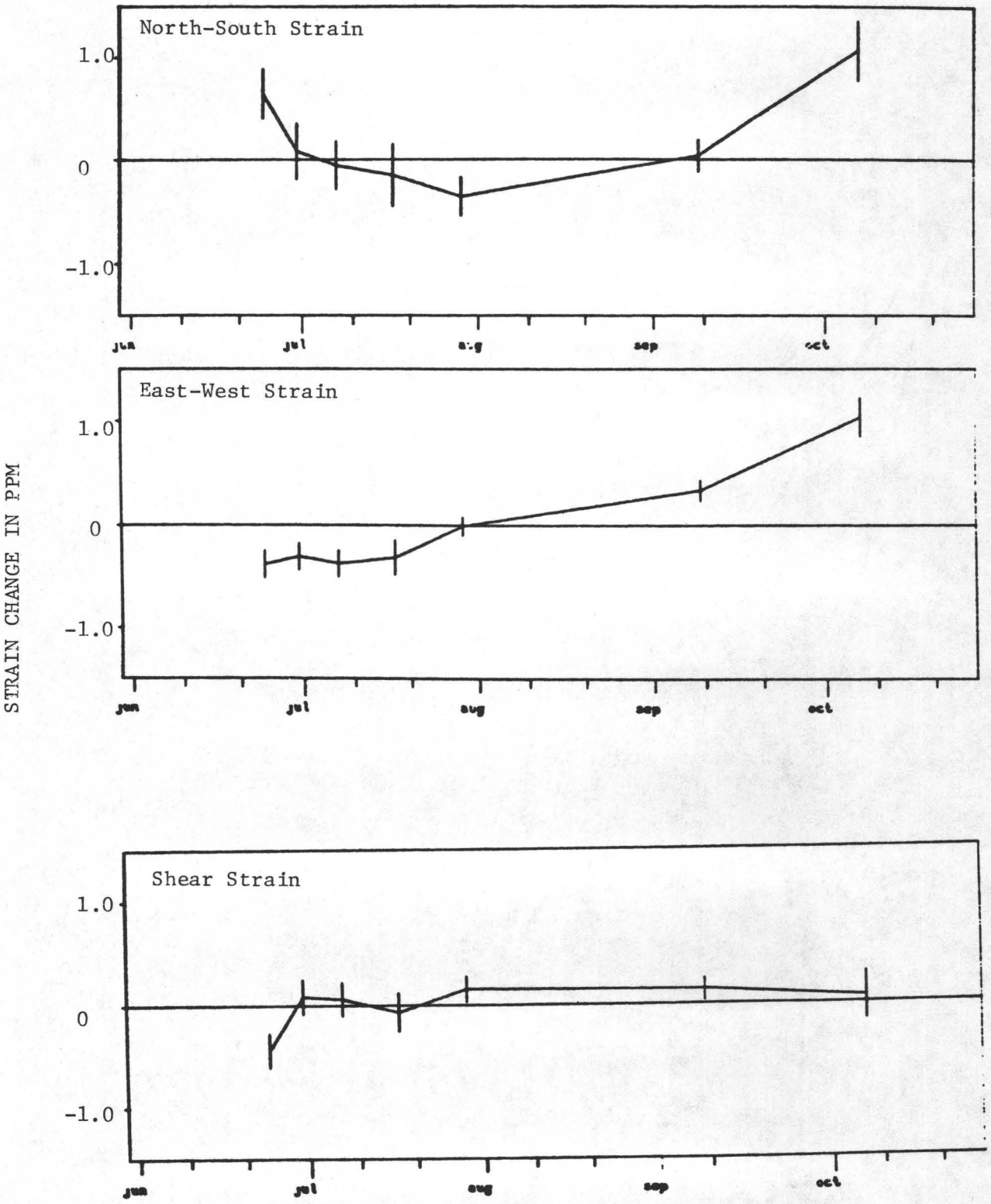

FIG 2: Strain accumulation within Mammoth Lakes network from instrument point CASA.

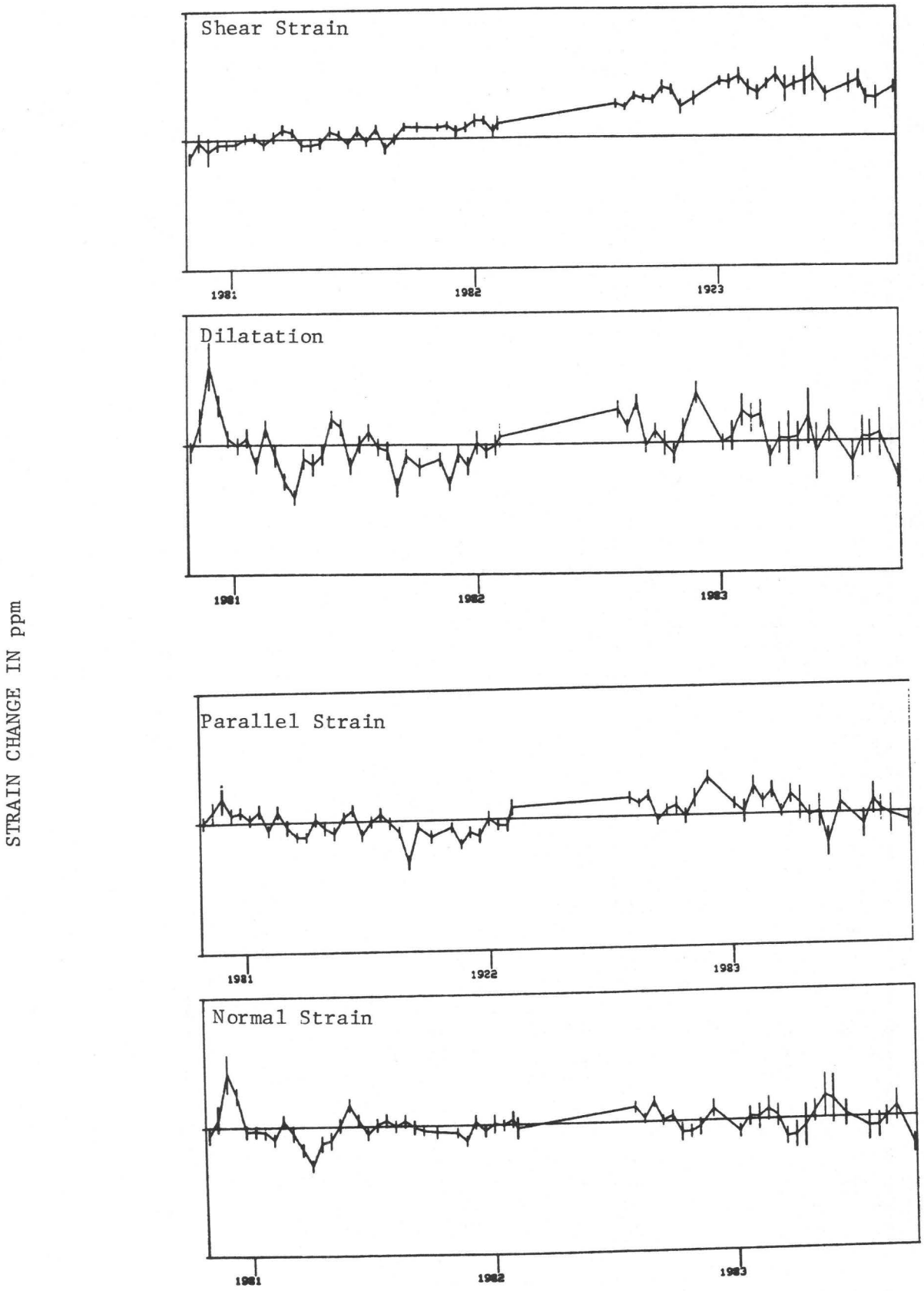

FIG 3: Strain accumulation within the Pearblossom network.

Determination of 'Whole Earthquake Cycle' Systematics: Continued Studies of Large Earthquakes (M_s 7-7.5) Along the Middle America Trench to Refine Methodologies and Models for Earthquake Prediction

14-08-0001-20511

Karen McNally
Earth Sciences Board
University of California, Santa Cruz
Santa Cruz, California 95064
(408) 429-4136

INVESTIGATIONS

Seismicity patterns (in time, space, energy release and mechanisms) which precede and follow each of six large earthquakes ($M_s \geq 7$) along the Middle America Trench offshore from Mexico are being analyzed with respect to mainshock source rupture parameters and source regions. The objectives are: (1) to determine whether seismicity patterns can be reliably used for earthquake prediction, i.e. that patterns can be found which are consistent and only occur prior to major earthquakes and which are recognizable relative to background activity, (2) to determine whether particular aspects of seismicity patterns (such as duration of seismic quiescence, etc.) correlate with mainshock source parameters (magnitude, stress drop, etc.), and (3) to determine whether the seismicity patterns are consistent with a model of strain accumulation and failure along a fault zone which is heterogeneous.

We are relocating all earthquakes ($m_b \geq 4.0$) along the Middle America Trench from 1964 to present, as well as selected earthquakes from 1928 to 1964, in order to make dependable interpretations of the spatio-temporal patterns in reference to mainshock rupture zones. ISC and USGS/NOAA catalogs have been synthesized for listings which are as complete as possible. Data from field array studies in Mexico are used as calibration events with the JHD method for relocations. (Standard catalog locations vary by as much as $\pm$ 30 km from the redetermined locations, an uncertainty which is unacceptable for associating seismicity patterns with mainshock rupture processes.) Waveform modeling is being used to study source rupture mechanisms for mainshocks ($M_s \geq 7.0$) and fault mechanisms are being constructed from P-wave first motions for earthquakes $m_b \geq 5.5$. A model of inhomogeneous faulting for seismic gaps, asperities, and fault barriers is being developed with J. Rundle and is being tested with the refined seismicity data. The combined case histories of seismic activity preceding and following the six mainshocks spans $\pm$ 15 years, a time period comparable to the average repeat time of 33 $\pm$ 8 years for this region, i.e. one "earthquake cycle."

A seismic quiescence ($m_b \geq 4$) SE of Acapulco is being monitored on an ongoing basis. Data from a field array study in the same region have been analyzed and indicate a relative seismic quiescence (at magnitudes $M \geq 2.5$) which is nearly coincident in location with that found from WWSSN data.

In order to incorporate more constraints on the model which we are developing, the study has been expanded to include the seismicity patterns prior to large normal fault earthquakes in Mexico. We hope to determine the relative influence of mainshock rupture mechanism (and inferred stress field) on the systematics of prior seismicity patterns.

RESULTS

Ten separate projects have been conducted under this contract and are nearing completion, with several manuscripts being submitted for publication. Due to space limitations for this summary, interested persons are referred to the following references for results which have been obtained to date.

REPORTS

Manuscripts

Tajima, F., and K. C. McNally, 1983, Seismic rupture patterns in Oaxaca, Mexico, J. Geophys. Res., v. 88, n. B5, p. 4263-4275.

Eissler, H. K., and K. C. McNally, Seismicity and tectonics of the Rivera Plate and implications for the 1932 Jalisco, Mexico Earthquake, J. Geophys. Res., submitted.

Nava, F. A., K. C. McNally and G. Beroza, 1983, Seismicity of the Acapulco, Mexico, quiescent zone, Geophys. Res. Lett., submitted.

Gonzalez, J. and K. C. McNally, 1983, Influence of earthquake fault mechanism, depth and distance on damage in Mexico, Seismol. Soc. Am Bull., submitted, and Proc. VI Congress Soc. Seism. Eng. Mexico, in press.

Beroza, G., J. A. Rial and K. C. McNally, 1983, Source mechanisms of the June 7, 1982 Pinotepa, Mexico earthquakes, Geophys. Res. Lett., submitted.

Lefevre, L. V., and K. C. McNally, 1983, Stress distribution and subduction of aseismic ridges in the Middle America subduction zone, J. Geophy. Res., to be submitted.

Beroza, G., Gonzalez-Ruiz, J. R., K. C. McNally and F. A. Nava, 1983, Seismicity and seismic potential of the Acapulco, Mexico region, J. Geophys. Res., to be submitted.

Brown, E. D., and K. C. McNally, 1983, Spatial and temporal patterns

of seismicity associated with the 1973 Colima, Mexico earthquake (M_s = 7.5), J. Geophys. Res., to be submitted.

Abstracts

Beroza, G., J. A. Rial and K. C. McNally, 1982, Source mechanism of the June 7, 1982, Mexico earthquakes, EOS Trans., AGU, 63, 1040.

Brown, E., and K. C. McNally, 1982, Spatial and temporal seismicity patterns associated with the 1973 Colima, Mexico earthquake M = 7.5, EOS trans., AGU, 63, 1040.

Gonzalez, J., and K. C. McNally, 1982, Recent seismic patterns in the Acapulco-Pinotepa area of the Middle America Trench, southern Mexico, EOS Trans., AGU, 63, 1040.

Harlow, D., J. A. Rial and K. C. McNally, 1982, The June 19, 1982, earthquake near El Salvador: A double event double mechanism earthquake, EOS Trans., AGU, 63, 1040.

Lefevre, L. V., and K. C. McNally, 1982, Stress distribution in the Mexican subduction zone, EOS Trans., AGU, 63, 1039.

Nava, F. A., G. Beroza and K. C. McNally, 1982, Microseismicity of the Acapulco quiescent zone, EOS Trans., AGU, 63, 1040.

Rial, J. A., J. Gonzalez and K. C. McNally, 1982, Two recent large normal fault earthquakes in south central Mexico, EOS Trans., AGU, 63, 1040.

Rundle, J. B., K. C. McNally and H. Kanamori, 1982, Seismic triggering of earthquakes, EOS Trans., AGU, 63, 1028.

Gonzalez-Ruiz, J. R., and K. C. McNally, 1983, Influence of earthquake fault mechanism, depth and distance on damage in Mexico, Proc. VI Congress Soc. Seism. Eng. Mexico, in press.

Nava, F. A., K. C. McNally and J. R. Gonzalez-Ruiz, 1984, Digital monitoring of gaps and prediction: The Acapulco quiescent zone and the 1982 Pinotepa, Mexico earthquakes, Proc. 27th. International Geol. Congress, Moscow, U.S.S.R., in press.

Reevaluation and Interpretation of Releveling Observations in the Western U.S.: Implications for Earthquake Prediction

20585

Jack Oliver and Robert Reilinger
Department of Geological Sciences
Cornell University
Ithaca, NY 14853
(607) 256-2377

Investigations

This research program is designed to clarify the nature and causes of contemporary vertical movements of the crust primarily as evidenced by precise releveling in seismically active areas of the western U.S. with emphasis on southern California. Recent investigations include: 1) Analysis and interpretation of tectonic deformation in the Imperial Valley, California; 2) Identification of regions undergoing subsidence due to fluid withdrawal throughout the U.S. with emphasis on southern California; 3) Analysis of recent releveling around the Rio Grande Rift, New Mexico; 4) U.S. National Report to IUGG 1979-1982 on Crustal Movements.

Results

1) Coseismic and Postseismic Vertical Movements Associated with the 1940, M7.1 Imperial Valley, California Earthquake

Elevation changes derived from precise leveling surveys conducted by the National Geodetic Survey in 1931, 1941, and 1972 along two routes crossing the Imperial fault in southern California represent the first documented examples of spatially coherent vertical movements associated with a purely strike-slip fault. The leveling routes cross the northern section of the fault that broke at the time of the 1940, M7.1 Imperial Valley earthquake. The observed vertical movements, which extend approximately 25 km east and west of the fault, are among the largest observed anywhere in the U.S. These movements are consistent with simple elastic models of coseismic and postseismic "secondary" vertical deformation due to right-lateral, strike slip movement along a finite length fault. The spatial and temporal patterns of deformation suggest a simple scenario consisting of large coseismic slip on the southern part of the Imperial fault which transferred stresses to the northern part of the Imperial fault and the Brawley fault (enechelon fault northeast of Imperial fault). These stresses were subsequently released primarily by aseismic creep. The estimates of coseismic faulting determined from the leveling observations are roughly consistent with field observations of horizontal surface offset made after the earthquake as well as with some estimates derived from triangulation measurements. The postseismic fault offsets reported here suggest slip to shallower levels than those determined from repeated triangulation measurements. Other geophysical observations in this part of the Imperial Valley (fault creep, seismicity, seismic faulting) suggest that stick-slip on the southern part of the Imperial fault and creep on the northern part of this fault and the Brawley fault may characterize the long term fault behavior in the Imperial Valley.

The overall shallow slip (coseismic plus postseismic) required by the leveling observations on the southern part of the Imperial fault is larger than that required on the northern part of this fault and the Brawley fault. This difference may have contributed to the 1979, M6.6 Imperial Valley earthquake which caused surface offsets on the northern part of the Imperial fault and the Brawley fault.

2) Subsidence Due to Groundwater Withdrawal in Many Parts of the U.S.: Impact on Tectonic Movements in Southern California

Analysis of repeated levelings conducted by the National Geodetic Survey indicates many locations of relative subsidence in the United States. In addition to confirming subsidence in previously reported areas, over 35 new locations of subsidence, possibly due to water withdrawal, have been identified. The best documented of these include: Ventura, Ontario, and San Pedro-Santa Monica, California; Monroe and Alexandria, Louisiana; and Jackson, Mississippi. Subsidence may also have occurred in other groundwater basins where water levels have been drawn down, and remained undetected because of a lack of repeated levelings. It is important to be aware of and to continue to monitor such effects because of increasing rates of utilization of groundwater resources and the potential for significant engineering problems due to surface movements. Perhaps more importantly for the purposes of this study, identifying cases of subsidence due to water withdrawal is essential in order to use effectively releveling observations for investigating tectonic deformation. Along these lines, our analysis suggests that some of the releveling observations used to define the southern California uplift more likely reflect subsidence due to water level declines within sedimentary basins around the periphery of the presumed zone of uplift.

3) Recent Measurements of Crustal Deformation Related to the Socorro Magma Body, New Mexico

New releveling measurements conducted by the National Geodetic Survey during 1980 in the vicinity of the Socorro magma body indicate substantial vertical movement from 1951 to 1980. These data are consistent with previously published results of crustal uplift (1912 to 1951) above the magma body (Reilinger et al., Geology, 1980) and, in addition, define a prominent zone of subsidence bordering and to the south of the main zone of uplift. While unusually rapid movement apparently related to magma migration has occurred during the most recent interval around the Socorro area, the average rate of deformation from 1951 to 1980 (1.8 mm/yr) is slower than that from 1912 to 1951 (3.4 mm/yr) which is consistent with an apparent reduction in seismic activity.

4) U.S. National Report to IUGG 1979-1982: Crustal Movement

This report reviews progress by U.S. investigators in applying geodetic techniques to the study of crustal movements. The report is divided into the following general catagories: 1) the southern California uplift, 2) the San Andreas Transform system, 3) earthquake deformations, 4) magma induced

deformations, 5) the northwestern U.S., 6) subsidence due to fluid withdrawal, 7) the eastern U.S., and 8) diagnosis and prognosis. A fairly complete bibliography of U.S. studies is included.

Reports

Reilinger, R.E., Coseismic and postseismic vertical movements associated with the 1940, M7.1 Imperial Valley, California earthquake, J. Geophys. Res., submitted, 1983.

Chi, S.C., and R.E. Reilinger, Geodetic evidence for subsidence due to groundwater withdrawal in many parts of the U.S., J. of Hydrology, v. 67, n. 1/4, 1984.

Brown, L.D., and R.E. Reilinger, Crustal movement, Rev. of Geophys. and Space Phys., v. 21, 553-559, 1983.

Reilinger, R.E., M. Bevis, and G. Jurkowski, Tilt from releveling: an overview of the U.S. data base, Tectonophysics, submitted, 1983.

Larsen, S., and R. Reilinger, Recent measurements of crustal deformation related to the Socorro magma body, New Mexico, New Mexico Geological Society Guidebook: Socorro, New Mexico, in press, 1983.

Seismicity and Earthquake Source Properties in the Yakataga Seismic Gap, Alaska

9940-03005

R. A. Page
Branch of Seismology
U. S. Geological Survey
345 Middlefield Road, Mail Stop 77
Menlo Park, California 94025
(415) 323-8111, ext. 2567

Investigations

1. Seismicity in and around the Yakataga seismic gap was reviewed to assess the significance of recent moderate-to-large earthquakes around the gap with regard to the imminence of a major earthquake in the gap.

2. R. A. Page coordinated planning within the Geologic Division for a multi-disciplinary investigation of the crustal structure of Alaska along a north-south transect following the route of the trans-Alaska oil pipeline and extending offshore across the Pacific and Arctic continental margins. The transect study will feature acquisition of extensive state-of-the-art seismic data (including refraction/wide-angle reflection and vertical reflection data) and coordinated geologic, aeromagnetic, and gravimetric mapping and studies. A two-year plan of investigations was prepared to initiate the transect along the southern segment of the route between Valdez and the Denali fault in the Alaska Range. Four seismic refraction/wide-angle reflection profiles within the Chugach, Peninsular and Wrangellia tectonostratigraphic terranes, and crossing their common boundaries, were reconnoitered in anticipation of shooting in 1984.

3. J. R. Pelton pursued the determination of accurate ($\pm$ 3 km) focal depths for 30 moderate-sized ($m_b \geq 5$) earthquakes in and around the Yakataga seismic gap. The WWSSN film chip library was searched for depth phases (pP,sP) on long-period and short-period vertical components over a range of azimuths that was as broad as possible. Selected long-period records with good S/N ratios were digitized and processed to remove the long-period instrument reponse and to obtain displacement and velocity seismograms. Final depth phase identification and focal depth determination are now being completed using the original long-period and short-period seismograms, the displacement and velocity seismograms, and synthetic long-period P-waveforms.

4. In cooperation with George Zandt at SUNY-Binghamton, J. R. Pelton completed a manuscript on the 3-D inversion of teleseismic P-wave residual for crust and upper mantle structure beneath southern coastal Alaska.

5. J. R. Pelton completed, for journal publication, a manuscript describing the computer-based, four-film digitizing system used for interactive timing and location of Alaskan earthquakes.

Results

1. In the first nine months of 1983, seven earthquakes of magnitude m_b 5.0 or larger have occurred within about 150 km of the Yakataga seismic gap. This is the largest number to occur within any one year interval since 1970-71, when the Pamplona Ridge sequence occurred on the southeastern edge of the gap. Moreover, these seven shocks include two events (M_s 6.3 and 6.1) near Columbia Bay--the largest shocks in Prince William Sound since the great (M_w 9.2) 1964 earthquake--and an m_b 5.9 event in the aftershock zone of the 1979 St. Elias earthquake (M_w 7.6) -- the largest shock in the sequence following the main earthquake.

   The occurrence of the Columbia Bay earthquakes in July and September caused us to question whether the increased number of moderate-to-large earthquakes indicates that a gap-filling earthquake is imminent. We conclude from considerations of seismotectonics and seismicity patterns that there is no compelling evidence that a major earthquake is substantially more likely to occur in the next several months than in the next decade or two. However, in view of the recent spate of sizeable earthquakes, we are keeping close watch on the seismicity in and around the gap.

   The Columbia Bay shocks are tentatively interpreted to be down-dip extensional faulting within the subducted oceanic lithosphere (see report by Lahr and Stephens, this volume). It is doubtful that these two earthquakes would significantly effect the stress conditions on the megathrust inferred to underlie the Yakataga gap, or therefore, the short-term earthquake potential within the gap. The postulated mechanism for a gap-filling earthquake is interplate thrusting, whereas the Columbia Bay earthquakes are thought to be extensional failures within the subducted plate. The Columbia Bay shocks are about 100 km west of the gap and, perhaps more importantly, lie west of a pronounced northwest-trending discontinunity in seismicity that reflects severe complications in the subduction tectonics between the Columbia Bay region and the Yakataga region and that is especially prominent in the Benioff zone seismicity. Moreover, even within a simple subduction zone, earthquakes within the subducting plate, at least those deep enough to be clearly distinguished from megathrust or overriding plate events, seem to occur largely independently of major interplate thrust earthquakes.

A review of the activity in and around the Yakataga gap for shocks of m_b 4.5 or larger for the interval 1960 to the present (Figures 1 and 2) shows that the great 1964 Prince William Sound earthquake stimulated a flurry of shocks within the Yakataga gap to the east, but that since 1966 only one event has occurred distinctly within the gap, an m_b 4.9 event in 1967. Numerous shocks have occurred on the periphery of the gap including the prominent 1970 Pamplona Ridge and 1979 St. Elias sequences on the southeastern and eastern boundaries, respectively. Thus, for shocks of m_b 4.5 or larger, the seismic gap has been quiet since probably 1967 and at least since 1970, but significant activity has occurred on and beyod its boundaries. The uniqueness of the observed increase of seismicity around the gap in 1983, is difficult to evaluate because the historical record of seismicity at this magnitude level encompasses only two decades.

The microseismicity of the region shown in Figure 2 was also reviewed for the interval since 1974 when the USGS regional seismograph network was extended into the region. For this entire interval the microseismicity within the gap has been characterized by a persistent, diffuse concentration of seismicity in the middle of the gap beneath Waxell Ridge (at about 60.5°N, 143°W) and less frequent events elsewhere in the gap. (See Figure 1 in the report by Lahr and Stephens, this volume, for a typical example of the microseismicity in and around the gap.) From the currently available data, we cannot resolve whether the Waxell Ridge earthquakes are confined to the inferred megathrust, or whether some or all of the shocks occur in the overriding or subducting plates; nor can we determine whether the Waxell Ridge area is a high-strength patch locking the Yakataga segment of the megathrust, or whether it is a weak zone. Only a very few microearthquakes have been located along the northern boundary of the gap, which is perhaps the most likely location for the epicenter of a gap-filling earthquake based on experience in the adjacent 1964 and 1979 earthquakes as well as large thrust earthquakes in subduction zones elsewhere. While the number of earthquakes of m_b 5.0 or larger in the area surrounding the gap has increased in 1983, the rate of microseismicity in and adjacent to the gap has remained at normal levels except where aftershock sequences have followed the larger earthquakes.

Reports

Fogleman, K. A., Stephens, C. D., Lahr, J. C., and Page, R. A., 1983, Recent seismicity in and around the Yakataga seismic gap, southern Alaska [abs.]: EOS, Transactions, American Geophysical Unon, v. 64, in press.

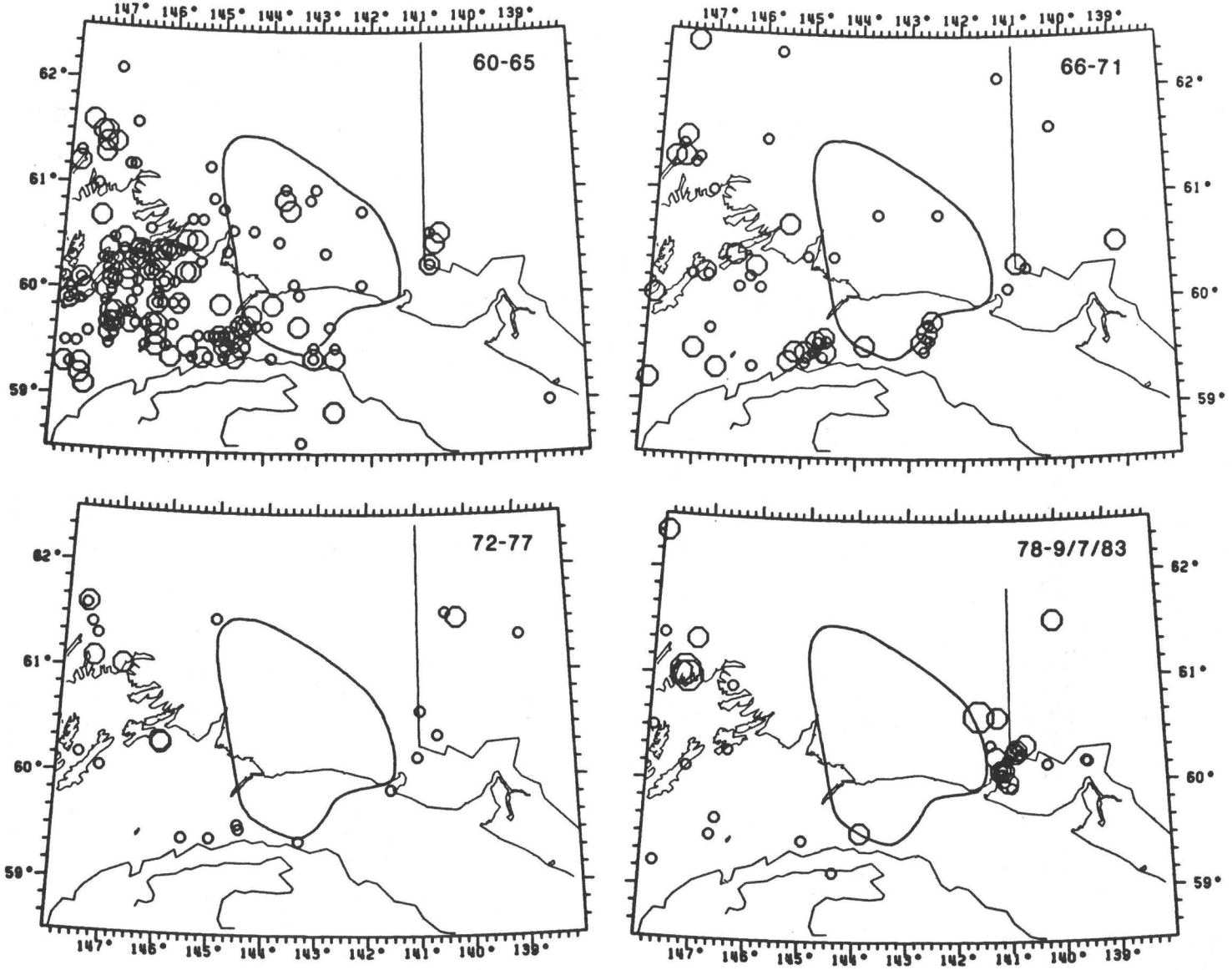

Fig. 2. Epicenter maps of earthquakes plotted in Figure 1 for four consecutive 6-year intervals. The most recent interval only extends through 7 September 1983. Symbols as in Figure 1. The area of the Yakataga gap is indicated in the center of the maps.

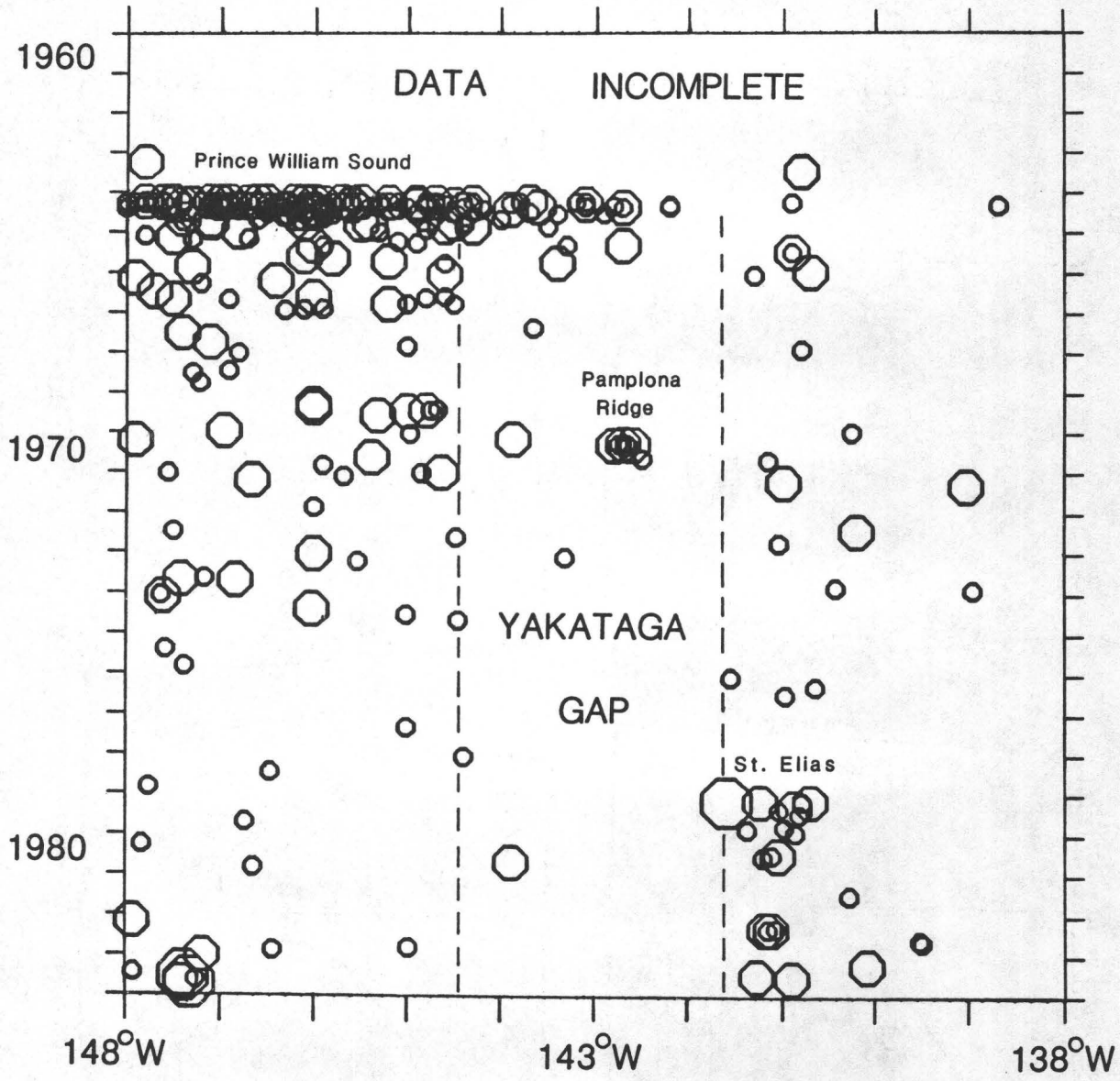

Fig. 1. Longitude-time plot of earthquakes in the Yakataga region (see Fig. 2) with magnitudes m_b 4.5 or larger from the interval 1 January 1960-7 September 1983, as reported in the PDE files. The data are incomplete before 1964; body-wave magnitudes have been routinely computed by the PDE program since April 1963. Symbol size is proportional to magnitude; small, 4.5-4.9; intermediate, 5.0-5.9; and large, 6.0 or greater. Three prominent earthquake sequences are observed: 1964 Prince William Sound, 1970 Pamplona Ridge, and 1979 St. Elias. The approximate extent of the Yakataga gap is shown.

CRUSTAL STRAIN

9960-01187

W.H. Prescott, J.C. Savage, M. Lisowski, and N. King
Branch of Tectonophysics
U.S. Geological Survey
345 Middlefield Road, MS/77
Menlo Park, California 94025
(415) 323-8111, ext. 2701

Investigations

The principal subject of investigation was the analysis of deformation in a number of tectonically active areas in the western United States.

1. Deformation in the Long Valley, California, caldera, 1982-83

The deformation across the Long Valley caldera in the interval August 1982 to August 1983 has been deduced from leveling and trilateration surveys. Most of the deformation apparently occurred prior to the end of January 1983 and possibly principally at the time of the January earthquake swarm. The observed deformation can be attributed to two sources: Continued inflation (about 0.014 km^3) of the magma chamber beneath the resurgent dome and right-lateral slip (0.20 m) and dike injection (about 0.013 km^3) along the 8.5 km-long and 8-km-deep rupture zone defined by the January 1983 swarm. This model requires that the magma chamber beneath the resurgent dome be represented by a sill-like chamber rather than the spherical chamber previously used.

2. Leveling across the Long Valley, California, caldera, 1932-1983.

The elevation changes indicated by leveling surveys along Highway 395 from Toms Place to Lee Vining in 1932, 1957, 1980 (Toms Place to Crestview only), 1982, and 1983 are shown in the accompanying figure. The uppermost plot shows the topographic profile along the leveling route, and the true lower plots show the elevation changes for various epochs. The curve labeled 82-83, for example, shows the 1983 elevation less the 1982 elevation for each of the bench marks along the line. In plotting these data it has been assumed that the bench mark at Lee Vining remained fixed in elevation except for the 75-80 elevation change plot in which Toms Place was held fixed inasmuch as the

1980 leveling did not extend to Lee Vining. The leveling suggest that both Toms Place and Lee Vining have remained stable in elevation; the failure of the 1932 and 1982 leveling to close exactly at Toms Place (i.e., indicated elevation change at Toms Place in the 32-75, 75-82, and 82-83 plots) is probably simply a product of survey error. The third plot from the top clearly shows the development of the uplift centered at Casa Diablo within the Long Valley caldera. The uplift is attributed to reinflation of the magma chamber beneath the resurgent dome within the caldera.

3. Strain accumulation in the Shumagin Island, Alaska, seismic gap.

The Geodolite network established in the Shumagin Islands in 1980 and 1981 was resurveyed in June 1983. The principal strain rates deduced for the 1980-1983 interval are $\dot{\varepsilon}_1 = -0.04 \pm 0.07$ μstrain/a N76W ± 16 and $\dot{\varepsilon}_2 = -0.14 \pm 0.07$ μstrain/a N14°E ± 16° (extension reckoned positive). The strain accumulation rate predicted from a dislocation model of the subduction process would be a uniaxial compression ($\dot{\varepsilon}_1 = 0.0$ μstrain/a N60°E and $\dot{\varepsilon}_2 \sim 0.1$ μstrain/a N30°W). Thus, only a marginally significant measurement of strain accumulation has been obtained, but it is clear that the strain rate is not anomalously high.

4. Deformation between San Francisco Bay and Cape Mendocino

Although the San Andreas fault is commonly referred to as the boundary between the Pacific and North American plates, in reality the boundary is not a single fault trace but rather a broad deforming zone. In the Coast Ranges of California north of San Francisco Bay, the deforming zone extends at least from the submarine trace of the San Andreas fault inland to the Coast Range thrust. Geodetic measurements of crustal strain have been made at 6 sites in this zone between the Mendocino triple junction and San Francisco Bay. At one of the 6 sites no detectable strain is occurring - the rate is less than about 0.1 μrad/yr (engineering shear strain). At all of the other sites strain is accumulating at rates varying from about 0.3 μrad/yr to about 0.7 μrad/yr with standard deviations around 0.1 μrad/yr. For two of the sites the data consist of repeated triangulation spanning the time period 1942 to 1964. A third triangulation site spans the time period 1925 to 1949, and this site is the only one that did not exhibit strain accumulation. At the remaining three sites, the observations consist of repeated distance measurements observed during the last 10 years. For these sites it is possible to estimate the dilatation as well as the shear.

None of the three sites indicates that any detectable dilatation is occurring. The northern-most site is located onshore directly opposite the Mendocino triple junction. The dilatation here is poorly resolved because of the short time span of the observations, but even here there does not appear to be any dilatation occurring. A possible explanation for the absence of strain at one site may be that the time period covered by measurements at this site is earlier than at the other sites.

5. Precision of 2-color distance measurements.

The errors in distance measurements made with 2-color laser geodimeters were found to have a distribution with standard deviation $\sigma = (a^2 + b^2 L^2)^{1/2}$. For three years of data collected by CIRES at Pearblossom, California a = 0.4 mm and b = 0.16×10^{-6}. For 3 months of data collected by the USGS at Long Valley, a = 0.4 mm and b = 0.20×10^{-6}. For both data sets the total error is better determined than either of the length-dependent (b) or length-independent (a) parts. For the pearblossom daa set this total error is 0.9 mm and for the Long Valley data set it is 1.0 mm.

These estimates of errors in the observations were used to estimate the minimum amount of slip on the Parkfield fault plane, that would be detectable by a 2-color network located at Parkfield. We conclude that one or two centimeters of fault slip will be detectable if it occurs near the surface under the network or if it extends over a length of fault that is large relative to the size of the network. Localized slip in other locations will be detected only if it exceeds 5 to 10 cm.

Reports

Savage, J. C., Strain accumulation in western United States, Ann. Rev. Earth Planet. Sci., 11, 11-43, 1983.

Savage, J. C., A dislocation model of strain accumulation and release at a subduction zone, J. Geophys. Res., 88, 4984-4996, 1983.

Prescott, W. H. and J. D. Davis, Geodolite observations near Hanford, Washington, Rockwell Hanford Operations Tech. Mem. No. RHO-BW-CR-132P, Richland, WA, 1983.

Prescott, W. H. and M. Lisowski, Strain accumulation along the San Andreas fault system east of San Francisco Bay, California, Tectonophysics, 97, 41-56, 1983.

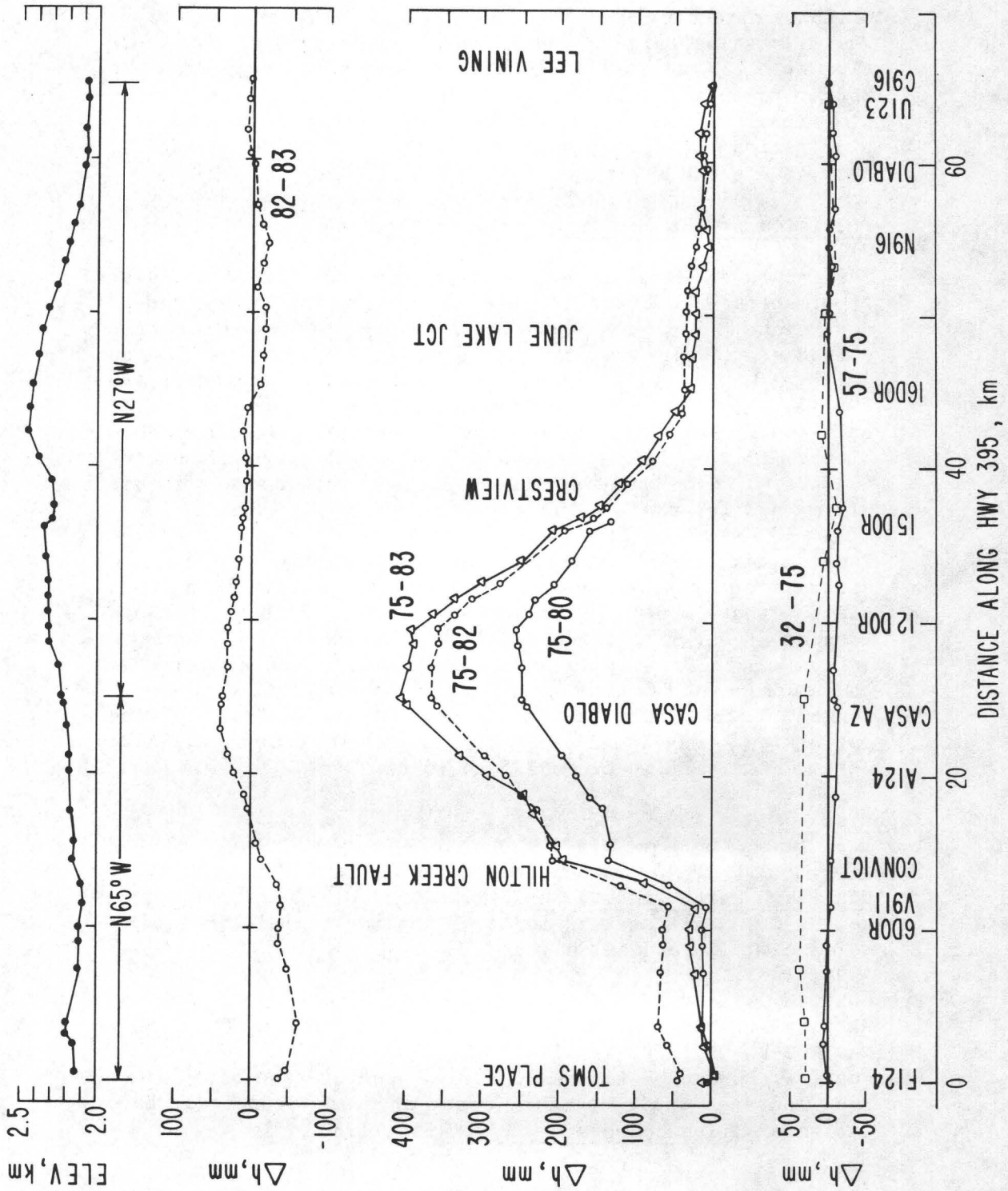
ELEV, km
2.5
2.0
N65°W
N27°W
Δh, mm
100
0
-100
82-83
Δh, mm
400
300
200
100
0
TOMS PLACE
HILTON CREEK FAULT
CASA DIABLO
CRESTVIEW
JUNE LAKE JCT
LEE VINING
75-83
75-82
75-80
Δh, mm
50
0
-50
32-75
57-75
F124
6DOR
V911
CONVICT
A124
CASA AZ
12DOR
15DOR
16DOR
N916
DIABLO
U123
C916
0
20
40
60
DISTANCE ALONG HWY 395, km

A Crustal Deformation Observatory near the San Andreas Fault in Central California

21300

L.E. Slater
CIRES
Campus Box 449
University of Colorado
Boulder, Colorado 80309
(303) 492-8028

Investigations

1. A cooperative U.S. Geological Survey - University of Colorado effort to monitor crustal deformation near Pearblossom in Southern California has been underway since late 1979.

2. The CIRES multiwavelength EDM instrument is going to be installed at a new site near Parkfield in central California where it will be used to measure crustal deformation.

3. A back-up electro-optic modulator is being produced for use in the CIRES multiwavelength EDM instrument.

Results

1. The CIRES multiwavelength EDM instrument has been used to monitor approximately a dozen lines near Pearblossom, California since late 1979. The lines are arranged in a radial array and are measured approximately twice a week. The lines range in length from 2 km to 9 km with about half of them crossing the San Andreas fault. The results of these measurements indicate that the accumulation of strain in the earth's crust is not a simple linear phenomena. There appear to be periods of time (weeks or months) when the accumulation of strain may proceed at rates 2 to 5 times that of the long-term average. Whether these episodes of increased strain rate indicate periods of increased seismic risk is not yet certain. We expect to move the CIRES multiwavelength EDM instrument from the Pearblossom site to central California before the end of 1983.

2. We have begun installation of a new multiwavelength array in central California. The array will be radial in design with the instrument site on a hilltop approximately 1 km south of the town of Parkfield. The array will span the transition portion of the San Andreas fault between the northern end of the 1857 earthquake that is now locked and the central portion that is currently undergoing aseismic fault slip. The array will consist of about 12 lines that will allow the calculation of the strain field and fault slip in this region. Several researchers have identified this portion of the San Andreas fault as the most likely site of the next magnitude 6 to 7 earthquake along the San Andreas.

3. The heart of the CIRES multiwavelength EDM instrument is the electro-optic modulator. If this element was to fail unexpectedly we would suffer several months of down-time. For this reason, we have begun the construction of a spare unit. The design is nearly complete and we expect to complete work by the end of 1983.

Sesismic Studies of Fault Mechanics

9930-02103
Paul A. Reasenberg
U. S. Geological Survey
345 Middlefield Road, Mail Stop 77
Menlo Park, California 94025
(415) 323-8111, ext. 2049

Investigations

1. Analysis of the second-order moment (2-point correlation function) of the U. S. Geological Survey's central California earthquake catalog for the period 1969-1982 continued.

2. A preliminary analysis of the hypocentral distribution of aftershocks of the M 6.5 earthquake near Coalinga, California, that ocurred May 2, 1983, was undertaken with Donna Eberhart-Phillips, and Paul Segall (both at the U. S. Geological Survey).

Results

1. The second-order moment of a point process represents the statistical distribution of event pairs and thus provides a measure for evaluating the process with respect to models of event independence (random model) and interaction. The second-order moment for a subset of the U. S. Geological Survey's central California catalog including 40,000 earthquakes was formed with respect to a magnitude threshold of M 4.0, resulting in 1,857,000 pairs of events. In terms of number of pairs, the apparent dominant process of earthquake interaction is the aftershock process. This process dominates the entire second-order moment, including that portion which could, in the absence of the aftershock process, reveal a pre-mainshock pattern (e.g., gap, donut, migration), if one exists. Therefore, a new approach to removing aftershocks from the catalog was developed in which clusters are defined by the data rather than by the conventional fixed space-time window method. The resulting de-clustered catalog is Possionian in time. Tests for the existence of spatial and bivariate patterns in the de-clustered catalog are in progress.

2. Nine hundred thirty-nine aftershocks for the 10-day period ending 12 May, 1983 (2251 GMT) were relocated using P-wave arrivals from 22 stations of the USGS central California telemetered network. Hypocenters were determined with a velocity model obtained by Walter and Mooney (1980) from refraction data. Station corrections were determined by linear inversion of a subset of the P-wave data. Resulting location uncertainty is estimated to be less than 1.5 km (epicenter) and 2.0 km (depth).

   In map view (fig. 1) the distribution of aftershock epicenters is an elongate zone striking approximately N 30° W, with approximate length 32 km and breadth 16 km. The zone is wider in the northwest portion than in the southeast. The epicenters of both the mainshock and the largest aftershock (9 May, 0249 GMT; M_L 5.1) are located near the center of the zone, beneath Anticline Ridge (fig. 2). The strike of the aftershock

zone parallels the regional strike of the Diablo Range to the west, and more locally, of the anticlinal structure composed of Anticline Ridge and Kettleman Hills. The aftershock epicenters are essentially confined to the anticline.

Vertical cross sections AA' and BB' (fig. 3) show the depth distribution of hypocenters in vertical planes along the transverse to the strike of the zone, respectively. The depth of the mainshock (approximately 10 km) and that of the largest aftershock (approximately 12 km) are near the bottom of the aftershock zone. The deeper aftershocks are confined to the volume near the mainshock hypocenter, within 5-7 km distance along the strike, and predominatly southwest of the mainshock. Aftershocks above 4 km depth are confined to the northwest portion of the aftershock zone. The densest concentration of aftershocks occurs between 6 and 9 km depth, near the mainshock hypocenter. In transverse cross section (BB') a weakly defined linear trend apparently dips toward the southwest, somewhat above the mainshock hypocenter. The possibility of inferring a steeply northeast-dipping plane passing through the densest part of the distribution is also noted. The location of the M 5.1 aftershock relative to the mainshock hypocenter would support the northeast-dipping plane if this aftershock were a continuation of the main rupture. However, resolution of any planar features in the aftershock pattern is poor in this hypocenter set.

In figure 4, subsets of aftershocks occurring in the first 21 hours of the sequence with lower magnitude thresholds of 1.5, 2.0, 2.5 and 3.0 are shown in transverse cross section (BB'). The larger magnitude events suggest a southwest-dipping plane. The temporal development of the sequence during the first 24 hours (fig. 5) suggests that during the first 18 hours aftershocks defined a southwest-dipping structure.

References

Fowkes, E. J., 1982, An Educational Guidebook to the Geologic Resources of the Coalinga District, California, Westhills College, Coalinga, CA.

Walter, A. W., and Mooney, W. D., 1980, Crustal structure of the Diablo and Gabilan Ranges, central California: a reinterpretation of existing data: Bulletin, Seismological Society of America, v. 72, no. 5, p. 1567-1590.

Reports

Reasenberg, P., D. Eberhart-Phillips, and P. Segall, 1983, Preliminary views of the aftershock distribution of the May 2, 1983, Coalinga Earthquake, U. S. Geological Survey Open-File Report 83-511, 27-37.

Reasenberg, P., D. Eberhart-Phillips, and P. Segall, 1983, (in) The Coalinga, California earthquake of May 2, 1983: a reconaissance report, Earthquake Engineering Research Institute, Berkeley, CA.

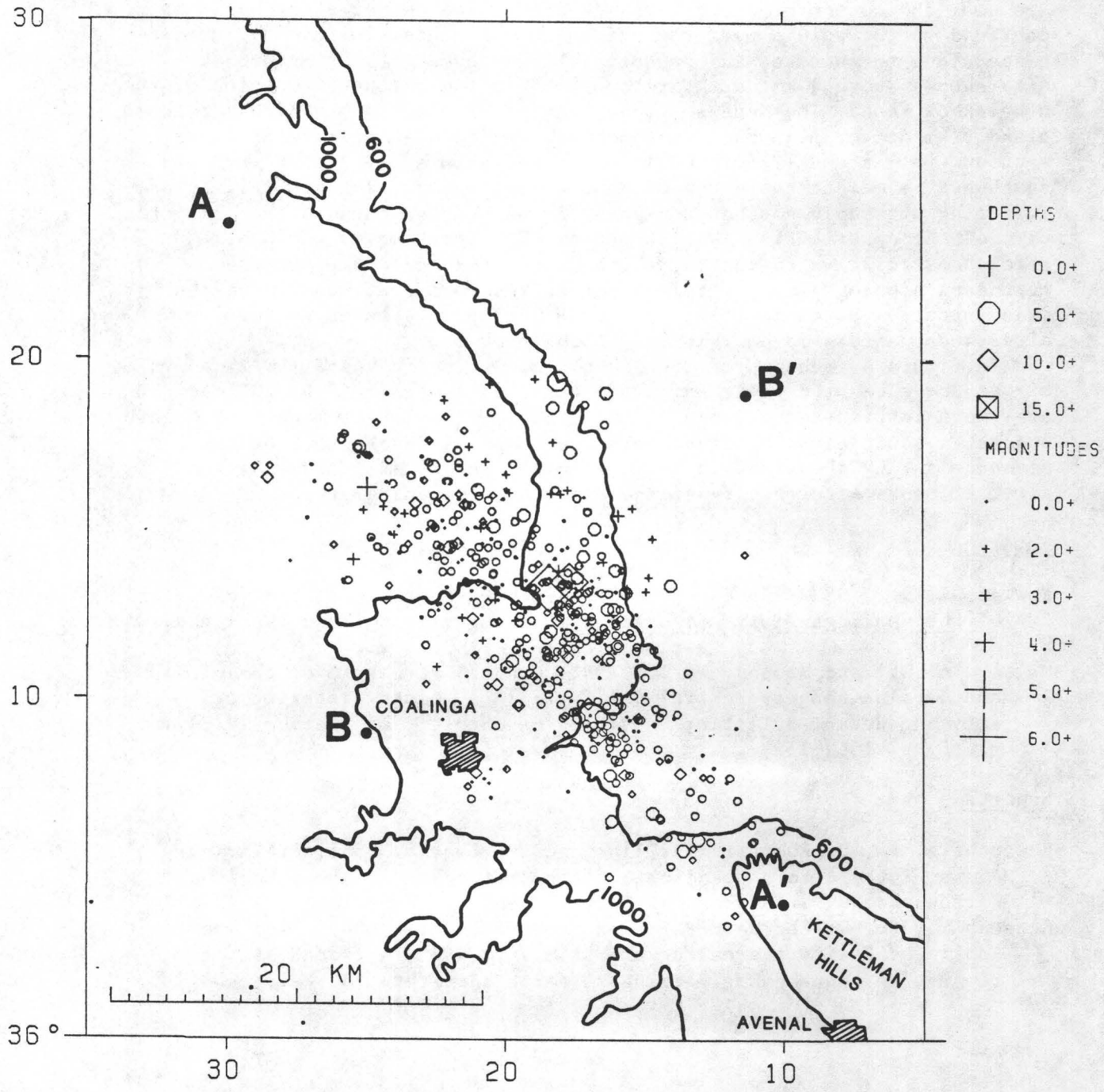

Figure 1. Epicenters of the mainshock (largest diamond symbol) and selected aftershocks for the period May 2-12, 1983. Aftershocks selected were observed on at least 10 seismograph stations in the USGS telemetered network. Symbol type represents hypocentral depth range as indicated in key. Generalized 600-foot and 1000-foot elevation contours are shown.

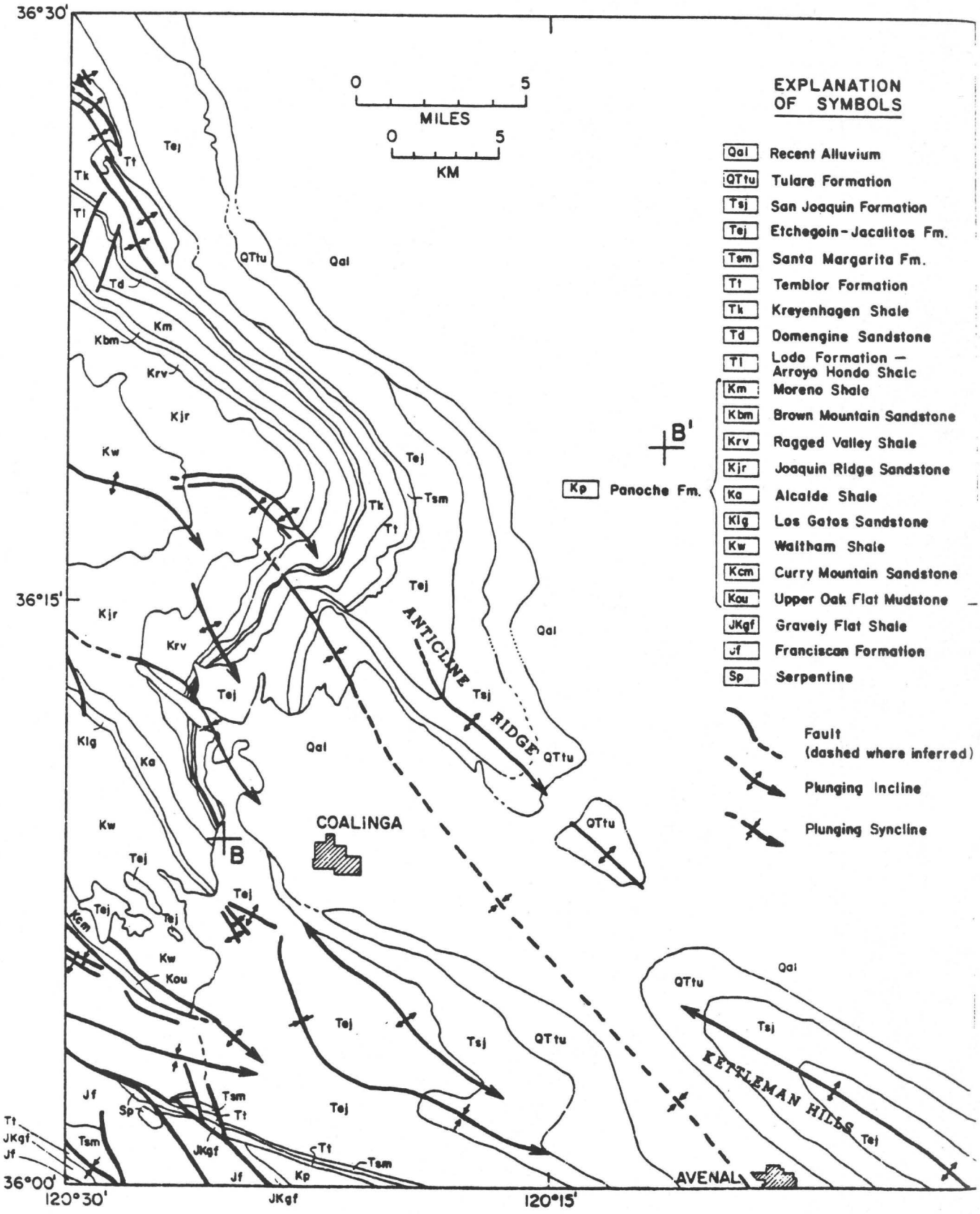

Figure 2. Simplified geologic map of the Coalinga area generalized from E. J. Fowkes, An Educational Guidebook to the Geologic Resources of the Coalinga District, California, Westhills College, Coalinga, CA (1982).

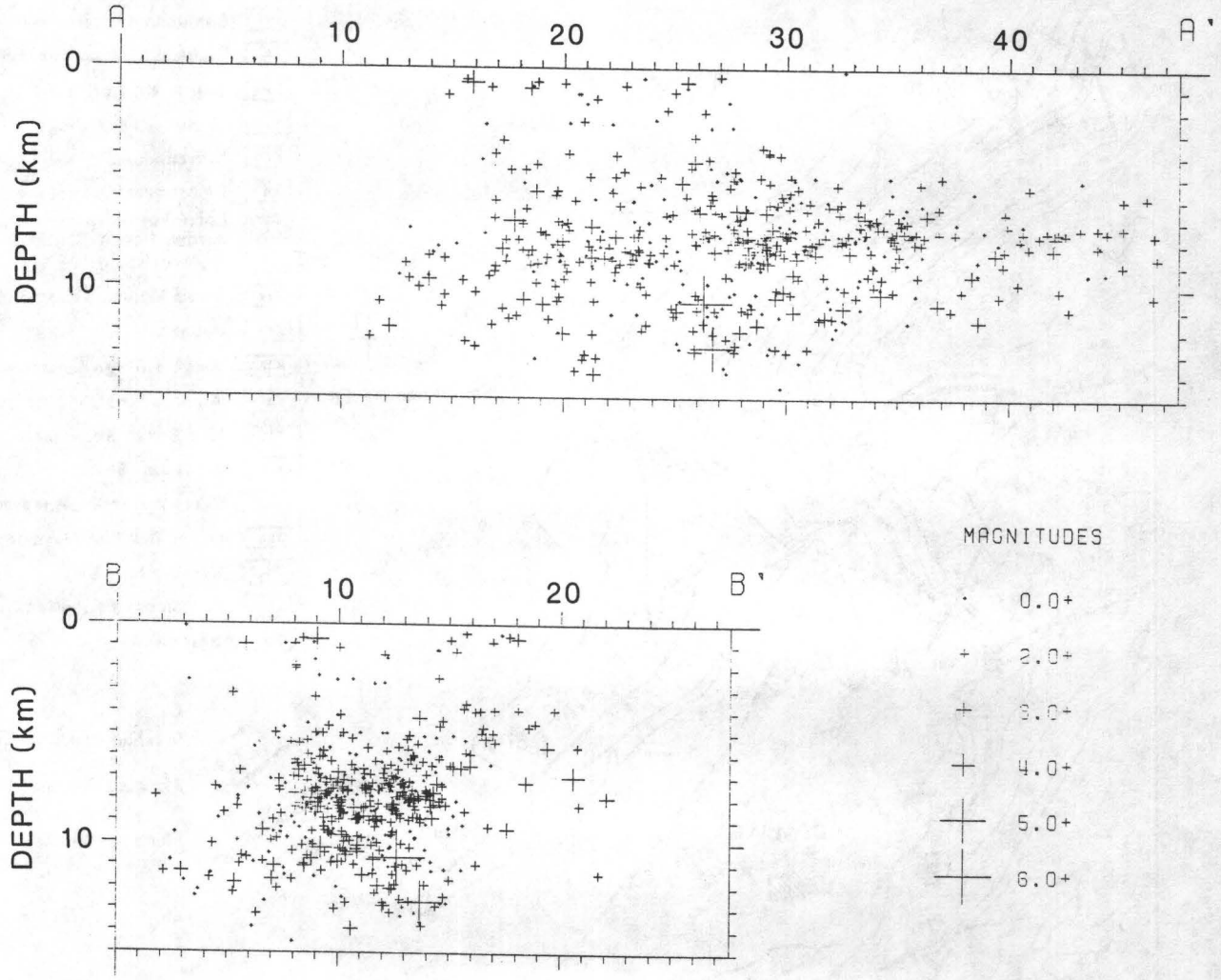

Figure 3. Cross-sectional views without vertical exaggeration of the earthquake set shown in figure 1. Hypocenters are projected onto vertical planes defined by the endpoints shown in figure 1.

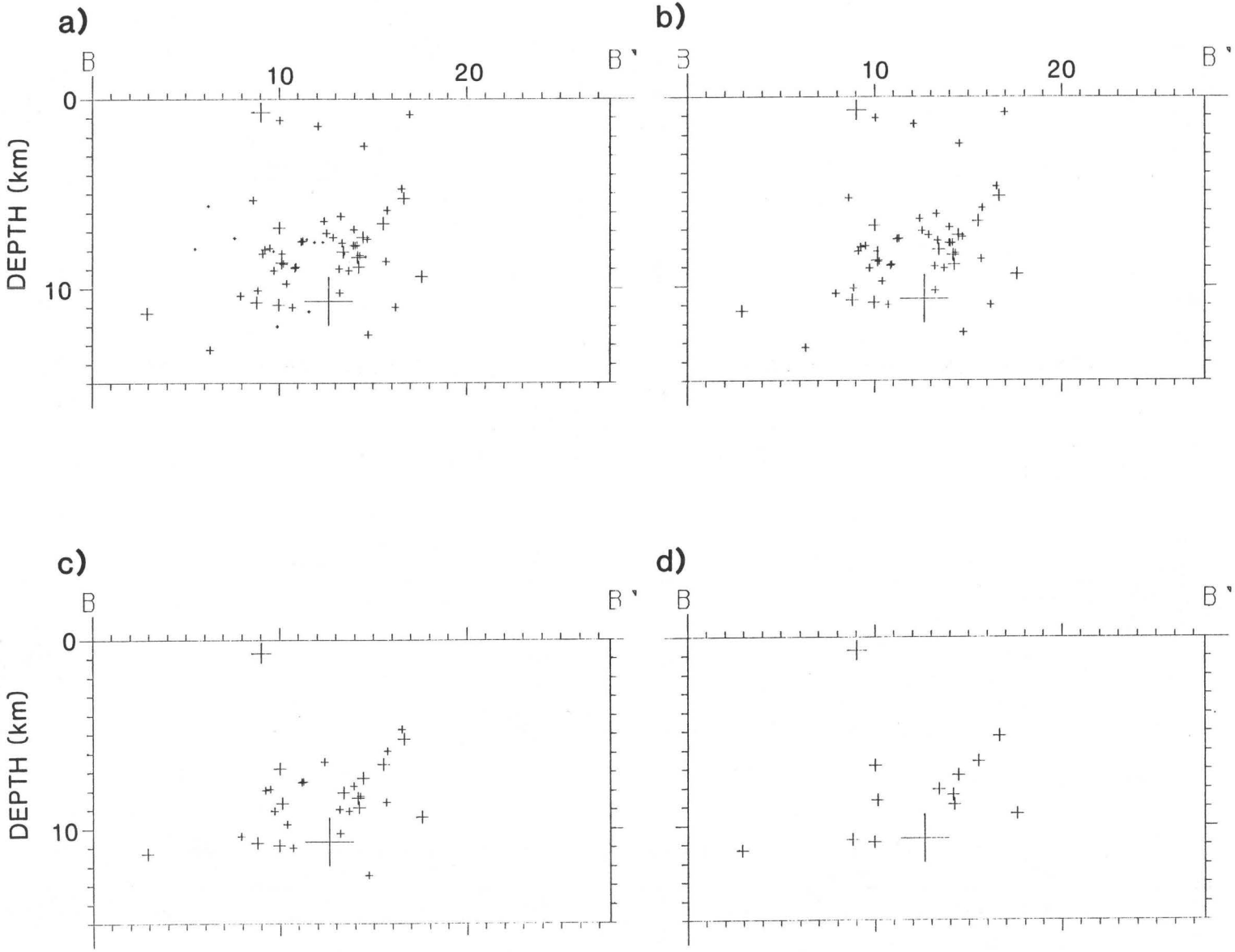

Figure 4. Transverse cross-sectional view of aftershocks for the first 21 hours of the sequence for selected lower magnitude thresholds. (a) $M \geq 1.5$; (b) $M \geq 2.0$; (c) $M \geq 2.5$; (d) $M \geq 3.0$.

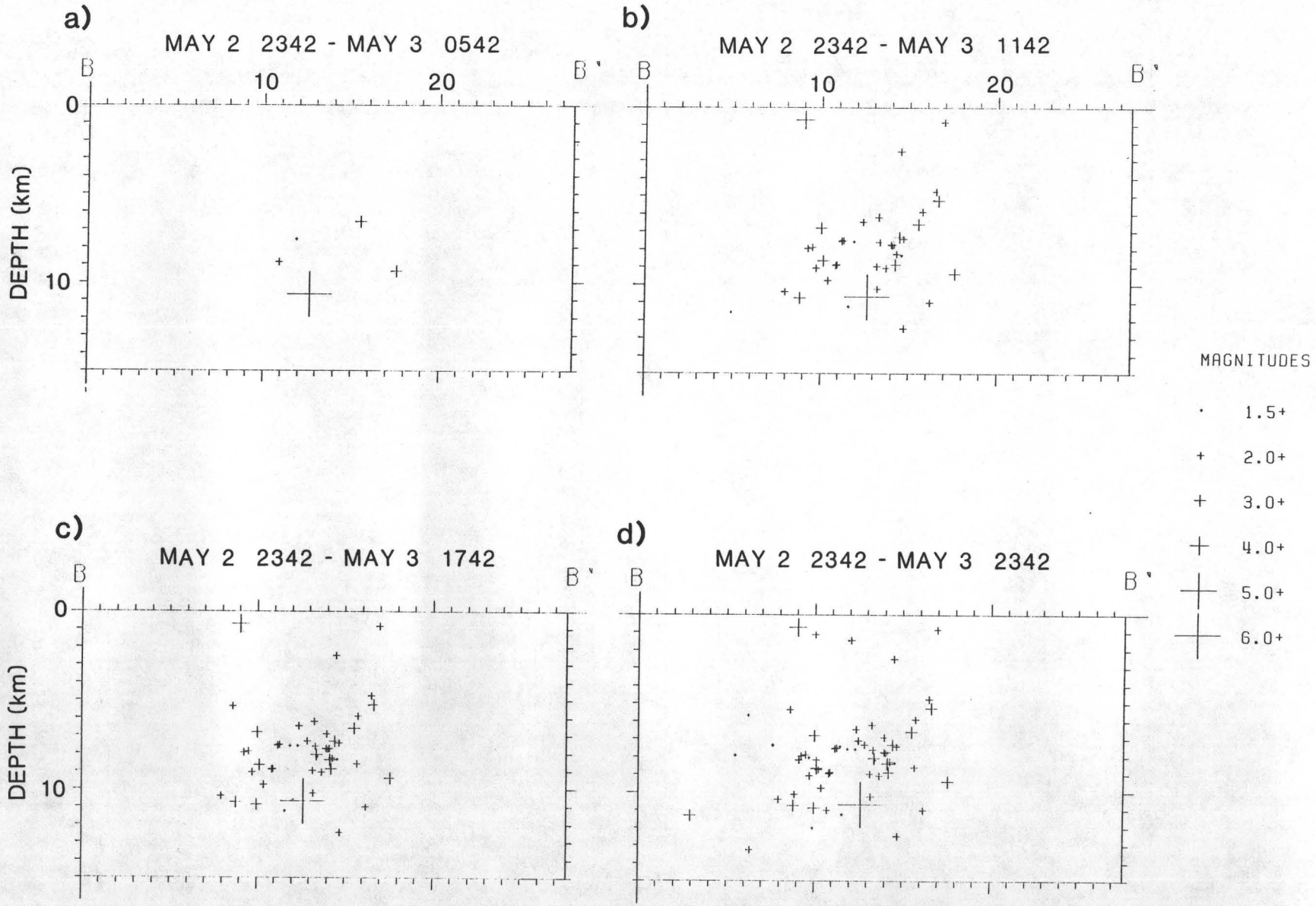

Figure 5. Transverse cross-sectional views of aftershocks ($M \geq 1.5$) during the first 24 hours of the sequence. (a) first 6 hours; (b) first 12 hours; (c) first 18 hours; (d) first 24 hours.

Consolidated Digital Recording and Analysis

9930-03412

Sam W. Stewart
Branch of Seismology
U. S. Geological Survey
345 Middlefield Road M/S 77
Menlo Park, California 94025
(415) 323-8111, Ext. 2577

Investigations

1. The goal is to develop and operate a computer-automated system that will detect and process earthquakes occurring within the USGS Central California Micro-earthquake network (aka CALNET). Presently the network telemeters the output from more than 400 short-period seismometers to a central recording point in Menlo Park, California. A DEC PDP 11/34 computer is used for online, realtime detection of events, and a DEC PDP 11/44 computer is used for processing and archiving. Both computers use the DEC RSX11M operating system.

   Software has been developed largely by Carl Johnson, but with some contributions from Bob Dollar, Peter Johnson and myself.

Results

1. The online event detection and recording system has worked well during this report period. Presently we are digitizing and processing 424 short-period seismic network stations, at a 100 Hertz rate for each station, using the DEC 11/34 computer.

   Two significant improvements were made to the system. First, the detection algorithm was greatly speeded up, principally by analyzing only half of the incoming data points for each station, and by checking for subnetwork triggers less often. Second, the online detection system can now run on the DEC 11/44 computer as well. The conversion involved taking into account the 22-bit address space on the 11/44 as compared to 18 bits on the 11/34. When our 11/34 gets upgraded to an 11/44 (early FY-84) then we will be able to do additional processing on the online computer. The additional processing will involve preparing the data for analysis and timing on the offline computer. For example, the data can be searched for triggers and demultiplexed at the same time.

2. The system for offline timing, locating and archiving of the detected events is running, but needs to be speeded up because of the large amounts of data to be processed. The system being used in Menlo Park was developed by Carl Johnson for the Southern California network.

Reports

None.

Great Earthquakes and Great Asperities, Southern California: A Program of Data Analysis

14-08-0001-21286

L. R. Sykes and L. Seeber
Lamont-Doherty Geological Observatory of Columbia University
Palisades, New York 10964
(914) 359-2900

Investigations

1. Analysis of recent seismic activity in both space and time along the San Andreas fault, with special emphasis on the Eastern Transverse Ranges between Riverside and Desert Hot Springs. This includes determination of the three-dimensional configuration of seismicity, its relation to regional tectonics and surface geology, as well as the orientation of slip along faults through the use of hypocentral locations and first-motion studies.

2. Analysis of the historical record to determine the long term behavior in California for large plate rupturing earthquakes.

Results

1. Probabilities of large plate rupturing events over the next 20 years have been estimated for the San Andreas, San Jacinto and Imperial Faults. Several segments along these faults have well constrained probabilities, whereas, several have large uncertainties. Nine of the 19 possible segments, constituting about 40% of the total lengths of the three faults, have moderate to high probability. In some cases the probabilities are such that two adjacent segments may be close enough in their loading history to break in a single event. The segment of the San Andreas that broke less than 1.5 m in 1906, from opposite San Jose to San Juan Bautista, is calculated to have a moderate to high probability for an earthquake of magnitude 6 3/4 to 7 1/4 during the next 20 years. A 325 km segment of the southern San Andreas, between Tejon Pass and the Salton Sea is the only segment along the three faults that appears to have other than a small chance of rupturing in a shock of magnitude near 8 during this time interval.

2. The long-range forerunning activity to the magnitude 6.5 Desert Hot Springs earthquake of 1948 has been found to exhibit unusual spatial and temporal variations (Figure 1). The most obvious pattern is the occurrence of seven magnitude 5 or greater earthquakes, all within a 50 mile radius, and all within a period of eight years just prior to the 1948 event. This pattern is unique within the historical record of California seismicity and suggests that the effects of high strain accumulation are observable over large areas near this segment of the San Andreas fault. Since this region is the potential site of a great earthquake, there is the likelihood that such a large event may have similar forerunning effects that can be identified.

3. Results using hypocentral locations from the southern California network indicate features in crustal structure defined by boundaries between seismic and aseismic regions. Other spatial geometries are used to identify coherent groups of earthquakes for composite focal mechanism studies. Preliminary analysis of first-motion data in the region that includes the San Bernadino Mountains and San Gorgonio Pass indicates several different types of focal mechanisms are present. The predominant style of faulting appears to be oblique right-lateral strike-slip with a significant thrust component. This component of thrust decreases with increasing focal depth consistent with the increase in vertical stress due to overburden. Several events, however, exhibit left-lateral motion on nearly identical nodal planes. This mixed pattern of seismicity resembles the regional pattern of both left- and right-lateral surface faults.

Reports

Sykes, L. R., and Seeber, L., 1982, Great earthquakes and great asperities along the San Andreas fault, Southern Califoria, EOS, v. 63, no. 45, p. 1030.

Nishenko, S. P., and Sykes, L. R., 1983, Probabilities of occurrence of large plate rupturing earthquakes for the San Andreas, San Jacinto and Imperial Faults, California, 1983-2003, EOS, v. 64, no. 18, p. 258.

Sykes, L. R., and Nishenko, S. P., 1983, Probabilities of occurrence of large plate rupturing earthquakes for the San Andreas, San Jacinto and Imperial Faults, California, 1983-2003, submitted to J. Geophys. Res.

Nicholson, C., Williams, P., Seeber, L., and Sykes, L. R., 1983, San Andreas seismicity and fault tectonics through the Eastern Transverse Ranges, EOS, v. 65.

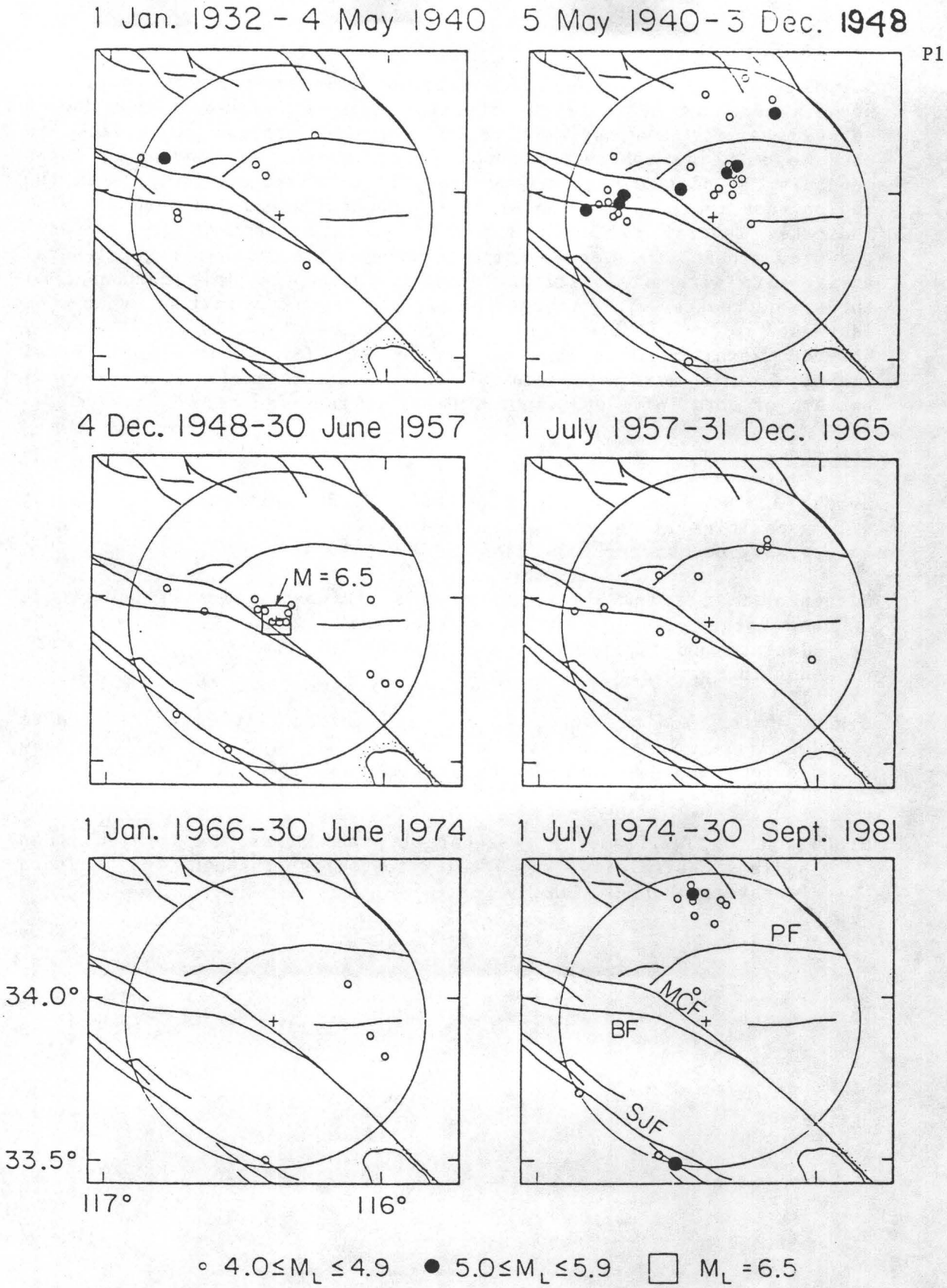

Figure 1. Earthquakes of magnitude larger than 4.0 within 50 km radius of Desert Hot Springs earthquake of 1948, M = 6.5. Data from Caltech catalogue. Note very high level of activity for eight years preceeding 1948 event and much lower levels in other comparable time intervals. Also note that all of long-term forerunning activity is situated to the north of the Banning (BF) and Mission-Creek faults (MCF). PF = Pinto fault. SJF = San Jacinto fault. Quaternary faults from Jennings (1975).

Nearfield Geodetic Investigations of Crustal Movements in Southern California

14-08-0001-21218

Arthur G. Sylvester
Department of Geological Sciences, and
Marine Science Institute
Santa Barbara, California 93106
(805) 961-3156

INVESTIGATIONS

During the past decade we have established and repeatedly surveyed short leveling, trilateration and alignment arrays across several kinds of active and potentially active faults in diverse tectonic regions of California to determine the spatial and temporal nature of nearfield strain accumulation and release, if any, which may be associated with those faults. These investigations are intermediate in scale between the infrequent regional geodetic surveys traditionally done by the National Geodetic Survey and point measurements by continually recording instruments such as creepmeters, borehole tiltmeters and strainmeters. The intermediate scale of this work strongly complements both the regional and point scale studies of many other investigators in California. Thus we have established 38 short leveling arrays ranging in length from 200 m to 2400 m across normal, reverse and strike slip faults. We have 12 small aperture trilateration arrays across faults not being monitored by other investigators; we monitor two alignment arrays and four nail lines. All surveying is done according to First Order standards.

Surveys of most of our leveling arrays are done at least annually, in some cases quarterly. The objective is to document in time and space the vertical movements that occur near different kinds of active faults. For example, our line at San Juan Bautista is across a 15 m high scarp of the San Andreas fault where horizontal creep at each end of the scarp is documented on creepmeters (Sylvester, Brown and Riggs, 1980); level lines in Death Valley and Long Valley are across youthful normal fault scarps; our line at Pallett Creek in the San Andreas fault zone is across the Punchbowl fault, a high-angle reverse, oblique-slip fault; we are monitoring nontectonic subsidence caused by withdrawal of groundwater for irrigation in Fremont Valley near the Garlock fault; the line at Grapevine is across the Pleito thrust fault; we have a level line and small aperture trilateration array across the San Jacinto fault at Anza; the array at Pinyon Flat Geophysical Observatory provides geodetic control for arrays of long-base fluid tiltmeters and other strain measurement instrumentation. We have also run our own set of levels across National Geodetic Survey benchmarks across the San Andreas fault at Palmdale and at Reyes Station. Location and historical data for our leveling arrays are given in Table I.

In addition to these traditional geodetic endeavors, we have 45 dry tilt arrays located mainly along the San Andreas fault between Reyes Station and Cajon Pass and along the southern front of the San Gabriel Mountains to document crustal tilt (Table II). We surveyed those arrays from 6 to 8 times per

year from 1976 to 1981. In 1982 and 1983 they were resurveyed only once each year. In response to the heightened concern over the possibility of a volcanic eruption in the Long Valley area, we established 8 dry tilt arrays in Long Valley to complement 5 arrays established by the Cascades Volcano Observatory in May 1982 to provide documentation of tilt related to domal deformation and earthquakes. These arrays have been resurveyed approximately every other month.

RESULTS

Leveling and trilateration arrays show little or no significant movement across faults during the past year of study. Most height changes among benchmarks are barely above the noise level with notable exceptions described below.

The only vertical fault displacement of probable tectonic origin we have documented in 1982-83 is that on the Hilton Creek fault south of Long Valley caldera in McGee Creek. A resurvey in August 1983 of our 628 m long line of 30 permanent benchmarks shows a small but clear height change across the fault of less than 3 mm relative to the previous survey in August 1982. The time period brackets much seismic activity in the area, including the unusually intense earthquake swarm of January 1983. Thus, we must conclude that tectonic activity has not extended to or affected the Hilton Creek fault south of Long Valley caldera.

We have evidence of minor dynamically-triggered slip on two faults and just as clear evidence that two other faults did not move as a result of moderate earthquakes on other nearby faults. Fresh ground cracks were observed along an unnamed fault 4 km south of Lompoc immediately after shaking associated with the Coalinga earthquake of 2 May 1983 was felt at the site. Shortly afterwards, we resurveyed our leveling array across that fault and found about 2 mm of displacement across some segments of the fault. Following a M 4.9 earthquake in November 1981, 10 km northwest of our line across the Pleito thrust, we found the hanging wall had uplifted 2 mm relative to the footwall. The uplift recovered to datum, however, by June 1983. On the other hand, we were in the process of leveling across the San Jacinto fault at Anza in June 1982 when we felt rather strongly a M 4.9 earthquake located beneath Anza, 3 km south of our array. Careful search of leveling data obtained before, during and 3 days after the earthquake failed to reveal any anomalous height changes. The same is true of our level line in Fish Lake Valley in eastern California where an M 5 earthquake at the north end of the valley failed to have any effect on our line at the south end across the Furnace Creek fault.

Groundwater and associated subsidence effects are seen only in four of our lines. By far the most spectacular is the 35 mm/yr offset we have been monitoring since 1974 across an unnamed fault through Duravan Ranch on the south edge of Fremont Valley, 40 km northeast of Mojave. There the cause is withdrawal of groundwater for irrigation. With dry tilt arrays at Duravan Ranch we have also documented 135 rad/yr tilt of the downdropped block and 68 rad/yr tilt of the relatively uplifted block, both toward the center of subsidence, but not parallel to each other. Over the 5 years of dry tilt measurements, however, the azimuth of tilt of each block varies less than 5

degrees. We have maintained that the 90 mm of height change we have measured progressively across the San Andreas fault at San Juan Bautista is also related to withdrawal of groundwater in San Juan Bautista Valley. During the past year, the height change stopped, perhaps in response to the heavy rainfall and recharge combining to equal withdrawal. At Anza we saw the northeast, upstream fault block uplifted 2 mm relative to the southwest block, evidently as a result of minor recharge of the watertable by the very heavy rains of winter 1982-83. Resurveys in spring and summer show that the uplift has recovered to datum.

Benchmarks located on or very near the most recently active trace of the San Andreas fault at Palmdale and Tejon Pass show unusually large height changes relative to neighboring benchmarks only 20-30 m away. From 1977 to 1979 a benchmark in the Tejon Pass line rose 6 mm; it recovered to datum from 1979 to 1981; then in 1982 it dropped 8 mm; by July 1983 it recovered to datum, but in September 1983 it had begun to drop again. In the Palmdale area, benchmark 0428 of the National Geodetic Survey's array has risen 13 mm since 1978. All other benchmarks of both lines are otherwise motionless. We have no ready explanation for this behavior yet.

Nail lines at San Juan Bautista have slowed to a crawl from rates measured there from 1968 to 1979. The nail line established across the San Andreas fault in 1966 at Cholame continues to show creep of about 1 mm/yr; and a new nail line established across the San Andreas fault in the Carrizo Plain in 1981 shows no change in 1983.

TABLE I. UCSB SHORT LEVEL LINES

LOCATION	LATITUDE	LONGITUDE	QUADRANGLE	INITIAL SURVEY	MOST RECENT SURVEY	TOTAL # SURVEYS
SANTA BARBARA						
Cook	34 25'10"	119 43'00"	Santa Barbara	8/70	8/82	11
Cabrillo	34 22'20"	119 41'25"	Santa Barbara	9/70	6/82	16
Lorinda	34 25'20"	119 43'25"	Santa Barbara	8/70	8/82	7
Castillo Connect	34 25'00"	119 43'25"	Santa Barbara	10/73	8/82	5
Portesuelo	34 25'20"	119 43'35"	Santa Barbara	8/70	8/82	8
Bath	34 24'10"	119 41'40"	Santa Barbara	4/71	8/82	8
Chapala	34 24'50"	119 41'30"	Santa Barbara	4/71	8/82	8
Natoma	34 24'50"	119 41'25"	Santa Barbara	8/70	6/82	8
Castillo	34 24'50"	119 41'35"	Santa Barbara	2/72	8/82	6
Yanonali	34 25'00"	119 41'10"	Santa Barbara	7/70	8/82	8
State	34 24'55"	119 41'55"	Santa Barbara	10/70	8/82	8
SAN ANDREAS FAULT ZONE						
San Juan Bautista	36 50'48"	121 32'00"	San Juan Bautista	9/75	8/83	16
Wallace Creek	35 16'09"	119 49'27"	McKittrick Summit	7/83	7/83	1
Camp Dix	34 57'48"	119 26'41"	Ballinger Canyon	7/82	7/82	1
Caballo	34 52'97"	119 13'02"	Sawmill Mountain	8/82	6/83	2
Mesa Valley	34 48'46"	118 54'20"	Frazier Mtn.	2/77	9/83	16
Una Lake	34 33'00"	118 06'15"	Palmdale	8/79	9/83	4
47th St. East	34 31'03"	118 02'47"	Palmdale	12/76	9/83	12
Big Rock Springs	34 26'04"	117 50'00"	Valyermo	10/80	9/83	8
Pallett Creek	34 25'10"	117 54'00"	Juniper Hills	6/78	6/83	12
Llano	34 31'06"	117 47'53"	Lovejoy Buttes	3/81	6/83	3
Painted Canyon	33 36'15"	116 01'20"	Mecca	9/83	9/83	1
DEATH VALLEY						
Triangle Spring	36 42'40"	117 07'20"	Stovepipe Wells	10/70	4/78	4
Sewage Treatment	36 30'20"	115 52'25"	Chloride Cliff	10/70	9/74	4
Artists Drive	36 25'00"	116 51'00"	Furnace Creek	4/70	4/78	8
Hanaupah	36 14'05"	116 53'00"	Bennett's Well	10/70	4/78	7
Fish Lake Valley	37 24'28"	117 51'47"	Soldier Pass	9/71	10/82	5
SAN JACINTO FAULT ZONE						
Pinyon Flat	33 35'00"	116 26'00"	Palm Desert	10/79	8/83	12
Anza	34 35'00"	116 39'35"	Idyllwild	1/81	9/83	16
TRANSVERSE RANGES						
JM Quarry	34 36'30"	120 26'44"	Lompoc Hills	8/81	9/83	6
Juncal	34 29'00"	119 30'15"	Carpinteria	8/70	8/80	7
Grapevine	34 55'30"	118 55'30"	Grapevine	7/79	5/83	7
San Fernando	34 18'03"	118 25'35"	San Fernando	2/71	12/76	9
Dalton Canyon	34 10'09"	117 48'04"	Glendora	6/81	6/83	7
LONG VALLEY						
McGee Creek	37 33'39"	118 47'08"	Mt. Morrison	7/82	8/83	3
MOJAVE DESERT						
SNORT	35 44'52"	117 45'00"	Ridgecrest North	7/83	9/83	2
Airport	35 42'41"	117 43'16"	Ridgecrest North	7/83	7/83	2
Duravan	35 17'05"	117 53'25"	Cantil	9/74	9/83	13

TABLE II. UCSB DRY TILT ARRAYS

NAME	MAP#	LATITUDE	LONGITUDE	QUADRANGLE	ESTABLISH DATE	INITIAL SURVEY	MOST RECENT SURVEY	TOTAL SURVEYS
UCSB	1	35 24'54"	119 50'10"	Goleta	12/76	4/77	6/83	39
Jeffrey Pine Flat	2	34 48'26"	119 06'08"	Cuddy Valley	10/76	4/77	6/83	22
Cuddy Flat	3	34 50'25"	118 59'51"	Frazier Mountain	11/76	4/77	6/83	26
Hungry Valley	4	34 44'15"	118 52'05"	Black Mountain	10/76	2/77	9/83	27
Oso Pumping Station	5	34 48'44"	118 42'50"	La Liebre Ranch	12/76	4/77	9/83	19
Sawmill	6	34 41'52"	118 34'08"	Burnt Peak	11/76	3/77	9/83	25
Rye Canyon Road	7	34 25'30"	118 35'08"	Newhall	11/76	1/77	9/83	30
Drinkwater Flat	8	34 34'06"	118 27'49"	Green Valley	4/77	5/77	9/83	23
Indian Springs	9	34 42'12"	118 42'12"	Lake Hughes	11/76	4/77	9/83	25
Elizabeth Lake	10	34 40'03"	118 22'54"	Lake Hughes	11/76	4/77	11/80	28
Live Oak	11	34 22'45"	118 24'06"	Mint Canyon	12/76	1/77	9/83	35
Wentworth	12	34 15'29"	118 22'22"	Sunland	12/76	3/77	9/83	34
Escondido	13	34 30'00"	118 15'20"	Agua Dulce	8/77	8/77	9/83	22
Rose Bowl	14	34 09'25"	118 10'05"	Pasadena	12/76	3/77	9/83	34
Ave 25 East	15	34 33'21"	118 05'04"	Palmdale	11/76	1/77	9/83	34
Pearblossum Cutoff	16	34 31'21"	118 05'45"	Palmdale	11/76	1/77	9/83	34
Soledad Pass	17	34 29'59"	118 07'08"	Pacifico Mountain	11/76	1/77	9/83	35
90th St. East	19	34 39'58"	117 58'05"	Littlerock	3/77	4/77	6/83	32
Longview	20	34 27'23"	117 54'02"	Juniper Hills	7/77	7/77	9/83	31
Azusa*	21	34 09'41"	117 54'04"	Azusa	7/77	8/77	9/80	19
Aerojet	22	34 07'38"	117 55'38"	Azusa	7/77	8/77	9/83	26
Saddleback Butte	23	34 48'00"	117 41'30"	Hi Vista	12/76	3/77	6/83	33
Largo Vista	24	34 27'13"	117 45'55"	Valyermo	11/76	1/77	9/83	35
Blue Ridge*	25	34 22'27"	117 41'20"	Mt. San Antonio	7/77	7/77	8/82	18
Upper Cajon Creek	26	34 22'36"	117 34'06"	Phelan	11/76	1/77	6/83	28
Cucamonga South	27	34 09'44"	117 31'05"	Cucamonga Peak	6/77	8/77	9/83	22
Cucamonga North*	32	34 10'28"	117 32'11"	Cucamonga Peak	6/77	7/78	9/80	11
Cima Mesa	34	34 27'50"	117 57'30"	Juniper Hills	1/78	1/78	9/83	33
Murphy Lane	36	34 26'02"	117 54'00"	Juniper Hills	1/78	3/78	9/83	31
Punchbowl Park	37	34 25'07"	117 57'30"	Juniper Hills	1/78	3/78	9/83	32
VABM Ward	38	34 27'50"	117 57'30"	Juniper Hills	1/78	4/78	9/83	30
Buck Canyon*	39	34 20'26"	118 19'48"	Sunland	2/78	4/78	8/81	24
Wilson Canyon	40	34 27'11"	118 20'38"	San Fernando	2/78	3/78	9/83	26
Barrel Springs	41	34 32'16"	118 04'58"	Palmdale	5/78	6/78	9/83	23
Llano	42	34 29'50"	117 50'00"	Valyermo	5/78	6/78	6/83	28
Lone Tree	43	34 18'19"	117 30'29"	Telegraph Peak	5/78	6/78	9/83	15
Lovejoy	44	34 35'11"	117 48'24"	Lovejoy Buttes	5/78	6/78	6/83	20
Sheep Creek	45	34 21'36"	117 36'13"	Telegraph Peak	5/78	6/78	6/83	16
Old Lady	49	35 17'13"	117 53'24"	Cantil	4/78	8/78	8/83	6
Honeycup	50	35 17'06"	117 53'17"	Cantil	4/78	8/78	8/83	6
Kentucky Springs	52	34 26'24"	118 06'07"	Pacifico Mountain	12/78	1/79	6/83	13
Cowhead Potrero	53	34 52'30"	119 17'25"	Apache Canyon	12/78	4/79	6/83	15
Mill Potrero	54	34 51'00"	119 11'07"	Sawmill Mountain	12/78	4/79	6/83	14
Penny Pines	55	34 50'04"	119 05'14"	Cuddy Valley	12/78	4/79	6/83	15
Quail	56	34 45'29"	118 47'36"	Lebec	12/78	4/79	9/83	11
Baughman Spring	57	34 22'00"	118 06'19"	Chilao Flat	12/76	3/77	6/83	24
Pinyon Flat East	58	33 35'00"	116 26'00"	Palm Desert	9/79	9/79	8/81	8
Pinyon Flat West	59	33 35'00"	116 26'00"	Palm Desert	9/79	9/79	8/81	6

*Array destroyed, site abandoned

Crustal Deformation Observatory, Part B: Precise Leveling

#14-08-001-21234

Arthur G. Sylvester
Department of Geological Sciences, and
Marine Science Institute
University of California
Santa Barbara, California 93107
(805) 961-3156

Investigations

Two complete and one partial resurveys were done of the leveling array at Pinyon Flat Geophysical Observatory in 1982-83. Ties were made among benchmarks on piers of UCSD and LDGO long-base fluid tiltmeters as well as NASA benchmarks.

Results

Changes in heights of benchmarks did not exceed 1 mm in any of the surveys; most were less than 0.4 mm, and between tiltmeters the height change did not exceed 0.2 mm. A comprehensive statistical and correlation analysis is in progress by Dr. D. D. Jackson under another contract.

Earthquake Hazard Research in the Greater Los Angeles Basin and its Offshore Area

14-08-0001-21224

Ta-liang Teng and Thomas L. Henyey
Center for Earth Sciences
University of Southern California
Los Angeles, CA 90089-0741
(213) 743-6124

Investigations

Continued seismic monitoring of the greater Los Angeles basin area has two principal objectives:

1) Investigating relationships between microearthquakes and oil field operations (principally water flooding), and

2) Compiling earthquake statistics for coastal zone faults, principally the Newport-Inglewood, Palos Verdes, and Santa Monica-Malibu Coast faults.

Results

The University of Southern California has monitored seismicity in the Los Angeles Basin since 1971 with particular attention to the activities associated with oil exploration. However, because of unknowns in the velocity structure and noise problems in the urban environment it is often difficult to determine locations with the precision needed to identify the causal faults.

In a Ph.D. dissertation by Ken Piper, we are currently finishing a study of the three-dimensional velocity structure of the Los Angeles basin and to make use of that revised structure in the relocation of all earthquakes during the past decade. By doing so, it is hoped that an improvement in the hypocentral determination of these earthquakes will aid in the identification of the involved faults and thus help in the evaluation of seismic risk analysis.

At present, the method used to locate earthquakes in the Los Angeles basin and for most other local networks assumes a flat layered structure with seismic velocity varying only in the vertical direction. Because the velocity most often varies laterally, the assumption of lateral homogeneity leads to systematic errors in earthquake hypocenter location. For example, a seismometer located on rocks with relatively high seismic velocity will have an arrival time which is earlier than would be expected by assuming lateral homogeneity. In order to minimize station residuals, the location program will place the hypocenter closer to such a station, resulting in a systematic error. Similarly, hypocenters will be "pushed" away from stations which receive signals through rocks with relatively slow seismic velocity.

The use of station delays is the current technique to correct for this error by simply adding to or subtracting from the observed arrival times at each station. If all of the anomalous velocity were localized in the immediate vicinity of the station, the solution to the problem would have been

quite simple. However, velocity anomalies may also arise elsewhere along the ray path that are not so easily accounted for.

Several attempts have been made to resolve these problems. For example, a simple scheme used by McElrath and Teng (1980) applies a station delay which is a function of azimuth and distance from a given event. This was used in a relocation of events in the Los Angeles basin. An inherent weakness with this approach is that it assumes lateral velocity anomalies are constant as a function of depth. Another problem is that because of uneven distribution of earthquakes and stations, large areas are poorly constrained.

This new study is divided into two parts. In the first part, explosion data is used to invert for an improved velocity structure of southern California and the borderland. Then, in the second part, the velocity structure obtained in the southern California inversion is used as a starting point for a simultaneous inversion for velocity structure and improved earthquake locations within the Los Angeles basin.

In order to make use of available explosion data in improving the seismic velocity structure of the Los Angeles basin and surrounding areas, the program SIMUL 3B (Thurber, 1981) is being modified to allow its use in a larger area. The approximate ray tracing routine used by Thurber in the original program is not applicable for ray paths longer than a few tens of kilometers (Thurber, personal communication, 1983). Instead, a routine designed by R. Comer is being substituted and other necessary modifications are being made.

In order to study the three-dimensional seismic velocity structure of southern California, P-wave arrival times from known explosion sources within the area have been compiled. Simultaneous inversion as used in this work is a method for determining both the hypocentral parameters of a set of local earthquakes and the seismic velocity structure of the earth in the vicinity of the seismic array. This differs from a standard earthquake location program which uses an assumed velocity structure and inverts simply for the hypocentral parameters (location and origin time). It also differs from three-dimensional velocity inversions which use teleseismic data (e.g. Aki et al., 1977), or explosion data as described above. The steps involved in simultaneous inversion are similar to those in an iterative earthquake location program.

In order to determine a more precise velocity model for the Los Angeles basin, the program SIMUL 3B (Thurber, 1981) is being applied to Los Angeles area earthquake data for the period 1973 to 1982.

To study the three-dimensional seismic velocity structure of the Los Angeles basin, P-wave arrival times from local earthquakes and one explosion have been compiled. The earthquakes were chosen from the earthquake list of the University of Southern California for the period 1973 to 1982. Only events with eight or more P-wave arrivals were chosen. The earthquakes were carefully relocated using the standard location program HYPO 71R (Lee and Lahr, 1975). In order to assure high quality of chosen events, the list was further culled to eliminate questionable loctations. We expect to complete this 3-D inversoin and relocation study during this contract year. The result will be a comprehensive analysis of the structure and seismicity of the Los Angeles basin.

GEODETIC MODELING AND MONITORING

9960-01488

Wayne Thatcher
Branch of Tectonophysics
U.S. Geological Survey
345 Middlefield Road, MS/77
Menlo Park, California 94025
(415) 323-8111, ext. 2120

Investigations

Analysis and interpretation of repeated geodetic survey measurements relevant to earthquake-related deformation processes operative at or near major plate boundaries. Principal recent activities have been:

1. The viscoelastic coupling effects on repeated earthquakes at subduction zones is critically compared to postearthquake effects due to transient aseismic slip, in light of the geodetic record of great earthquakes and interseismic strain accumulation.

2. A multi-disciplinary analysis of the coseismic and Quaternary deformation at the site of the 2 May 1983 Coalinga, California earthquake was conducted to model the seismic fault geometry and slip, the long-term fault slip rate, and the earthquake repeat time.

Results

1. Vertical displacements due to periodic reverse faulting events in an elastic plate overlying a viscoelastic (Maxwell) half-space are obtained and compared with the observed deformation cycle (coseismic strain release, postseismic transients, interseismic strain accumulation) from Japan. The viscoelastic effects, including the influence of buoyant restoring forces, are obtained using the method developed by Rundle, and plate convergence by Savage. The resulting deformation cycle is compared with that of an analogous elastic half-space dislocation model in which postearthquake effects are due to transient aseismic slip below the coseismic fault.

   Cyclic deformation is similar but not identical for the two models, and observations from southwest Japan suggest the superiority of the viscoelastic coupling model. In particular, inclusion of the effects of steady-state flow in the asthenosphere overcomes a defect of the elastic

half-space model and results in agreement with the observed interseismic movement pattern. Several aspects of the postseismic deformation, its landward migration, and its transition to the interseismic phase of the cycle are explained as well, but the short duration of near-trench transients relative to those observed farther inland is not matched. The success of a buried slip model in explaining early postseismic near-trench movements and asthenospheric flow in accounting for cumulative postearthquake transient motions suggests the existence of a transition zone between lithosphere and asthenosphere whose behavior is brittle/elastic in the short-term and ductile for longer term deformation, and such a modification may reconcile remaining discordant observations. However, reasonable variations in coupling model parameters cannot account for observed differences in the deformation cycle in other parts of Japan and these regional differences remain unexplained. (W. Thatcher and J. Rundle)

2. The Coalinga earthquake (M_L = 6.2-6.7) uplifted Anticline Ridge one half meter, but caused no fault rupture at the ground surface, demonstrating that folding and faulting of the eastern margin of the California Coast Ranges are coincident and continuing. Elevation changes associated with the earthquake enable an estimate of the fault attitude, geometry, and slip. Small topographic relief over the route minimizes systematic leveling errors. Artificial subsidence due to fluid withdrawal is more significant, although it is still small in relation to the earthquake changes. Deep-well compaction monitors and the record of fluid pumping are used to remove the subsidence. A steeply dipping reverse fault is well fit by the geodetic and seismic data, whereas a gently dipping thrust fault is less compatible with the location and depth of the mainshock. For a N53°W strike and a 67°NE dip, the best-fit earthquake parameters are: 1.8±0.5 m of dominantly reverse dip slip on a fault extending from a depth of 10-13 km to within 3-5 km from the ground; M_o = 6.7 x 10^{25} dyne-cm. The deformation caused by the 1983 earthquake looks strikingly like the present-day topographic form of Anticline Ridge. About 2 km of cumulative buried fault slip during the last million years would account for this similarity.

   The beds and terraces of two antecedent streams are uplifted where they cross the anticline. In one place a ^{14}C date indicates that an uplift of about 10 m has occurred within a period of 2,500 years. A repeat time of about 350 years for the Coalinga event can be determined from the uplifted terrace and the ^{14}C data. Much of the topography of Anticline Ridge is late-Pleistocene and this

provides a second method of estimating recurrence periods. On this basis a longer period of 1,000 years is estimated. The form of the observed uplift differs in some respects from that to be expected from many repetitions of the Coalinga event, suggesting that other deformation processes occur; a shallow angle, southwest dipping fault is hypothesized. The presence of such a structure is supported by the reflection data in the Kettleman Hills to the south of the epicentral area. Although the observations in this work are restricted to the epicentral region of the Coalinga earthquake, it is apparent that the structures of the northwestern Diablo Range front have developed by earthquake-related folding. (R. Stein and G. King)

Reports

Thatcher, W., and J. B. Rundle, 1984, A viscoelastic coupling model for the cyclic deformation due to periodically repeated earthquakes at suduction zones, J. Geophys. Res., submitted.

Thatcher, W. and N. Fujita, 1983, Deformation of the Mikita Rhombus: Strain buildup following the 1923 Kanto earthquake, Central Honshu, Japan, ibid, in press.

Thatcher, W., 1983, The earthquake deformation cycle, recurrence, and the time predictable model, ibid, in press.

Stein, R. S., 1983, Reverse slip on a buried fault during the 2 May 1983 Coalinga earthquake: Evidence from Geodetic elevation changes, The 1983 Coalinga, California Earthquake: California Div. Mines & Geol. Spec. Pub. 66.

King, G. and R. S. Stein, 1983, Surface folding, river terrace deformation rate and earthquake repeat time in a reverse faulting environment: The Coalinga, California earthquake of May 2, 1983, ibid.

McTigue, D. F., and R. S. Stein, Topographic amplification of tectonic displacement: Implications for geodetic measurement of strain changes, J. Geophys. Res., in press.

Abstracts

Thatcher, W., 1983, Geodetic measurement of active tectonic processes, EOS, 65, in press.

Thatcher, W., 1983, Earthquake deformation cycle, recurrence an the time predictable model, ibid.

Stein, R. S., 1983, The 2 May 1983 Coalinga Earthquake: Evidence for reverse slip on a buried fault from geodetic elevation changes, ibid.

King, G. and R. S. Stein, 1983, Surface folding, river terrace deformation rate and earthquake repeat time: The Coalinga, California, Earthquake of May, 1983, ibid.

Stein, R. S., 1983, Historical vertical deformation in southern California: Removal of systematic errors in geodetic leveling, Canadian Geophys. Union Annual Meeting, Program with abstracts, 8.

Stein, R. S., 1983, Implications of off-fault aftershocks for pre-earthquake stress, ibid.

Data Processing Center Operations

9930-01499

John Van Schaack
Branch of Seismology
U. S. Geological Survey
345 Middlefield Road MS/77
Menlo Park, California 94025
(415) 323-8111, ext. 2584

Investigations

This project has the general housekeeping, maintenance and management authority over the Earthquake Prediction Data Processing Center. Its specific responsibilities include:

1. Day to day operation and performance quality assurance of 5 network magnetic tape recorders.
2. Day to day management, operation, maintenance, and performance quality assurance of 2 analog tape playback stations.
3. Day to day management, operation, maintenance and performance quality assurance of the U.S.G.S. telemetered seismic network event library tape dubbing facility (for California, Alaska, Hawaii, and Oregon).
4. Projection of usage of critical supplies, replacement parts, etc., maintenance of accurate inventories of supplies and parts on hand, uninterrupted operation of the Data Processing Center.

Results

Procedures and staff for fulfilling assigned responsibilities have been developed, and the Data Processing Center is operating smoothly and serving a large variety of scientific user projects.

Field Experiment Operations

9930-01170

John Van Schaack
Branch of Seismology
U. S. Geological Survey
345 Middlefield Road MS/77
Menlo Park, California 94025
(415) 323-8111, ext. 2584

Investigations

This project performs a broad range of managment, maintenance, field operation, and record keeping task in support of seismology and tectonophysics networks and field experiments. Seismic field systems that it maintains in a state of readiness and deploys and operates in the field (in cooperation with user projects) include:

a. 5-day recorder portable seismic systems.
b. Smoked paper-recorder portable seismic systems.
c. "Cassette" seismic refraction trucks.
d. Portable digital event recorders.

This project is responsible for obtaining the required permits from private landowners and public agencies for installation and operation of network sensors and for the conduct of a variety of field experiments including seismic refraction profiling aftershock recording, teleseism P-delay studies, volcano monitoring, etc.

This project also has the responsibility for managing all radio telemetry frequency authorizations for the Office of Earthquakes, Volcanoes and Engineering and its contractors.

Results

Seismic Refraction. Three experiments were conducted using 120 seismic cassette recorders. The first experiment consisted of two reversed profiles running North-South and East-West through the Coalinga California earthquake epicenter region. The second experiment was carried out in the Long Valley Caldera area of California . It consisted of 12 shots fired in a series of profiles and fan spreads. The third experiment was carried out in the area of Newberry Crater, Oregon and consisted of 10 shots in 2 reversed East West profiles.

Telemetry Networks. Modifications were made to the Southern Oregon Net which allows signals to be recorded at Oregon State University and at Menlo Park, Caliornia. Modifications were made to the Mammoth Lakes Net to increase reliability and improve coverage. Work has begun on installing a backbone microwave data network extending from Mt. Tamalpais to Paso Robles.

Portable Network. Fifteen 5-day records were operated for about 1 month recording aftershocks of the Coalinga earthquake of May 2, 1983. Five 5-day recorders were diployed for two series of aftershocks of earthquakes near Valdez Alaska in July and September.

Earthquake Process
9930-03483

Robert L. Wesson
Branch of Seismology
U.S. Geological Survey
922 National Center
Reston, Virginia 22092
415/860-7481

Investigations

1. Analysis of theoretical and numerical models of the processes active in fault zones leading to large earthquakes.

2. Analysis of seismological and other geophysical data pertinent to the understanding of the processes leading to large earthquakes.

Results

1. A computer program has been developed and debugged to calculate the displacements, strains and stresses at any location in an elastic half-space surrounding a buried or unburied, dipping rectangular fault. The program follows the formulation of Mansinha and Smylie (1971) for the displacements and numerical differentiation to obtain strains and stresses. In collaboration with Mark Zoback, this program has been used to interpret in-situ stress measurements in a 600 m deep borehole drilled through the Cleveland Hills Fault as reflecting a coseismic stress change causd by the M_L = 5.7 Oroville earthquake. Hydraulic fracturing measurements of the least principal horizontal compressive stress in the well show a linear increase with depth, reaching about 160 bars at a depth of 600 m. However, the measured values of the least principal stress deviates by about + 20 bars from this trend in the interval immediately above the fault zone, and about -25 bars immediately beneath the fault zone. Stress changes were calculated for plausible distributions of slip on the fault. Fault dip was constained to be 50-60°, in accord with fault plane solutions and the distribution of aftershocks. Previous wave-form modelling results suggest an average slip during the main shock of about 200 mm, but the maximum slip observed at the surface was les than 60 mm. Calculations are highly dependent upon the manner in which the fault slip tapers from a mean value to that measured at the surface. However, the observed least principal stress deviations can be explained by models of faulting in which the slip decreases from the average value of 20 cm at a down-dip depth of 0.5-2 km to the observed value at the surface.

2. Numerical techniques have been developed to calculate the time-dependent displacement on an infinite strike-slip fault which has experienced a uniform slip along an infinite strip at $t = 0$, assuming any desired transient creep law to characterize the

rheological behavior of the fault zone. The methods are based on the formulation of Ida (1974) and utilize the numerical evaluation of Hilbert transforms using the method of subtracting the singularity (Davis and Rabinowitz 1967) and numerical quadrature. Calculations have been made using viscous and quasi-plastic flow laws. Good agreement between calculations and observations of afterslip and the expansion of the aftershock zone of the 1972 San Juan Bautista, California, earthquake have been obtained.

3. Observations of aftershocks and afterslip following moderate earthquakes in California support a conceptual model of an active fault in which significant earthquakes represent the breaking of lock points or asperities; incontrast, afterslip represents continuing and spreading slip controlled by the time-dependent reheology of the surrounding fault zone. Aftershocks are caused by the breakage or slippage of minor asperities. The afterslip process controls the rate of occurrence of aftershocks and the growth of aftershock zones. The presence within the surrounding fault zone of additional siginificant lock points limits or retards the growth of aftershock zones and retards development of afterslip. Lock points may represent the ends of individual fault segments, other geometric irregularities, or areas of high effective strength. Distant from, or in the absence of lock points, the growth of aftershock zones and afterslip proceed t an initially high rate which decays with time. Numerical simulations of these phenomena, based on dislocation theory and assuming a distribution of lock points surrounded by a fault zone characterized by a quasi-plastic or other time-dependent relaxation rehology, are in good agreement with observations. Aftershock sequences studied include those of the 1966 Parkfield, 1968-1969 Borrego Mountain-Coyote Mounain, 1971 San Fernando, 1971-1973 Bear Valley-San Juan Bautista, 1974 Bush fault, 1975 Oroville, 1979 Coyote Lake, 1979 Imperial Valley and 1980 Livermore earthquakes.

4. Analyses of travel-time from explosions in the vicinity of the 1971 San Fernando, California, earthquake and of the detailed space-time behavior of the aftershocks of the earthquake are nearing completion.

References

Davis, P.J. and P. Rabinowitz, 1967, Numerical Intergration: Waltham, Massachusetts. Blaisdell Publishing Company, 230 p.

Ida, Y., 1974, Slow-moving deformation pulses along tectonic faults: Phys. Earth Planet. Interiors, v. 9, p. 328-337.

Mansinha, L., and D.E. Smylie, 1971, The displacement fields of inclined faults, Bull. Seismol. Soc. Am., v. 61, p. 1433-1440.

Reports

Wesson, R.L., 1983 Physical processes responsible for successive earthquakes [abs]: SSA Annual Meeting, May 2-4, 1983, Salt Lake City, Utah.

Wesson, R.L., 1983, Aftershocks and afterslip, [abs]: AGU Fall Meeting, San Francisco, California.

Wesson, R.L. and R.E. Wallace, in press, Preparing for the next great earthquake in California, Scientific American.

Zoback, M., and R.L. Wesson, 1983, Modelling of coseismic stress changes associated with the 1975 Oroville earthquake [abs]: AGU Fall Meeting, San Francisco, California.

CENTRAL AMERICAN SEISMICITY AND HAZARDS

9930-01163

Randall A. White
David H. Harlow
Branch of Seismology
U. S. Geological Survey
345 Middlefield Road, MS 77
Menlo Park, CA 94025
(415) 323-8111, x 2570

Investigations

The long-term goal of this project is to study and evaluate the risk in northern Central America from earthquakes (displacements, shaking, and liquifaction) and from the many active volcanoes, and to obtain pertinent geophysical observations that may be useful for the prediction of damaging earthquakes or eruptions at analogous tectonic settings within the United States.

1. Begin the first phase of a cooperative effort between the USGS and the Guatemalan geophysical observatory (INSIVUMEH), titled Cooperative Investigations in Earthquake Hazard Reduction in Guatemala.

2. Begin the first phase of a cooperative effort between the USGS and the geophysical observatory of El Salvador (CIG), titled Cooperative Investigations in Earthquake Hazard Reduction in El Salvador.

Results

1. The facilities at the Guatemalan geophysical observatory (INSIVUMEH) were inspected during July and August 1983. About 1/2 of the 25 seismic stations that compose the Guatemala National Seismic Network were inspected in the field. Recommendations for extensive equipment purchases for the renovation and expansion of the network were worked out with INSIVUMEH personnel. The daily data reduction routine for calculating epicenter locations was analysed, recommendations were made, several days of training were given, with the immediate result being the reduction in the turnaround time from a few months to a few days. Completeness of the catalog for the first half of 1983 was found to be excellent for the interior of the country where the vast majority of the population lives. The formation of a national committee on seismic hazards and seismic engineering was begun. Three Guatemalan technicians and two junior scientists were identified for further training at USGS facilities on the installation and maintainance of standard seismic and strong motion stations, and graduate level seismology respectively.

2. The facilities at the geophysical observatory of El Salvador (CIG) were inspected during October 1983. Three existing low-gain Weicherts seismographs were inspected and recommendations were made for their renovation, establishment of coordinated universal time and a back-up power system. The 20 seismic stations purchased in 1979 (but never installed by the vendor because of political turmoil) were inspected and determined to be of appropriate design for the environment, and six of these stations were subsequently installed. Recommendations for equipment purchases for the expansion of the network were worked out with CIG personnel. The daily data reduction routine for calculating epicenter locations was established, several days of training were given, and a catalog of micro-seismicity was begun for the interior of the country where the most of the population lives. The formation of a national committee on seismic hazards and seismic engineering was begun. Two El Salvadorean technicians and one scientist were identified for further training at USGS facilities, on the installation and maintainance of standard seismic and strong motion stations, and graduate level seismology respectively.

3. Analysis of intensity data and newly discovered Weicherts seismograms from Guatemala City for the 1942 Guatemala Earthquake (Ms = 7.9) show that the earthquake rupture zone, as determined from both the area of greatest damage and the area of aftershocks (revised locations), is considerably different from previous estimates. The rupture zone was centered about 80 km west of Guatemala City, not 80 km south. Taken together with other historical data for subduction zone earthquakes along the Pacific coast of northern Central America, the relocation of the 1942 earthquake implies that the previous location of the 1942 earthquake, ie Escuintla province, should now be reconsidered as the site of greatest potential for a Ms = 8+ earthquake in Guatemala.

4. Identification of harmonic tremor and increased fumarolic activity at Fuego Volcano in Guatemala have prompted the forecast of a major eruption for late 1983 or 1984. Harmonic tremor of the magnitude currently being observed has not occurred since the most recent major eruption of Fuego Volcano in 1974. Small ash eruptions have been occurring sporadically since then.

Cooperative Earthquake Prediction Research with Institute of Geophysics & Center for Analysis & Prediction of Earthquakes, SSB, PRC

14-008-0001-19860
14-008-0001-21341

Francis T. Wu
Department of Geological Sciences
State University of New York
Binghamton, New York 13901
(607) 798-2512

Ta-liang Teng
Department of Geological Sciences
University of Southern California
Los Angeles, California 90008

Investigations

1. Updating and automation of Beijing Seismic Network.
2. Installation of water well level sensors in four wells in Beijing Area.
3. Analysis of water well level and short baseline survey data before and after the 1976 Tangshan earthquake.

Results

1. The first stage of hardware development and installation for the Beijing network have been completed. All together 15 sets of RF (230 mHa) transmiters and receivers (manufactured by Monitorn (2 sets) and (13 sets) have been provided through this contract. The VCO/ amplifiers designs were also provided through this contract to the Institute of Geophysics, SSB, units have been manufactured there for use in the automated processing of network data. The Institute has now expanded the network to 33 stations from 20, including down hole stations in the Plain. A number of additional stations have been installed but are awaiting phone lines for transmission to Beijing telemetering network center. USGS personnel will install on-line seismic monitoring system in October, 1983. Analysis of first batch of network data is planned for late Spring, 1984 by the PI's and a graduate student.
2. Four water level sensors and 4 1/2 digit printing recording system have been designed, manufactured and installed (September, 1983) in four areas around Beijing (see figure 1). All wells record earth tides clearly. At the deepest wells (Gaochung) response of water level to a wide excitation frequency band - from seismic (.5 Hz - .01 Hz), earth tides to atmospheric pressure - has been noted from previous records. Some improvement in timing system is to be incorporated in the near future such that the phase of various signals can be accurately determined.

2. Kalman filter has been applied to the study of 17 water well level records in the Beijing-Tianjin area before and after the 1976 Tangshan earthquake. As figure 2 shows, residual well level fluctuations (subtracting predicted level from the observed level) became noticeable two years before the earthquake for six brackish water wells in Tianjin area while before that period, the residual levels remained stable. For 17 wells in the vicinity of Beijing though, only slight variations in one well were detected; other fluctuations closely related to rainfalls can be clearly discerned. The results will be published shortly in the Proceedings of a meeting held in Beijing in 1982.

Reports

Wu, F.T., Han, D.Y., and Zheng, Z.Z., Filtration of short baseline and water level data before and after the Tayhan Earthquake. Proc. of ISSEP, Beijing, to be published in late 1983.

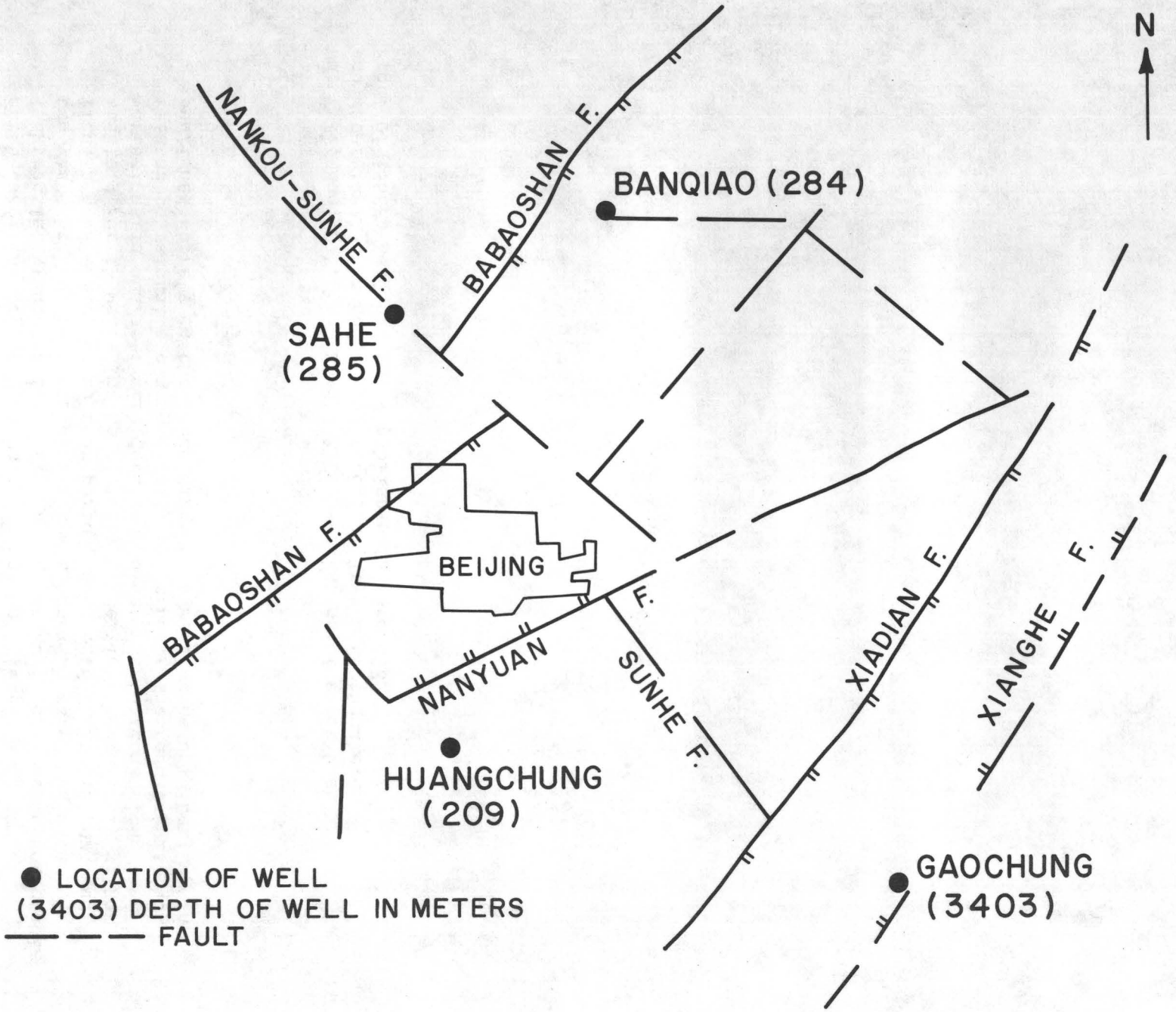
N
NANKOU-SUNHE F.
BABAOSHAN F.
BANQIAO (284)
SAHE
(285)
BABAOSHAN F.
BEIJING
F.
NANYUAN
SUNHE F.
XIADIAN F.
XIANGHE F.
HUANGCHUNG
(209)
GAOCHUNG
(3403)
● LOCATION OF WELL
(3403) DEPTH OF WELL IN METERS
— — — FAULT

Figure 1

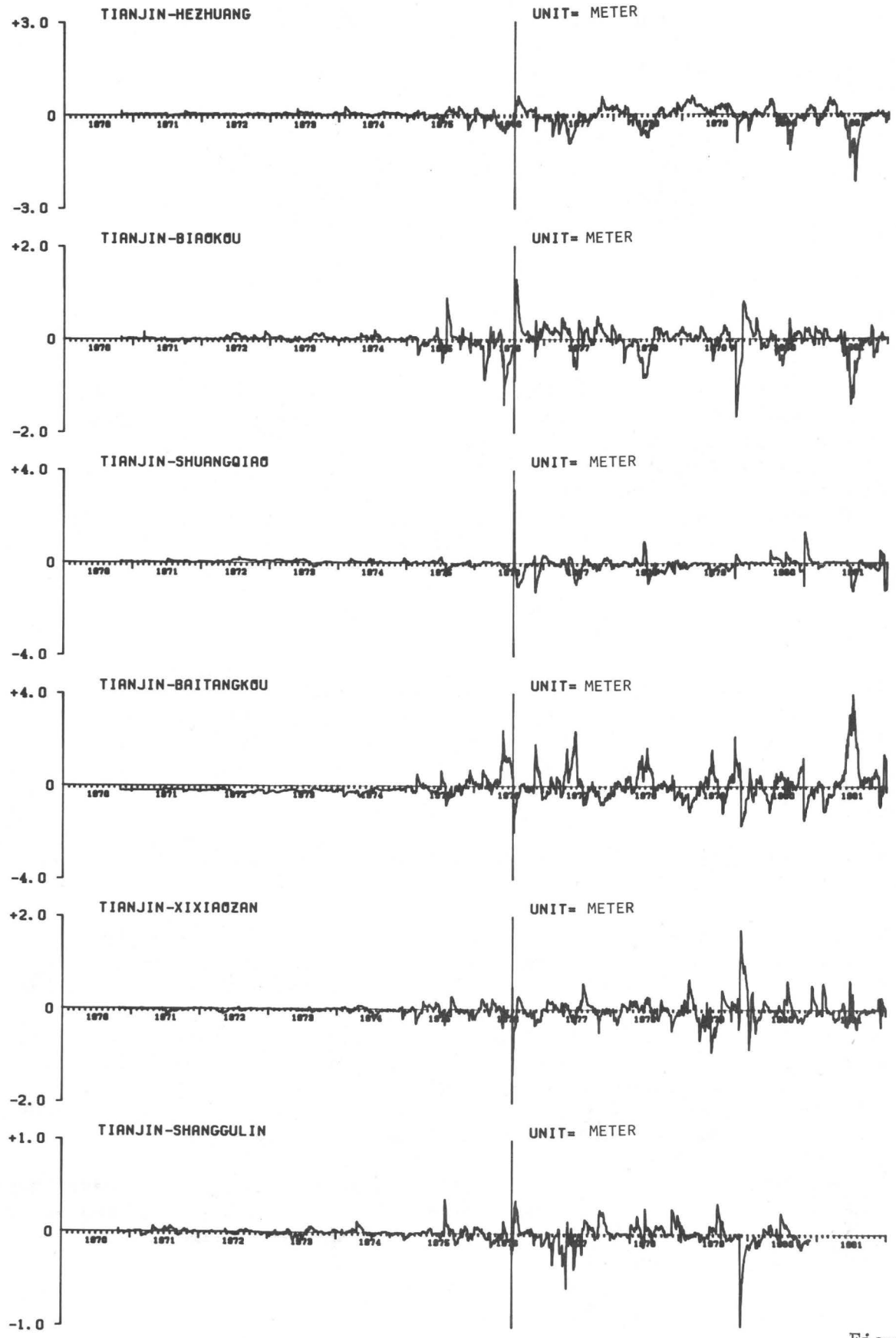
TIANJIN-HEZHUANG
UNIT= METER
+3.0
0
-3.0
TIANJIN-BIAOKOU
UNIT= METER
+2.0
0
-2.0
TIANJIN-SHUANGQIAO
UNIT= METER
+4.0
0
-4.0
TIANJIN-BAITANGKOU
UNIT= METER
+4.0
0
-4.0
TIANJIN-XIXIAOZAN
UNIT= METER
+2.0
0
-2.0
TIANJIN-SHANGGULIN
UNIT= METER
+1.0
0
-1.0

Figure 2

Crustal Deformation Observatory
Part D

14-08-0001-21254

Frank Wyatt, Duncan Carr Agnew, Jonathan Berger
Institute of Geophysics & Planetary Physics
Scripps Institution of Oceanography
University of California, San Diego
La Jolla, CA 92093
(619) 452-2019

Investigations

This report covers the six-month period from November 1982 through April 1983. The purpose of this contract is to provide research coordination, operational support, data recording, and preliminary data analysis for the investigators participating in the Crustal Deformation Observatory (CDO) program at Piñon Flat Observatory. The CDO program is a cooperative effort, designed to evaluate existing and proposed instrumentation for measuring very long period ground deformation in an area of ongoing tectonic activity.

Results

CDO Program:

1. Cambridge University. The 535 m long differential-pressure tiltmeter required very little attention in this period, although higher frequency noise (.1-.2 μrad at periods of an hour) has increasingly obscured the tidal quality records. We believe that much of this noise is due to environmental effects. Tim Owen intends to modify the instrument to attenuate the undesirable temperature sensitivity of .35 μrad/°C.

2. CIRES. Although progress has been made, the initial measurements from this two-fluid differential tiltmeter have yet to be recorded.

3. Lamont-Doherty Geological Observatory. Beginning in November 1982, a number of substantial changes were made to this equipotential fluid tiltmeter by Roger Bilham and John Beavan of L-DGO. New displacement transducers were added to the end-point-monitoring vertical strainmeters, the entire electronics assembly reworked, optical length modulators introduced, new lasers installed, and, finally, a secondary absolute tilt sensor added. The absolute measurement is based on monitoring the differential fluid height using manually read micrometers. The result of this work has been a highly accurate tiltmeter capable of running for many weeks without adjustment.

4. University of California, Los Angeles. Under the direction of Dave Jackson, Calum Macdonald has edited the past 1.5 years of observations produced by the CDO project. These results have served to identify the needed improvements in the existing instrumentation.

5. University of California, Santa Barbara. In December 1982, the array of benchmarks at PFO were surveyed for the twelfth time.

6. University of California, San Diego. After correcting for motion of the end-points, the UCSD tiltmeter indicates a tilt rate of .3 μrad/yr, down to the WNW for this period. The record is remarkably linear (deviations less than .15 μrad) considering the magnitude of the weather-induced apparent (i.e., uncorrected) tilt of 1 μrad in six months.

Projects Related to the CDO Program:

1. California Institute of Technology. Site preparations were completed at the CIB borehole for the installation of a continuously recording radon monitor.

2. Carnegie Institution of Washington, DTM. The three volumetric strainmeters installed in April 1982 continued to work well in the period. Analysis of the tidal signals has yielded some important results (F. Wyatt, D. Agnew, A. Linde and S. Sacks, Carnegie Institution of Washington Year Book 82). Our first discovery is that the earth (at least at this one site) is uniformly straining in response to the tides even when averaged over baselengths as short as a few meters (the length of the instrument). And second, we find that these signals are about 1.4 times larger than expected. This suggests that the modulus of the instrument is less than that of the rock, thereby allowing an amplified signal within the borehole. In softer rock we would anticipate a greatly reduced response to tectonic strains.

3. Leighton & Associates: Bruce Clark has continued to operate his intermediate depth (∿14 m) borehole stressmeter without assistance.

4. NASA/NGS National Crustal Movement Network. In February 1983, the 50 m-wide observation area was prepared for occupation by JPL's MV-3 VLBI antenna. The instrument was installed, measurements made, and the equipment disassembled in little more than a day.

5. University of California, San Diego. Yu-Chia Chung installed an experimental well-water gas monitoring transducer in the CIA borehole in April 1983. This well is connected to a major hydraulically-conductive fracture at a depth of 100 m.

6. University of Queensland. Drilling began in February 1983 for the installation of two directional borehole strainmeters designed by Michael Gladwin. Following the drilling, conducted by the USGS drill crew, the sites were prepared with well-head enclosures, electrical power, and signal wiring.

7. U.S. Geological Survey. During this period a survey gravity measurement was made at our absolute gravity station by Carter Roberts, a telemetry link for monitoring the Sacks-Evertson strainmeters installed by Doug Myren, and the water level in the CIC borehole monitored by Dick Moyle.

Studies of the Seismic and Crustal Deformation Patterns of an Active Fault: Piñon Flat Observatory

14-08-0001-21270

Frank Wyatt, Duncan Carr Agnew, Jonathan Berger
Institute of Geophysics & Planetary Physics
Scripps Institution of Oceanography
University of California, San Diego
La Jolla, CA 92093
(619) 452-2019

Investigations

This contract supports the ongoing research program at Piñon Flat Observatory. The objectives of this program are: 1) To provide a common location with shared facilities for the research and development of precision geophysical instrumentation; 2) To establish the accuracy with which each of these instruments measure the different geophysical quantities by operating the best available reference standards; 3) To monitor reliably the state of tectonic strain in the lithosphere within the neighborhood of the observatory, a region of imminent seismic activity.

Results

1. Table 1 lists those investigations which are currently underway at Piñon Flat Observatory. Most of these studies are conducted independently, requiring little support by our staff. Members of a second group, called the Crustal Deformation Observatory project, are formally assisted in the operation and evaluation of their projects. (This effort is being supported by separate contract.) The intercomparison of all these observations promotes an understanding of the merits of the differing techniques and provides the means of establishing the reliability of the individual measurements.

2. Figure 1 presents nearly 1.5 years of data recorded by the three 730 m laser strainmeters at PFO. Each of these records has been heavily edited (denoted by gaps in the records) and, to various degrees, corrected for weathering-induced motions of the end monuments. Better results are possible, and we are continuing to improve these instruments. Nevertheless, these continuous recordings show very low strain rates: North-South, .18 $\mu\varepsilon$/yr; East-West, -.17 $\mu\varepsilon$/yr; Northwest-Southeast, -.30 $\mu\varepsilon$/yr. Unfortunately, these recent observations do not agree in sign with the earlier data, from the period 1974 through 1980 (Summary of Technical Reports, Volume XIII), nor do they agree in magnitude with the data published recently by King and Savage (*Geophysical Research Letters*, 10, January 1983). The Geodolite records indicate an average (1973-81) right-lateral shear strain rate of about .05 $\mu\varepsilon$/yr at Pinyon Flat, compared with -.45 $\mu\varepsilon$/yr deduced from the laser strainmeter records. We are currently investigating whether this represents a recent change in the strain rate, a local adjustment of the regional deformation pattern, or simply an instrumental artifact.

Table 1.

Cooperative Studies at Piñon Flat Observatory August 1983

Investigator	Affiliation	Program
Independent Investigations		
D. Agnew	UC San Diego	IDA global seismic network Seismometer testing
J. Berger J. Brune	UC San Diego	Anza seismic array
Y. Chung	UC San Diego	Borehole gas monitor
B. Clark	Leighton and Associates	Borehole stressmeters
D. Garbin	Sandia Laboratories	NTS seismic monitoring
M. Gladwin	Univ. of Queensland	Borehole strainmeter
J. Healy	US Geological Survey	Borehole surveys
L. Hothem	NGS	Satellite Doppler survey Global Positioning System
R. Jachens	US Geological Survey	Survey gravity meter
A. Lachenbruch	US Geological Survey	Heat flow measurements
A. Linde S. Sacks	Carnegie Institution of Washington — DTM	Borehole strainmeters
J. Melvin M. Shapiro	California Institute of Technology	Borehole radon monitor Water level recording
D. Moyle	USGS/WRD	Water well recording
P. Pammel	DMA — Geodetic Survey	Survey gravity meter
C. Parkin	Hunter Geophysics	SQUID magnetometer
A. Reed	USGS/Stanwick	Strong motion recorder
D. Trask	NASA	VLBI/ARIES
J. Whitcomb	CIRES	Survey gravity meter
F. Wyatt A. Harvey	UC San Diego	Long baseline tiltmeters Long baseline strainmeters Laser optical anchors
M. Zumberge	UC San Diego	Absolute gravity meter
Crustal Deformation Observatory Project		
R. Bilham J. Beavan	Lamont-Doherty Geological Observatory	Long baseline tiltmeter Benchmark stability
J. Cipar	AF Geophysics Laboratory	Borehole tiltmeter
D. Jackson	UC Los Angeles	Data analysis and distribution
T. Owen	Cambridge University	Long baseline tiltmeter
L. Slater	CIRES	Long baseline tiltmeter Benchmark stability
A. Sylvester	UC Santa Barbara	Precision levelling array Benchmark stability
F. Wyatt D. Agnew	UC San Diego	Coordination of research Environmental monitoring Data collection Preliminary data analysis

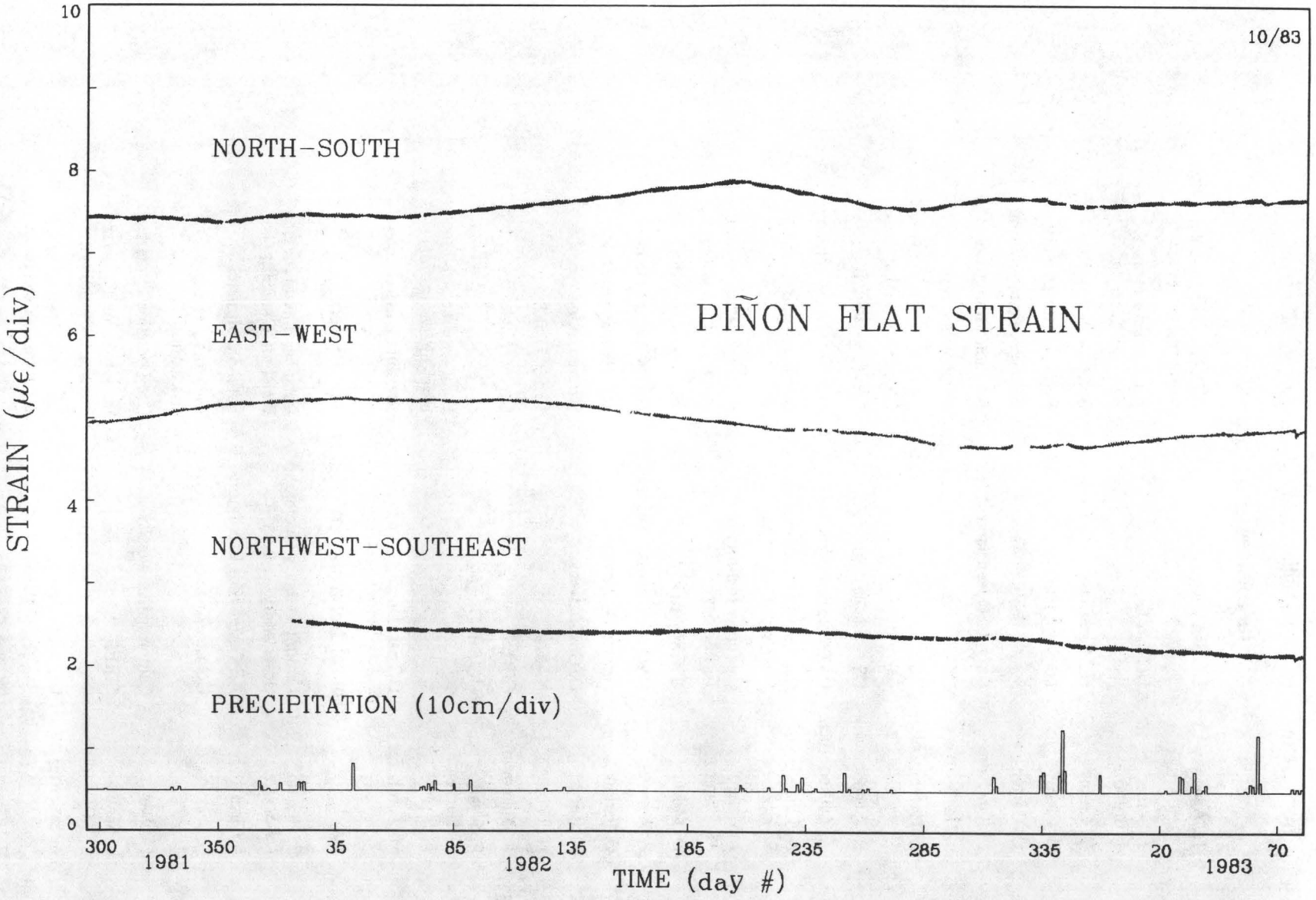
10/83
NORTH-SOUTH
EAST-WEST
NORTHWEST-SOUTHEAST
PRECIPITATION (10cm/div)
PIÑON FLAT STRAIN
STRAIN (με/div)
10
8
6
4
2
0
300
350
35
85
135
185
235
285
335
20
70
1981
1982
1983
TIME (day #)

Figure 1.

PRECURSORY SEISMICITY PATTERNS

14-08-0001-21324

M. Wyss and R. E. Habermann
CIRES/ Dept. of Geological Sciences
University of Colorado
Boulder, Colorado 80309

The homogeneity of seismicity catalogues is crucial to the whole problem of defining seismicity patterns quantitatively. We have found that changes in the reporting frequency of small earthquakes can produce artificially the impression of seismicity rate changes. If such changes were interpreted in terms of precursory changes, serious mistakes could result. We have shown that in the PDE catalogue the total number of small ($m_b \leq 4.5$) earthquakes reported for the entire world during the 1970ies was about 50% of the annual numbers reported during the 1960ies. This change appears to have been due to the closing of US seismograph arrays. Therefore the change did not affect all tectonically active areas in the same way.

We concluded that the minimum magnitude of homogeneity must first be determined before a catalogue can be used for a seismicity rate study. The method developed for this purpose is to make magnitude signatures of the data. Using this method we search the data set by algorithm for significant rate changes as a function of time and within a number of magnitude windows. We then compare the rate stability of larger events to that of smaller ones. Assuming that the larger earthquakes have been reported completely at all times, we will make a decision which smaller magnitude bands may have experienced a reporting change.

Using this method we found that the catalogues for northern as well as southern California have surprisingly high values for the minimum magnitude of homogeneity.

The main thrust of our research remained directed at the systematic and quantitative evaluation of seismicity rate changes in large tectonic units. The steps that we follow in this procedure and the rational upon which our methods are based are explained below.

(1) First we select a region for study which constitutes a seismo-tectonic unit to some degree, but which is sufficiently large such that background rates and minimum magnitude of homogeneity can be determined.

(2) The minimum magnitude of homogeneity is obtained using magnitude signatures. Shocks with smaller magnitudes are removed from the catalogue.

(3) Aftershocks are removed next. In some of our studies we have used statistical criteria to distinguish dependent from independent events. However we found that in teleseismic data sets the simple removal of aftershocks by eye (judging the separation in space and time subjectively) leads to the same results. With very few exceptions (some very great ruptures) aftershock removal poses no problem at all.

(4) The search for seismicity rate changes associated with large earthquakes which have occurred recently in the study area is designed to test the hypothesis that seismic quiescence may precede mainshocks. The source volume and the immediate surrounding area is examined for seismicity rate changes judged to be statistically significant by an algorithm using the z-test.

Various subvolumes may be analyzed separately in order to define the spatial extent of an anomaly, or in order to test the hypothesis that segments of the source volume may experience quiescence while others do not. Successes (precursory quiescence demonstrated) and failures (constant rate before mainshock) are published alike. The duration of quiescence as well as it's spatial and temporal relationship to the mainshock are of special interest.

(5) If precursory anomalies are found in endeavor (4) we proceed to test their uniqueness in the tectonic unit chosen for analysis. We will call an anomaly "unique" if we cannot find another volume of the same dimensions with a period of quiescence at least as long as that of the precursor anomaly, and equaling (or exceeding) the latter in statistical significance. If we find such an anomaly which is not related to a mainshock we call it a false alarm, and we include its characteristics in the publication. The search for false alarms is done by computer, subdividing the study area in a number of overlapping test-volumes (10 to 30 volumes). Using the time window which defines the background and the anomalous period for the precursor, we then search the data as a function of time in all of these test-volumes for possible false alarms by sliding the window through the data set from beginning to end. This means that we end up testing a few thousand different (but overlapping) data sets. If we do not find any false alarms by this method we have not proven that absolutely none exist (perhaps a specially shaped volume of certain dimensions placed in a specific location may show a false alarm). However, we may conclude that false alarms of the type we searched for are extremely rare if they exist at all.

(6) If we find cases of statistically highly significant rate decreases, but which fail to exceed in significance our precursory anomaly, we will discuss these observations along with the false alarms. Such instances do not violate the uniqueness of precursory anomalies, but they must be taken seriously as potential sources for false alarms.

(7) Next the seismicity data from seismic gaps are searched for significant quiescence which may extend from the recent past to the present. If such an anomaly is found and substantiated as unique the gap in question may be called a "mature gap", and the potential of a mainshock in it may be discussed.

The identification of major asperities and the relationship between tectonic lineaments and seismicity patterns has become a new focus of our attention. Lines of study aimed at understanding these problems are the following.

(1) Determination of the properties of asperities is not easy. Opinions are divided as to what properties one should expect. Therefore we have examined the segments of plateboundaries, which ruptured recently in large events, for evidence of asperity related anomalies. In a couple of cases (New Hebrides, Kermadec) we have found small volumes which seem to be good candidates for asperities. They had the following properties: (a) Excess rate of seismicity compared to the average of the tectonic unit. (b) Excess numbers of $m_b \geq 6$ events. (c) Initiation of mainshock rupture. (d) Stopping of mainshock rupture. (e) High average stress-drops compared to surrounding volumes. (Note: not all of these properties, but several of them, were present simultaneously in any one volume proposed as an asperity).

(2) Searches for asperities which may play an important role in future mainshocks were made. It was assumed that the properties listed above were to be expected. (a) Small segments of excess activity were identified as those volumes within which the rate exceeded the average rate of the entire tectonic unit by a highly significant amount. (b) Volumes which contained more than average numbers of $m_b \geq 6$ events were also singled out. (c) An attempt was made to identify volumes with larger than average mean stress-drop, which was

estimated on the bases of the m ratio. (d) Areas which possessed some of these qualities were then examined for tectonic lineaments offsetting the plate boundary. (If segments can be found which exhibit some of these properties they may be proposed as asperities. However, we don't feel certain that they are asperities, and we doubt that all asperities can be found in the way described above.)

The triggering of increased seismicity rate is a phenomenon that may happen during the preparation stage of great earthquakes. We have noticed a couple of cases (New Hebrides, Kermadec) where precursory periods of quiescence were terminated before the mainshock occurred. In these cases the onset of renewed activity coincided with fairly large (M_S = 7) shocks near the future mainshock volume. While the connection between an outer rise rupture and increased seismicity rate on the megathrust plane seems plausible, more data are needed before the idea of precursory triggering can be accepted as valid.

Recent Publications

Conversion of m_b to M_s for estimating the recurrence time of large earthquakes, (M. Wyss and R. E. Habermann), **Bull. Seism. Soc. Amer., 72,** 1651-1662, 1982.

Precursory seismicity quiescence in the New Hebrides arc, (M. Wyss, R. E. Habermann and C. L. Heiniger), **Bull. Seism. Soc. Amer., 73,** 219-236, 1983.

Large earthquakes, mean sea level and tsunamis along the Pacific coast of Mexico and Central America, (G. Cruz and M. Wyss), **Bull. Seism. Soc. Amer., 73,** 553-570, 1983.

Local seismic activity in the region of the Assam Gap, northeast India, (K. Khattri, M. Wyss, V. K. Gaur, S. N. Saha, and V. K. Bansal), **Bull. Seism. Soc. Amer., 73,** 459-470, 1983.

Precursory seismicity quiescence in the Tonga-Kermadec arc, (M. Wyss, R. E. Habermann and J. C. Griesser), **J. Geophys. Res.,** in revision.

Earthquake triggering during preparation for great earthquakes, (R. E. Habermann and M. Wyss), **Geophys. Res. Lets.,** submitted.

Consistency of Teleseismic Reporting since 1963, **Bull. Seis. Soc. Amer., 72,** 93-, 1982. (R. E. Habermann).

Seismicity rates in the Kuriles Island Arc. **Earthquake Prediction Research, 1,** 73-94, 1982. (R. E. Habermann).

Teleseismic detection in the Aleutian Island Arc, **J. Geophys. Res., 88,** 5056-5064, 1983. (R. E. Habermann).

A gap is ..., (with R. E. Habermann, W. R. McCann and S. Nishenko), **Bull. Seism. Soc. Amer., 73,** 1485-1486, 1983.

Spacial seismicity variations and asperities in the New Hebrides seismic zone, in press, **J. Geophys. Res.** (R. E. Habermann).

A quanitative examination of the seismic detection history of California, (R. E. Habermann), **Bull. Seism. Soc. Amer.,** submitted.

Recognition of Individual Earthquakes on Thrust Faults

14-08-0001-21379

Robert S. Yeats and Kelvin R. Berryman
Earth Deformation Section
New Zealand Geological Survey
P.O. Box 30368
Lower Hutt, New Zealand
(011-644) 699-059

Investigations

We plan to follow up our trenching and surface mapping on the Dunstan reverse fault in central Otago with work on the Nevis-Cardrona fault system to the west, where young fault scarps cut late Quaternary surfaces and are associated with strongly deformed Tertiary strata (S. Beanland and R. Thomson, personal commun., 1983). Much of the region has been under snow, and we have been waiting for spring to begin trenching with a bulldozer from the Ministry of Works and Development. Trenching is now scheduled to begin in November. Following the Recent Crustal Movements Symposium in Wellington in February, we plan to do additional trenching at critical localities on the Dunstan fault identified by the earlier trenching in 1982 (Officers of the Geological Survey, 1983). Our object is (1) to establish the recurrence intervals of several active reverse faults in central Otago rather than restrict our investigations to the Dunstan fault and (2) to characterize individual reverse fault events.

In addition, we will summarize existing evidence for recurrence intervals of reverse-fault earthquakes in Otago and northern Westland, South Island, building on the work of Berryman (1980). This will be compared with the limited data available for fault recurrence intervals along the Alpine fault and strike-slip faults in the eastern North Island. These data sets may be used to compare recurrence intervals on reverse faults in the Transverse Ranges with that on the San Andreas fault.

References

Berryman, K. R., 1980, Late Quaternary movement on White Creek fault, South Island, New Zealand: New Zealand Jour. Geol. Geophysics, v. 23, p. 93-101.

Officers of the Geological Survey, 1983, Seismotectonic hazard evaluation of the Clyde dam site: N.Z. Geol. Survey Report EG-375.

Crustal Deformation Observatory: Part F

USGS 14-08-0001-21231

Roger Bilham and John Beavan
Lamont-Doherty Geological Observatory of Columbia University
Palisades, New York 10964
(914) 359-2900

Investigations

1. The 532 m long water-tube tiltmeter installed in 1980 by LDGO at Pinon Flats Observatory has been maintained and improved. The instrument is modelled on a 130 m long tiltmeter operated for a short time by Michelson between 1915 and 1919. Two other tiltmeters of similar length are operated at PFO in the same azimuth; one, constructed by Cambridge, shares the same end-mounts but operates on a pressure-sensing principle. The other, constructed by IGPP, is similar to the Michelson tiltmeter but uses different transducing principles. We are investigating the response of the three instruments to thermal, hydraulic and tectonic signals (Figures 1 and 2).

2. We have identified periods during which the fringe-counter in one or other of the water-height interferometers failed due to light intensity fluctuations associated with laser malfunction. The resulting loss of fringe datum is usually monotonic and causes an apparent D.C.-drift to appear in the tilt signal. The fringe following, white-light interferometer in the IGPP tiltmeter does not suffer from this problem and can always recover its datum after power interruptions. To overcome the fringe datum uncertainty in the LDGO tiltmeter we have investigated methods to improve the reliability of the fringe-counter, to simplify tiltmeter maintenance and to provide an independent check on datum stability using an "absolute" method of water height measurement.

Results

1. Long term data from three tiltmeters are presented in Figure 3. The LDGO and IGPP half-filled pipe tiltmeters are less affected by thermal effects than is the Cambridge central-pressure tiltmeter. Periods of large drift or high noise level on the LDGO tiltmeter correspond to periods during which the fringe-counters were malfunctioning. New lasers were inserted after day 400 resulting in correct operation of the tiltmeter until premature failure of the lasers in June 1983. New, more reliable plasma tubes have been incorporated into these lasers which have been reinstalled in the tiltmeter.

2. Narrow-band filters and revised collimators have been installed on the interferometer detectors to render them more robust during routine maintenance. Plane-polarised lasers were installed in December 1982 to reduce the adverse phase affects of random polarisation on the quadrature signal that feeds the fringe-counter. Mode jumps in the new lasers are less frequent and no loss of fringe-count

datum has occurred during their operation. To facilitate maintenance at PFO we have installed circuitry to observe the quality of the fringe quadrature signal remotely. Finally, a pair of high-quality LVDT transducers and electronics have been installed to replace the original LVDT sensors that monitor vertical strain in the 30 m deep boreholes beneath each tiltmeter end-mount.

3. We have attached two micrometer sensors to the end-mounts of the tiltmeter in order to relate fringe-count to the "absolute" height of the water at each end. The micrometer to which a slender conical point has been fixed, is driven from beneath the water-surface to meet its reflected image. The moment of contact may be viewed from below with a low power microscope. To assist the setting of the digital micrometer to $\pm 1\mu m$ we have installed a Ronchi ruling in the path of the white light source that illuminates the pointer from behind. The parallel line image of the ruling reflected from the water surface is distorted in proportion to the amount of penetration of the pointer through the water surface. The micrometer reading and the instantaneous fringe-count reading are noted and used in subsequent analysis to reconcile any fringe jumps that might have occurred due to power failures.

4. We have neared completion of an alternative water-height transducer that is expected to be much more reliable than the present interferometers at PFO. It uses a similar optical arrangement to the existing interferometer but incorporates automatic circuitry and microprocessor control to retain operation over a much wider range of physical conditions. The laser intensity required by the interferometer is 100 times less than that required in the present system. Fringe subdivision to $\lambda/20$ is possible providing a tilt resolution of 10^{-10} radians. Vertical motion of the water in the reservoirs of the LDGO tiltmeter at PFO at periods of a few minutes or less corresponds to tilt amplitudes of the order of several parts in 10^{-10} radians.

Reports

Bilham, R., J. Beavan, and K. Evans, Long baseline fluid tube tiltmeter geometry and the detection of flexure and tilt, Proc. 9th Int. Symp. on Earth Tides, New York, Aug. 17-22, 1981, ed. J.T. Kuo, 85-94, Schweizerbartsche Verlagsbuchhandlung D-7000 Stuttgart, pp. 747, 1983.

Bilham, R., D. Lentrichia, and R. Garner, Xerox mice in water-tube tiltmeter - VLSI in interferometer sensors, EOS, Trans. AGU, 63, 1982.

Cheng, A., D. Jackson, F. Wyatt, G. Cabaniss, T. Owen, and R. Bilham, Tiltmeter observations at Pinon Flats Observatory, California, EOS, Trans. AGU, 63, pp. 1107, 1982.

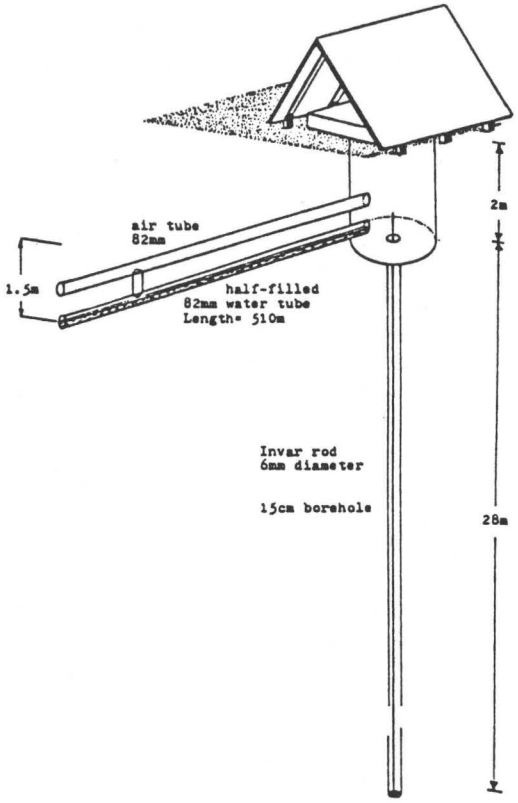

Figure 1: View of one end of the Lamont/Cambridge tiltmeters. The end mount is referred to the base of a 30 m borehole via a 6 mm invar rod held in tension. The "A" frame protects the vicinity of the end mount from the direct effects of solar radiation.

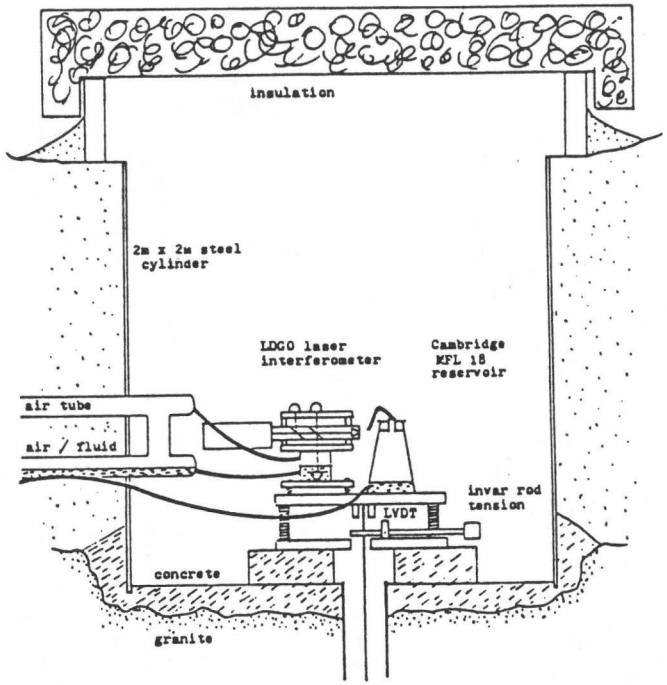

Figure 2: Arrangement of tiltmeter end units relative to the invar reference rod. An LVDT monitors vertical displacements of the end units relative to a point 30 m below ground level. A benchmark is fixed to the end-mount base-plate so that its height can be referenced to a local levelling network.

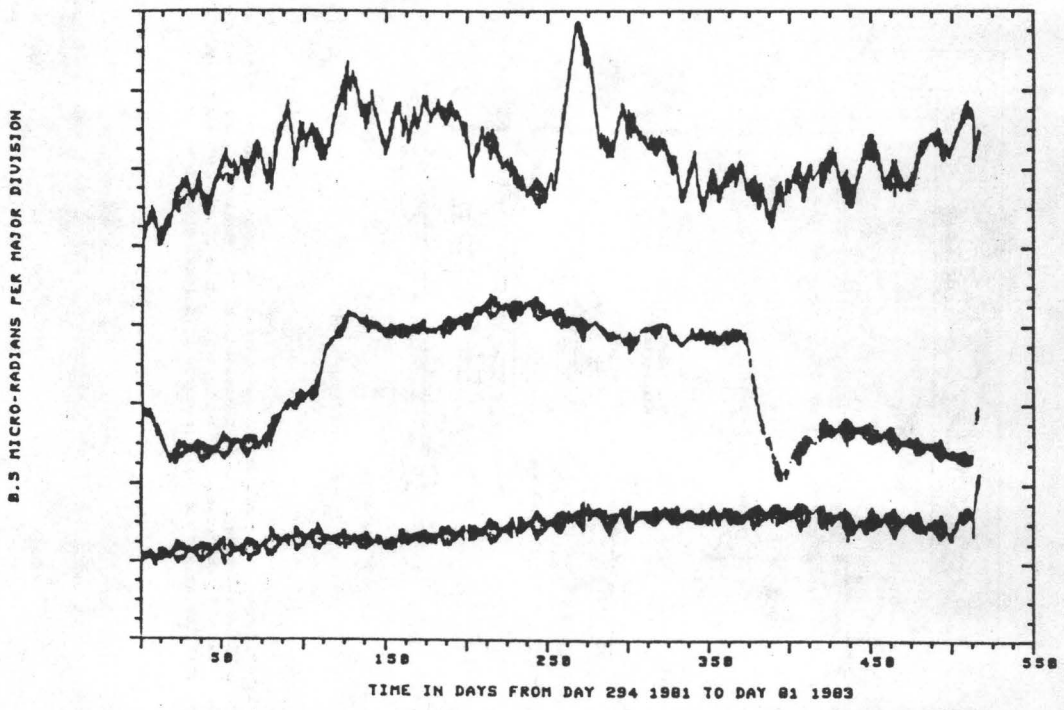

Figure 3: Tilt data from the Cambridge (top), LDGO (center) and IGPP (lower) tiltmeters. The low noise level and drift of the IGPP tiltmeter contrasts strongly with the thermal noise on the Cambridge tiltmeter and noise generated by fringe-miscounts on the LDGO tiltmeter prior to about day 400. The LDGO and IGPP data are in closer agreement from day 440 onward following modifications to the LDGO lasers and fringe-counters.

Investigation of Radon and Helium as Possible Fluid-Phase Precursors to Earthquakes

14-08-0001-21186

Y. Chung
Scripps Institution of Oceanography
University of California, San Diego
La Jolla, California 92093

(619) 452-2662

Investigations

1. Monitoring radon, helium, and other relevant geochemical parameters in a southern California network of hot springs and wells along the San Andreas, San Jacinto, and Elsinore faults for their temporal variations which may display anomalies in response to pre-seismic events.

2. A general study of the relationships between these components, their origin, and variations due to flow rate changes, seasonal effects, atmospheric contributions, and variable crustal and mantle sources.

3. Monitoring radon continuously (on an hourly interval) with field-installed Continuous Radon Monitors (CRM's) for possible short-term anomalies which may be precursory to earthquakes.

4. Comparison of the CRM data with the discrete data which are collected less frequently at the same site for their compatibility in long-term variations.

5. Direct comparison of the CRM variations with the Rn variations obtained from a Caltech Radon-Thoron Monitor at the Pinon Flat Geophysical Observatory.

6. Testing the performance of a field pH meter and a field conductivity meter.

Results

1. During the past six months (April 1 to September 30, 1983), we have observed no significant variations in Rn, He or other parameters within our network except for the Arrowhead site. The discrete Rn data at Arrowhead show a continual increase to a maximum in May and June which is about 60% above the baseline level. Similar increase was observed in He between February and June. After June both He and Rn dropped by about 20%. The magnitude of increase is comparable to that observed prior to the Big Bear earthquake in 1979. However, only a few shocks (M=3.0 to 3.5) occurred nearby during this period. The CRM data (see below) does not show a parallel increase.

2. Plots of Rn-He and He-N_2 for all the data available at Arrowhead show that they are linearly correlated with a Rn/He slope of about 4×10^4 dpm/cc and a He/N_2 slope of about 4.3×10^{-3} cc/cc. The He/N_2 slope does not go through the origin; it intercepts at 4.5 cc/kg N_2 at zero He. The CH_4-N_2 plots are

quite scattered with no apparent linear correlation. At the Hot Mineral Well, the Rn-He plots are clustered in an area with no linear trend. The Rn/He ratio is about 1.2×10^7 dpm/cc or about 3 orders of magnitude greater than that at Arrowhead due to extremely high Rn in association with low He at the Hot Mineral Well.

3. There were three CRM's in operation during the report period. The first CRM was installed at Arrowhead to monitor the gas-phase radon in September, 1982. After various technical and field problems were solved during 1982, we were able to obtain good quality data from January to early July, 1983. A 15% increase was observed within a few days between February and March, but no environmental effects or earthquakes were noticed during this increase. The Rn level was quite constant at the higher level until July, 1983 when the electronic system malfunctioned. This CRM was out of commission during August and part of September. The September data show that the Rn level has returned to the pre-February baseline. The second CRM was installed at Murrieta Hot Springs in March, 1983. Similar to Arrowhead, gas bubbles are collected for monitoring. The data fluctuated with large amplitudes at lower level during the first couple of months and then became stable and fairly constant at higher level after May, 1983. A third unit on loan from USC was connected with a Caltech Radon-Thoron Meter at Pinon Flat in June for direct comparison. The preliminary results indicate very little or no correlation between the two sets of Rn data. The Caltech Rn data show much larger amplitudes of fluctuation than the CRM data in temporal variations in terms of percentage.

4. The CRM detector cells were calibrated against an NBS Ra-226 standard previously prepared for oceanographic work. The efficiency was determined to be at 78% for both the Arrowhead and Murrieta units. Based on this efficiency and the known volume of the cell, one can calculate the Rn concentration in the gas bubbles. At Arrowhead, this Rn concentration ranges from 8 to 9.5 dpm/cc at about 30°C. The Rn dissolved in the spring water is about 0.34 to 0.47 dpm/g. Thus the Rn activity ratio between the liquid- and gas-phase on per unit volume basis is about 0.05, i.e. only about 5% of Rn is dissolved in the Arrowhead water at 80°C. This amount is less than half of what is expected from the Rn solubility in fresh water at this temperature. Although the dissolved constituents or salts may have lowered the expected solubility by about 20%, it is not sufficient to account for the low dissolved-phase Rn measured from discrete samples. The loss of Rn in the liquid phase is probably due to stripping effect of the ascending bubbles or non-equilibrium between the two phases. At Murrieta, the gas-phase Rn is about 11 to 12 dpm/cc, while the liquid-phase Rn ranges from 0.41 to 0.51 dpm/g. The activity ratio between these two phases indicates that only 4% of Rn is dissolved in the 55°C water. This is about one third of the equilibrium value. These results suggest that the stripping of the dissolved Rn by the ascending bubbles is more effective at Murrieta than at Arrowhead. Since the activity ratio of Rn between the two phases is fairly constant, Rn in either phase can be monitored for temporal variations. However, it seems that the gas-phase Rn has a faster or shorter response time than the liquid-phase Rn based on our time-series data obtained from the CRM and discrete Rn measurements.

5. The CRM on loan from USC was installed at Pinon Flat in June. It was attached to the Caltech Radon-Thoron Monitor for direct comparison of temporal variations. The well assigned for this experiment is CIB which has a depth of 800 feet with steel casing down to 197 feet. The water level is at 88 feet;

the gas bubbler is at 215 feet or 18 feet below the casing. With an ID of 6 inches, the total volume of water under stripping is about 25 cubic feet or 700 liters. However only 14% of the water is directly in contact with the bedrocks for exchange and replenishment. The CRM is monitoring the Rn level inside the Caltech monitor vault which contains Rn stripped from the well water by the bubbling and circulating system. The Rn activity level is extremely low, only about 4 times above the background level. Little or no correlation has been observed so far between the two Rn monitors.

6. A field pH meter and a conductivity meter purchased recently from the IBM Instruments, Inc. on another grant were tested at field and in laboratory. Both instruments can also measure temperature to ±1°C. The upper temperature limit recommended for the pH meter is 80°C; the conductivity meter should be used below 50°C. The tests show that the pH values may be higher by 0.5 pH unit if measured at room temperature rather than at the higher in situ water temperature. The conductivity depends on the water temperature: it may drop by one third to one half when the water is at room temperature. Thus the conductivity meter is not suitable for our field use on hot spring waters. Collecting samples for laboratory measurements defeats the purpose of a field instrument.

Reports

Chung, Y., and Craig, H., 1983, Monitoring of dissolved gases in southern California groundwaters for earthquake prediction. Symposium on ultra-deep and fault related gases, 186th Am. Chem. Soc. National Meeting, Washington, D.C. (with published abstract).

Investigation of extensive-dilatancy anisotropy

Contract No. 110196

Stuart Crampin
Institute of Geological Sciences,
Murchison House, West Mains Road,
Edinburgh EH9-3LA, SCOTLAND UK
(031)-667-1000

Investigations

1. The hypothesis of extensive-dilatancy anisotropy, EDA, (Crampin, Evans & Atkinson 1982, 1984) suggests that crack-induced anisotropy may occur at low deviatoric stresses by subcritical crack growth during the slow build-up of strain before earthquakes. This would cause effective anisotropy at substantial distances from impending epicentres, so that the build-up of strain could be monitored by analysing shear-wave splitting in the wavetrains of local earthquakes. This would appear to be a possible technique for earthquake prediction. To test this hypothesis, shear-wave splitting must be analysed on records of local earthquakes from closely spaced networks of digital or digitizable instruments surrounding earthquake epicentres. Very few suitable seismic networks exist. Present investigations have been restricted to the Turkish Dilatancy Projects (TDP1 and TDP2), where temporary networks were sited over a persistent swarm of earthquakes near the North Anatolian Fault in Turkey for a few months in 1979 and 1980 (Crampin, Evans & Üçer 1984), and the seismic network of the Lawrence Livermore Laboratory, California. There will be a further TDP experiment in 1984 (Crampin, Üçer, Evans, Miller & Kafadar 1984).

Results

1. Various earthquake parameters necessary for investigating shear-wave splitting have been determined for the TDP swarm, including hypocentre locations in effectively anisotropic structures (Doyle, McGonigle & Crampin 1982; Doyle, Crampin, McGonigle & Evans 1984), and fault-plane mechanisms (Evans, Asudeh, Crampin & Üçer 1984). The TDP events have focal depths between six and twelve kilometres and include a variety of mechanisms, consistent with a zone containing many fault facets subjected to a consistent right-lateral strain imposed by the adjacent North Anatolian Fault system.

2. Preliminary observations indicated pronounced shear-wave splitting (Crampin et al. 1980). However, shear-waves incident at a free surface with incidence angles greater than than a critical angle arcsin(Vs/Vp) suffer phase and amplitude changes, and S to P conversions, that make it difficult to infer the incident waveform from observations at the surface (Crampin 1983; Booth & Crampin

1984). These surface interactions include arrivals that could be misinterpreted as anisotropy-induced shear-wave splitting. Only for arrivals within the shear-wave window, where incidence is less than critical, are the shear waves at the surface similar to the incident waveforms. Even within this window, in undulating topography as in the TDP experiment, a horizontally propagating P-headwave, the local SP-phase, may sometimes be focused towards a site so that it appears as a large, sometimes dominant, signal on the radial component of the seismogram (Crampin 1983, Booth & Crampin 1984).

3. Consequently, shear-wave analysis has been restricted to observations from within the shear-wave window, that is to records from instruments very close to the epicentre, and care taken to recognize locally generated phases. The polarizations are complicated and display considerable scatter, but the polarizations of the faster split shear-wave show, with one exception, approximately the same orientation pattern at each of the recording sites. This would not be expected from the polarizations of shear waves radiated from a range of directions and incidence angles from a variety of double-couple sources, but would be expected for waves propagating through an effectively anisotropic structure. Thus, we suggest that, anisotropy is directly indicated by the shear-wave polarizations (Booth, Crampin, Evans & Roberts 1984).

4. It should be noted that, whereas the polarizations display consistent patterns, the observed delays between the split shear-waves do not appear to follow any recognizable pattern. However, patterns in the delays would not necessariy be expected. Numerical experimentation with synthetic seismograms indicates that the polarizations of the faster shear-waves split by crack-induced anisotropy are a comparatively stable phenomenon: polarizations are locally generated by the symmetry of the anisotropy (the crack alignments) immediately adjacent to the observation point. In contrast, delays are determined by properties of the domain and may well vary considerably as different ray paths traverse different cracked structures, even though the cracks may have similar orientations due to the overall stress field and yield consistent polarizations.

5. With the one exception, the patterns at the recording sites have the same azimuthal orientations at all sites both in 1979 and 1980. The exception is a site on the edge of the network which has polarization orientations n/2 different from the other sites in 1979, but reverting to approximately the same orientation as the other sites in 1980. In all other respects the behaviour of the polarizations at this exceptional site appear to be similar to those at the other sites. Stress orientations in fault zones and the consequent anisotropy is poorly understood at present (Evans 1984), and the cause of the changed pattern at this site has not yet been investigated in detail. However, some form of crack-induced anisotropy appears to be the only mechanism that can cause temporal changes in the anisotropic symmetry orientations. The EDA hypothesis of subcritical crack

growth is the only hypothesis yet suggested for strain-induced cracking in comparatively low-stressed regions surrounding a fault so that splitting could be observed on seismic shear-waves (Booth, Crampin, Evans & Roberts 1984).

6. Analysis of data from the network at Livermore has only just begun, but preliminary observations indicate that the polarizations of the faster split shear-waves appear to behave in much the same way as those in the TDP experiments.

7. This Report was submitted with the approval of the Director of the Institute of Geological Sciences (NERC), UK.

References (Reports marked *)

*Booth, D.C., and Crampin, S., 1984. Shear-wave polarizations on a curved wavefront at an isotropic free surface, Geophys.J.R.astr.Soc., submitted.

*Booth, D.C., Crampin, S., Evans, R., and Roberts, G., 1984. The effects of extensive-dilatancy anisotropy in observed shear-wave polarizations, Geophys.J.R.astr.Soc., in preparation.

*Crampin, S., 1983. Shear-wave polarizations: a plea for three-component recording, Extended Abstracts, SEG, 53rd Annual International Meeting, Las Vegas, 1983, 425-428.

Crampin, S., Evans, R., and Atkinson, B.K., 1982. A new physical basis for prediction, EOS, 63, 370.

*Crampin, S., Evans, R., and Atkinson, B.K., 1984. Earthquake prediction: a new physical basis, in Proceedings of the First International Workshop on Seismic Anisotropy, Suzdal, 1982, editors S.Crampin, E.M.Chesnokov, & R.G.Hipkin, Geophys.J.R.astr. Soc., 76, in press.

*Crampin, S., Evans, R., and Üçer, S.B., 1984. The analysis of records of local earthquakes: the Turkish Dilatancy Projects (TDP1 and TDP2), Geophys.J.R.astr.Soc., submitted.

Crampin, S., Evans, R., Üçer, B., Doyle, M., Davis, J.P., Yegorkina, G.V., and Miller, A., 1980. Observations of dilatancy-induced polarization anomalies and earthquake prediction, Nature, 286, 874-877.

Crampin, S., Üçer, S.B., Evans, R., Miller, A., and Kadafar, N., 1984. The Turkish dilatancy project (TDP3) - March to November 1984, D.Fizik,Boğaziçi Üniv., submitted.

Doyle, M., Crampin, S., McGonigle, R., and Evans, R., 1984. The joint inversion of arrival times in a region of possible dilatancy anisotropy, Geophys.J.R.astr.Soc., in preparation.

Doyle, M., McGonigle, R., and Crampin, S., 1982. The effects of crack anisotropy on the hypocentral locations of local earthquakes, Geophys.J.R.astr.Soc., 69, 137-157.

*Evans, R., Asudeh, I., Crampin, S., and Üçer, S.B., 1984. Tectonics of the Marmara Sea region of Turkey: new evidence from micro-earthquake fault plane solutions, Geophys.J.R.astr.Soc., submitted.

Evans, R., 1984. Anisotropy: a pervasive feature of fault zones? in Proceedings of the First International Workshop on Seismic Anisotropy, Suzdal, 1982, editors S.Crampin, E.M.Chesnokov, & R.G. Hipkin, Geophys.J.R.astr.Soc., 76, in press.

DEEP BOREHOLE CONTINUOUS PLANE STRAIN MONITORING

14-0800001-21228

Michael T. Gladwin
Department of physics
University of Queensland
St.Lucia,4067
AUSTRALIA

1.INVESTIGATIONS. The object of this project is the installation of three continuous plane strain monitors in medium depth holes in California. The instrument was developed in 1972 for monitoring of deep underground pillars in mining environments. It provides, by the use of three gauges oriented at 120 degrees to each other, redundant data for the determination of the plane strain components. The major advantage over volume strain meters is that the instrument allows isolation of the shear strain, which at reasonable depths is independent of many sources of noise which make interpretation of volume strain data difficult. The gauges used for this experiment have a sensitivity of approximately 0.3 nanostrain, and a dynamic range of about 10**-4. Installations for the present experiment have been planned so that the instrument performance can be compared with the D.T.M. Sacks-Everton volume strainmeters, with each site selected in very close proximity to D.T.M. installations. D.T.M. installation procedures including choice of grout have been used with the close co-operation of Carnegie Institute staff. The instrument makes measurements every eighteen minutes on all axes, including an inbuilt reference gauge. The data stream, which is rich in station performance diagnostics, is returned to the laboratory via a satellite, and selected results are recorded on site in case of failure of this telemetry.

2.RESULTS . Two sites were instrumented during September, 1983. The first, at Pinyon Flat Observatory with the co-operation of staff of UC, San Diego, will provide reliable calibration of the instrument against the broad range of instrumentation at the observatory, in particular the long baseline strain interferometer. The second installation was at San Juan Baptista, in sedimentary materials. The object of this installation was to determine the viability of the installation technique in non crystalline rock materials. The rock type chosen was a poorly sorted "sandstone" rich in clay materials. Early non-coherent response of the three components of this instrument verified previous measurements by D.T.M. which indicate that reliable volume strain measurements in such materials are probably impossi-

ble. The instrument has recently gone into compression on all axes so that it may be possible to isolate some shear data in the next several months. The figure below shows data from one of the three components at the P.F.O. installation beginning two days after installation. The upper trace shows the raw data dominated by the compression generated by curing of the expansive grout. The second trace is produced from the first by simple removal of a linear trend line. The solid earth tides are well sampled. No formal reduction of the data will be attempted until the curing process is complete.

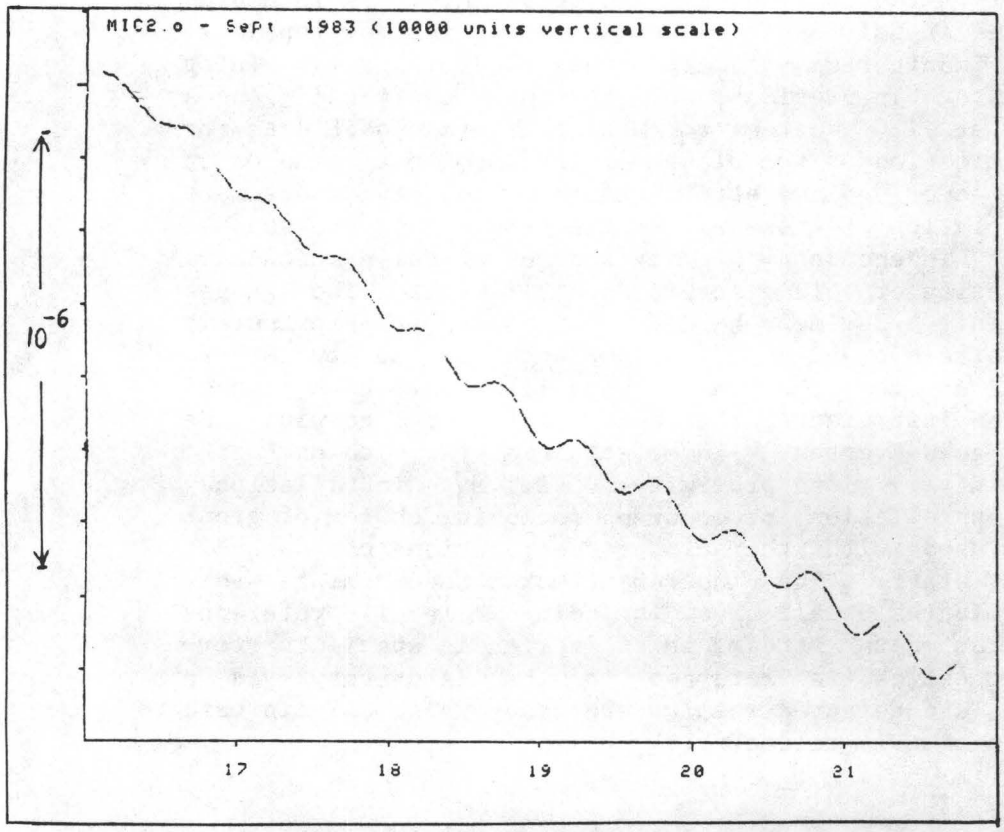

SEPTEMBER 1983.

Figure 1 Raw strain data from component 2 at the UQB site at Pinyon Flat Observatory. The data shows the compression caused by grout curing, with earth tide superimposed.

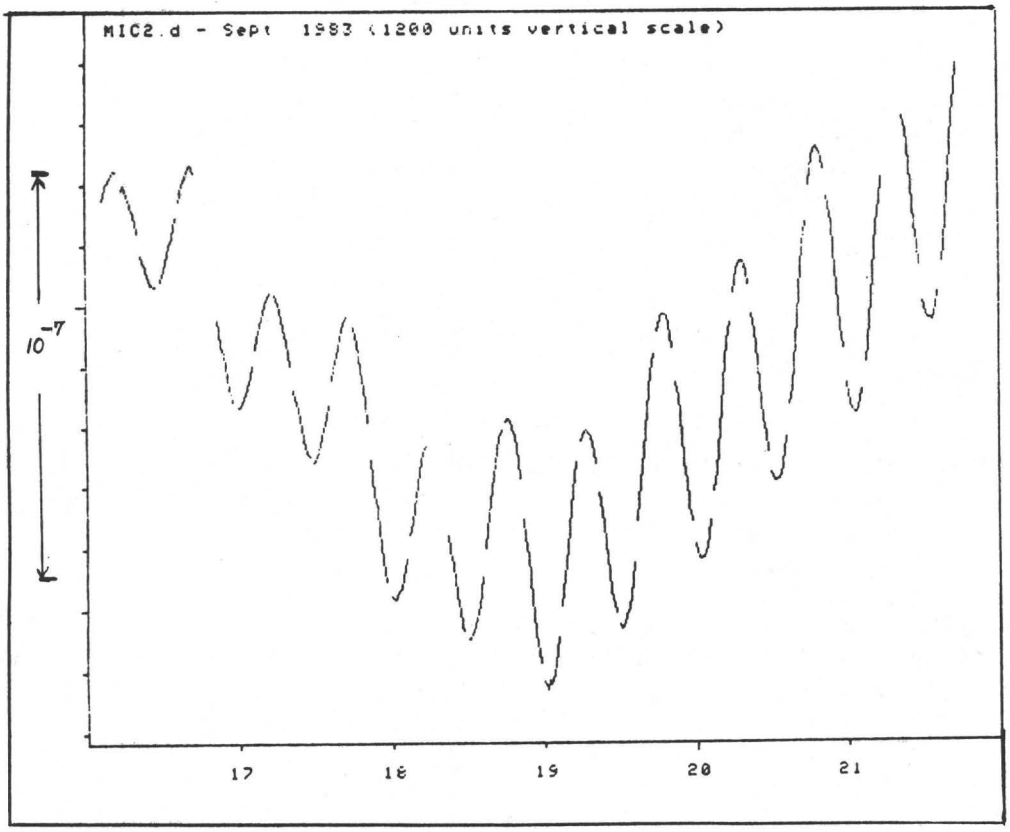

SEPTEMBER 1983.

Figure 2 The same data with a linear trend removed to show the earth tide .

Deepwell Monitoring Along the Southern San Andreas Fault

14-08-0001-21273

Thomas L. Henyey and Steve P. Lund
University of Southern California
Center for Earth Science
Los Angeles, California 90089-0741
(213) 743-6123

Investigations

A group of deep, abandoned, wildcat wells in the locked portion of the San Andreas Fault between Gorman and San Bernardino have been instrumented with continuously recording high-precision water-level transducers and thermal sensors to monitor changes in groundwater parameters which may be sensitive to regional strain or precursory to seismic slip.

Results

Figure 1 shows daily averaged water-level data for four representative wells through August, 1983.

The data reflect the large atmospheric pressure variations and heavy rainfall during the winter of 1983. The rise in groundwater is particularly impressive at the Crystallaire site, perhaps due to its proximity to a major ephemeral drainage system. Note that the vertical scale is different on each plot (Figures 1b to 1e).

Investigation of the solid earth tidal response of the well is the first step to "clearing" of the data in a search for stress-induced water level change. Figures 2-5 provide background to work on tidal and barometric pressure response currently underway. Figure 2 represents a digitized data set (every 4 hours) for the theoretical dilatational tides between May 1, 1983 and July 24, 1983. Figure 3 is the MEM spectra (lag = 128) for these data. Figure 4 is a similarly digitized data set (same time period) for the water level in the Crystallaire well. The diurnal and semi-diurnal tides show up well and agree closely in period with the theoretical tides but differ in relative amplitudes (Figure 5). This may be a function of either well response or data set inadequacy. Finally the fortnightly and monthly tidal peaks which are clearly seen in the theoretical spectra, are highly contaminated by barometric pressure effects in the well spectra. Longer data sets should improve the resolution.

Multiyear, high-quality, continuous data sets will be required to adequately account for barometric pressure and rainfall effects. Such data are just now coming on line for the southern California deep well network.

st/93

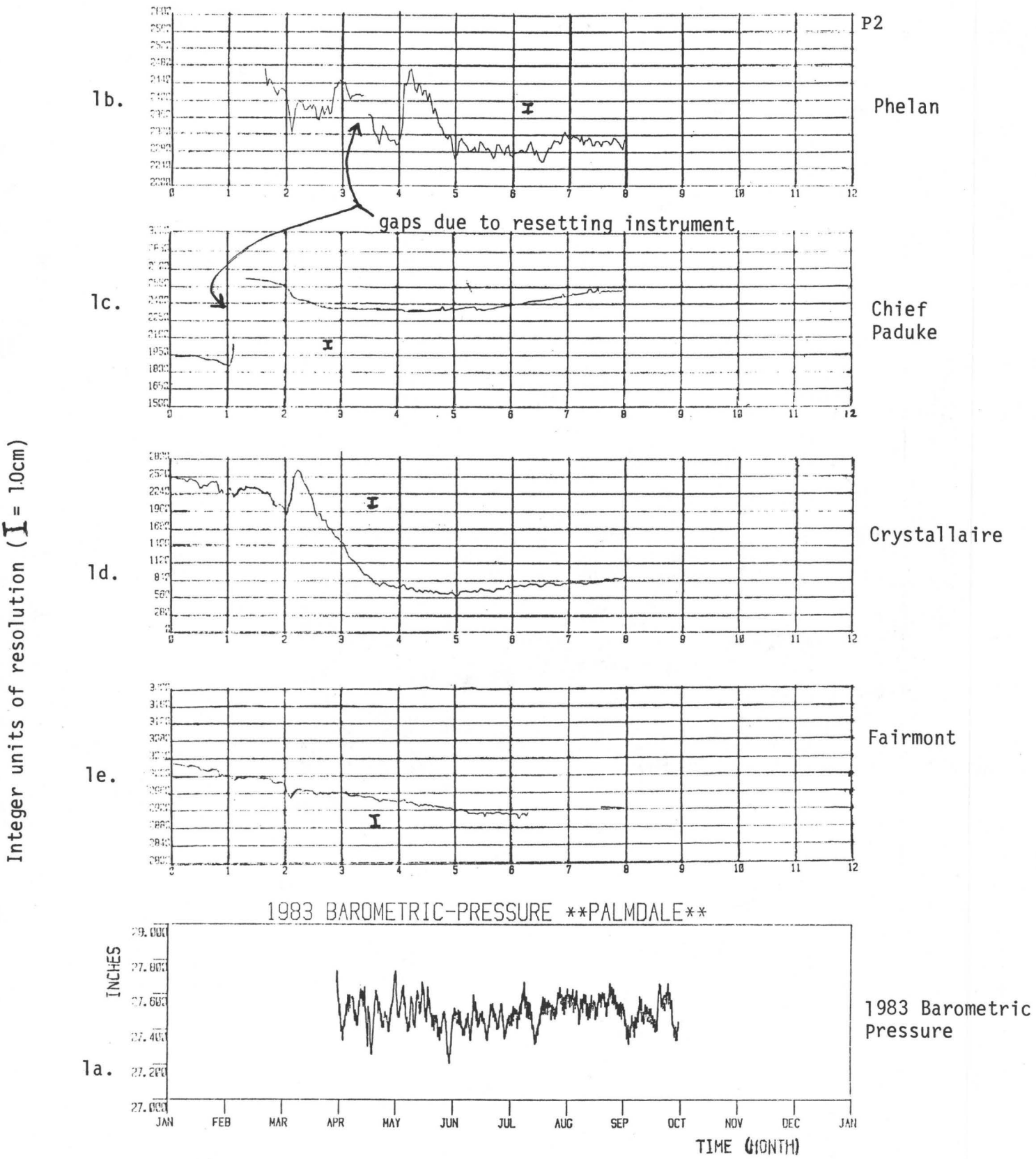

Figure 1. 1983 daily average water level from selected well of the Palmdale region. Water level on b-e increase downward.

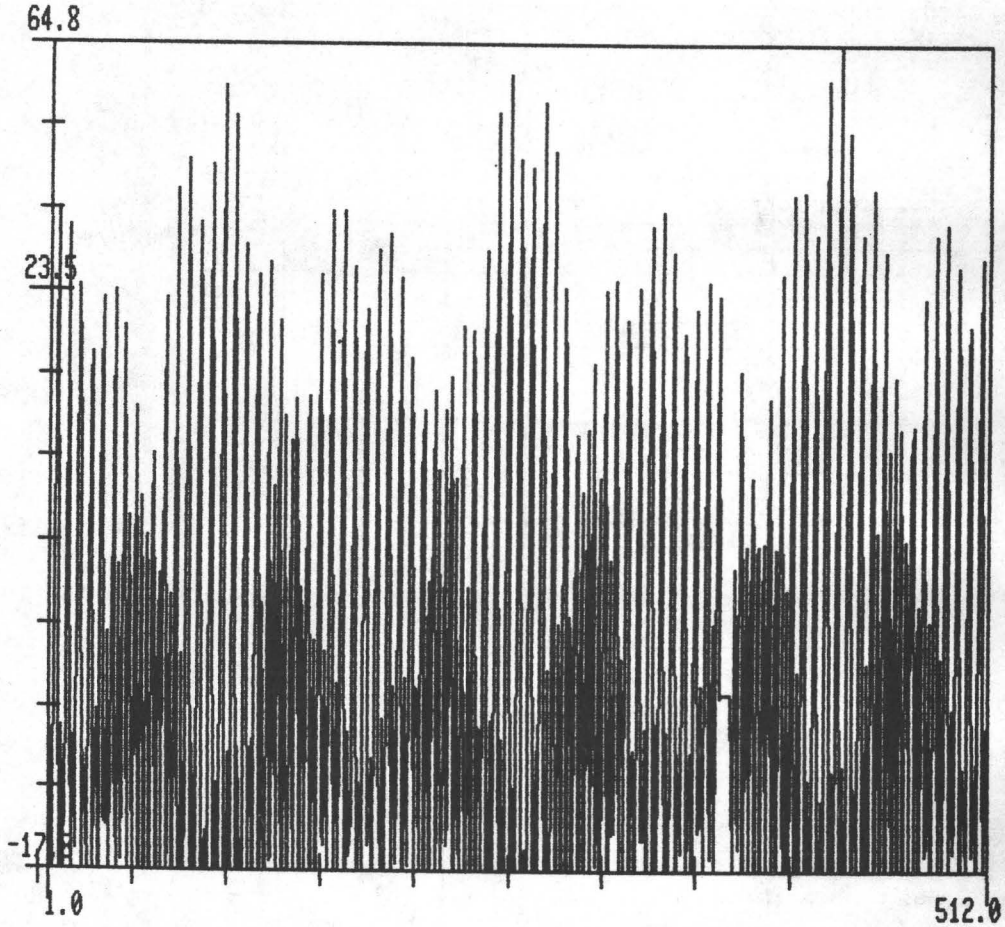

Theoretical dilitation tides

512 data points
4 hour sample interval

FIGURE 2

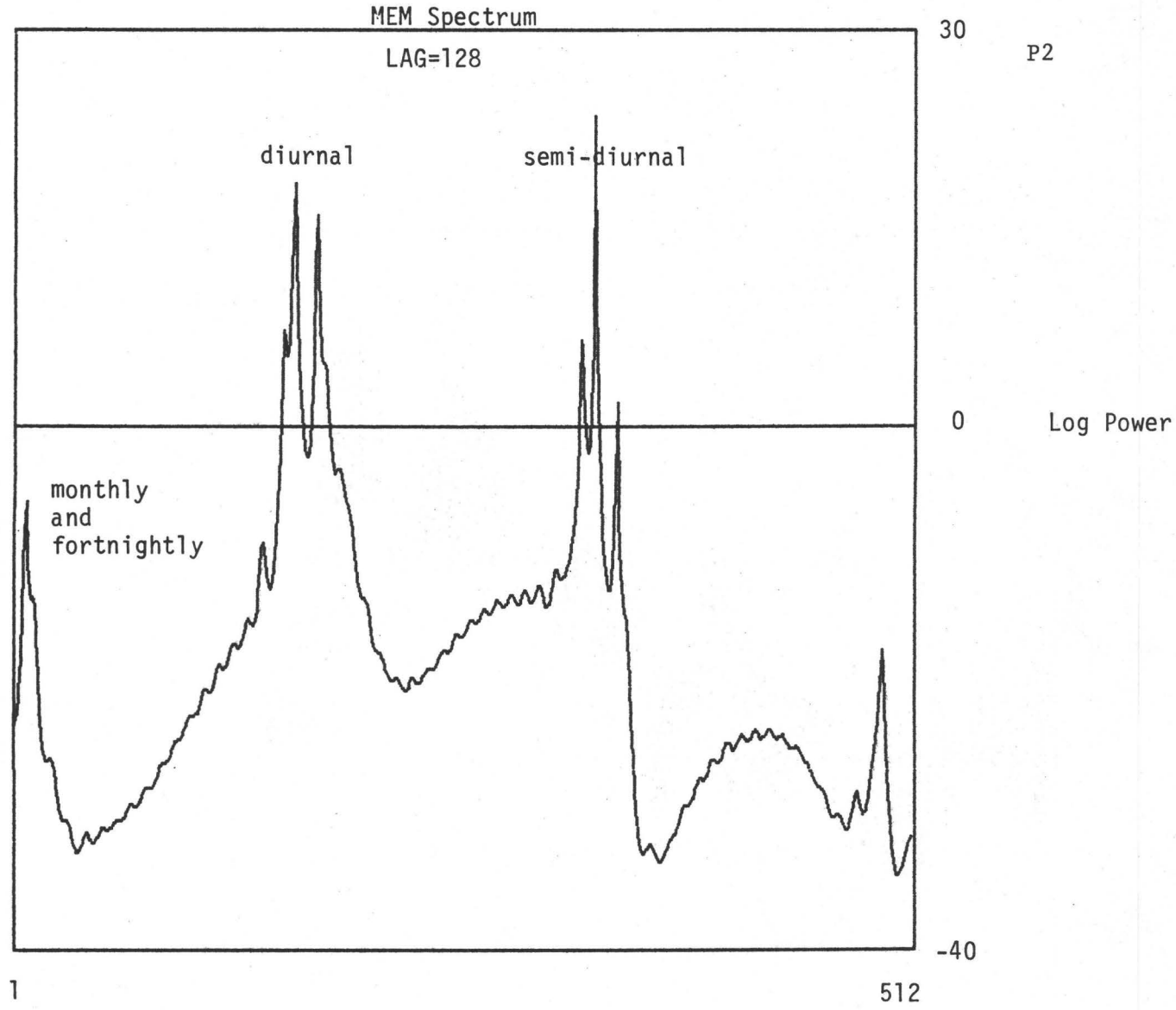
MEM Spectrum
LAG=128
30
P2
diurnal
semi-diurnal
0
Log Power
monthly
and
fortnightly
-40
1
512
FREQUENCY NUMBER

FIGURE 3

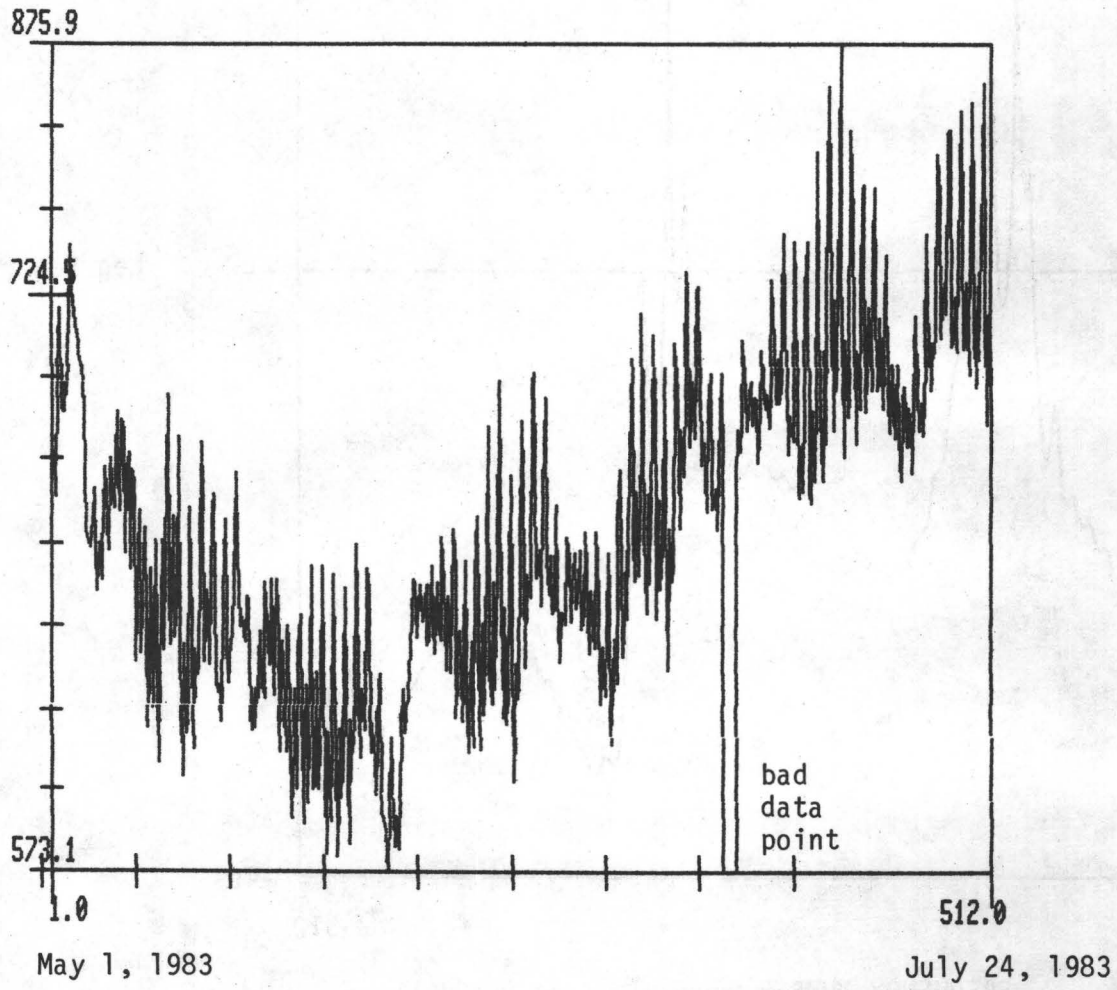

FIGURE 4

Relative water level from Cystallaire Well

512 data points
4 hour sample interval

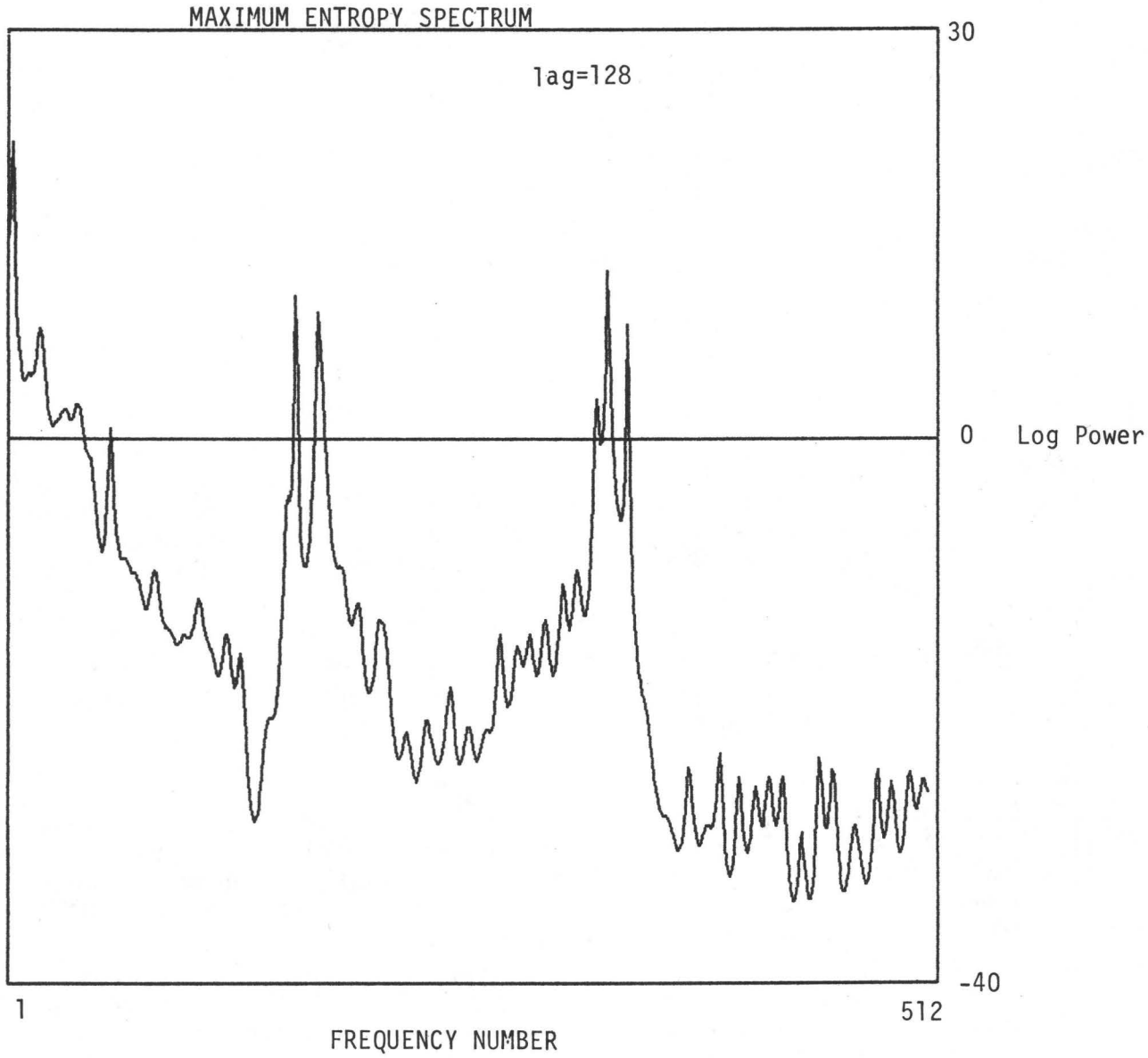
MAXIMUM ENTROPY SPECTRUM
lag=128
30
0
Log Power
-40
1
512
FREQUENCY NUMBER

FIGURE 5

Low Frequency Data Network

J. Herriot, K. Breckenridge, S. Silverman
Branch of Tectonophysics
U. S. Geological Survey
Menlo Park, California 94025
415/323-8111, ext 2932
10 October 1983

9960-01189

Investigations

[1] Real-time monitoring, analysis, and interpretation of tilt, strain, creep, magnetic, and other data within the San Andreas fault system and other areas for the purpose of understanding and anticipating crustal deformation and failure.

[2] Compilation and maintenance of long-term data sets free of telemetry-induced errors for each of the low frequency instruments in the network.

[3] Development and implementation of real-time algorithms for the purpose of detecting earthquake precursors in the low frequency data.

Results

[1] Data from low frequency instruments in Southern and Central California have been collected and archived using the Low Frequency Data System. In the six months three million measurements from 125 channels have been received and subsequently transmitted on the Low Frequency 11/44 UNIX computer for archival and analysis.

[2] The project continues to operate a configuration of one PDP 11/44 computer running the UNIX operating system and two PDP 11/03 running real-time data collection software. This 11/44 has been operational as our analysis machine with less than 1% down time. The two 11/03 machines operate redundantly for robustness. Accordingly, our real-time collection has had 0% down time.

[3] The data from the Network have been made available to investigators in real time. Data only minutes old can be plotted. Events such as creep events can be monitored while they are still in progress.

[4] The working prediction group of the Branch has made extensive use of the timely plots which are produced routinely by the project.

[5] A network connection has been completed between the Low Frequency PDP 11/44 and the UNIX PDP 11/70 of the Branch of Seismology. Files can be transferred quickly between the two machines.

[6] Graphics on the UNIX system have been improved with the addition of a fast and easy to use program. This new software allows plotting of data in various forms including the System's special data base form as well as universal ascii data. In addition, the software has been expanded to incorporate map projections used in real-time seismic and low frequency data display. This new graphics software is machine-independent as well as (graphics) device independent. Therefore, in an effort to standardize software we have installed this package on the Office's VAX 11/780 machine as well as both UNIX computers.

[7] The project continues to develop color graphics and color hardcopy capabilities for use in real-time seismic displays. Using the advanced graphics software with color graphics devices we have demonstrated our real-time seismic and low frequency data monitoring ability to visiting government officials, scientific investigators, and public interest groups.

[8] Real-time monitoring of designated suites of instruments in particular geographical areas is now operational. Terminals may to be dedicated to real-time graphics displays of low frequency data plotted as a time series or seismic data plotted in map or cross-sectional view. For additional clarity these plots can be optionally displayed in color.

[9] Retrieval of GOES satellite telemetry data from various locations in Alaska and California has been automated with the development of new software and dial-out capabilities on the PDP 11/44. This allows increased flexibility in timely data acquisition, as well as a higher quality of data reception.

INTERPRETATION OF DATA
14-08-0001-21243

David D. Jackson
Institute of Geophysics and Space Physics
University of California
Los Angeles, California 90024
(213) 825-0421

REFRACTION ERROR IN SOUTHERN CALIFORNIA LEVELING

Refraction error in leveling depends on sight length, elevation difference, and the second vertical derivative of temperature. NGS and USGS conducted a refraction experiment from Saugus to Palmdale in California, during 1981. The total elevation difference over the 45km profile is about 536m; estimates of this quantity by long and short sight-length surveys differ by 38mm. The mean temperature T, and its first and second vertical derivatives T' and T", were estimated from measured temperatures at 0.5, 1.5 and 2.5m above the ground.

Furthermore, the refraction error can be estimated well using T' or T in place of T", and the observed regression coefficients agree with theory. Refraction corrections using observed temperatures or gradients reduce the residual error to less than 10mm for the refraction test. Observed temperatures on pre-1978 surveys might be used to make reasonably accurate refraction corrections. Uncorrected refraction, rod calibration errors, subsidence and junction point instability can account for the previously reported "aseismic uplift" in Southern California.

TECTONICS AND TEMPERATURE EFFECTS IN TRILATERATION DATA

We examined trilateration data from the USGS Palmdale, Hollister, Salton, and Loma Prieta networks for evidence of temperature dependence and time dependent bias. We fit the data for each line with the regression equation

$$l(j) = l(0) + a\,t(j) + b\,T(j) + e(j)$$

where j is a time index, l(j) and T(j) are the observed line length and temperature at time t(j), and e(j) is a random error. The trend a, and the temperature sensitivity b were determined by least squares. Many lines showed significant temperature dependence. The temperature sensitivity decreases with line length, from 0.13 mm/deg at 6 km to -0.39 mm/deg at 40 km. We suggest that this temperature sensitivity reflects a systematic measurement error. A few lines showed extreme and highly significant temperature sensitivity, near + or - 1 mm/deg, possibly caused by thermal displacement of the monuments. The average residual over all lines was significantly negative during the time period from 1977.5 to 1979.5, suggesting a time dependent bias. The estimated linear trend for each line was hardly affected by the temperature sensitivity or the temporal bias. Thus these possible errors should not influence any estimates of secular strain rate, especially shear strain rates, if the temperature has a small trend. However, these and other systematic errors could partly explain the apparent

episodic dilatations at Palmdale and Hollister reported by Savage et al. (1983)

BAYESIAN ADJUSTMENT OF TRILATERATION DATA

We adjusted the 1977 line length data for Hollister including prior elevation estimates as data. The final elevations indicate a residual correction resulting from errors in the reported elevations. The rms elevation correction is about 0.6m. The rms line length residual is 1.5mm, consistent with experimental precision.

Using a similar adjustment procedure, we adjusted the temperature sensitivities of the lines at Hollister and Palmdale. Our model includes an additive temperature dependent bias, a uniform thermal expansion proportional to line length, and temperature dependent displacements specific to each station. For Palmdale we find a significant bias term of 0.137+0.007 mm/deg. For Hollister we find a bias term of 0.035+/-0.087 mm/deg, not significant but consistent with the Palmdale value. At Hollister, monuments show significant temperature dependent displacement (up to 0.9mm/deg) but not at Palmdale. The uniform thermal expansion was not significant at either network. The temperature dependent bias and the thermal displacement of some monuments may partly explain the apparent episodic dilatations reported for Palmdale and Hollister.

INVERSE DISLOCATION MODEL FOR HOLLISTER TRILATERATION DATA

We developed a systematic method for analyzing trilateration data on the basis of a new algorithm of nonlinear inversion. Aseismic crustal deformation associated with strain accumulation on a plate boundary is modeled by a relative block motion and a negative dislocation on the locked part of the boundary. We applied the method to the trilateration data (1971-1978) of the Hollister network which spans the Sargent, Calaveras and San Andreas faults in central California. We estimated the rate of relative motion between the Pacific and North American plates to be 44 mm/yr in a direction N34!0W. For every segment, the predominant fault motion is right-lateral strike slip on a nearly vertical plane. Tectonic stress caused by the relative plate motion appears to be rapidly accumulating on the Sargent fault, which is locked to a depth of 2.5 km, and on the southern segment of the Calaveras fault, locked to a depth of 15 km.

TILT, STRAIN, AND MAGNETIC MEASUREMENTS

9960-02114

M.J.S. Johnston, R. Mueller, C. Mortensen
D. Myren, A. Jones and V. Keller
Branch of Tectonophysics
U.S. Geological Survey
345 Middlefield Road, MS/77
Menlo Park, California 94025
(415) 323-8111, ext. 2132

Investigations

1. To investigate the mechanics of failure of crustal materials using deephole and surface strainmeters, tiltmeters and arrays of absolute magnetometers.

2. To investigate real-time records of these and other parameters for indications of incipient failure of the earth's crust.

Results

1. As part of the current Scientific Exchange Program between the United States and the Peoples Republic of China, arrays of differential magnetometers and intermediate-baseline geodetic lines have been installed at the northern end of the Red River fault in Yunnan Province and on the Da chang fault near Beijing. Since 1980, all lines in the arrays at Dengchaun and Liantie to the north of Er Hai Lake in Yunnan Province show compression of between 1 and 6 ppm. This appears to result from almost equal parts of right-lateral shear and negative dilatation. 2σ for these data is 3.6 ppm. Magnetic measurements in the high magnetization environment on the west side of the fault show an increase in local magnetic field of as much as 5 nT over sites on the east side of the fault at Dengchaun. An earthquake M_L 4.9 occurred at Madaoyu on December 10, 1982. This is just north of Beijing and within 20 km of the array on the Da chang fault where 5 days of data were recorded in early October, 1982. Differences in the data taken before and after the earthquake show changes from -1.4 to 2.9 nT.

2. The measurement precision of the U.S. Geological Survey proton magnetometer (PM) array in central California was determined using self-calibrating rubidium magnetometers (SCRs) having 10 times greater acccuracy. It was found that sensitivity to transient magnetic events with periods less than 4 minutes is 20dB greater for the SCRs than for

the PMs. This presents an opportunity to improve the sensitivity to short period events by an order of magnitude. In addition, instrument precision and local noise are determined from short baseline tests in Colorado. It is found that the high frequency local noise is 30 dB below the PM noise for periods less than one hour. For periods greater than two hours and site separations of 10 km, externally fluctuations in geomagnetic field limit the measurement precision of both SCRs and PMs.

3. Ten years of continuous strain data have been obtained on an extensometer installed in the Presidio near San Francisco at a distance of 8 km from the San Andreas fault. The instrument is 14.4 m long and measures strain with a differential capacitance type of displacement transducer. It is mounted in an old ammunition bunker at a depth of about 10 m below ground surface. The mean compressive strain rate obtained by a least-square linear fit to these data is 0.245 μstrain/year. While this is in good agreement with the geodetically determined regional strain rate for this area, more variable results are obtained with this type of instrument at sites quite close to the fault. The main features of the data other than the linear strain change are earth tides and teleseisms in the short term, and an annual variation which is most likely of topographic and thermoelastic origin. Noise power decreases from -100 dB at a period of 100 days (0.01 c.p.d.) to -150 dB at a period of several hours (10 c.p.d.). Since these and other data are comparable to the best obtained in aseismic areas from either down-hole strainmeters or long-baseline strainmeters with evacuated travel paths, and since spectra from other areas are much worse, we conclude (1) the spectrum of crustal noise has apparently a strong spatial dependence, (2) this spatial dependence may result from geometry, geology and the effect of meteological parameters, (3) the spectrum from instruments at depths of 10 meters or greater, is likely to be quieter than that obtained near the surface of the earth.

4. Continuous measurements of near-field tilt (4 instruments) and strain (1 instrument) was obtained at a sensitivity of less than 0.01×10^{-6} prior to the 1983 Coalinga earthquake ($M_L = 6.7$). Near-field dilational strain (3 instruments) has previously been reported for the 1978 Izu earthquake ($M_L = 7.0$). The state of strain during the last few hours to the last few seconds is remarkably noneventful in both cases after earthtides and other periodic signals have been removed. Large-scale strain redistribution at longer periods may occur and, if so, could be used for prediction of earthquakes but resolution at these longer periods is uncertain. Final failure apparently occurs in a small

localized zone(s) that rapidly expands, triggering failure over the entire rupture plane. Simultaneous brittle failure of the entire hypocentral area seems unlikely.

5. Much effort this summer has been required to complete installation of two 3-component strainmeters constructed by M. Gladwin of the Physics Department at the University of Queensland and several Carnegie dilatometers.

6. Measurements of charge-drop size distributions in active thunderclouds indicate that electrostatic forces become important in controlling drop size distributions. In highly charged regions of thunderclouds, electrostatic forces on individual drops will exceed surface tension forces, making large drops unstable and inhibiting particle growth. With the neutralization of charge accompanying a lightning stroke, droplets will grow rapidly and a rain gush will ensue.

Reports

Dvorak, J., Okamura, A.T., Johnston, M.J.S., Mortensen, C.E., Mueller, R.J. and Furukawa, Tiltmeter and Magnetometer Measurements on Mt. St. Helens, Washington: 1980-1981, USGS Open File Report 83- .

Johnston, M.J.S., 1983, The Approach to Catastrophic Crustal Failure - Inference from Two Earthquakes with M_L > 6.5., Trans. A.G.U. (in press).

Johnston, M.J.S., Chen, Z., Jiang, K., Mueller, R.J., Keller, V.G., and Zhan, Z., 1983, Magnetic and Fault Crossing Geodetic Arrays in the Peoples Republic of China, Trans. A.G.U., (in press).

Jones, A.C. and Johnston, M.J.S., 1983, Continuous Strain Measurements at the Presidio, California: 1973-1983, Trans. A.G.U., (in press).

Lockner, D.A., Johnston, M.J.S., and Byerlee, J.D., 1983, Charge Density, Drop Size, Lightning, and Rainfall Gushes, Nature (in press).

Ware, R.H., Johnston, M.J.S., and Mueller, R.J., 1983, The Detection Threshold for Short Period Seismomagnetic Events, J. Geomag. Geoelec. (in press).

Cooperative Study of Short Term Precursors to the Songpan-Pingwu Earthquakes of August 1976 in Sichuan Province, China

14-08-0001-20620

Lucile M. Jones and Egill Hauksson
Lamont-Doherty Geological Observatory of Columbia University
Palisades, New York 10964
(914) 359-2900

Investigations

Analyze and interpret the seismicity and possible precursory activity associated with the Songpan-Pingwu earthquakes in Sichuan, China.

Results

The precursory swarm, three mainshocks (M = 7.2, 6.7, 7.2) and aftershocks of the Songpan earthquakes have been reanalyzed using both local and teleseismic data. The three mainshocks of this sequence occurred on the Huya fault over a seven day period. Relocations of the aftershocks using local arrival times show that three fault strands were activated during this sequence. Each mainshock occurred on a separate strand, each one south of the strand activated in the previous mainshock, and the aftershock zones of each mainshock appear to abut rather than overlap. Fault plane solutions determined by matching teleseismic P-waveforms at WWSSN stations with synthetic seismograms are consistent with the observed aftershock zones. The first and third mainshock (M_o = 1.3 x 10^{26} and 8.4 x 10^{25} dyne-cm, respectively) showed almost identical senses of motion, a combination of reverse and left-lateral strike-slip motion, on parallel strands, striking N 15° W, that were separated by a large right-stepping en echelon offset. The second mainshock (M_o = 4.0 x 10^{25} dyne-cm), occurred in this offset on a fault at an angle of 125° to the other two strands and showed almost pure reverse motion. Differences in the orientations of the slip vectors of the three mainshocks show that the first mainshock increased the normal and shear stresses on the fault segment that moved in the second mainshock and that the second mainshock decreased the normal stress on the fault segment activated by the third mainshock. These changes in normal stresses may have given rise to the longer time between the first and second events (5 days) as compared with the time between the second and third events (30 hours). A precursory swarm that preceded the Songpan sequence by three years occurred in a volume that surrounded the northernmost part of the planar aftershock zone. The time between the start of the swarm and the mainshocks and the magnitude of the largest event in the swarm are similar to those seen for precursory swarms in Soviet Central Asia.

Reports

Jones, L.M., W. Han, E. Hauksson, A. Jin, Y. Zhang, and Z. Luo, Focal mechanisms and aftershock locations of the Songpan earthquakes of

August 1976 in Sichuan, China, submitted to J. Geophys. Res., 1983.

Jones, L.M., W. Han, E. Hauksson, A. Jin, Y. Zhang, and Z. Luo, Focal mechanisms and aftershock locations of the Songpan earthquakes of August 1976 in Sichuan, China, submitted for 1983 Fall AGU Meeting, 1983.

FAULT ZONE WATER AND GAS STUDIES

9960-01485

C.-Y. King
Branch of Tectonophysics
U.S. Geological Survey
345 Middlefield Road, MS/77
Menlo Park, California 94025
(415) 323-8111, ext. 2706

Investigations

1. Water temperature and radon content were continuously monitored at two water wells in San Juan Bautista, CA. A third continuous radon monitor was installed at another well (Limekiln A) where gas bubbles out nearly continuously.

2. Water level was continuously recorded at seven other wells.

3. Water samples were periodically taken from most of these wells for chemical analyses.

4. A laboratory faulting model was reconstructed and a series of experiments were run.

Results

Several large impulsive increases in radon emanation were recorded by two of a set of four continuous radon monitors deployed in a closely spaced linear array of shallow holes, which crossed a creeping section of the San Andreas fault at Melendy Ranch in central California. Each of these radon increases lasted for less than a few hours, similar in appearance to the spiky radon changes in ground waters observed in China. One of the increases was followed 10 hours later by a local creep event of 2.6 mm. Another increase occurred at about the same time as a magnitude 3.4 earthquake about 40 km away. A third increase was followed by a magnitude 3.3 earthquake the next day 5 km away. No impulsive radon increase was recorded during another creep event of 2.3 mm nor at the time of two other earthquakes of comparable magnitude (3.0, 3.1) and distance. The observed radon increases may be the result of a sudden burst of ground gas triggered by crustal deformation or vibration.

Reports

King, C.-Y., 1983, Impulsive radon emanation on a creeping fault [Abst], EOS, Trans. Am. Geophys. Un., in press.

Air-gun Seismic Velocity Measurements

9960-02413
Hsi-Ping Liu
Branch of Tectonophysics
U. S. Geological Survey
345 Middlefield Road, MS-77
Menlo Park, California 94025

Investigations

1. Tidal stress variation of seismic traveltimes in shallow crust.

2. Elastic properties of rocks: development of a method to determine quasi-statically the absolute strain on the order of 10^{-8} - 10^{-7} in rock samples under uniaxial compression. This method is to be used for determining the effects of cracks and rock fabric on the elastic anisotropy and, by comparison with ultrasonic velocity measurements, determine the Young's modulus dispersion. (In collaboration with Lou Peselnick 9960-01490)

Results

1. Precise seismic traveltime measurements over a period of 48 hours from August 18 to August 20, 1983 have been conducted at the Le Masurier granite quarry in North Chelmsford, Massachusetts in order to compare results with those obtained by Reasenberg and Aki (1974). A 656 cm^3 air gun fired in a mud-filled pit 2 m deep provided a repeatable seismic source. Seismic trveltimes along three baselines, one of which, the South-East line, coincides with that chosen by Reasenberg and Aki (1974), were determined by subtracting the traveltime to a seismometer located ~ 5 m from the source from the traveltime recorded by the seismometer located at the far end of the baseline ~ 200 m from the source. Details of instrumentation and data reduction techniques have been described previously (Liu et al., 1983). Data analysis has been carried out for the first P-arrival with a velocity of 5.5 km/s and for a later arrival with a phase velocity of 1.7 km/s over the South-East baseline which shows traveltime constant to ± 0.1 ms ($|\Delta t/t| < 4.5 \times 10^{-3}$ for the first P-arrival and $|\Delta t/t| < 9.8 \times 10^{-4}$ for the later arrival) for the first 12 hours for both these phases. Data reduction for the remaining 36 hours of data and for the other 2 baselines are currently under progress.

2. Work is continuing on the apparatus which measures quasi-statically the Young's modulus of rocks at small strains (10^{-8} - 10^{-7}). A single crystal quartz rectangular plate oriented to generate piezoelectrically a pure longitudinal displacement along its maximum plate dimension has been tested satisfactorily as a displacement calibrator. As a result, strains as small as 2×10^{-8} can be measured reliably on rock samples 3.81 cm x 15.24 cm long. Work is currently

under progress to achieve a state of uniform compression by loading the sample ends with hydrostatically generated pressure.

References Cited

Liu, H.-P., R. E. Westerlund, and J. B. Fletcher, Precise measurement of seismic traveltimes - investigation of variation from tidal stress in shallow crust, Geophys. Res. Lett., 10, 377 - 380, 1983.

Reasenberg, P., and K. Aki, A precise continuous measurement of seismic velocity for monitoring in situ stress, J. Geophys. Res., 79, 399 - 406, 1974.

Report

Liu, H.-P., R. E. Westerlund, and J. B. Fletcher, Precise measurement of seismic traveltimes - investigation of variation from tidal stress in shallow crust, Geophys. Res. Lett., 10, 377 - 380, 1983.

HIGH SENSITIVITY MONITORING OF RESISTIVITY AND SELF-POTENTIAL VARIATIONS IN THE HOLLISTER AND PALMDALE AREAS FOR EARTHQUAKE PREDICTION STUDIES

Contract No. 14-08-0001-19249

P.I.: T.R. Madden
Department of Earth, Atmospheric, and Planetary Sciences
Massachusetts Institute of Technology
Cambridge, MA 02139
(617) 253-6384

We are continuing our monitoring of telluric signals on the Hollister and Palmdale arrays (Fig. 1) in order to observe resistivity and self-potential changes and to study their association with earthquake phenomena. The entire Palmdale data set has been reprocessed and the results are presented in Fig. 2. The data were first edited to remove data points that appeared to hold non-stationary or non-Gaussian noise. The remaining data was analyzed in terms of two reference dipoles C and D, and the variations of the principal reference eigenvector are plotted. Actually the plot shows the variations in the C and D contributions separately, but since only one eigenvector is used the variations are correlated. The editing did not use any a priori bias and the analysis for the principal eigenvector did not use any damping so we believe the resistivity variations inferred from the variations in the analysis results, excepting for dipoles A and F, are representative of the true resistivity variations. Dipoles A and F use telemetering links which have not performed completely satisfactorily and most of the large variations shown are associated with high noise levels.

Dipole H has remained very stable during the entire period. Some small jogs in 1978 and 1979 are associated with changes in the recording arrangements and probably represent errors in the old calibration system. One can probably state that dipole H has remained constant relative to dipole D to within 0.1% for more than 5 years. Dipoles B and E show variations of $\pm$ 0.3 to 0.5% during 1978-1980 which though at times of lower data quality seem to be real. Since 1981 only a drift is seen which appears to be about 0.2%/year. These changes can be attributed either to changes in the Mohave region perpendicular to the fault or to changes along the fault. The data from dipoles A and F are not very satisfactory but the net change for dipole A during this 5-year period is probably within 1%. Dipole G is constructed from C and D and is therefore only a test of the electronics. Before 1982 it was not even recorded and is purely ficticious. The relative dipole amplitudes have not been corrected for their pre-amp gains, which are 10, 5, 3, 1, 2, 10, 1, and 1 for dipoles A, B, C, D, E, F, G, and H, respectively.

At present we have no reason to believe that anomalous changes are occurring in the Palmdale region. The Hollister data was also reprocessed but here we are having more noise problems associated with new electrodes installed in 1982. We are presently trying to separate out this electrode noise from the telluric signals.

Fig. 3 shows the first three years of digital data from Hollister. Changes of about 0.5% can be seen in early 1980 which must be due to dipole A. The only other significant changes are slow changes of 0.3 to 0.4% on dipoles F and H that might represent some recovery from effects associated with the Coyote Lake event and subsequent creep. Unfortunately we do not have earlier data for these dipoles and the changes are barely discernable in the noise. The preamp gains which are reflected in the relative dipole amplitudes shown are 1, 10, 10, 2, 10, 10, 2 and 10 for A through H, respectively.

The second reference eigenvector variations are not shown since they are noise-dominated, but they also show systematic variations which we do not fully understand at present. We believe these variations are associated with finite source wavelength effects and we are investigating if the telluric relationships between Palmdale and Hollister can be used to correct for this effect.

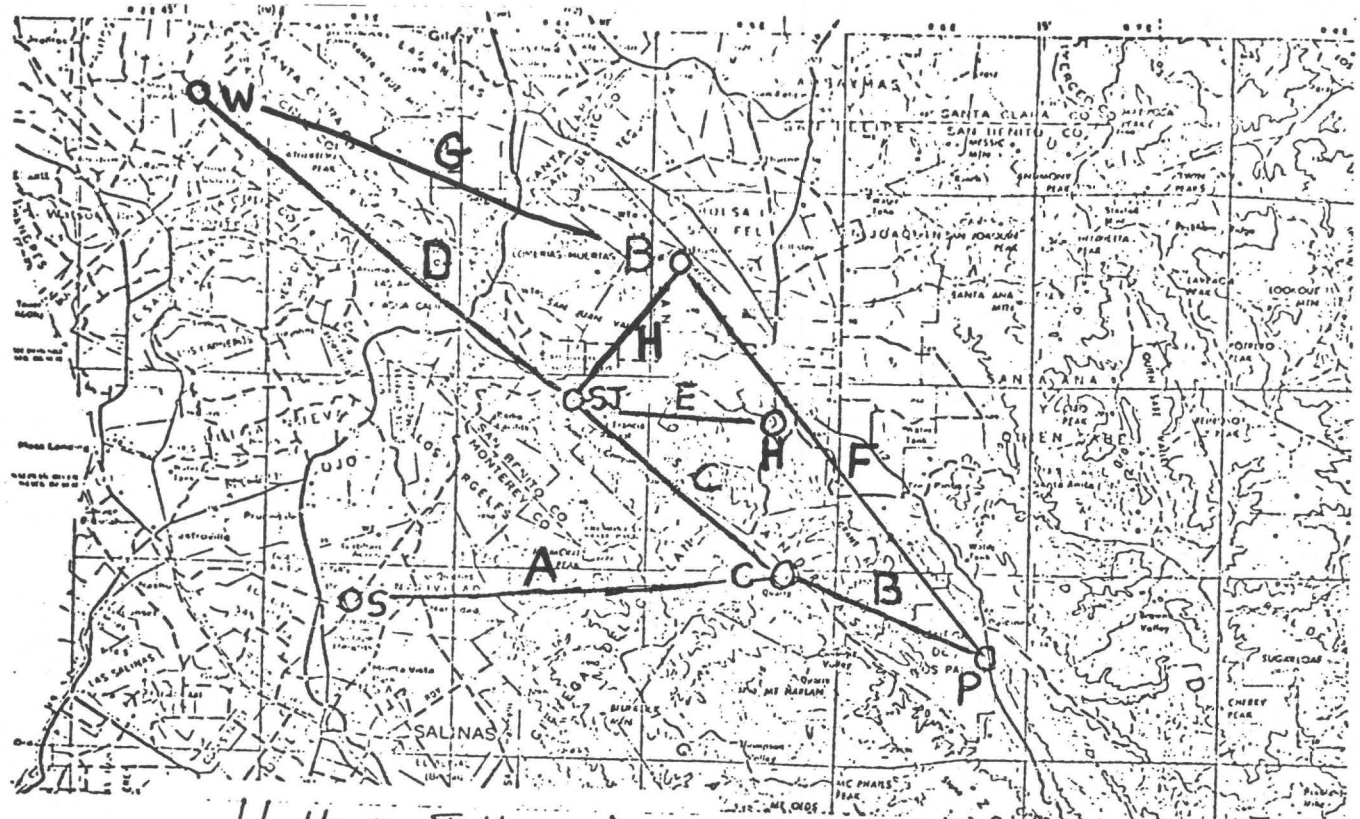

Hollister Telluric Array

Palmdale Telluric Array

Fig 1

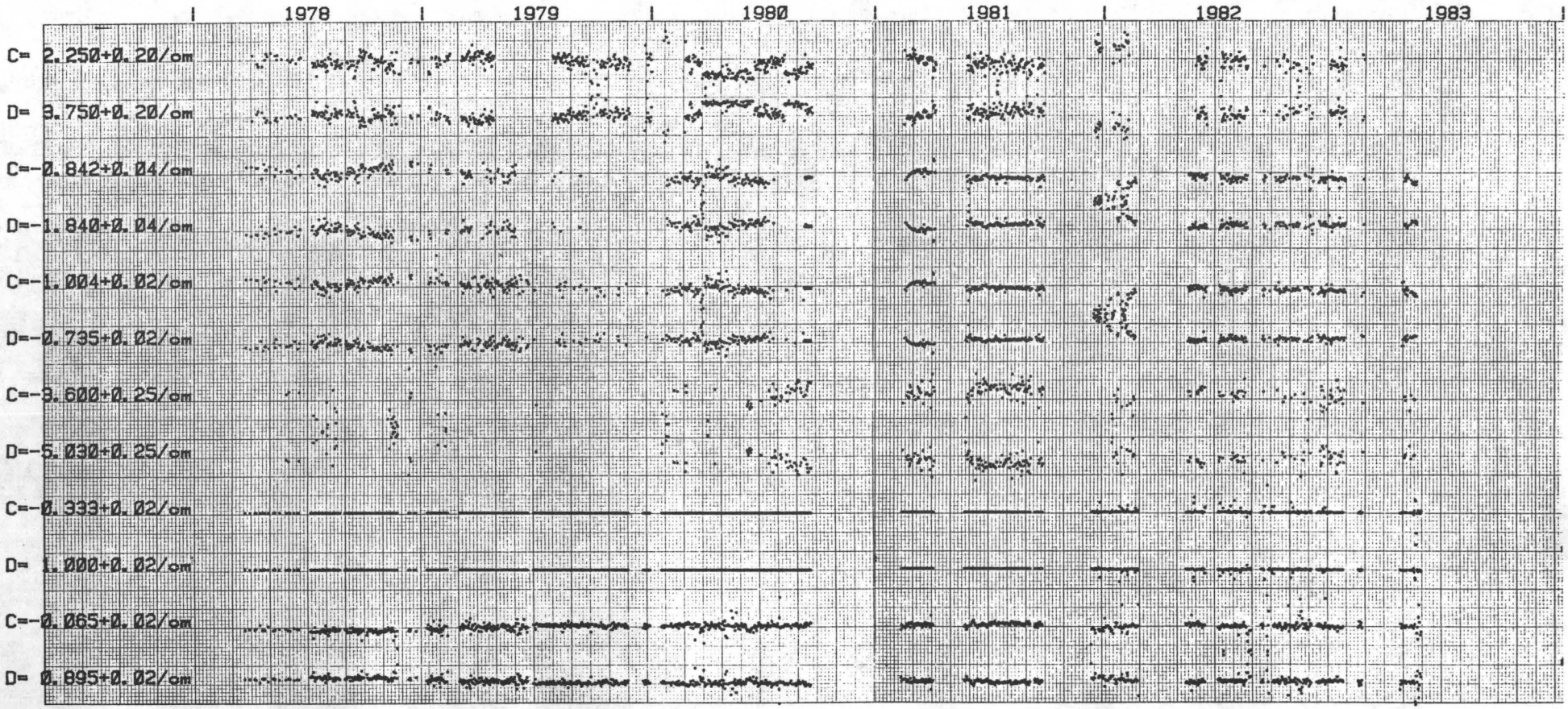

357

Palmdale Telluric Array Resistivity Variations

each point represents analysis of 24 hours of data

horizontal scale 6days/smallest division

vertical scale 0.2%

except for A&F 0.5%

P2

Fig. 2

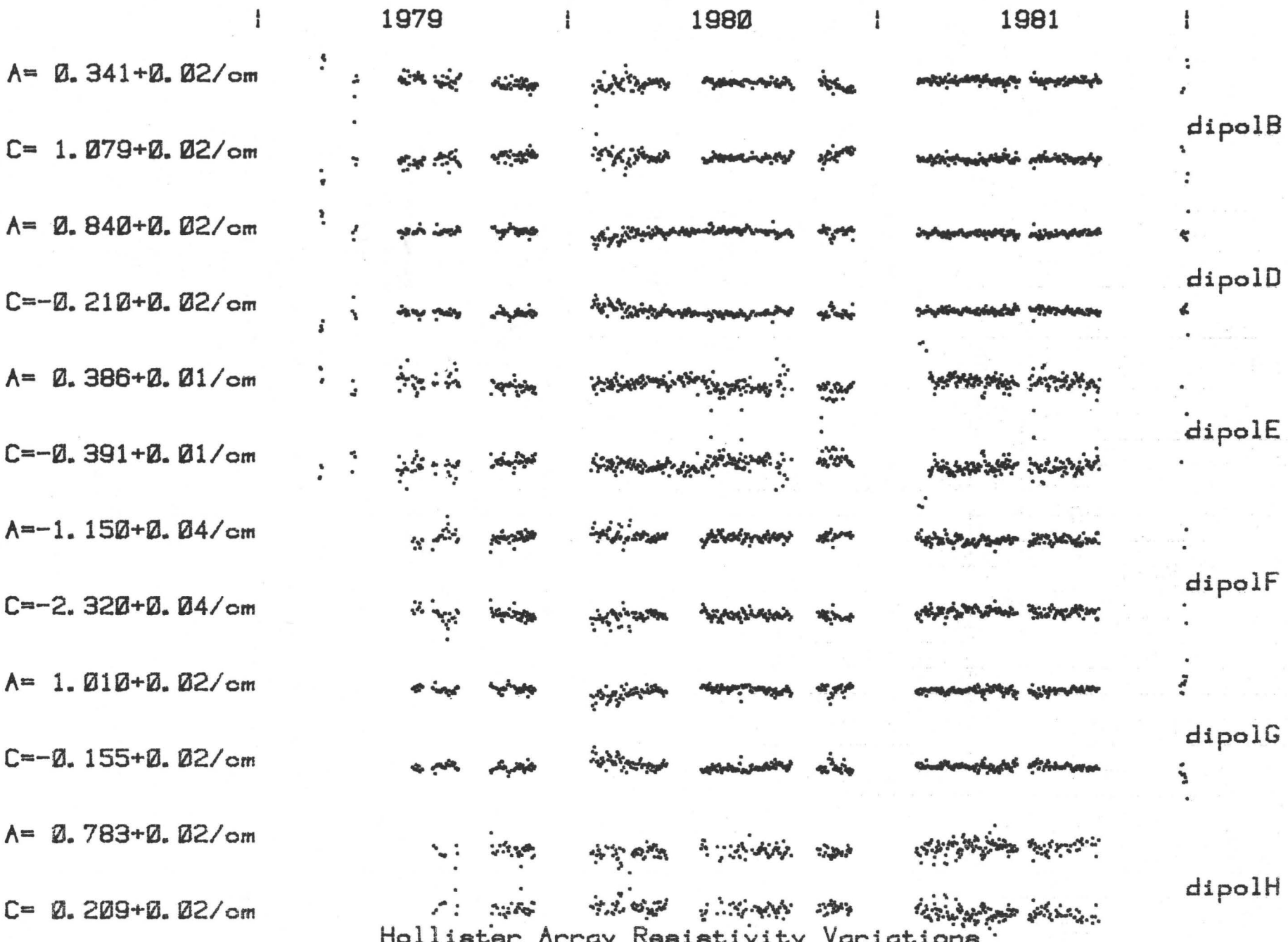

Hollister Array Resistivity Variations

Fig 3

FAULT ZONE TECTONICS

9960-01188

Gerald M. Mavko, Beth D. Brown, Sandra S. Schulz
Branch of Tectonophysics
U.S. Geological Survey
345 Middlefield Road, MS/77
Menlo Park, California 94025
(415) 323-8111 x 2756, 2763

Investigations

1. Maintained and upgraded creepmeter arrays in California.

2. Updated archived creep data on PDP 11/44 computer.

3. Developed experimental procedures aimed at an operational prediction program.

4. Monitored and modeled effects of 1983 Coalinga earthquake sequence on creep along the San Andreas fault.

5. Established an alinement array network on central and northern California faults.

Results

1. Currently 28 extension creepmeters operate; 22 of the 28 have on-site strip recorders; and 18 of the 22 are telemetered to Menlo Park (locations shown on Figure 1). A new creepmeter was installed on the Hayward Fault in Berkeley.

2. Fault creep data from all 28 USGS creepmeter sites on the San Andreas, Hayward and Calaveras faults have been updated (through September 1983) and stored in digital form (1 sample/day).

3. More frequent examination of daily creepmeter data has begun in order to document and analyze the relation between fault creep and earthquakes. This was prompted by (1) the accumulation of nearly 15 years of creepmeter data, (2) the increased occurrence of moderate central California earthquakes, and (3) our desire to develop imputs to an operational prediction program. Experimental algorithems are being tested against past creep data to identify possible anomalies preceding earthquakes.

4. USGS creepmeter along the San Andreas fault in central

California recorded coseismic steps at the time of the Coalinga earthquake on May 2, 1983. Steps range in size from 0.1 mm to 8.7 mm. All the coseismic steps were right-lateral except for the southernmost two sites (Gold Hill, Twisselman Ranch) near the southern end of the creeping fault. Additional coseismic steps were observed with some of the larger aftershocks. Creepmeters on the San Andreas fault near Parkfield (Slack Canyon southward to Twisselman Ranch) have shown slower than average creep rates since the May 2 earthquake. At two of the sites (Slack Canyon and Middle Mountain) the slow rates are unprecedented in our recording history. At the remaining sites the slow rates resemble seasonal patterns but are more pronounced than in the past. Comparison of the creep data with dislocation models suggests that the coseismic steps were induced by coseismic accelerations. The residual slow rates indicate a static strain change from the Coalinga events, but a quantitative measure of the change can be made only after the resumption of normal slip.

5. Currently 17 alinement arrays (locations shown in Figure 2) have been established and surveyed across active faults in central and northern California. Each site will be remeasured approximately every 120 days. The arrays will be used for siting and checking creepmeters as well as for monitoring fault creep where creepmeters are impractical or logistically impossible. Expansion of the alinement network will continue as is practical. Results are being computed and analyzed. A program is being written to allow processing of data by the computer.

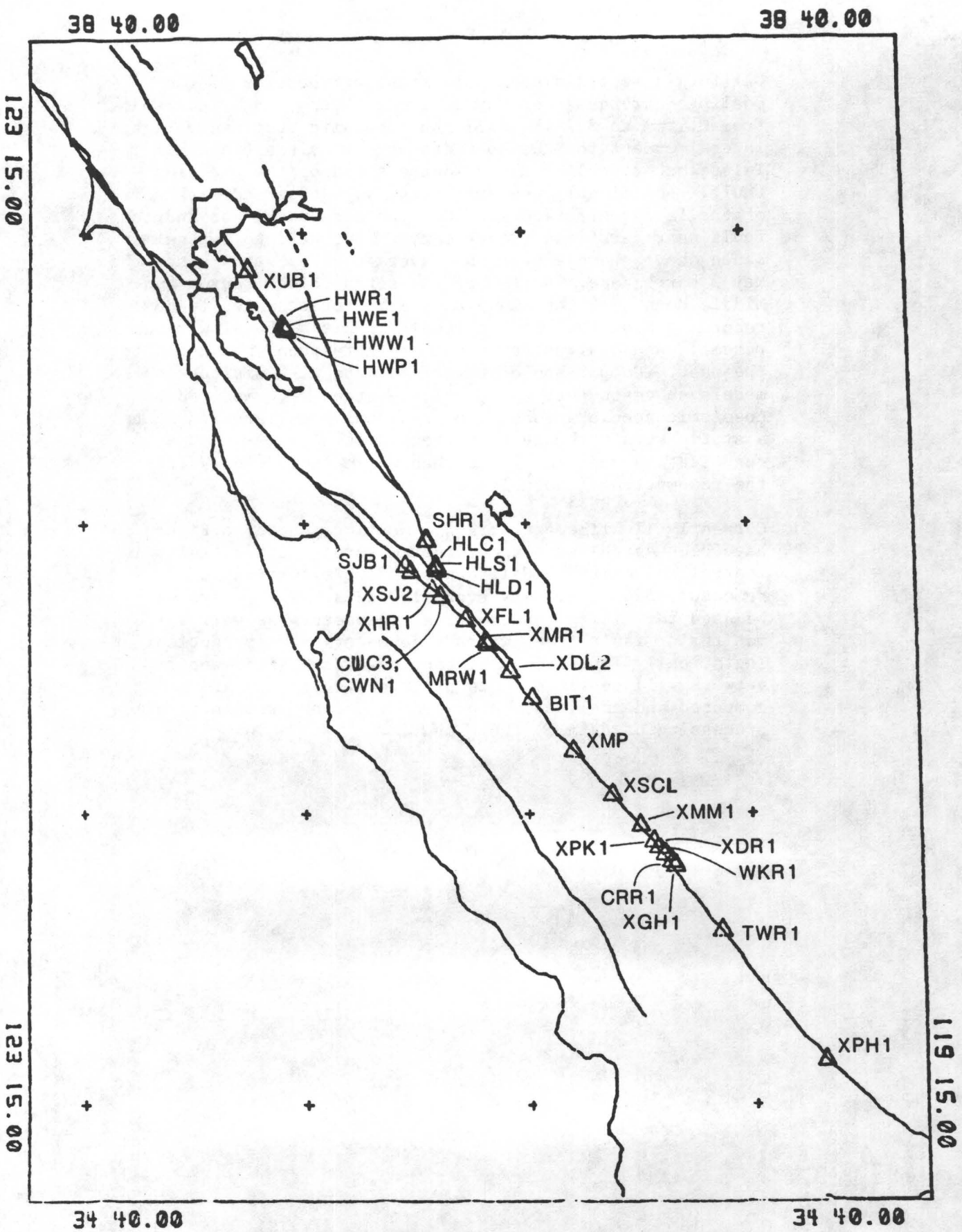

Figure 1 - USGS CREEPMETER LOCATIONS IN CENTRAL AND NORTHERN CALIFORNIA.

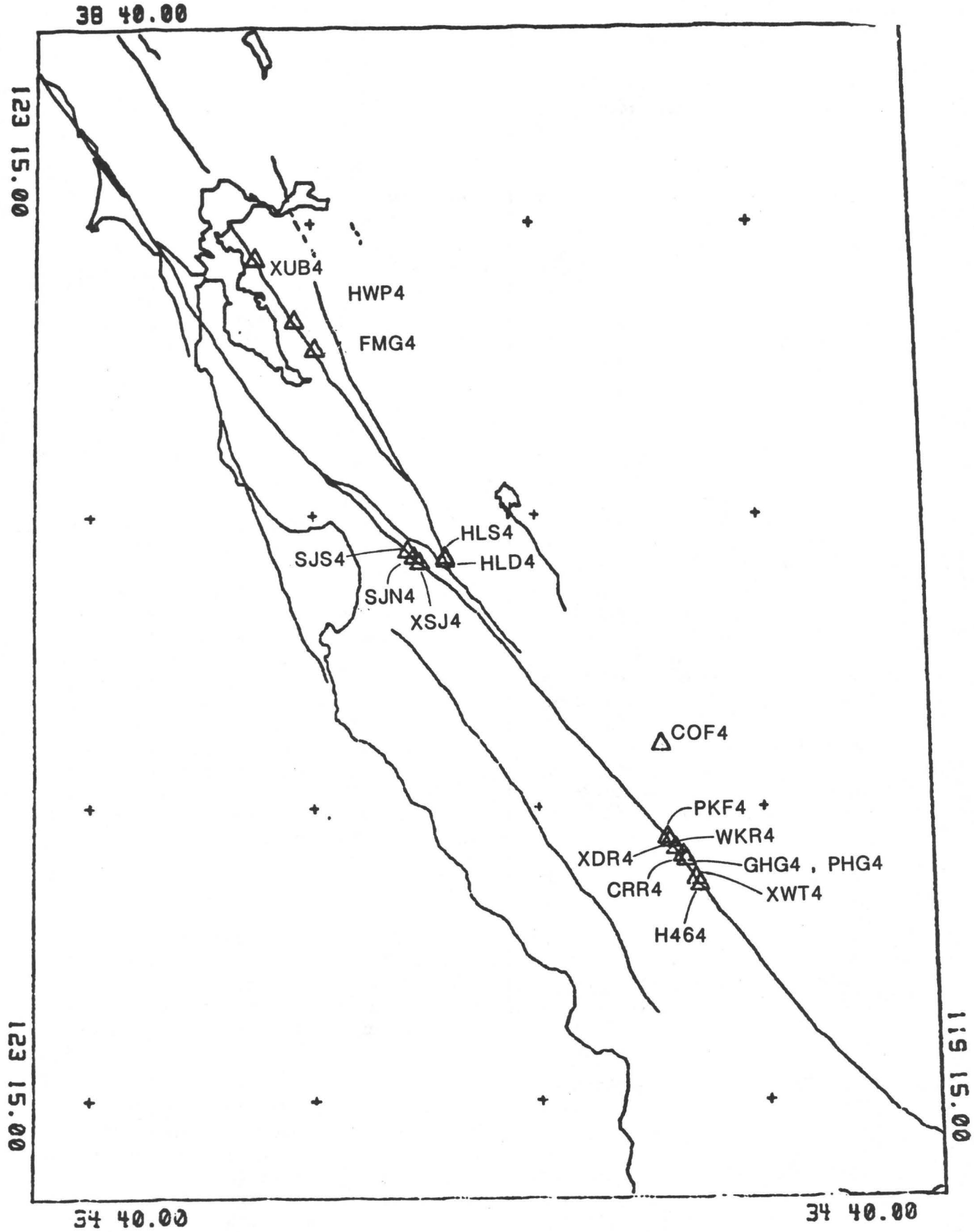

Figure 2 - U.S.G.S THEODOLITE ALINEMENT ARRAYS ACROSS MAJOR FAULTS IN CENTRAL AND NORTHERN CALIFORNIA

Seismicity Studies for Earthquake Prediction in Southern California Using a Mobile Seismograpic Array

14-08-0001-20546

Karen C. McNally
Earth Science Board
University of California, Santa Cruz
Santa Cruz, California 95064
(408) 429-4136

INVESTIGATIONS

During the time period of this report, we have concentrated our efforts on the rupture mechanism and seismicity patterns preceding the Coalinga, California earthquake. This event is significant for earthquake prediction studies both by virtue of its size (M_L = 6.7) as one of the larger recent earthquakes in California, and due to the pattern of earthquake clustering from 1975 to 1982 which surrounded the subsequent rupture zone (McNally and McEvilly, 1975; Eaton, 1983). Currently we are documenting the details of this sequence (Beroza et al., 1983, Sherburne and McNally, 2983; Sherburne et al., 1983; Rial and Brown, 1983; Brown and McNally, 1983). The patterns of prior seismicity and rupture mechanism will then be compared with other earthquakes in California, as well as large thrust earthquakes in Mexico, in order to determine the influence of tectonic environment vs. mainshock rupture mechanism on the process of strain accumulation and release, as inferred by the prior seismicity patterns in time, space, and fault mechanism.

RESULTS

Within 24 hours of the May 02, 1983 Coalinga earthquake the University of California, Santa Cruz and California Division of Mines and Geology combined efforts and equipment to install a dense, 13 station aftershock array within a radius of 25 km of the epicenter. Data from this array shows a number of interesting spatial and temporal characteristics of the aftershock zone.

The mainshock faulting mechanism has been determined by Rial and Brown, 1983, Eaton, 1983, Hartzell and Heaton, 1983 to have a strike N 58 W to N 60 W while the trend of the entire aftershock zone determined by this array is more northerly at about N 35 W. The size and spatial definition of the aftershock zone changed markedly during the time of our observations, however. Prior to 40 hrs after the mainshock the activity ($M_L \geq 3$) is distributed in a relatively small region 5 km NW and 5 km SE of the mainshock, with a steep dip down to the NE, and a

strike of about N 60 W. This suggests bilateral rupture of the mainshock and a stress drop of about 100 - 150 bars. Within the following 44 hrs (a) the initial N 60 W zone extends an additional 5 km to the NW. (b) Scattered smaller events occur at S 25 E from the mainshock epicenter at a distance of 5 to 10 km. Twelve to 14 days after the mainshock a secondary zone breaks the region between initial rupture and the events to the south, along a trend of S 25 E. Additional differences between the NW and SE sections of the aftershock zone are: Depths along the NW half of the aftershock zone range from about 3 km to 12 km. Most of the larger events ($M_L \geq 4.0$) occur in this area. In contrast, depths along the SSE half of the aftershock zone range from about 5 to 8 km. Aftershocks in this area are primarily of magnitude less than 4.0. Prior seismicity (Beroza et al, 1983) shows the NW half of the aftershock zone to have been devoid of earthquakes (magnitude ≥ 3.0) since 1930 while the SSE area showed a swarm of activity with largest event $M_L = 4.7$ in the early part of 1976. Intense swarm activity also occurred 10 km NW of the aftershock zone in 1975 with largest events $M_L = 4.9$ and 4.5 (McNally and McEvilly, 1975).

REPORTS

Manuscripts

Beroza, G. C., E. Brown, and K. C. McNally, Report to: Southern California Data Review Group.

Rial, J. A., and E. Brown, Waveform modeling of long period p-waves from the Coalinga earthquake of May 2, 1983, California Division of Mines and Geology Special Reports, in press.

Sherburne, R., K. C. McNally, E. Brown, and A. Aburto, 1983, The mainshock-aftershock sequence of 2 May 1983: Coalinga, California, Calif. Div. Mines and Geology Spc. Rpt., in press.

Sherburne, R. W., and K. C. McNally, 1983, CDMG-UCSC aftershock studies, Coalinga, California Earthquake, May 2, 1983, Eqke, Eng. Res. Inst. Spc. Rpt., in press.

Brown, E., K. C. McNally and J. A. Rial, Aftershock Sequence of the May 02, 1983 Coalinga Earthquake: Details of the Rupture Process, J. Geophys. Res., manuscript in preparation.

Abstracts

Brown, E., K. C. McNally and J. A. Rial, 1983, Mainshock-aftershock sequence of the May 02, 1983 Coalinga Earthquake: Details of the Rupture Process, EOS Trans., AGU, in press.

Deardorff, D. G. and K. C. McNally, 1982, Seismic slip patterns of three possible asperities in California, EOS Trans., AGU, 63, 1030.

Delsemme, Jacques, 1983, Migration of moderate earthquakes in Central California, Earthquake Notes, Seismological Society of America, 54, 38.

Hydrological/Geochemical Monitoring Along San Andreas and San Jacinto Faults, Southern California, During Fiscal Year 1983

P. M. Merifield and D. L. Lamar
Lamar-Merifield Geologists, Inc.
1318 Second Street, Suite 25
Santa Monica, California 90401
(213) 395-4528
Contract 14-08-0001-20660

Investigations

Water levels in more than thirty wells along the San Andreas and San Jacinto fault zones were monitored during the current reporting period. Water levels in seven wells, barometric pressure at three wells and temperature and conductivity at one well were monitored by the Caltech Remote Observatory Support System (CROSS). Another ten wells were monitored continuously with Stevens Type F recorders, two being maintained by W. R. Moyle, Jr., of the Geological Survey. The remaining wells were probed monthly, weekly, semiweekly or daily with the aid of volunteers. Water-level data are displayed on computer-generated hydrographs for each well. Rainfall and earthquakes are plotted on the graphs for direct comparison with water levels. Temperature, salinity, and conductivity were measured in ten selected wells at the time the water-level charts were changed, and radon was mesured in one well by the Track Etch technique.

Results

No earthquakes of M 3.0 or greater occurred in the past twelve months within 13 miles (20 km) of an observation well along the Palmdale-Valyermo segment of the San Andreas fault. The largest event along the San Jacinto fault zone was M 4.1 on 8 January 1983 about 24 miles (38 km) northwest of our nearest observation well with a continuous recorder in San Jacinto Valley. Other events of M 3.0 - 3.7 occurred as close as 3.7 miles (6.0 km) to our observation wells. Neither the long-term hydrographs nor the continuous records show any variations which are interpreted to be precursors of these earthquakes.

Comparison of rainfall data and the times of water-level spikes in well 5N/12W-14C1 south of Palmdale indicates that all but two of the spikes may be explained by rainfall. Previously, these spikes had been tentatively interpreted as caused by tectonic creep events. Flooding, and complete filling of well 11S/8E-33P1, Ocotillo Wells, occurred in August 1983 during a rainstorm. Thus, a previously reported rise in July 1979 was probably also due to a rainstorm, rather than a possible precursor of the M 6.6 Imperial Valley earthquake of 15 October 1979 (Merifield and Lamar, 1981). During early 1983 water levels in well 5N/10W-30L1 in the Valyermo area rose abruptly, like a similar rise in early 1979 (Fig. 1). Thus, we have less reason to believe that the 1979 rise was related to a change in crustal strain pattern, as previously suggested (Merifield and Lamar, 1981).

These new interpretations demonstrate the necessity for long-term records to understand the significance of water-level changes. As the recording period increases, so does our confidence in identifying anomalous water-level changes which may be precursors of earthquakes.

Reference

Merifield, P. M. and D. L. Lamar, 1981, Anomalous water-level changes and possible relation with earthquakes: Geophys. Research Letters, v. 8, p. 437-440.

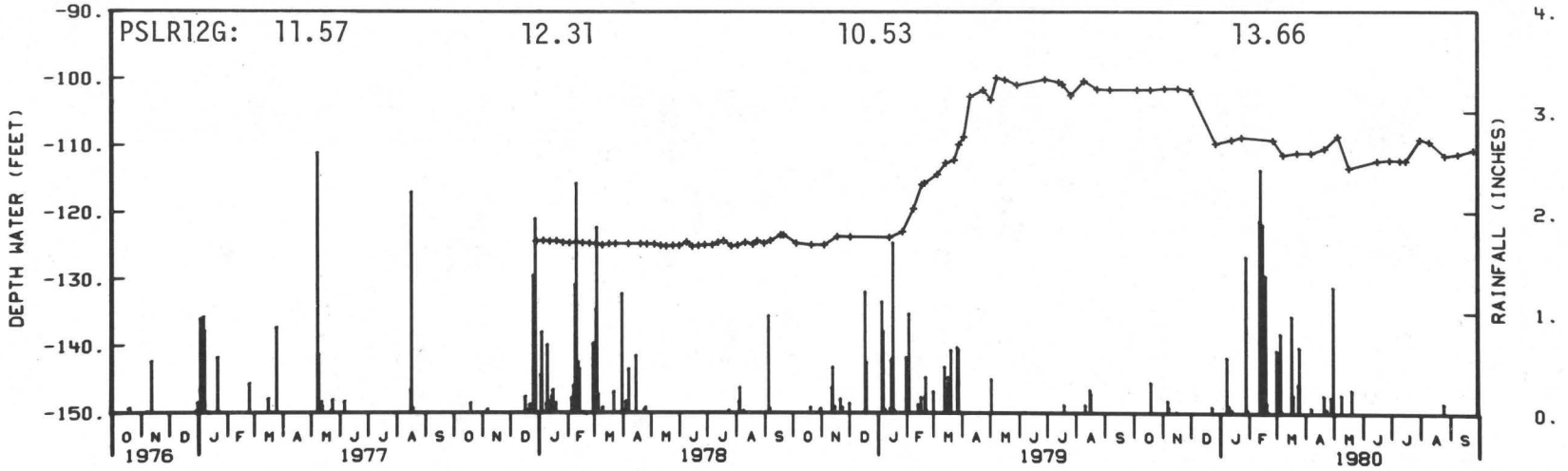

FIGURE 1A -- WEEKLY OBSERVATIONS OF WATER LEVEL (+) AND RAINFALL (.) IN WELL NUMBER 05N/10W-30L01 DURING 1976-1980, VALYERMO AREA
SEASONAL RAINFALL AT ADJACENT STATIONS IN INCHES ACROSS TOP

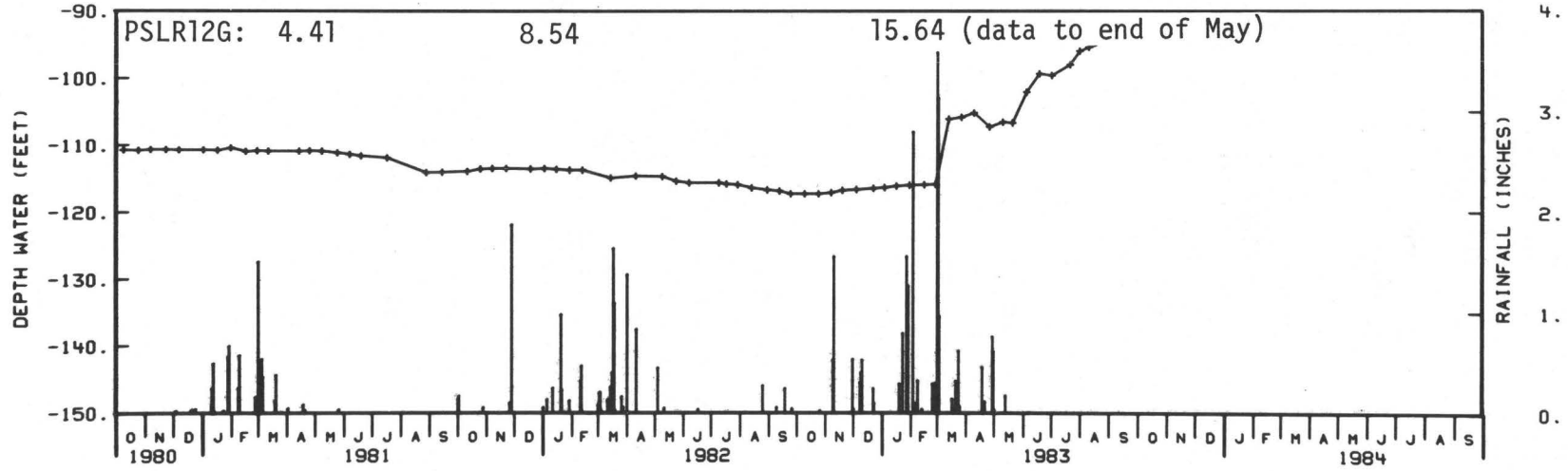

FIGURE 1B -- WEEKLY OBSERVATIONS OF WATER LEVEL (+) AND RAINFALL (.) IN WELL NUMBER 05N/10W-30L01 DURING 1980-1984, VALYERMO AREA
SEASONAL RAINFALL AT ADJACENT STATIONS IN INCHES ACROSS TOP

PSLR12G: Average rainfall 1976-83: 10.95

Tiltmeter and Earthquake Prediction Program in S. California and at Adak, AK

14-08-0001-21244

Sean-Thomas Morrissey
Saint Louis University
Department of Earth and Atmospheric Sciences
P.O. Box 8099 - Laclede Station
St. Louis, MO 63156
(314) 658-3129

I: Task 1: The Tiltmeter System

Objective: To continue to improve the performance of bubble-sensor tiltmeter systems and to investigate alternative methods of detecting tilt in moderate depth boreholes, with low-cost, readily deployed instrumentation.

Accomplishments: The new tiltmeter electronics has proved quite reliable and consistent in its performance with regard to a temperature stability of 3 to 5 nanoradians/^{o}C. All eight tiltmeters at Adak have been upgraded by installing the new electronics unit, with notable improvements in long term stability. Figure 1 is a sample of the Adak South site, West tiltmeter data around the time the electronics was changed. Notice the thermal contamination on the left, and the relatively clean earth tide data on the right. The six predominant earth tide harmonics are readily resolved by spectral analysis of the data.

In other improvements, a gearmotor driven zeroing potentiometer is being evaluated in place of the Heath servo motor, which has been a point of weakness in the system. The gearmotor potentiometers have counter dials that will read directly in net tilt in nanoradians. Also, due to a lightning strike at Adak in late January that disabled almost everything, a report "Field Servicing of Tiltmeter Systems" was prepared to enable our local observer to make diagnostics and repairs, since there were no travel funds to go there. It is specifically designed for servicing units equipped with the new electronics. A circuit card equipped with two edge meters plugs into the front pc socket of the mother board and provides all the system diagnostics. Our observer was able to get all 8 tiltmeters operating again using the Service Guide to localize failed circuit cards and replace them. Net tilt values with respect to the zero tilt "bubble box" were also obtained.

II: Task 2: The Installation Method

Objective: To improve the installation methods for borehole instruments, with a goal of installing them as deep as 100 meters.

Accomplishments: After several experiments in a "simulated" 30 cm diameter by 10 meter deep hole at the CCMO test site, installations at that depth were determined to be feasible, with the bubble sensor mounted to the new tapered housing that engages the end of the installation control rod with a cable-released fitting. The only problem is that the 5%

hydraulic cement in the bonding sand makes dust that obscures the view of the downhole TV camera for about a minute. (The sand/cement is delivered through garden hoses to fixed fittings on either side of the tiltmeter installation hole; the water uses a third pipe.) It was also found that two tamping rods facilitated installation, since they did not have to be maneuvered around as much as a single rod.

Consequently, the holes for the tiltmeters at Adobe Mountain (3) and Saddleback Butte (2) were drilled in the Mojave Desert in April. These holes are 12" diameter to 35 feet, with an additional 3 feet of 4-1/2" hole for the tiltmeter. They are cased the first 12 feet, and the rest is in solid granite. The third site at Valermo proved unusable because of large gravel filled voids in the rock.

The installation tests at CCMO indicate that 10 meters is about the limit of being able to control the tiltmeter to within several ppm of vertical with the long control rod, so a biaxial gearmotor driven arrangement has been devised to warp a short section of rod above the tiltmeter. The system can be lowered by cable to any reasonable depth, and has a range of about ± 5 degrees, and a control resolution of about 5 ppm/sec. A prototype has been constructed.

III: Task 3: The Digital Data System

Objective: To continue to develop and operate a digital data acquisition system to acquire geodetic data and to thoroughly monitor the environment of the instrument installations.

Accomplishments: The digital data system at Adak continues to operate well. Much of it was damaged by the lightning strike, but repairs were made by shipping up replacement units. Although Adak has lightning rarely (last was in 1976), it does lots of damage because the volcanic soils do not provide a reasonable ground. Lightning suppressors were installed in all the FM and digital telemetry lines. These modules pass up to 5 volts of carrier, but will withstand 20 kv when tested with an electric fence transformer.

An experiment in heat flow measurement was installed in August 1982 at Adak, and the results were recently looked at. The sensor is a flat 3.5 cm x 3.5 cm array of thermopiles that produces 2.7 $(cal/cm^2 - hr)/mv$. It is buried 0.5 meter, and has a DC amplifier with a gain of 2 K. Figure 2 is a sample of the heat flow data plotted with some of the meteorology. Notice how it integrates the rainfall effects. Overplotted on Figure 2 is the companion tiltmeter data. Notice how the "bumps" in the tiltmeter data resemble those in the heat flow. An additional heat flow unit was installed in August 1983 at Adak. Two sensors will be used in the Southern California array.

The digital data system for Southern California is nearing completion. Without an existing observatory to be an "add on" to, the system has to be designed as a self-contained stand-alone system, complete with power control and timing systems, in addition to the receive/logging microcomputer. The system has been mounted in a large glass fronted stereo cabinet, and will be installed in the Visitor's Center at the

Saddleback Butte State Park.

Processing of the incoming data disks is kept current, with the raw data plotted the day it arrives (to stay on top of problems), and cummulative plots are made periodically. The water tide gauge at Adak has completed one year of operation with no problem. It is a self contained pressure gauge designed for remote shallow offshore installation. It has a range of 10 meters and a resolution of 1 mm, and compares exactly with the digital data from the NOAA standard bubble gauge.

IV: Task 4: Data Interpretation

Objective: To process the digital data and make efforts to remove the environmental noise from the data, so as to establish the intrinsic long term stability of the tiltmeters. Various analysis techniques are then utilized to present the data in the meaningful formats such that any precursory tilt events would become evident.

Accomplishments: At the suggestion of several colleagues at the last AGU meeting, the Adak tilt data was analyzed for variations in the amplitude of the M2 tidal harmonic. There is evidence that this will change in amplitude in response to changes in stress in the earth's crust in the near field of earthquakes. Although the tiltmeters were not really designed to record earth tides, but do (as a handy way of proving that they're working), and the earlier digital data had serious gaps because the receive microcomputer kept crashing, an analysis was performed anyhow, with no special effort made to clean up the data. Figure 3 shows the results of averaging the data from all 8 tiltmeters; earthquakes greater than m_b 4.5 within 100 km of the array are noted, with those with coherent co-seismic tilts asterisked. (No further co-seismic events have been detected since that reported last time on 04 June 1982.) Currently, the analysis procedure is being redesigned to clean up the data. Figure 4 is an example of how the earth tides are recovered from the raw tiltmeter data.

The long term stability of the tiltmeters is a major concern, and it is indicated in the cumulative data plots as in Figure 5, which shows more than two years of data from the East tiltmeter. The annual cycle is obvious, and the level agrees with the net annual tilt measured with regard to the electronically level "bubble box." Net annual (1982-1983) tilt (drift) averaged 12.1 ppm, with the most stable unit being the West site, west unit, at 1.8 ppm down to the NE.

Currently efforts are being made to remove the effects of thermal, barometric, and other measured environmental noises from the tiltmeter data. The analysis is utilizing Fourier transformations to the frequency domain. Once the environmental effects are removed, such as the obvious annual thermal cycle of Figure 5, the rate vector plots should show considerably more actual geodetic tilt activity that can be related to the larger near field earthquakes.

10/14/83

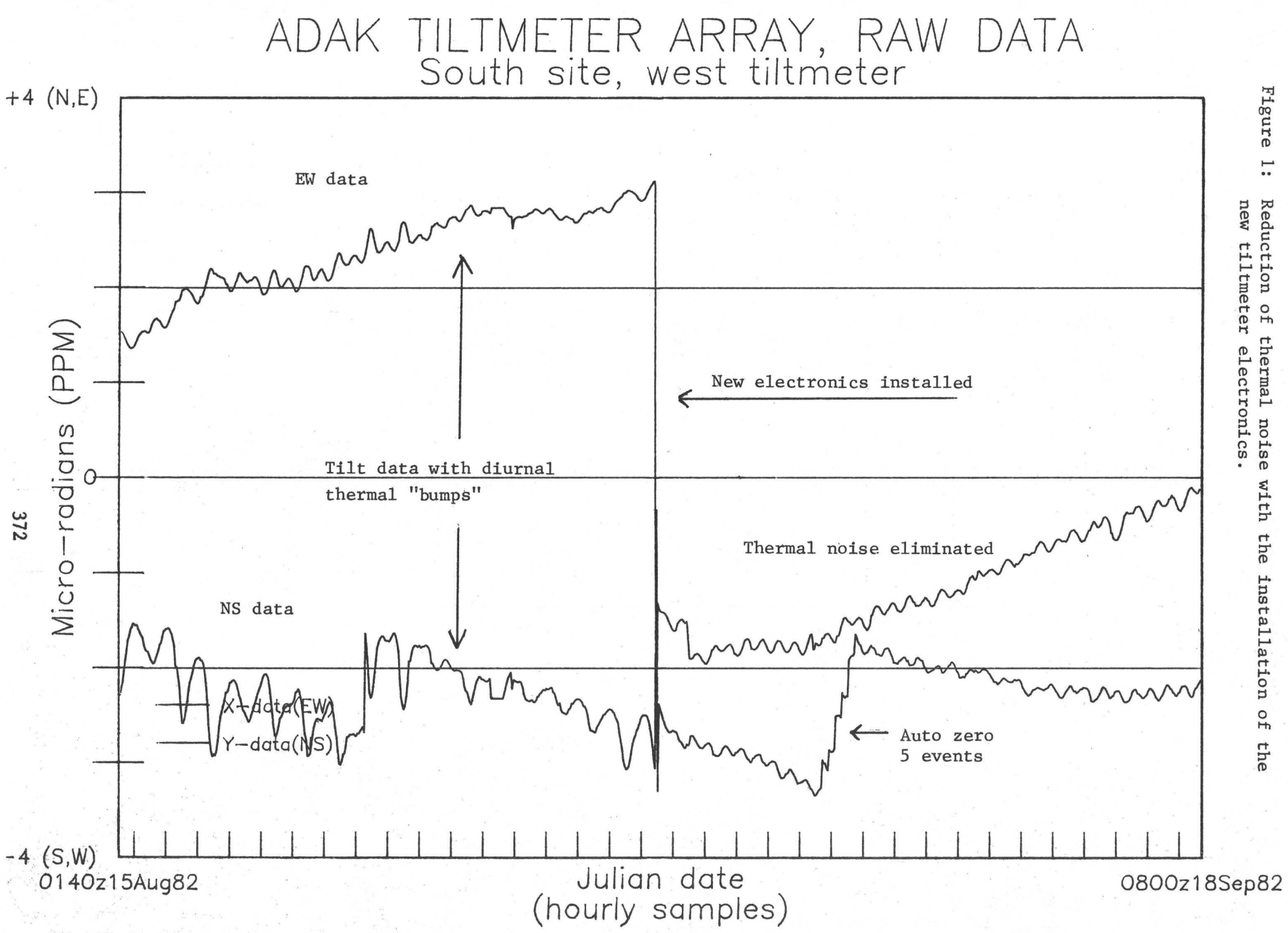

Figure 1: Reduction of thermal noise with the installation of the new tiltmeter electronics.

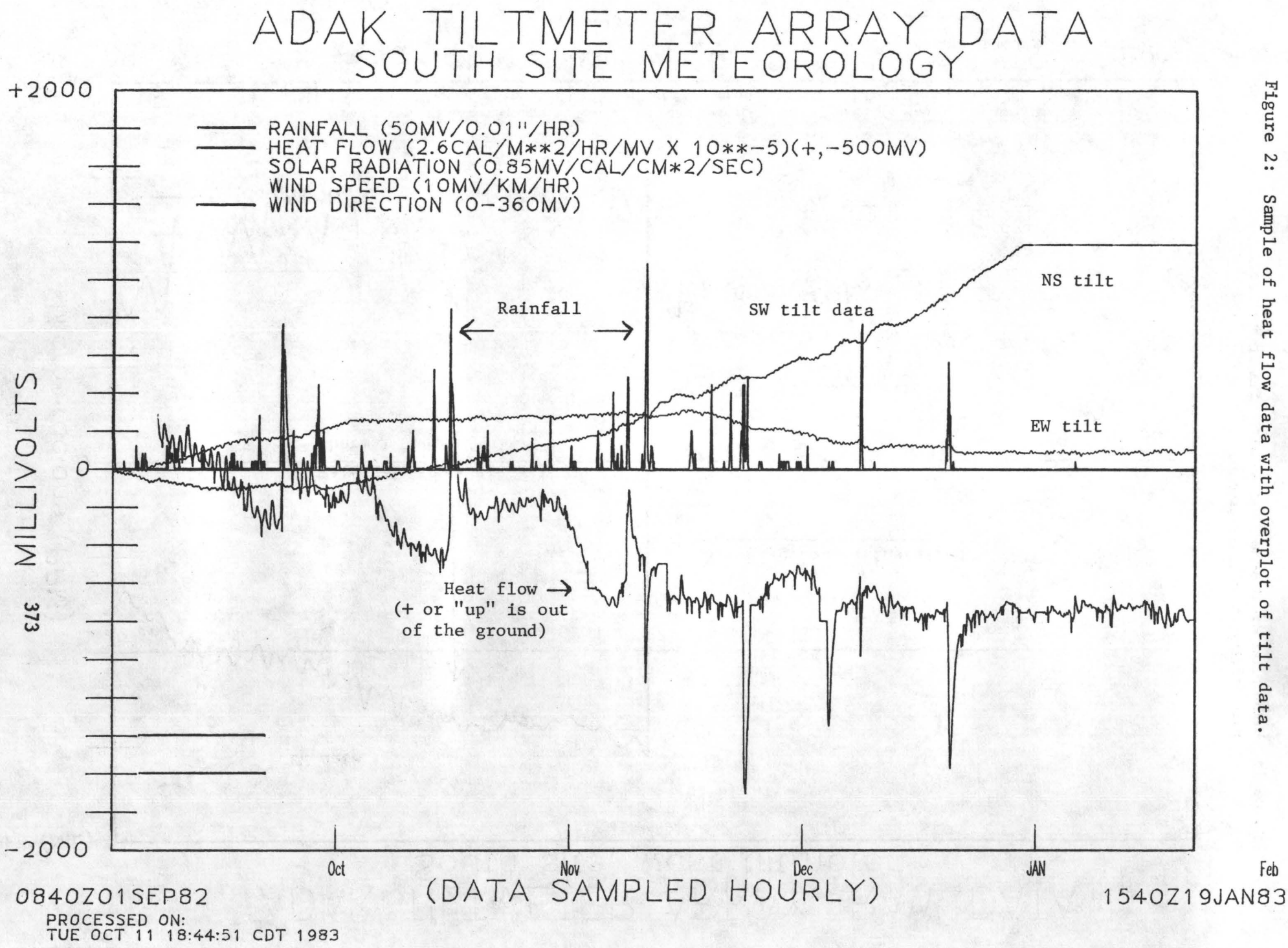

Figure 2: Sample of heat flow data with overplot of tilt data.

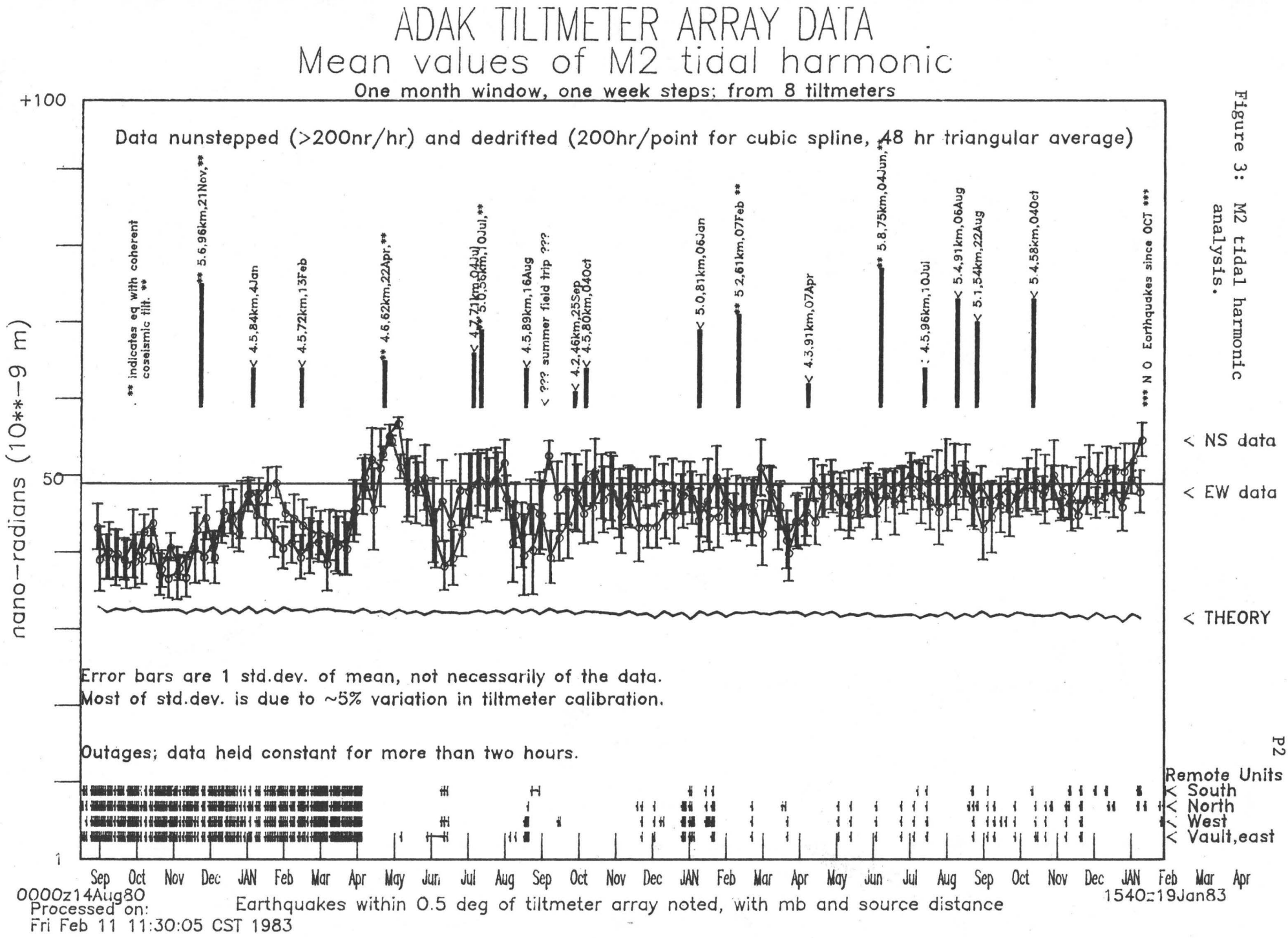

Figure 3: M2 tidal harmonic analysis.

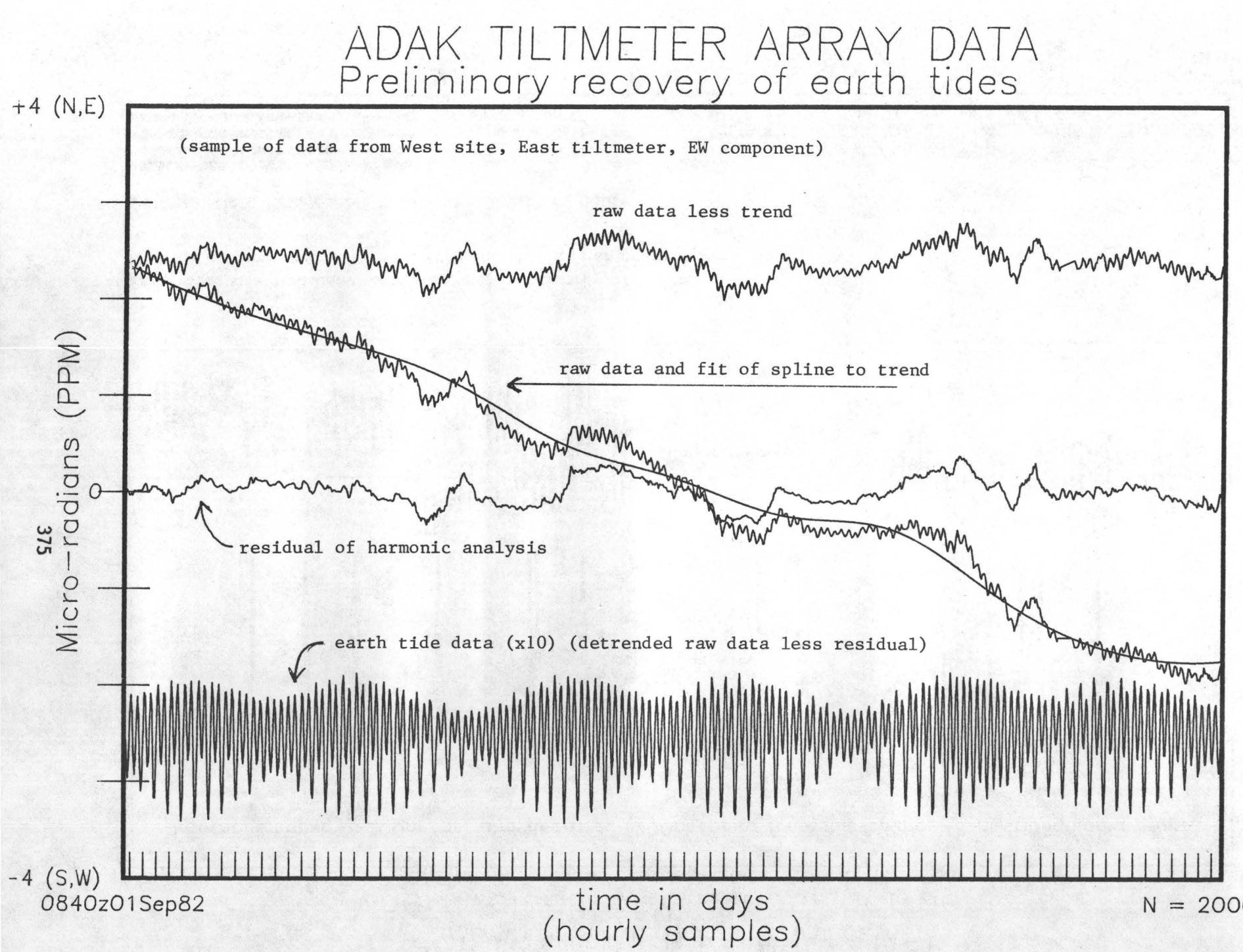

Figure 4: Samples of data in the process of recovering earth tides from borehole tiltmeters. (A special figure for the report; this data is generally not plotted.)

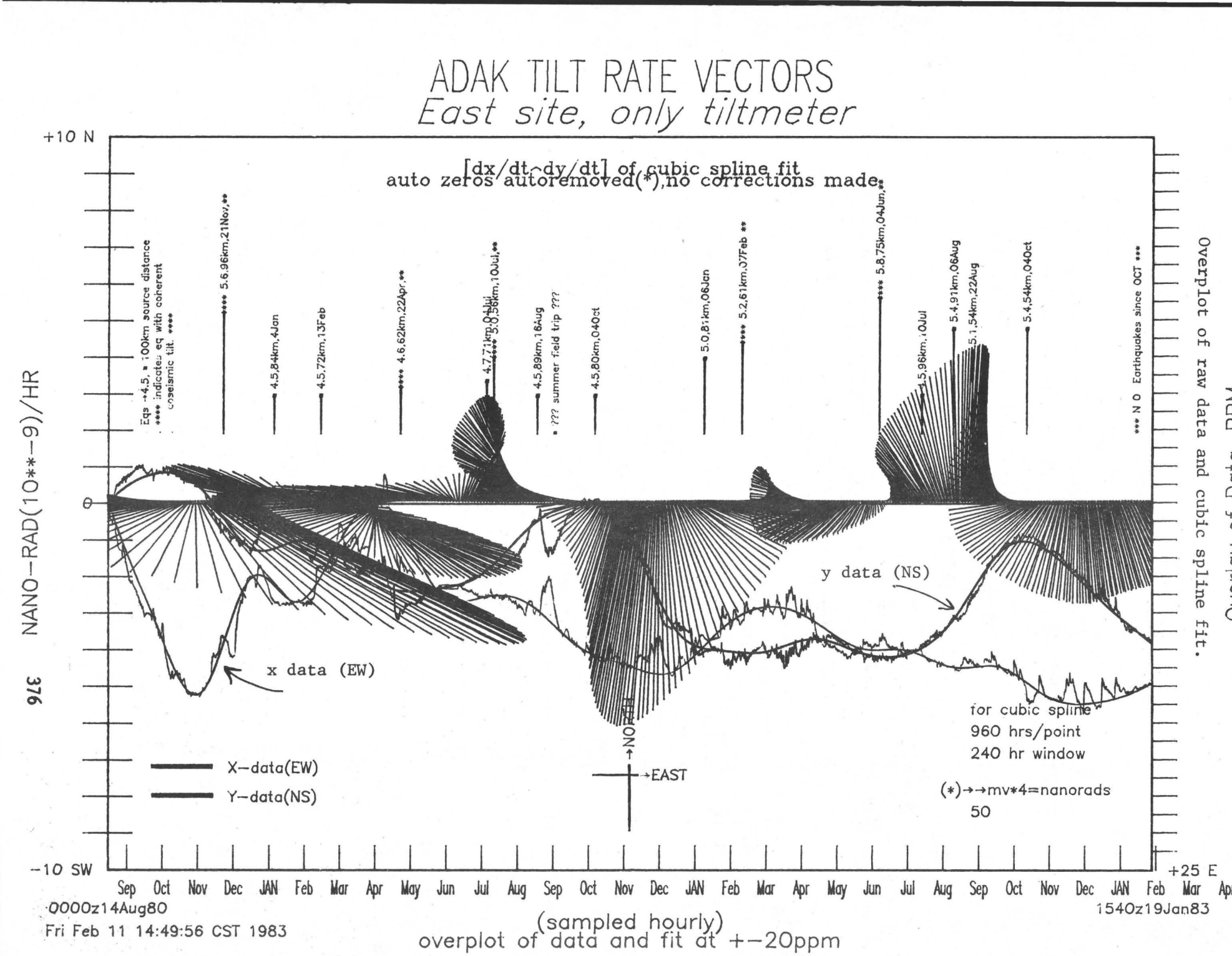

Figure 5: Tilt dynamics: plot of azimuth and amplitude of tilt change in time.

Overplot of raw data and cubic spline fit.

EXPERIMENTAL TILT AND STRAIN INSTRUMENTATION

9960-01801

C.E. MORTENSEN, G.D. MYREN, R.P. LIECHTI, AND V. KELLER
Branch of Tectonophysics
U.S. Geological Survey
345 Middlefield Road, MS/77
Menlo Park, California 94025
(415) 323-8111, ext. 2583

Investigations

1. This project operates and maintains a small network of shallow-borehole tiltmeters at 8 sites in central California. These instruments monitor crustal deformation in seismically active regions in order to detect changes in surface deformation that may be related to earthquakes.

2. Twelve boreholes having depths of 20 feet were drilled and readied for tiltmeters in the Long Valley caldera, near Mammoth Lakes, California. Two boreholes were drilled at each of six sites. The locations of the six sites were chosen to provide coverage of the resurgent dome area and the region of dense epicenters near the town of Mammoth Lakes, which may represent a possible position for future dike intrusion. At each site a Kinemetrics or Rockwell tiltmeter was installed at depths ranging from about 12 to 18 feet. Tiltmeters having somewhat greater dynamic range were also installed at each of the six sites by Jim Westphal of Cal Tech, who developed the instrument, and Dan Dzurisin of Cascade Volcano Observatory. Each tiltmeter site is bounded by or proximate to a level array of 100 to 500 m on a side. Data from the tiltmeters, along with temperature, will be telemetered by 12-bit digital telemetry to Menlo Park.

Results

1. The tiltmeter located near Mt. Hamilton, east of San Jose, California, recorded tilt signals that closely resembled signals observed on other tiltmeters at the times of nearby surface creep events. These signals were recorded on 28 April, 1 May and 5 May, prior to an earthquake (M_L = 3.5, on 19 May) in Halls Valley on the Calaveras fault, about 5 km from the tiltmeter. This observation was similar to two observations reported previously, but the quality of the observation was not as good because of a period of instrument malfunction prior to the onset of the

signals. If these observations continue to be repeated in the future there will be fairly compelling evidence suggesting a direct relationship between buried creep and earthquakes on this section of the Calaveras fault.

2. The first month of data, recorded onsite by stripchart, from four tiltmeters installed in the Long Valley caldera in August, showed that the instruments settled in very quickly. Solid earth tides can be seen in some portions of the records although the dominant signal is thermal or thermoelastic with diurnal periodicity. Figure 1 shows the locations of the tiltmeters with respect to the Long Valley caldera and some of the faults that exist within the region. The zone of epicenters during the January 1983 earthquake swarm was in the region around the Casa Diablo tiltmeters, labelled CA1 and 2 in Figure 1, the Valentine tiltmeters (VA1, 2 and 3 in Figure 1) and the Sherwin Creek tiltmeters (SH1 and 2). The resurgent dome is approximately centered on the Little Antelope Valley tiltmeters, labelled LA1 and 2 in Figure 1. For the period August 8 to September 22 the tiltmeters at Hot Creek, labelled HC1 and 2, recorded approximately 1 microradian tilt down to the northeast, an amount that is not significantly above the noise level for those instruments. The other instruments may still be undergoing a "settling in" period. Data from these instruments may be reliably interpreted by the time the telemetry installation is completed.

Reports

Mortensen, C. E., 1982, Short-term tilt events preceding some local earthquakes on the central Calaveras fault: additional evidence: in Proceedings, Conference on Earthquake Hazards in the Eastern San Francisco Bay Area 1982, California Department of Conservation, Division of Mines and Geology Special Publication 62, p. 289-298.

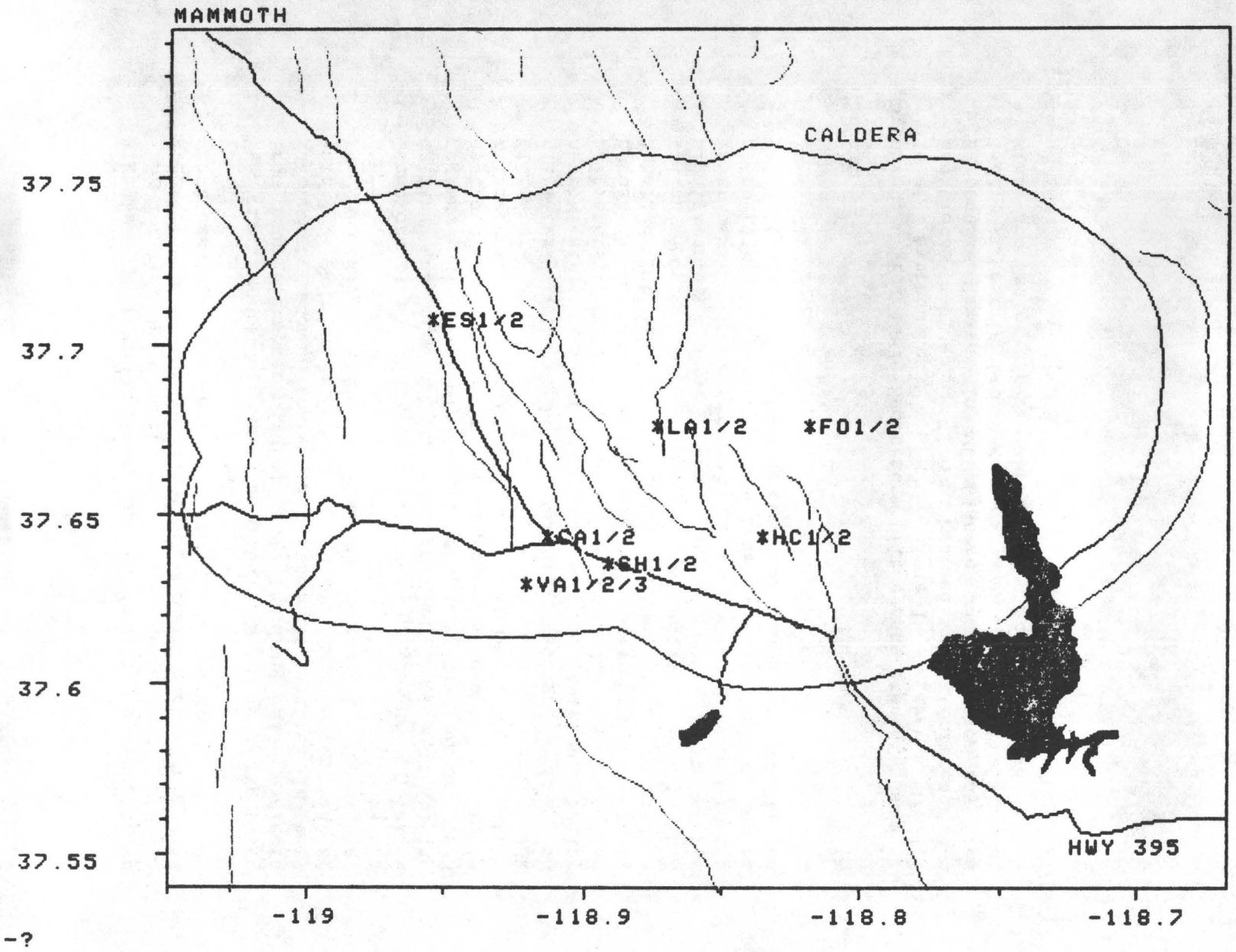
MAMMOTH
CALDERA
*ES1/2
*LA1/2
*FO1/2
*CA1/2
*HC1/2
*GH1/2
*VA1/2/3
HWY 395
37.75
37.7
37.65
37.6
37.55
-119
-118.9
-118.8
-118.7
P2
-?

Fault demarcation from helium soil-gas profiles near Oroville, California

9570-01376

G. M. Reimer
U.S. Geological Survey
Denver Federal Center, Mail Stop 963
Denver, Colorado 80225
(303) 234-5531

Investigations

A helium soil-gas survey was performed in May, 1983 near Oroville, California. The purpose of this study was to determine if the helium technique could delineate a northern extension of the Cleveland Hill Fault. Traverses were run over the area of the known fault, as defined by surface cracking and after-shocks following the August 1, 1975 earthquake, and the data compared to that for traverses run north of the known fault. A preliminary study in August, 1982 revealed a zone of higher soil-gas helium concentrations and it was this area in which sampling was conducted for the May survey.

Results

Six east-west traverses were run perpendicular to the trend of the known fault. Three were actually over the known fault and three were to the north in the direction of the Oroville Dam. Figure 1 shows the sample localities. The helium concentrations that are defined as anomalous, those being in the upper 10 percent or greater than 100 parts per billion above background for each traverse, are shown by larger circles. The distribution of these anomalous samples is diffuse in the southern traverses then diverges northward to define two trends, one a projection of the surface cracking, the other located several kilometers westward on the down dip side of the fault.

The location of the anomalous helium concentrations is consistent with a model illustrated by Figure 2. The fault acts as a conduit for the flow of gases. There may be some optimum thickness of ground cover for higher helium soil-gas concentrations; less cover results in more atmospheric dilution, more cover creates a greater dispersion volume for the gas. The fault may be a source of ground water recharge and an interaction of ground water and gas along the dip of the fault at depth may prevent higher helium concentrations from being observed in certain surface zones. Finally, seismic activity may have created subsurface fractures or regions of greater permeability facilitating vertical migration of gas.

Assuming a dip of 62° for the fault, the westward high-helium trend projects to the top of the aftershock zone (3 km depth) as depicted by Savage and others, 1975.

This survey revealed two very anomalous areas, shown by highlighted circles on Figure 1, where the helium excess in the soil-gas approached 10 times that of the other anomalous areas. Typically, these are concentrations that may be expected when sampling near natural gas pipelines; there is commonly a trace helium component in the methane. However, there were no evident markings that pipelines were present in the area. The exact source remains unexplained at this time.

The results of this study indicate that the soil-gas helium technique can be successful in tracing faults and that, in this case, there is the geochemical evidence that the Cleveland Hill Fault extends northward toward the Oroville Reservoir.

Reference

Savage, William U., Tocher, Don, and Birkhahn, P. C., 1975, Micro-aftershock study of the Oroville, California, earthquake of August, 1975 in Oroville, California, Earthquake 1 August 1975, Sherburne, R. W. and Hauge, C. J., editors, California Division of Mines and Geology Special Report 124, p. 123.

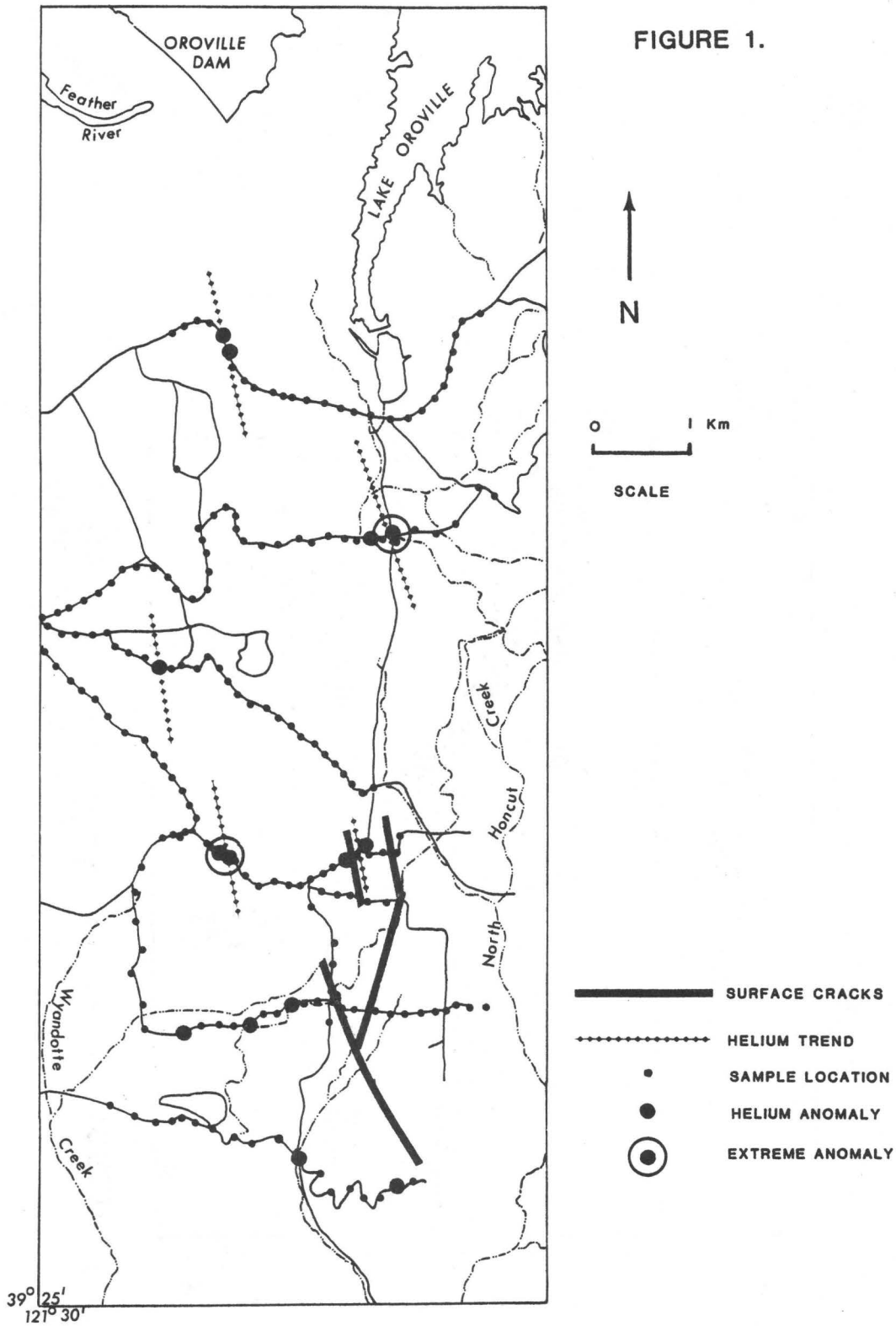

Figure 1.--Location of helium soil-gas samples and helium anomalies near Oroville, California. The trend of the anomalies, paralleling the surface cracks extends northward toward the Oroville Reservoir.

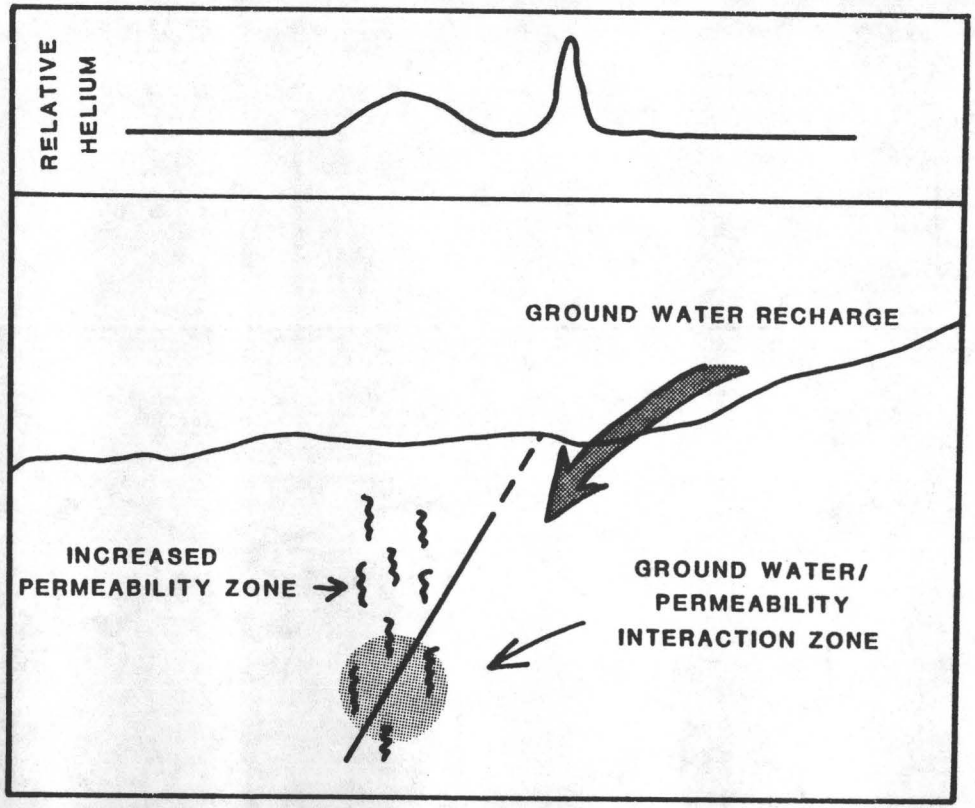

FIGURE 2.--Illustration of a model depicting the relative helium concentrations in soil-gas in the vicinity of a fault.

THE EXTENSION AND OPERATION OF A COMPUTER-CONTROLLED MONITORING NETWORK FOR RADON AND OTHER GEOCHEMICAL PRECURSORS, AND LABORATORY STUDIES ON SEISMO-GEOCHEMICAL PRECURSORS

14-08-0001-21268

M.H. Shapiro, A. Rice, J.D. Melvin, and T.A. Tombrello
Div. of Physics, Mathematics, and Astronomy - Caltech
Pasadena, CA 91125
(213) 356-4277

INVESTIGATIONS

During the first half of FY83 radon and other geochemical data were collected from the 10 operating stations in the Caltech automated geochemical network. An additional station was added at Pinon Flat later in the year. Radon, thoron, and air temperature data are collected from all stations. CO_2 is monitored at 4 stations of the network, helium at 2 stations, hydrogen at 4 stations, hydrocarbon gases at 1 station, water level at 6 stations, water temperature at 5 stations.

The Anza monitoring site was brought on-line at the beginning of 1983, and has operated nearly continuously since then. Pinon Flat was added to the network during the summer, and has operated continuously since then. The Pinon Flat unit is recording radon and thoron from a borehole that also houses a dilatometer and another type of continuous radon monitor. Upgrading of field monitors continued through FY83. During the second half of FY83 the two old version monitors (Stone Canyon and Dalton) still in operation on the network were upgraded to Version 3 instruments. A set of multiple temperature sensors was installed at Sky Forest to examine the temperature profile in the borehole at that location in an attempt to understand the extreme annual cycle exhibited by that monitor.

Modifications to our computer software were started during this period in order to permit us to operate from a more extensive network of campus computers.

RESULTS

Although rainfall was heavy during the past winter, few of the stations on the network exhibited marked changes in radon level associated with the winter storms (in contrast to some previous winters). This may have been the result of more evenly spaced rainfall and fewer intense storms than in previous high rainfall winters. At most stations on the network (see Fig. 1) the radon signals have been relatively quiet. Summarizing our measurements during the first half of FY83, we find: (1) Kresge - radon level normal and quiet, (2) Dalton - radon level normal, (3) Lytle Creek - radon level somewhat below normal and quiet, (4) Stone Canyon - radon level normal and quiet, (5) Pacoima - radon level above normal during the winter and noisy -- now returning to normal, (6) Lake Hughes - radon level normal and quiet, (7) Sky Forest - radon level above normal and noisy, (8) Ft. Tejon - radon

level normal, (9) Alandale - quiet and normal most of period -- large spikes of short duration recorded for a few days before a 3.7 M local event (12 km) at the north end of ANZA gap, (10) Anza - radon level noisy -- not enough data to determine normal range.

The two sites showing above normal radon for most of the first part of FY83 probably are responding to the winter rains. Water storage at Pacoima was very high this winter. The spikes at Alandale appear to be a genuine precursor, water level fluctuations also were noted. After a few days of very high radon spikes, the water level in the borehole had risen to about the 25 ft. level. Because of the long bubbler tube in use at Alandale, this resulted in water entering the instrument vault during the pump cycle. The unit stopped operating at that point, but was not seriously damaged. Repairs were made and the unit was reinstalled with the air pump reconfigured to pump at 1/3 the usual rate and 3 times the usual pumping duration. This prevents water from reaching the instrument vault. The data returned to normal after the earthquake, and these repairs and modifications to the unit.

During the second part of FY83 there was very little change in the pattern of radon signals from stations on the network. Some spiking has been observed at Ft. Tejon, but this appears to correlate with heavy pumping of the well at that site. The Alandale data has shown a gradual increase, but at this time is considered to be within normal limits. Generally, the data from the new Pinon Flat site has been quiet during this period.

Data from the Sky Forest temperature probe array confirmed our hypothesis that temperature inversion in the borehole was responsible for the extreme annual cycle. Installation of a longer, rigid bubbler tube and modification of the air pump cycle appears to have evened out some of the annual variation.

The archive plots of radon data from the network are shown in figures 1a and 1b.

REPORTS

M.H. Shapiro, J.D. Melvin, A. Rice, and T.A. Tombrello, Automated geochemical monitoring for earthquake prediction in southern California (invited paper presented at the Joint Italian-Soviet Symposium on Geochemical Monitoring of Seismic and Volcanic Hazards, Palermo, Italy - May, 1983)

M.H. Shapiro, J.D. Melvin, A.P. Rice, and T.A. Tombrello, Comparison of two radon anomalies (paper presented at the annual meeting of the American Chemical Society, Washington, D.C. - August, 1983)

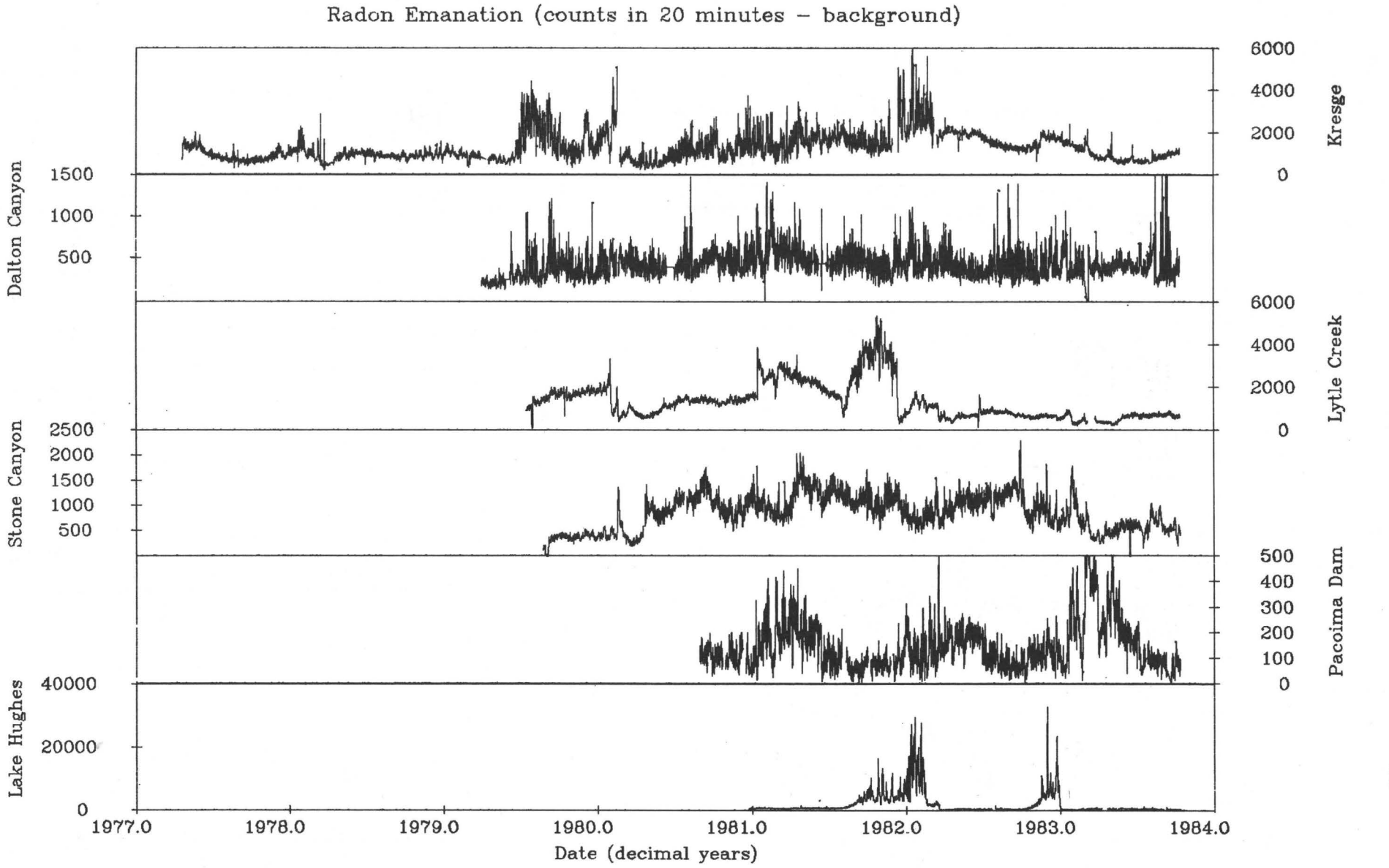

Figure 1a: Caltech Radon Monitoring Network Data Archive

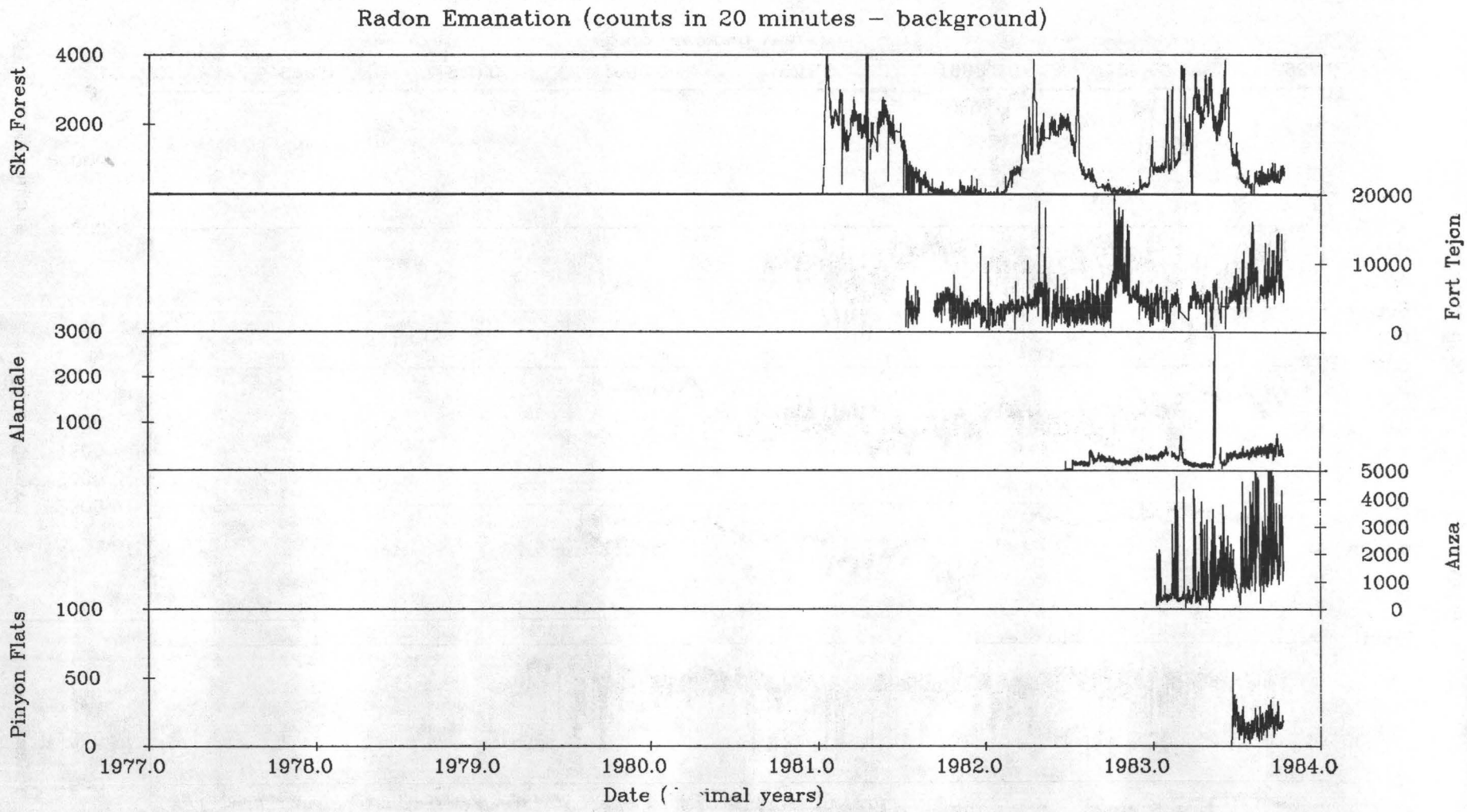

Figure 1b: Calte adon Monitoring Network Data Archive

CARBON FIBER STRAINMETER STUDIES NEAR PALMDALE, CALIFORNIA

14-08-0001-21240

Peter C. Leary and Thomas L. Henyey

A MULTI-PURPOSE CRUSTAL STRAIN OBSERVATORY, DALTON TUNNEL COMPLEX SAN GABRIEL MOUNTAINS

14-08-0001-21217

Thomas L. Henyey and Peter C. Leary

Center for Earth Science
University of Southern California
Los Angeles, CA 90089-0741
(213) 743-8034

Investigations - Observation of short baseline (20 meter) strain (sensitivity ~ 1% tidal amplitude) at mine sites in the San Gabriel Mountains near San Andreas fault.

Results - Seven strainmeters (Figure 1) at four sites [TS, BQ, JK, DT] returned data for a good part of 1982-1983. However, considerable recording time and instrument performance was lost to heavy winter rains. JK was completely flooded due to hillside runnoff water entering the tunnel mouth; BQ water levels rose high above the steady seepage level (Figure 2); TS suffered continually from rainfall induced drift. As a result of the meterological incursions strain sensitivity was reduced to permit a higher dynamic range. Systematic comparison of strain at different sites was not possible.

The rationale for a strainmeter net is wide sampling of crust. Wide sampling is necessary because of the fundamental ignorance of the surface manifestations of earthquake related stress build-up. In this regard it is interesting to note that USC identified four spring 1979 precursory deflections in a USGS creepmeter (XWR) located on the trace of the 1857 break of the San Andreas fault near Palmdale. Three strain steps preceded local seismic events, while the fourth preceded the Homestead Valley earthquake. These events are summarized in Table 1. It is important to note that the Bouquet strainmeter record of this era, despite its greater sensitivity showed no unusual behavior at a distance of 5 km from the fault (Figure 3). These observations may be an indication that significant strain is highly localized near the fault zone.

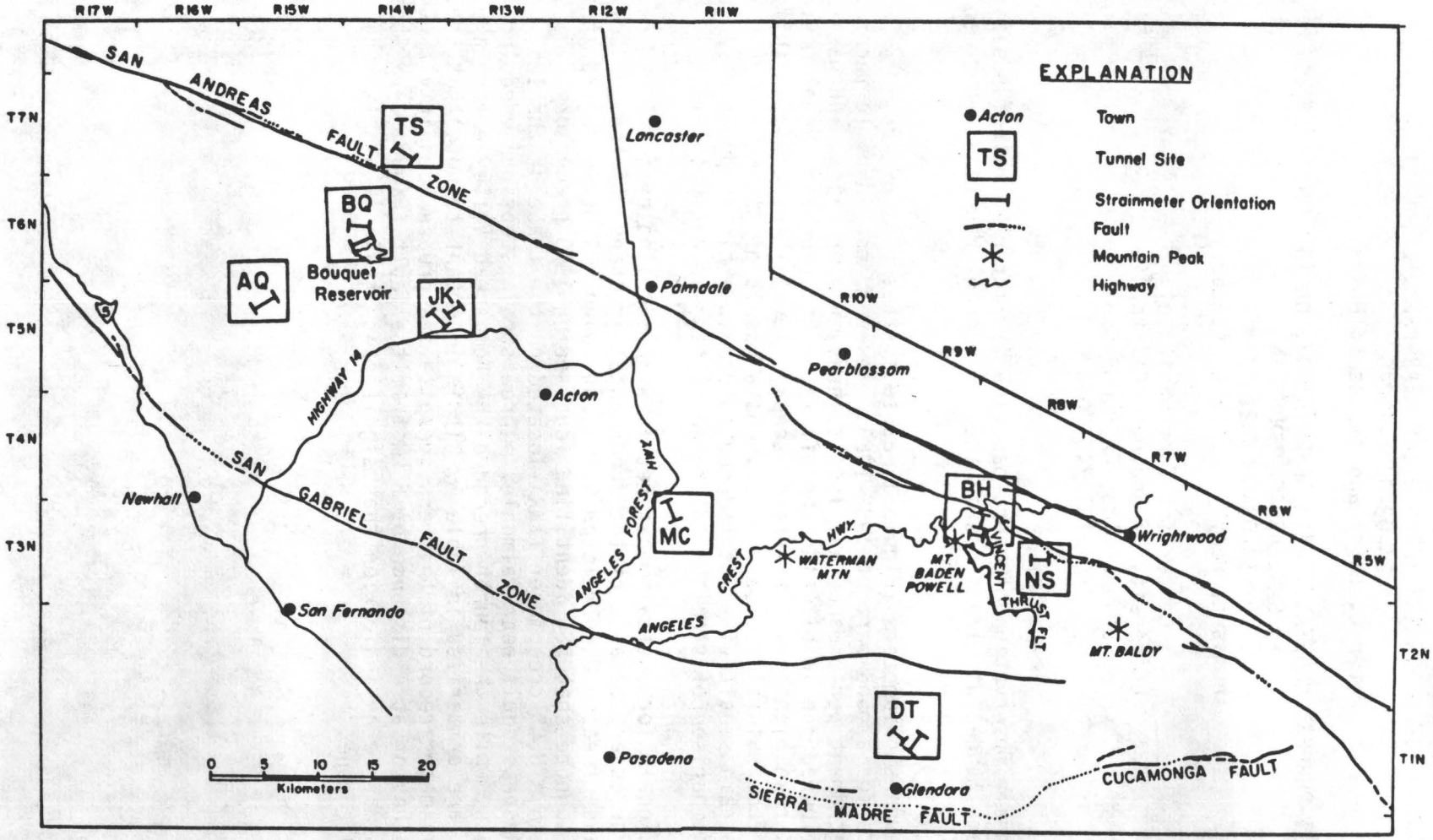

Figure 1. Location map for carbon fiber strainmeter array in San Gabriel Mountains of southern California.

Figure 2a. Rainfall recovery strainmeter signal for Bouquet #1; period is late May to early October, 1983; strain sense is contraction up.

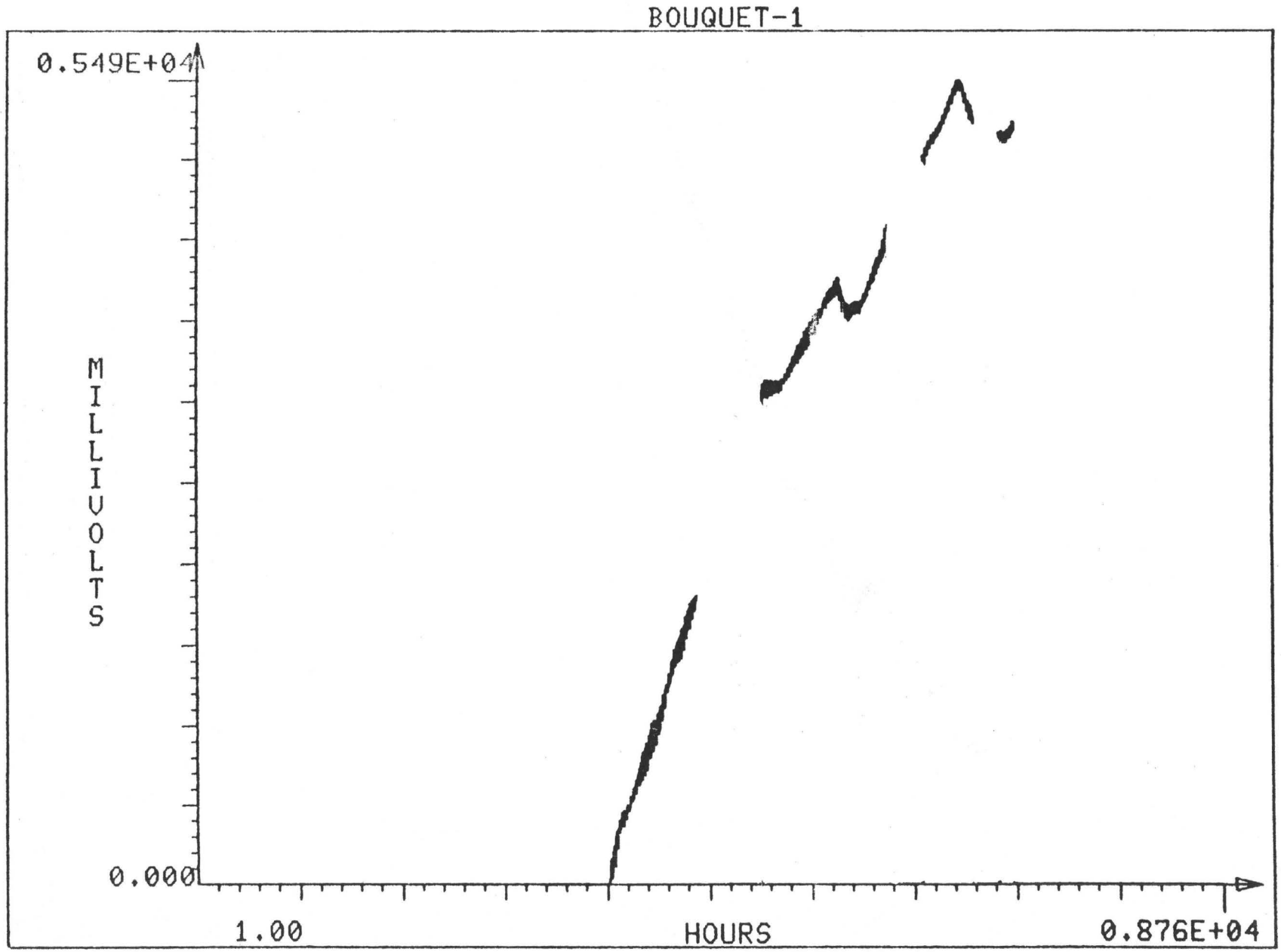

Figure 2b. Rainfall recovery strainmeter signal for Bouquet #2; period is late May to early October, 1983; strain sense is contraction up.

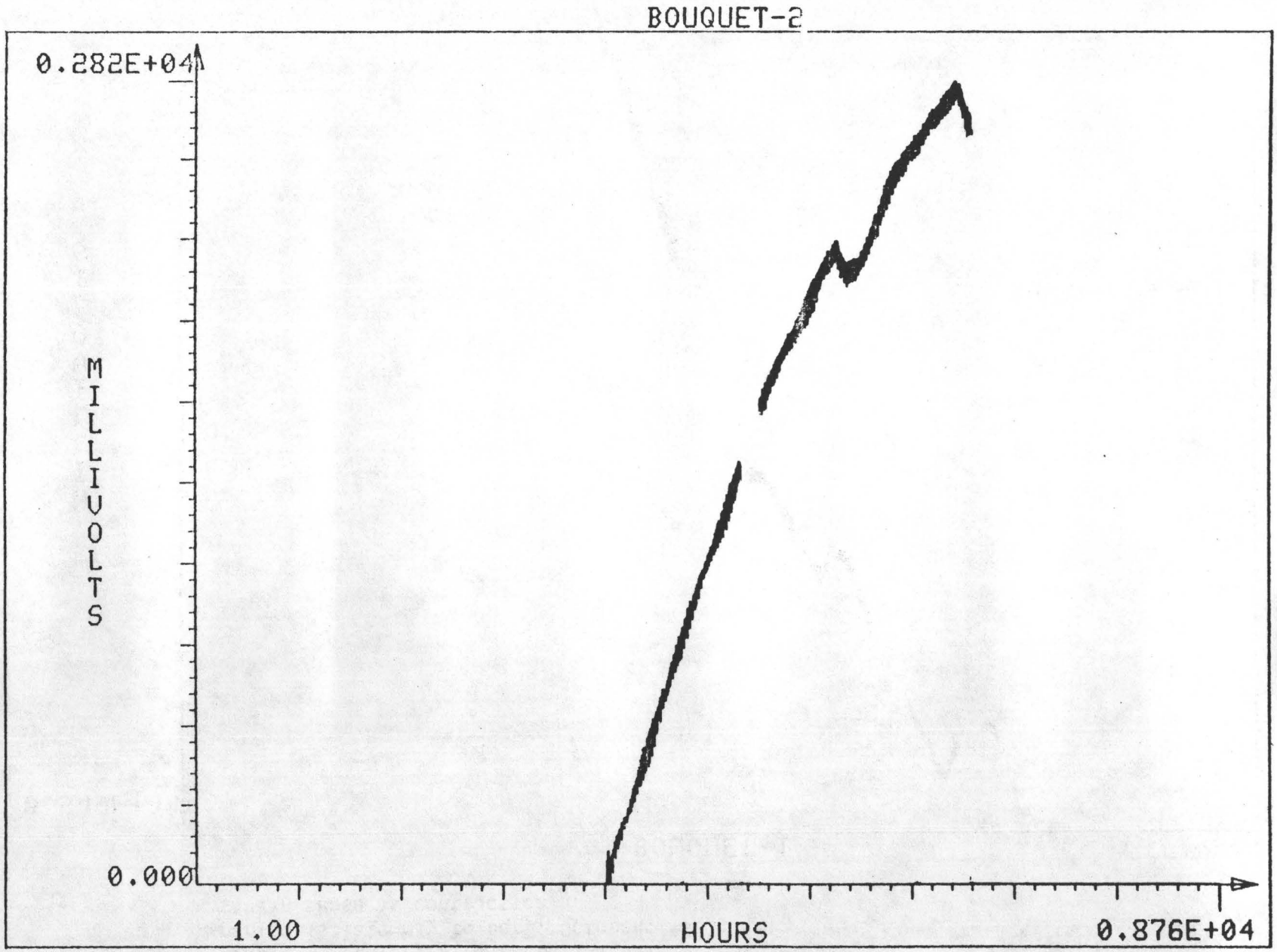

TABLE 1

Correlation of creepmeter anomalies and local seismicity (local seismic data from Sauber et al., JGR, 88, B3, 1983).

Creepmeter Events	Seismic Events			
Hour, Date(GMT)	Hour, Date(GMT)	Magnitude	Depth	Distance from Creepmeter (km)
0000 1/20	1611 1/21	3.1	6.4	25
0400 2/12	1236 2/17	2.0	11.6	10
2000 3/7	2231 3/9	2.4	1.8	25
0000 3/15	2000 3/15	5.1*	5	150

*Homestead Valley Earthquake

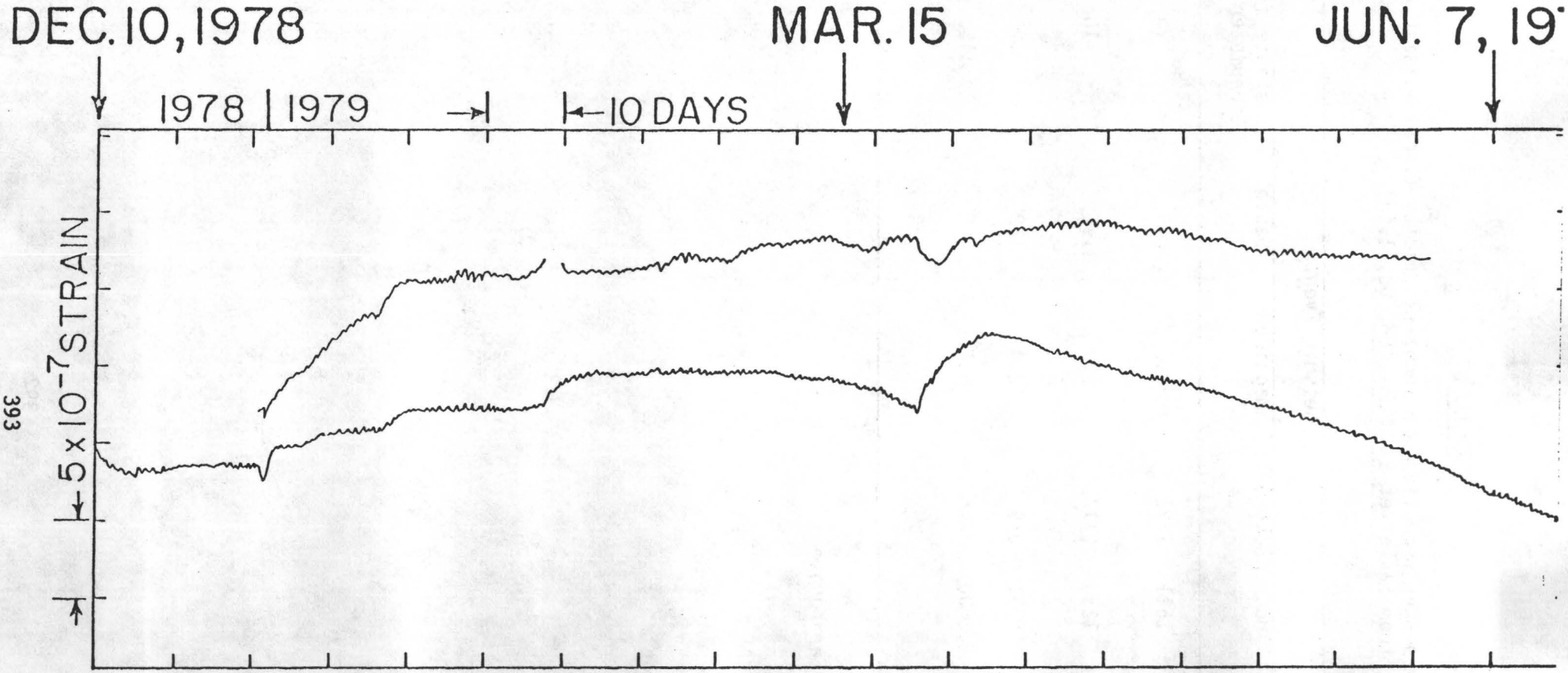

Figure 3. BQ strainmeter records for first half of 1979, during which the geodetic extensional anomaly and local seismic activity occurred. Strainmeter deflections are related to rainfall.

P2

Groundwater Radon Studies for Earthquake Precursors

14-08-0001-21193

Ta-liang Teng
Center for Earth Science
University of Southern California
Los Angeles, California 90089-0741
(213) 743-6124

Investigations

A fourteen station network of hot and cold springs and deep wells have been sampled since the late 1970's to study the relationship between changes in groundwater radon content and nearby earthquakes. During the past two years, the main emphasis has been to improve our capability of continuous monitoring. Previous results have been published in Teng (1980, JGR, vol. 85; p. 3089) and Teng et al. (1981, GRL, vol. 8, p. 441).

Results

Two major efforts have been continuous in the program during the past year. One is to bring on line a series of continuous groundwater radon monitors. Through an independent contract, a production run of a dozen continuous groundwater radon monitoring (CRM) systems has been completed. This change of emphasis, from discrete to continuous monitors, results from the P.I.'s findings during his recent visits to China where many reported radon anomalies before large earthquakes are found to be spike-like with short duration (about a day or so). If radon anomalies of similar nature were to occur in California, they might easily be missed by a practice of weekly or monthly sampling. The second change is the augmentation of the monitoring activity to include studies of other parameters associated with the groundwater hydrology; these include temperature, conductivity and pH value. This additional effort, brought on line this coming year, should increase our insight into the mechanisms responsible for radon fluctuations.

Figure 1 gives the results of one year operation of two CRM units independently monitoring the same warm spring site at the Haskell Ranch. It is reassuring to find that the outputs of the two units track each other closely, giving a high degree of repeatability. Figures 2 through 5 show the data from CRMs at four other sites. At Seminole Hot Springs (Figure 2) the data are offset due to a new unit being installed in late March, 1983. There are no anomalous features to the data so far collected by the new CRMs since their deployment.

As the stepped-up effort in the installation of CRMs pushes ahead, we are gradually reducing the number of sites at which discrete radon sampling work is being carried out. This is a long-range effort to improve the efficiency on the operation of the radon monitoring program. Parallel to this effort but funded by an independent source, we are installing five CRMs in Taiwan -- a cooperative research with Professor Ben Tsai to enhance our chance of success in this type of premonitory program.

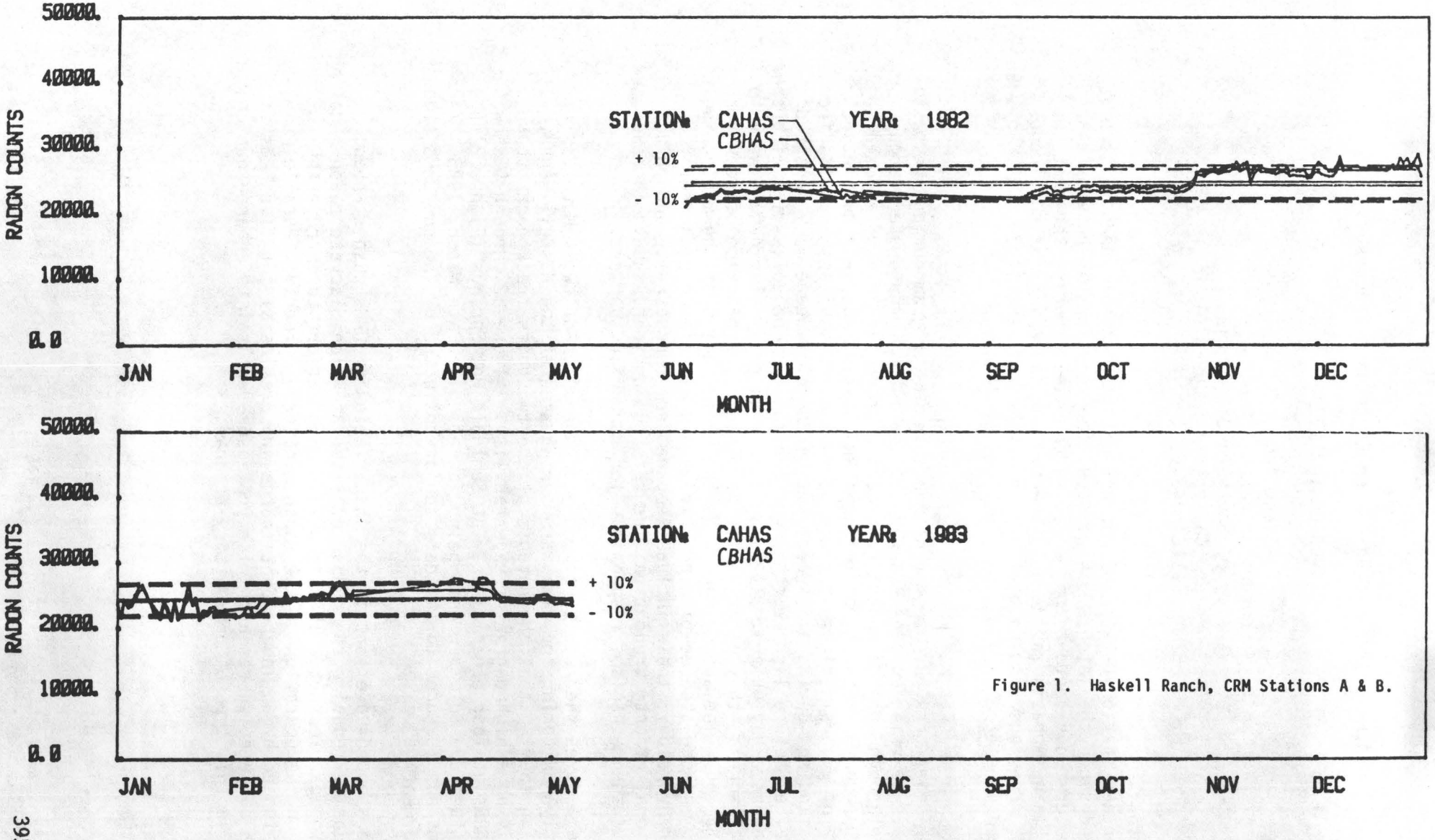

Figure 1. Haskell Ranch, CRM Stations A & B.

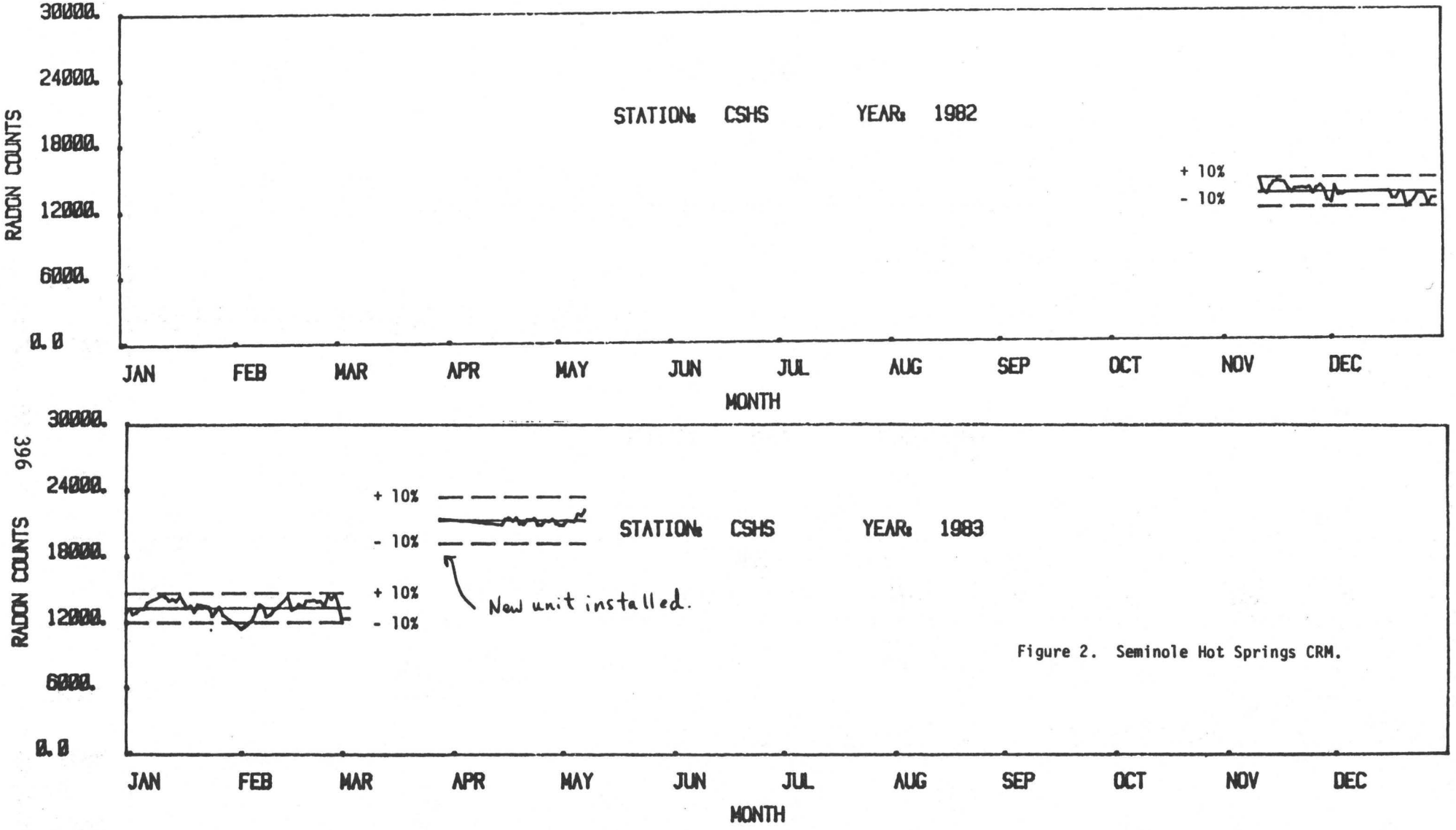

Figure 2. Seminole Hot Springs CRM.

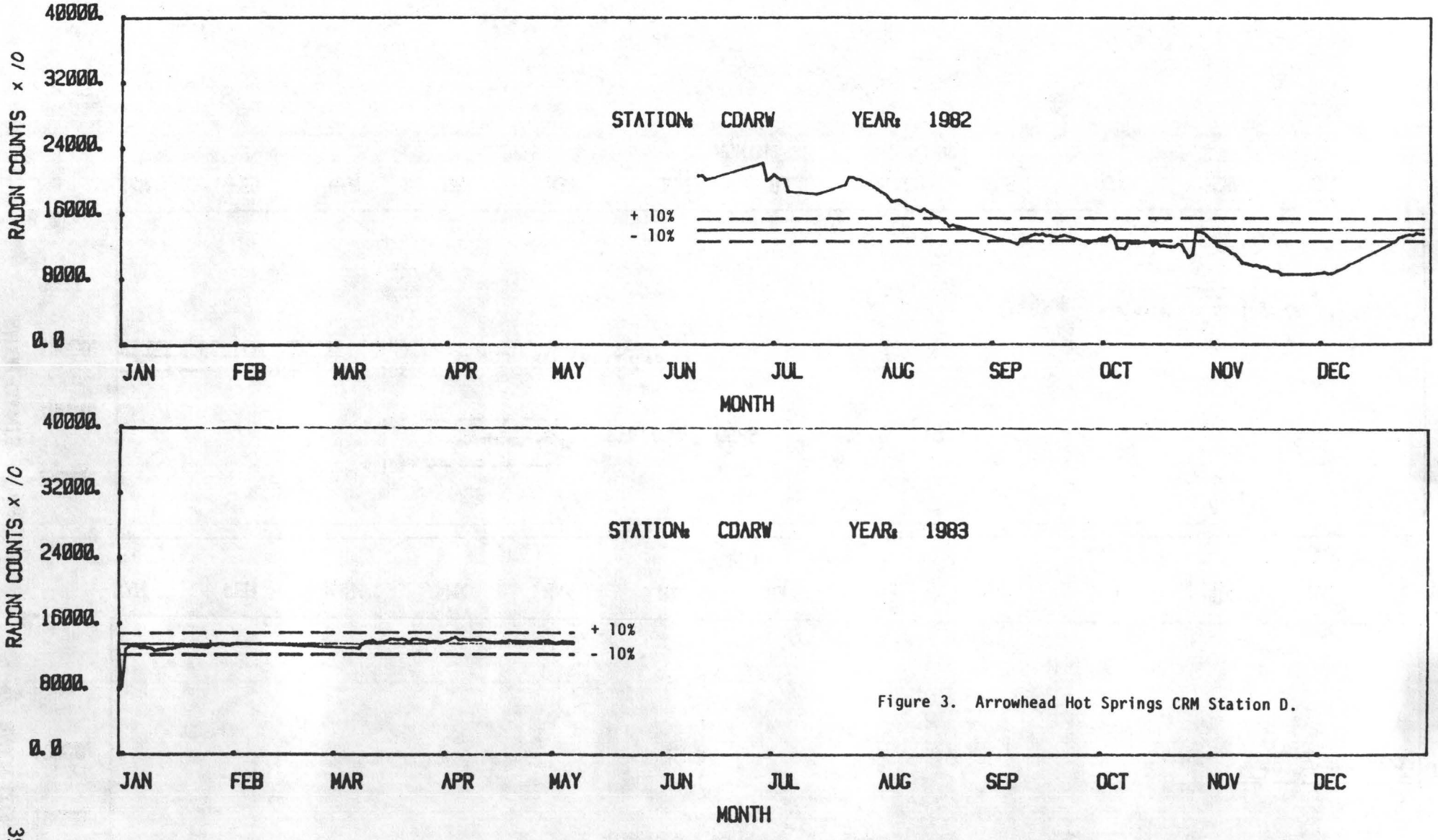

Figure 3. Arrowhead Hot Springs CRM Station D.

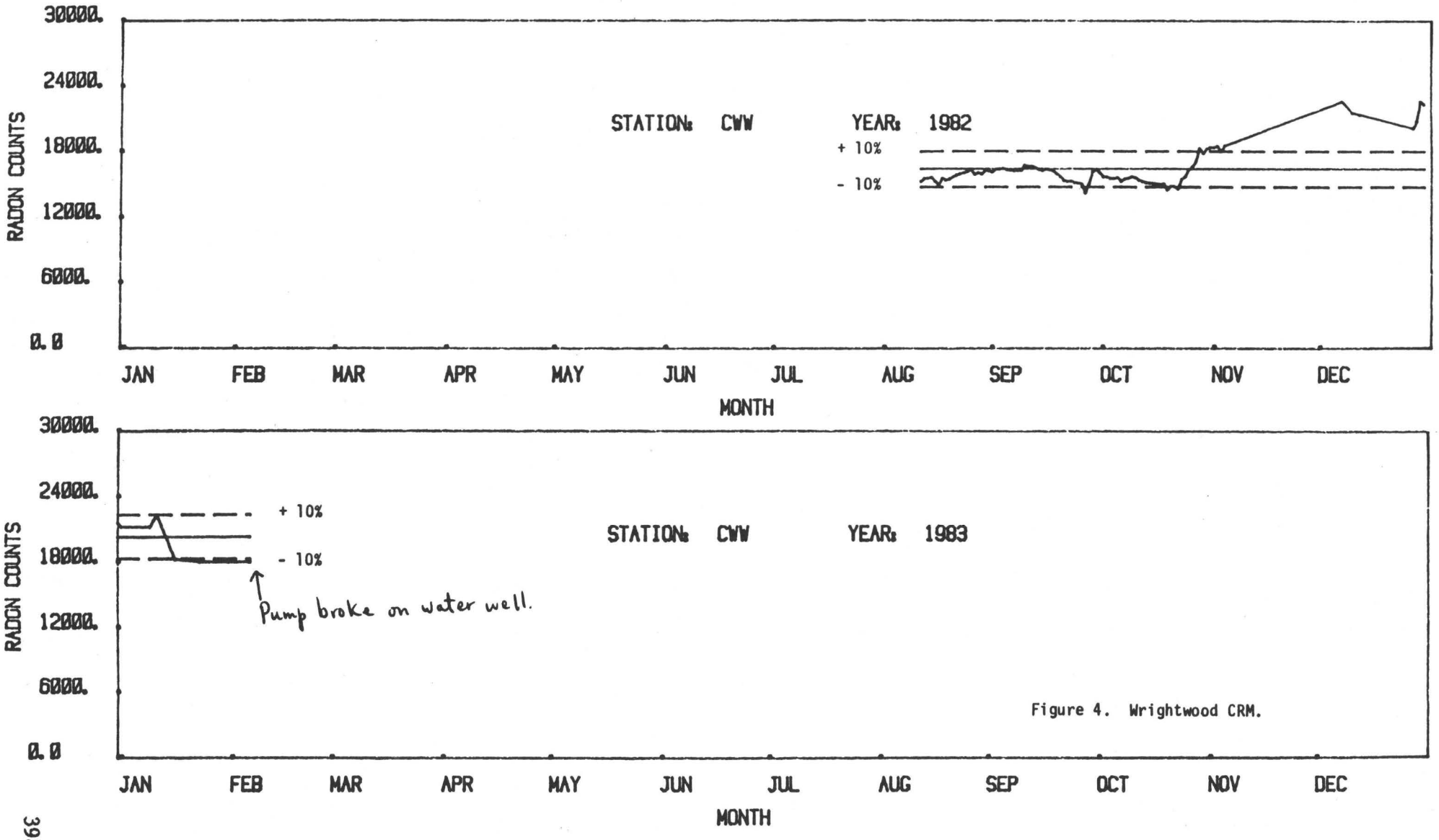

Figure 4. Wrightwood CRM.

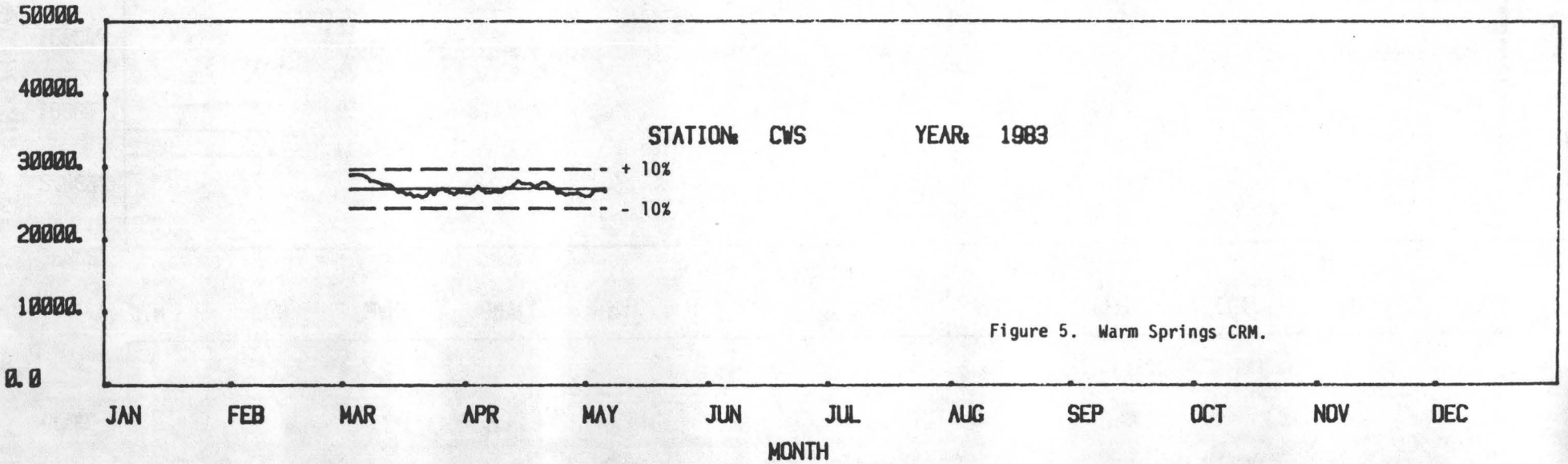

Figure 5. Warm Springs CRM.

USGS Contract # 14-08-0001-21280

STATISTICAL ANALYSIS OF PRECURSOR DATA USING A PHYSICAL MODEL OF FAULT MECHANICS

Principal Investigator: Keiiti Aki
Department of Earth, Atmospheric, and Planetary Sciences
Massachusetts Institute of Technology
Cambridge, Massachusetts 02139
Tel. (617) 253-6397

Co-Investigator: Victor Li
Department of Civil Engineering
Massachusetts Institute of Technology
Cambridge, Massachusetts 02139

Co-Investigator: Steven Ellis
Department of Mathematics
Massachusetts Institute of Technology
Cambridge, Massachusetts 02139

Investigation

During the present reporting period, we have focused on investigating the physical mechanism of precursory seismicity patterns. We have used different friction laws on stick-slip faults to numerically simulate their seismicity. This was done by using a finite difference technique. For nonlinear cases, we used an iterative approach. We use these calculations to quantitatively assess the friction law that could account for various precursory seismicity patterns, in particular the quiescence phenomena before large earthquakes.

Results

Various seismicity patterns were simulated using a simple deterministic numerical model for stick-slip faulting. In this model, the fault friction is given by displacement hardening-softening, described by $\tau = s \exp\left[-\left(\frac{2\omega - 2\omega_b}{a}\right)^2\right]$, which was first proposed by Stuart (1979). Here, τ is the shear stress on the fault; 2ω is the total fault slip; s, ω_o and a are constants. We found that this friction law is similar to Dietrich's time-dependent friction law (1972, 1978a, 1978b, 1979), which was derived from experiments. Although a model

having the frictional characteristics given simply by Byerly's law could not simulate the quiescence, our model, using Stuart's law, could.

The quiesence phenomenon has been intensively discussed and modeled by Kanamori (1981) and Mikumo and Miyatake (1978, 1979, 1983). In their modeling, the frictional strength distribution on the fault is a bi-model Weibull type. Our approach does not require such an ad-hoc assumption in order to simulate the quiesence.

On the other hand, our model has many features that are simular to the model of Mikumo and Miyatake (1983). First, more heterogeneous fault strength distribution leads to larger b-value. Second, on faults with relatively uniform properties, a large event suddenly occurs, rupturing the entire fault plane. After the main rupture, there is again a long temporal seismic gap and a similar large event occurs.

We have also simulated the seismicity patterns for the San Andreas and North Anatolian faults. In our model of the San Andreas fault, the locked section is connected with the creep section. Large earthquakes occurred only at the locked section. In our model of the North Anatolian fault, large earthquakes broke the fault successively from one segment to another.

This model can provide some insight into the physical mechanism of precursory seismicity patterns.

IMPERIAL COLLEGE OF SCIENCE AND TECHNOLOGY

Department of Geology, Royal School of Mines
Prince Consort Road, London SW7 2BP
Telephone: 01-589 5111 Telex: 261503

STRESS CORROSION AND MICROSEISMIC ACTIVITY DURING FAILURE OF ROCKS

CONTRACT No: 14-08-0001-21287

Principal Investigators: B. K. ATKINSON, N. J. PRICE

Report Prepared by: B. K. ATKINSON, S. M. DENNIS, P. G. MEREDITH

Investigations

The continuing aim of this project is to understand more about the chemical effects of pore water on the long-term strength of rocks in the upper levels of the Earth's crust. To this end triaxial deformation experiments on hot, wet rocks at low strain rates are being run as well as fracture mechanics studies of subcritical cracking in rocks under conditions of geophysical interest. Additionally, various studies are in progress of the microstructural aspects of chemically-enhanced weakening of rocks. These include, acoustic emission studies, ion microprobe analyses, and electron microscopy.

Results

1. Further long-term relaxation experiments on wet, faulted rocks at high temperatures have been conducted to elucidate the nature of water-induced chemical weakening. Rock types studied in this report period were Preshal More basalt, Haast greywacke, and Arkansas novaculite. These studies complement earlier work done on Tennessee sandstone, Mojave quartzite, and Westerly granite.

Specimens were prefaulted at a confining pressure of 200 MPa and at a strain rate of $10^{-5}s^{-1}$ at 20°C. They were then unloaded and the confining pressure adjusted to give an effective pressure of 150 MPa. Three pore fluid conditions were studied: oven dry, and with a pore fluid pressure of 20 MPa or 100 MPa. The temperature was raised to 300°C or 400°C, the samples were reloaded and stress relaxation initiated once stable sliding was achieved.

Results are described for each material tested below.

Preshal More basalt - At 300°C this plagioclase/olivine basalt shows no significant strength reduction when dry even at strain rates as low as $10^{-10}s^{-1}$. On wetting, however, it is considerably weakened at strain rates less than $10^{-7}s^{-1}$. In the wet state the relaxation behaviour is similar to that of Westerly granite. Increasing the pore fluid pressure does not seem to influence the relaxation rate, in contrast to the behaviour of Westerly granite. The reason for this is unclear. Experiments at 400°C give similar relaxation rates to those at 300°C, but the sliding stress is not reproducible enough even in the same specimen to give reliable activation enthalpies.

Haast greywacke - Preliminary results from Haast greywacke (a quartz-feldspar rock) show little relaxation behaviour when dry or at a pore fluid pressure of 20 MPa. At 400°C and a pore fluid pressure of 60 MPa it shows a similar relaxation rate and weakening as did the basalt and granite at 20 MPa fluid pressure.
Arkansas novaculite - Characterization experiments performed on the novaculite (a microcrystalline quartz rock with less than 1% phyllosilicates) showed that it was exceptionally strong. e.g. a fracture stress of ca. 1500 MPa at 100 MPa confining pressure. This necessitates that lower confining pressures than with the other rock types are used for prefracturing and for relaxation experiments. 100 MPa will be used for prefracturing because 60° fractures are not common below this pressure. For stress relaxation an effective confining pressure of 75 MPa will be used so that the sliding stress and its variation with time can be more easily monitored by the deformation apparatus.

2. Most fracture mechanics testing employs rocks with a small grain size relative to the sie of the specimen. We have run some experiments to see what is the specimen size dependence of fracture toughness for the coarse-grained Merrivale granite (grain size = 1-2 cm). K_Q, the apparent fracture toughness, was determined using short rod tests and three sizes of double torsion specimens. The only reasonable correlation between specimen dimensions and K_Q was obtained for the maximum crack length. As the maximum crack length changed from 2.5 cm to over 60 cm, the K_Q changed from approximately 1.8 MPa.$m^{\frac{1}{2}}$ to 3.6 MPa.$m^{\frac{1}{2}}$. Even at the longest crack lengths the tendency for K_Q to increase with crack length increase had not completely levelled off. Hence, even larger values of K_Q might be expected for very large (natural size) specimens. We attribute this increase in K_Q with crack length increase to the development of a large non-linear process zone of diffuse microcracking at the macrocrack tip. Conventional linear elastic fracture mechanics may not be applicable to this material and an R-curve or J-integral approach may be more suitable.

Reports

Meredith, P.G. and Atkinson, B.K. 1984. Fracture toughness and subcritical crack growth during high-temperature tensile deformation of Westerly granite and Black gabbro. To be submitted to Phys. Earth. Planet Int.

Meredith, P. G. and Atkinson, B. K. 1983. Stress corrosion and acoustic emission during tensile crack propagation in Whin Sill dolerite and other basic rocks. Geophys. J. R. Astr. Soc. v75, 1-21.

Crampin, S., Evans, R., and Atkinson, B.K. 1984. Earthquake prediction: a new physical basis. Geophys. J. R. Astr. Soc. (in press).

Digital Signal Processing of Seismic Data

9930-02101

W. H. Bakun
U. S. Geological Survey
345 Middlefield Road, Mail Stop 77
Menlo Park, California 94025
(415) 323-8111, ext. 2777

Investigations

1. Coda-duration τ at 42 of the stations in the U. S. Geological Survey's central California seismic network (CALNET) for earthquakes in five source regions of central California -- the Parkfield and San Juan Bautista sections of the San Andreas fault, the Sargent fault, the Coyote Lake section of the Calaveras fault, and the Livermore area -- are used to obtain empirical formulae relating local magnitude M_L and seismic moment M_0 to τ and epicentral distance Δ.

Results

1. Empirical formulae with $\log^2\tau$ fit the data better than those assuming a $\log \tau$ dependence. For 55 earthquakes with $0.8 \leq M_L \leq 5.6$, $M_L = 0.69 + 0.655(\pm 0.006) \log^2\tau + 0.00321(\pm 0.00010)\Delta$. For 53 earthquakes with $18.4 \leq \log M_0 \leq 22.3$, $\log M_0 = 17.97 + 0.719(\pm 0.007)\log^2\tau + 0.00319(\pm 0.00013)\Delta$. These relations provide unbiased estimates of M_L for $1.5 \lesssim M_L \lesssim 5.6$ and $19 \lesssim \log M_0 \lesssim 22.3$. Station corrections can significantly improve the accuracy and precision of M_L and $\log M_0$ estimates, particularly if τ from a small number of stations are used. Regional variations in station corrections reflect an increase in coda duration toward the south within the CALNET.

Reports

Bakun, W. H., Magnitudes and moments of duration (abs.): EOS, in press.

Scofield, C. P., W. H. Bakun, and A. G. Lindh, The M_L = 5.4 Idria, California, earthquake of October 25, 1982 (abs.): EOS, in press.

ROCK MECHANICS

9960-01179

James Byerlee
U.S. Geological Survey
Branch of Tectonophysics
345 Middlefield Road, MS/77
Menlo Park, California 94025
(415) 323-8111, ext. 2453

Investigations

Laboratory experiments are being carried out to study the physical properties of rocks at elevated confining pressure, pore pressure and temperature. The goal is to obtain data that will help us to determine what causes earthquakes and whether we can predict or control them.

Results

Measurements of charge separation in rock during stable and unstable deformation give an unexpectedly large decay time of 50 s. Time domain induced polarization experiments of wet and dry rocks give similar decay times and suggest that the same decay mechanisms operate in IP response as in the relaxation of charge generated by mechanical deformation. These large decay times require low frequency relative permittivity to be very large - in excess of 10^5. A consequence of large decay times is that a significant portion of any electrical charge generated during an earthquake can persist for tens or hundreds of seconds afterwards. As a result, electrical disturbances associated with earthquakes should be observable for these lengths of time rather than the milliseconds previously suggested.

Reports

M.H. Bakiev, J. Byerlee, V.C. Kuksenko, 1982, Electrical phenomena of frictional sliding of rocks under high confining pressure, Report of the Academy of Science of U.S.S.R., v. 266, No. 6, p. 1347-1348.

D. Moore, R. Summers, J. Byerlee, 1983, Strengths of clay and non-clay fault gouges a elevated temperatures and pressures, Proceedings of the 24th U.S. Symposium of rock mechanics, p. 489-500.

PERMEABILITY OF FAULT ZONES

9960-02733

James Byerlee
Branch of Tectonophysics
U.S. Geological Survey
345 Middlefield Road, MS/77
Menlo Park, California 94025
(415) 323-8111, ext. 2453

Investigations

Laboratory studies of the permeability of fault gouge were carried out to provide information that will assist us in evaluating whether in a given region, fluid can navigate to a sufficient depth during the life-time of a reservoir to trigger a large destructive earthquake.

Results

Permeability of westerly granite has been measured under confining pressure ranges from 160-960 bars, pore pressure ranges from 0-850 bars, with constant pore pressure gradient. Experimental results show that the cube root of permeability change with logrithm of effective pressure is consistent with the theoretical model proposed by Walsh.

Reports

C. Morrow, D. Moore, J. Byerlee, 1983, Permeability and pore fluid chemistry of the Bullfrog tuff in a temperature gradient, Proceedings of the 24th U.S. Symposium of rock mechanics, p. 819-829.

Joint Work with Professor B. V. Kostrov on Fundamental Studies of Spontaneous Fracture Processing and Earthquake Fault Mechanics

USGS 14-08-0001-21294

S. Das
Lamont-Doherty Geological Observatory of Columbia University
Palisades, New York 10964
(914) 359-2900

Investigations

Under this contract, which supports joint work with Professor B. V. Kostrov of the Institute of Physics of the Earth, Moscow, on spontaneous fracture propagation, we have studied how ellpitical asperities rupture. We use a truly three-dimensional numerical boundary integral method, originally developed by Das (1980, 1981), to solve for the fracture process. The initial static stress distribution was determined using the results of Mindlin (1946) and discretized for input into the numerical method.

Results

Several cases were studied, with the direction of initial stress on the asperity being at different angles to the axes of the ellipse. It is found that for elliptic asperities of all aspect ratios and for all directions of applied stress, the stress concentration is always stronger at the end of the major axis. Elliptic asperities of aspect ratios of 3:1 were studied. It was found that when the applied stress is along the major or minor axis, the fracture can propagate dynamically only if the first point that fractures is at or very close to the end of the major axis. The fracture front is found to propagate at a constant speed of half the P-wave velocity of the medium, as an almost straight line from one end of the major axis to the other. If the applied stress is at 45° to the axes of the ellipse, the fracture can propagate dynamically by breaking a point anywhere along the edge of the ellipse. If the first broken point is at the end of the major axis, the fracture front behaves as described above. If, however, the first broken point is at one end of the minor axis, the fracture propagates as two fronts forming a V-shape, which moves away from the initially fractured point, with a variable fracture velocity that is different in the different directions of fracture propagation.

References

Das, S., (1980). A numerical method for determination of source time functions for general three-dimensional rupture propagation, Geophys. J. Roy. Astr. Soc., 62, 591-604.

Das, S., (1981). Three-dimensional rupture propagation and implications for the earthquake source mechanism, Geophys. J. Roy. Astr. Soc., 67, 375-393.

Mindlin, R. D. (1949). Compliance of elastic bodies in contact, J. Appl. Mechanics, 16, 259-0268.

Effects of Pore Fluid Chemistry on Fault Stability

Contract #14-08-0001-21263

J. D. Dunning, Department of Geology,
Indiana University, Bloomington, IN 47405

Investigations

Four series of laboratory friction experiments were performed on 35° sawcut cylinders of Berea Sandstone and Deadwood Sandstone in the presence of eight aqueous chemical environments. The tests were carried out at an effective confining pressure of 50 MPa and at an axial strain rate of 10^{-5} cm s^{-1}. Berea Sandstone is a clean well-sorted, friable sandstone with high porosity and permeability; Deadwood Sandstone is a well indurated orthoquartzite with lower porosity and permeability. Both of these sandstones have similar gross mineralogical composition and grain size.

The chemical environments used in this study were: the ambient atmosphere (R.H. 60-90%), distilled deionized water, two cationic surfactants in aqueous solution (10^{-4}M, FC 750 and 10^{-4}M, and 10^{-3}M dodecyl trimethyl ammonium bromide), an anionic surfactant (10^{-4}M sodium dodecyl sulfate), in aqueous solution, a nonionic surfactant (10^{-4}M Triton X-100), a concentrated inorganic brine, and a low concentration inorganic brine. The surfactants were chosen because the cationic varieties have demonstrated an ability to weaken quartz and sandstone whereas the anionic and nonionic varieties have little or no effect on the strength of these materials. Furthermore, the surfactants display a broad range of variation in such properties as interfacial surface tension and heat of adsorption onto quartz. The inorganic brines were chosen in order to compare the effects of analogs of natural aqueous chemical environments to the synthetic surfactant environments.

The salient goals of this study were to: 1) ascertain whether fluids, which chemically weaken quartz and sandstone, produce a change in the frictional properties of sandstone, 2) determine the nature of the mechanism or mechanisms of these changes (i.e. are they related to chemical weakening of the asperities and gouge or are they due to a purely mechanical lubrication effect), and 3) evaluate the potential relationship between reduction in the surface free energy of the minerals in the sandstone (due to adsorption of species from the chemical environments onto the surface of the minerals) and observed variations in frictional behavior.

Test Series 1: Berea Sandstone Friction Tests

Cylinders of Berea Sandstone with 35° sawcuts were saturated with the various aqueous environments and deformed at an effective confining pressure of 50 MPa. Each sample was allowed to undergo 2-2.5% axial shortening after yield.

The effect of most of the chemical environments on the frictional behavior of Berea Sandstone was negligible. Samples deformed in the presence of the ambient atmosphere displayed stable sliding behavior subsequent to yield with the frictional coefficient (μ) between 0.69 and 0.70. The observed μ value did not vary significantly with axial strain (during these tests). Distilled water and 10^{-4} M Triton X-100 produced a reduction in the initial coefficient of friction (μ) of about 5-8%, although the μ value increased slightly with increasing axial strain, especially in the presence of water. Dodecyl trimethyl ammonium bromide (10^{-4}M) produced a 5-8% increase in the coefficient of friction (μ) over that obtained in the ambient atmosphere. The other environments demonstrated no statistically significant differences in behavior or μ values relative to those obtained in the presence of an ambient atmosphere.

Test Series 2: Deadwood Sandstone Friction Tests

The experimental procedure in these tests was identical to that in Series 1. The effects of distilled water and the other aqueous chemical environments on the frictional behavior of Deadwood Sandstone were extensive. The dry samples of Deadwood Sandstone failed by low stress-drop stick slip events. Additional axial strain was accommodated by continuous (low stress drop) stick slip events. The coefficient of friction varied from 0.61-0.62 at yield to about 0.65 at axial strains of 2-2.5%. The coefficient of friction at the yield point for the Deadwood samples was reduced substantially in the presence of all the aqueous environments with values varying from a high of (0.36-0.37) for water to a low value of (0.30-0.31) for the concentrated brine solution. The coefficient of friction (μ) increased substantially after yield in all samples deformed in each of the chemical environments. The most striking increase occurred in the samples saturated with 10^{-4} M Triton X-100 (μ = 0.33-0.34 at yield with an increase to 0.45-0.46 at 2.5% axial strain) and 10^{-4} M DTAB.

The striking differences between the frictional behavior of the Berea and Deadwood Sandstones in the presence of aqueous chemical environments suggests that the chemical effects that are being observed are extremely complex.

Test Series 3: Berea Sandstone Cyclic Friction Tests

In this test series 35° sawcut samples of Berea Sandstone subjected to an effective confining pressure of 50 MPa were deformed in four cycles of: loading to yield, axial shortening of 2.5% and unloading. The purpose of these tests was to evaluate the effects of aqueous chemicals on gouge behavior and gouge production.

Dry samples of Berea Sandstone displayed small ($\leq 5\%$) increases in the coefficient of friction after yield in all of the cycles and the yield stresses and μ values for all cycles were statistically identical. Water and most of the other chemical environments displayed similar behavior. Dodecyl trimethyl ammonium bromide (10^{-4} M) displayed markedly different behavior. During the first cycle the coefficient of friction value increased by over 10% from yield to 2.5% axial strain. In the ensuing cycles the μ value at yield was the same as the highest value during the first cycle and remained constant throughout the cycles. In dodecyl trimethyl ammonium bromide some decrease in μ was noticed during the last (fourth) cycle.

These results suggest that DTAB, which has been shown in a number of studies to weaken quartz, enhances the comminution of the gouge and by doing so increases the effective contact area of the surfaces in a manner analogous to that described by Dieterich (1979). This possibility is now being evaluated by comparing the grain size distribution of gouge generated in the presence of DTAB and the other environments in a scanning electron microscope and by elutriation grain size evaluation techniques.

Test Series 4: Acoustic/Microseismic Emissions

The Kaiser effect is an acoustic/microseismic stress memory. A pre-stressed rock will not emit significant acoustic signals upon reloading along the axis of pre-stressing until the initial load level is exceeded. The Kaiser effect was investigated in two series of frictional sliding experiments utilizing 35° sawcut cylinders of Berea Sandstone and Deadwood Sandstone.

In one experimental series jacketed samples, under a confining pressure of 50 MPa were loaded along the axis of the cylinder until yield occurred along the sawcut, unloaded, and then reloaded until failure reoccurred. During the loading cycles acoustic signals were monitored at 30 kHz, 175 kHz and 375 kHz. In the other experimental sequence samples of each sandstone were loaded, unloaded and reloaded to 60% of their yield points. Acoustic signals were monitored in several threshold counting modes.

Deadwood Sandstone displayed a moderate stress memory when loaded to failure and then reloaded, with the acoustic rate much diminished during the second loading cycle. The Kaiser effect was much better developed in the Deadwood Sandstone samples cycled to 60% of the yield point, with no acoustic emissions occurring during the second load cycle except at very low loads (during sample reseating). Berea Sandstone displayed a strong acoustic stress memory in both types of tests.

Other Test Series Nearing Completion

A series of calorimetric tests is being completed in which the heats of desorption of the environments employed in this project on ground samples of Berea Sandstone are being measured in a differential scanning calorimeter (DSC). The heat of desorption value normalized to the surface area of the sample, can be used to estimate the degree by which the environment of interest reduces the surface free energy of the test material used in this study. This information will allow me to evaluate one of the important possible mechanisms of chemical weakening of asperities, surface energy reduction.

Compressive strength tests are being carried out at atmospheric pressure on cylinders of the Berea and Deadwood Sandstones which have been saturated with the environments employed in the friction tests described above. These results will give me the opportunity to further assess the role of chemical weakening of asperities.

Elutriation analysis and scanning electron microscopy are being utilized to determine the morphology and grain size distribution of gouge generated in samples deformed in the presence of each of the environments used in this study. The purpose of these tests is to evaluate the relative ease of comminution of the gouge material in each of the environments, as is discussed above in the Test Series 3 section.

References

Dieterich, J., Modeling of rock friction 1, Experimental results, J. Geophys. Res., 84 (5), 2161-2168, 1979.

Reports

Dunning, J. and Miller, M.E., The effects of pore fluid chemistry on stick-slip/stable sliding in sandstones, submitted to Amer. Geophys. Union, for presentation at the National Meeting in December 1983 in San Francisco, CA.

Leaird, J., Dunning, J., and Miller, M., The Kaiser effect in sandstone undergoing stable sliding and stick-slip, submitted to Amer. Geophys. Union, for presentation at the National Meeting in December 1983 at San Francisco, CA.

Earthquakes and the Statistics of Crustal Heterogeneity

9930-03008

Bruce R. Julian

Branch of Seismology
U.S. Geological Survey
345 Middlefield Road - MS77
Menlo Park, California 94025
(415) 323-8111 ext. 2931

Investigations

Both the initiation and the stopping of earthquake ruptures are controlled by spatial heterogeneity of the mechanical properties and stress within the earth. Ruptures begin at points where the stress exceeds the strength of the rocks, and propagate until an extended region ("asperity") where the strength exceeds the pre-stress is able to stop rupture growth. The rupture termination process has the greater potential for earthquake prediction, because it controls earthquake size and because it involves a larger, and thus more easily studied, volume within the earth. Knowledge of the distribution of mechanical properties and the stress orientation and magnitude may enable one to anticipate conditions favoring extended rupture propagation. For instance, changes in the slope of the earthquake frequency-magnitude curve ("b-slope"), which have been suggested to be earthquake precursors and which often occur at the time of large earthquakes, are probably caused by an interaction between the stress field and the distribution of heterogeneities within the earth.

The purpose of this project is to develop techniques for determining the small-scale distributions of stress and mechanical properties in the earth. The distributions of elastic moduli and density are the easiest things to determine, using scattered seismic waves. Earthquake mechanisms can be used to infer stress orientation, but with a larger degree of non-uniqueness. Some important questions to be answered are:

** How strong are the heterogeneities as functions of length scale?

** How do the length scales vary with direction?

** What statistical correlations exist between heterogeneities of different parameters?

** How do the heterogeneities vary with depth and from region to region?

Scattered seismic waves provide the best data bearing on these questions. They can be used to determine the three-dimensional

spatial power spectra and cross-spectra of heterogeneities in elastic moduli and density in regions from which scattering can be observed. The observations must, however, be made with seismometer arrays to enable propagation direction to be determined. Three-component observations would also be helpful for identifying and separating different wave types and modes of propagation.

The stress within the crust is more difficult to study. Direct observations require deep boreholes and are much too expensive to be practical for mapping small-scale variations. Earthquake mechanisms, on the other hand, are easily studied and reflect the stress orientation and, less directly, its magnitude, but are often not uniquely determined by available data.

This investigation uses earthquake mechanisms and the scattering of seismic waves as tools for studying crustal heterogeneity.

Results

Dike-intrusion earthquake mechanisms

Most of effort during the last six months has been concentrated on studying the mechanisms of the earthquakes that have been occurring since 1978 in and near Long Valley caldera. These studies have been carried out in cooperation with Stuart Sipkin, from the Branch of Global Seismology in Golden, Colorado. A paper on this work was presented in May at the 1983 National meeting of the AGU, which was held in Baltimore.

In addition to two of the earthquakes of May, 1980, the 1978 Wheeler Crest earthquake now has been identified as having a large non-double-couple (CLVD) component. In addition, the event of 1944 UTC May 25, 1980 turns out to have a predominantly strike-slip mechanism. The occurrence of this double-couple earthquake spatially surrounded by CLVD events virtually rules out any possibility that the CLVD mechanisms could be an artifact of wave-propagation anomalies. Another possibility that cannot be ruled out, however, is that the CLVD mechanisms are actually superpositions of double-couples caused by simultaneous slip on distinct faults. Such a hypothesis might be able to explain the long-period first-motion, waveform, and amplitude observations, but short-period first motions should reflect the initiation of rupture, and indicate double-couple mechanisms. They do not do this, however, but rather yield large CLVD components in agreement with long-period data. The multiple-rupture hypothesis, therefore, is considered dubious.

A critical test may be provided by the mechanisms of small earthquakes. Differentiating between double-couple (shear faulting) and CLVD mechanisms, however, is difficult and requires station coverage denser than that currently installed in Long Valley. Several more short-period seismometers are now being installed in the area of highest activity, and data from them should help to resolve the mechanisms of small earthquakes.

In another attempt to gather data bearing on the earthquake mechanisms, a Sacks-Evertson dilatometer is being installed near the Devil's Postpile, immediately southwest of the caldera. This instrument will provide high-sensitivity measurements of areal strain changes, and can also be used as a high-quality seismometer, if the data are recorded with adequate bandwidth. Such instruments have proven powerful tools for monitoring dike propagation in Iceland and other volcanic areas. A hole for the dilatometer has been drilled, and we hope to cement the instrument into it before winter, so that the cement will have set and useful data can be obtained by springtime.

Reports

Julian, Bruce R., 1983, Evidence for dyke intrustion earthquake mechanisms ear Long Valley caldera, California, Nature, v. 303, no. 5915, p. 323-325.

S. W. Sipkin and B. R. Julian, Evidence for non-double couple earthquake mechanisms (abstract) EOS, v. 64, no. 8, p. 262.

Experimental Rock Mechanics

9960-01180

Stephen Kirby
Branch of Tectonophysics
U.S. Geological Survey
345 Middlefield Road, MS/77
Menlo Park, CA 94025
(415) 323-8111, Ext. 2872

Investigations

We continue our research on the rheology of the lithosphere and the strength of rocks and minerals of the continental crust. This work is focused on establishing the laws governing flow of earth materials. These flow laws enable one to model geophysical processes involving flow and to estimate stress differences which can be supported within the earth.

Results

The important role of transient creep in the deformation of the lithosphere has been emphasized in a thorough review of the topic [Kirby, 1983b]. Rocks are softer at low strain than at high strain, hence the overall resistance to the bending of the oceanic lithosphere at trench-rise systems, where strains are low, is expected to be less than predicted for steady state flow. In addition, the deformation at transform faults is likely to involve a complex brittle-ductile transition zone [Kirby, 1983b; Kirby and Kronenberg, 1983].

Under low-grade metamorphic conditions, crustal rocks commonly display evidence for extreme ductility under low inferred differential stress. Dry rocks tested in the laboratory under these conditions of temperature and pressure are in general very strong and brittle even when due account is made for differences in laboratory and natural strain rates. The key factor in promoting ductility at low temperatures and pressures appears to be the chemical role of water in promoting crack growth, mass solute transfer in solution and hydrolytic weakening. Kirby and Scholz have organized and edited a special JGR issue on this topic. It is our common conviction that the stress differences supported by the upper 20 km of the continental crust and the basic time and temperature effects on rock strength in the crustal area are governed by the important chemical processes that occur in rock-water systems. This conclusion has obvious implications for the occurrence and time-dependent aspects of earthquakes.

Reports

Kirby, S. H., Flexure of the oceanic lithosphere at trench-rise systems: the importance of transient creep, Trans. Am. Geophys. Union, v. 64, p. 311, 1983a.

Kirby, S. H., Rheology of the lithosphere, Rev. Geophys. and Space Phys., v. 21, p. 1458-1487, 1983b.

Kirby, S. H., and McCormick, J. W., Inelastic properties of rocks and minerals: strength and rheology, v. 3 of CRC Handbook of Physical Properties of Rocks, R. S. Carmichael, editor, (In Press), 1983.

Lee, R. W., and Kirby, S. H., Experimental deformation of topaz crystals: possible embrittlement by ultracrystalline hydrogen, J. Geophys. Res., (In Press), 1983.

Linker, M. F., Kirby, S. H., Ord, A., Christie, J. M., Effects of compression direction on the plasticity and rheology of hydrolytically-weakened synthetic quartz crystals, J. Geophys. Res., (In Press), 1983.

Kirby, S. H., and Kronenberg, A. K., Deformation of clinopyroxenite: evidence for a transition in flow mechanisms and semibrittle behavior, J. Geophys. Res., v. 88, (In Press), 1983.

Durham, W. B., Heard, H. C., and Kirby, S. H., Experiments of polycrystalline ice at high pressure and low temperature: preliminary results, J. Geophys. Res., v. 88, (In Press), 1983.

Kirby, S. H., and Scholz, C. H., eds., Chemical role of water in the strength of rocks under crustal conditions, J. Geophys. Res., v. 88, (In Press), 1983.

LABORATORY AND FIELD STUDIES OF CONSTITUTIVE RELATIONS AND FAULT ZONE PROPERTIES

14-08-0001-21181

John M. Logan
Center for Tectonophysics
Texas A&M University
College Station, TX 77843
(409) 845-0312

Investigations

The overall objective of this project is to investigate fault-zone mechanics of gouge-host rock systems through controlled laboratory experiments and associated field studies. Laboratory investigations have been conducted to (1) investigate the effect of normal stress on the frictional behavior; (2) determine the mechanical properties of simulated quartz gouge at temperatures to 900°C; (3) assess the relationship between fault-zone fabric and constitutive relations; and (4) investigate the frictional behavior of ductile fault gouge. Field work in southern California has attempted to characterize the character and physical properties of a natural fault zone and correlate these with the laboratory investigations.

Results

Normal Stress and Frictional Behavior. Behavior of simulated faults upon the reduction in the confining pressure, Pc, has been studied experimentally in order to separate the mechanical effects of changing pore pressure on fault motion from the chemical ones. Experiments were performed on cylindrical specimens of Tennessee sandstone with a 35° precut in a triaxial apparatus. The loading motor is turned off at some points in ordinary friction experiments, and then Pc is lowered from 65-100 down to 0 MPa at various rates. This Pc reduction brings about an increase in the shear stress, τ, and in a decrease in the normal stress, σ_n, and the differential stress supported by the specimen is released mostly by a sequence of abrupt slip events.

Major results: (1) Behavior during ordinary friction experiments compares well with that in the Pc reduction experiments; that is, chlorite gouge (dry) shows only stable slip, violent slip is observed for a wet specimen with no gouge, and the behaviors of quartz gouge (wet) and of halite gouge (dry) are intermediate between the two, in both tests. It might not be easy to release the stored strain via fluid injection into faults. (2) $\Delta\tau = \alpha\ \sigma_n^{\beta}\ t^{\gamma}$ holds; α, β and γ are constants depending at least on materials and displacements. Qualitatively, the greater the σ_n, or normal stress, and/or the longer the time in stationary contact, t, the greater is the shear-stress drop, $\Delta\tau$. The result fits the idea that the coefficient of static friction increases with increasing contact time. (3) At very low normal stresses, only a small drop in Pc induces many small slip events that are somewhat similar to earthquake swarm.

High Temperature Deformation of Artificial Quartz Gouge. Artificial quartz gouge, with an initial grain size of 60-130μm, was sheared between 35° precuts in cylindrical specimens. Pc = 200-300 MPa, Pp = 0-265 MPa, T = 600-950°C, and shear strain rates of 2×10^{-6}-10^{-5} s^{-1}.

Dry specimens exhibit (1) higher strengths than wet counterparts, (2) stable, aseismic sliding, (3) Reidel shears marked by extreme grain comminution along narrow zones inclined 10-20° to the shear zone boundary, and (4) sinuous stringers of opaque impurities. Cataclasis dominates, but undulatory extinction and deformation bands in porphyroclasts are also observed.

Wet tests are done at effective pressures Pe = 0-200 MPa, T = 900°C. Ultimate strengths decrease with decreases in Pe. At Pe > 50 MPa stress-strain curves are characterized by an elastic interval, followed by an initial stress drop, then stable sliding with periodic, small amplitude stress rises and drops. The Riedel geometry is only slightly developed and very fine-grained neoblasts and partially recrystallized porphyroclasts occur particularly along the shear zone boundary. Fine-grained neoblasts also form recrystallized pods within the shear zone surrounded by relatively undeformed grains.

At Pe > 50 MPa the initial stress drop is surpressed and stable sliding occurs early in the test. The deformation is homogeneously distributed across the shear zone. Porphyroclasts remain unstrained, but matrix grains are equant, have a homogeneous grain size, and a preferred orientation. They are probably syntectonic neoblasts.

Fault-Zone Fabric and Constitutive Relations. Theoretical models are the major tools in an earthquake prediction effort. They ideally permit consideration of boundary conditions, geometric effects, variations along strike and dip of mechanical properties, changes in country rock, etc., along faults. Unfortunately, to attain such a sophisticated level they must have imput from laboratory and field studies; particularly they require realistic constitutive relations, as determined in the laboratory. Attempts to approach this problem experimentally have been complicated by the questions of geometric, kinematic and dynamic similarity between the laboratory experiments and natural fault zones. Unless the issues can be evaluated, and the problems of similarity shown to be minimal, it is questionable whether experimentally derived constitutive relations will be viable in the immediate future.

Arguments for the importance of this question comes from both field and laboratory studies: (1) There is evidence that interfaces between the country rock and gouge may be highly irregular, introducing a major geometrical component into fault movements. (2) Laboratory experiments have clearly shown that under some conditions there is interaction between gouge and the country rock (Byerlee et al., 1976; Logan and Teufel, 1978).

To investigate this question, laboratory experiments have been conducted. The following conclusion appear warranted:

1. Fabric studies of experimentally deformed gouge have shown consistently developed fabrics. At critical amounts of shear strain, the sites of displacement shift from the gouge/country rock interface to the

"Y-fractures". Further displacement entails sliding gouge against gouge, and does not directly involve the country rock.

2. The above results have been obtained for relatively smooth gouge/country rock interfaces (specifically sawcuts), only partially addressing the problem of irregular interfaces. Laboratory specimens have been fractured, separated, and gouge material distributed along the surface. These were subsequently sheared, and behavior compared with sawcut interfaces. The character of the mechanical behavior is similar. Y fractures are dominantly confined to the gouge material. Invariably they develop as relatively smooth surfaces.

3. Field attempts to relate macro- and microscopic fabrics of laboratory experiments with those of natural fault zones have been encouraging (Dengo and Logan, 1979; Dengo, 1982; Chester, 1983). This validation of the laboratory-produced geometries is felt to be particularly important.

These results suggest that, although geometrical similarity has been used to construct the laboratory experiments, kinematic results are directly applicable to natural conditions, and valid constitutive relations may be achieved for gouge material.

Frictional Behavior of Ductile Fault Gouge. Cylindrical specimens of Tennessee Sandstone with dry, crushed halite between 35°-precut surfaces were deformed at 70-MPa confining pressure, at displacement rates from 10^{-1} to 10^{-6} cm/sec, and at 25°C. Under these conditions the fabric changes from elongate grains to equant neoblasts with increasing shear strain, indicative of a change in deformation mechanism from glide to recrystallization. A "ghost" structure of lineations (possibly the trace of a foliation), manifest by the alignment of crystals and of grain boundaries, and accentuated by impurities, is oriented at progressively smaller angles to the shear zone boundary as shear strain increases. The excellent correspondence between these angles and those calculated assuming simple shear combined with a constant thickness of the gouge, independent of displacement, indicates the deformation can be modeled as progressive, homogeneous simple shear. Although the external temperature of these tests is 25°C, thermally-activated dyes implanted within the gouge indicate the actual temperature is between 400° and 500°C. This temperature rise is supported by calculations of heat generated by crystal-plastic work, although frictional heating cannot be excluded as a possible heat source. In the slower rate tests, conduction plays a role in removing heat from the system. Changes in fabric and deformation mechanism with increasing shear strain are attributed to the corresponding increase in gouge temperature.

In some specimens porphyroblasts exhibit well defined euhedral {100} faces, particularly when bounded by a fine grained mosaic. Their boundaries become anhedral when there is interference of growth with neighboring porphyroblasts. It is proposed that the fine-grained mosaic represents small neoblasts formed by syntectonic recrystallization. This is based on their preferred orientation and a grain size independent of shear strain. The larger, euhedral porphyroblasts occur by (1) syntectonic recrystallization at the end of shearing, or (2) annealing or metadynamic recrystallization once shearing stops. The metadynamic case is preferred because it does not require extremely high temperatures or a nucleation interval post-shearing.

Slow displacement rate tests show an oscillation in strength somewhat similar to stick-slip events, but since the deformation is ductile, no acoustic emission is heard. For this reason they are more analogous to the phenomena of recrystallization waves found in metals, where stress oscillations are produced by repeated work hardening followed by recrystallization. These stress drops and the accelerating displacement rate associated with it may provide a model for the mechanism of deep-focus earthquakes.

Field and Laboratory Studies of the Punchbowl Fault, Southern California. Experimental deformation of naturally deformed rocks collected from the Punchbowl Fault, an inactive trace of the San Andreas, have been completed to determine the degree to which mechanical properties vary both along and across the fault. Chosen as an analog to active seismogenic faults, the Punchbowl Fault juxtaposes arkosic sandstones against igneous and metamorphic rocks along a continuous gouge zone. Field and petrographic observations demonstrate that (1) structures and fabrics within the fault zone are well preserved, (2) the sandstone is progressively more deformed towards the gouge, and (3) cataclasis was the dominant deformtaion mechanism. The compositions of the sandstone and the gouge samples are similar except for smectite content; typically 4% and 14%, respectively.

Texturally different gouges were particulated and sheared between precuts at a displacement rate of $3(10^{-4})$ cm s^{-1} and Pe = 50 MPa under both wet and dry conditions. The initial sliding strengths of the wet gouges are significantly lower than the dry gouges, but work harden at greater rates, suggesting that at some finite strain the coefficient of sliding friction for the two would be the same. Triaxial compression tests on naturally deformed samples, ranging from undeformed sandstone to intact gouge, under wet and dry conditions at a Pe = 50 MPa and strain rate of 10^{-7} show large variations in mechanical behavior; strength and modulus decreases while ductility increases with increasing natural deformation in the starting material. Water weakening also occurs in these tests with the greatest effect on the intact gouge, thus increasing the contrasts in response demonstrated under dry conditions. These experiments are consistent with previous reports demonstrating the influence of rock textures and fabrics, minor amounts of clay and water on the mechanical properties of rocks.

Reports

Shimamoto, T. and Logan, J. M., 1982, Stick-slip exhibited by simulated gypsum and serpentine gouges during their dehydration (Abstract): Program and Abstracts, Fall Ann. Mtg., The Seismological Society of Japan.

Chester, F. A. and Logan, J. M., 1982, Mechanical testing of fault zone materials (Abstract): EOS, Am. Geophys. Union Trans., v. 63, p. 1108.

Knapp, S. T., Friedman, M., and Carter, N. L., 1982, Gliding flow and recrystallization of halite gouge in experimental shear zones: EOS, Am. Geophys. Union Trans., v. 63, p. 1109.

Teufel, L. W., 1983, Frictional Instabilities in Rock: 24th U.S. Symposium on Rock Mechanics, Texas A&M Univ., p. 479-481.

Logan, J. M., Dengo, C. A., and Higgs, N. G., 1983, Experimental and Field Studies of Fault Gouge: Their Implications for Formulating Constitutive Relations: IUGG Meeting, IASPEI Program, p. 124.

Theoretical Mechanics of Earthquake Precursors

9960-02115

Gerald M. Mavko
Branch of Tectonophysics
U.S. Geological Survey
345 Middlefield Road, MS/77
Menlo Park, CA 94025
(415) 323-8111, Ext. 2756

Investigations

1. Modeled large-scale strike-slip earthquakes using a laboratory-inferred friction law.

2. Analyzed effects of micrometeorologic fluctuations on refraction leveling error.

Results

1. Numerical simulations of large-scale strike-slip earthquakes were made using a laboratory-inferred friction law. The simulations produce repeated unstable events followed by rapid postseismic slip, long periods of strain accumulation, and precursory accelerated slip. The simulations resemble observations of coseismic slip during the 1857 and 1906 great earthquakes on the San Andreas fault, and also roughly reproduce the observed apparent decrease in strain rate following those events. Variations in coseismic slip along strike can result from variations in stress or material frictional properties along strike, or from variations in the depth to the brittle-ductile transition. The simulations predict precursory accelerating slip and accompanying drops in strain rate that should be easily detectable with existing geodetic and creepmeter technology. The duration of the precursors, however, is model dependent. The parameter that determines the duration only weakly determines the coseismic and postseismic behavior, so it may be difficult to calibrate the precursory part of the models from past observations.

2. Traditional estimates of leveling refraction error are based on assumptions of laterally uniform thermal gradient and free-convection. Fluctuations in vertical temperature profile along the line of sight always occur due to variations in surface thermal properties and non-steady convection. Preliminary calculations indicate that these fluctuations tend to decrease the refraction error relative to the corresponding temporally and spacially averaged models.

INTERNAL FRICTION AND MODULUS DISPERSION

9960-01490

L. Peselnick and H.-P. Liu
Branch of Tectonophysics
U.S. Geological Survey
345 Middlefield Road, MS/77
Menlo Park, California 94025

Investigations

Elastic properties of rocks: Development of an apparatus for determining Young's modulus of rocks (as well as other solid materials) subjected to quasi-static stress and small (10^{-8}) strain. The objectives are (1) to investigate dispersion effects, specifically to compare 'zero-frequency', small strain elastic moduli of rocks with measurements from dynamic methods, and (2) to investigate small strain, quasi-static anisotropic elastic properties of rocks in terms of crack orientation and fabric. Such data, along with proposed Q measurements in rocks provide a means for investigating the anisotropy of internal friction at seismic strain amplitudes.

Results

A uniformily distributed load was applied to one end of an aluminum sample using the piston and cylinder arrangement shown in Figure 1. Low friction between the piston and cylinder walls was obtained by using a loose fitting "chevron" seal on the piston. The Young's modulus of the sample (10.27×10^6 psi ± 2%) was determined from measurements of P and S ultrasonic velocities and the sample density. Quasi-static measurements of displacement at a fixed (constant) location on the sample, as a function of load are reproducible to within 2 percent. The displacements when plotted against location on the sample show differences associated with stress concentrations for regions close to the granite surface plate. Calculations of the quasi-static Young's modulus from displacement data near the upper half of the sample, where the stress is more uniform, are reproducible to within 3 percent, and agree with the ultrasonically determined value of Young's modulus to 10 percent. The largest experimental uncertainty is non-uniform stress, especially at sample regions close to the granite surface plate. Both ends of the sample need to be uniformily loaded for further improvement of experimental accuracy.

The apparatus for investigating crack and fabric dependent quasi-static Young's modulus of rocks at stress levels as low as 10^{-8} is operational. Several measurements at strain amplitudes of 10^{-9} have also been obtained.

Figure 1. Sketch of the piston and cylinder for uniform loading at the top end of the sample. The lower end of the sample is cemented to a granite surface plate (G). The top of the sample (S) is fitted with a teflon piston (A) and cylinder (B) containing oil (E). This apparatus, including a capacitive displacement detector and piezoelectric quartz calibrating plate (not shown in the figure) are enclosed in a temperature controlled chamber supported by the table (T). The external weight (W) is transmitted via two flexible chains (C) through holes (H) to the loading pin (P) and piston. The displacement of the ledge (L) on the sample is measured by the stylus (D), capacitance detector and quartz calibrator.

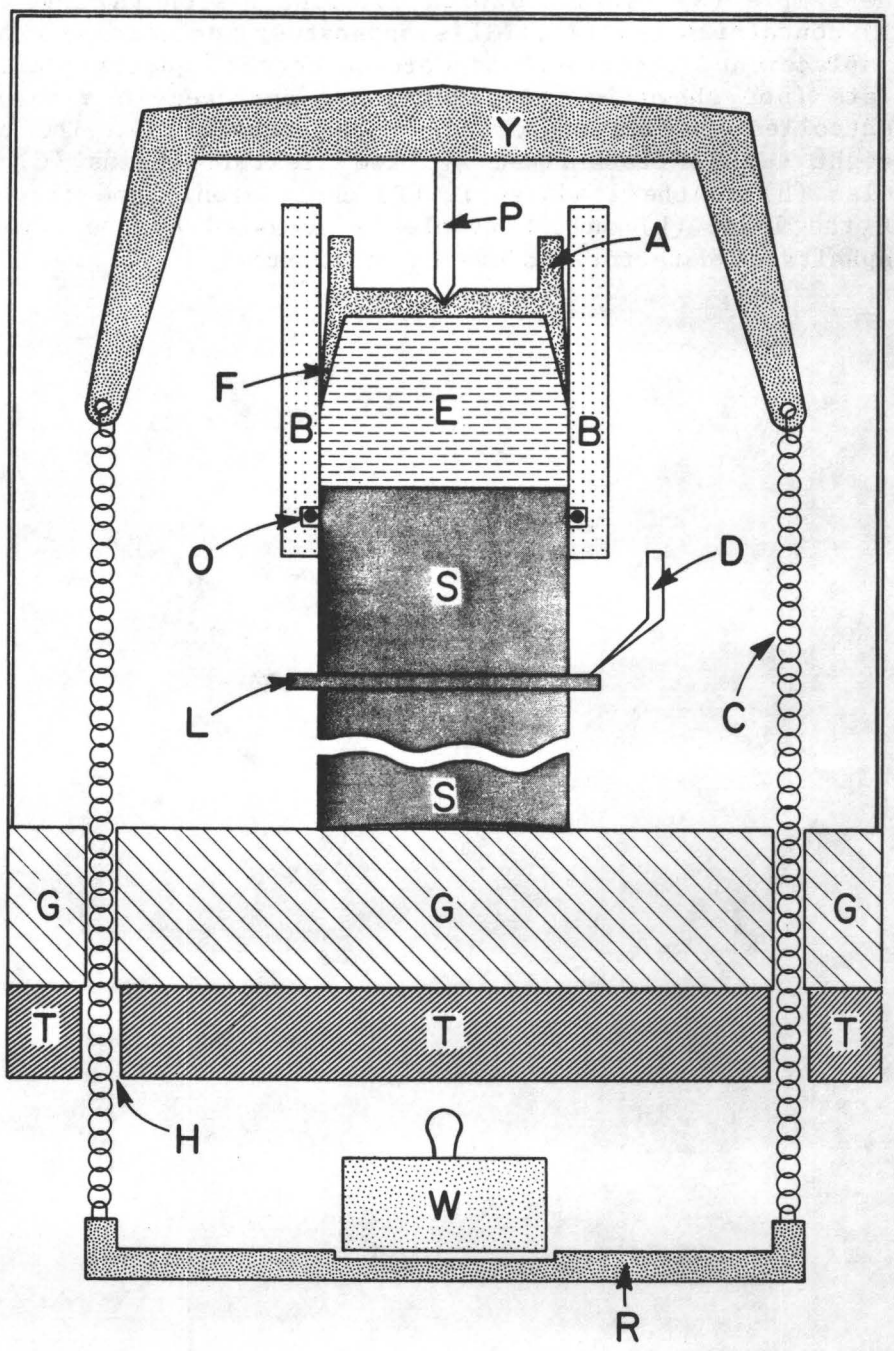
Y
P
A
F
E
B
B
O
S
D
L
C
S
G
G
G
T
T
T
H
W
R

Fault Mechanics and the Earthquake Generation Process

14-08-0001-20535

J.R. Rice (P.I.) and R. Dmowska
Division of Applied Sciences
Harvard University
Cambridge, MA 02138
(617) 495-3445

and

V.C. Li
Department of Civil Engineering
Massachusetts Institute of Technology
Cambridge, MA 02139
(617) 253-7142

Investigations

1. Stressing and rupture of slip deficient patches along transform plate boundaries is being studied. Creep, geodetic and seismic data are used to constrain the geometry of such patches along the creeping portion of the San Andreas fault near Parkfield, and thereby to infer loading rates and fracture parameters that are consistent with earthquake repeat times.

2. Time-dependent stress redistribution in the crust due to adjacent great earthquakes is being modelled in relation to shear relaxation in the asthenosphere and on downdip extensions of rupture surfaces in the lithosphere. Associated stress transfer and non-linear stress accumulation at a plate margin is being evaluated for the 1938-65 series of great Aleutian earthquakes.

3. Constitutive relations for fault slip, dependent on slip rate and evolving measures of surface state, are being used as a basis for fault instability modelling.

Results

1.1 An analysis is underway by Tse and Dmowska of the stressing of locked patches along a fault zone which is creeping elsewhere. The model consists of a faulted elastic lithospheric plate with finite thickness in a field of distant, uniform tectonic shear stress; the fault zone has an inhomogeneous strength distribution and is composed of locked patches and freely slipping parts modelled by cracks. The solution is given with the use of a "line-spring" model (Li and Rice, 1983) which treats the problem as a thickness averaged plane stress mode II cut coupled with an anti-plane strain mode III crack at each cross section along the fault trace.

The model is versatile. We have used it to analyze the stress distribution along a locked patch bordering regions carrying no stress, the locked area being a model of a seismic gap of the first kind (Mogi, 1979) surrounded by regions which slipped recently in great earthquakes and, for the first order of analysis, do not carry stress at present. The analysis shows stress concentrations at both ends of such a slip-deficient seismic gap, the stress distribution along the strike being dependent on the geometry of the locked region (i.e., its length, and depth of a slipping region below it). Further, the

model is used to evaluate the stress distribution in the stopping zone of a large earthquake, the region of the earthquake being modelled as a freely slipping crack, and the stopping part as a completely locked patch.

1.2 The model is further used to simulate slip and deformation processes along the San Juan Bautista to Cholame segment of the San Andreas fault in Central California. Matching the field measurements of surface creep along the San Andreas fault with the surface slip predicted by our model, and also taking into consideration the results of microseismicity studies in this region, we are able to place some geometric constraints on the locked patches. These are believed to be located near the Cholame to Parkfield section in the south and the Bear Valley to San Juan Bautista section in the north. As shown in Figure 1, we model the region of diminished slip close to Monarch Peak as being caused by a small locked patch located under it, although other interpretations are certainly plausible. The analysis shows dependences of surface slip on the geometry of locked patches, and allows us to quantify the stress concentrations at such patches (Fig. 1). Although the model is intended to stimulate the slip and stressing patterns for periods between earthquakes for the San Andreas fault segment considered, the results provide some understanding of the mechanics of the characteristic Parkfield earthquakes as well. For example, calculated stress accumulation and known repeat times suggest an effective fracture energy of 4×10^5 J/m^2.

2.1 Distant stress transfer in the seismogenic crust following large earthquakes has been evaluated by Rice and Gu. They compare coseismic static stress alterations, for which the Earth is assumed to respond elastically, to the long post-seismic alterations which will occur if there is relaxation of shear stresses on downdip extensions of the rupture plane, beneath the seismogenic layer, and (on what is thought to be a longer time scale) in the asthenosphere. For comparison, resulting alterations of crustal shear stress τ, at large distance r along strike from the center of a long strike slip rupture, with average slip D along length L and over the depth Z of the seismogenic layer, are:

$$\text{coseismic } \tau = \mu DLZ/2\pi r^3 \text{ , long post-seismic } \tau = 5\mu DLH/2\pi Zr^2 ,$$

where H is the lithosphere thickness and μ is the elastic shear modulus. The latter expression predicts considerably higher stresses and is discussed as a possible basis for distant earthquake aftereffects and delayed triggering of seismic events. Long term stress alterations greater than 0.5 bar are predicted out to approximately 150 km from representative M = 7 sources, and greater than 1 bar out to approximately 300 km of representative M = 8 sources.

2.2 The work of Lehner, Li and Rice (1981) was employed and extended by Li, in collaboration with C. Kisslinger, to analyze stress transfer along the Aleutian subduction zone in the most recent series of great ruptures there (Fig. 2a). It was found that the Shumagin (Fig. 2b) and the Unalaska gap have accumulated the highest stress changes according to a simulation which assumes that the whole subduction plate boundary had a uniform stress level in 1920. In general, the accumulation of stress at seismic gaps is highly non-linear due to coupling to the relaxing asthenosphere following each large rupture. Discontinuous jumps in stress due to adjacent ruptures further complicate the accumulation process. For example Figure 2c shows the stress in the 1938 rupture zone from 1920 to 1983. An important conclusion is that long term earthquake forecast models must account for such non-linear behavior over a complete earthquake cycle. Detailed discussion of stress accumulation in the

Aleutians is contained in a report by Li and Kisslinger (1983).

3. In an application and extension of recent work by Gu et al. (1983) on the stability of frictional slip, Rice and Gu have analyzed the response of a single degree of freedom fault model (spring-loaded sliding block) to perturbations representing coseismic changes in stress and post-seismic changes in stress rate on fault segments neighboring a prior earthquake. The work adopts the Ruina one state variable friction law, for which

$$A = (\partial\tau/\partial \ln V)_{instantaneous} \quad \text{and} \quad A-B = (\partial\tau/\partial \ln V)_{steady\text{-}state}$$

are taken as constants times normal stress, and there is exponential decay of stress with characteristic slip distance L for ongoing slip at fixed rate V. The heavy solid lines in fig. 3a show phase plane trajectories for an essentially stable [i.e., $\lambda \equiv -(A-B)/A < 0$] fault which is relaxing under a fixed spring-end displacement; τ_* is the strength for steady state slip at some reference rate V_*, the dashed line depicts the locus of steady states, and $k = KA/L$ is the spring stiffness. Sudden increases of shear stress, due to rapidly imposed fault loading, take place along 45° constant state lines. The situation depicted is regarded as an approximate model of the response of stable downdip extensions of brittle seismogenic zones to a crustal earthquake. Fig. 3b shows stability boundaries in the phase plane, for various values of dimensionless stiffness K, in the case of a potentially unstable fault segment ($\lambda>0$) subjected to steady motion of the spring end at rate V_*. Motions beginning in the region below the stability boundary remain there always and show stable approach of V to V_*. Those beginning above it exhibit continual increase of V with time and result ultimately in seismic instability. Sudden imposed changes in the loading result in changes along the 45° constant state lines; e.g., beginning at X_2 such change causes stable response if to point B but unstable if to point A when $K = 1.4$. All motions are ultimately unstable when $K < \lambda$.

In related work, Gu has integrated the one state variable friction law based on the assumption that the fault surface is subjected to a uniformly accelerated slip rate, and shows that the resulting τ versus slip relations resemble those recently reported by P. Okubo and J. Dieterich for dynamic stick slip events. Currently, Tse is developing numerical algorithms to deal (in a manner analogous to that in recent work by G. Mavko) with continuously distributed slip on an anti-plane shear model of a strike slip fault, with depth dependent transition from unstable ($\lambda>0$) to stable ($\lambda<0$) frictional constitutive properties.

Reports

Dmowska, R. and J.R. Rice, Fracture theory and its seismological applications, in Continuum Theories in Solid Earth Physics, ed. R. Teisseyre, Elsevier- in press, 1983.

Gu, J.-c., J.R. Rice, A.L. Ruina, and S.T. Tse, Slip motion and stability of a single degree of freedom elastic system with rate and state dependent friction, J. Mech. Phys. Solids - in press, 1983.

Li, V.C. and J.R. Rice, Pre-seismic rupture progression and great earthquake instabilities at plate boundaries, J. Geophys. Res. 88, pp. 4231-4246, 1983.

Li, V.C. and J.R. Rice, Precursory surface deformation in great plate boundary earthquake sequences, Bull. Seis. Soc. Amer. 73, pp. 1415-1434, 1983.

Li, V.C. and C. Kisslinger, Stress transfer and nonlinear stress accumulation at subduction-type plate boundaries, Applications to the Aleutians, submitted to Pure and Appl. Geophys., 1983.

Li, V.C., Estimation of in-situ diffusivity, submitted to Trans. A.S.C.E., 1983.

Rice, J.R. and A.L. Ruina, Stability of steady frictional slip, J. Appl. Mech. 50, pp. 343-349, 1983.

Rice, J.R. and J.-c. Gu, Earthquake aftereffects and triggered seismic phenomena, submitted to Pure Appl. Geophys., 1983.

Stopinski, W. and R. Dmowska, Rock resistivity in the Lubin (Poland) copper mine and its relation to occurrence of rockbursts, Proc. ISRM Seismicity in Mines Symp., ed. N.C. Gay - in press, 1983.

Tse. S.T., R. Dmowska and J.R. Rice, Stressing of locked patches along a creeping fault: San Andreas fault, Central California, presented at SSA Eastern Section annual meeting at Mohonk Mountain, September 18-21, 1983; full text in preparation.

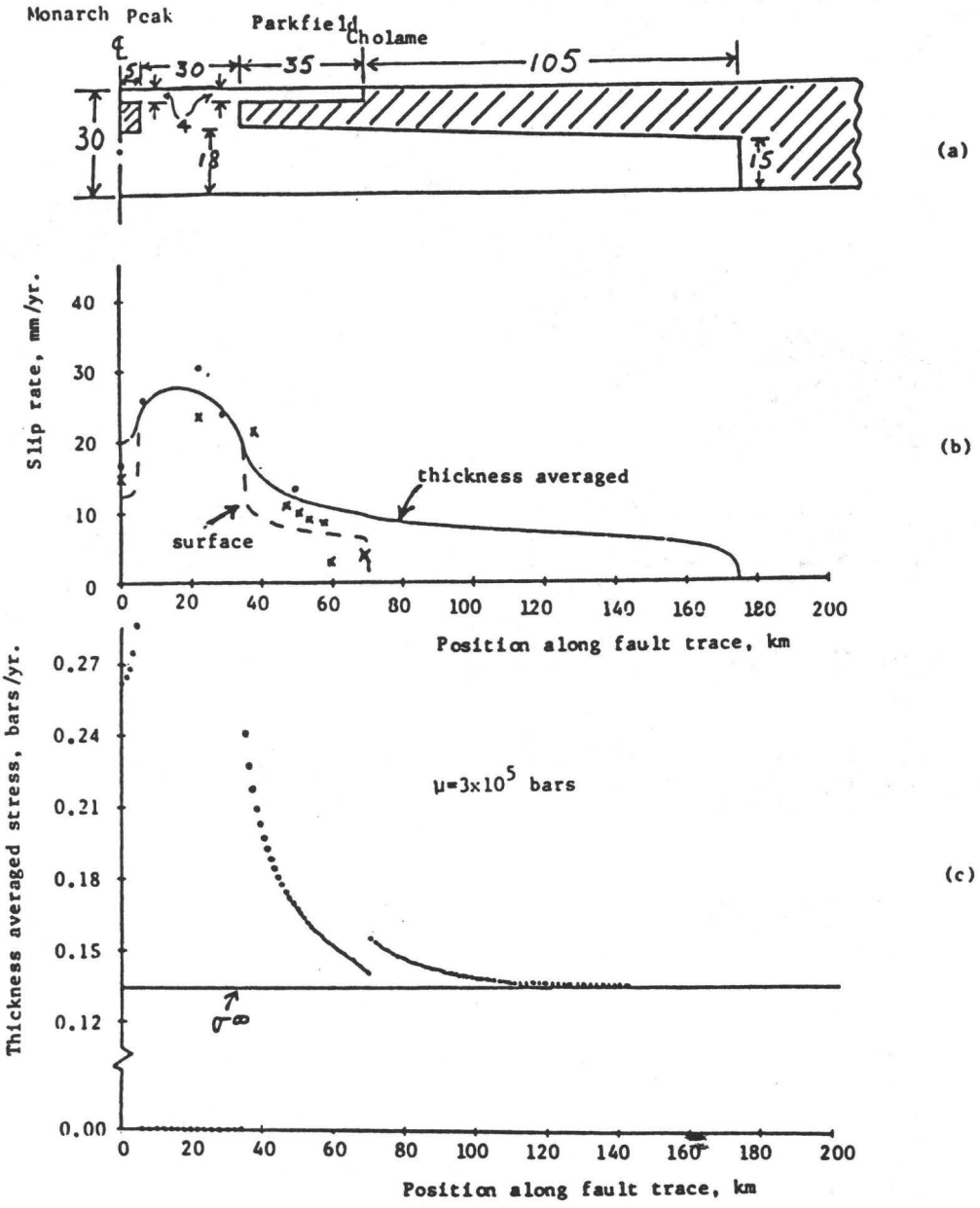

Fig. 1.

a) Distribution and geometry of locked patches (cross hatched) and slipping zones for section of San Andreas fault, b) thickness averaged (continuous line) and surface (broken line) slip rates, compared with geodetic (dots, after Burford and Harsh, 1980) and creep (crosses, after Schulz et al., 1982) measurements, c) thickness averaged stress distribution along the fault segment.

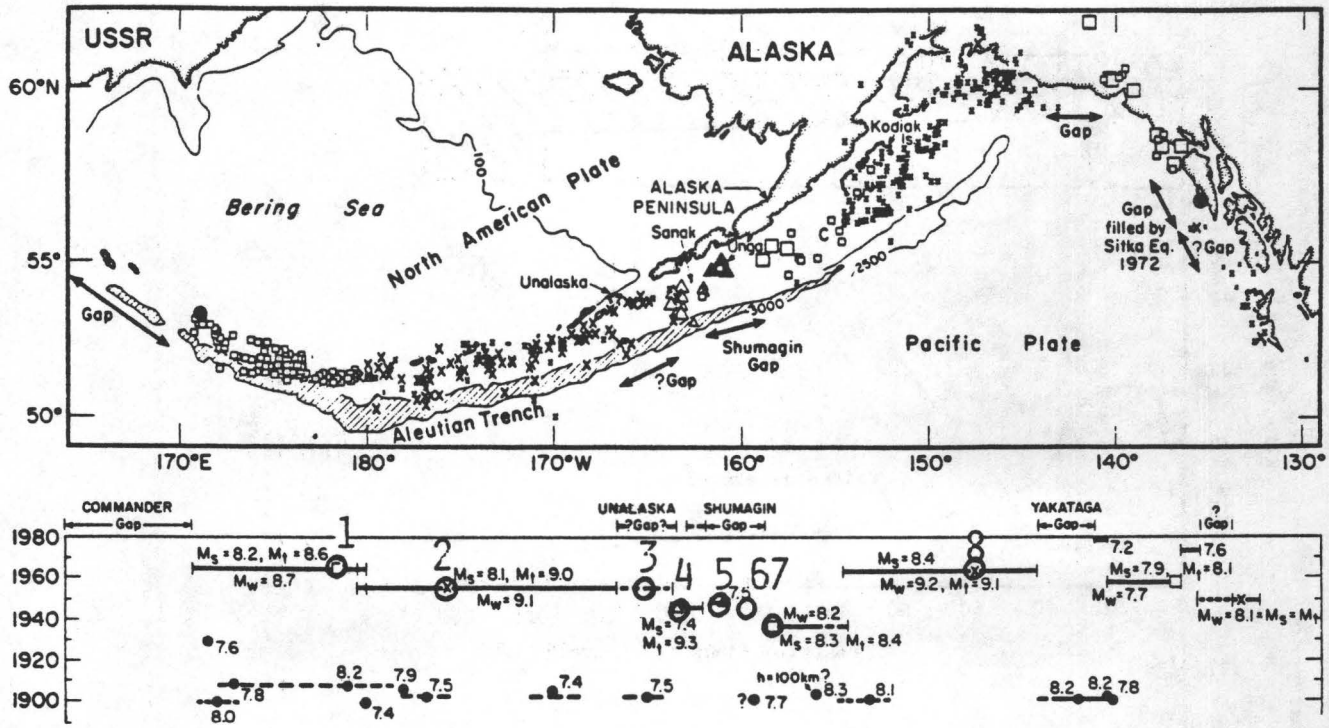

Fig. 2a.
Location and space-time of seismic rupture lineaments along the Aleutians (Sykes et al., 1981)

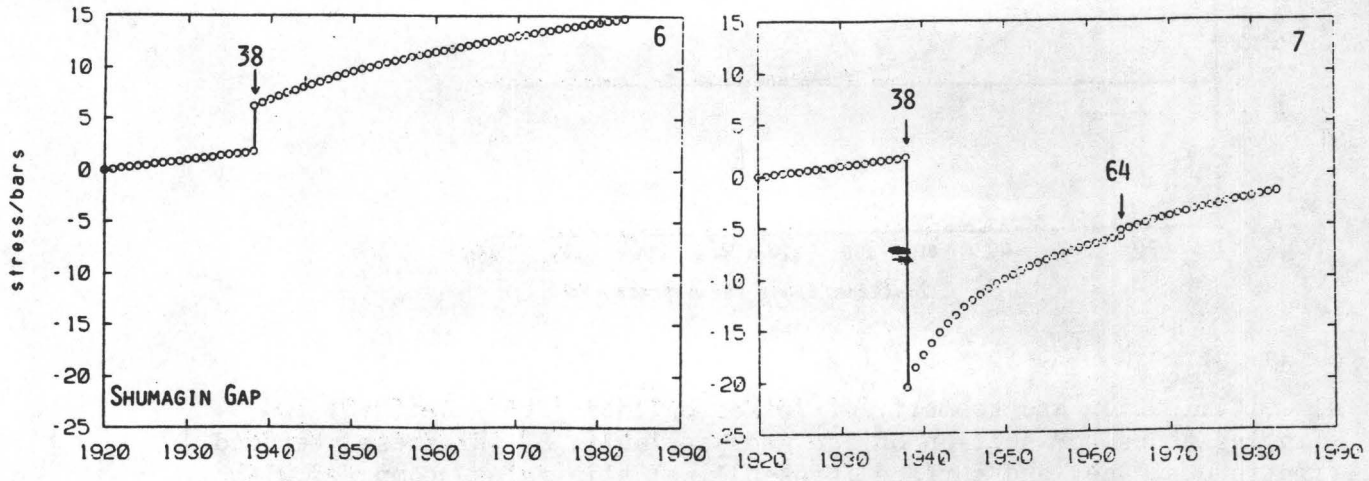

Fig. 2b.

Fig. 2c.

Stress alterations at Locations 6 and 7 since 1920. Note the high stress level and the accelerated accumulation rate in the Shumagin Gap, and the high nonlinearity in stress accumulation in an earthquake cycle in the rupture zone of the 1938 earthquake.

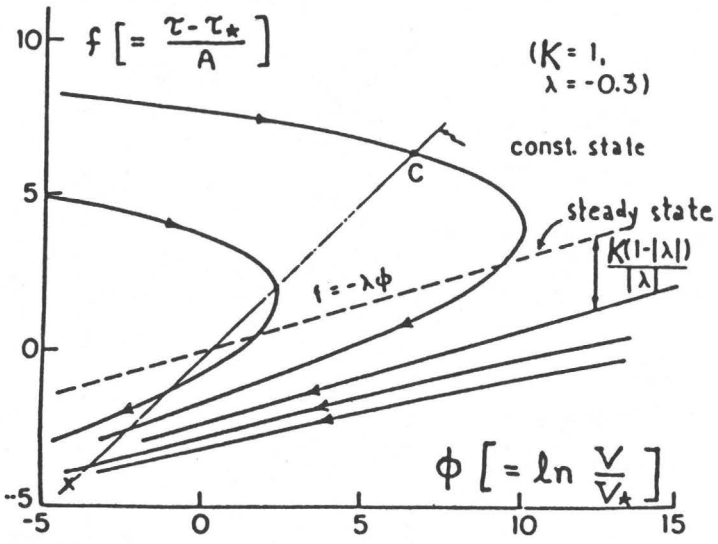

Fig. 3a. Trajectories for stable fault segment; fixed spring end.

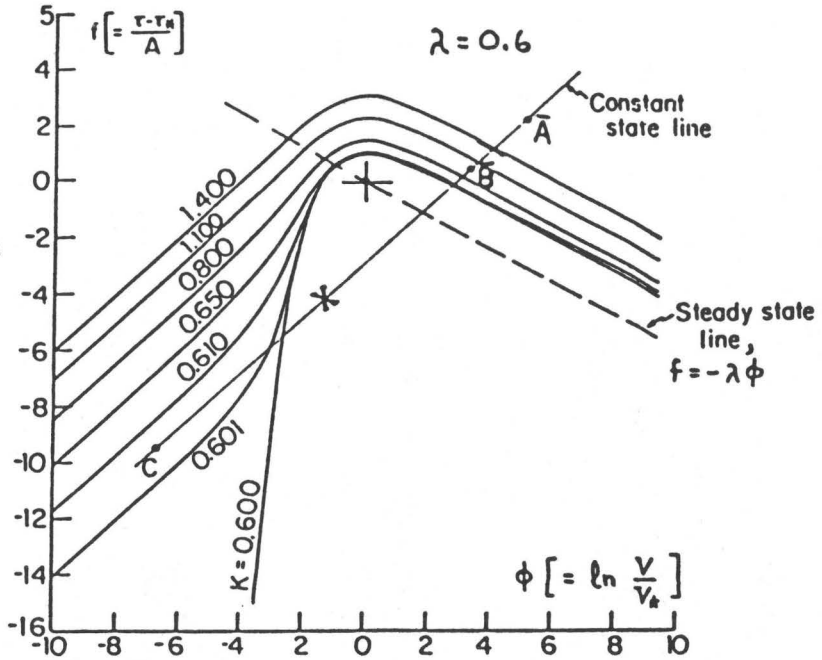

Fig. 3b. Stability boundaries for possibly unstable segment; imposed motion of spring end.

Theoretical Studies of Rupture Processes in Geological Material with Applications to Earthquake Faulting

14-08-0001-20577

John W. Rudnicki
Department of Civil Engineering
Northwestern University
Evanston, Illinois 60201
(312) 492-3411

Investigations

1. Effects of dilatant hardening on the inception of shear rupture.

2. Effects of slip zone interaction on moment, stress drop, and strain energy release.

Results

1. This analysis complements and extends Rice's study (JGR, 80, 1531-1536, 1975) of the effects of dilatant hardening on the development of concentrated shear deformation. The linearized analysis of Rice predicted that homogeneous dilatantly hardened deformation becomes unstable, in the sense that infinitesimal spatial nonuniformities grow exponentially in time, when the peak of the underlying drained (constant pore pressure) response is reached. The present analysis examines the rate at which instability develops by analyzing the shear of an unbounded layer containing a weakened sublayer of width h. The analysis is simplified by assuming that the deformation in each sublayer is homogeneous and that the change in fluid mass of the embedded layer is proportional to the difference in pore fluid pressures. The stress strain behavior of both the embedded layer and the surrounding material is assumed to be parabolic near peak stress and the weakened sublayer has a lower peak stress than the surrounding material.

The presence of the weakened sublayer causes localization instability, characterized by an unbounded ratio of the strain rate in the weakened layer to that in the farfield, to occur earlier than it would be predicted from the response of the material surrounding the embedded layer. The development of instability depends on the relative rates of imposed shear strain $\dot{\gamma}_\infty$ and the time scale of fluid mass exchange between the layers. The time scale is expressed as h^2/c where c is an effective diffusivity. In the limit $\dot{\gamma}_\infty h^2/c \to 0$, the pressure in the weakened sublayer is equal to that in the surrounding material and localization instability occurs at the peak of the drained response curve. For finite $\dot{\gamma}_\infty h^2/c$, localization instability is delayed until the material in the weakened sublayer has been driven to the peak of its undrained, dilatantly hardened response curve. The time delay between final instability and the time at which the weakened sublayer passes the peak of its drained stress strain curve is called the precursor time t_{pr} because rapid straining of the weakened sublayer occurs during

this period. For small $\dot{\gamma}_\infty h^2/c$, as appropriate for tectonic applications and most laboratory experiments, a nonlinear asymptotic analysis predicts that

$$t_{pr} \propto (\alpha h^2/c)^{2/3} (\lambda/\dot{\gamma}_\infty)^{1/3} \Delta^{-1/6}$$

where λ is the half-width of the peak of the stress strain curve, Δ is the difference in the peak stresses of the layers divided by λ times the elastic shear modulus and α is a nondimensional measure of the strength of dilatant hardening. For a wide range of numerical values, the precursor times are very short: less than a few hours for tectonic strain rates and less than a few tens of seconds for typical laboratory strain-rates. Consequently, the analysis suggests that, at least for this deformation state, discernable precursors due to dilatant hardening effects on the development of concentrated shear deformation are unlikely. Further analysis is needed to determine whether more easily observable effects occur for other deformation states, for example, axisymmetric compression, or are associated with dilation accompanying slip on a fault zone following the development of concentrated deformation in the weakened layer.

Rudnicki (Publication 3, below) has extended the formulation described above to arbitrary deformation states. Although the character of the governing equations is shown to be similar to that of the equations for the layer analysis, explicit results are not yet available.

2. Work in this area has been done in collaboration with J. D. Achenbach and K. Hirashima, who are not supported by this project. The following abstract from publication 4 summarizes this work:

> "Previous work of Rudnicki and Kanamori (JGR, 86, 1785-1793, 1981)which used collinear crack solutions to examine quantitatively the effects of fault slip zone interaction on moment, stress drop, and strain energy release, is extended by considering the effects of interaction between different size slip zones. The calculations demonstrate that the presence of a large pre-existing slip zone can substantially amplify the low frequency seismic signal due to slip on a nearby smaller slip zone. For example, if the length of the larger slip zone is ℓ, that of the smaller is $\ell/10$, and the distance between the nearest ends of the zones is $\ell/100$, the seismic moment due to slip on the larger zone induced by slip on the smaller zone is about 5 times that due to slip on an isolated zone of length $\ell/10$. Furthermore, because of the interaction between slip zones, the moment due to slip on the smaller zone is about 2.5 times the value for an isolated zone of the same size and subjected to the same effective stress. Conversely, estimates of stress drop based on the measured value of the moment and the total length on which slip occurs substantially underestimate the actual stress drop. Although the stress drop on the larger slip zone is zero, the induced slip there does contribute to W_0, the difference between the strain energy change and the frictional work. In fact, it is demonstrated that $W_0 = \tau_e M/2\mu$ where τ_e is the effective stress, M is the actual value of the seismic moment and μ is the shear modulus."

Publications

1. Rudnicki, J. W., A class of elastic-plastic constitutive laws for brittle rock, to appear in a special issue of the Journal of Rheology devoted to geological materials, 1983.

2. Rudnicki, J. W., Energy radiation from a spherically symmetric homogeneous source, BSSA, 73, 901-908, 1983.

3. Rudnicki, J. W., A formulation for studying coupled deformation - pore fluid diffusion effects on localization of deformation, in GEOMECHANICS, Proceedings of the Symposium on the Mechanics of Rocks, Soils and Ice (edited by S. Nemat-Nasser), Applied Mechanics Division, Vol. 57, American Society of Mechanical Engineers, New York, pp. 35-44, 1983.

4. Rudnicki, J. W., K. Hirashima and J. D. Achenbach, Amplification of moment and strain energy release due to interaction between different size fault slip zones, submitted to Journal of Geophysical Research for special issue on Fault Behavior and the Earthquake Generation Process, 1983.

5. Rudnicki, J. W., Effect of pore fluid diffusion on deformation and failure of rock, to appear in Mechanics of Geomaterials (edited by Z. P. Bazant), Proceedings of the IUTAM William Prager Symposium on Mechanics of Geomaterials: Rocks, Concretes, Soils, September 11-15, 1983, Northwestern University, Evanston. Publication by John Wiley, Ltd., London expected in 1984.

Earthquake Forecast Models

9960-03419

William D. Stuart
Branch of Tectonophysics
U.S. Geological Survey
Seismological Laboratory
California Institute of Technology
Pasadena, California 91125
(213) 356-6883

Investigations

The focus of this project is now the development of an earthquake instability model for seismic failure of the currently locked section of the San Andreas fault in southern California. The goal is to calculate the theoretical changes of fault slip and ground surface deformation that occur before instabilities analogous to great earthquakes on the fault.

Results

The current model contains a vertical strike-slip fault of variable strike embedded in a half space subject to remote forcing. The location, shape, and strength of strain softening fault patches allow unstable slippage comparable to slippage of great earthquakes. In particular, a simple model simulates the overall form and amount of slip for the 1857 earthquake inferred by Sieh. The model also approximately reproduces the earlier sequences of earthquakes inferred by Sieh.

Reports

Stuart, W.D., Use of instability models to forecast earthquakes in southern California (abs.), XVIII General Assembly IUGG/IASPEI, Hamburg, 1983.

Time and Environment Dependent Failure in Rock
14-08-0001-21354

P.L. Swanson, H.A. Spetzler and I.C. Getting
Cooperative Institute for Research in Environmental Sciences
University of Colorado
Boulder, CO 80309
(303) 492-8028

Investigations

Our overall objective is to understand the mechanisms responsible for time dependent phenomena that are precursory to or concomitant with the rock failure process. Laboratory studies of subcritical fracture were undertaken to understand this particular element of time and environment dependent deformation of upper crustal rocks. By varying the physical parameters which influence subcritical crack growth, namely temperature and environmental water content, we strive to identify specific mechanisms of subcritical rock fracture by comparison with simple materials such as glass or single crystals.

Results

The results of subcritical fracture experiments on five rock types under standard laboratory conditions are summarized in the plots of crack velocity versus applied stress intensity factor (mode I-tensile) in Figure 1. The apparent non-unique relationship between K_I and crack velocity, which is not observed for glass, is thought to be partly due to the measurement technique (relaxation form of double torsion testing). The slopes of the log K - log v curves seem to be fairly repeatable, however, and are a measure of the resistance to subcritical fracture. In glass the slope is controlled by the activation volume of the particular chemical reaction between the stressed crack tip and a reactant in the environment. The slope for the tests on rocks seems to be influenced by the the degree of heterogeneity in the microstructure (i.e., grain size, shape and mineral distribution). Irregularities in the K-v curves also seem affected by this. A search of the ceramics literature was made and it was found that synthetic materials also show this behavior. The schematic diagram in Figure 2 shows the effect of increasing microstructural complexity on the slope of the normalized K-v curves. It is apparent that the simpler the microstructure, the more susceptible the material is to subcritical fracture, i.e., there is a larger range of stress over which the fracture can extend subcritically. This subcritical fracture resistance - microstructure relation is largely a mechanical phenomena that exists independently of the particular chemical reaction responsible for the extension of single microcracks.

Before initiating the tests in which the environment (i.e., moisture) is changed by varying the partial pressure of water, tests were first run on glass with the apparatus in a vacuum chamber in order to repeat the results of S.M. Wiederhorn (1967). He has observed an increase in crack velocity at constant stress intensity factor of approximately one order of magnitude per order of magnitude increase in the partial pressure of water. Figure 3 shows four K-v curves obtained on a single glass microscope slide at room temperature and 40% relative humidity (~1.1 kPa partial water vapor pressure, data marked with X's). Three regions are shown associated with (I) the crack velocity limited by

the chemical reaction rate at the crack tip (lowest velocities), (II) a levelling-off region which represents the fluid transport rate-limited crack velocity regime and finally at the higher velocities, (III) the highly stress dependent but mostly environment independent region.

Lowering the partial pressure of water by ~5 orders of magnitude to $\sim 3\times10^{-2}$Pa (data marked by O's) did not produce the expected 5 order of magnitude decrease of crack velocity. Four tests were run on the same sample and the curves shifted to lower velocities as the time under vacuum increased. A furnace was constructed in order to bake out the specimens while in the apparatus under vacuum. The data marked with +'s were obtained from a sample baked out at 250°C and 1.5×10^{-1}Pa water vapor pressure and then tested at room temperature and 3×10^{-2}Pa water vapor pressure. The difference between these experiments and Wiederhorn's was that Wiederhorn conducted his tests in the same chamber that was used to anneal his crack guiding scribe line without any intermediate exposure to the atmosphere. No crack guide or annealment was used in the present experiments.

The conclusion from these tests is that the source of the reacting species for the chemical reaction at the crack tip does not have to be in the "atmosphere" or "environment". This means that once a material is wet it is susceptible, when under stress, to subcritical fracture even though the "environment" has been subsequently changed. We suggest that, under the assumption that silicate minerals behave similar to the silicate glass, interconnected cracks in the uppermost crustal rocks will always be susceptible to this effect unless some mechanism is available for removing surface adsorbed moisture. There is no need for free liquid water. Higher temperatures at depth, in the absence of confined liquid water or steam and dehydration reactions, would desorb exposed surfaces and reduce the possibility of this mechanism contributing to time dependent deformation.

Since the subcritical fracture resistance appears to be so strongly affected by the mechanics of the microstructure, the effect of temperature on crack propagation rates will not be be limited to the activated process responsible for crack extension in glass or single crystals. Temperature and pressure can affect the heterogeneity of the microstructure and this will also have to be taken into account when extrapolating expected fracture behavior to depth in the crust.

References

Wiederhorn, S.M., Influence of Water Vapor on Crack Growth in Soda Lime Glass, *J. Am. Ceram. Soc.*, 50, 407-414, 1967.

Reports

Swanson, P.L., Subcritical Crack Growth and Other Time and Environment Dependent Behavior in Crustal Rocks, submitted to *J. Geophys. Res.*.

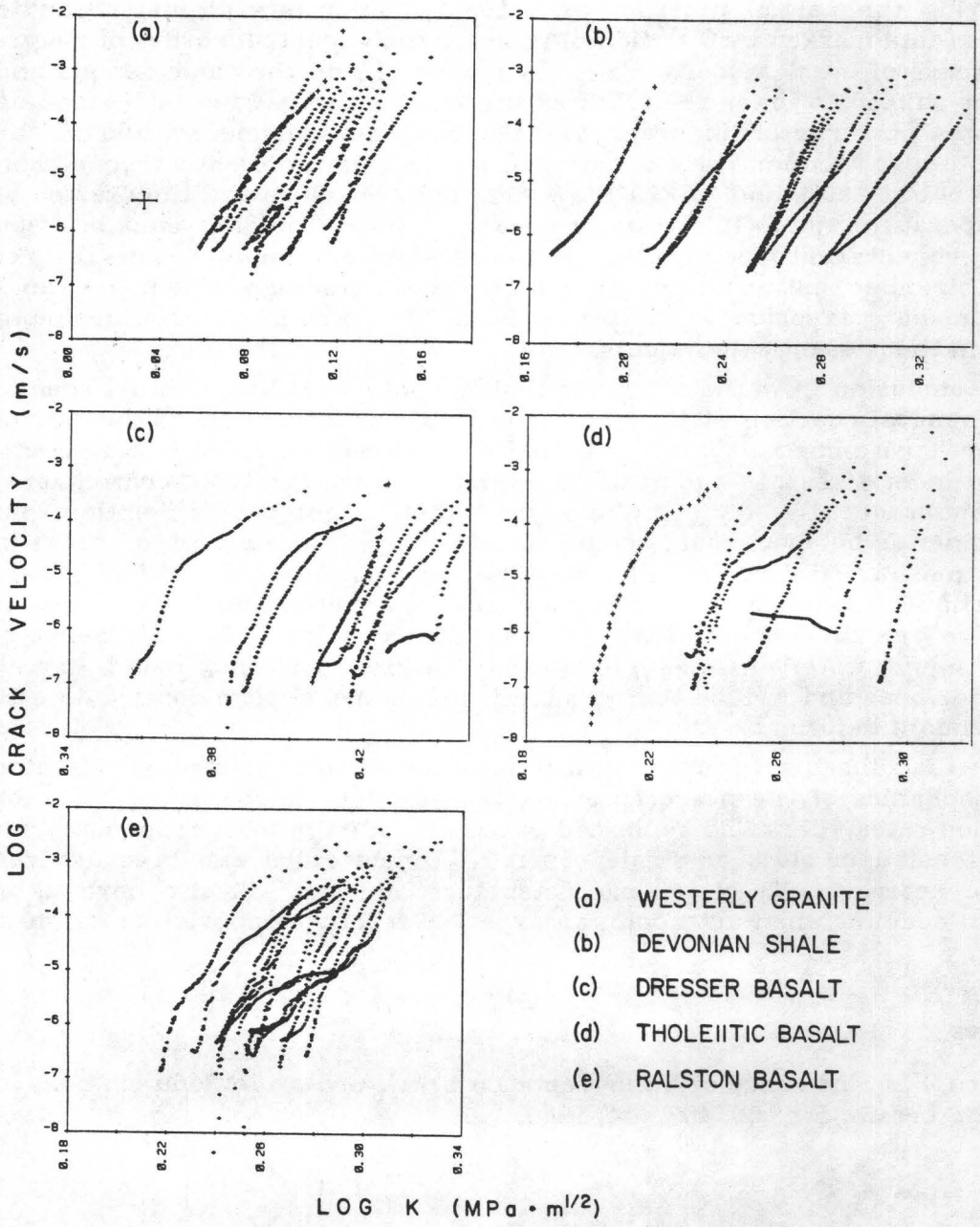

Fig. 1. Composite plot of stress intensity factor - crack velocity relations. Data obtained from relaxation form of double torsion testing. The sharp hooks at the lower end of several curves are artifacts of the 6th degree polynomial fit to the log force-log time data.

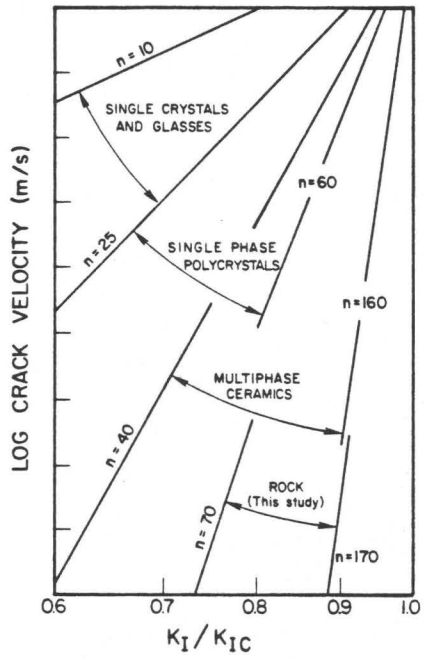

Fig. 2. A search of the synthetic materials literature shows a general trend toward greater resistance to subcritical fracture (higher n-values; $v \propto \left\{\frac{K}{K_c}\right\}^n$) with increasing microstructural complexity.

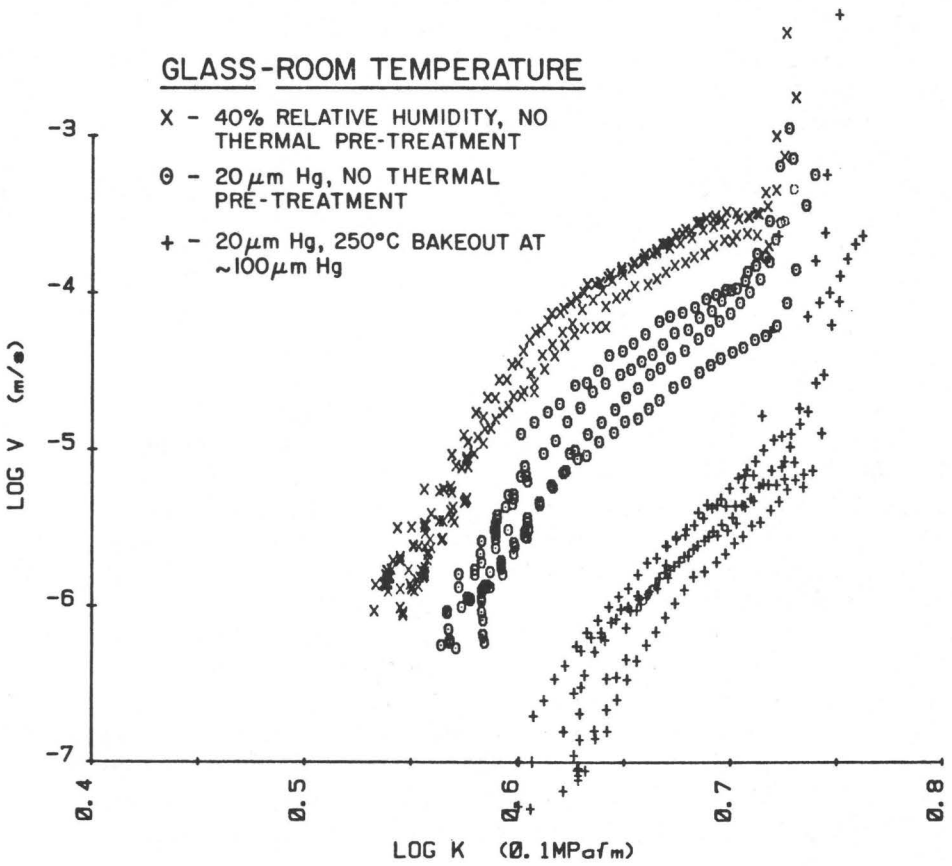

Fig. 3. Surface adsorbed moisture was found to maintain high crack velocities even at pressures 5 orders of magnitude less than atmospheric. High temperature bakeout while under vacuum was necessary to obtain large decreases in crack velocity at same K_I and room temperature.

Experiments on Rock Friction Constitutive Laws Applied to Earthquake Instability Analysis

14-08-0001-21227

Terry E. Tullis
John D. Weeks
Department of Geological Sciences
Brown University
Providence, RI 02912
(401) 863-3829

Investigations

1. We have investigated experimentally the dependence of frictional resistance on velocity of steady sliding at normal stresses up to 75 MPa. The purpose is to resolve existing controversy as to whether, for steady-state sliding, higher velocities result in higher or lower frictional resistance at normal stresses for which earthquakes occur. This information is a critical part of the constitutive description of frictional behavior.

2. Experiments were undertaken to determine whether the resistance to frictional sliding increases with time of truly stationary contact between sliding episodes. Previous experiments by Dieterich (1972) which demonstrated strengthening during nominally stationary contact involved small amounts of creep displacement. The purpose of this investigation was to determine whether the creep displacement was necessary to produce the strengthening. It is part of a larger study to determine what micromechanical processes occur on sliding surfaces during sliding and stationary contact, and to determine what constitutive description correctly describes the observed behavior.

3. We have begun investigation of the physical and chemical character of gouge developed by sliding on a rough ground surface of granite. Study of the gouge character will aid in understanding the processes that determine the constitutive laws for frictional sliding. Understanding of these processes is needed to scale laboratory results to natural faults.

Results

1. Results of a rotary shear experiment at 75 MPa normal stress are shown in Figure 1, together with the results from Dieterich (1978) at lower normal stress. Our results show that the same dependence of frictional resistance on sliding velocity is found at 75 MPa as at 2 MPa. They show that the frictional resistance for steady-state sliding decreases as the velocity of sliding increases. These results suggest that the contradictory results found by Solberg and Byerlee (1981) do not represent steady-state behavior. The amount of displacement needed in order to obtain steady-state behavior may depend on the initial roughness of the sliding surface and on the presence and thickness of an artificial gouge layer, although further experiments are needed to fully understand why different results have been obtained by different workers. We believe our recent results extend the applicability of Dieterich's constitutive description to normal stresses approaching those at which earthquakes usually occur, enhancing the value of instability analysis based on this theory to our understanding of earthquakes. Experiments at higher normal stresses will be undertaken to determine if the same effects are found at the actual normal stresses of typical crustal earthquakes.

2. Figure 2 shows the two similar types of experiments that we have done in studying the effect of time of contact on resistance to subsequent frictional sliding. The left plot shows

an experiment in which some creep displacement occurs on the sliding surface (internal displacement axis and matching middle curve) even though the point at which the load was applied was held fixed. This is the type of experiment done by Dieterich (1972) in which creep displacement occurs as a result of the (relaxing) shear stress on the sample during the hold interval. This is contrasted with the type of experiment illustrated in the right plot in which the shear stress is reduced to zero during the hold interval and only the normal stress on the sliding surface is maintained. In this case after the load point is moved back to reduce the shear stress to zero, no motion of the sliding surface occurs during the hold.

Results for three different hold times, with and without shear stress, are shown in Figure 3 for an experiment conducted at 22 MPa normal stress. A convenient measure of the strengthening is the magnitude of the delta mu peak labeled on the top right curve. As shown, this strengthening during the holds is found in the experiments in which there was no shear stress and thus no creep displacement during the hold as well as in those for which shear stress was present. The magnitude of the strengthening is similar with and without shear stress and it increases with the log of the hold time in a manner similar to that found by Dieterich (1972). Similar results were found in a separate experiment at 75 MPa normal stress in that strengthening occurred without shear stress as well as with it. At 75 MPa the amount of strengthening did not change appreciably with the length of hold time, a result we currently do not understand.

3. Examination of our samples using the scanning electron microscope and the petrographic microscope reveals some interesting structures which may help us understand the micromechanical processes occuring on the sliding surface. Our Westerly granite samples were first ground with a surface grinder to produce a flat surface and then hand-lapped with 80 grit alumina powder to increase their roughness. Sliding under 75 MPa normal stress produced a layer of gouge 0.1 to 0.25 mm thick after 18 mm of sliding. Optical and SEM study of the gouge reveals that it consists of flakes separated by discontinuities which appear to represent discrete sliding surfaces similar to those observed by previous workers. SEM shows that these flakes are composed of spherical particles less than 0.5 microns in diameter and isolated angular fragments larger than 5 microns. Several observations suggest that the minute gouge particles may be composed of amorphous siliceous material: 1) The sphericity of the particles, 2) their tendency to agglomerate into botryoidal masses, 3) their morphological resemblance to similarly sized opaline gel spheres, 4) preliminary powder diffraction in which gouge X-ray peaks are reduced and broadened relative to mortar ground Westerly granite. SEM observations of the truncation of globules at flake boundaries and lineations on flake surfaces indicate that they are the actual sliding surfaces in the gouge. The microscopic smoothness of flake surfaces and the truncation of globules indicate extreme localization of strain as Ruina (1980) predicted for velocity-weakening materials.

Reports

Weeks, J. D., and Tullis, T. E., 1983, Increase in Frictional Strength of Granite During Static Contact: *EOS*, v. 64, no. 18, p. 317.

Tullis, T. E., Weeks, J. D., and Bechtel, T. D., Inverse Dependence of Frictional Resistance on Sliding Velocity at Elevated Normal Stress: *EOS*, v. 64, no. 45, (submitted).

Weeks, J. D., Tullis, T. E., and Bechtel, T. D., Nonlinear Instability Effects in Experiments on Rock Friction: *EOS*, v. 64, no. 45, (submitted).

Bechtel, T. D., Weeks. J. D., and Tullis, T. E., Observations of Experimentally Produced Fault Gouge: *EOS*, v. 64, no. 45, (submitted).

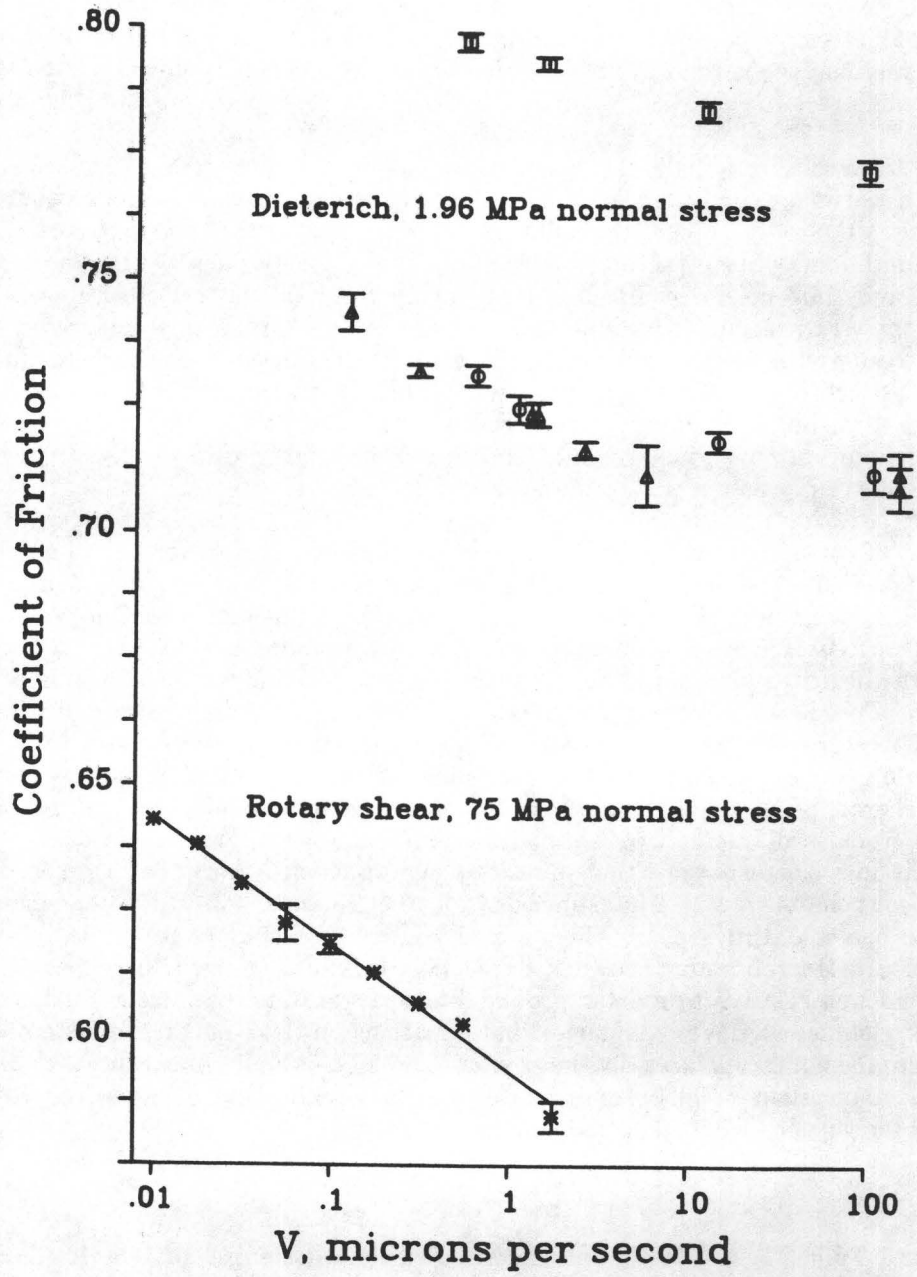

Figure 1. Coefficient of friction as a function of sliding velocity. The three different data point symbols at the top are for three experiments reported by Dieterich (1978); the important consideration is the slope defined by each set and not the offset between the data sets. The stars represent our data obtained at elevated normal stress, and the line is a least-squares fit to our data.

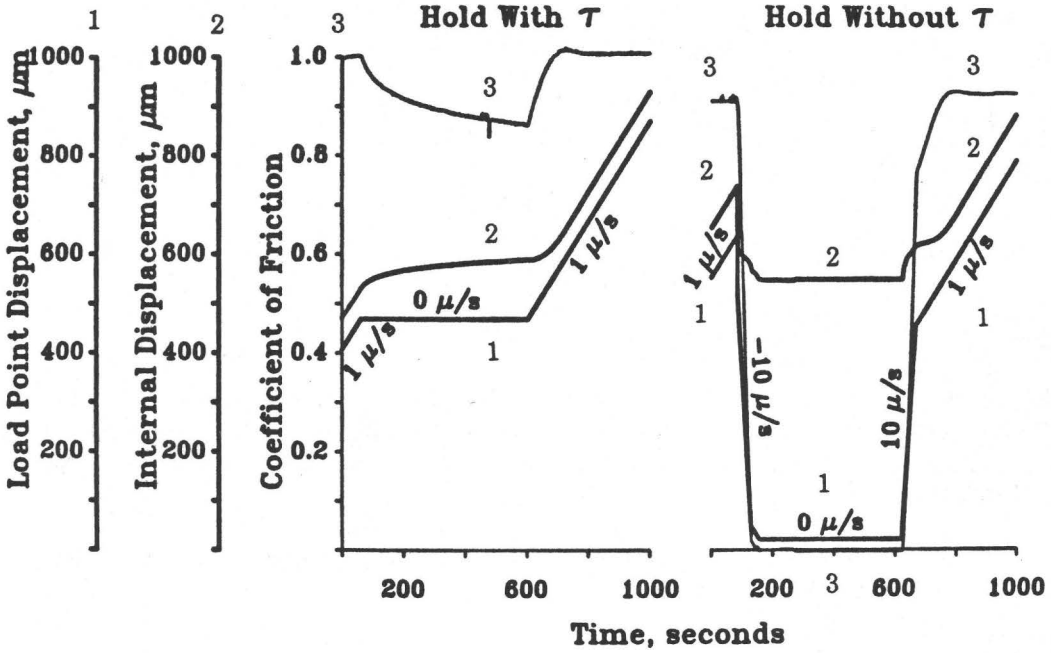

Figure 2. Illustration of the two different types of experiments conducted to investigate the effect of hold time on coefficient of friction. The correspondence between the three abcissas and the curves is given by the numbering.

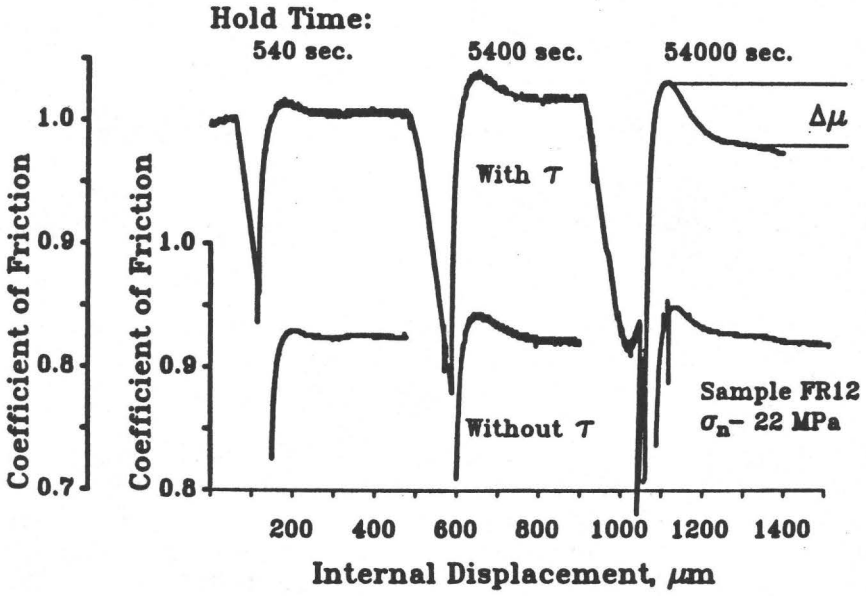

Figure 3. Strengthening of frictional surfaces after holds with and without shear stress as shown by magnitude of transient friction peak upon subsequent sliding. The normal stress decayed during the 54,000 second hold time without shear stress and was reset just prior to the resumed sliding. This may explain why the magnitude of the friction transient is smaller than was found for the same time with shear stress.

Time-dependent Constitutive Relation for the San Andreas and Hayward Fault Gouges

USDI 14-08-0001-21352

C.Y. Wang
Department of Geology and Geophysics
University of California, Berkeley 94720

Investigation

1. Laboratory experiments designed to provide data for determining the time-dependent constitutive relation for clayey gouge and gouge-like materials, at pressures equivalent to those at mid-crustal depths and at a broad range of strain rates.

2. A detailed gravity survey across the San Andreas fault zone near Bear Valley, California.

Results

1. A constitutive relation of saturated clayey gouge samples at high pressure is obtained from experimental results. These experiments were carried out at various strain rates and confining pressures, on saturated, clayey fault gouge from the San Andreas and Hayward fault zones in central California, as well as on API standard clays. This constitutive relation may be described by a spherical pore model for porous material, and may be presented in two different stress regimes:

   1) Before yielding $e + N \frac{\dot{e}}{e(e+1)} = A\tau + B \log(\sigma - P_w) + C$

   2) After yielding, $e + N' \frac{\dot{e}}{e(e+1)} = A' \log\tau + B' \log(\sigma - P_w) + C'$

   where N, A, B, C, and N', A', B', C' are empirical constants, e the void ratio, $\dot{e}$ the rate of change in e, τ the shear stress, σ the normal stress, P_w the pore pressure.

   As a test for the above constitutive relation, samples of different thicknesses were examined under the same conditions; it was shown that this constitutive relation satisfactorily predicts the experimental results.

2. Microscopic examination of some sheared samples showed that the experimentally observed work-hardening may be associated with cataclastic reduction in grain size, with corresponding reduction in pore space and increase in the number of grain-to-grain contact. We suggest that such processes may also occur in natural faults and the empirical relations shown above may have potential application in modeling the tectonic activities of clay-rich fault zones.

3. A detailed gravity survey across the San Andreas fault near Bear Valley was carried out, using a calibrated LaCoste-Romberg gravimeter. The data will be used to model the density structure of the fault zone, which would bear on the fault zone constitution at depth.

Reports

Chu, C. L., and Wang, C. Y., A constitutive relation of saturated clayey fault gouges at high pressures, (Abstract), EOS Trans. Am. Geophys. Union, 64, 1983 (in press).

Wang, C. Y., On the constitution of the San Andreas fault zone in central California (manuscript), submitted to J. Geophys. Res., 1983.

Seismic Source Mechanism Studies In The Anza-Coyote Seismic Gap

14-08-0001-21271

Jonathan Berger and James N. Brune
Institute of Geophysics and Planetary Physics
Scripps Institution of Oceanography
University of California, San Diego
La Jolla, CA 92093
(619) 452-2889

Investigations

This report covers the progress of the research investigating the Anza-Coyote Canyon seismic gap for the period of the first half of 1983. The objectives of this research are: 1) To study the mechanisms and seismic characteristics of small and moderate earthquakes; 2) To determine if there are premonitory changes in seismic observables preceeding small and moderate earthquakes. This work is carried out in cooperation with Tom Hanks, Joe Fletcher and Linda Haar, of the U.S. Geological Survey, Menlo Park.

Network Status

During the period of this report, up to eight stations of the Anza seismic network were telemetering three component data. The network was set at a low gain to try to record earthquakes up to magnitude 4 occurring inside the array. Access to some of the seismic stations was limited by the severity of the winter storms this year. We determined several aspects of operating the array which needed improvement. These included improving structurally the receiving antennas which were subjected to unexpectedly heavy icing and high winds, as well as making improvements to the system noise characteristics. With the last snow melting in early June, we started testing various modifications; formulating plans to make necessary changes during the summer.

Seismicity

In the six months of winter and spring, the Anza network recorded 192 earthquakes of various sizes. From the start of April until mid-July, nine magnitude M_L = 2 to 3 events and five M_L = 3 to 4 events were recorded inside the array dimensions. The largest of these measured M_L = 3.7. The seismicity (Figure 1) appears to be not at all associated with the main trace of the San Jacinto fault on the north-west half of the array, or with any of the three principal branches of the fault zone south-east of the trifurcation near the town of Anza. The depths of the events range from 18 km on the north-west end of the array near the Hot Springs fault and the San Jacinto fault, to less than a few kilometers near the south-west side of the array where no known surface faults exist. In the cross-section A-A′ (Figure 2), the shallow events trend to a depth of about 10-12 km on the main trace of the San Jacinto fault.

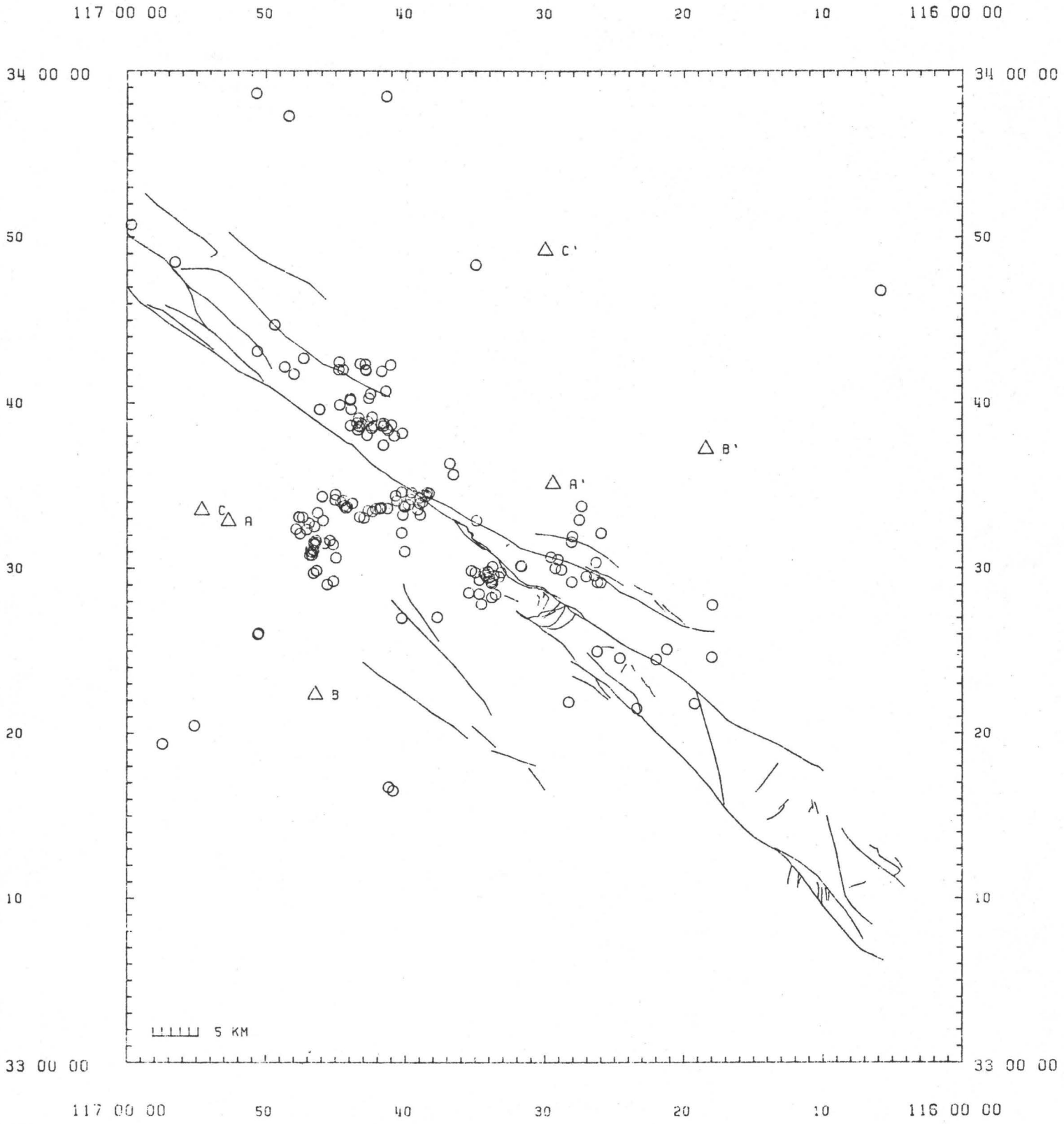

ANZA SEISMICITY OCT 82-AUG 83

Figure 1.

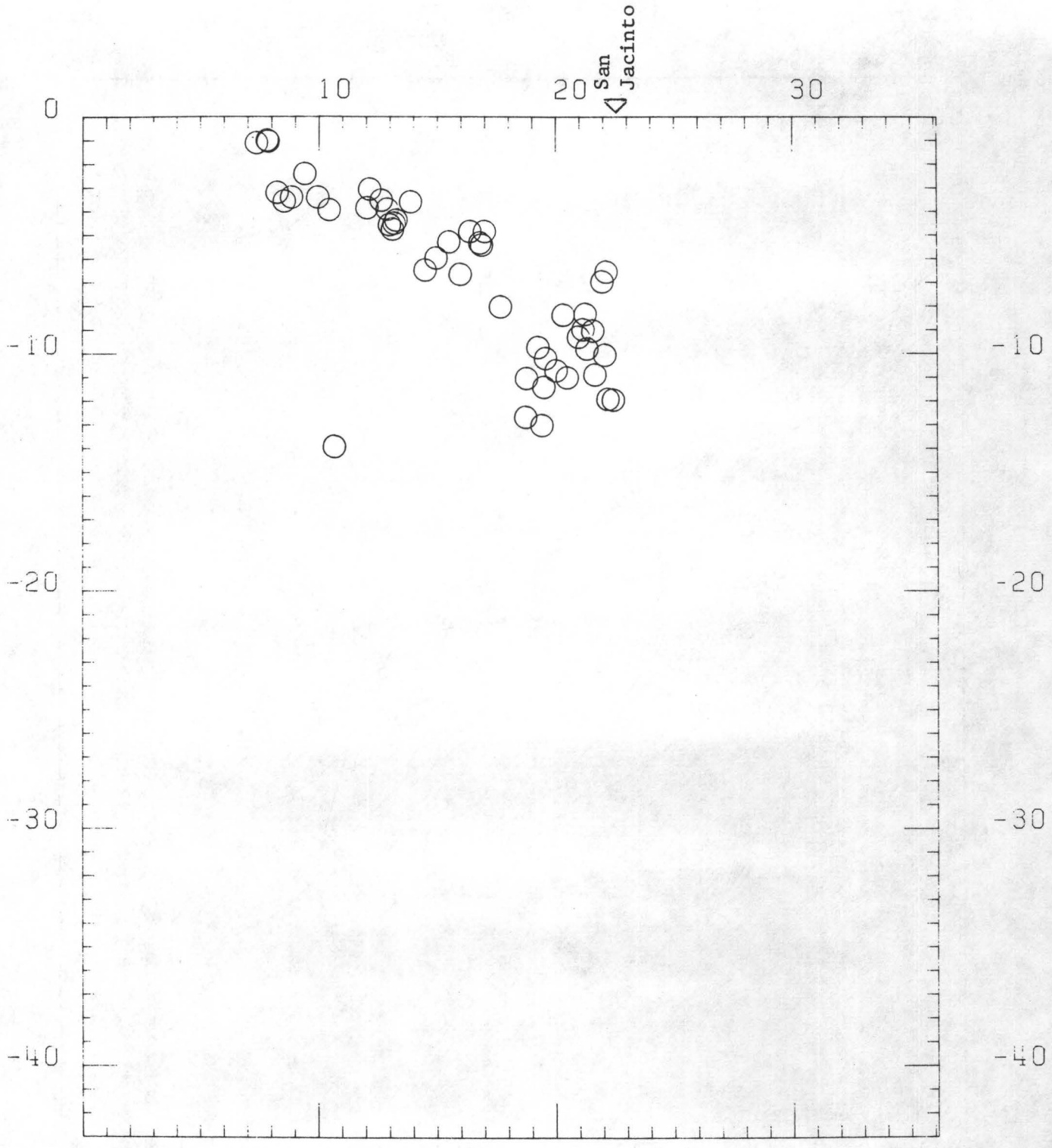

CROSS-SECTION A-A

Figure 2.

Experimental Study of Ultra Fine-Grained Granular Fault Gough

Contract No. 14-08-0001-19789
W. F. Brace
P4
Massachusetts Institute of Technology
Cambridge, Massachusetts 02139
617-253-3278

Experiments during this period concentrated on the sintering of ultra fine-grained (UFG) granular quartz and feldspar gouges at high temperatures and pressures. Investigations of frictional properties of UFG gouge and pore pressure generation during shear have been completed and will be summarized in the final technical report. A microscopy and surface area study of unaltered, natural quartz gouge was also completed.

UFG quartz powder (median sizes: 1.5, 3.5, and 6.5 μm) was hot pressed in an internally heated gas-medium pressure vessel at temperatures of 800-950°C, confining pressures of 300-650 mPa, pore pressures of 0 & 100 mPa, and times of 0-7 hrs. (Blendell, 1983). Porosities were measured by Archimedes' method in CCly and by point counting pores in scanning electron micrographs. The results are summarized in Table 1. The former method is believed to be inaccurate due to the presence of microcracks; introduced during unloading from pressure and by friction at the end pieces. Therefore, all porosities (Table 1) are from point counts. Porosity decreases as expected with increasing temperature, confining pressure, and time. The effect of particle size is a yet unknown. The primary densification mechanism is believed to be diffusion-enhanced plastic flow at grain-grain contacts. The dramatic decrease in porosity with increasing confining pressure when H_2O is present supports the hypothesis of hydrolytic weakening, lowering the yeild stress (for summary and reference list see Mainprice and Paterson, 1981).

UFG feldspar powder was prepared from polycrystalline rock of Amelia Courthouse albite. The rock was crushed into millimeter-sized particles in a jaw crusher and then pulverized in a shatterbox. The powder was then washed with HCl and HNO_3 solutions and rinsed in distilled H_2O. The final product was sized in an air centrifuge into median size distributions of 2, 5, 9, 16, and 25 μm. Sedigraph analyses of the 2, 5 and 25 μm fractions are shown in Figure 1 (solid lines). The 5 μm powder was re-centrifuged and then sieved through a 270 mesh screen to remove very large (30-70μm) anomalous particles. Most of these particles were removed but the mean particle size increased to 10 μm (dashed line in Figure 1).

Hot-pressing experiments were performed using this 10 μm albite powder. In both wet and dry experiments performed below the albite + H_2O solidus, porosities greater than 12% were obtained. The affect of H_2O on the densification of albite is unknown, but H_2O doesn't appear to enhance plastic flow at the low temperatures used to stay below the solidus.

As a supplimentary project to the main proposal, scanning and transmission electron microscopy (SEM and TEM) studies and surface area measurements of unaltered, natural UFG quartz gouge were also completed (Olgaard and Brace, 1983). Fault gouge collected from two mining-induced seismic shear fractures located in a deep gold mine near Johannesburg, South Africa was analyzed. Microscopy showed that: 1) the particles ranged in size from the initial grainsize of the source rock (500 μm) to less than 0.05 μm and 2) particles greater than 1 μm in size are slightly rounded and nearly equant while submicron-sized particles are highly angular and platey and commonly show basal plane cleavage. The average specific surface areas of the two gouge samples were 0.7 and 2.0 m^2/g indicating that the surface energy may be 1 to 10% of the toal energy released during an earthquake.

Figure 1. Particle size distributions for Amelia albite. Solid lines are for 2, 5, and 25 μm fractions that were air centrifuged once. Dashed line is from 5 μm fraction that was air centrifuged a second time and then sieved through a 270 mesh screen.

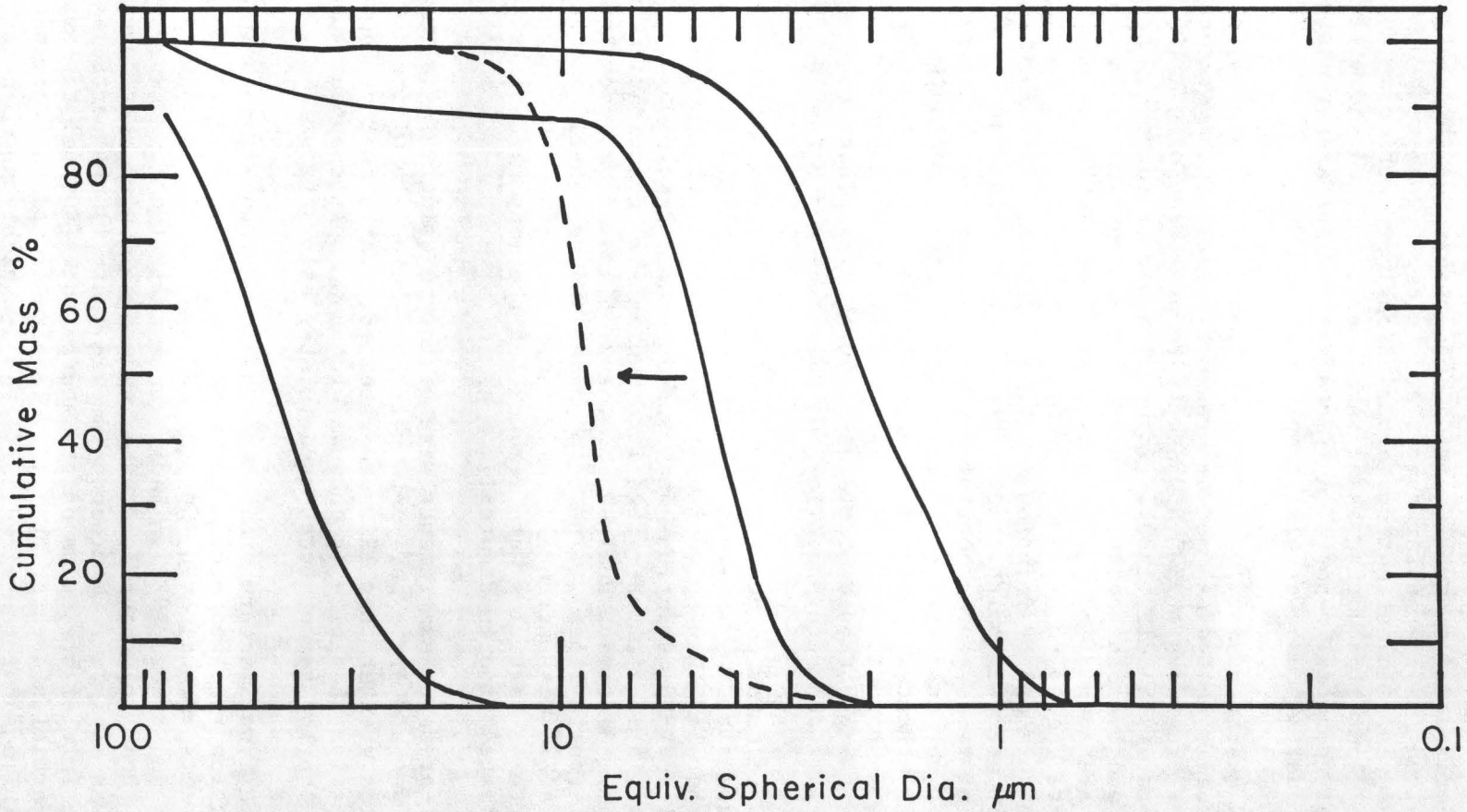

Bibliography

Blendell, J.E., Hot isostatic pressing of SiO_2, Am. Ceramic Soc. Bull. Abstr., 62, 382, 1983.

Mainprice, D.H. and M.S. Paterson, Experimental studies of the role of water in the plasticity of quartzites, U.S.G.S. workshop on Chemical Role of water in crustal deformation processes, Carmel, Calif., 1981.

Olgaard, D.L. and W.F. Brace, The microstructure of gouge from a mining-induced seismic shear zone, Int. J. Rock Mech. Min. Sci. & Geomech. Abstr., 20, 11-19, 1983.

Table 1

Particle Size (μM)	Temp. (C°)	Pres. (MPa)	Time (HRS)	Porosity (%)
6.5	800	400	1	10
1.5	850	400	0	11
3.5	850	400	3	8.5
3.5	850	500	3	7.5
3.5	900	400	7	8
3.5	900	650	5	2.5
		P_{H_2O} = 100mPa		
3.5	825	600	0	>15
3.5	900	300	1	>2.5
		P_{H_2O} = 0		

In Situ Stress Measurements

9960-01184

John H. Healy
Branch of Tectonophysics
U.S. Geological Survey
345 Middlefield Road MS 77
Menlo Park, CA 94025
415/323-8111, Ext. 2535

Investigations and Results

1. Development of instrumentation for and analysis of data from a 2,000' well near Hi Vista in the Mojave Desert. This well appears to be a particularly sensitive indicator of the Earth's stress. Water level changes in the well are caused by the solid earth tides and have an amplitude larger than 10 cm. About 85% of the tidal signal can be removed by subtracting the theoretical gravitational tide, suggesting that the well is behaving as a volumetric stress meter. The change in water level over a period of months is less than the tidal amplitude and it may be possible to extract signals from these data that reflect stress anomalies in the Earth that are more than a factor of 10 below the amplitude of the tidal signals. These exceptional results were achieved by processing the drill hole to seal off the effects of near-surface aquifers so that the water level changes reflect the stress changes in a deep fracture zone. These results can be extremely important for earthquake research as they demonstrate the feasibility of achieving stress measurements that are one or two orders of magnitude more sensitive than can be achieved with near-surface instrumentation.

2. Development of a new packer system to hold pressures to 10,000 psi. This system was developed for us by TAM International and gives us the capability of carrying out stress measurements efficiently in holes at depths between 6,000 and 10,000'. We have tested these packers in shallow holes and demonstrated that they offer significant operational advantages over our previous packer systems.

3. A major fraction of our time and effort has been spent developing holes for the installation of the Carnegie volumetric strain meters and the three-component strain meters developed by Mick Gladwin of the University of Queensland. The installation of these meters in holes near the San Andreas fault zone has proved to be a difficult and time consuming task. The holes must be logged and carefully studied to find a suitable and unfractured section of the borehole for the installation of these sensitive instruments. Frequently, the hole must be processed by cementing or redrilling to seal off water zones and keep the hole stable until the instrument can be installed. We believe that procedures for hole preparation and instrument installation have advanced significantly during the past year so that future installations will be more routine, although we expect that any instrument installed near a fault zone will always present unforeseen problems.

4. Prepared equipment for and are currently engaged in a cooperative stress measurement program with the People's Republic of China.

5. Time has been spent analyzing the data and attending meetings relating to the Yucca Mountain waste disposal site. This research will involve a major part of our time during the next reporting period.

6. We have given assistance to Peter Malin of the University of California at Santa Barbara in conducting a series of experiments in our drill hole in Oroville, California.

7. Contracts and Purchasing: Although not a scientific accomplishment, a major effort has been required to adapt our operating procedures to the new and more stringent purchasing procedures of Contracts and Purchasing. Our activities often require the purchase of expensive items on short notice. Procedures that were formerly accepted have been changed and make the procurement of our necessary supplies and equipment much more complicated and time consuming. While the new purchasing rules will always present a problem, we believe we have made some progress in adapting to these rules; hopefully more progress will be made in the future. This subject is important as it has required a large fraction of our working time.

Reports

Anderson, R. N., Zoback, M. D., Hickman, S. H., and Healy, J. H., In situ stress and physical property measurements in the Cleveland Hills fault zone, Oroville, California (abs.): EOS, Transactions of the American Geophysical Union, (Dec. 1983).

Healy, J., Stock, J., Svitek, J., and Hickman, S., 1983, Hydrofrac stress measurements on Yucca Mountan, Nevada (abs.): EOS, Transactions of the American Geophysical Union, v. 64, no. 18, p. 320.

Healy, J. H. and Urban, T. C., The application of deep boreholes to earthquake prediction (abs.): EOS, Transactions of the American Geophysical Union, (Dec. 1983).

Stock, J., Healy, J., and Svitek, J., 1983, The orientation of the current stress field on Yucca Mountain, Nevada, as determined from televiewer logs (abs.): EOS, Transactions of the American Geophysical Union, v. 64, no. 18, p. 319.

Urban, T. C. and Healy, J. H., Monitoring fluid pressure in fractures for earthquake prediction (abs.): EOS, Transactions of the American Geophysical Union, (Dec. 1983).

Zoback, M. D., Hickman, S. H., Moos, D., McGarr, A., and Healy, J. H., In situ stress and physical property measurements at depth near the San Andreas fault, California (abs.): EOS, Transactions of the American Geophysical Union, (Dec. 1983).

Fault Zone Structures

9930-01725

John H. Healy
Walter D. Mooney
Branch of Seismology
U.S. Geological Survey
345 Middlefield Road M/S 77
Menlo Park, California 94025
(415) 323-8111, ext. 2476

Investigations

1. Development of an automatic microseismic network in Jordan.

2. Interpretation of the deep crustal structure and tectonic evolution of the Mississippi Embayment, central United States.

3. Preparation of journal articles on the crustal structure of Saudi Arabia, based on U.S. Geological Survey Open-File Report OF-02-37 (Healy and others, 1982).

4. Interpretation of seismic refraction data in central California.

5. See project report 9930-02102: Active seismology in fault zones, Walter D. Mooney.

Results

1. For many years the Geological Survey has maintained scientific cooperation with the Government of Jordan, Natural Resources Authority (NRA), in the exploration of their natural resources and conventional energy sources. The most recent activity was sponsored by the Agency for International Development (AID) in the form of a Minerals Development Grant for a Kingdom-wide geophysical survey, designed and supervised by Geological Survey staff members.

   The present request for Office of Earthquakes, Volcanoes, and Engineering (OEVE) services is part of a follow-up program to the geophysical surveys to measure and record microearthquake activity along the Dead Sea rift zone. Resulting data is expected to provide valuable information on subsurface geologic structure related to possible geothermal energy sources of the numerous hot springs along the rift zone. The data would also provide important earthquake risk and earthquake prediction information for the Government or Jordan, particularly for AID Assistance programs for the construction of dams, roads, and other construction projects in the developing country.

Specifically, OEVE, at the request of AID, through the Office of International Geology (OIG), will assist in the design of an automated microseismic network observatory. The work includes design of state-of-the-art instrumentation for a 20-station network, site construction, telemetry to a central observatory, recording, playback and data display system, and operation and training programs for Jordanian seismologists.

The development and deployment is based on a new system concept that integrates seismic systems, telemetry, specialized computer hardware and software, and technical presonnel to produce high quality results with minimal cost of long-term monitoring. The system is named "JSS" (Jordan Seismic System) to identify its unique qualities and combination of components. Data will be gathered by clusters of as many as eight seismic stations, telemeterd by radio to a central collection point where routine, automatic analysis will take place by a data processing system. These results will then be transmitted to the Central Observatory for further analysis and display.

2. The seismicity of the Mississippi Embayment is the highest in the eastern U.S. We have examined both the seismicity and the crustal structure with the aim of improving the hypocentral locations and tectonic models for the area.

We have developed a tectonic model for the Mississippi Embayment based on new geophysical and ecisting geologic data. The model is constrained by two features of the crust: a high velocity, high density lower crust, interpreted to be a fossil rift cushion, and an upper crustal low velocity zone, interpreted to be a rift graben.

Based on the geophysical model for the crustal structure of the Embayment and on geologic evidence the following model for the evolution of the Embayment is proposed. The intrusion of mantle derived material into the lower crust occurred in the Late Precambrian causing the initiation of crustal rifting in the northern Embayment area. Isostatic subsidence caused by the cooling of the lower crustal intrusion created a broad, elongate basin in Cambro-Ordovician time that accumulated thick sequences of carbonate sediments. In the late Paleozoic, compressive tectonic forces from the south, at a high angle with the rift zone, caused uplift and igneous activity along previously faulted zones in the Embayment. Another phase of uplift was initiated before late Cretaceous time. This uplift and associated igneous activity was in response to isostatic recound forces caused by renewed injection of mantle material into the lower crust. Major subsidence followed in late Cretaceous and early Tertiary time due to cooling of the altered lower crust. It was during this time that the present configuation of the embayment was established.

3. Three manuscripts have been prepared (see 'Reports').

4. Several detailed profiles have been recorded in central California in areas of seismicity. For example, a magnitude 5.7 earthquake within the Calaveras fault zone near Coyote Lake of west-central California on August 6, 1979, motivated seismic-refraction investigations in this area. A northwest-southeast profile along the fault, as well as two fan profiles perpendicular to the main-profile line were recorded to axamine the three-dimensional velocity structure of this region.

   The area under investigations has a very complicated near-surface velocity structure, and strong lateral variations in all directions. The uppermost layers consist of recent sediments with seismic P-wave velocities of 2.6-3.2 km/s. The next deepest layer, with an average velocity of 4.5 km/s, is present along the whole profile and reaches a depth of 4.3-4.8 km in the northwest near Anderson Lake and in the southeast of the profile line near Hollister. In the middle of the profile near Coyote Lake, however, the 4.5 km/s layer is thinner and we find a laterally limited higher veocity layer (5.0-5.2 km/s) between the depths of 2.8-4.8 km just in the hypocentral area of the magnitude 5.7 earthquake and its aftershocks. The contrasting volume responsible for this high velocity zone is also expressed in a gravity high. We suggest that this zone constitutes as area of strength on the fault which failed in the magnitude 5.7 earthquake.

   According to two fan profiles, the velocity within the fault zone itself varies. In the northwest a pronounced delay in the first arrivals of the fan records indicates a 1-2 km wide near-surface low-velocity zone, whereas in the southeast the sruficially mapped fault is not correlate with the observed seismic data.

   The lower crust has a structure similar to the neighboring Diablo Range: a 8-9 km thick layer with a seismic velocity of 5.7-6.3 km/s is underlain by a 3 km thick later with velocity 6.8 km/s. In accordance with previous results in the Diablo Range, there are indications of a pronounced lower crustal low-velocity layer (LVL) between a depth of 17 and 23 km. If real, the presence of this LVL has important implications for the deep geologic structure of the Coast Ranges of California.

Reports

Blumling, P., Mooney, W. D., and Lee, W. H. K., Crustal strcuture of the southern Calaveras fault zone, central California, from seismic refraction investigations (in review).

Gettings, M. E., Mooney, W. D., Blank, H. R., and Healy, J. H., Saudi Arabian seismic deep-refraction profile: a traveltime interpretation of deep crustal structure: USGS-Saudi Arabian Mission Open-file Report 03-59 and in preparation for submission to Journal of Geophysical Rrsearch).

Ginzburg, A., Mooney, W. D., Walter, A., Lutter, W., and Healy, J. H., 1983, Deep crustal structure of the Mississippi Embayment, Am. Assoc. Pet. Geol. Bulletin (in press).

Healy, J. H., Mooney, W. D., Blank, H. R., Gettings, M. E., Kohler, W. L., and Leone, L. E., 1982, Saudi Arabian deep-seismic refraction profile, Final Progest Report, USGS- Saudi Arabian Mission Open-file 02-37, 432 pp.

Mooney, W. D., Andrews, M. C., Ginzburg, A. Petes, D., and Hamilton, R. M., 1983, Crustal strcuture of the northern Mississippi Embayment and a comparison with other continental rift zones: Tectonophysics, v. 94, pp. 327-348.

Mooney, W. D., and Colburn, R. H., A seismic-refraction profile across the San Andreas Sargent, and Calaveras faults, west-central California (in review).

Mooney, W. D., Fuis, G. S., and Healy, J. H., Seismic refraction studies of a sedimentary basin, southern California, USA: Methods and results (A.E.G., Hydrabad, India, in review)

Mooney, W. D., Gettings, M. E., Blank, H. R., and Healy, J. H., Saudi Arabian seismic-refraction profile: A traveltime interpretation of crustal and upper-mantle structure (Tectonophysics, in press).

Mooney, W. D., and Prodehl, C., Preceedings of the IASPEI Workshop on the interpretation of the 1978 Saudi Arabian refraction profile (USGS circular, in press).

Milkereit, B., Mooney, W.D ., and Kohler, W. M., Tau-p inversion for laterally-varying structure (in review).

Walter, A.W ., and Mooney, W. D., Preliminary report on the crustal report on the crustal velocity struture near Coalinga, California, as determined from seismic refraction surveys in the region (Calif. Div. Mines and Geol. Spec. Report, in press).

Wentworth, C. M., Walter, A.W ., Bartow, J. A., and Zoback, M. D., Evidence on the tectonic setting of the 1983 Coalinga earthquakes from deep reflection and refraction profiles across the southeastern end of the Kittleman Hills, (Calif. Div. Mines and Geol. Spec. Rept., in press).

Heat Flow and Tectonic Studies

9960-01176

Arthur H. Lachenbruch
Branch of Tectonophysics
U.S. Geological Survey
345 Middlefield Road
Menlo Park, California 94025
(415) 323-8111, ext. 2272

Investigations:

1. Heat flow and tectonics of the western United States: Eleven wells were drilled in the unconsolidated sediments of the western Imperial Valley to extend the areal coverage of the Salton Trough. A group of seven heat-flow holes was drilled in granitic rocks of the Southern Sierra Nevada at ~latitude 36°. Additional thermal data were obtained at Yucca Mountain, Nevada, the Vekol Valley, Arizona, and at the USBR's Brantley Dam site near Carlsbad, New Mexico.

2. Heat flow and tectonics of Alaska: Additional temperature logs were obtained at all accessible wells at the National Petroleum Reserve, Alaska. Heat flows were calculated for nine sites in Southeastern Alaska.

3. Thermal studies related to nuclear waste isolation: Equilibrium temperature measurements have been completed on most wells in the Yucca Mountain area. Additional conductivity data are being obtained, and interpretation is continuing.

Results:

1. Heat flow and tectonics of the western United States: Eleven wells ranging in depth from 110 to 140 meters were drilled in the unconsolidated sediments of the Western Imperial Valley. Temperatures and thermal conductivities were measured "in situ" during the drilling process. The 44 values of thermal conductivity averaged 1.89 ± 0.05 (SE) $Wm^{-1} K^{-1}$, in excellent agreement with the mean of 49 values (1.87 ± 0.05) from the Glamis - East Brawley region in the eastern part of the valley. Heat flows from these wells ranged from 46 to 142 mWm^{-2} with a mean of 102±8 (SE), significantly lower than the average heat flow in the eastern part of the valley. The combined mean in situ thermal conductivity (1.88 $Wm^{-1} K^{-1}$) was used to re-evaluate heat flow from the USBR test wells at East Mesa and to calculate heat flow from temperature-gradient data obtained by industry, primarily in the eastern part of the valley, average heat flow were then calculated for 3' × 3' elements (approximately 5 × 5 km). With the exception of a few very high values associated with near-surface anomalies, the heat flows are normally distributed with mean of about 140 mWm^{-2}. (The mean of all 100 3' × 3' elements is 166 ± 10 (SE).)

Preliminary results from the Southern Sierra Nevada indicate typical Sierran heat flows west of the Kern River; to the east, the preliminary heat flows are somewhat higher.

Heat flow in seven wells with casing grouted in along the proposed abutments for Brantley Dam ranges from 26 to 43 mWm^{-2} over a very small area. Regional heat flow is in the range 42 to 45 mWm^{-2}. It appears that the thermal regime beneath wells with depressed heat flows is being affected by lateral water movement with a downward vertical component of velocity.

In contrast with the Santa Maria basin, where temperature profiles seem to be significantly affected by the drilling-production history, apparently undisturbed temperature profiles have been obtained from a number of wells in the Ventura and neighboring basins. No information on thermal conductivities is as yet available; however, from the generalized lithology, it appears that the heat flow from the Ventura Basin is moderate--in the range 45 to 65 mWm^{-2} (1 to 1.5 HFU).

2. Heat flow and tectonics of Alaska: Heat flow was measured at nine sites in crystalline and sedimentary rocks of southeastern Alaska (Figure 1). Seven of the sites, located between 115 and 155 km landward of the Queen Charlotte-Fairweather transform fault, have an average heat flow of 59 ± 6 mWm^{-2}. This value is significantly higher than the mean of 42 mWm^{-2} in the coastal provinces between Cape Mendocino and Queen Charlotte Islands and lower than the mean of 72 ± 2 mWm^{-2} for 81 values within 100 km of the San Andreas transform fault. This intermediate value suggests the absence of significant heat sinks associated with Cenozoic subduction and of heat sources related to either late Cenozoic tectonomagmatic events or significant shear-strain heating. At Warm Springs Bay, 75 km from the plate boundary, an anomalously high heat flow of 150 mWm^{-2} can most plausibly be ascribed to the thermal spring activity from which its name is derived. At Gold Hill, 240 km landward of the plate boundary, a value of 115 mWm^{-2} might indicate a transition to a province of high heat flow resulting from Late Tertiary extension and dike intrusion.

3. Thermal studies related to nuclear waste isolation: For sites in the Paradox Basin of Utah, all yield moderate values of heat flow ($\sim$60 mWm^{-2}). The thermal data also indicate no vertical fluid movement within the Paradox Salt at any of the sites. This is in contrast to Yucca Mountain, where our research to date indicates a complex hydrologic system in the upper kilometer of the tuffs, and perhaps within the pre-Tertiary basement as well.

Reports:

Bills, D. J., and Sass, J. H., 1984, Hydrologic and near-surface thermal regimes of the San Francisco volcanic field: U.S. Geological Survey Professional Paper, in press.

Chapman, D. S., Howell, J., and Sass, J. H., 1983, A note on drillhole depths required for reliable heat-flow determinations: Tectonophysics, in press.

Lachenbruch, A. H., Sass, J. H., Galanis, S. P., Jr., and Marshall, B. V., 1983, Heat flow and crustal extension in the Salton Trough [abs.]: International Union of Geodesy and Geophysics, XVIII General Assembly, Hamburg, Germany, 1983, Programme and abstracts, v. 1, p. 504.

Lachenbruch, A. H., Sass, J. H., Lawver, L. A., Brewer, M. C., and Moses, T. H., Jr., 1983, Depth and temperature of permafrost on the Alaskan Arctic Slope: U.S. Geological Survey Professional Paper, in press.

Sass, J. H., Lachenbruch, A. H., and Smith, E. P., 1983, Temperature profiles from Salt Valley, Utah, thermal conductivity of 10 samples from drill hole DOE 3, and preliminary estimates of heat flow: U.S. Geological Survey Open-File Report 83-455, 22 p.

Sass. J. H., Lachenbruch, A. H., and Smith, E. P., 1983, Thermal data from well GD-1, Gibson Dome, Paradox Valley, Utah: U.S. Geological Survey Open-File Report 83-476, 15 p.

Sass, J. H., Stone, C., and Munroe, R. J., 1984, Thermal conductivity determinations on solid-rock--A Comparison between a steady-state divided-bar apparatus and a commercial transient line-source device: Journal of Volcanology and Geothermal Research, in press.

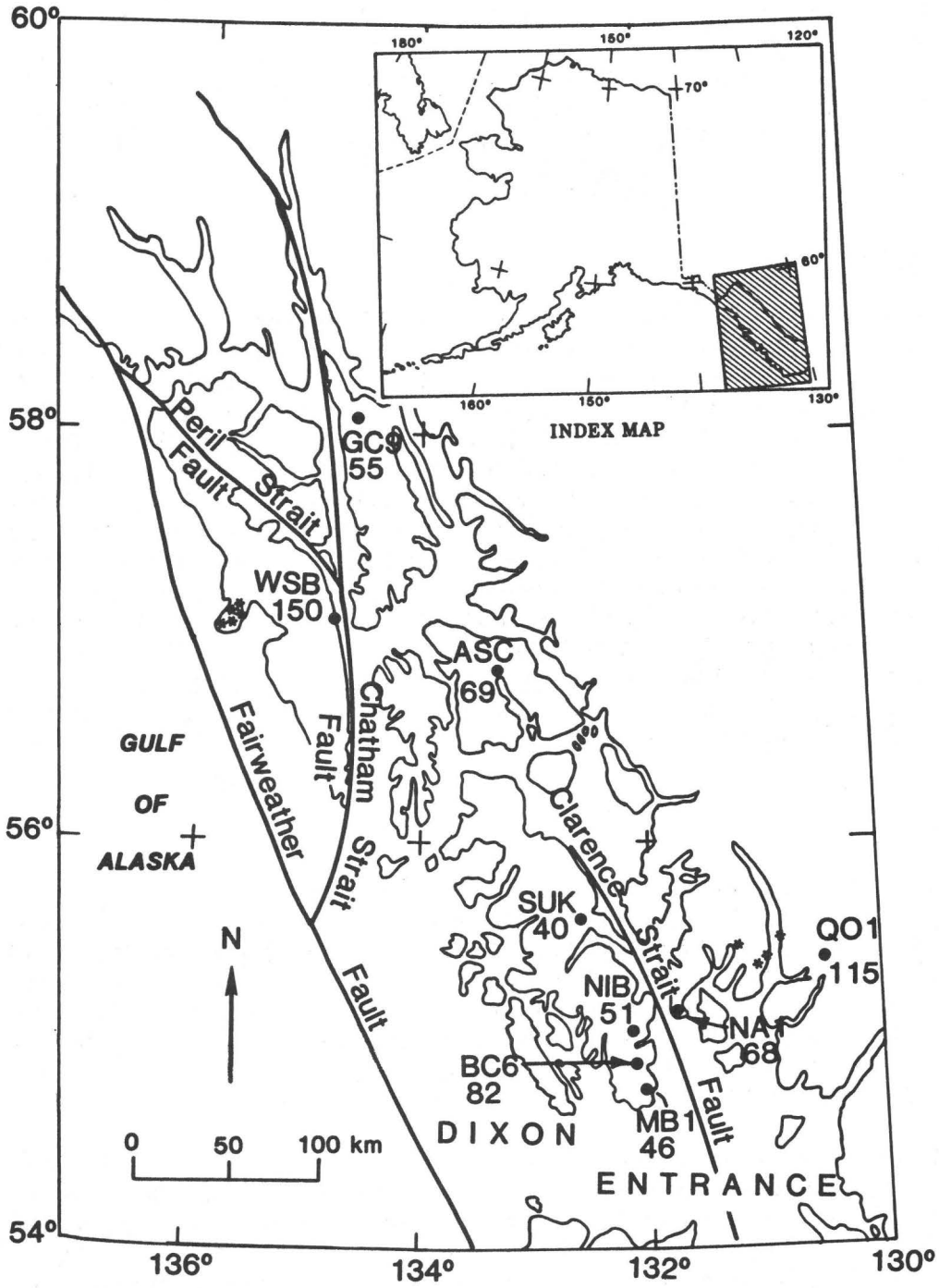

Figure 1. Sketch map of southeastern Alaska showing site locations, heat flow (in mWm^{-2}) and major faults. Asterisks are Quaternary volcanic centers. Cross-hatched area of index map indicates study area.

P_n Anisotropy and Subcrustal Deviatoric Stress in Southern California

20520

J. B. Minster, W. L. Rodi, and A. H. Olson
S-CUBED
3398 Carmel Mountain Road
San Diego, CA 92121-1095
(619) 453-0060

Investigations

This study is aimed at the determination of horizontal anisotropy of material near the crust-mantle boundary by inversion P_n travel-times across an array of stations. An initial study of this problem was performed by Vetter and Minster (1981) for a region near the central Transverse Ranges, Southern California. Their results indicate an average anisotrpy of P_n propagation consistent with simple shear in a vertical plane subparallel to the direction of relative plate motion. We utilize the very large CEDAR data base archived at Caltech in a systematic inversion of P_n travel-times across the SCARLET network to produce an image of a Moho dip, P_n anisotropy, and their lateral variations. The variation in degree and orientation of P_n anisotropy as a function of geographical location places constraints on the geometry and lateral extent of the plate boundary below the seismogenic layer, and ultimately constraints on mechanical models of this layer and its state of stress.

Results

1. Tomographic inversion of anisotropic fields -

In the present context, tomography is the imaging of a planar slice of a three-dimensional body from data corresponding to line integrals across the plane. The image parameter is the anisotropic P-wave horizontal slowness and the plane corresponds to the crust-mantle interface. The data are differences in P_n arrival times across an array stations above the study area and correspond to straight line integrals of the horizontal slowness.

Rather than divide the plane into a set of cells and "invert" the resulting matrix system, we have chosen to extend the Fourier transform methods currently used in the medical X-ray field (Swindell and Barrett, 1977) to include the effects of anisotropy. For the isotropic problem, a result known as the Projection-Slice Theorem shows how to construct the two-dimensional Fourier transform of the slowness field when travel-times across the array are available for sources at all azimuths. Inverting this data simply requires performing an inverse two-dimensional Fourier transform.

We derive an extension of The Projection-Slice theorem for anisotropic fields by allowing the slowness to be a sum of fields, each modulated by a different order harmonic function to account for the direction of propagation.

2. Decoupling of the data field -

Moho topography (dip for example) and crustal anomalies give rise to the odd-order harmonic dependence in the slowness field since they cause the travel time to be greater in one direction than in the opposite direction. Material anisotropy on the other hand is related to the even-order harmonics. The isotropic component of the slowness field is the zero'th order harmonic since it is independent of direction. The data is decomposed into two parts: one relating to the even harmonics and the other relating only to odd harmonics. In this way, material anisotropy is solved for independently.

3. Computation of a fast inverse -

A motivation in our application of Fourier theory to the anisotropic problem is that the inverse is known. The Fourier transform however must be computed numerically from sample values on a polar grid (f,θ). The θ-integral can be done exactly as a convolution of two band-limited periodic functions using an FFT algorithm. The convolution kernal is shown to be band-limited in θ to machine precision. The f-integral is then done by trapezoidal rule. Tests with a normalized Gaussian function show that a frequency sampling finer than the usual DFT sampling is required. A precision of 10^{-4} requires eight times the number of DFT sample points in f.

4. Nonuniqueness -

The extended Projection-Slice Theorem shows that the resolution between isotropy and anisotropy is poor at short spatial wavelengths. That is, short wavelength features in the anisotropic field can be traded off for short wavelength isotropic ones and vice versa. On the other hand, it shows that zero frequency (i.e., constant part) components of the anisotropic field can be uniquely determined in principle. This means that travel-time residuals due to a constant anisotropic field cannot be fit with an isotropic model.

5. Collation and culling of P_n arrival times -

Some 4000 P_n arrival times at 200 stations in the SCARLET network have been collected along with epicenter locations and times. Latitude and longitude coordinates have been converted to Cartesian coordinates using a Universal Transverse Mercator Projection.

6. Plotting software -

We have developed a plot code which displays the Southern California area and SCARLET stations along with major faults. A contour algorithm is incorporated into the program to plot contours of constant P_n velocity for each component of anisotropy.

We are currently inverting the SCARLET data using these Fourier techniques. These results are not available at this time.

Abstract

Olson, A. H., J. B. Minster, and W. L. Rodi. "A Tomographic Analysis of P_n for Upper-Mantle Anisotropy," accepted for presentation at the Annual Meeting of the AGU, December 1983.

References

Vetter, U. and J. B. Minster (1981), "P_n Velocity Anisotropy in Southern California," BSSA, 71, No. 5, pp. 1511-1530.

Swindell, W. and H. H. Barrett (1977), "Computerized Tomography: Taking Sectional X-Rays," Physics Today, December, pp. 32-41.

Active Seismology in Fault Zones

9930-02102

Walter D. Mooney
Gary S. Fuis
U. S. Geological Survey
Branch of Seismology
345 Middlefield Road, Mail Stop 77
Menlo Park, California 94025
(415) 323-8111, ext. 2569

Investigations Undertaken

1) Analysis and interpretation of a 1981 seismic refraction experiment in northeastern California (Zucca, Fuis, Catchings, Milkereit and Mooney).

2) Continued time-term analysis of a 1979 seismic refraction experiment in the Imperial Valley region, California (Kohler and Fuis).

3) Planning and execution of an earthquake aftershock study and of a seismic-refraction experiment in the Coalinga, California, region following the May 2, 1983, earthquake, M 6.5 (Fuis and Walter) .

4) Field planning of a 1983 seismic-refraction experiment in southern Alaska--the first project in a multi-year Trans-Alaska Crustal Transect (TACT) program (Fuis, Mooney, Page, Criley).

5) Participation in a workshop by the International Commission on Controlled Source Seismology (CCSS) in Zurich, Switzerland (Fuis, Mooney, and Zucca).

6) Continued analysis of seismic refraction and reflection data from central California (Walter, C. Wentworth, and others).

Results

1) In 1981, the U. S. Geological Survey conducted a seismic-refraction experiment in northeastern California that included 95-km-long north-south lines in the Klamath Mountains (KM) and on the Modoc Plateau (MP), and a 275-km-long east-west line from the KM to the California-Nevada state line. Instrument spacing averaged 1 km, and shotpoint spacing 50 km. The KM and MP lines yielded the simplest models. The KM line is underlain by relatively flat high-velocity layers (6.1, 6.5, 6.7 and 7.0 kms) with low-velocity layers between them. Layer thicknesses range from 1 to 3 km; the 7.0-km/s-velocity layer is 14 km deep. The MP line is underlain by 4-1/2 km of relatively low-velocity (3.5-4.5 km/s) material over a 6.2 km/s-velocity basement. A small velocity step (to 6.4 km/s) occurs

at 11-km depth, a velocity step to 7.0 km/s occurs at 25-km depth, and mantle is estimated to be 38-45 km deep. On the east-west line, the KM and MP models are juxtaposed in the vicinity of the Cascade Range.

The fact that the velocity-depth curve for the MP is virtually identical, beneath its surficial layers, to that determined by other workers for the Sierra Nevada leads us to conclude that the MP is underlain, beneath its volcanic and sedimentary rocks, by a basement of granitic and metamorphic rocks that are the roots of magmatic arcs. The finely layered velocity-depth curve in the KM can be related, with the help of independent modeling of aeromagnetic data, to the structural imbrication of oceanic pates that is mapped at the surface. We conclude that the volcanic Cascade Range overlies a complex suture region between the KM, underlain by imbricate oceanic plates, and the MP, underlain by the roots of magmatic arcs.

These results are of value to earthquake studies in the area, as well as geologic studies. Interest in the seismicity of northeastern California was heighted by the 1978 earthquake swarm near Tenant, California.

2) The deep crustal structure of the Imperial Valley, southern California, has been investigated thoroughly and these results reported (e.g., Fuis and others, 1982). In order to extend the coverage possible in our previous interpretations, the time-term mthod has been applied to the 1979 seismic refraction data. All of the traveltime data were next integrated to produce a time-term map, which in principle eliminates distortions of features seen on traveltime maps and can be converted to a sediment isopach map. Striking features seen on this map include the following: 1) A complex buried scarp along the west side of the Imperial Valley. This feature, seen on the earlier traveltime maps, trends roughly north-south; it appears to be terraced and also segmented. The Superstition Hills fault and Superstition Mountain fault bound one segment and northwest-striking buried faults (?) farther south appear to bound other segments. 2) A prominent scape is also seen northest of the Salton Sea and appears to be a continuation of the modern mountain front beneath the sediments. (We had surmised earlier than such a scarp existed about 10 km farther southwest, along the San Andreas fault). 3) Geothermal areas are reflected on the maps as areas of relatively low time-terms. These areas have varied shape and relief on the map. The Salton geothermal area has the strongest relief and is the largest areally. In conjunction with this investigation a computer program was written for machine contouring of data points.

3) The May 2, 1983, Coalinga earthquake, M 6.5, caused extensive damage in Coalinga, California, and precipitated a strong aftershock sequence. This earthquake and its aftershocks were the subject of concern and numerous investigations by the USGS. G. Fuis and P. Berge represented the USGS in Coalinga at an emergency information and planning center set up by the CDMG. Activities included answering questions for the news media and residents, and coordination of field aftershock studies and ground breakage investigations. A. Walter and G. Fuis planned and conducted both an aftershock study and a seismic refraction study using our 120 portable refraction instruments. These instruments were deployed along a 90 km-long east-west line through the main-shock epicenter on Anticline Ridge, and later along a 120 km-long northwest-southeast line through Pleasant Valley, immediately west of the main-shock epicenter, extending southeastward to Antelope Plain. The instruments recorded aftershocks during intervals of time totaling about 1 hour for each line in the first week of the aftershock sequence. The instruments were subsequently redeployed in late May and explosions were fired at 4 shotpoints along the east-west line and 5 shotpoints along the northwest-southeast line.

4) In 1984 the USGS will conduct an extensive seismic refraction experiment in southern Alaska, as the first major project of the Trans-Alaska Crustal Transect (TACT) program. TACT's a multi-year, multi-disciplinary effort to investigate the crustal structure along a route paralleling the Alaska oil pipeline (fig. 1). The program includes many investigations including seismic refraction, seismic reflection, geologic mapping, and gravity and aeromagnetic studies. The 1984 seismic refraction experiment will consist of four profiles designed to investigate in various ways the accreted terranes of southern Alaska (fig. 1) and their sutures, including the current Benioff zone(s) extending northwestward under the Kenai Peninsular and northward under the Wrangell volcanoes, and the active Denali fault zone. One profile extends along the Glenn Highway from Tahneta Pass to Mentasta Pass near the Denlai fault (225 km), crossing the Peninsular and Wrangellia terranes more or less diagonally; shotpoint spacing will average about 45 km. A second profile extends southward along the Richardson Highway from the Denali fault to the Tiekel River and thence cross-country to the Tasuuna River (260 km), crossing numerous terranes roughly perpendicular to strike. Shotpoint spacing wil average 25 km to deal with expected rapid near-surface velocity variation in this direction. A third profile extends eastward cross-country from Valdez to the Tana River (200 km) sampling the Chugach terrane parallel to strike.

Shotpoint spacing will average 50 km. We hope to see the subducted slab clearly along this profile. A fourth profile extends southeastward along the Edgerton Highway from Copper Center to a point east of Chitina (100 km) crossing the prominent surture between the Peninsular and Wrangellia terrances in a second place. (The Richardson Highway profile crosses this surture to the west.) Shotpoint spacing will be 50 km.

The results of this experiment will be important not only to geologic framework studies, but also to earthquake and volcanic hazards studies in that they will provide a velocity structure and calibration for more precise earthquake location.

4) Participants in the workshop meeting of the Commission on Controlled Source Seismology in Zurich, Switzerland analyzed a number of synthetic record sections generated from an undisclosed model having both vertical and lateral velocity variations, including a local low-velocity zone. Most participants converged closely on the real model and methods of analysis were compared. The remarkable convergence to the real model by different approaches was encouraging, indicating the strength of modern refraction seismology in dealing with 2-dimensional velocity variations.

6) Preliminary interpretation of seismic reflection and refraction profiles across the southeastern end of Kettleman Hills, 65 km southeast of the Coalinga epicentral area, suggests that presence of both northeast-dipping reverse faults and southwest-dipping thrust fault beneath the Kettleman Hills anticline. Two deep reverse faults are inferred to dip steeply northeastward beneath the anticline and offset basement at a depth of about 9 km. One of these faults is alined with a shallow northeast-dipping reverse fault in the southwest limb of the anticline that offsets upper Miocene strata about 200 m; we assume that these two faults are connected. The reverse faults have an orientation beneath the anticline approximately equivalent to that of one plane of the focal mechanism solution for the Coalinga main shock, which is the plane preferred from surface deformation studies.

The thrust fault is inferred to dip gently southwestward from 3 km beneath the north-east limb of the anticline to a depth of 10 km beneath the Diablo Range. The thrust shows about 10 km of post-late Miocene dip slip that has repeated the Tertiary and upper Mesozoic section and the underlying Franciscan essemblage.

Mafic basement unconformably underlying the Great Valley sequence beneath the San Joaquin plunges southwestward at 40° to a depth of 15 km beneath the Diablo Range, rather than following the base of the Great Valley sequence up to the surface. If this is a single, continuous basement surface, as eastward-thinning wedge of Franciscan rock is defined that lies between the basement and the overlying Great Valley sequence. Farther east, however, the Great Valley sequence was deposited directly on the same mafic basement.

Reports

Blumling, P., Mooney, W. D., and Lee, W. H. K., Crustal strcuture of the southern Calaveras fault zone, central California, from seismic refraction investigations (in review).

Fuis, G. S., 1982, Crustal structure of the Majave Desert, California (abs.): Geological Society of America Abstracts with Programs, v. 14, no. 4, p. 164.

Fuis, G. S., Mooney, W. D., Healy, J. H., McMechan, G. A., and Lutter, W., 1982, Crustal structure of the Imperial Valley region, in The Imperial Valley Earthquake of 1979: U.S. Geological Survey Professional Paper 1254, p. 64.

Fuis, G. S., Zucca, J. J., Mooney, W. D., and Milkeret, B., 1983, Crustal structure of the Klamath Cascade, and Modoc regions of northeastern California from seismic-refraction data (abs.): EOS Transactions of AGU (December meeting).

Fuis, G. S., Zucca, J. J., Mooney, W. D., and Milkereit, B., A geologic interpretation of seismic-refraction results in northeastern California: (submitted to GSA)

Milkereit, B., Mooney, W.D ., and Kohler, W. M., Tau-p inversion for laterally-varying structure (in review).

Mooney, W. D., Andrews, M. C., Ginzburg, A., Peters, D. A., and Hamilton, R. M., 1983, Crustal structure of the northern Mississippi Embayment and a comparison with other Continental rift zones: Tectonophysics, v. 94, 327-348.

Mooney, W. D., and Colburn, R. H., A seismic-refraction profile across the San Andreas Sargent, and Calaveras faults, west-central California (in review).

Mooney, W. D., Fuis, G. S., and Healy, J. H., Seismic refraction studies of a sedimentary basin, southern California, USA: Methods and results (A.E.G., Hydrabad, India, in review)

Mooney, W. D., Gettings, M. E., Blank, H. R., and Healy, J. H., Saudi Arabian seismic-refraction profile: A traveltime interpretation of crustal and upper-mantle structure (Tectonophysics, in press).

Mooney, W. D., and Prodehl, C., Preceedings of the IASPEI Workshop on the interpretation of the 1978 Saudi Arabian refraction profile (USGS circular, in press).

Walter, A.W ., and Mooney, W. D., Preliminary report on the crustal report on the crustal velocity struture near Coalinga, California, as determined from seismic refraction surveys in the region (Calif. Div. Mines and Geol. Spec. Report, in press).

Wentworth, C. M., Walter, A.W ., Bartow, J. A., and Zoback, M. D., Evidence on the tectonic setting of the 1983 Coalinga earthquakes from deep reflection and refraction profiles across the southeastern end of the Kittleman Hills, (Calif. Div. Mines and Geol. Spec. Rept., in press).

Zucca, J. J., Fuis, G. S., Milkereit, B., Mooney, W. D., and Catchings, R. D., Crustal structure of northeast California from seismic refraction data: (submitted to JGR).

Figure 1. Route of the Trans-Alaska Crustal Transect (heavy line) and seismic refraction/wide-angle reflection profiles to be shot in 1984 (dotted lines) in relation to tectonostratigraphic terranes taken from Jones and Silberling (1979, USGS Open-File Report 79-1200). Terranes along transect: (1) North America, (3) Endicott, (4) Ruby, (5) Angayucham, (6) Innoko, (7) Livengood, (8) Yukon-Tanana, (9) 70-Mile, (11) Pingston-McKinley, (24) McLaren, (25) Wrangellia, (26) Peninsular, (27) Chugach, and (28) Prince William.

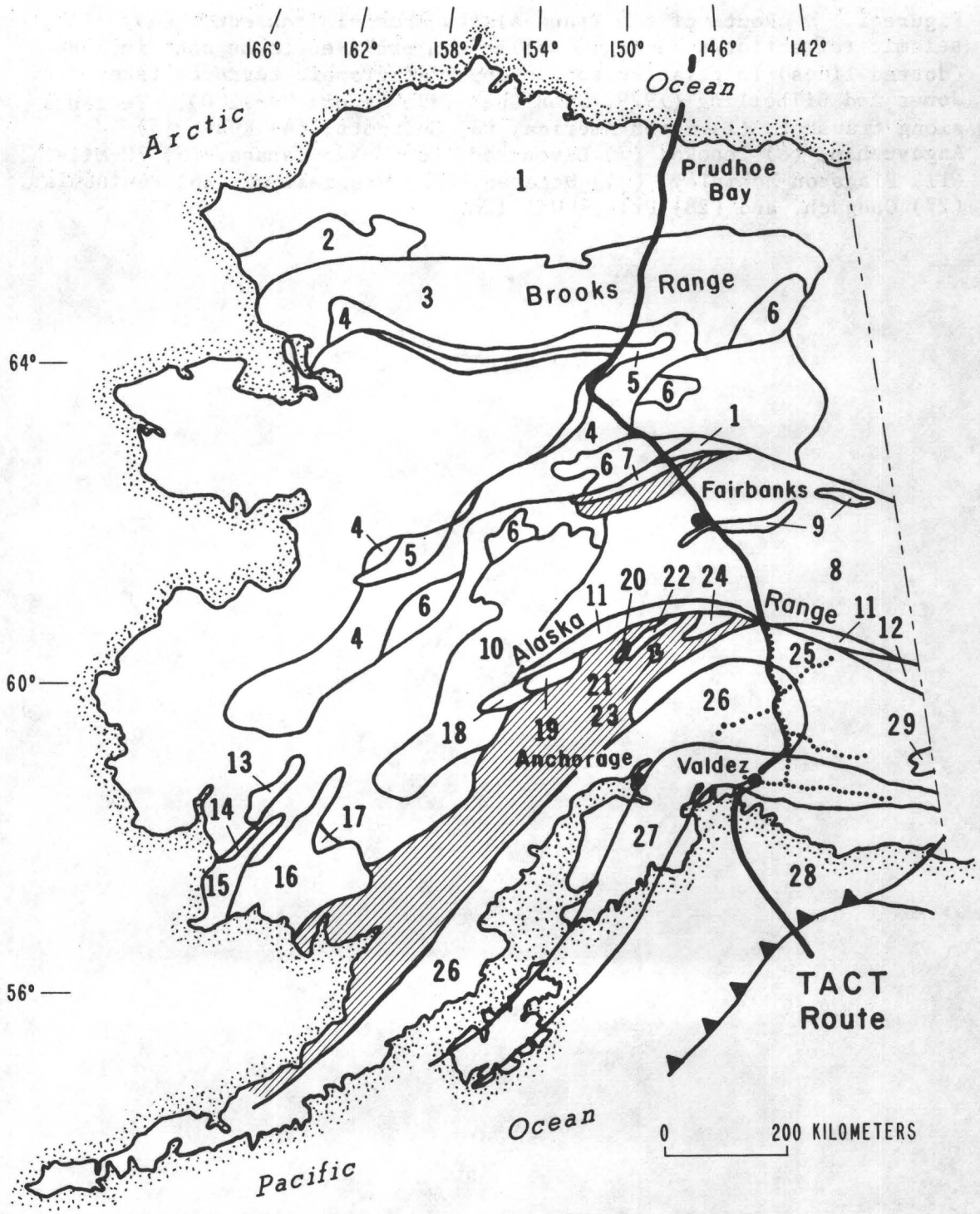

EXPLANATION

1 Tectonostratigraphic terrane

Deformed upper Jurassic and Lower Cretaceous Flysch

Undifferentiated Upper Cretaceous and Cenozoic deposits

Crustal Changes North of San Francisco Bay

9930-03353

Peter L. Ward
U.S. Geological Survey
Branch of Seismology
345 Middlefield Road - M/S 77
Menlo Park, California 94025
(415) 323-8111, ext. 2838

Investigations

1. Completed documentation of GEOPLOT, An Advanced Graphics Package for Minicomputers.

2. Finishing up a paper on "The Feasibility of Developing Magma Energy".

Results

Geoplot is an advanced graphics package that runs interactively, from command files, or as a subroutine package on 16 bit microcomputers. Geoplot contains many features usually found only in graphics packages on larger computers. A geoplot user can draw lines, symbols, and letters of any pattern, size, thickness, and orientation, using 29 idfferent transformations, including 16 map transformations. Great circle and rhumbline paths are easily drawn. Two sets of world coastline data are available in files containing 5,000 and 80,000 points. Map data can be digitized using an X-Y table-top digitizer. Map coordinates can be rotated and shifted about any arbitrary sequence of poles. Complex plots can be generated simply using high-level routines or the user may access low-level calls. Plots may be stored in disk files and output to a wide variety of vector or raster graphics devices.

Development of Geoplot began in 1978 but was severly curtailed in 1981 for economic and political reasons. The published version consists of all improvements as of September 14, 1983. Several advanced features such as multiple fonts, shading of arbitrary areas, and placing rectangular blank areas within plots, were planned but never completed. Most of the existing code has been tested, but not extensively. This version runs as a child process under the UNIX Operating System on a Digital Equipment Corp PDP 11/70 using an overlay scheme available in the Berkeley 2.9 version of UNIX. The overlays are only required for the transformations and the package could me made significantly smaller by omitting some transformations. The full power of geoplot is best utilized through the interactive command language Geolab developed simultaneously be James Herriot.

Reports

Ward, Peter L., 1983, GEOPLOT, An Advanced Graphics Package for Minicomputers, Part 1: User's Guide, Part 2: Computer Source Code, U.S. Geological Survey Open-File Report 83-807, 277 p.

Seismicity and Structure of the San Pablo Bay-Suisin Bay Seismic Gap from Calnet and Explosion Data

9930-02938

David H. Warren
Branch of Seismology
U. S. Geological Survey
345 Middlefield Road M/S 77
Menlo Park, California 94025
(415) 323-8111, ext. 2531

Investigations

Study was continued of the nature of the 1977 deep earthquake swarm just east of Suisin Bay.

Considerable time was spent on the Willits aftershock study to refine it and produce a manuscript.

Results

It has been previously reported that the earthquake swarm just east of Suisin Bay is elongated vertically from about 15 to 25 km depth. This result was acheived using data from the Calnet catalog. But earlier analysis by J. Eaton featuring picks from magnetic tapes rather than film records, station corrections tailored to the region, and limited distance range of stations used results in a very tight clustering of the swarm with only a 3 km vertical extent, 17 to 20 km depth.

Major conclusions of the Willits study are as follows. The Willits earthquake and its aftershocks may be the manifestation of the northeast component of a right-stepping strike-slip couple, on the northeast side of a pull-apart basin under Little Lake Valley. Focal mechanisms are right-lateral strike slip and agree with the faulting which trends N 26° W, except for a small patch of 8 events on the southwest side of the aftershock zone whose solution is strike slip, but rotated about 45° from the faulting. Stereo plots of the attershocks and simplified surface faulting projected downward show the aftershocks and faulting to be related in a complex way.

Recrystallized Grainsize in Ductile Fault (Mylonite) Zones as an Indicator of Palaeostress Magnitudes during Faulting

14-08-0001-19797

A. Ord, B.E. Hobbs, M.A. Etheridge and G.H. Edward
Department of Earth Sciences
Monash University
Clayton 3168, Australia
(03) 541-3791

In a recent paper, Edward, Etheridge and Hobbs (1982), an equation relating subgrain size to stress has been derived and tested against some of the published experimental data for both metal and non-metals. The basic equation is:

$$gA\left(\frac{\sigma}{G}\right)^n = \frac{2\ell}{d}\left(\frac{32}{\pi(1-\nu)}\right)\frac{D_2}{D_1}\,bc_j\left[\left(\frac{b}{d}\right)^3 + \frac{kT}{D_1Gb}\,\dot{\theta}\right] \quad - \quad (1)$$

where A is the Stocker and Ashby (1971) constant, σ is differential stress, G is the shear modulus of the material, ℓ is the effective slip distance of creep dislocations, d is subgrain size, ν is Poisson's ratio, D_1 and D_2 are the diffusion coefficients for dislocation climb in the body of the crystal and the subgrain boundary respectively, b is the Burgers vector of slip dislocations, c_j is the number of jogs per unit dislocation length, n is the creep stress exponent, and $\dot{\theta}$ is the rate of change of misorientation across the subgrain boundary. If it is assumed that $\dot{\theta}$ is very small, the second term in the square brackets can be neglected, and equation (1) reduces to the conventional form:

$$\frac{\sigma}{G} = K\left(\frac{b}{d}\right)^p \quad - \quad (2)$$

where

$$K = \left(\frac{64}{\pi gA(1-\nu)}\,\frac{D_2}{D_1}\,bc_j\,\frac{\ell}{b}\right)^{\frac{1}{n}}$$

$$p = {}^4/_n$$

For a creep stress exponent of between 3 and 5, as is generally found, σ is approximately inversely proportional to d, as predicted by other theoretical models and a number of experimental studies (Twiss, 1977). However, there is a dependence on creep exponent, as well as on other parameters related to the details of the creep process (e.g., A, D_1, D_2, b, ℓ, c_j). In particular we have been able to incorporate the dependence on temperature (small) and chemical environment predicted from an extensive compilation of grainsize data from natural mylonite zones (Etheridge and Wilkie, 1979, 1981).

An expression relating recrystallized grainsize to stress is still being developed but it promises to involve the same range of parameters as does the subgrain size/stress relationship.

An experimental program aimed at examining and testing these relationships has concentrated to date on the influence of both stress and chemical environment upon subgrain and recrystallized grain size.

In particular it now appears that both the fugacity of oxygen (f_{O_2}) and the fugacity of water (f_{H_2O}) have an influence on recrystallized grain size.

Experiments have been conducted in a modified Griggs apparatus on specimens from a single crystal of natural quartz from Victoria, Australia. Infrared (IR) spectroscopy reveals spectra for various positions within the crystal similar in form and in intensity to IR spectra for Brazilian quartz. The crystal was cut and diamond cored to provide cylinders 6.4 mm in diameter and 15.0 mm in length, oriented such that the compression direction (σ_1) would be normal to m $\{10\bar{1}0\}$. The deformed specimens were ground and cut after deformation to provide IR spectra with the beam normal to $\underset{\sim}{c}$, and thin sections of $\{11\bar{2}0\}$ orientation.

The confining medium for the experiments is household salt. The ramped graphite furnaces are protected from the salt by soft-fired pyrophyllite sheaths. Two Pt-Pt/10% Rh thermocouples are placed diametrically opposite each other against the base of the specimen. One of these is used with a Eurotherm for controlling the temperature within 30°C of that required. Temperature, confining pressure, and load are measured continuously on a W + W chart recorder. Displacement is measured at intervals from a dial gauge placed on top of the load piston. The load is corrected for apparatus distortion which was calibrated for the same confining pressure, displacement rate, and confining medium, as used in the experiments.

All the experiments reported here were conducted at a confining pressure of 1500 MPa and at 800°C. Specimens were kept at these conditions for 20 ± 1 hours before deformation began. The load piston was run at a constant displacement rate providing a strain rate of approximately 1.3×10^{-5} s^{-1}. The pistons either side of the quartz specimens were of alumina rod and did not deform during the experiments.

The chemical environment of the specimens during deformation was controlled by use of solid oxygen buffers. The metals Cu, Ni and Mo, with their oxides, provide buffering capabilities for oxygen at similar pressures, temperatures, and resultant oxygen fugacities to the geologically-relevant buffers of magnetite-hematite, quartz-fayalite-magnetite, and quartz-fayalite-iron, respectively. Extreme oxidising and reducing environments are produced by Mn_3O_4 - Mn_2O_3, and Ta-Ta_2O_5. These five buffers provide an overall fange of f_{O_2} from $10^{-30.3}$ to $10^{-2.2}$MPa at the experimental conditions described. The equivalent range of hydrogen fugacities (f_{H_2}) is from $10^{+4.3}$ to $10^{-4.9}$ MPa. The water fugacity is almost constant for the three more oxidised buffers at $10^{+3.7}$ MPa, changing to $10^{+3.6}$ MPa for Mo-MoO_2, and to $10^{-1.4}$ MPa for Ta-Ta_2O_5.

The oxygen buffers were encapsulated in silver together with the quartz specimen and 50µl of water. The temperature required to weld silver is sufficiently high that water is lost from the capsule even when held in a water bath. Hence a cap was welded to each of two sections of silver tube of wall thickness 0.1mm, one compressed so as to slide inside the other. The specimen, buffer, and water were then placed inside the lower, narrower section and the other section brought down around it to provide metal-metal contact for about 14 mm length. Once the capsule is loaded, assembly of the pressure vessel and application of the confining pressure and temperature required for the experiments is completed as fast as possible. The specific volume for water was always below that

required to rupture the capsule. The compositions of the solid oxygen buffer reactants and products were checked by optical microscopy, X-ray powder diffraction, and electron microprobe analyses.

The mechanical results show that the strength of quartz single crystals decreases steadily and dramatically, from 1500 to 200 MPa, with an increasing oxidising environment, and that these results are reproducible. A sharp break in slope between the Ni-NiO and Mo-MoO_2 buffers on a graph of f_x versus flow strength is interpreted as reflecting the sharp decrease in f_{H2O} under reducing conditions.

Recrystallization is well-developed in the low strength, high fO_2 specimens, decreasing in proportion with the increase of deformation lamellae as fO_2 decreases and the flow strength increases. The orientations of the deformation lamellae (about 50° to σ_1 on $\{11\bar{2}0\}$) in the specimen with highest strength are consistent with slip on r and/or z parallel to $\langle \underline{c} \pm \underline{a} \rangle$, the system with the highest resolved shear stress for deformation in this orientation. Lamellar structures normal to σ_1 may represent slip on m parallel to $\underline{a}$, the next most highly stressed system.

Recrystallized grain sizes vary from 5-10μm in the specimens buffered by Mn_3O_4-Mn_2O_3 to 15-35μm in the specimens buffered by Cu-Cu_2O, Ni-NiO, and Mo-MoO_2. This is the inverse of the expected recrystallized grain size/flow stress relationship. However, subgrain size appears to conform to the predicted subgrain size/flow stress relationship. Experimental results show that the flow strength of quartz is dependent on fO_2 but there is insufficient evidence to demonstrate its effect on the microstructure/flow stress relationships. Information on this problem is being gathered from a new sequence of creep experiments on quartz under controlled chemical environments.

References

Edward, G.H., Etheridge, M.A. and Hobbs, B.E. On the stress dependence of subgrain size. Textures and Microstructures, 5, 127-152, 1982.

Etheridge, M.A. and Wilkie, J.C. Grain size reduction, grain boundary sliding and the flow strength of mylonites. Tectonophysics, 58, 159-178, 1979.

Etheridge, M.A. and Wilkie, J.C. An assessment of dynamically recrystallized grainsize as a palaeopiezometer in quartz-bearing mylonite zones. Tectonophsyics, 78, 475-508, 1981.

Stocker, R.L. and Ashby, M.F. On the rheology of the upper mantle. Rev. Geophys., 11, 391-497, 1973.

Twiss, R.J. Theory and applicability of a recrystallized grain size palaeopiezometer. Pure Appl. Geophys. 115, 227-244, 1977.

Worldwide Standardized Seismograph Network (WWSSN)

3-9920-01201

O. J. Britton

Branch of Global Seismology and Geomagnetism
U. S. Geological Survey
Albuquerque Seismological Laboratory
Building 10002, Kirtland AFB-East
Albuquerque, New Mexico 87115
(505) 844-4637

Investigations

1. Technical and operational support was provided to each station in the Worldwide Standardized Seismograph Network (WWSSN) as needed and required.

2. During this period 195 components and modules were repaired, and 420 separate items were shipped to various stations in the network. Emergency shipments of photographic supplies were made to several stations. This was necessary because of ordering difficulties resulting from new procurement regulations in G.S.A.

3. The Balboa Heights, Canal Zone (BHP) discontinued operation in July 1979. This station has been relocated at the University of Panama (UPA). It began operation at the new location in September 1983. Likewise, the station at Natal Brazil discontinued operation in January 1980. It was relocated and reinstalled in Caico, Brazil (CAI) in August 1983.

4. Training was provided to Mr. Terry Hardiman on the Worldwide Seismic instrumentation for a two weeks period in September 1983. Mr. Hardiman will be the Observer-in-Charge of the San Juan, Puerto Rico (S.J.G.) Observatory.

Results

A continuous flow of high quality seismic data from the cooperating stations within the network is provided to the users in the seismological community.

Glen Canyon Dam

9920-01211

Marvin A Carlson
Branch of Global Seismology and Geomagnetism
U.S. Geological Survey
National Earthquake Information Service, MS 967
Box 25046, Denver Federal Center
Denver, Colorado 80225
(303) 234-3994

Investigation

Glen Canyon Dam - Recorded, compiled, interpreted and reported local earthquakes in the vicinity of the dam and reservoir to attempt to determine whether there are detectable influences on the seismicity by the dam and/or reservoir.

Reservoir induced seismicity appears to have increased as a result of the record Colorado river runoff during the summer of 1983.

Results

Glen Canyon Dam - Memorandum-Type reports are being submitted to the Bureau of Reclamation periodically concerning status of local earthquakes recorded at seismograph station "GCA."

The goal of the Glen Canyon Project is to record, compile, interpret, and report local earthquakes in the vicinity of the dam and reservoir to accumulate data to aid in determining whether there are detectable influences on the seismicity by changes in water level in the reservoir.

U.S. Seismic Network

9920-01899

Marvin A. Carlson
Branch of Global Seismology and Geomagnetism
U.S. Geological Survey
National Earthquake Information Service, MS 967
Box 25046, Denver Federal Center
Denver, Colorado 80225
(303) 234-3994

Investigations

U.S. Seismicity. Data from the U.S. Seismic Network are used to obtain a preliminary location of significant earthquakes worldwide.

Results

As an operational program, the U.S. Seismic Network operated normally throughout the report period. Data were recorded continuously in real time at the NEIS main office in Golden, Colorado. At the present time, 100 channels of SPZ data are being recorded at Golden on develocorder film. This includes data telemetered to Golden via satellite from both the Alaska Tsunami Warning Center, Palmer, Alaska and the Pacific Tsunami Warning Center, Ewa Beach, Hawaii. A representative number of SPZ channels are also recorded on Helicorders to give NEIS real time monitoring capability of the more active seismic areas of the United States. In addition, 12 channels of LPZ data are recorded in real time a multiple pen Helicorders.

Data from the U.S. Seismic Network are interpreted by record analysts and the seismic readings are entered into the NEIS data base. The data are also used by NEIS standby personnel to monitor seismic activity in the U.S. and worldwide on a real time basis. Additionally, the data are used to support the Alaska Tsunami Warning Center and the Pacific Tsunami Warning Service. At the present time, all earthquakes large enough to be recorded on several stations are worked up using the "Quick Quake" program to obtain a provisional solution as rapidly as possible. Finally, the data are used in such NEIS publications as the "Preliminary Determination of Epicenters" and the "Earthquake Data Report."

On July 6, 1983, the Delores River/Paradox Valley seismographic network began operation. The new network is located in Western Colorado and operated by the USGS for the Bureau of Reclamation. The data are telemetered to Golden and recorded on develocorder film and helicorders which are maintained by U.S. Seismic Network personnel. The data are also processed, along with data from the Nevada Test Site, by a PDP 11/34 computer. At this time, data from 10 sites are being telemetered to Golden.

Objectives

The U.S. Seismic Network is an operational program as the data generated are routinely used to support the NEIS operational requirement of timely location and publication of earthquakes worldwide. Also, the network data directly support the NEIS standby

personnel who are responsible for locating and reporting to the media, disaster agencies and other organizations all significant earthquakes worldwide. Thirdly, support is given to the Alaska Tsunami Warning Center and the Pacific Tsunami Warning Service as network data are exchanged with both organizations.

Remote Monitoring of Source Parameters for Seismic Precursors

9920-02383

George L. Choy
Branch of Global Seismology and Geomagnetism
U.S. Geological Survey
Denver Federal Center, MS 967
Denver, Colorado 80225
(303) 234-4041

Investigations

1. Rupture process of moderate-sized earthquakes. We are examining the rupture characteristics of important moderate-sized earthquakes using digitally recorded broadband waveforms. Earthquakes currently under study are the Yemen earthquake of December 13, 1982 and the Coalingua earthquake of May 2, 1983.

2. Rupture process of large earthquakes. We are examining the rupture process of large complex earthquakes (magnitude greater than 7.0). In addition we are looking at pre- and post-seismicity to develop a time-dependent delineation of the process preparatory to an earthquake. We have been analyzing the Samoa earthquake of September 1, 1981.

Results

1. From broadband waveforms we have determined the depth of the Yemen event and determined several other static parameters (moment, depth, stress drop). The rupture was a complex double event. Although both events occurred on the same fault plane, the slip vectors were updip in different directions. The resultant aftershock activity strongly suggests triggered faulting on a conjugate plane. The resolution possible with broadband data shows that in general moderate-sized earthquakes do exhibit complex behavior.

2. We are developing methods of generating synthetic waveforms that correctly incorporate effects of propagation and source complexity in the broadband frequency range. The methods are being used to resolve the details of the large (MS 7.8) Samoa earthquake of September 1, 1981. The earthquake occurred in two stages, rupturing two separate segments in an en echelon pattern. The first stage consisted of a cluster of three events. The second stage consisted of four events linearly aligned. The separation between the rupture zones is interpreted as a barrier which remains unfractured even as its transmits a stress pulse from the first rupture zone to the next. We are interpreting this process and observed pre- and post-seismicity patterns in terms of a time-dependent rupture model.

Reports

Choy, G. L. and M. Zirbes (1983). Broadband body wave analysis of a complex rupture: the Samoa earthquake of September 1, 1982, EOS, Trans. A. G. U., 64, 264.

Choy, G. L. (1983). On the calculation of source parameters from broadband waveforms. IASPEI Program and Abstracts, 47.

DATA PROCESSING SECTION

3-99920-02217

John P. Hoffman
Branch of Global Seismology and Geomagnetism
U.S. Geological Survey
Albuquerque Seismological Laboratory
Building 10002, Kirtland AFB-East
Albuquerque, New Mexico 87115
(505) 844-4637

Goals

1. Data Management Center for the China Digital Seismograph Network: A new project to install a data processing system in Beijing, China to process digital data from a network of nine stations in China has been initiated. A cooperative agreement between the USGS and the People's Republic of China was signed in May, 1983 to design and install a digital network in China. The data management center, which will be the responsibility of the Data Processing Section, will include a PDP 11/44 computer system plus the necessary software to read the station tapes and assemble the data into network-day tapes. The Data Management Center should be installed by October or November, 1984.

Investigations

1. Data Management Center for the China Digital Seismograph Network: The data processing equipment necessary to process the station tapes must be purchased, assembled, and completely tested prior to shipment to China. Software programs required to read the station tapes and to assemble the data into network-day tapes must be written and tested at the Albuquerque Seismological Laboratory before the hardware is shipped.

2. Data Processing for the Global Digital Seismograph Network: All of the digital data received from the global network and other contributing stations are reviewed and checked for quality.

3. Network-Day Tape Program: Data from the global network of stations are assembled into network-day tapes which are distributed to regional data centers and other Government agencies.

4. Event Detection Program for the Global Network: This program has undergone substantial revisions and upgrading and has been installed (May 1983) at all SRO/ASRO installations.

Results

1. Data Management Center for the China Digital Seismograph Network: Since the agreement of understanding between the People's Republic of China and the Geologic Survey was signed in May, 1983, all of the hardware for the data

management center has been specified and ordered. A visit was made to Beijing, China, where the equipment will be installed, to discuss the details of the hardware and software with the Chinese engineers and technicians. All questions from both sides were answered to their satisfaction, and the project is progressing according to schedule. A training program is being planned to provide the Chinese with an extensive background in both hardware, maintenance, and software proficiency. Training will start in April, 1984. Copies of station tapes and network-day tapes from the China Digital Network will be forwarded to the ASL for distribution.

2. Data Processing for the Global Digital Seismograph Network: During the past six months, 417 digital tapes (153 SRO/ASRO, 219 DWWSSN, and 45 RSTN) from the global network and other contributing stations were edited, checked for quality, corrected when feasible, and archived at the Albuquerque Seismological Laboratory. The global network is now comprised of 11 SRO stations, 5 ASRO stations, and 15 DWWSSN stations, which comprise the Global Digital Seismograph Network (GDSN) and are supported by the ASL. In addition, there are six contributing stations which include Glen Almond, Canada and the five RSTN stations installed and supported by Sandia National Laboratories.

3. Network-Day Tape Program: The Network-Day Tape Program is a continuing program which assembles all of the data recorded by the Global Digital Seismograph Network plus the contributing stations for a specific calendar day onto one magnetic tape. This tape includes all the necessary station parameters, calibration data, frequency response, and time correction information for each station in the network. A third edition of a Network-Day Tape Newsletter containing information on all of the global stations and also on the Network-Day Tape Program was distributed in May, 1983. A fourth edition of this newsletter will be issued in November, 1983. A surplus PDP 11/70 computer system has been obtained from the Defense Advanced Research Projects Agency (DARPA). After installation is completed, this computer system will be used in assembling and copying the Network-day tapes and for other research projects at the ASL.

4. Event Detection Program: This algorithm has been implemented (May, 1983) on all of the SRO and ASRO stations. An Open-File Report No. 83-785 by James N. Murdock and Charles R. Hutt describing this algorithm has been published. The abstract of this report is reproduced below.

ABSTRACT

A new short-period event detector has been implemented on the seismic research observatories. For each signal detected, a printed output gives estimates of the time of onset of the signal, direction of the first break, quality of onset, period and maximum amplitude of the signal, and an estimate of the variability of the background noise. On the SRO system, the new algorithm runs approximately 2.5 times faster than the former (power level) detector. This increase in speed is due to the design of the algorithm: all operations can be performed by simple shifts, additions, and comparisons (floating point operations are not required). Even though a narrow

band recursive filter is not used, the algorithm appears to detect events competitively with those algorithms that employ such filters. Tests at Albuquerque Seismological Laboratory on data supplied by Blanford suggest performance commiserate with the on line detector of the Seismic Data Analysis Center, Alexandria, Virginia.

Reports

1. Open-File Reports:

Murdock, James N. and Charles R. Hutt. A New Event Detector Designed for the Seismic Research Observatories. USGS Open-File Report 83-785, 37 pp.

2. Newsletter:

Hoffman, J. P., R. Buland, and M. Zirbes, Network-Day Tape Newsletter, May, 1983, V. 2, No. 1, 11 pp., available from Albuquerque Seismological Laboratory, Albuquerque, New Mexico.

Socorro Magma Bodies

3-9920-03379

Lawrence H. Jaksha
Branch of Global Seismology and Geomagnetism
U.S. Geological Survey
Albuquerque Seismological Laboratory
Building 10002, Kirtland AFB-East
Albuquerque, New Mexico 87115
(505) 844-4637

Investigations:

1. Earthquakes in New Mexico - 1981.

2. Albuquerque Basin Seismicity 1976-1981.

3. Source Spectra.

4. Crustal Structure.

5. Instrumentation.

Results:

1. We have completed an analysis of earthquakes in New Mexico during 1981 that attained magnitudes (M_L) $\geq$ 1.5. The most significant feature of the 1981 seismicity was a long swarm of eathquakes near Lordsburg, New Mexico. This sequence lasted 12 days and generated 22 events with $M_L > 1.5$. The largest earthquake in the series had $M_L = 2.8$.

2. Hypocenters for $\sim$ 1200 earthquakes that were recorded by a seismic network near Albuquerque (1976-1981) have been obtained using the computer program HYPO 71. Most of the earthquakes occurred near Socorro, New Mexico. The seismicity there for the 66 month observation period is described by: $\log_{10} N = 2.81 - .87M$.

A portion of the Jemez Lineament northeast of Grants, New Mexico contained the next most active area. The relationship: $\log_{10} N = 2.63 - .91M$. was derived for that source.

Outside of those two zones (and disregarding two swarm sequences), the seismicity is diffuse and is described by: $\log_{10} N = 1.90 - .69M$.

3. We studied several hundred microearthquakes beneath Socorro mountain that had magnitudes ranging from -0.6 to 1.8. Cross correlation of the first 0.6 seconds of digital seismograms with a characteristic P phase wave form for the swarm produced high correlation coefficients for earthquakes up to but not beyond magnitude 1.2. We concluded that for events with magnitudes less than 1.2 the spectra of the P phase contains no information on the source.

4. We are using the time term method to invert P wave travel times into velocity structure beneath the Socorro Region. Preliminary results suggest a P wave velocity of 8.08 ± .13 Km./s along the top of the mantle. Data sets for the P_g and P_c refractors are presently being compiled.

Our papers summarizing crustal structure beneath northwestern New Mexico (San Juan Basin) have received the Director's approval.

5. We have installed a permanent station at Magdalena, New Mexico. This is the tenth station in the local network.

Frequency response curves were obtained for all of the telemetered stations last summer.

Field equipment is being prepared for experiments utilizing large chemical explosions due to be detonated on White Sands Missile Range (October 26) and Kirtland AFB (October 25).

Reports:

Jarpe, S., Sanford, A., Jaksha, L., and Ake, J., 1983, Earthquakes in New Mexico, 1981. Geophysics Open-File Report No. 44, New Mexico Tech, Socorro, N.M., 12 pp.

Jaksha, L. H., 1983, Earthquakes Near Albuquerque, N.M. 1976-1981, EOS Abstracts for Fall Meeting.

Sanford, A. R., Ake, J. P., Jarpe, S. P., Carpenter, P.J., and Jaksha, L. H., 1983, Source Independent Spectra Up To M = 1.2 Implied From Duplication of P Phase Wave Forms in a Rio Grande Rift Microearthquake Swarm, EOS Abstracts for Fall Meeting.

Evans, D. H., and Jaksha, L. H., 1983, Seismic Refraction Studies in the San Juan Basin, Northwest New Mexico, U.S. Geological Survey Open-File Report No. 83-416, 4 pp.

A Report Entitled: USGS Seismic Studies in New Mexico was presented at a meeting of the Albuquerque Geological Society.

Seismic Observatories

3-9920-01193

Leonard Kerry
Branch of Global Seismology and Geomagnetism
U.S. Geological Survey
Albuquerque Seismological Laboratory
Building 10002, Kirtland AFB-East
Albuquerque, New Mexico 87115
(505) 844-4637

Investigations

Recorded and provisionally interpreted seismological and geomagnetic data at observatories operated at Newport, Washington; Cayey, Puerto Rico; and Guam. At Guam, 24-hour standby duty was maintained to provide input to the Tsunami Warning Service operated at Honolulu Observatory by NOAA and to support the Early Earthquake Reporting function of the NEIS.

Results

Continued to provide data on an immediate basis to the National Earthquake Information Service and the Tsunami Warning Service. Supported the Puerto Rico Project of the Branch of Engineering Geology and Tectonics. Responded to requests from the public, interested scientists, state and federal agencies regarding geophysical data and phenomena.

During this reporting period, the Branch of Global Seismology and Geomagnetism terminated a contract to Nero & Associates of Portland, Oregon to supply one technical person to operate the San Juan Observatory. Date of termination of this contract was September 30, 1983. A Geological Survey Geophysicist will assume this position on October 1, 1983.

Albuquerque Observatory

3-9920-01260

Leonard Kerry
Branch of Global Seismology and Geomagnetism
U.S. Geological Survey
Albuquerque Seismological Laboratory
Building 10002, Kirtland AFB-East
Albuquerque, New Mexico 87115
(505) 844-4637

Investigations:
Recorded seismological data at Albuquerque Observatory, Albuquerque, New Mexico on a continuing basis.

Results:
Continued to send seismograms to the National Earthquake Information Service for use in ongoing USGS programs. Responded to requests from the public, interested scientists, state and federal agencies regarding geophysical data and phenomena.

Seismic Review and Data Services

9920-01204

R. P. McCarthy
Branch of Global Seismology and Geomagnetism
U.S. Geological Survey
Denver Federal Center, MS 969
Denver, Colorado 80225
(303) 234-5080

Investigations and Results

Technical review and quality control were carried out on 514 station-months of seismograms generated by the Worldwide Standardized Seismograph Network (WWSSN). Seventy-two station-months of the ASRO and SRO network analog seismograms were provided on a current basis to the National Earthquake Information Service (NEIS) for their PDE programs. These, as well as, the WWSSN recordings are forwarded to the microfilming service: weekly schedule for the WWSSN; and as released by the NEIS for the SRO and ASRO recordings.

The special microfilming project was temporarily halted due to the contractor's business problems (unrelated to this project), but some effort though limited has been carried out with inhouse help until a new contractor takes over. The experimenting with the short period filming parameters in hopes of improving the microfiche quality was also sidelined. Initial results from changing the reduction ratios were not encouraging. This work will be resumed under the new contractor.

Fifty-seven WWSSN station performance reports were sent to directors during this period. No reduction in the overall high standards was noted. Chiang Mai, Thailand (CHG) has a polarity difference on all six components compared to the SRO station at Chiang Mai (CHTO). This is to be checked by Seismological Laboratory personnel as soon as someone is in the area. Bulawayo, Zimbabwe (BUL) continued to operate the short period's calibration in reversed polarity. Ogdenburg, N.J. (OGD) was transferred to Palisades, N.Y. (PAL) by Lamont-Doherty but conversion to a WWSSN station has not been completed. The last OGD recordings were in February 1980. Tasmania (TAU) which had opted for microfich copies of the TAU records instead of the return of its original seismograms has now asked that the originals be returned in view of the inadequacy of the fiche in their studies of regional earthquakes.

Consultations regarding station data and operations were provided to government officials, and to researchers as needed. Up-to-date monthly reports on the analog and digital data collected from the GSN were distributed to USGS, NOAA, and DOD officials, and Branch of Global Seismology and Geomagnetism researchers.

National Earthquake Information Service

9920-01194

Waverly J. Person
Branch of Global Seismology and Geomagnetism
U.S. Geological Survey
Denver Federal Center, MS 967
Denver, Colorado 80225
(303) 234-3994

Investigations and Results

The weekly publication, Preliminary Determination of Epicenters (PDE), continues to be published on a weekly basis, averaging about 60 earthquakes. The PDE, Monthly Listings, and Earthquake Data Reports (EDR) have been on the VAX for some time and are continuing to work very well with very little down time encountered. We have had no appreciable improvements on rapid data flow from our foreign contributors.

The personal contacts with many of our foreign visitors explaining the need for faster reporting of data have been helpful. We continue to receive telegraphic data from the U.S.S.R. on most magnitude 6.5 or greater earthquakes and some damaging earthquakes with magnitudes less than 6.5 data from the PR China via the American Embassy are being received in a very timely manner and in time for the PDE publication. We are presently receiving 4 stations on a weekly basis from the PR of China and about 22 from SSB by mail in time for the Monthly.

The Monthly Listings of earthquakes are up to date. To date the Monthly Listings and Earthquake Data Report (EDR) have been completed through May 1983. Fault Plane Solutions are being determined when possible and published in the Monthly Listing and EDR for any earthquake having a MB magnitude $\geq$ 5.8. Centroid Moment Tensor Solutions from Harvard University continue to be published in the Monthly Listing and EDR. Moment Tensor Solutions are being computed by the USGS and are also published in the Monthly Listing and EDR. Digital Waveform plots continue to be published in the Monthly Listing which provides an opportunity for graphically displaying focal parameters presented within the text of the publication. Waveform plots are being published for selected events having MB magnitudes $\geq$ 5.8.

The Earthquake Early Alerting Service continues to provide services on recent earthquakes on a 24-hour basis to scientists, news media, and the general public. Fifty-four releases were made from April 1, 1983, through September 30, 1983. The largest earthquake released during this time was a magnitude 7.7 in Japan on May 26. In the United States the largest was a magnitude 6.5 in Coalinga, California on May 2.

Reports

Preliminary Determination of Epicenters (PDE) (25 weekly publications April 6, 1983 to September 28, 1983--Numbers 11-83 through 36-83). Compilers: W. Leroy Irby, Willis Jacobs, John Minsch, Waverly Person, Bruce Presgrave, William Schmieder.

Monthly Listing of Earthquakes and Earthquake Data Reports (EDR) (6 publications--December 1982 through May 1983). Compilers: W. Leroy Irby, Willis Jacobs, John Minsch, Russell Needham, Waverly Person, Bruce Presgrave, William Schmieder.

Seismological Notes, BSSA: Waverly J. Person
July-August 1982
September-October 1982
November-December 1982

Earthquake Information Bulletin:
Vol. 14, no. 6, Earthquakes, Waverly J. Person, May-June 1982
Vol. 15, no. 1, Earthquakes, Waverly J. Person, July-August 1982
Vol. 15, no. 2, Earthquakes, Waverly J. Person, September-October 1982
Vol. 15, no. 3, Earthquakes, Waverly J. Person, November-December 1982

Global Seismograph Network Evaluation and Development

3-9920-02384

Jon Peterson
Branch of Global Seismology and Geomagnetism
U.S. Geological Survey
Building 10002, Kirtland AFB-East
Albuquerque, New Mexico 87115

(505) 844-4637

Investigations

1. Simple numerical noise models representing ambient earth background at hypothetical quiet and noisy sites, and quiet sites during a microseismic storm were developed from straight-line approximations of composite power spectral density plots obtained from the Global Digital Seismograph Network and other sources.

2. Work began in accordance with a Protocol Agreement between the State Seismological Bureau (SSB) of the People's Republic of China and the U.S. Geological Survey, signed in May 1983, in which the USGS will assist the SSB in the establishment of a China Digital Seismograph Network (CDSN).

Results

1. The earth noise models have been defined and illustrated in a draft report that also presents some applications. The noise models may easily be placed in a computer program. By correcting the models with an appropriate transfer function, they can be used to predict the ambient spectral output of a seismograph, or other instrument sensitive to earth motion, at quiet and noisy sites. The models are also useful for defining instrument characteristics, such as maximum tolerable level of self noise, sensitivity, and dynamic range, and as baselines for comparative evaluation of recording sites. They can also be used to predict the peak-to-peak amplitude of ambient background over a specified bandwidth.

2. The CDSN will initially consist of nine field systems, to be installed at stations that have been selected by the SSB, a data management system, and a depot maintenance center, both of which will be installed in Beijing. Agreement has been reached on system design and major components have been selected. Signals will be derived from PRC-manufactured short-period seismometers and a triaxal set of Strecheisen (Wielandt) broadband seismometers. Four data bands will be recorded: short period, broadband, long period, and very long period, the first two in a triggered mode and the second two in a continuous mode. The digital data will be recorded on high-density tape cartridges. The cartridges will be sent to the data management system in Beijing where the station data will be assembled into network-day tapes. The data management system is modeled on the USGS facility used to assemble network-day tapes from the global digital network. Selected data from the CDSN will be placed on the USGS network-day tapes. Detailed system design is underway, as is the procurement of network hardware.

Global Digital Network Operations

3-9920-02398

Robert D. Reynolds
Branch of Global Seismology and Geomagnetism
U. S. Geological Survey
Albuquerque Seismological Laboratory
Building 10002, Kirtland AFB-East
Albuquerque, New Mexico 87115
(505) 844-4637

Investigations

The Global Network Operations continued to provide technical and operational support to the SRO/ASRO/DWWSSN observatories which include operating supplies, replacement parts, repair service, redesign of equipment, training and on-site maintenance, recalibration and installation. Maintenance is performed at locations as required when the problem cannot be resolved by the station personnel.

The O&M contract was awarded to Bendix Corp. effective October 1, 1983. The same personnel were retained consisting of a team leader and three field engineers.

Several major procurements were undertaken during this period as part of the SRO enhancement program. A contract was awarded to Inland Assoc. of Manchester, Mo. to provide DEC LA-12 matrix printers as replacements for the ASR 33 teletypes at all SRO/ASRO stations. Teledyne-Geotech of Garland, Texas received a contract to provide 20 model 38850 S.P. filters. These filters are to be used to upgrade the SRO stations to 3 channels of S.P. data. Also, an uninterruptible power system was ordered for the DWWSSN station at Toledo, Spain.

The following station maintenance activity was accomplished:

ANMO - Albuquerque - SRO
One maintenance visit.

ANTO - Ankara, Turkey - SRO
No maintenance visit.

BCAO - Bangui, Central African Republic - SRO
No maintenance visit.

BOCO - Bogota, Colombia - SRO
One maintenance visit.

CHTO - Chiang Mai, Thailand - SRO
One maintenance visit.

CTAO - Charters Towers, Australia - ASRO
No maintenance visit.

GRFO - Grafenberg, W. Germany - SRO
No maintenance visit.

GUMO - Guam - SRO
No maintenance visit.

KONO - Kongsberg, Norway - ASRO
One maintenance visit.

KAAO - Kabul, Afghanistan - ASRO
No maintenance visit.

MAJO - Matsushiro, Japan - ASRO
No maintenance visit.

MAIO - Mashhad, Iran - SRO
Out of operation.

NWAO - Mundaring, W. Australia - SRO
No maintenance visit.

SHIO - Shillong, India - SRO
No maintenance visit.

SNZO - Wellington, New Zealand - SRO
No maintenance visit.

TATO - Taipei, Taiwan - SRO
No maintenance visit.

ZOBO - La Paz, Bolivia - ASRO
One maintenance visit.

DWWSSN

GDH - Godhavn, Greenland
Two maintenance visits.

BER - Bergen, Norway
One maintenance visit.

KEV - Kevo, Finland
One maintenance visit.

BDF - Brasilia, Brazil
One maintenance visit.

SLR - Silverton, S. Africa
One maintenance visit.

AFI - Afiamalu, W. Samoa
One maintenance visit.

LEM - Lembang, Indonesia
One maintenance visit.

ASL Repair Facility

A minimum amount of routine repair was done during this period due to maximum effort being in field work.

Special Activity

An analog telemetry system was installed at Peldehue, Chile along with a satellite telemetry system for rapid reporting of seismic event parameters.

Two WWSSN systems were reinstalled after having been moved from former locations. One system is now operating in Caico, Brazil and the other at the University of Panama.

A noise survey was started in three African countries for potential GTSN locations. The countries are South Africa, Kenya, and Ivory Coast.

Results

The digital network continues with a combined total of 30 SRO/ASRO/DWWSSN stations. The maximum effort now is to perform as much on site maintenance and training as possible to provide as much quality digital data as possible for the worldwide digital data base.

United States Earthquakes

9920-01222

Carl W. Stover
Branch of Global Seismology and Geomagnetism
U.S. Geological Survey
Denver Federal Center, MS 967
Denver, Colorado 80225
(303) 234-3994

Investigations

1. Seventy-five earthquakes in 18 states were canvassed by a mail questionnaire for felt and damage data. Forty-three of these occurred in California. The most significant event for the period was the Coalinga, California earthquake of May 2, 1983 located at 36.24°N., 120.30°W., depth 12 km, magnitude 6.2 mb, 6.5 MS, and 6.5 ML. There were seven events that caused damage in the United States; four in California (3 in Coalinga), two in alaska, and one in Illinois. The alaska events, magnitude 6.3 MS and 6.1 MS on July 12, 1983 and September 7, 1983 respectively, occurred in the same areas as the 1964 earthquake.

2. The United States earthquakes for the period April 1, 1983 to September 30, 1983, have been located and the hypocenters, magnitudes, and maximum intensities have been published in the Preliminary Determination of Epicenters.

3. The seismicity map of New Mexico, MF 1660, has been printed at a scale of 1:1,000,000.

Results

The maximum Modified Mercalli intensity of VIII was assigned to the Coalinga, California earthquake of May 2, 1983. One death was attributed to earthquakes and 47 people were injured. Most of the downtown business area was destroyed and many homes were damaged. Damage was estimated at $31 million. Two aftershocks, one on May 9 the other on July 21, caused additional minor damage.

United States earthquake data for January-March 1982 has been published in circular 895A. The data for April-June 1982 has the Director's approval is being printed.

Reports

Stover, C. W., Minsch, J. H., Reagor, B. G., and Baldwin, F. H., 1983, Earthquakes in the United States, January-March 1982: U.S. Geological Survey Circular 895A, 42 p.

Reagor, B. G., Stover, C. W., Minsch, J. H., and Brewer, L. R., 1983, Earthquakes in the United States, April-June 1982: U.S. Geological Survey Circular 895-B, 27 p.

Stover, C. W., 1983, Intensity distrubution and isoseismal map: in the 1983 Coalinga, California earthquakes, California Division of Mines and Geology, Special Report (in press).

Stover, C. W., Reagor, B. G., and Algermissen, S. T., 1983, Seismicity map of the State of New Mexico: U.S. Geological Survey Miscellaneous Field Studies Map MF-1660

Digital Data Analysis

9920-01788

Ray Buland
Branch of Global Seismology and Geomagnetism
U.S. Geological Survey
Denver Federal Center, MS 967
Denver, Colorado 80225
(303) 234-4041

Investigations

1. Moment Tensor Inversion. Apply methods for inverting body phase waveforms for the best point source description to research problems.

2. Computation of Free Oscillations. Develop practical methods for computing free oscillations of the Earth and combining them to construct synthetic seismograms.

3. Near Source Structure. Study the effects of near source structure on teleseismic body waves recorded on broadband instruments.

4. Post Seismic Deformation. Study the behavior of model rheologys on time scales of days to months.

5. Earthquake Location Technology. Study techniques for improving the robustness, honesty, and portability of earthquake location algorithms.

6. Detection Capabilities. Study the seismic event detection capability of each proposed station in the Southern Hemisphere Seismic Net (SHSN) now under development.

7. Network Day/Event Tapes. Support and enhance portable software for retrieving data from the Global Digital Seismograph "Network Day Tapes." Develop software for creating "Network Event Tapes."

8. Special Event Reports. Contribute to NEIS publications pertaining to selected events.

9. NEIS Monthly Listing. Contribute both fault plane solutions (using first-motion direction) and moment tensors (using long-period body-phase waveforms) for all events of magnitude 5.8 or greater when sufficient events exist. Contribute waveform/focal sphere figures of selected events.

Results

1. Moment Tensor Inversion. Careful study of the three largest Mammoth Lakes earthquakes indicates that two of the three have large non-double couple components which are consistent with a compensated linear vector dipole source. That is, these events seem to arise directly from the extensional tectonics of the region. The other event was determined to be a pure double couple, probably due to stress imposed on the region by the extension. A technical artcle is being prepared on these findings.

2. Computation of Free Oscillations. Work on a standaard normal mode program is proceeding slowly. Calculations are currently being done for the normal modes of a viscoelastic Earth. By performing the calculation directly from a model rheology rather than by first order perturbation theory, the quality of the perturbation theory may be tested. Finally, project personnel have been consulting on the calculation of the normal modes of neutron stars. These calculations may be able to explain the high frequency oscillations modulating the x-ray radiation from bursters.

3. Near Source Structure. Recently, the timing, shape, amplitude, and duration of multiple body wave arrivals observed on broadband instruments at teleseismic distances have been used to interpret source complexity. Model studies examine the effect of near source structure on this interpretation. Preliminary conclusions are that the timing and interpretation of P, pP, and sP from multiple events of comprable size is unaffected. However, the body wave shapes, amplitudes, and durations must all be treated with caution.

4. Post Seismic Deformation. Currently no deformational mechanisms are known to have time scales between the free oscillations of the Earth (periods shorter than one hour) and the quasi-static post glacial rebound modes (periods longer than 100 years). We have examined the secular determinant of a homogeneous Earth assuming a model rheology. Preliminary results are that deformation at these intermediate time scales are probably controlled by both viscous normal modes and by branch cuts.

5. Earthquake Location Technology. The NEIS location algorithm has been modified to incorporate step length damping. This new version, now in routine production, determines whether an event is shallow or deep much more reliably and eliminates non-optimal solutions. The travel-time algorithm of Buland and Chapman is being extended to compute P_g, P_b, P_n, P, Pdiff, PKP, pP, sP, PcP, SKP, ScP, PKKP, SKKP, PP, P'P', S_g, S_b, S_n, Sdiff, and SKS. It is hoped that these travel-times may be applied to routine NEIS locations within the next six months. Investigation of robust location techniques continues with the current emphasis on scale invaraiant M-estimators and on R-estimators.

6. Detection Capabilities. Each of the ten stations comprising the proposed SHSN network is to be studied in detail for ability to well record seismic events. To date the study of two stations, described in internal reports, have been completed and a third is under way.

7. Network Day/Event Tapes. The third release of the portable Network Day Tape software and documentation has been distributed. A new product, the Network Event Tape, has been specified and preliminary coding of computer programs to produce them is nearing completion.

8. Special Event Reports. The mechanism of the Western Arabian Peninsula event of December 13, 1982, has been studied for a forthcoming special report.

9. NEIS Monthly Listing. Since May 1981, fault plane solutions for large events have been contributed to the Monthly Listing. Beginning in November 1982, moment tensors and waveform/focal sphere plots are also being contributed. In the last six months the fault plane solutions and moment tensors of approximately 75 events were published. Catalogs of all fault plane solutions along with first motions data is being prepared for publication as a USGS circular.

Reports

Needham, R. E., 1983. Preliminary Report on the Detection Capabilities of the SHSN Stations: Station ANT-Antofagasta, Chile; Internal Report.

Needham, R. E., 1983. Preliminary Report on the Detection Capabilities of the SHSN Stations: Station SPA-South Pole: Internal Report.

SYSTEMS ENGINEERING

3-9920-01262

Harold E. Clark, Jr.
Branch of Global Seismology and Geomagnetism
U. S. Geological Survey
Albuquerque Seismological Laboratory
Building 10002, Kirtland AFB-East
Albuquerque, New Mexico 87115
(505) 844-4637

Investigations

1. Design, develop, and test microprocessor based seismic instrumentation.

2. Design, develop, procure, and test special electronic systems required by seismic facilities.

3. Design, develop, and test microprocessor/computer software programs for seismic instrumentation and seismic recording systems.

Results

1. The Digital Recording System and the Depot Repair Instrumentation Plans for the China Digital Seismograph Network (CDSN) have been completed. The China Digital Recording System will be based on the DWWSSN Digital Recording System with additional tasks and features required by the China Digital Seismograph Network. During this time period, the purchase and contracting for all developmental test systems and equipment, the parts and equipment for the demonstration system, and most of the parts and equipment for the remaining field systems were the primary efforts which required most of the Systems Engineering time.

2. During September 11th through September 30th, detailed technical discussions were held with the Peoples Republic of China (PRC) in Beijing, China. Final design considerations and site technical specifications were discussed and approved by both the PRC and the USGS personnel. Training requirements for PRC personnel were discussed. Extensive training by the PRC personnel in CDSN system operation, maintenance, and repair will be required for successful network operation.

3. Four man-months were devoted to the Panama Project. A list of seismic equipments for Phase One was completed. Radio frequency requirements for the proposed David City and Panama City seismograph network were completed. No other Panama Project work is scheduled by Systems Engineering personnel in the future because of the large commitment to the China Network Program.

Earth Structure and its Effects Upon Seismic Wave Propagation

9920-01736

George L. Choy
Branch of Global Seismology and Geomagnetism
U.S. Geological Survey
Denver Federal Center, MS 967
Denver, Colorado 80225
(303) 234-4041

Investigations

1. Effect of source complexity on inversions for earth structure. Many studies of earth structure have dismissed frequency-dependent effects of the source as secondary to propagation effects. (For example, many long-period studies use a point source on the assumption that the wavelengths involved are much longer than the source dimension.) We have been developing methods of generating synthetic waveforms that correctly incorporate the frequency dependent effects that arise from source directivity and propagation through the earth. We are using these methods to examine the possible bias in determining earth structure that results from neglect of actual source functions.

2. Source parameters from GDSN data. Extract source parameters from digitally recorded data of the GDSN by determining corrections to waveforms to distinguish source effects from propagation effects.

Results

1. Recent studies of source mechanism using broadband body waves indicates that even moderate-sized earthquakes (mb between 5.8 and 6.5) rupture in complex fashion. Besides a number of shallow earthquakes, we have looked at 20 deep earthquakes. Only about one of every ten deep events generated relatively simple waveforms. All other events had varying degrees of complexity. We are evaluating the bias that complexity might had on some studies of earth structure that presumed simplicity in source functions.

2. After correcting broadband waveforms for propagation effects, we were able to detail source parameters for earthquakes in Samoa (September 1, 1981; MS 7.8) and Yemen (December 13, 1982; MS 6.0). Stations at distances for body waves that were diffracted, that interacted with the earth's core and that touched internal caustics provided crucial azimuthal control on the rupture processes.

Reports

Choy, G. L. and M. Zirbes (1983). Broadband body wave analysis of a complex rupture: the Samoa earthquake of September 1, 1981, EOS, Trans. A. G. U., 64, 264.

Choy, G. L. (1983). On the calculation of theoretical seismograms by the full wave method, IASPEI Programme and Abstracts, 46.

Choy, G. L. (1983). On the calculation of source parameters from broadband waveforms, IASPEI Programme and Abstracts, 47.

Seismicity and Tectonics

9920-01206

William Spence
Branch of Global Seismology and Geomagnetism
U.S. Geological Survey
Denver Federal Center, MS 967
Denver, Colorado 80225
(303) 234-4041

Investigations

Studies carried out under this project focus on detailed investigations of large earthquakes, aftershock series, tectonic problems, and earth structure. Studies in progress have the following objectives:

1. Provide tectonic setting for and analysis of the 1977 Sumba earthquake series (W. Spence).

2. Provide tectonic setting for and analysis of the 1974 Peru gap-filling earthquake (W. Spence, C. J. Langer, and J. N. Jordan).

3. Provide an integrated seismicity and tectonic study for the country of Panama (C. Mendoza).

4. Determine the maximum depth and degree of velocity anomaly beneath the Rio Grande rift and Jemez lineament by use of a 3-D, seismic ray-tracing methodology (W. Spence, R. S. Gross, and L. H. Jaksha).

Results

1. The great $M_0 = 4 \times 10^{28}$ dyne-cm), normal-faulting Sumba earthquake of 1977 occurred at the Java Trench, just west of the zone where the Australian continental lithosphere is in collision with the Java arc. Aftershocks of the Sumba earthquake have been relocated by the joint hypocenter method and occur in two zones: an east-west trending zone, mostly east of the main shock, and a triggered northwest-southeast-trending zone located about 180 km northwest of the main shock. The focal mechanism data for the main shock zone combined with its detailed tectonic setting support the conclusion that the Sumba main shock occurred directly as a result of slab pull and moreover that the displacement in the main shock zone may be part of a continuing process of detachment of the subducted oceanic lithosphere from the Australian continental lithosphere, rather than the main shock being a simple plate-bending event. The space-time character and right-lateral, strike-slip focal mechanisms for earthquakes in the second zone imply a postseismic rebound of the overriding wedge of continental shelf, and in turn compression of this wedge coseimically with the occurrence of the main shock.

2. The great 1974 Peru thrust earthquake (M_S 7.8, M_W 8.1) occurred in a documented seismic gap, between two earthquakes to the north occurring in 1940 (M_S 8.0) and 1966 (M_S 7.5) and one earthquake to the south, occurring in 1942 (M_S 8.1). The stress release of the October 3, 1974 main shock and aftershocks occurred in a spatially and temporally irregular pattern.

The multiple-rupture main shock produced a tsunami with wave heights of 0.6 ft at Hawaii and which was observed, for example, at Truk Island and at Crescent City. The aftershock series essentially was ended with the occurrence of a M_S 7.1 aftershock on November 9, 1974.

3. As part of a cooperative program between the University of Panama and the USGS to assess earthquake hazards in Panama, historical information on past Panamanian earthquakes is being collected. A comprehensive catalog of historic earthquakes is being compiled and will be used to develop cumulative intensity maps, to be used in assessing earthquake hazard in Panama. An examination of regional seismicity, initially through a teleseismic analysis and to be followed by regional network coverage, is also being conducted. This seismicity study should lead to further insight on tectonically active structures in Panama and into the nature of the plate interaction process in the vicinity of the Cocos-Nazca-Caribbean triple junction.

4. To a depth of about 160 km, the upper mantle P-wave velocity beneath the Rio Grande rift and Jemez lineament is 4-6 percent lower than the corresponding upper mantle velocity beneath the High Plains Province. The 3-D, P-wave velocity inversion shows scant evidence for pronounced low P-wave velocity beneath the 240-km-long section of the Rio Grande rift covered by our array. However, the inversion shows a primary trend of 1-2 percent lower P-wave velocity underlying the northeast-trending Jemez lineament, down to a depth of about 160 km. The Jemez lineament is defined by extensive Pliocene-Pleistocene volcanics and late Quaternary faults. The upper mantle low-velocity segment beneath the Jemez lineament is at most 100 km wide and at least 150-200 km long, extending in our inversion from Mt. Taylor through the Jemez volcanic center and through the Rio Grande rift. A Backus-Gilbert resolution calculation indicates that these results are well-resolved.

Reports

Engdahl, E. R., Dewey, J. W., and Billington, S., 1983, Features of subduction-zone seismicity in the central Aleutian Islands: Program and Abstracts, IUGG Interdisciplinary symposia, Hamburg, p. 39.

Fracture Mechanics Analysis Of The Validity Of Hydraulic Fracturing As A Technique Of In Situ Stress Determination

14-08-0001-20516

Charles Fairhurst and Gideon Leonard
Department of Civil & Mineral Engineering
500 Pillsbury Drive S.E.
University of Minnesota
Minneapolis, MN 55455
(612) 373-2968

Investigations

Careful laboratory experiments were conducted on quartz glass samples in order to understand better the mechanics of initiation and early stages of propagation of hydraulic fracturing as well as to test the validity of this method as a technique of in-situ stress determination.

This work was motivated by recent experimental (Mizuta and Kobayashi - 1980) and theoretical (Cleary - 1979) developments. The former has clearly demonstrated that for the general case where the principal compressive stresses are inclined to the borehole axis, the hydraulic fracture is always coaxial with the borehole axis in its early stages of development and then re-orients itself to the direction of minimum compression in the far field. The latter has suggested that fracture initiation and propagation do not occur simultaneously and symmetrically on each side of the borehole.

The results of this work bring into question some of the basic conclusions underlying this technique. Specifically, the practical outcome from field tests may be that the measured fracture direction along the borehole surface does not coincide with a principal stress direction and hence the calculated maximum principal stress magnitude would be incorrect. This is due to the fact that where a fracture initiates along a non-principal direction, the fracture plane is subjected to a combination of tensile and shear stresses which could result in an influence on the breakdown pressure and the indicated tensile strength. In addition it becomes unclear whether the breakdown pressure is related to the primary or secondary fracture initiation.

Results

The selection of glass as a model testing material made it possible to examine carefully on both sides of the borehole; the location and dimensions of the critical flaw, the influence of the shear stresses on the critical flaw geometry, and the fracture front geometry and dimensions at each increment of the fracture growth.

The main conclusions that can be drawn from such a detailed experimental analysis are:

1) The hydraulic fracture does not initiate, nor propagate simultaneously and symmetrically across the borehole.

2) Initiation -

- Initiation is governed by one single "best oriented, best sized" penny shaped flaw located anywhere within the packed-off section and at any place around the borehole surface where the hoop stress is tensile and not necessarily the maximum.

- The average flaw to borehole radius ratio did not exceed 6%.

- In cases where anti-plane shear stresses (formed when principal stress directions are inclined to the borehole axis) acted along the borehole surface the critical flaw retained its penny shaped geometry. However, this flaw did not always lie in the plane of fracture propagation.

3) Propagation -

- Early stages of propagation are influenced directly by the borehole geometry, i.e. length of packed-off (pressurized) region compared to the borehole diameter, which constrains the fracture to be axial. This holds for vertical or inclined boreholes with respect to principal stress directions.

- During the first stage of fracture growth, the initial crack front moves much faster along the borehole surface than it does into the far field, forming a narrow semi-elliptical crack whose major axis coincides with the borehole surface.

- During this stage of growth, a secondary fracture is formed across the borehole (not necessarily along a diametrical line) and propagates in the same manner as the primary fracture.

- At the time where the semi-major axes of both fronts exceed the pressurized borehole length, the rate of growth of the fractures into the far field increases.

4) The breakdown pressure is related to the primary fracture initiation and not influenced by the anti-plane shear stresses.

In conclusion an improved understanding of the mechanics of hydraulic fracturing has been achieved. However, the validity of this technique with regard to the measured principal stress directions is still unconfirmed.

Reports

Mizuta, Y. and Kobayashi, H., (Fairhurst, C. and Santich, J., Co-Principal Investigators), Improved Stress Determination Procedures By Hydraulic Fracturing, Final Report to the U.S. Geological Survey, Grant No. USDI-14-08-0001-17775, 1980.

References

Cleary, M.P., Rate and Structure Sensitivity In Hydraulic Fracturing of Fluid-Saturated Porous Formations, the 20th U.S. Symposium on Rock Mechanics, 1979.

DEVELOPMENT OF IMPROVED HYDROFRACTURING INSTRUMENTATION AND ITS APPLICATION AT THE SITE OF INDUCED SEISMICITY NEAR THE MONTICELLO RESERVOIR, SOUTH CAROLINA

Contract No. 14-08-0001-20537

Bezalel C. Haimson

University of Wisconsin-Madison

1509 University Avenue

Madison, Wisconsin 53706

(608)262-2563

Hydrofracturing is todate the most widely accepted method of estimating the in situ state of stress at depths larger than a few tens of meters. However, many opportunities of measuring rock stresses have been passed over because of the high costs involved in conducting hydrofracturing tests. Thus, a large number of induced seismicity site evaluations are conducted without the benefit of, perhaps, the most important parameter, namely the in situ stress. The high costs of hydrofracturing result mainly from the use of drilling rig and drill-rod for tripping the test probe. Not only are drilling rig mobilization costs and daily charges often considered excessive, but the slow process of lowering and lifting of the pipes is inefficient and adds considerably to the test budget.

Under the current USGS contract, we have developed a new hydrofracturing field technique which renders the measurement of stress considerably faster and less expensive. The major improvement is the conversion of hydrofracturing from a drill-rod to a wire-line method using separate flexible hydraulic lines for the packers and for the test interval. The newly designed fracturing tool accommodates downhole pressure transmitters and allows the attachment of caliper, temperature or other logging probes. The downhole electronic instrumentation is connected to surface power supplies and recorders via the 7 conductors located in the wire-line. The drilling rig has been replaced by an easy-to-assemble tripod and a hoist located in a specially equipped truck. Hydrofracture delineation and orientation are determined by a wire-line impression packer and orienting tool. The tripping of the hydrofracturing probes is now continuous and fast. Depths previously reached in hours are now arrived at in minutes. Transducer measurements previously conducted by necessity on the surface, now are carried out at the depth of interest.

We have employed the new system to carry out stress measurements in Mont 2, a 1.1 km hole in the area of seismic activity near the Monticello Reservoir, South Carolina. This hole was previously tested by Zoback and Hickman [J. Geophys. Res. 6859-6974, 1982]. The objectives of our tests

were: (1) to evaluate the suitability of our newly designed wireline hydrofracturing system for conducting stress measurements in deep holes, and (2) to obtain additional stress magnitudes and previously unavailable stress directions at different depths in the hole, and relate them to the local seismicity which was apparently induced by the reservoir impoundment. The wire-line method of testing performed flawlessly during the tests, but proved to be considerably more sensitive than the drill-rod method to minor irregularities along the borehole wall. Seven complete tests were conducted between the depths of 75 to 360 m. In general accord with previous results [Zoback and Hickman, J. Geophys. Res., 87, 6959-6974, 1982] the least principal stress (σ_{min}) in the range of depths tested was approximately equal or somewhat smaller than the density-based calculated vertical stress (σ_v). Linear regression shows $\sigma_v = 0.0265\ D$ and $\sigma_{min} = 0.5 + 0.020\ D$ for this depth range (where stresses are in MPa and D is depth in m). Extremely thin but clear packer impressions of the induced hydrofractures were obtained in each of the tests. All the fractures were inclined, four dipping more than 60°, and three - 30° to 45°. The mean strike direction of five hydrofractures dipping 45° or more is N78°W ± 20°. The unexpected occurrence of inclined hydrofractures in granite is somewhat puzzling. Additional testing at greater depths in the hole for further confirmation of our results is recommended. Parts of Zoback and Hickman's [1982] analysis, which was based on the common assumption of vertical hydrofracturing, may have to be reexamined. Although the classical method of calculating the maximum stress fails when the hydrofracture is not vertical, our estimation of this value indicates that at any particular depth all three principal stresses are close in magnitude yielding an almost negligible maximum shear stress. This suggests stress relaxation resulting from the reservoir-induced seismicity.

Seismic Monitoring of the Richard B. Russell Dam Impoundment

3-9900-01268

L. T. Long
School of Geophysical Sciences
Georgia Institute of Technology
Atlanta, Georgia 30332
(404) 894-2860

Investigations

1. The first objective of the project is to develop three instruments to site in the Richard B. Russell Lake area. This will augment an existing four-station net to seven stations should reservoir induced seismicity be detected.

2. The second objective is to obtain a set of unique data which can be used to study, in detail and with precision, a small sub-area of induced seismicity. The data set will allow precision determination of depth, focal mechanism, and spectra for small shallow events.

3. The third objective has been to investigate the relation between high-frequency spectral slope and depth of focus. The objective of this investigation is to relate the spectral properties of reservoir induced earthquakes to the state of stress and perhaps be able to estimate the largest event that might be induced in a particular reservoir area.

Results

1. We have three stations on hold for possible installation in the Richard B. Russell area should induced seismicity be detected.

2. The components for six systems have been purchased, and we are in the process of assembling the components.

3. The frequency content of earthquakes recorded in the Monticello, South Carolina, and the Mammoth Lakes, California, areas have been examined as a function of depth of focus. For each event we determined the depth-of-focus and slope of the displacement spectra above the corner frequency. In the Monticello, South Carolina, area the range of depths was too narrow to determine a relationship with spectral slope. However, in the Mammoth Lakes area a relation between slope above the corner frequency and depth-of-focus was observed. Spectra which decay at a rate of ω^{-3} or higher were predominantly observed for shallow events. Events with a deeper focus typically had a displacement spectra decay rate less than ω^{-3}. The relation is shown in Figure 1.

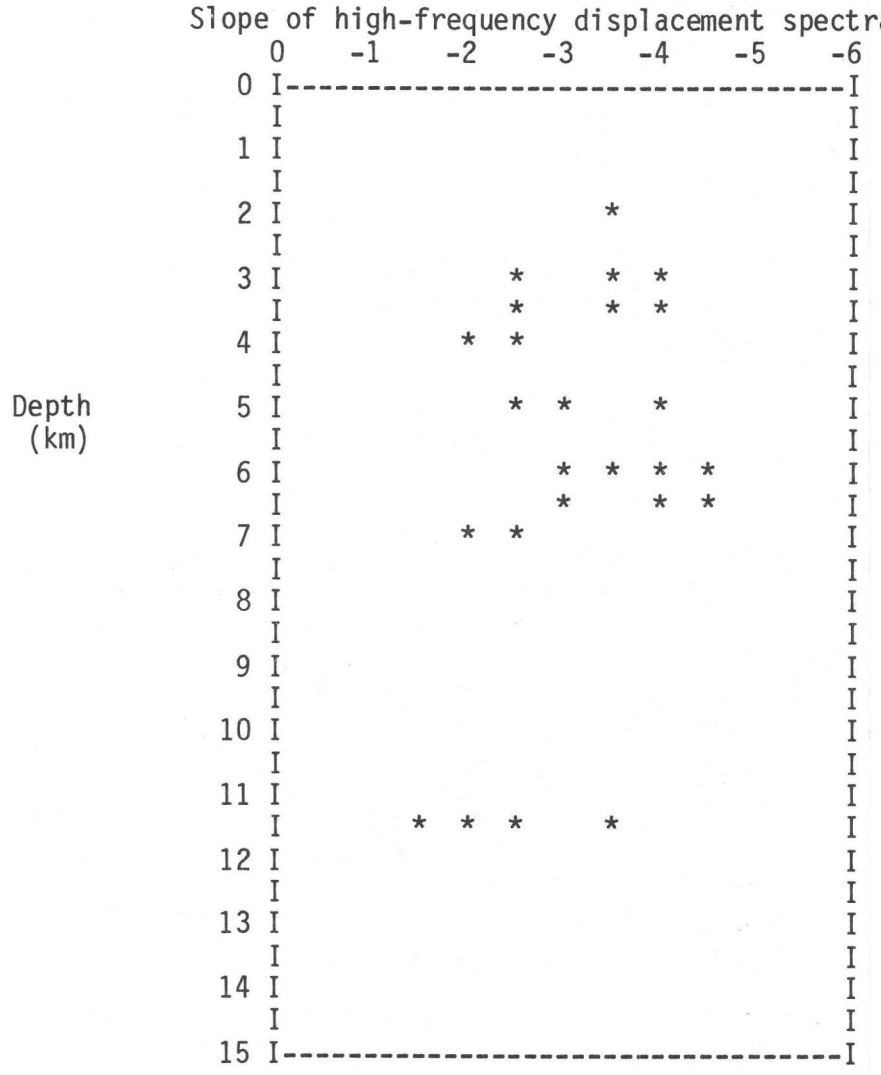

Figure 1. Relation between depth of focus and spectral slope above the corner frequency. Depth of focus is computed indirectly from the direction of propagation.

Reports

Long, L. T., and Wilson, Jeffrey, 1983, Investigation of high-frequency spectral slope versus depth (Abstract): Earthquake Notes, v. 54, no. 1, p. 32.

THE OROVILLE VERTICAL SEISMIC PROFILING EXPERIMENT

USGS CONTRACT NO. 14-08-0001-21238

P.E. Malin
W.A. Waller
Marine Sciences Institute
Dept of Geological Sciences
University of California
Santa Barbara, Ca. 93108
ph. (805) 961 3520

Investigations

In 1982 the USGS drilled a 500m deep well on the Cleveland Hills, south of Oroville Dam in northeastern California. The well penetrated the high angle Cleveland Hills fault at a depth of approximately 350 m. In April 1983 we deployed a Vertical Seismic Profiling string of geophones in this well with the intent of studying the local sub-micro and micro earthquake activity, and as a first step in characterizing the attenuation of earthquake s waves at the earth's surface. The string contained 3 sets of 3 component geophones (4.5 hz, 1.5k +10% coils), one set at the bottom of the well, one just above the fault zone and the third set at the ground surface. Four vertical component geophones (4.5 hz, 9.5k +10% coils) were spaced at 100 m intervals between the 3 component instruments (see Figure 1).

The output of the downhole geophones was recorded on USGS GEOS digital event recorders, at a sampling rate of 200 samples per second per channel. The GEOS systems were set up to trigger on the vertical component at the bottom of the well. The high cut filters of the recorders were set at 50 hz. In October 1983, after successfully collecting a catalogue of some 30 local and regional events, the vsp string was removed from the well.

Results

Despite being next to a light traffic country road (1 vehicle every 5 to 10 min), the GEOS / downhole sensor triggering system recorded only a few dozen cultural events. One of these events, the moving of a 10 ton trailer around the well site, allowed us to establish the downhole noise reduction as a function of frequency in the band 6 to 50 hz. The maximum noise reduction, which was on the order of 24 db, occurred at the higher frequencies. This noise reduction allowed us to record several -1 magnitude events that occurred a few km below and away from the well site. It appear at this time that the background seismicity of this site at magnitudes less than or equal to 0 is smaller than might be expected from previous work.

We have analyzed several of the nearby microearthquakes for spectral content as a function of recording depth in the well. For these events the p and s wave corner frequencies at the bottom of the well are beyond the high cut filters set in the GEOS recorders. The three component record immediately above the fault zone establishes, however, that substantial high frequency s wave loss occurs over this interval. The character of

this frequency dependant loss can be seen in Figure 2. Shown in the latter Figure is the ratio of horizontal motion power spectra for the 3 component geophones above and below the fault.

We suggest that this apparent attenuation is due to two mechanisms. First the overall decreasing ratio with increasing frequency may indicate intrinsic attenuation along the ray path. Second, the local maximum at about 35 hz may result from frequency dependent reflection/transmission through the fault zone. We are currently attempting to model this feature and will report on it in a future publication.

Publications

Waller, J.A. and P.E. Malin, 1983, Shallow Vertical Seismic Profile Observation of Earthquake Wave Attenuation, EOS, San Francisco AGU meeting December, 1983.

FIGURE 1

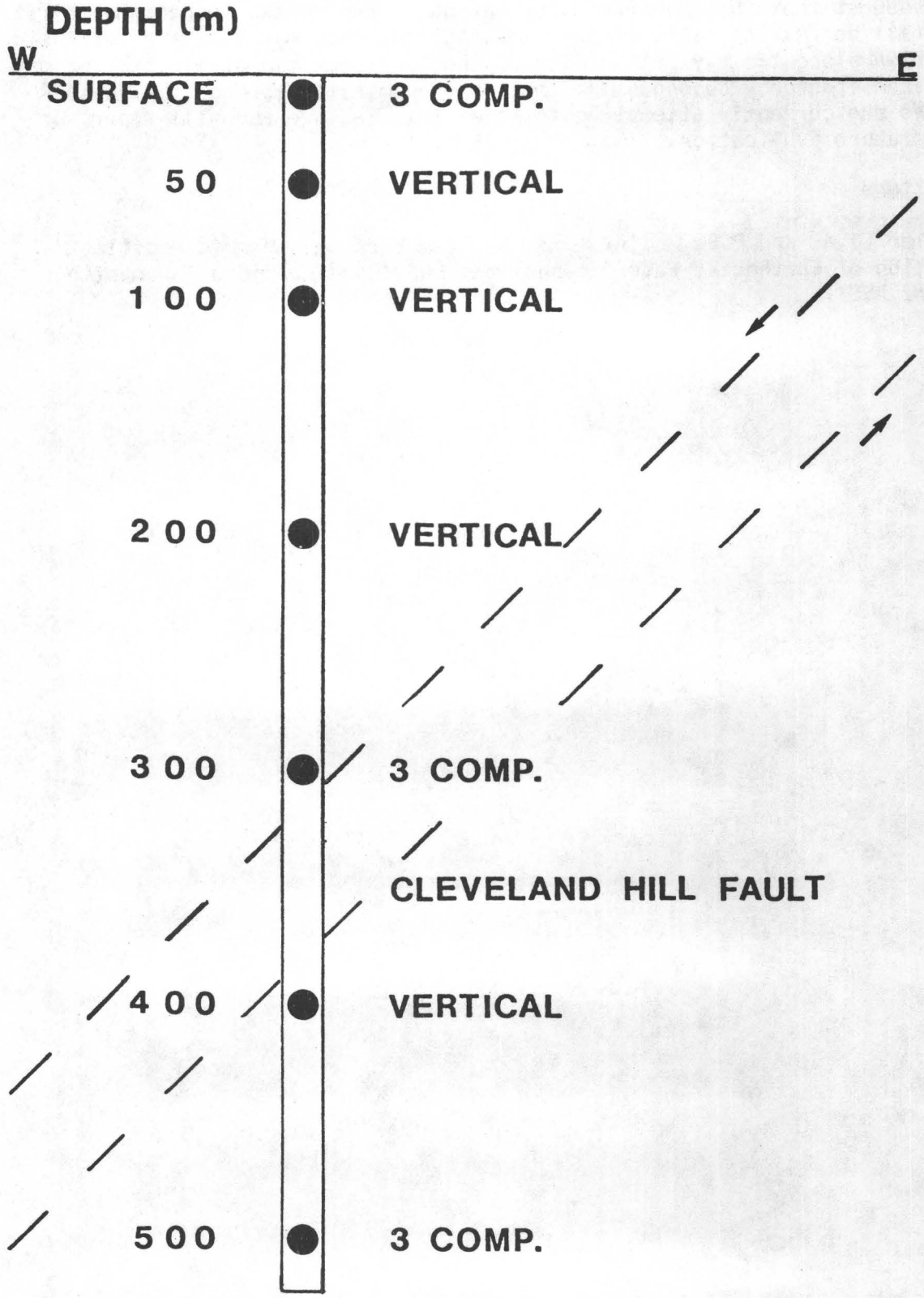
DEPTH (m)
W
E
SURFACE
3 COMP.
50
VERTICAL
100
VERTICAL
200
VERTICAL
300
3 COMP.
CLEVELAND HILL FAULT
400
VERTICAL
500
3 COMP.

HORIZONTAL AT 300M/HORIZONTAL AT 500M (S PHASE)

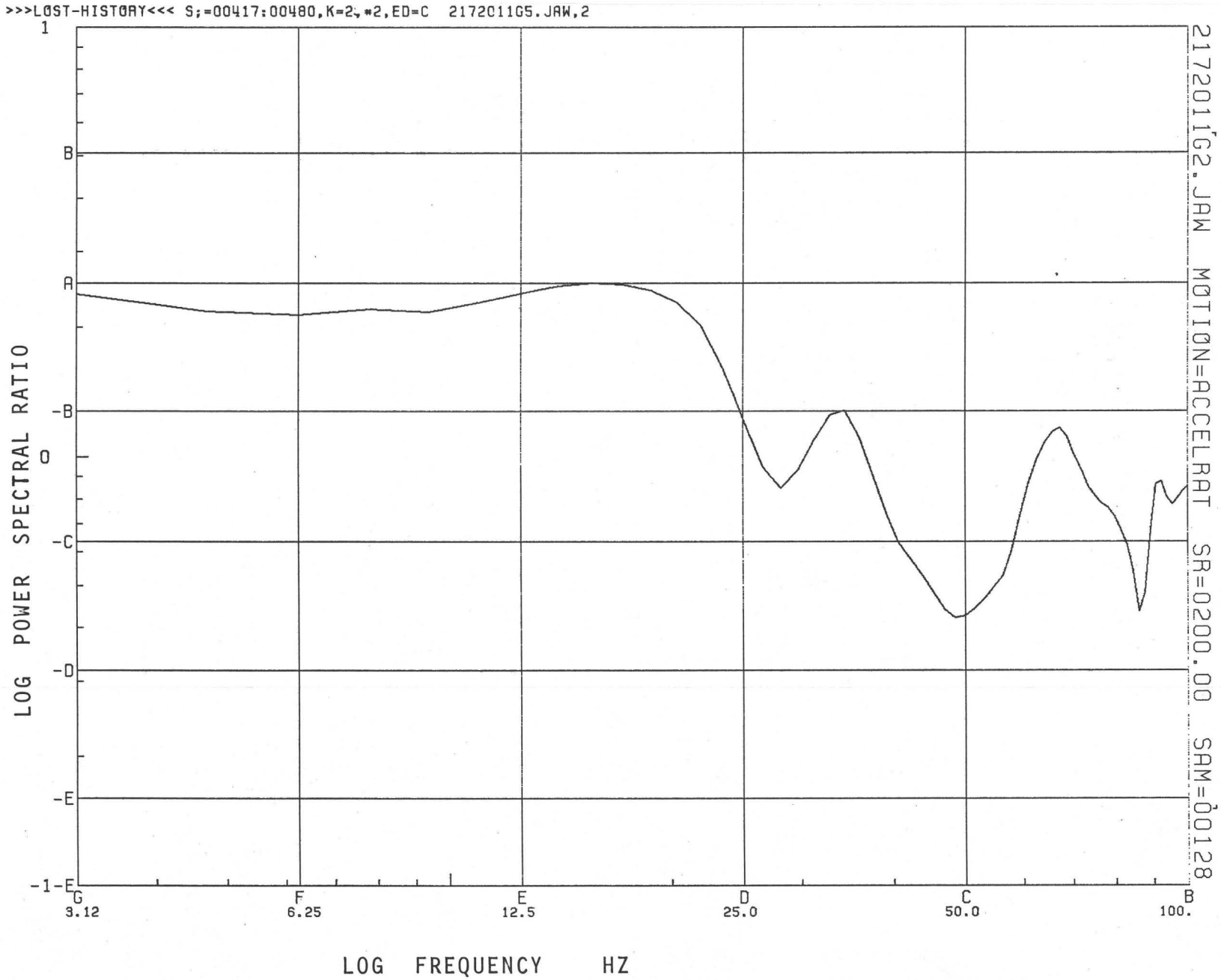

FIGURE 2

IS

PRESSURE TRANSIENT ANALYSIS OF MINI-FRAC EXPERIMENTS FOR IN-SITU STRESS MEASUREMENTS

T. N. Narasimhan
Earth Sciences Division
Lawrence Berkeley Laboratory

The Problem

A widely used technique for in situ stress measurement in rock formations is that of hydraulic fracturing, utilizing controlled, low-volume cyclic injection of water with intervening periods of shut-in and bleed off. The pressure transient data collected during these experiments is used to estimate a) the minimum horizontal stress, S_h and b) the maximum horizontal stress, S_H. The estimation of S_h is based on the instantaneous shut-in Pressure (ISIP) while that of S_H is based on the Fracture Opening Pressure (FOP). Experience of several researchers indicates that considerable judgement is required to read the correct value of the ISIP from the rapid pressure transients that follow shut-ins. In regard to the FOP, there exists an uncertainty as to whether the start of the deviation of the pressure-time curve from a linear relation during repressurization following fracture initiation represents fracture reopening or whether it represents other effects such as well-bore storage. An understanding of ISIP as well as FOP is critical for founding the interpretation technique on a sound base.

Progress

The purpose of the present work is to mathematically simulate the hydraulic fracturing process focussing attention on the hydrodynamics of the mechanisms involved. The model used for this purpose includes a number of relevant factors such as rock toughness, variable fracture geometry, fracture stiffness, variable fracture permeability, minimum fracture aperture subsequent to initiation, permeable rock matrix and the compliance of the hydraulic system and well bore cavity. The notions of ISIP and FOP will be critically examined on the basis of panametric numerical experiments conducted with the model.

So far, literature survey has been completed and the model updating has been completed. Parametric studies is in progress.

Earthquake Studies in The Geysers Area

9930-02106

David H. Oppenheimer
U. S. Geological Survey
Branch of Seismology
345 Middlefield Road, Mail Stop 77
Menlo Park, California 94025
(415) 323-8111, ext. 2791

Investigations

1. Relocate earthquakes in the Clear Lake, CA, area for the period 1975-1983.

2. Test 3-D velocity inversion program with synthetic traveltime data prior to inversion of microearthquake traveltime data collected at The Geysers geothermal field.

3. Model crustal velocity structure from arrival time data collected on four refraction profiles extending across the Coast Ranges from Stewart's Point near the Pacific coast to the western edge of the Great Valley.

4. Relocate seismicity at The Geysers on weekly basis for new evidence of induced seismicity.

5. Model Pn traveltime data recorded by 238 stations of the CALNET for 77 regional earthquakes for changes in crustal thickness, upper mantle velocity and associated anisotropy, and lower crustal velocity.

6. Analyze aftershock distribution of May 2, 1983 Coalinga earthquake.

7. Maintain Terratech digital event recorders and service field installations in Parkfield, CA, area.

Results

1. Pattern of seismicity in the Clear Lake area is diffuse, with the area southeast of the lake having the highest concentration of activity. Swarms including events with $M \geq 3.5$ occur along the Konocti Bay fault zone, but no activity is observed along the Collayomi fault zone. A 10-km wide, southwest-northeast trending zone of seismicity exists from The Geysers to Konocti Bay but is not correlated with any known geologic feature. Earthquake depths in the region do not exceed 6 km,

substantially more shallow than in the surrounding region. Focal mechanisms show predominant right-lateral strike-slip movement, consistent with the San Andreas system, with a significant component of normal dip-slip movement.

2. Synthetic traveltime data generated by approximate ray tracing (ART) for various 3-D velocity configurations were inverted to test the ability of an inverse program to resolve 3-D velocity structure. Improved results are obtained by first performing a 1-D velocity inversion to obtain the initial 3-D model and hypocenters. Velocity nodes located deeper than most earthquakes as well as along the model edge are poorly modeled. In general, the program is more likely to generate spurious velocity anomalies than to neglect true velocity anomalies. Hypocentral distributions do not appear to affect the solution except for those where hypocenters are located primarily on the network edge.

3. Arrivals from the shotpoints south of Clear Lake and near Bartlett Springs did not propagate beyond 10 km. Elevation changes of as much as 1 km over distances of 10 km, together with non-linear station profiles make interpretation of the data difficult. A 14, 000 lb. explosion was detonated at a depth of 1.7 km to stimulate a geothermal well in The Geysers field, and the resulting traveltime data indicate traveltime delays of approximately 0.5 s west of the Maacama fault and northwest of the Collayomi fault, marking the location of the Coast Range thrust. Between these two faults the Franciscan melange at the depth of the well stimulation has a velocity of approximately 5.5 km/s, with no observable traveltime delay associated with the boundaries of The Geysers steam field. Northeast of the Collayomi fault the Great Valley Sequence is modeled with velocities of 3.3, 4.0, and 5.1 km/s. West of Maacama fault the basement velocity is 5.5 km/s.

4. Microearthquake activity continues to be induced adjacent to steam production and fluid injection wells at The Geysers, Previous studies have shown that seismicity commences in previously aseismic regions within 1 year after nearby geothermal activity begins. As production activities continue to expand into new areas at The Geysers, we expect to observe a corresponding increase in seismicity.

5. Inversion of relative Pn travel times for the Moho orientation shows that the Moho dips between 3 and 6 degrees NE beneath the Coast Ranges, 8 to 17 degrees benath the Great Valley, and is horizontal beneath the Sierra Nevada foothills. An upper mantle velocity of 8 km/s adequately explains most Pn data when the traveltime effect of dipping structure is removed. No significant upper mantle velocity anisotropy is observed in the

azimuthal distribution of apparent velocities corrected for dip, although evidence exists for lateral velocity variations beneath the Coast Ranges. Beneath the Great Valley a 7.4 km/s layer is proposed to explain the arrival times observed in the Coast Range stations from the Oroville, Winters and Mt. Shasta earthquakes.

6. The 5,000 aftershocks of the Coalinga earthquake recorded by the USGS telemetered seismic network define a broad elongate zone 30 km long trending NNW-SSE from 2.5 km to 13 km deep. Most activity south of the mainshock locates at depths 5-11 km, while north of the mainshock the depths range from 2.5 to 13 km. The northern zone is twice the width of the southern zone and contains most of the large aftershocks. A compressive tectonic environment is indicated by the focal mechanisms, permitting reverse or thrust faulting. The inferred orientation of maximum compressive stress from P axes is NE to ENE, rotated 10 to 60 degrees E from that inferred for the San Andreas fault. The aftershock pattern is complex and does not define a single fault plane.

7. Thirteen digital seismic event recorders are now routinely maintained and in service in the Parkfield region. Among numerous earthquake recordings from Parkfield, the May 2, 1983 Coalinga earthquake was recorded by these instruments, providing on-scale recordings of the first few cycles of the waveform.

Reports

Eberhart-Phillips, D., 1983, Seismicity in the Clear Lake area, 1975-1982, in Sims, J., ed. Cores from Clear Lake; Late Quaternary Record of Climate, Tectonics, and Lake Sedimentation in the Northern California Coast Ranges, Geol. Soc. Am., Special Paper (in press), 29 manuscript pages.

Eberhart-Phillips, D., 1983, Seismicity in the Clear Lake area, 1975-1982, Geol. Soc. Am., Abstracts with Programs, 15, 279.

Oppenheimer, D. H., and J. P. Eaton, 1983, Moho orientation beneath central California from Pn traveltime analysis, EOS, Trans. Am. Geophys. Un., 64, (in press).

Eberhart-Phillips, D., and D. H. Oppenheimer, 1983, Induced seismicity at The Geysers geothermal area, California, Program and Abstracts, 58th Annual Meeting Pac. Sect. AAPG, Sacramento, CA.

Eberhart-Phillips, D., R. Stein, and J. Eaton, 1983, Source parameters and aftershock distribution for the May 2, 1983 Coalinga Earthquake, Coalinga Earthquake Symposium, 26th Annual Meeting Ass. Eng. Geol., San Diego, CA.

Reasenberg, P., D. Eberhart-Phillips, and P. Segall, 1983, Preliminary views of the aftershocks distribution of the May 2, 1983, Coalinga earthquake, U. S. Geol. Surv. Open-File Rep. 83-511, 27-29.

INDUCED SEISMICITY - SLEEPY HOLLOW OIL FIELD

14-08-0001-20544

George H. Rothe
Geophysics Program, Dept. of Geology
The University of Kansas
Lawrence, Kansas 66045
(913) 864-4974

INVESTIGATIONS

1) Continue to monitor seismicity and locate earthquakes in the Sleepy Hollow Oil Field.
2) Determine focal mechanisms for Sleepy Hollow earthquakes.
3) Correlate earthquake occurences with injection data.

RESULTS

The Sleepy Hollow Seismographic Network became operational 1 April 1982. Through 1 September 1983 a total of 130 earthquakes had been recorded in or near the Sleepy Hollow Oil Field. None of these events has located deeper than five kilometers, although most occur within the Precambrian granite basement (i.e. $z > 1.1$ km). The largest event recorded by the Sleepy Hollow network is a $M_c = 1.80$ earthquake on 24 May 1983. In the twenty-four hours following this earthquake 6 aftershocks ($M_c = -0.30$ to $M_c = 0.85$) were recorded. The epicenters for this sequence of events are clustered near the northern end of the network in an area of relatively high seismic activity.

To refine the velocity model, we are modifying a group hypocenter location program. With the modifications the program will invert for the velocity of the sediment layer while holding constant the layer thickness (constrained by well-hole data) and half-space velocity (constrained by refraction data). The modifications are currently being tested before implementation.

Recent experiments to determine station polarities resolved previous polarity ambiguities. We are correcting the phase data accordingly.

AMOCO Production Company continues to provide injection data which is being entered into our computer.

The recent installation (15 June 1983) of an additional solar panel (provided by the USGS) at the radio repeater site has improved network reliability in the last few months.

REPORTS

Rothe, George H. and Chung-Yao Lui (in press). Possibility of induced seismicity in the vicinity of the Sleepy Hollow Oil Field, southwestern Nebraska, BULL. SEISM. SOC. AM. [A report reviewing the results of the 4-station array that preceeded the Sleepy Hollow Network]

Geological Studies in an Area of Induced Seismicity at Monticello Reservoir, South Carolina

14-08-0001-19833

Donald T. Secor, Jr.
Department of Geology
University of South Carolina
Columbia, SC 29208
(803) 777-4516

Investigations

1. Preparation of geologic maps of six 7½' U.S.G.S. quadrangle maps in the vicinity of Lake Monticello, SC.

2. Detailed geologic mapping of the Wateree Creek fault zone in the region southeast of Monticello Reservoir.

3. Measurement of 110 km of magnetic profile in the vicinity of Lake Monticello.

4. $^{40}Ar/^{39}Ar$ dating of breccia from within the Wateree Creek fault zone.

Results

1. The induced seismicity is occurring in a heterogeneous quartz monzonite pluton of Carboniferous age.

2. Lithologic inhomogeneities and small faults and joints, together with an irregular stress field, are thought to control the diffuse seismic activity.

3. The Wateree Creek fault zone is a late Paleozoic or Mesozoic brittle fault. It is not present in the immediate vicinity of Monticello Reservoir.

4. In view of the apparent antiquity of the Wateree Creek fault zone, and the apparent absence of long faults in the region of active seismicity, it seems unlikely that a large magnitude earthquake will occur in response to the stress and pore pressure changes related to the impoundment of Monticello Reservoir.

Reports

Secor, D.T., Jr., Peck, L.S., Pitcher, D.M., Prowell, D.C., Simpson, D.H., Smith, W.A., and Snoke, A.W., Geology of the area of induced seismic activity at Monticello Reservoir, South Carolina: J. Geophys. Res., 87, 6945-6975, 1982.

Deep Hole Desalinization of the Dolores River

9920-03464

William Spence
Branch of Global Seismology and Geomagnetism
U.S. Geological Survey
Denver Federal Center, MS 967
Denver, Colorado 80225
(303) 234-4041

Investigations

This project provides monitoring and interpretation of the seismicity in the region of the intersection of the Dolores River and Paradox Valley, southwest Colorado. This project is a part of the Paradox Valley Unit of the Colorado River Basin Salinity Control Project and is being performed for the U.S. Bureau of Reclamation with support from the Induced Seismicity program of the USGS. In this desalinization project it is proposed to pump approximately 30,000 barrels/day from brine-saturated rocks beneath the Dolores river through a borehole to the Madison-Leadville limestone formation of Mississippian age, some 15,000 feet below the surface. There is a possibility of seismicity being induced, especially in the long term, by this desalinization procedure. The project objectives are to establish a pre-pumping seismicity baseline and, during the pumping phase, to closely monitor the discharge zone for possible induced seismicity. If induced seismicity does occur it should be possible to relate it to formation characteristics and to the pumping pressure and discharge rates.

Results

A ten-station seismograph network has been installed, centered on the location of the proposed pumping station. This high-gain network has a diameter of about 60 kilometers. Seismic data are presently being brought to Golden, Colorado, via microwave and phone line transmission. These data are fed through an A/D converter and then through an event detection algorithm. Final installation of the network was complete in September, 1983 and detected seismic events, which include many blasts, are presently being studied.

Study of Reservoir Induced Seismicity and Earthquake Prediction in South Carolina

Contract No. 14-08-0001-21229

Pradeep Talwani
Geology Department
University of South Carolina
Columbia, S.C. 29208
(803) 777-6449

Investigations

1. Continue to monitor seismic activity near Monticello Reservoir, near Newberry, S.C., and Lake Jocassee.

2. Development of a theoretical model for RIS.

Results

1. Induced seismicity at Monticello Reservoir, South Carolina and its vicinity.

More than half of the seismic activity in 1982, as well as all eight events with magnitudes greater than 2.0, in the Monticello Reservoir area occurred during the three month period from February to April. The activity was widespread but concentrated in a broad east-west band located in the center and the western side of the reservoir (Fig. 1). After several years of relatively shallow activity, this activity was also associated with an increase in depth (Fig. 2).

Two swarms occurred outside the Monticello Reservoir area. On May 7, 1982, a swarm of seven events, the largest of which was of magnitude 2.1, occurred in Blair, S.C., approximately 10 km northwest of the reservoir (Fig. 1). Near Newberry, S.C., approximately 25 km west of the reservoir, a swarm of 14 events, the largest of which was of magnitude 2.3, occurred in July and August, 1982. The Newberry activity was sporadic until April 28, 1983, when the level picked up again. In a swarm of more than 100 events in the following two weeks (Fig. 3), two larger, felt events ($M_L > 2.0$) occurred on April 28 ($M_L = 2.2$) and May 7 ($M_L = 2.5$), and were accompanied by 16 smaller events ($1.0 < M_L < 2.0$). The activity was monitored on portable seismographs for six weeks, supplementing Monticello network data. The portable instruments were removed when the level of activity appeared to have died down. The felt events were also accompanied by sharp sounds and are all shallow ($Z < 3$ km). The activity appears to be located on the flanks of the Newberry pluton, and it is not clear if it is associated with the Monticello Reservoir.

2. Induced seismicity at Lake Jocassee, South Carolina

Seismicity at Lake Jocassee has been monitored since 1975, first with portable instruments, and now three permanent stations. One of these stations, SMT, was connected to the state seismographic network in February, 1980, but disconnected in March, 1983, due to lack of funding. In 1982, there were four events with magnitudes greater than 2.0, and none in the first six months of 1983.

As can be seen from Figure 4, the seismicity has been fairly widespread in 1982 and the first half of 1983, but generally the spatial extent of the seismic activity has been confined within the epicentral area defined in the first year of activity.

3. Theoretical model for RIS

Additional literature has been reviewed and a draft on the mechanism of RIS is under preparation.

Reports

Talwani, P., 1983, Clays, pore pressure diffusion, and the mechanism of reservoir induced seismicity: Spring meeting of American Geophysical Union, Baltimore, Maryland, EOS Trans. Am. Geophys. Union 64 (18), p. 268.

Talwani, P., 1983, Pore pressure diffusion, clays and the mechanism of reservoir induced seismicity: International Association of Seismology and Physics of the Earth's Interior, Hamburg, West Germany, August 1983.

Blair

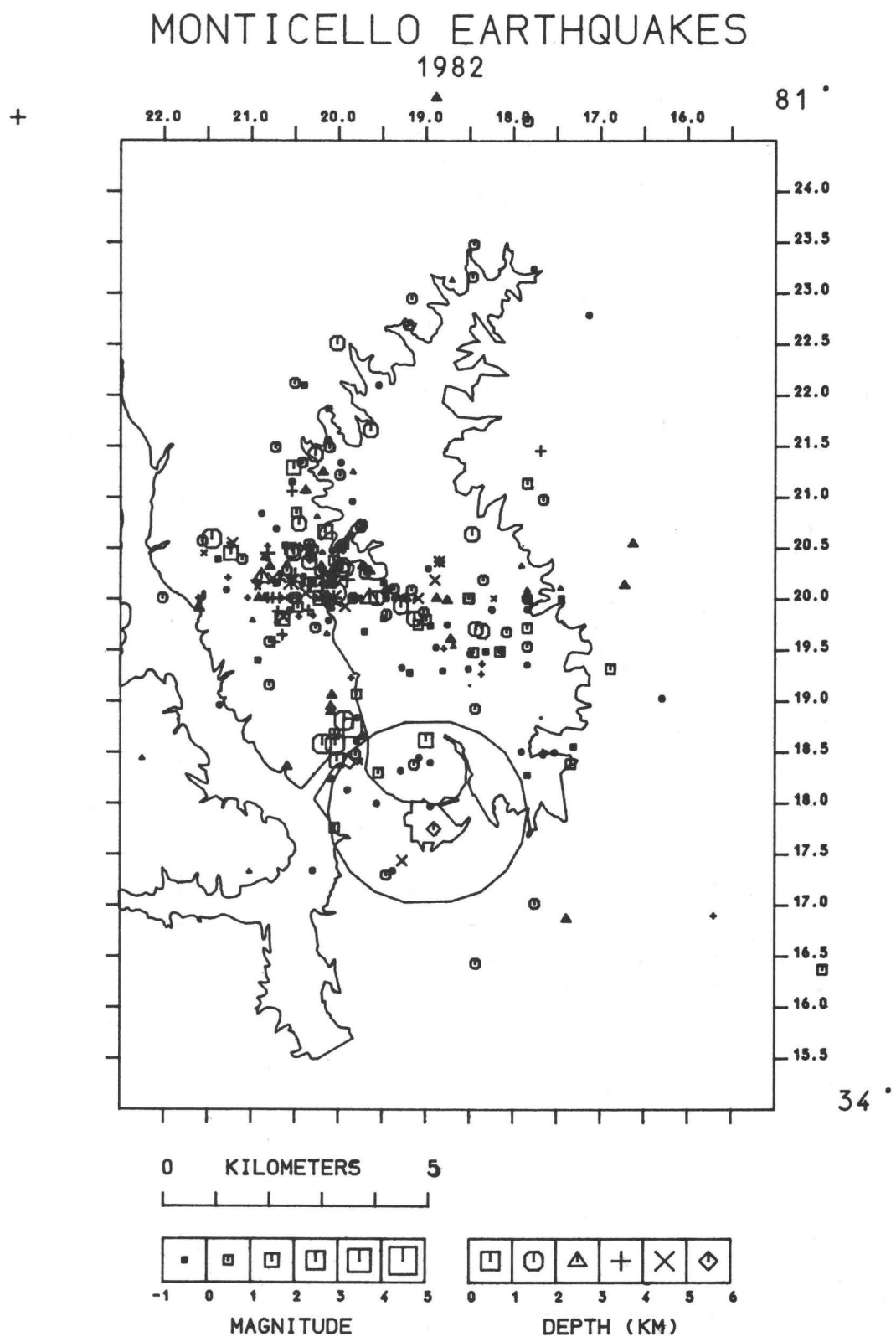

Figure 1. Earthquakes at Monticello.

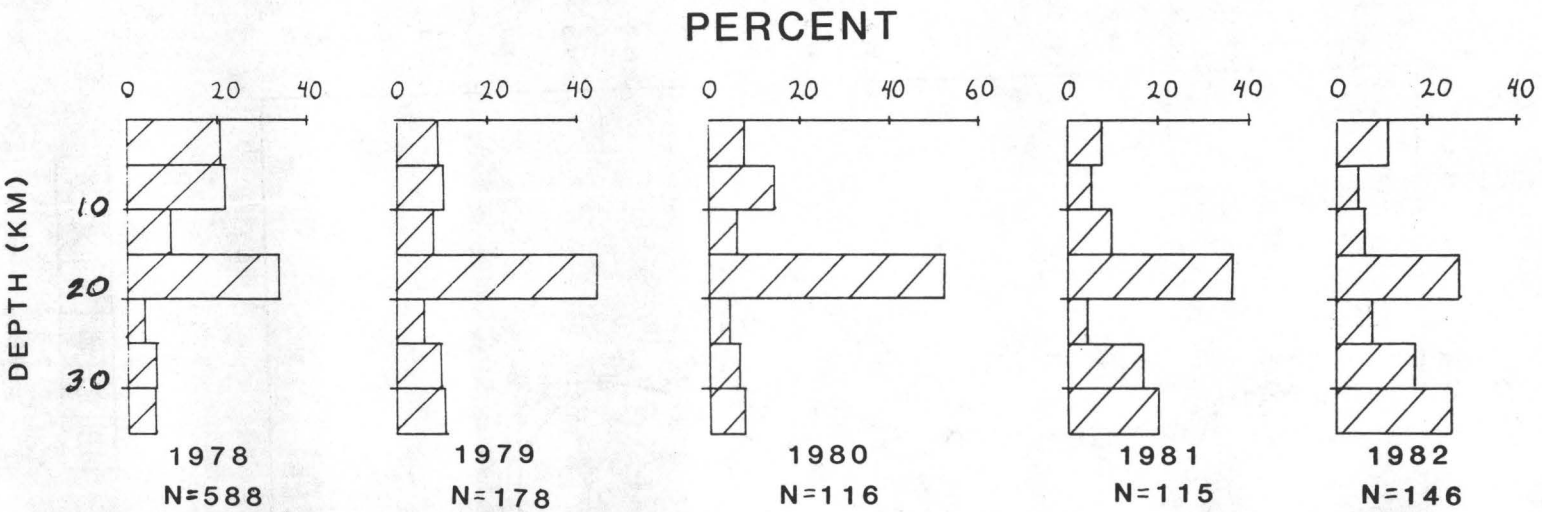

Figure 2. Change in depth with time.

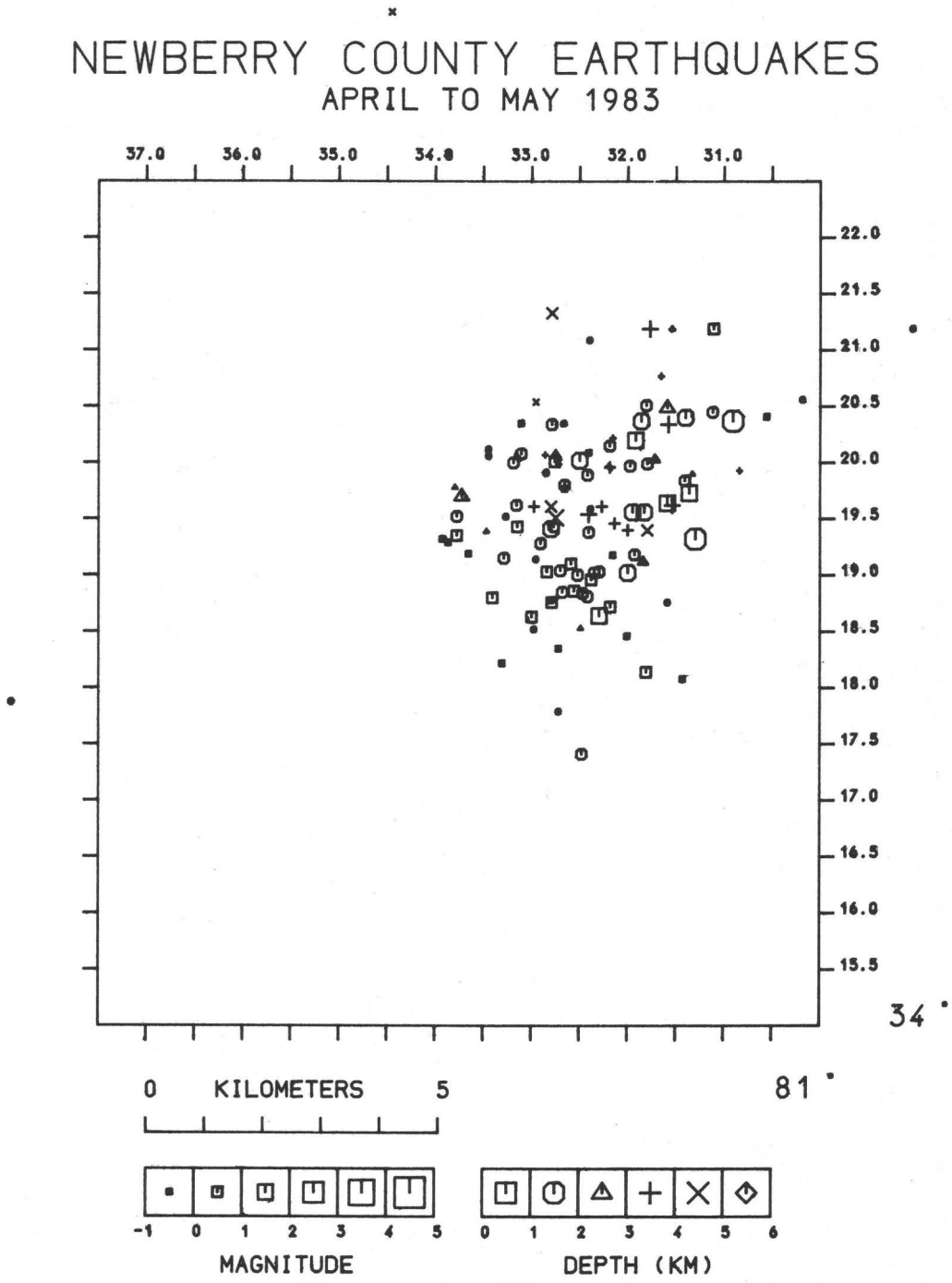

Figure 3. Earthquakes in Newberry County, S.C.

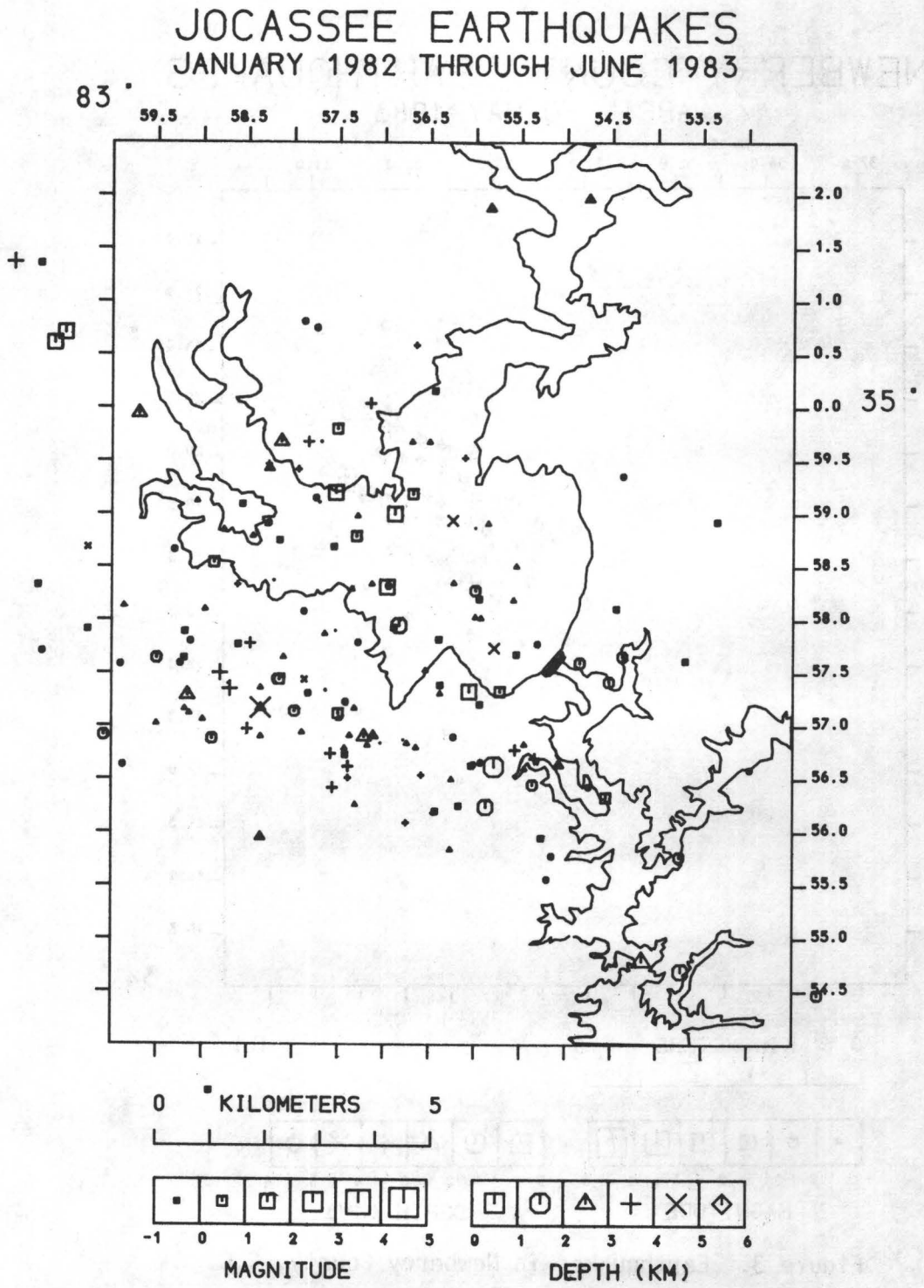

Figure 4. Earthquakes near Lake Jocassee.

Induced Seismicity at Lake Oroville, California
Contract No. 14-08-0001-20531

T.R. Toppozada and C.H. Cramer

California Division of Mines and Geology
2815 O Street
Sacramento, CA 95816
(916) 322-9309

Historical Seismicity

Within 60 km of Oroville, earthquakes of magnitude (M)4 or greater are quite rare, only one such earthquake having occurred during the twenty years before filling Lake Oroville. That earthquake occurred on the Foothills fault system of the Sierra Nevada, where M > 5 earthquakes had previously occurred.

First filling of Lake Oroville was accompanied by a M4.7 earthquake in April 1968. This earthquake occurred 40 km west of Oroville in the Great Valley where M > 4.5 earthquakes were previously unknown. The rarity of a M4.7 event in the Great Valley suggests that filling Lake Oroville triggered the 1968 earthquake. However, it appears unlikely that filling could trigger an event 40 km away.

No other significant earthquakes occurred until the M5.7 earthquake of 1975. That earthquake occurred 10 km south of Lake Oroville following an unprecedented fluctuation in lake storage. The aftershock zone of the M5.7 earthquake was not the site of any pre-1975 earthquakes.

Seismicity After 1975

Improved seismographic coverage following the M5.7 earthquake of 1975 permits a detailed comparison of seismicity to the seasonal fluctuations in water level in the lake. Toppozada and Morrison (California Geology, June 1982) have shown that earthquakes near Oroville occur mainly in the summertime when the reservoir is drawing down, and that the local seismicity decreases markedly during refilling in the winter and spring.

Hypocentral locations for the post-1975 seismicity are available partly from the California Department of Water Resources and partly from the U.S. Geological Survey. These locations were combined into a uniform dataset to determine the spatial distribution of the seismicity and its relation to the seasonal variations in reservoir storage.

The area of the 1975 mainshock has apparently been relieved of stress, few earthquakes of M > 2 having occurred within 3 km of the mainshock epicenter since 1977. Post-1977 seismicity is concentrated at the ends of the aftershock zone and ranges in size up to M3. Most of the seismicity is located at the southern end of the aftershock zone, 12 km south of Lake Oroville, and occurs mainly during periods of drawdown. The seismicity at the northern end of the aftershock zone, nearest Lake Oroville, occurs mainly at the ends of large fillings such as in June 1975, May 1978, and June 1982, and at the ends of large drawdowns such as in December 1976, January 1979, and in October and November 1980.

Comparison to Neighboring Reservoir

New Bullards Bar Reservoir is located 30 km southeast of Lake Oroville in the historically active Foothills fault system. Maximum reservoir depth and capacity are 191 meters and 1,196 million cubic meters compared to 220 meters and 4,299 million cubic meters for Lake Oroville. Within 20 km of New Bullards Bar Dam (NBBD) no earthquakes of M > 3 have been located, even after filling in 1969. Since the seismographic network was improved following the 1975 Oroville earthquake, earthquakes of M > 2 were recorded three times within 20 km of NBBD: (1) in February 1976 following unprecedented drawdown, (2) in June 1978 following the refilling at the end of the drought, (3) in May and August 1981 after the reservoir was drawn down to a level even lower than during the 1976-1977 drought, and then refilled. Thus, it appears that large fluctuations in storage behind NBBD might have triggerred earthquakes in the M2 to 3 range.

Seismicity Near Aswan Dam, Egypt, with Application to Induced Seismicity in California

Contract No. 14-08-0001-21266

T. R. Toppozada, C.H. Cramer, D.L. Parke

California Division of Mines and Geology
2815 O Street
Sacramento, CA 95816
(916) 322-9309

On 14 November 1981, a magnitude (M)5 1/2 earthquake occurred 50 km upstream from Aswan High Dam, under a large western branch of the lake. Although the lake started filling in 1964, the mainshock epicentral area became submerged only in late 1975 when the maximum water depth behind the dam first exceeded 90 m, making the 150 cubic km reservoir the second largest in the world. Since 1976, the maximum depth of the reservoir has varied seasonally between 86 m and 92.5 m. Earthquakes of M 5 or larger were previously unknown within 100 km of the reservoir, suggesting that the M 5 1/2 event was triggered by reservoir filling.

The large western branch of the reservoir, where the seismicity occurred, is underlain by porous sandstone. The delay of six years between the submergence of the epicentral area in 1975, and the occurrence of the mainshock in 1981, might be related to the gradual saturation of the sandstone.

A month after the mainshock, the Egyptian Geological Survey (EGS) deployed five MEQ-800 seismographs in the aftershock area. This portable network was operated by EGS in difficult field conditions from 12 December 1981 to 6 July 1982 when Helwan Institute of Astronomy and Geophysics installed a permanent telemetry network in cooperation with Lamont Doherty Geological Observatory. The EGS portable network adequately surrounded the seismic zone from 24 December 1981 to 11 June 1982 providing a unique data set that is being analyzed and interpreted by EGS in cooperation with California Division of Mines and Geology.

Confirmed quarry blasts were used to determine the velocity structure appropriate for earthquake location. Four-hundred and fifty earthquakes have been located. The seismicity is concentrated under the large western branch of the lake in three zones. The main zone is located at Gebel Marawa at the intersection of east-west and north-south faults. Well determined focal depths range from 15 to 25 km, which are greater than depths previously reported for induced seismicity. The mainshock was accompanied by a zone of cracking trending westward from Gebel Marawa. The second seismic zone is located 20 km to the east of Gebel Marawa, towards the main reservoir, also near the intersection of east-west and north-south faults. The third seismicity zone is located

some 10 to 15 km northeast of Gebel Marawa in an area of north-south faults. Focal mechanisms suggesting right-lateral strike-slip on easterly planes or left-lateral strike-slip on northerly planes occur in all three seismic zones. In addition, focal mechanisms suggesting normal faulting on an easterly plane occur at Gebel Marawa. Outside the western branch, minor seismicity occurs in the main part of the reservoir, and includes a few events within 10 km upstream from the dam.

The focal depths of the mainshock and of the aftershocks during the following ten weeks are unconstrained because seismographic coverage was sparse at that time. It is unknown whether focal depths before adequate seismographic coverage became available on 25 January 1982 were shallower than the 15 km to 25 km range determined for the later period.

Efforts are under way to locate all earthquakes of magnitude 2 or greater that occurred within 60 km of Aswan Dam during the six months that the network was operating. The spatial and temporal characteristics of the seismicity will be determined and compared to the geology and to the reservoir operations.

INDEX 1

INDEX ALPHABETIZED BY PRINCIPAL INVESTIGATOR

		Page
Ahrens, T. J.	California Institute of Technology	186
Aki, K.	Massachusetts Institute of Technology	192
Aki, K.	Massachusetts Institute of Technology	400
Algermissen, S. T.	U.S. Geological Survey	9
Allen, C. R.	California Institute of Technology	93
Allen, C. R.	California Institute of Technology	197
Allen, C. R.	California Institute of Technology	199
Allen, R. V.	U.S. Geological Survey	203
Anderson, L. R.	Utah State University	167
Anderson, L. R.	Utah State University	169
Anderson, R. E.	U.S. Geological Survey	96
Andrews, D. J.	U.S. Geological Survey	145
Atkinson, B. K.	Imperial College	402
Baker, L. M.	U.S. Geological Survey	146
Baker, L. M.	U.S. Geological Survey	147
Bakun, W. H.	U.S. Geological Survey	404
Bekins, B.	U.S. Geological Survey	204
Berger, J.	California, University of, San Diego	447
Bilham, R.	Lamont-Doherty Geological Observatory	324
Biswas, N. N.	Alaska, University of	148
Bonilla, M. G.	U.S. Geological Survey	98
Borcherdt, R. D.	U.S. Geological Survey	149
Brace, W. F.	Massachusetts Institute of Technology	450
Britton, O. J.	U.S. Geological Survey	479
Brune, J. N.	California, University of, San Diego	206
Buland, R.	U.S. Geological Survey	500
Byerlee, J. D.	U.S. Geological Survey	405
Byerlee, J. D.	U.S. Geological Survey	406
Cann, L. R.	Leighton Associates, Inc.	99
Carlson, M. A.	U.S. Geological Survey	480
Carlson, M. A.	U.S. Geological Survey	481
Chen, A. T. F.	U.S. Geological Survey	151
Choy, G. L.	U.S. Geological Survey	483
Choy, G. L.	U.S. Geological Survey	504
Chung, Y.	California, University of, San Diego	328
Clark, H. E., Jr.	U.S. Geological Survey	503
Clark, M. M.	U.S. Geological Survey	100
Colquhoun, D. J.	South Carolina, University of	66
Cotton, W. R.	Foothill-DeAnza Community College	103
Cotton, W. R.	Foothill-DeAnza Community College	107
Counselman, C. C., III	Massachusetts Institute of Technology	207
Crampin, S.	Institute of Geological Sciences	331
Daily, W. D.	Lawrence Livermore National Laboratory	210

Das, S.	Lamont-Doherty Geological Observatory	407
Dewey, J. W.	U.S. Geological Survey	1
Diment, W. H.	U.S. Geological Survey	68
Dunning, J. D.	Indiana University	408
Ebel, J. E.	Boston College	69
Espinosa, A. F.	U.S. Geological Survey	12
Fairhurst, C.	Minnesota, University of	507
Felson, L. B.	Polytechnic Institute of New York	152
Galehouse, J. S.	San Francisco State University	211
Gladwin, M. T.	Queensland, University of	214
Gladwin, M. T.	Queensland, University of	334
Guptill, P. D.	Woodward-Clyde Consultants	109a
Hadley, D. M.	Sierra Geophysics, Incorporated	153
Haimson, B. C.	Wisconsin, University of, Madison	509
Hall, N. T.	Foothill-DeAnza Community College	110
Hall, W.	U.S. Geological Survey	218
Harding, S. T.	U.S. Geological Survey	13
Harkrider, D. G.	California Institute of Technology	219
Hauksson, E.	Lamont-Doherty Geological Observatory	221
Healy, J. H.	U.S. Geological Survey	453
Healy, J. H.	U.S. Geological Survey	455
Henyey, T. L.	Southern California, University of	337
Herriot, J.	U.S. Geological Survey	343
Herrmann, R. B.	Saint Louis University	71
Hoffman, J. P.	U.S. Geological Survey	484
Irwin, W. P.	U.S. Geological Survey	112
Isacks, B. L.	Cornell University	225
Isacks, B. L.	Cornell University	228
Jackson, D. D.	California, University of, Los Angeles	230
Jackson, D. D.	California, University of, Los Angeles	345
Jaksha, L. H.	U.S. Geological Survey	487
Jensen, E. G.	U.S. Geological Survey	234
Johnson, C.	U.S. Geological Survey	235
Johnston, A. C.	Memphis State University	236
Johnston, M. J. S.	U.S. Geological Survey	347
Jones, L. M.	Lamont-Doherty Geological Observatory	350
Joyner, W. B.	U.S. Geological Survey	156
Julian, B. R.	U.S. Geological Survey	412
Kanamori, H.	California Institute of Technology	240
Kanamori, H.	California Institute of Technology	242
Keefer, D. K.	U.S. Geological Survey	171
Kelleher, J.	Redwood Research	244
Kerry, L.	U.S. Geological Survey	489
Kerry, L.	U.S. Geological Survey	490
King, C. -Y	U.S. Geological Survey	352
King, K. W.	U.S. Geological Survey	16

Kirby, S.	U.S. Geological Survey	415
Kiremidjian, A. S.	Stanford University	181
Kissingler, C.	Colorado, University of	245
Kustu, O.	URS/ John A. Blume	184
Lachenbruch, A. H.	U.S. Geological Survey	459
Lahr, J. C.	U.S. Geological Survey	17
Lajoie, K. R.	U.S. Geological Survey	116
Langer, C. J.	U.S. Geological Survey	157
Langston, C. A.	Pennsylvania State University	159
Leary, P. C.	Southern California, University of	388
Lee, W. H. K.	U.S. Geological Survey	249
Lee, W. H. K.	U.S. Geological Survey	250
Lester, F. W.	U.S. Geological Survey	251
Lindh, A. G.	U.S. Geological Survey	258
Liu, H. -P	U.S. Geological Survey	353
Logan, J. M.	Texas A & M University	417
Long, L. T.	Georgia Institute of Technology	511
Machette, M. N.	U.S. Geological Survey	119
Madden, T. R.	Massachusetts Institute of Technology	355
Malin, P. E.	California, University of, Santa Barbara	513
Mark, R. K.	U.S. Geological Survey	23
Martin, G. R.	Ertec, Incorporated	174
Matti, J. C.	U.S. Geological Survey	24
Mavko, G. M.	U.S. Geological Survey	359
Mavko, G. M.	U.S. Geological Survey	422
McCarthy, R. P.	U.S. Geological Survey	491
McGarr, A.	U.S. Geological Survey	260
McGuire, R. K.	Dames & Moore	160
McKeown, F.	U.S. Geological Survey	72
McNally, K.	California, University of, Santa Cruz	265
McNally, K.	California, University of, Santa Cruz	363
Merifield, P. M.	Lamar-Merifield	366
Minster, J. B.	S-Cubed	463
Mooney, W. D.	U.S. Geological Survey	466
Morrissey, S-T.	Saint Louis University	369
Mortensen, C. E.	U.S. Geological Survey	377
Narasimhan, T. N.	Lawrence Berkeley Laboratory	517
Nason, R.	U.S. Geological Survey	161
Oliver, J.	Cornell University	268
Oppenheimer, D. H.	U.S. Geological Survey	518
Ord, A.	Monash University	476
Page, R. A.	U.S. Geological Survey	271
Park, R. B.	U.S. Geological Survey	14
Perkins, J. B.	Association of Bay Area Governments	29
Person, W. J.	U.S. Geological Survey	492
Peselnick, L.	U.S. Geological Survey	423
Peterson, J.	U.S. Geological Survey	494
Power, M. S.	Woodward-Clyde Consultants	175
Prescott, W. H.	U.S. Geological Survey	276

Ratcliffe, N. M.	U.S. Geological Survey	74
Reasenberg, P. A.	U.S. Geological Survey	281
Reimer, G. M.	U.S. Geological Survey	380
Reynolds, R. D.	U.S. Geological Survey	495
Rial, J. A.	California, University of, Santa Cruz	162
Rice, J. R.	Harvard University	426
Ross, D. C.	U.S. Geological Survey	124
Rothe, G. H.	Kansas, University of	521
Rudnicki, J. W.	Northwestern University	433
Ryall, A.	Nevada, University of	33
Sarna-Wojcicki, A. M.	U.S. Geological Survey	126
Secor, D. T., Jr.	South Carolina, University of	522
Shapiro, M. H.	California Institute of Technology	384
Sharp, R. V.	U.S. Geological Survey	130
Sieh, K.	California Institute of Technology	134
Sieh, K.	California Institute of Technology	135
Sims, J. D.	U.S. Geological Survey	137
Singh, S.	Dames & Moore	178
Slater, L. E.	Colorado, University of	280
Smith, R. B.	Utah, University of	38
Spence, W.	U.S. Geological Survey	505
Spence, W.	U.S. Geological Survey	523
Spudich, P.	U.S. Geological Survey	164
Stauder, W.	Saint Louis University	77
Stewart, S. W.	U.S. Geological Survey	288
Stover, C. W.	U.S. Geological Survey	498
Street, R. L.	Kentucky, University of	4
Stuart, W. D.	U.S. Geological Survey	436
Swanson, P. L.	Colorado, University of	437
Sykes, L. R.	Lamont-Doherty Geological Observatory	289
Sylvester, A. G.	California, University of, Santa Barbara	292
Sylvester, A. G.	California, University of, Santa Barbara	297
Taggart, J. N.	U.S. Geological Survey	8
Talwani, P.	South Carolina, University of	80
Talwani, P.	South Carolina, University of	524
Teng, T.	Southern California, University of	298
Teng, T.	Southern California, University of	394
Thatcher, W.	U.S. Geological Survey	300
Tinsley, J. C.	U.S. Geological Survey	42
Toksoz, M. N.	Massachusetts Institute of Technology	87
Toppozada, T. R.	California Division of Mines and Geology	530
Toppozada, T. R.	California Division of Mines and Geology	532
Tullis, T. E.	Boston University	441
Updike, R. G.	Akaska, State of	44
Van Schaack, J.	U.S. Geological Survey	304
Van Schaack, J.	U.S. Geological Survey	305
Wallace, R. E.	U.S. Geological Survey	139

Wang, C. Y.	California, University of, Berkeley	445
Ware, R. H.	Colorado, University of	47
Ward, P. L.	U.S. Geological Survey	474
Warren, D. H.	U.S. Geological Survey	475
Warrick, R. E.	U.S. Geological Survey	166
Weaver, C. S.	U.S. Geological Survey	49
Wesson, R. L.	U.S. Geological Survey	306
Wheeler, R. L.	U.S. Geological Survey	91
White, R. A.	U.S. Geological Survey	309
Wood, S. H.	U.S. Geological Survey	52
Wyatt, F.	California, University of, San Diego	315
Wyatt, F.	California, University of, San Diego	317
Wyss, M.	Colorado, University of	320
Wu, F. T.	New York, State University of, Binghamton	311
Yeats, R. S.	Oregon, State University	56
Yeats, R. S.	Oregon, State University	323
Yerkes, R. F.	U.S. Geological Survey	57
Youd, T. L.	U.S. Geological Survey	179
Yount, J. C.	U.S. Geological Survey	60
Ziony, J. I.	U.S. Geological Survey	64
Zoback, M. L.	U.S. Geological Survey	142

INDEX 2

INDEX ALPHABETIZED BY INSTITUTION

		Page
Alaska, University of	Biswas, N. N.	148
Alaska, State of	Updike, R. G.	44
Association of Bay Area Governments	Perkins, J. B.	29
Boston College	Ebel, J. E.	69
Boston College	Tullis, T. E.	441
California Division of Mines and Geology	Toppozada, T. R.	530
California Division of Mines and Geology	Toppozada, T. R.	532
California Institute of Technology	Ahrens, T. J.	186
California Institute of Technology	Allen, C. R.	93
California Institute of Technology	Allen, C. R.	197
California Institute of Technology	Allen, C. R.	199
California Institute of Technology	Harkrider, D. G.	219
California Institute of Technology	Kanamori, H.	240
California Institute of Technology	Kanamori, H.	242
California Institute of Technology	Shapiro, M. H.	384
California Institute of Technology	Sieh, K.	134
California Institute of Technology	Sieh, K.	135
California, University of, Berkeley	Wang, C. Y.	445
California, University of, Los Angeles	Jackson, D. D.	230
California, University of, Los Angeles	Jackson, D. D.	345
California, University of, San Diego	Berger, J.	447
California, University of, San Diego	Brune, J. N.	206
California, University of, San Diego	Chung, Y.	328
California, University of, San Diego	Wyatt, F.	315
California, University of, San Diego	Wyatt, F.	317
California, University of, Santa Barbara	Malin, P. E.	513
California, University of, Santa Barbara	Sylvester, A. G.	292
California, University of, Santa Barbara	Sylvester, A. G.	297
California, University of, Santa Cruz	McNally, K.	265
California, University of, Santa Cruz	McNally, K.	363
California, University of, Santa Cruz	Rial, J. A.	162
Colorado, University of	Kissingler, C.	245
Colorado, University of	Slater, L. E.	280
Colorado, University of	Swanson, P. L.	437
Colorado, University of	Ware, R. H.	47

Colorado, University of	Wyss, M.	320
Cornell University	Isacks, B. L.	225
Cornell University	Isacks, B. L.	228
Cornell University	Oliver, J.	268
Dames & Moore	McGuire, R. K.	160
Dames & Moore	Singh, S.	178
Ertec, Incorporated	Martin, G. R.	174
Foothill-DeAnza Community College	Cotton, W. R.	103
Foothill-DeAnza Community College	Cotton, W. R.	107
Foothill-DeAnza Community College	Hall, N. T.	110
Georgia Institute of Technology	Long, L. T.	511
Harvard University	Rice, J. R.	426
Indiana University	Dunning, J. D.	408
Imperial College	Atkinson, B. K.	402
Institute of Geological Sciences	Crampin, S.	331
Kansas, University of	Rothe, G. H.	521
Kentucky, University of	Street, R. L.	4
Lamar-Merifield	Merifield, P. M.	366
Lamont-Doherty Geological Observatory	Bilham, R.	324
Lamont-Doherty Geological Observatory	Das, S.	407
Lamont-Doherty Geological Observatory	Hauksson, E.	221
Lamont-Doherty Geological Observatory	Jones, L. M.	350
Lamont-Doherty Geological Observatory	Sykes, L. R.	289
Lawrence Berkeley Laboratory	Narasimhan, T. N.	517
Lawrence Livermore National Laboratory	Daily, W. D.	210
Leighton and Associates, Inc.	Cann, L. R.	99
Massachusetts Institute of Technology	Aki, K.	192
Massachusetts Institute of Technology	Aki, K.	400
Massachusetts Institute of Technology	Brace, W. F.	450
Massachusetts Institute of Technology	Counselman, C.C., III	207
Massachusetts Institute of Technology	Madden, T. R.	355
Massachusetts Institute of Technology	Toksoz, M. N.	87
Memphis State University	Johnston, A. C.	236
Minnesota, University of	Fairhurst, C.	507

Monash University	Ord, A.	476
Nevada, University of	Ryall. A.	33
New York, State University of, Binghamton	Wu, F. T.	311
Northwestern University	Rudnicki, J. W.	433
Oregon, State University	Yeats, R. S.	56
Oregon, State University	Yeats, R. S.	323
Pennsylvania State University	Langston, C. A.	159
Polytechnic Institute of New York	Felson, L. B.	152
Queensland, University of	Gladwin, M. T.	214
Queensland, University of	Gladwin, M. T.	334
Redwood Research, Inc.	Kelleher, J.	244
Saint Louis University	Herrmann, R. B.	71
Saint Louis University	Morrissey, S-T	369
Saint Louis University	Stauder, W.	77
San Francisco State University	Galehouse, J. S.	211
Sierra Geophysics, Incorporated	Hadley, D. M.	153
South Carolina, University of	Colquhoun, D. J.	66
South Carolina, University of	Secor, D. T., Jr.	522
South Carolina, University of	Talwani, P.	80
South Carolina, University of	Talwani, P.	524
Southern California, University of	Henyey, T. L.	337
Southern California, University of	Leary, P. C.	388
Southern California, University of	Teng, T.	298
Southern California, University of	Teng, T.	394
Stanford University	Kiremidjian, A. S.	181
S-Cubed	Minster, J. B.	463
Texas A & M University	Logan, J. M.	417
U.S. Geological Survey	Algermissen, S. T.	9
U.S. Geological Survey	Allen, R. V.	203
U.S. Geological Survey	Anderson, R. E.	96
U.S. Geological Survey	Andrews, D. J.	145
U.S. Geological Survey	Baker, L. M.	146
U.S. Geological Survey	Baker, L. M.	147
U.S. Geological Survey	Bakun, W. H.	404
U.S. Geological Survey	Bekins, B.	204

U.S. Geological Survey	Bonilla, M. G.	98
U.S. Geological Survey	Borcherdt, R. D.	149
U.S. Geological Survey	Britton, O. J.	479
U.S. Geological Survey	Buland, R.	500
U.S. Geological Survey	Byerlee, J. D.	405
U.S. Geological Survey	Byerlee, J. D.	406
U.S. Geological Survey	Carlson, M. A.	480
U.S. Geological Survey	Carlson, M. A.	481
U.S. Geological Survey	Chen, A. T. F.	151
U.S. Geological Survey	Choy, G. L.	483
U.S. Geological Survey	Choy, G. L.	504
U.S. Geological Survey	Clark, H. E., Jr.	503
U.S. Geological Survey	Clark, M. M.	100
U.S. Geological Survey	Dewey, J. W.	1
U.S. Geological Survey	Diment, W. H.	68
U.S. Geological Survey	Espinosa, A. F.	12
U.S. Geological Survey	Hall, W.	218
U.S. Geological Survey	Harding, S. T.	13
U.S. Geological Survey	Healy, J. H.	453
U.S. Geological Survey	Healy, J. H.	455
U.S. Geological Survey	Herriot, J.	343
U.S. Geological Survey	Hoffman, J. P.	484
U.S. Geological Survey	Irwin, W. P.	112
U.S. Geological Survey	Jaksha, L. H.	487
U.S. Geological Survey	Jensen, E. G.	234
U.S. Geological Survey	Johnson, C.	235
U.S. Geological Survey	Johnston, M. J. S.	347
U.S. Geological Survey	Joyner, W. B.	156
U.S. Geological Survey	Julian, B. R.	412
U.S. Geological Survey	Keefer, D. K.	171
U.S. Geological Survey	Kerry, L.	489
U.S. Geological Survey	Kerry, L.	490
U.S. Geological Survey	King, C. -Y.	352
U.S. Geological Survey	King, K. W.	16
U.S. Geological Survey	Kirby, S.	415
U.S. Geological Survey	Lachenbruch, A. H.	459
U.S. Geological Survey	Lahr, J. C.	17
U.S. Geological Survey	Lajoie, K. R.	116
U.S. Geological Survey	Langer, C. J.	157
U.S. Geological Survey	Lee, W. H. K.	249
U.S. Geological Survey	Lee, W. H. K.	250
U.S. Geological Survey	Lester, F. W.	251
U.S. Geological Survey	Lindh, A. G.	258
U.S. Geological Survey	Liu, H. -P.	353
U.S. Geological Survey	Machette, M. N.	119
U.S. Geological Survey	Mark, R. K.	23
U.S. Geological Survey	Matti, J. C.	24
U.S. Geological Survey	Mavko, G. M.	359
U.S. Geological Survey	Mavko, G. M.	422
U.S. Geological Survey	McCarthy, R. P.	491
U.S. Geological Survey	McGarr, A.	260
U.S. Geological Survey	McKeown, F.	72
U.S. Geological Survey	Mooney, W. D.	466

U.S. Geological Survey	Mortensen, C. E.	377
U.S. Geological Survey	Nason, R.	161
U.S. Geological Survey	Oppenheimer, D. H.	518
U.S. Geological Survey	Page, R. A.	271
U.S. Geological Survey	Park, R. B.	14
U.S. Geological Survey	Person, W. J.	492
U.S. Geological Survey	Peselnick, L.	423
U.S. Geological Survey	Peterson, J.	494
U.S. Geological Survey	Prescott, W. H.	276
U.S. Geological Survey	Ratcliffe, N. M.	74
U.S. Geological Survey	Reasenberg, P. A.	281
U.S. Geological Survey	Reimer, G. M.	380
U.S. Geological Survey	Reynolds, R. D.	495
U.S. Geological Survey	Ross, D. C.	124
U.S. Geological Survey	Sarna-Wojcicki, A. M.	126
U.S. Geological Survey	Sharp, R. V.	130
U.S. Geological Survey	Sims, J. D.	137
U.S. Geological Survey	Spence, W.	505
U.S. Geological Survey	Spence, W.	523
U.S. Geological Survey	Spudich, P.	164
U.S. Geological Survey	Stewart, S. W.	288
U.S. Geological Survey	Stover, C. W.	498
U.S. Geological Survey	Stuart, W. D.	436
U.S. Geological Survey	Taggart, J. N.	8
U.S. Geological Survey	Thatcher, W.	300
U.S. Geological Survey	Tinsley, J. C.	42
U.S. Geological Survey	Van Schaack, J.	304
U.S. Geological Survey	Van Schaack, J.	305
U.S. Geological Survey	Wallace, R. E.	139
U.S. Geological Survey	Ward, P. L.	474
U.S. Geological Survey	Warren, D. H.	475
U.S. Geological Survey	Warrick, R. E.	166
U.S. Geological Survey	Weaver, C. S.	49
U.S. Geological Survey	Wesson, R. L.	306
U.S. Geological Survey	Wheeler, R. L.	91
U.S. Geological Survey	White, R. A.	309
U.S. Geological Survey	Wood, S. H.	52
U.S. Geological Survey	Yerkes, R. F.	57
U.S. Geological Survey	Youd, T. L.	179
U.S. Geological Survey	Yount, J. C.	60
U.S. Geological Survey	Ziony, J. I.	64
U.S. Geological Survey	Zoback, M. L.	142
URS/ John A. Blume	Kustu, O.	184
Utah State University	Anderson, L. R.	167
Utah State University	Anderson, L. R.	169
Utah, University of	Smith, R. B.	38
Wisconsin, University of, Madison	Haimson, B. C.	509
Woodward-Clyde Consultants	Guptill, P. D.	109a
Woodward-Clyde Consultants	Power, M. S.	175